ISBN: 978-3-95450-191-5 doi:10.18429/JACoW-SRF2017-MOXA02

THE COMMISSIONING OF THE EUROPEAN-XFEL LINAC AND ITS PERFORMANCE*

D. Reschke†, W. Decking, N. Walker, H. Weise, European XFEL Accelerator Consortium and Commissioning Team, Deutsches Elektronen-Synchrotron DESY, Hamburg, Germany

Abstract

The main linac of the superconducting accelerator of the European XFEL presently consists of 96 accelerator modules, each housing eight 1.3 GHz TESLA-type cavities, with an average design gradient of 23.6 MV/m. The performance of each individual module has been tested after module assembly in the Accelerator Module Test Facility (AMTF) at DESY. The 2-year period of module installation to the accelerator tunnel was finished in August 2016. In order to recheck and re-establish the performance of the input power couplers, warm processing of nearly all installed modules was performed before the first cool-down during Dec 2016 / Jan 2017. Four consecutive modules are connected to one 10 MW klystron and form a so-called RF station, which is powered and controlled individually during operation. By June 2017 23 of 25 RF stations have been commissioned for beam acceleration including frequency tuning, various calibrations and LLRF adjustments. A preliminary beam energy of 14 GeV was achieved, which is sufficient for first lasing experiments. No significant performance degradation has been observed so far. The commissioning experience and the available RF performance data will be presented.

INTRODUCTION

The European XFEL aims at delivering X-rays from 0.25 to up to 25 keV out of 3 SASE undulators [1, 2]. The radiators are driven by a superconducting linear accelerator based on TESLA technology with a design energy of 17.5 GeV [3]. The linac operates in 10 Hz pulsed mode (1.4 ms RF pulse length) and can deliver up to 2700 bunches per pulse. Electron beams will be distributed to the 3 different beamlines within a pulse, thus being able to operate three experiments in parallel.

The accelerator of the European XFEL and major parts of the infrastructure are contributed by the accelerator construction consortium, coordinated by DESY. The consortium consists of CNRS/IN2P3 (Orsay, France), CEA/IRFU (Saclay, France), DESY (Hamburg, Germany), INFN-LASA (Milano, Italy), NCBJ (Świerk, Poland), WUT (Wrocław, Poland), IFJ-PAN (Kraków, Poland), IHEP (Protvino, Russia), NIIEFA (St. Petersburg, Russia), BINP (Novosibirsk, Russia), INR (Moscow, Russia), CIEMAT (Madrid, Spain), UPM (Madrid, Spain), SU (Stockholm, Sweden), UU (Uppsala, Sweden), and PSI (Villigen, Switzerland). DESY will also be responsible for the operation, maintenance and upgrade of the accelerator.

Construction of the European XFEL started in early 2009. In 2010 the 800 series cavities have been ordered and the assembly of the first prototype module took place at CEA/IRFU. Series cavity delivery started in late 2012, ramping up to full production rate in Oct. 2013 and continued until end of 2015 [4, 5]. The assembly of the 102 series modules at CEA/IRFU [6] and testing at AMTF [7, 8] began in 2013 and finished in 2016. The commissioning of the linear accelerator started end of 2016.

SRF FACILITY LAYOUT

The main linac is constructed underground, in a 5.2 m diameter tunnel about 25 to 6 m below the surface level and fully immersed in the ground water. The 50 m long injector occupies the lowest level of a seven-story underground building that also serves as the entry shaft to the main linac tunnel. Next access to the tunnel is about 2 km downstream at the bifurcation point into the beam distribution lines. The beam distribution provides space for 5 undulators (3 being initially installed), each feeding a separate beamline so that a fan of 5 almost parallel tunnels with a distance of about 17 m enters the experimental hall 3.3 km away from the electron source.

The European XFEL photo-injector consists of a normal-conducting 1.3 GHz 1.6 cell accelerating cavity with a Cs2Te-cathode [9, 10, 11]. The photo-injector is followed by a standard superconducting 1.3 GHz accelerator module and a 3rd-harmonic linearizer, consisting of one 3.9 GHz module – also superconducting – containing eight 9-cell cavities. A laser-heater, a diagnostic section and a high-power dump complete the injector.

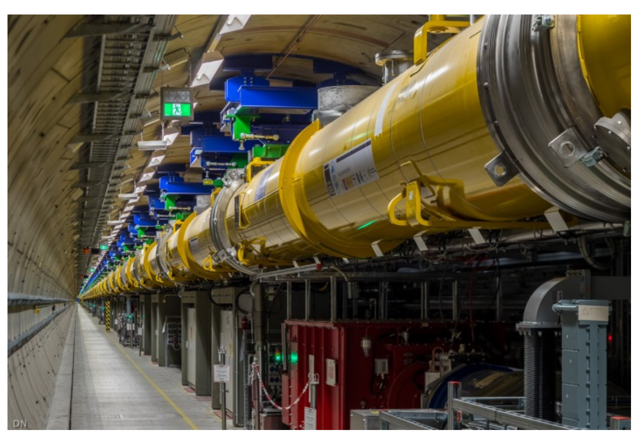

Figure 1: View into the linac tunnel with the accelerator modules suspended from the ceiling and the RF infrastructure placed below on the floor.

* Work supported by by the respective funding agencies of the contributing institutes; for details please see http://www.xfel.eu
† detlef.reschke@desy.de

Content from this work may be used under the terms of the CC BY 3.0 licence (© 2017). Any distribution of this work must maintain attribution to the author(s), title of the work, publisher, and DOI.

ISBN: 978-3-95450-191-5 doi:10.18429/JACoW-SRF2017-MOXA03

THE 30 MeV STAGE OF THE ARIEL E-LINAC

R.E. Laxdal, Z. Ang, T. Au, K. Fong, O. Kester, S.R. Koscielniak, A. Koveshnikov, M. Laverty, Y. Ma, D.W. Storey, E. Thoeng, Z. Yao, Q. Zheng, V. Zvyagintsev
TRIUMF, 4004 Wesbrook Mall, Vancouver B.C., V6T 2A3, Canada

Abstract

A MW class cw superconducting electron linac (e-Linac) is being installed at TRIUMF as a driver for radioactive beam production as part of the ARIEL project. The e-linac final configuration is planned to consist of five 1.3GHz nine-cell cavities housed in three cryomodules with one single cavity injector cryomodule (ICM) and two double cavity accelerating cryomodules (ACM1 and ACM2) to accelerate in continuous-wave (cw) up to 10mA of electrons to 50MeV. The e-Linac is being installed in stages. A demonstrator phase (2014) consisting of a 300kV electron gun, ICM, and a partially outfitted ACM1 with just one accelerating cavity was installed for initial technical and beam tests to 22.9MeV. A Stage 2 upgrade now installed has a completed ACM1 to reach an operational goal of 3mA of electrons to 30MeV for first science from the ARIEL ISOL targets. A single 290kW klystron is used to feed the two ACM1 cavities in vector-sum closed-loop control. The paper is focused on the SRF challenges: systems design, cavity and cryomodule performance, rf ancillaries preparation and performance, LLRF and RF system performance and final beam test results.

INTRODUCTION

ARIEL[1,2] (the Advanced Rare IsotopE Laboratory) is a decade-long project with the objective to provide three simultaneous rare isotope beams (RIB) to the ISAC facility. ARIEL-I (2010-2015) was dedicated to the construction of the e-linac and a new target hall, mass separator room, and laboratory space. ARIEL-II (2016-2022) is centred around construction of a 100 kW capable electron target station, mass separators, RIB transport to ISAC. This paper is focused on the build out of the electron-driver-beam linac to 30 MeV.

The ARIEL electron linac is housed in a pre-existing shielded experimental hall adjacent to the TRIUMF 500MeV cyclotron that has been re-purposed as an accelerator vault. The e-linac presently consists of three 1.3GHz nine-cell cavities housed in three cryomodules with one single cavity injector cryomodule and one double cavity accelerating cryomodule. An rf frequency of 1.3GHz is chosen to take advantage of the considerable global design effort at this frequency both for pulsed machines (ILC) but also for cw ERL applications (KEK c-ERL, Cornell ERL and bERLinPro).

E-LINAC DESIGN

The linac architecture is determined by the choice of the final CW beam power and the available commercial cw rf couplers at the design rf frequency of 1.3GHz. The CPI produced coupler developed with Cornell for the ERL injector cryomodule is capable of operation at ~65kW cw [3]. The cavity design assumes two CPI couplers per cavity delivering a total of 100kW of beam loaded rf power. This sets a maximum gradient per cavity at 10MV/m for the maximum beam intensity of 10mA. Final beam specifications are set at 50MeV and 10mA with five cavities installed in three cryomodules. The e-linac is being installed in a staged way with the stages shown schematically in Fig. 1.

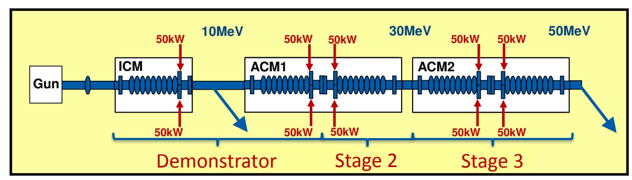

Figure 1: Schematic of the ARIEL e-Linac with staging.

The present installation is designed to accelerate in continuous-wave (cw) mode up to 10mA of electrons to 30MeV but the initial beam dumps and production targets will only be compatible with 10kW and 100kW operation respectively. First science from the targets will be produced during this stage. Stage 3, pending funding, will see the addition of a second accelerating module and a ramp up in beam intensity to the full 50MeV, 0.5MW capability.

The electron hall is shown in Fig. 2 in the present configuration. It is our intention to install a future ERL ring with injection and extraction between 5-10MeV. The angular off-set between the injector and the main linac allows accommodation of the future ring.

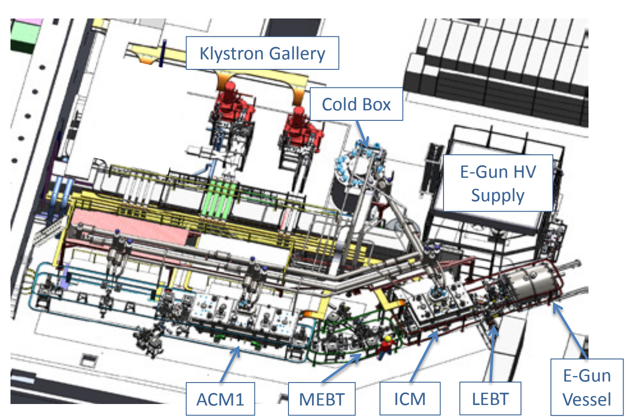

Figure 2: The present configuration of the e-Linac.

Content from this work may be used under the terms of the CC BY 3.0 licence (© 2017). Any distribution of this work must maintain attribution to the author(s), title of the work, publisher, and DOI.

ISBN: 978-3-95450-191-5 doi:10.18429/JACoW-SRF2017-MOXA04

SUPERCONDUCTING ACCELERATOR FOR ERL BASED FEL EUV LIGHT SOURCE AT KEK

H. Sakai†, E. Kako, T. Konomi, T. Kubo, K. Umemori, KEK, Tsukuba, Japan
M. Sawamura, QST, Tokai, Naka, Ibaraki, Japan
T. Ota, Toshiba Corporation, Yokohama, Japan

Abstract

An energy recovery linac (ERL)-based free electron laser (FEL) is a possible candidate of a tens of kW EUV source and open the era for next generation EUV-lithography. We have designed the 10 mA class ERL-based EUV-FEL light source to generate more than 10 kW power [1]. One of the key technologies is the CW superconducting cavity to realize the energy recovery of high beam current of more than 10 mA by suppressing HOMs and high gradient acceleration of more than 12 MV/m. This CW superconducting cavity had been developed through the construction of the Compact ERL (cERL) facility in KEK and it successfully achieved the energy recovery of 1 mA CW beam until now [2,3]. However, the accelerating gradient of main linac was limited at 8.3 MV/m due to heavy field emission during the long-term CW beam operation [4]. In this paper, first we express our design strategies of SRF cavities of the main linac of ERL-EUV light sources not only to suppress the HOMs but also to overcome the field emission problem by modifying the main linac cavity of cERL more sophisticatedly. Next we show the recent development works for ERL-EUV superconducting cavity about HOM damper and the reliable cryomodule operation by using new horizontal test stand.

INTRODUCTION

Lithography for LSI needs shorter wavelength and high power to meet the Moore's law. The intense EUV (Extreme Ultra-violet) light source around 13.5 nm wavelength is the strongest candidate for new generation light source for Lithography. And high power EUV source is required for mass production. Up to now, 250 W high power EUV source of 13.5 nm wavelength by using LPP (Laser Produced Plasma) has been developed for 30 years. However, EUV light source of more than 10 kW is required for mass production of LSI.

In order to obtain more than 10 kW EUV light source, the accelerator-based EUV light source was proposed [1]. Figure 1 shows the conceptual design of 10 kW EUV light source. The design of this light source is based on SASE-FEL scheme. This accelerator consists of the high-brightness DC-gun that can produce ultra-low emittance beams with a high average current of about 10 mA with drive-laser system, superconducting RF cavities for injector that can provide high RF power to beam up to 10 MeV beam energy and main linac that can accelerate up to 800 MeV energy under the energy recovery condition, a recirculating loop to achieve the energy recovery and to maintain the beam quality and compress the bunch length to increase the peak current of beam, the long undulator section to make a SASE-FEL of more than 10 kW with EUV regime, and the beam dump of the decelerated beam. The detailed beam parameters are summarized in Table 1. The total beam power of 8 MW is needed from the RF power and it is difficult to damp this beam power of 8 MW if we do not apply energy recovery scheme. Therefore, energy recovery is necessary to save the RF power to the beam and much reduce the beam power to the damp. Therefore, it is necessary to use the well-designed superconducting RF cavities in main linac section.

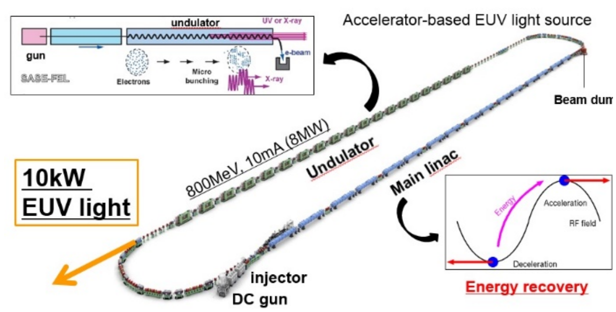

Figure 1: Conceptual layout of accelerator-based EUV light source of more than 10 kW.

Table 1: Main Parameters of Accelerator-based EUV Light Source of 10 kW

Wave length of light	13.5 nm
Power of EUV light	10 kW
Total beam energy	800 MeV
Bunch charge	60 pC
Beam current (CW)	9.75 mA (162.5MHz rep rate)
Normalized emittance	0.6 mm mrad
Bunch length	1 – 3 ps (usual) 100 fs (bunch compression)

To realize this high-power EUV light source, a stable beam operation is needed with this high CW current beam of more than 10 mA. It is important for main-linac superconducting cavities to not only achieve a high accelerating gradient (Eacc) in beam operation but to also strongly damp higher-order modes (HOMs), because the suppression of beam-breakup (BBU) instability and heat load due to the HOMs is one of the key issues for high-current operation. Furthermore, it is important to overcome

† hiroshi.sakai.phys@kek.jp

Content from this work may be used under the terms of the CC BY 3.0 licence (© 2017). Any distribution of this work must maintain attribution to the author(s), title of the work, publisher, and DOI.

ISBN: 978-3-95450-191-5 doi:10.18429/JACoW-SRF2017-MOXA07

DEVELOPMENT OF THE C-ADS SRF ACCELERATOR AT IHEP*

Fang Yan†, Huiping Geng, Cai Meng, Yaliang Zhao, Huafu Ouyang, Shilun Pei, Rong Liu, Feisi He, Tongming Huang, Rui Ge, Yanfeng Sui, Qiang Ye, Xiaoping Jing, Fengli Long, Jungang Li, Quanling Peng, Dizhou Guo, Zusheng Zhou, Haiyin Lin, Xinpeng Ma, Qunyao Wang, Guangwei Wang, Hua Shi, Gang Wu, Shengchang Wang, Ningchuang Zhou, Qiang Ma, Zhenghui Mi, Peng Sha, Xinying Zhang, Yaoyao Du, Jun He, Huizhou Ma, Lingda Yu, Ying Zhao, Xiaoyan Zhao, Fang Liu, Yanhua Lu, Lin Bian, liangrui Sun, Rui Ye, Xiaohua Peng, Dayong He, Ouzheng Xiao, Yao Gao, Zhenghua Hou, Yuan Chen, Xiangchen Yang, Hongyan Zhu, Bo Li, Lan Dong, Heng Li, Xitong Sun, Linglang Dong, Ping Su, Jianping Dai, Jianli Wang, Shaopeng Li, Jianshe Cao, Yunlong Chi, Weimin Pan
Key Laboratory of Particle Acceleration Physics and Technology
Institute of High Energy Physics (IHEP), Chinese Academy of Science, Beijing 100049, China

Abstract

The 10 MeV accelerator-driven subcritical system (ADS) Injector I test stand at Institute of High Energy Physics (IHEP) is a testing facility dedicated to demonstrate one of the two injector design schemes [Injector Scheme-I, which works at 325 MHz], for the ADS project in China. The ion source was installed since April of 2014, periods of commissioning are regularly scheduled between installation phases of the rest of the injector. Early this year, continuous wave (CW) proton beam has been successfully obtained with energy of 10 MeV and average beam current around 2 mA. The single spoke cavities with smallest developed beta ($\beta_g = 0.12$) were applied on Injector-I and successfully commissioned. Single spoke cavities with higher beta ($\beta_g = 0.21$) were also adopted for the last cryomodule of 25 MeV proton linac, and 150~200 μA CW proton beam were shooting through recently. This contribution reports the details of the development of the C-ADS SRF accelerator at IHEP and the challenges of the CW machine commissioning.

INSTRUCTION

ADS project in China was launched in year of 2011 intending to develop the concept and design of a 1.5 GeV high intensity SC linac with the aim of building a demonstration facility for accelerator-driven subcritical system (ADS) in multiple phases. The driver linac will be operating in continuous wave (CW) mode and delivering 15 MW beam power eventually. The linac includes two major sections: the injector section and the main linac section. The injectors accelerate the proton beams up to 10 MeV and the main linac boost the energy from 10 MeV up to 1.5 GeV.

In the first five year stage: 2011 to 2016, the injector on basis of two different frequencies have been developed in IHEP and IMP independently to demonstrate two different design schemes of the injector [1,2]. Scheme I (so-called Injector I) is on basis of 325 MHz Room-Temperature (RT) RFQ and single spoke type cavity with same frequency and scheme II (so-called Injector II) is on basis of 162.5 MHz RT RFQ and HWR cavity with the same frequency.

The specifications of the injector-I are listed in Table 1. Although the injector is designed to be operated on CW mode with average beam current of 10 mA, considering of the CW operation difficulty for high intensity proton linac and experience lacking with newly developed spoke cavities, the CW operation is not the acceptance goal for the first five year. However we still pursue to achieve CW proton beam with energy of 10 MeV and average beam current as high as possible.

Table 1: ADS Injector-I Test Facility Specifications

ADS Injector-I test facility specifications	
Particle	Proton
RF frequency (MHz)	325
Output Energy (MeV)	10
Average Current (mA)	10
Beam power (kW)	100
Duty factor (%)	100

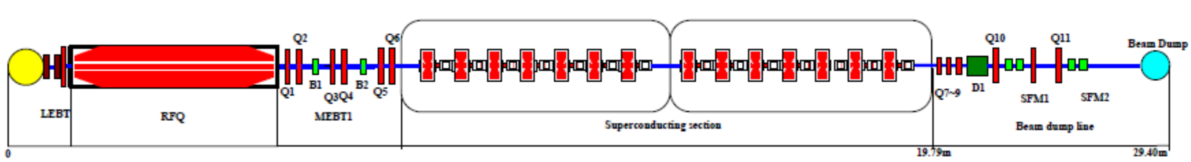

Figure 1: The schematic layout of the 10 MeV test stand in IHEP.

*Work supported by CAS Strategic Priority Research Program-Future Advanced Nuclear Fission Energy (Accelerator-Driven Sub-critical System) and National Natural Science Foundation of China, under contract NO. of 11405190.
†yanfang@ihep.ac.cn

Content from this work may be used under the terms of the CC BY 3.0 licence (© 2017). Any distribution of this work must maintain attribution to the author(s), title of the work, publisher, and DOI.

ISBN: 978-3-95450-191-5 doi:10.18429/JACoW-SRF2017-MOYA01

Content from this work may be used under the terms of the CC BY 3.0 licence (© 2017). Any distribution of this work must maintain attribution to the author(s), title of the work, publisher, and DOI.

THE SUPERCONDUCTING ACCELERATOR FOR THE ESS PROJECT

F. Schlander*, C. Darve, N. Elias, M. Lindroos, C. G. Maiano
European Spallation Source ERIC, Lund, Sweden
P. Bosland, CEA/DRF/IRFU, Gif-sur-Yvette, France
P. Michelato, INFN/LASA, Segrate, Italy
G. Olry, Institut de Physique Nucléaire, CNRS/IN2P3, Université Paris Sud, Orsay Cedex, France
M. Ellis, STFC/ASTeC, Daresbury, UK
R. Ruber, Uppsala University, Uppsala, Sweden

Abstract

The European Spallation Source, ESS, is under construction in Lund since 2014. While the installation of the source and the normal conducting part will start in this autumn, the production and testing of cryomodules and cavities for the superconducting accelerator is in full swing at the partner laboratories. The spoke cavities and cryomodules will be provided by IPN Orsay and the testing of those modules will take place at Uppsala University. Prototyping and assembly of the elliptical cryomodules series is occurring at CEA Saclay, and the modules will be tested at a new test stand at ESS. The fabrication and test of the medium beta cavities is provided by INFN Milan and STFC Daresbury for the high beta cavities respectively. An overview of the current activities and test results will be presented in this paper.

INTRODUCTION

The proton accelerator of the European Spallation Source (ESS) [1] consists of several sections as depicted in Fig. 1, beginning with the so-called warm front end. It consists of the proton source, low energy beam transport, radio frequency quadrupole, medium energy beam transport as well as the drift tube linac. The cold section will contain spoke cryomodules, medium-beta cavity cryomodules and high-beta cavity cryomodules to provide an optimised energy gain pattern [2]. The performance of the linac will be 5 MW average proton beam power with 62.5 mA current at 4 % duty cycle with a repetition rate of 14 Hz. This beam will be led to a tungsten target to generate neutrons for various experiments. To achieve these parameters, there are demanding requirements on the accelerator and its components. An overview of the requirements on the superconducting cavities is given in Table 1.

As the ESS is a European project, a large share of the components to be installed are provided by partner laboratories all around Europe via in-kind contributions. In-kind contributions are not limited to the provision of hardware, they also include the use of equipment at partner labs and installation/commissioning work force at the ESS site. This includes the three types of cryomodules, where an overview of the activities during the design and particularly the prototyping phase can be found in [3, 4]. The current status and recent test results will be described in the subsequent sections.

Table 1: Requirements on Superconducting Cavities

Requirement	**Spoke**	**medium-β**	**high-β**
Frequency / MHz	352.21	704.42	704.42
Optimum β	0.5		
Geometric β		0.67	0.86
E_{acc} / MV m^{-1}	9.0	16.7	19.9
E_{Pk} / MV m^{-1}	39	45	45
B_{Pk}/E_{Acc} / mT/(MV/m)	6.80	4.79	4.3
E_{Pk}/E_{Acc}	4.28	2.36	2.2
Iris diameter / mm	56	94	120
RF peak power / kW	335	1100	1100
G / Ω	130	196.63	241
maximum R/Q / Ω	425	394	477
Q_{ext} / 10^5	1.75-2.85	7.5	7.6
min $Q_0(E_{acc})$ / 10^9	1.5	5	5

SPOKE CRYOMODULES

The first part of the superconducting linac consists of 13 spoke cryomodules, housing two double spoke cavities each with an optimal beta of $\beta = 0.5$, whose main requirements are shown in Table 1. This section of the linac allows to increase the energy of the proton beam from 90 MeV to 216 MeV. A 3D model of the cryomodule is shown in Fig. 2.

The design of the cavities [5] and cryomodules [6] as well as testing the cavities of the series is in the hands of IPN-Orsay. In addition, the cryogenic tests to qualify the prototype valve box and prototype cryomodule are also carried out at IPN-Orsay. Nevertheless, cryogenic and high power RF tests of the cryomodule prototype and series will take place at the FREIA laboratory at the University of Uppsala [7].

Spoke Cavities

Three double spoke prototype cavities have been manufactured in 2014 and have been tested succesfully in the vertical cryostat at IPNO in 2015 [3]. The cavities were treated by BCP in three steps using different cavity orientations with the goal of a minimum removal of 200 µm, followed by four high pressure rinsing cycles taking three hours each. With-

* felix.schlander@esss.se

ISBN: 978-3-95450-191-5 doi:10.18429/JACoW-SRF2017-MOYA02

BESSY VSR: SRF CHALLENGES AND DEVELOPMENTS FOR A VARIABLE-PULSE LENGTH NEXT-GENERATION LIGHT SOURCE

A. Vélez†, H. W. Glock, F. Glöckner, B. Hall, A. Neumann, E. Sharples, P. Schnizer, A. Tsakanian, J. Knobloch
Helmholtz-Zentrum Berlin, Albert-Einstein-Str. 15, 12489 Berlin, Germany

Abstract

The BESSY VSR project represents an exciting alternative to diffraction limited storage rings in the development of a next generation light source. Such a system should be capable to store "standard" (some 10 ps long) and "short" (ps and sub-ps long) pulses simultaneously in the storage ring opening the door to picosecond dynamic and high-resolution experiments at the same facility [1]. This unique feature can be created by the introduction of the beating effects produced by higher harmonic SRF cavity systems (1.5 GHz & 1.75 GHz). The challenging design specifications as well as the technological demands on the SRF system make BESSY VSR a defiant project where non-standard techniques such as waveguide-damped cavities have been further developed. This talk focuses on the new SRF developments that include waveguide-damped cavities, high-power couplers and higher-order mode absorbers that must handle nearly 2 kW of HOM power. The cryomodule design and its interaction with the beam will also be discussed.

INTRODUCTION

The BESSY VSR module is designed to run CW with a 300 mA high current beam. With a quite exotic filling pattern, impedance control plays a key role when avoiding CBIs [2]. Therefore the longest low-β straight section in the BESY ring has been chosen as the only feasible module location. The cavity design was recently changed from a 5-cell to a 4-cell cavity since the available space is insufficient to accommodate the original 5-cell cavity based module design. As a result the total module voltage drops in 20% (29.71 MV) with respect to 37.2 MV originally specified for BESSY VSR. Thus a 10% reduction in the expected VSR bunch compression is obtained. That is a VSR short bunch length of 1.87 ps instead of 1.7 ps for the standard BESSY optics.

COLD STRING DEVELOPMENTS

Several recently identified important issues such as HOM power damping or incoming synchrotron light generated in the closest dipole magnet upstream to the VSR module have been studied and are presented on this paper. In addition the hard length restriction demands for unusual cavity connections. These are required to provide the system with the mechanical flexibility imposed by cooling shrinkage and, meanwhile, providing fundamental mode shielding to avoid overload of the cooling system and non-acceptable Q-value reduction. Thus designed solutions and actions taken to mitigate all such effects are presented in this paper.

Warm HOM Waveguide Loads

As a first measure to optimize the module length the number of cells per cavity (Fig.1) was decreased from 5 to 4. This variation results in a positive 15% reduction off the total HOM power and also improves the damping capabilities of the cavities. Consequently full EM validation of the new shortened cavity version by means power propagation studies through the module were performed [3].

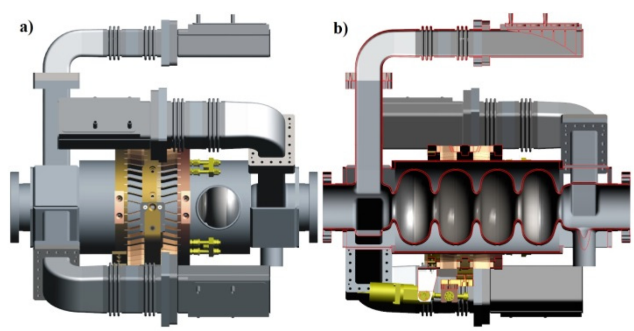

Figure 1: 4-cell 1.5 GHz cavity design equipped with He-vessel and blade tuner (a). Cut plane view showing waveguide (WG) HOM loads design details (b).

As it was designed for the VSR 5-cell cavities and presented in [4], the main HOM damping is performed by means of 20 warm water-cooled WG HOM loads. These are Silicon-Carbide (SiC) based loads with a maximum power specification of 460 W (10% overhead included) per load at room temperature. The design of these loads is being performed in collaboration with JLab [5]. The first prototypes are currently under fabrication and will be shortly tested in Jefferson Laboratory facilities. A detailed view of the load design and the calculated temperature on the absorbing tiles is shown in Fig. 2.

Content from this work may be used under the terms of the CC BY 3.0 licence (© 2017). Any distribution of this work must maintain attribution to the author(s), title of the work, publisher, and DOI.

ISBN: 978-3-95450-191-5 doi:10.18429/JACoW-SRF2017-MOYA03

PROGRESS OF THE RAON

D. Jeon†, H.C. Jung, H.M. Jang, Y.K. Kwon, S.C. Jeong, S.J. Choi, H.J. Jang, J.H. Jang, T.K. Ki, J.H. Kim, Y.K. Kim, S.I. Lee, B.S. Park, H.J. Cha, B.H. Choi, C.J. Choi, J.W. Choi, O.R. Choi, Y.J. Choi, I.W. Chun, I.S. Hong, M.O. Hyun, H.Y. Jeong, H.C. Jin, H.C. Jo, Y.B. Jo, Y.W. Jo, J.D. Joo, M.J. Joung, Y.C. Jung, I.I. Jung, J.S. Kang, D.G. Kim, D.M. Kim, H.J. Kim, H.T. Kim, J.W. Kim, W.K. Kim, Y.H. Kim, D.Y. Lee, J.W. Lee, K.W. Lee, M.K. Lee, S.B. Lee, S.H. Nam, M.J. Park, K.T. Seol, I.K. Shin, J.H. Shin, C.W. Son, H.J. Son, K.T. Son, K.S. Yang, S.W. Yoon, A. Zaghloul
Institute for Basic Science, Daejeon, Korea

Abstract

Construction of the RAON is under way in Korea building a heavy ion accelerator based on low beta superconducting cavities. The 81.25-MHz RFQ was fabricated and a beam test was conducted confirming beam acceleration. Major accelerator subsystems such as superconducting cavities are under development. QWR cryomodule test was conducted achieving the design field gradient and Q and HWR cryomodule test is planned shortly. SSR1 cavity is under development in collaboration with the TRIUMF. High Tc superconducting quadrupole prototype was successfully tested which is used in the IF separator.

INTRODUCTION

Construction of the RAON is in progress in Korea. The driver linac of the RAON is to accelerate uranium to proton beam up to 200 MeV/u and 600 MeV respectively, delivering 400-kW beam power to the target [1]. Site preparation is near completion. Figure 1 shows the bird's-eye view of the RAON facility.

Figure 1: Bird's-eye view of the RAON.

Prototyping and testing of subsystems are in progress. The injector consists of 28-GHz ECR ion source [2,3] and 81.25-MHz RFQ. The RAON superconducting linac (SCL) consists of SCL1, SCL2 and SCL3 and adopts a design that separates superconducting cavities and magnets. The lattice is robust and flexible in operation. The SCL consists of QWR (Quarter Wave Resonator), HWR (Half Wave Resonator) and SSR (Single Spoke Resonator). Superconducting cavities, couplers and tuners are fabricated and tested. High Tc superconducting quadrupole magnet prototype was fabricated in collaboration with domestic research institutes and successfully tested meeting the design requirement.

SRF Test Facility was constructed [4] and began operation from June 2016 and the SCL Demo facility is set-up.

DRIVER LINAC

The SCL Demo facility is set up to perform various tests which consists of the 28-GHz ECR ion source, LEBT, RFQ, MEBT and one QWR cryomodule. This facility is located in the SRF Test Facility at KAIST campus. At present the QWR cryomodule is being installed and the beam test is planned in September 2017.

The four-vane type 81.25 MHz RFQ was fabricated through a domestic vendor and accomplished successful beam acceleration in November 2016 accelerating the $^{16}O^{7+}$ beam from the 28-GHz ECR ion source to 0.516 MeV/u in the test facility [5].

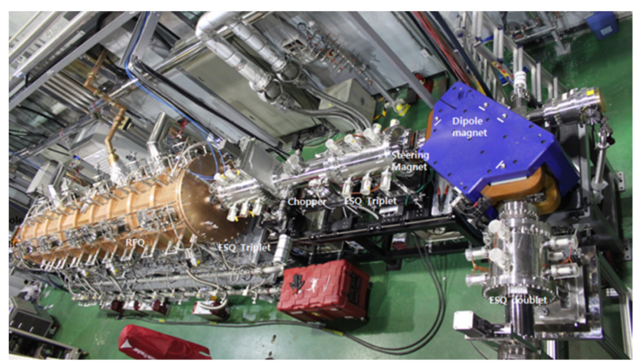

Figure 2: Photograph of the SCL Demo facility showing the RFQ installed.

Vertical test and horizontal test of QWR cavities and HWR cavities are in progress. Superconducting cavities are fabricated through domestic and international vendors. For the QWR cavities, following the vertical test of the bare cavity, vertical test of the jacketed test and an integrated test in a cryomodule were conducted. Figure 3 shows the Q vs E curves of the vertical test and horizontal test of a QWR in a cryomodule.

The total thermal load of the QWR cryomodule at the operating gradient was measured to be 9.9 W which is below 25 W of the design. The alignment was measured with

†jeond@ibs.re.kr

Content from this work may be used under the terms of the CC BY 3.0 licence (© 2017). Any distribution of this work must maintain attribution to the author(s), title of the work, publisher, and DOI.

ISBN: 978-3-95450-191-5 doi:10.18429/JACoW-SRF2017-MOPB001

CONCEPTS AND DESIGN FOR BEAMLINE HOM DAMPERS FOR eRHIC*

P. Kolb†[1], Y. Gao[1,2], D. Holmes[1], K. Smith[1], and W. Xu[1]
[1]Collider-Accelerator Department, Brookhaven National Laborarory, Upton, NY 11973, USA
[2]Institute of Heavy Ion Physics, School of Physics, Peking University, Beijing 100871, China

Abstract

In the design of eRHIC at BNL, HOM power plays a major role for the SRF installation. Depending on the final accelerator design and choice of cavity, up to 100kW of HOM power is estimated to be generated, presenting a big challenge for the HOM damping concept. Due to this high amount of HOM power, all current concepts for eRHIC would use room temperature beam line absorbers equipped with silicone-carbide dielectrics to absorb HOM power. Concepts, designs and simulations for these beam line absorbers will be presented.

INTRODUCTION

eRHIC is an electron-ion Collider proposed by the Collider-Accelerator Department at Brookhaven National Lab. The goal is to collide polarized electron with an energy form 5 to 18 GeV with the polarized proton beam from RHIC. For this a new electron accelerator will be build in the existing RHIC tunnel.

Two concepts for the electron accelerator are being considered. The Linac-Ring (LR) version [1] uses an Energy Recovery Linac (ERL) to accelerate the electrons up to collision energy and after collision decelerate them to recover their energy and drive the Linac. The Ring-Ring (RR) version [2] uses an recirculating Linac to inject the beam into a storage ring to collide with the ion beam. Both concepts will use SRF technology in their respective RF cavities. The LR eRHIC will use 647 MHz five-cell cavities and the RR-eRHIC 563 MHz two-cell cavities. In both concepts, room temperature beam line absorbers will be utilized to extract HOM power. In addition, the LR-cavity will have waveguide HOM dampers to extract power [3,4]. The absorber will be made out of silicone carbite (SiC), similar to the absorber used in Cornells ERL [5] and ANL APS upgrade [6]. The mechanical design of the beam line absorbers for both LR and RR is set to follow the ANL path with shrink-fitting the SiC into a copper sleeve with water cooling channels.

LINAC-RING

In the Linac-Ring (LR) (schematical layout can be seen in Fig. 1), concept of eRHIC a 1.67 GeV/turn ERL accelerates the beam up to its collision energy. The 647 MHz five-cell cavity will operated at a cw gradient of 16 MV/m. Since the straight section in the tunnel is limited to 200 m, the real estate needs to be conserved. For this reason most of the HOM power is extracted away from the beamline via waveguides with a SiC termination [7]. The rest of the HOM power is extracted with warm beam line absorbers between cryomodules. The cavity is designed with a beam pipe diameter of 104 mm, resulting in a cutoff frequency for TM01 modes of 2.2 GHz. As the bunch spectrum peaks at $n \cdot 2 \cdot 647$ MHz, the HOM power peaks at these frequencies too. The absorber is therefore optimized for frequencies around

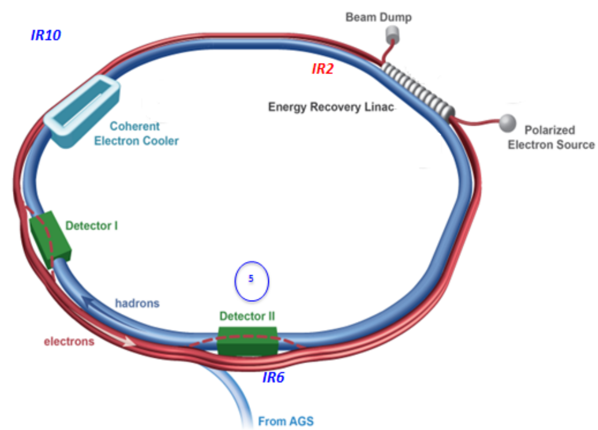

Figure 1: Layout for the Linac-Ring eRHIC with the existing "blue" hadron ring and the electron ring in red. The SRF Linac is located at IP2.

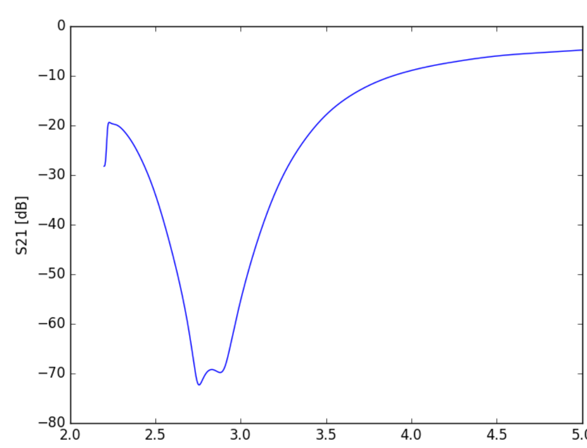

Figure 2: Tranmission simulation for the LR beam line absorber with a resonance around 2.7 GHz to cover the peak in bunch spectrum power.

---

* Work supported by LDRD program of Brookhaven Science Associates, LLC under Contract No. DE-AC02-98CH10886 with the U.S. DOE.
† pkolb@bnl.gov

Content from this work may be used under the terms of the CC BY 3.0 licence (© 2017). Any distribution of this work must maintain attribution to the author(s), title of the work, publisher, and DOI.

ISBN: 978-3-95450-191-5 doi:10.18429/JACoW-SRF2017-MOPB002

eRHIC CRAB CAVITY CHOICE for RING-RING DESIGN

Q. Wu†[1], I. Ben-Zvi[1,2], Y. Hao[1,3], S. Verdu-Andres[1], B. Xiao[1]

[1]Brookhaven National Lab, Upton, NY, USA
[2]Stony Brook University, Stony Brook, NY, USA
[3]Michigan Stata University, Lansing, MI, USA

Abstract

The future electron ion collider eRHIC adopts large crossing angle (22 mrad) to allow fast separation of two beams in the ring-ring scheme. Crab cavities are required to recover the luminosity from geometric losses. Initial calculation shows that the frequency of the cavities for the ion beam is no more than 338 MHz. In this paper, we discuss the crab cavity related lattice parameters for both ion and electron beams in ring-ring design, the frequency choice, and the cavity design considerations.

INTRODUCTION

The proposed electron-ion collider at Brookhaven National Laboratory (eRHIC), as shown in Figure 1, is designed for high luminosity in the range from 10^{32} to 10^{33} cm^{-2}s^{-1} over a center-of-mass energy range from 30 to 140GeV [1].

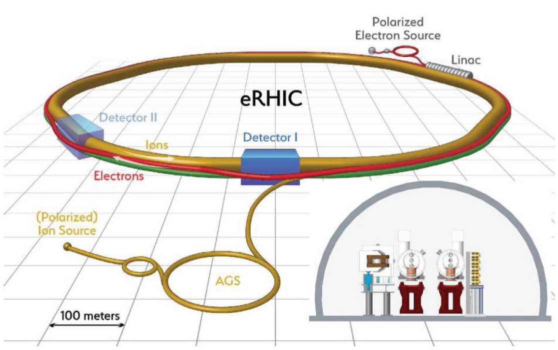

Figure 1: Schematic overview of the eRHIC facility.

To achieve such high luminosity, eRHIC adopted fast separation between the ion and electron beam lines after the interaction point. A careful study took into account the physics objectives of an EIC and constraints on the detector layout [2]. This included issues like separation of the forward hadron beam from neutral particles coming from the IP, synchrotron radiation issues and more. The study established that a separation dipole is incompatible with the physics and detector constraints. Therefore, a crossing angle is the only solution (as is present in all eRHIC designs) and thus, some form of crab cavities must be used to overcome the luminosity penalty introduced by the crossing angle.

* This work was supported by Brookhaven Science Associates, LLC under Contract No. DE-AC02-98CH10886 with the U.S. DOE.
† email address qiowu@bnl.gov

Different types of crab cavities have been designed over the past 25 years [3]. In 2007, the High Energy Accelerator Research Organization in Japan for the electron-positron collider (KEKB) demonstrated the first operation of crab cavities in colliders, and a corresponding luminosity increase was observed. The squashed elliptical single cell crab cavity at 509 MHz for KEKB achieved a deflecting voltage of 2.8 MV at 2.8 K [4][5].

For the LHC HiLumi upgrade program, beam studies showed that applying local crabbing at interaction region would boost the luminosity by 70% [3]. The location for crab cavity installation was limited due to existing beamline layouts. In demand for a compact crab cavity, the Double Quarter Wave Crab Cavity (DQWCC) at 400 MHz was designed to provide 3.4 MV at 2 K for vertical crabbing. The proof-of-principle DQWCC successfully reached 4.6 MV at 1.9 K [6], with a dimension much more compact than the KEKB design as shown in Figure 2.

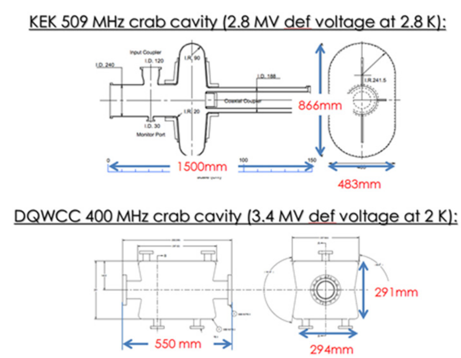

Figure 2: Dimension comparison of the DQWCC and the commissioned crab cavities at KEK.

Two DQWCCs were built at CERN to be tested in the Super Proton Synchrotron (SPS) in 2018. For fabrication and processing studies, two prototypes were built, cleaned, and tested in the US in advance. The bare cavity cryogenic tests of all four cavities reach > 4.5 MV, with field emission onset at 3.2 MV or beyond [7][8]. The current status of the crab cavity development for HiLumi LHC upgrade can be found in Ref. [9].

For eRHIC, lower frequency is required due to more than 30 times larger crossing angle compared to HiLumi LHC. Therefore, the compact size of DQWCC would benefit all aspects, including cost, fabrication, post-processing, installation, and beam dynamics.

Content from this work may be used under the terms of the CC BY 3.0 licence (© 2017). Any distribution of this work must maintain attribution to the author(s), title of the work, publisher, and DOI.

ISBN: 978-3-95450-191-5 doi:10.18429/JACoW-SRF2017-MOPB003

A NEW HIGH RESOLUTION OPTICAL SYSTEM FOR INSPECTION OF GUN- AND MULTI-CELL RESONATORS IN ISO-4 CLEANROOMS

Marco Schalwat, Ruediger Bandelmann, Alexej Daniel, Nicolay Krupka, Axel Matheisen, Sven Sievers, DESY, Hamburg, Germany

Abstract

Optical inspection of the inner surface of superconducting resonators was established during European XFEL cavity production by usage of the so called OBACHT optical inspection [1]. In addition to the surface inspection by OBACHT a new optical inspection system with integrated high resolution camera is set up at DESY. It allows inspection of multi-cell resonators as well as gun cavity resonators with only single side accessibility to the inner surface. A prototype was commissioned and optical inspections were done with OBACHT and the new system in parallel. Two SRF gun cavities were inspected by this optical system and origin of limitations of the resonators were identified.

INTRODUCTION

After the European XFEL had been commissioned, tests with SRF gun cavities were done at DESY. These tests have not been as successful as expected. The origin of the problems has been presumed in the welds or inner surface of the cavity. This assumption initiated the development of a new optical inspection system.

If the OBACHT system is used successfully in non-standard cavities it will be necessary to perform a new system without referencing. For the basic settings at the standard OBACHT system, the cavity is needed to be opened on both beam tube flanges, to allow the camera to pass it completely. Our first requirement of the new system was a free view on the back plate of a SRF gun cavity (Fig. 1) or with blind flange closed cavities. Up to now such actions are not feasible with the existing OBACHT system.

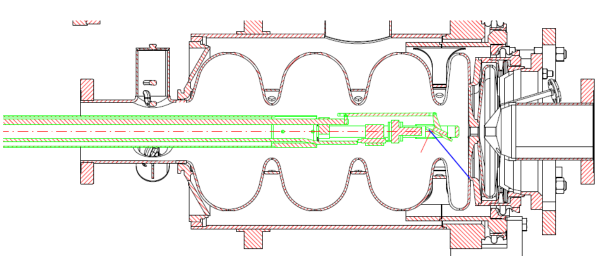

Figure 1: Drawing of 3.5 cell SRF gun cavity with optical inspection system.

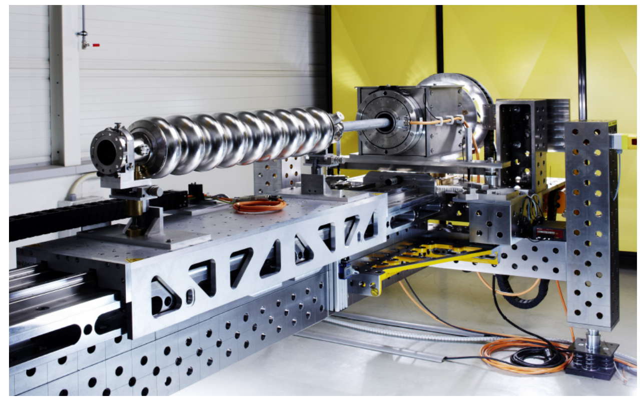

Figure 2: Picture of the OBACHT optical inspection system.

The second purpose was the installation of the new system in a cleanroom. The DESY OBACHT system (Fig. 2) is currently installed in a non-cleanroom area. At the moment it is necessary to transport cavities over long distances within DESY premises for the inspection of the inner surface. After each transport and OBACHT inspection an ultrasonic and UPW rinsing has to be done before the cavity can be used for further actions.

We established a test installation for the inspection of the inner surface of cavities outside the cleanroom to gain experiences on how to set up the new system. The existing devices for the installation of the field profile measurement system (FMS) was modified (Fig. 3).

With the FMS device it was possible to align the camera for the inspection in the centre of the beam tube.

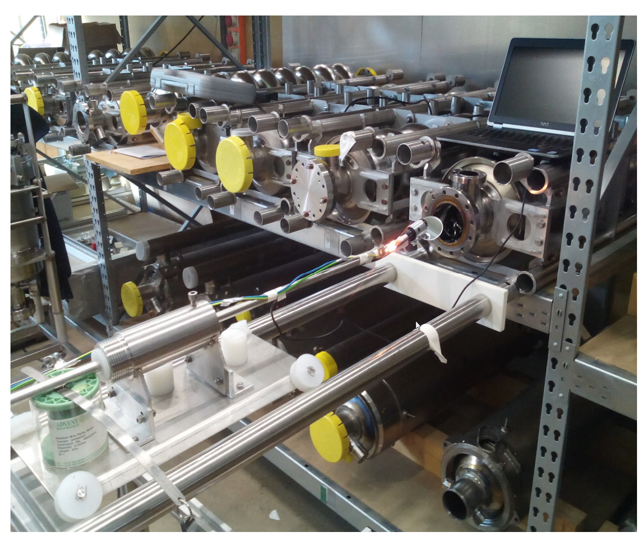

Figure 3: First steps to establish the new system.

Content from this work may be used under the terms of the CC BY 3.0 licence (© 2017). Any distribution of this work must maintain attribution to the author(s), title of the work, publisher, and DOI.

ISBN: 978-3-95450-191-5 doi:10.18429/JACoW-SRF2017-MOPB004

DESIGN OF A RF QUADRUPOLE RESONATOR FOR LANDAU DAMPING IN HL-LHC

K. Papke* and A. Grudiev, CERN, Geneva, Switzerland

Abstract

The design and optimization of a quadrupole resonator for transverse Landau damping in the High Luminosity Large Hadron Collider (HL-LHC) is presented. Two different cavity types are considered whose shape is determined by the quadrupolar strength, surface peak fields, and beam coupling impedance. The lower order and higher order mode spectra of the optimized cavities are investigated and different approaches for their damping are proposed. Furthermore, the required RF power and optimal external quality factor for the input coupler are derived.

INTRODUCTION

The betatron frequency spread in circular accelerators yield a natural effect of suppressing transverse collective instabilities, the so-called Landau damping [1]. The incoherent frequency or tune spread is caused by non-linearities in the machine. To ensure this mechanism dedicated nonlinear elements, typically octupole magnets, also known as Landau Octupoles (LO) are installed in the accelerator [2]. However, adiabatic damping and increased beam rigidity reduce their efficiency at higher energies. Future accelerators may call for more efficient devices in order to satisfy the beam requirements at higher energies.

Recently in [3], a superconducting RF quadrupole resonator was proposed as an alternative to the LOs. Its performance is affected likewise by beam rigidity but not by the adiabatic damping since in contrast to magnets, a RF quadrupole resonator introduces a longitudinal instead of a transverse betatron tune spread. The stabilization mechanism of a quadrupole resonator has been proven experimentally by using Q'' which likewise introduces a longitudinal betatron tune spread [4].

The variation of the betatron frequency due to quadrupolar focusing (so-called detuning) is proportional to the integrated quadrupolar strength b_2 which again is correlated to the transverse kick $\Delta\mathbf{p}^i_\perp$ that a particle i experiences while traversing the cavity (Fig. 1).

In [3], it has been demonstrated that an RF quadrupole resonator can result in a significantly more compact solution than a comparable set of octupole magnets providing the same tune spread. In this paper we present the first detailed design and optimization studies of a RF quadrupole resonator for Landau damping based on two types of cavities: the elliptical and the so-called four-vane cavity whose cross sections are shown in Fig. 1.

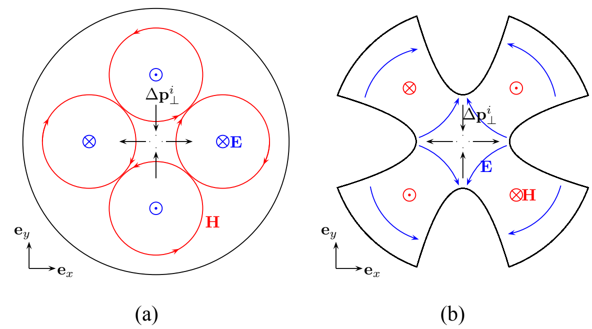

Figure 1: Cross section of quadrupolar field profiles providing the transverse kick to the particle. The force directions corresponds to a negative charge. a) Pillbox with TM-type mode. b) Four-Vane-Cavity with TE-type mode.

CAVITY DESIGN PARAMETERS

The parameters used to optimize the SC cavity can be differentiated into two categories. First, parameters that are derived from eigenmode simulations such as b_2 and second, parameters derived from wakefield simulations such as the transverse and longitudinal impedance. The latter is considerably more time-consuming than eigenmode calculations, hence, it is desirable to minimize the number of wakefield simulations. We propose, first, to optimize the designs independently of the impedance but with varying aperture which has the main influence on the impedance and, second, to calculate the impedance as a subsequent step for each pre-optimized design.

Integrated Quadrupolar Strength b_2

The integrated quadrupolar strength b_2 [5] should be as high as possible to minimize the total number of cavities. The values shown in Table 1 provide an equivalent stabilization effect as the LOs in HL-LHC at a specific chromaticity [6]. They are obtained from macro particle tracking simulation comprising 6×10^5 turns. Though only for a specific case of instability, we use these results as a reference for the cavity design in this paper.

* kai.papke@cern.ch

Content from this work may be used under the terms of the CC BY 3.0 licence (© 2017). Any distribution of this work must maintain attribution to the author(s), title of the work, publisher, and DOI.

ISBN: 978-3-95450-191-5 doi:10.18429/JACoW-SRF2017-MOPB005

BEAM DYNAMICS SIMULATIONS FOR THE NEW SUPERCONDUCTING CW HEAVY ION LINAC AT GSI*

M. Schwarz[†1], W. Barth[2,3,4], M. Basten[1], M. Busch[1], F. Dziuba[2], V. Gettmann[2], M. Heilmann[3], T. Kürzeder[2], M. Miski-Oglu[2], H. Podlech[1], U. Ratzinger[1], R. Tiede[1], S. Yaramyshev[3,4]
[1]IAP, Goethe University, Frankfurt am Main, Germany, [2]HIM, Mainz, Germany
[3]GSI Helmholtzzentrum, Darmstadt, Germany, [4]MEPhI, Moscow, Russia

Abstract

For future experiments with heavy ions near the coulomb barrier within the super-heavy element (SHE) research project a multi-stage R&D program of GSI, HIM and IAP is currently in progress. It aims at developing a superconducting (sc) continuous wave (CW) LINAC with multiple CH cavities as key components downstream the upgraded High Charge Injector (HLI) at GSI. The LINAC design is challenging, due to the requirement of intense beams in CW-mode up to a mass-to-charge ratio of 6 while covering a broad output energy range from 3.5 to 7.3 MeV/u with minimum energy spread. After successful tests with the first CH cavity in 2016 demonstrated a promising maximum accelerating gradient of E_a = 9.6 MV/m, recently first beam tests have been started as next milestone at GSI, confirming its flawless functionality [1].

INTRODUCTION

In the last decades the periodic system was essentially extended up to the nuclei with proton number $Z = 118$ and neutron number $N = 177$. Compared to the heaviest known stable nuclei, $^{208}_{82}$Pb and $^{209}_{83}$Bi, the mass of the overall heaviest nuclei was continuously increased. Most recently by more than 40 % with the discovery of $^{294}_{118}$Og [2]. It turned out, that the most successful methods for the laboratory synthesis of heavy elements are fusion-evaporation reactions using heavy-element targets, recoil-separation techniques and the identification of the nuclei by known daughter decays [3]. As an example for the production of SHE, hot fusion reactions with ^{48}Ca projectiles and targets made of actinide elements ranging from ^{231}Pa to ^{254}Es are considered very promising.

To sum it up, all of the experiments have the common challenge of very low cross sections and therefore require the separation of very rare events within weeks of beamtime from intense backgrounds. Fortunately, the yield of SHE respectively the number of events per time unit depends not only on the cross section but also on the projectile beam intensity, overall beam quality and target thickness. Thus, progress in SHE research is highly driven by technical developments in this fields [4].

At GSI a comprehensive upgrade programme is performed. In this context, the UNILAC (Universal Linear Accelerator) is upgraded to the requirements of FAIR and will be used as injector [5]. The duty factor will be relatively low (below 1 %). Conversely, for SHE experiments a high duty factor is required, which is why the presently available duty cycle of 25 % (5 ms pulse length @50 Hz) will be upgraded to CW-mode (duty cycle = 100 %) [6, 7]. Consequently the superconducting CW-LINAC was proposed [8] and is further investigated [9–11].

BEAM DYNAMICS

The beam dynamics concept for the CW-LINAC is based on multicell CH-DTL cavities, operating at 216.816 MHz (f_{HLI} = 108.408 MHz). The main requirements and boundary conditions for the LINAC design are as follows:

- ⊕ W_{in} = 1.4 MeV/u (at the HLI exit)
- ⊕ W_{out} = 3.5–7.3 MeV/u
- ⊕ $\Delta W_{\mathrm{out}} = \pm 0.003$ MeV/u
- ⊕ $I \leq 1$ mA
- ⊕ $A/q \leq 6$

With a relatively low beam current, CW-operation and limited longitudinal space, this LINAC is predestined to be operated in the superconducting mode. Further thoughts on the choice of technology with regard to superconducting or room-temperature operation can be found at [12].

A revised cryomodule (CM) layout is currently being studied. It comprises three CH-DTL cavities, two solenoids and a short buncher DTL-cavity (see Fig. 1). This approach partly reduces the overall drift lengths compared to the former consideration of CMs equipped with 2 CH-cavities.

Enabling First Experiments with 1 CM

By increasing the accelerating gradient and the RF-phase of the buncher (to use it for acceleration), LORASR simulations (100,001 particles, I = 1 mA, A/q = 3) show that the minimum output energy of the full CW-LINAC could already be reached in this early intermediate expansion stage. Instead of halving the accelerating gradient due to the halved mass-to-charge ratio, increasing E_a for CH1 and CH2 up to

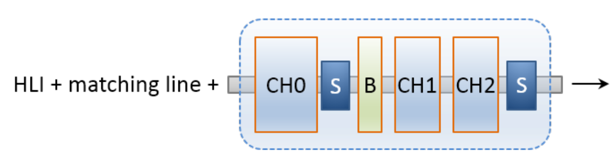

Figure 1: Proposed Layout for the first cryomodule of the CW-LINAC with 3 CH-DTLs, 2 solenoids and 1 buncher cavity. The flange-to-flange length is nearly 4.5 m.

* Work supported by BMBF contr. No. 05P15RFRBA
† schwarz@iap.uni-frankfurt.de

Content from this work may be used under the terms of the CC BY 3.0 licence (© 2017). Any distribution of this work must maintain attribution to the author(s), title of the work, publisher, and DOI.

ISBN: 978-3-95450-191-5 doi:10.18429/JACoW-SRF2017-MOPB007

DESIGN OF THE SUPERCONDUCTING QUARTER WAVE RESONATORS FOR HIAF

C. Zhang†, Y. He, S. H. Zhang, Y. M. Li, S. X. Zhang, R. X. Wang, W. M. Yue, A. D. Wu, T. C. Jiang, T. Tan, Y.L. Huang, S. C. Huang, F. Pan, L. Chen, Q. W. Chu, L. Li, H. Guo, P. R. Xiong, Q. J. Wu, Institute of Modern Physics, Lanzhou, China

Abstract

A heavy ion accelerator facility (HIAF) is under development in the Institute of Modern Physics. For the low energy superconducting accelerating section, two types of quarter wave resonators with frequency of 81.25 MHz and β of 0.05 and 0.09 have been proposed. The electromagnetic design has been optimized in order to reach the high accelerating voltage, and the optimization also included the drift tube face tilting to compensate for the beam steering caused by the asymmetry in the quarter wave resonator geometry.

INTRODUCTION

HIAF is a high intensity heavy ion multi-function research facility, and it contains a linac as injector and several rings. The HIAF Linac will accelerate ions from H to U, and it contains ECR, LEBT, RFQ, low energy superconducting section (QWRs) and the high energy superconducting section(HWRs). For the low energy superconducting section, f=81.25 MHz, β_{opt}=0.05 and 0.10 QWRs have been proposed consistent with beam dynamics [1].

ELECTRO-MAGNETIC DESIGN

With Microwave Studio of CST [2], the cavity optimization has been done in order to minimize the surface electro-magnetic field and keep high R_a/Q_0 and G values. Using the QWR in the ATLAS upgrade design for reference [3], tapered inner and outer conductors have been adopted (Figure 1). There are two ports on the top and on the bottom, respectively, for the cavity surface treatment. And there are two coupler ports on the outer conductor. The final design of the RF parameters has been presented in Table 1, and the RF field distributions have been shown in Figure 2.

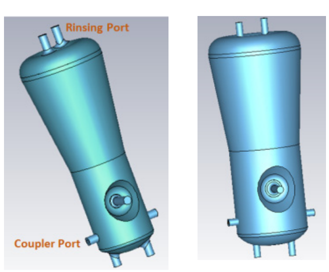

Figure 1: f=81.25 MHz, βopt=0.05, 0.10 QWR cavity model (from MWS of CST).

† zhangcong@impcas.ac.cn

Table 1: Design RF Parameters of the QWR

Cavity Type	QWR-0.05	QWR-0.10
Frequency (MHz)	81.25	81.25
β_{opt}	0.05	0.10
L_{eff} (β*λ,mm)	185	369
E_{peak}/E_{acc}	5.65	5.17
B_{peak}/E_{acc} (mT/(MV/m))	5.52	7.35
G (Ω)	28	39
R_a/Q_0 (Ω)	548	550

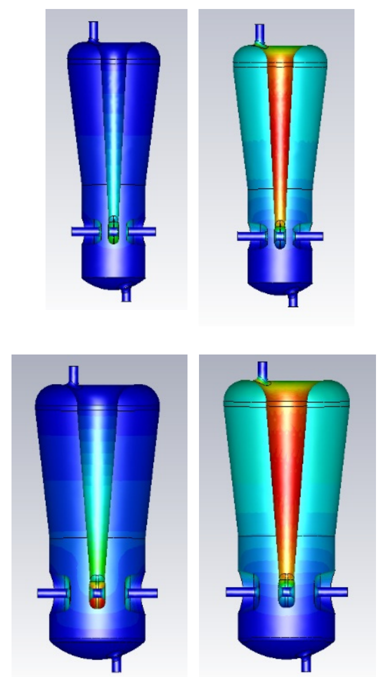

Figure 2: QWR surface fields (upper for QWR-0.05, nether for QWR-0.10).

CORRECTIONS OF THE BEAM STEERING EFFECT

The beam steering caused by the up-down asymmetry with respect to the beam axis needs to be compensated. Generally, three correction methods can be applied [4]: (I) donut-shaped axisymmetric drift tube used to reduce the magnetic field in the gap; (II) beam offset used to introduce the RF defocus field to counteract the electric and magnetic field effects; (III) beam port tilting used to create the artificial E_y to counteract the steering. In our design, the third method was employed (Figure 3). By properly tilting the beam ports, it's possible to create new E_y components (Figure 4), and adjusting the tilting angle

Content from this work may be used under the terms of the CC BY 3.0 licence (© 2017). Any distribution of this work must maintain attribution to the author(s), title of the work, publisher, and DOI.

ISBN: 978-3-95450-191-5 doi:10.18429/JACoW-SRF2017-MOPB008

INPUT POWER COUPLER FOR NICA INJECTOR COAXIAL QUARTER WAVE SC CAVITY

T. A. Bakhareva*, M. A. Gusarova, M. V. Lalayan, S. V. Matsievskiy,
National Research Nuclear University MEPhI , Moscow, Russia
V. Zvyagintsev, TRIUMF, Vancouver, Canada

Abstract

Nuclotron-based Ion Collider fAcility (NICA) is being built in Dubna, Russian Federation [1]. Usage of the accelerator superconducting QWR cavities for the proposed injector part of the accelerator upgrade is considered. These cavities along with auxiliary RF systems are under development by collaboration of Russian and Belorussian research institutions. In this paper the results on power coupler R&D for the 162 MHz QWR are presented and discussed. According to technical requirements power coupler should be able to transmit 20 kW of RF power. Additionally, external Q-factor tuning in small range should be possible.

DESIGN OVERVIEW

Nuclotron-based Ion Collider fAcility (NICA) injector upgrade plans comprise superconductintg QWR cavities (Fig. 1) for the acceleration of particles at velocity about 0.12 c. These cavities will operate in the pulsed mode [2, 3].

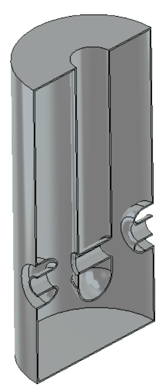

Figure 1: QWR cell.

Size of the 162 MHz rectangular waveguide is unacceptably big so the coaxial power input type was chosen. Outer and inner conductors of the coupler will be made of steel. Optional thin layer of plated copper is considered for better electrical and thermal conductivity. Accelerating system layout consists of 5 identical QWRs having the same beta value. This design was chosen because of low overall cost and cavity production capabilities despite the phase slipping occurred. It was decided to develop one power coupler suitable for all cavities. It require cavity external Q-factor value to be varied for different cavities in string. Power coupler antenna is of cylindrical shape and it couples to electric field in cavity. The required external Q-factor tuning range was calculated to be covered by the antenna with total tip penetration is varied within ±10 mm (Fig. 2).

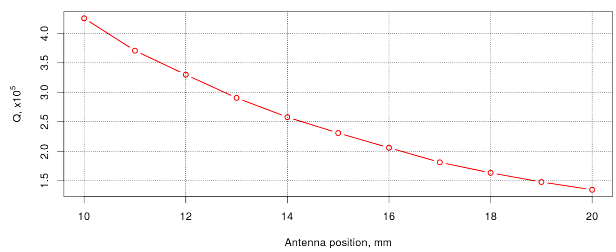

Figure 2: External Q-factor of the cell vs antenna position.

RF WINDOW

Conventional two-window power input design was chosen. It provides some protection from cavity contamination in case of mechanical failures and is not too complicated. First window isolates the high-vacuum cavity volume and contacts to the 70 K heat sink. Second window operates at higher temperatures. Usually, these windows would be half of the wavelength apart, but in this case it is unpractical. Both windows have the similar design providing them to be matched with reflection less than -45dB. Overview of the RF window design is shown in Figure 3.

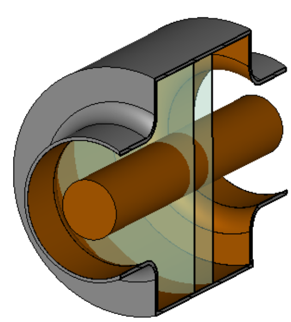

Figure 3: RF window overview.

In simulations 95% alumina ceramics was used. It is frequent to be employed in this kind of applications because of its good loss to cost ratio. Windows were tuned to achieve low reflection at operating frequency and in broad frequency range (Fig. 4).

In order to decrease the possibility of the breakdown, some rough window edges were smoothed. Due to rounded edges in transition from cylinder coax to pillbox volume the overvoltage factor is 1.3. (It equals to the maximal surface

* tatyanabasha@gmail.com

Content from this work may be used under the terms of the CC BY 3.0 licence (© 2017). Any distribution of this work must maintain attribution to the author(s), title of the work, publisher, and DOI.

ISBN: 978-3-95450-191-5 doi:10.18429/JACoW-SRF2017-MOPB009

Content from this work may be used under the terms of the CC BY 3.0 licence (© 2017). Any distribution of this work must maintain attribution to the author(s), title of the work, publisher, and DOI.

PROGRESS OF 650 MHz SRF CAVITY FOR ERHIC SRF LINAC*

Wencan Xu†, I. Ben-Zvi[1], Y. Gao, D. Holmes, P. Kolb, G. McIntyre, C. Pai, R. Porqueddu, K. Smith, R. Than, J. Tuozzolo, F. Willeke, A. Zaltsman, Collider-Accelerator Department, Brookhaven National Laboratory, Upton, NY, USA
[1]also at Physics &Astronomy Department, Stony Brook University, Stony Brook, NY, 11794, *USA*

Abstract

A high-current, well-damped 5-cell 647 MHz cavity was designed for ERL-Ring based eRHIC. Two prototype cavities were contracted to RI Research Instruments GmbH: one copper cavity with detachable beampipes for HOM damping study, and one niobium cavity for performance study. The performance study includes high-Q study for ERL-Ring eRHIC design and high gradient study for Ring-Ring eRHIC design. This paper will present the preliminary results of the HOM study, progress on Nb cavity fabrication and preparation for vertical test.

INTRODUCTION

An electron-ion collider, named eRHIC, is proposed by Collider-Accelerator Department at Brookhaven National Lab. A new electron accelerator will be built to provide polarized electron beams with an energy range from 5 to 18 GeV to collide with the existing polarized proton beams in RHIC. This electron accelerator will be placed in the existing RHIC tunnel and the SRF linac at IP2, where the length of the available straight section is 200m, as shown in Figure 1.

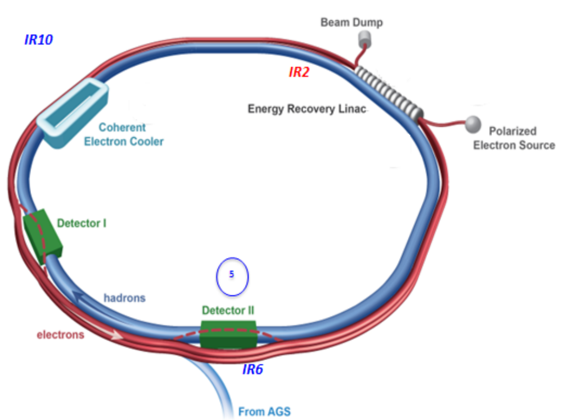

Figure 1: Layout eRHIC. Existing "Blue" hadron ring (center); Electron ring and SRF linac at IP2.

There are two technologies to build electron accelerator for eRHIC: one is to use ERL (Energy Recovery Linac) technology [1], which high current CW electron beam is accelerated by the same SRF cavities multiple times to reach a collision energy, and after colliding with, the electron energy is given back to the SRF cavities for the acceleration of following electron bunches; the other one is to use the storage ring technology [2], which electron bunches is accelerated by recirculating linac to the collision energy and injected into a storage ring to collide with proton beams. The design based on these two technology is called ERL-Ring eRHIC and Ring-Ring eRHIC, respectively.

The 5-cell 647 MHz cavity was originally designed for ERL-Ring eRHIC, which uses an enlarged beam tube to propagate all the HOMs but attenuate the fundamental mode. More detail of the cavity design can be found in reference [3]. A copper cavity was fabricated to study the performance of the HOM damping, and a niobium cavity is being fabricated to study post-processing and cavity performance. This paper will briefly describe cavity design, including the fundamental parameters and the different requirements of SRF cavity for ERL-Ring and Ring-Ring eRHIC. Then we will discuss the Cu cavity fabrication, and results of the HOM damping measurement and progress of the niobium cavity fabrication.

CAVITY DESIGN

Cavity Design for the ERL-Ring SRF Linac

The main objective for designing the 647 MHz 5-cell cavity was to damp well the HOMs, which includes both longitudinal modes and transverse modes. The 5-cell 647 MHz cavity uses the same idea of the previous BNL 5-cell cavities, i.e., enlarged beam tube to propagate all the HOMs but attenuate the fundamental modes. There is a taper at each side of the cavity to reduce the cross-talk between cavities and avoid RF heating on the cavity's gaskets. Figure 2 shows the Superfish code model of the cavity and its parameters are listed in Tab. 1.

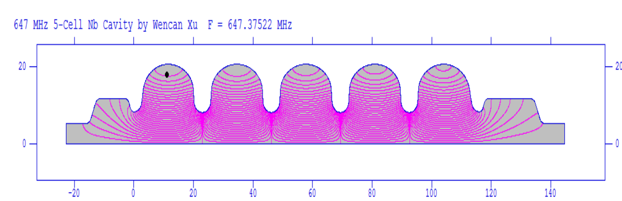

Figure 2: Superfish code model of BNL4 cavity.

During the cavity design, the loss factor, HOM damping capability was optimized to generate low monopole HOM power and increase the transverse beam-break-up (BBU) at the same time. More details of the cavity design are presented in reference [4].

Due to the wide range of the proton energy (40 GeV to 275 GeV), ERL-Ring SRF cavity is required to be able to tune up to 174 kHz. Following extensive mechanical-RF simulations [3], we decided that the wall thickness of the cavity would be 4.4 mm and there would not be any stiff-

* Work supported by LDRD program of Brookhaven Science Associates, LLC under Contract No. DE-AC02-98CH10886 with the U.S. DOE.
† email: wxu@bnl.gov

ISBN: 978-3-95450-191-5 doi:10.18429/JACoW-SRF2017-MOPB010

DESIGN OF THE 2×4-CELL SUPERCONDUCTING CRYOMODULE FOR THE FREE-ELECTRON LASER *

X. Luo, K. Zhou†, C. L. Lao, L. J. Shan, T. H. He,
X. M. Shen, L. D. Yang, H. B. Wang, X. F. Yang, M. Li
Institution of Applied Electronics, CAEP, Mianyang, China
X. Y. Lu, S. W. Quan, F. Wang, Peking University, Beijing, China

Abstract

A 2×4-cell superconducting linac module for the THz-FEL facility has been developed at the China Academy of Engineering Physics, which is expected to provide 6~8 MeV quasi-CW electron beams with an average current of 1~5 mA. The design of the cryomodule is presented in this paper. The dynamic and static heat load have been evaluated to reasonable level. The temperature distribution inside the cryomodule has been optimized by simulation, as well as mechanical structure and the magnetic shielding.

INTRODUCTION

A high average power THz free-electron laser facility developed by the China Academy of Engineering Physics (CAEP) [1] is under construction at Chengdu, China. Figure 1 shows the simplified layout of the THz-FEL facility. The designed frequency of the THz radiation is 1-3 THz with the average output power beyond 10 W. Owing to the advantages of SRF technology in CW mode operation, a 2×4-cell superconducting linac module has been adopted to accelerate 300 keV, 1~5 mA electron beams from a DC-Gun up to an energy of 6~8 MeV.

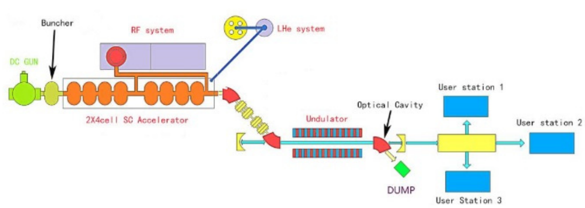

Figure 1: Layout of the CAEP THz-FEL facility.

CRYOMODULE DESIGN

In order to guarantee the SRF cavities have a good performance, the cryomodule must provide stable cryogenic temperatures, extremely low ambient magnetic fields and a stable mechanical support. The 2×4-cell cryomodule is designed to minimize thermal loss and fabrication cost. As shown in Fig. 2, the 2×4-cell cryomodule is consist of 2 K liquid helium layer, 80 K liquid nitrogen layer, vacuum vessel, magnetic shielding and cavity surport structure.

THERMAL OPTIMIZATION

A simplified model (see Fig. 3) in ANSYS Workbench

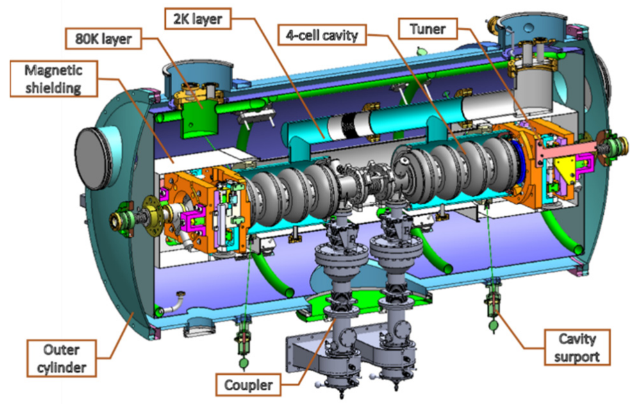

Figure 2: Schematic of the 2×4-cell module.

was used for thermal analysis of the cryomodule. Different thermal conditions were considered by this simulation, such as thermal radiation flux, HOM coupler power dissipation and coupler power dissipation. Figure 4 shows the simulated temperature distribution inside the cryomodule, including (a) the copper 80 K layer, (b) the connecting beam pipe, (c) the outer beam pipe and (d) the HOM couplers. Appropriate thermal insulations or insertions are used to cool down beam pipes and HOM couplers effectively.

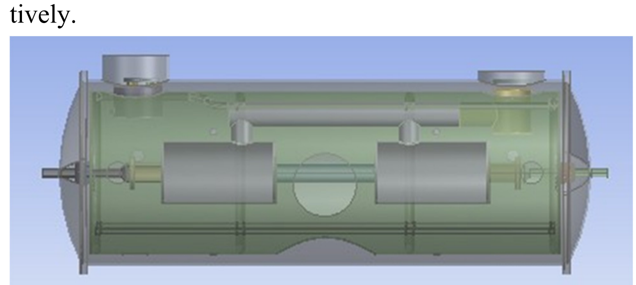

Figure 3: The simplified model in ANSYS Workbench.

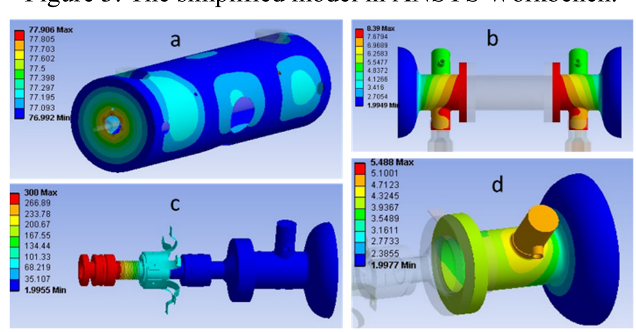

Figure 4: Simulated temperature distribution inside the cryostat.

* Work supported by National Natural Science Foundation of China with grant (11605190) and China National Key Scientific Instrument and Equipment Development Project (2011YQ130018).
† Email address: zhoudakui@163.com

Content from this work may be used under the terms of the CC BY 3.0 licence (© 2017). Any distribution of this work must maintain attribution to the author(s), title of the work, publisher, and DOI.

ISBN: 978-3-95450-191-5 doi:10.18429/JACoW-SRF2017-MOPB011

Content from this work may be used under the terms of the CC BY 3.0 licence (© 2017). Any distribution of this work must maintain attribution to the author(s), title of the work, publisher, and DOI.

CEA CRYOMODULES DESIGN FOR SARAF PHASE 2

C. Madec, N. Bazin, R. Cubizolles, D. Chirpaz, P. Hardy, F. Leseigneur, T. Plaisant, J. Plouin, P. Bredy, R. Bruce, CEA, Saclay, France

Abstract

CEA is committed to delivering a Medium Energy Beam Transfer line and a SuperConducting Linac (SCL) for SARAF accelerator in order to accelerate 5mA beam of either proton from 1.3MeV to 35MeV or deuterons from 2.6 MeV to 40.1MeV. The SCL [1,2] consists in 4 cryomodules separated by warm section housing beam diagnostics. The first two identical cryomodules host 6 half-wave resonator (HWR) low beta (0.091) cavities 176 MHz. The two last identical cryomodules are equipped with 7 HWR high beta (0.181) cavities, 176 MHz. The beam is focused through solenoids located between cavities housing steering coils. A beam position monitor is placed upstream each solenoid. The warm section contains a beam profiler and a vacuum pump will be placed at the end of each cryomodule. The cryomodules and warm sections are being designed. These studies will be presented in this poster.

INTRODUCTION

The SARAF-Phase II cryomodule design [2] is based on CEA experience on designing QWR and HWR cryomodule (SPIRAL2 and IFMIF). Figure 1 presents the SARAF Phase 2 cryomodule and its main components.

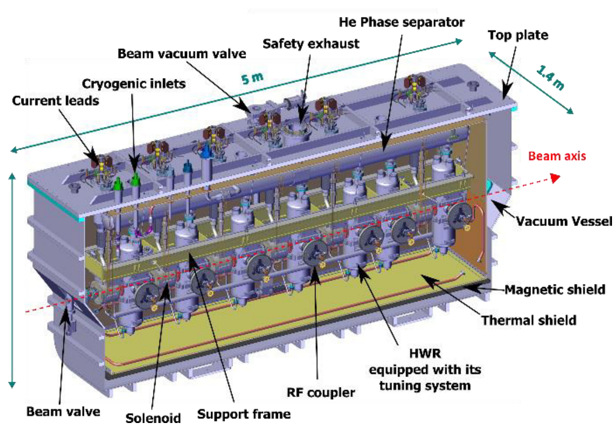

Figure 1 : SARAF phase 2 low beta cryomodule.

The infrastructures impose the lateral dimensions of the cryomodules since during the installation and maintenance, the cryomodules need to be moved freely in the beam corridor without disassembling any components of the accelerator line. Thus, the cavities have been placed vertically and the power coupler horizontally. In order to ease the assembly of the cryomodule, the cold mass will be hung on the top plate and top loaded into the vacuum vessel. The interfaces will be gathered on the top plate. Beam dynamics studies have determined the number of solenoids and cavities for the two types of cryomodules as well as the length of the string (cavities and solenoids) to 4.5 m for the low beta and 4.9 for the high beta. If the cavities performance are not reached in the first cryomodule, a free space for an optional cavity has been placed between the 5th and 6th cavity of the second low-beta cryomodule Figure 1. Moreover, the beam dynamic studies also impose a limitation on the cavity string misalignment at cold of +/- 2 mm. Hence, due to the impact on the cavity string alignment of the support frame, top plate and vacuum vessel, these components have been designed in order to ensure the alignment specifications and the results were presented in [3] together with the simulations and results on the top plate, support frame and vacuum vessel. Studies and simulations on the thermal and magnetic shield, phase separator, beam vacuum and assembly process were carried out. All those studies are presented in this contribution. Following simulations were performed with the finite elements software Cast3M.

THERMAL SHIELD

The thermal shield aims at reducing the radiative heat load from the room temperature parts of the cryomodule on the cold mass which is at liquid helium temperature. Indeed, the radiative heat flux between 300 K and 4 K is around 52 W/m² without a thermal intercept. With a thermal shield whose temperature is around 80 K, the value is reduced to 0.18 W/m² if no multi-layer insulation is installed on the 4 K parts. The thermal shield is also used to heat sink the components where one end is at room temperature and the other at liquid helium temperature, such as the RF power couplers, the current leads of the solenoid packages, the warm-cold transitions, etc. The heat loads on the Lβ and Hβ thermal shield are similar (respectively about 230 W and 220 W). Hence, the presented studies are based on the dimension of the Lβ thermal shield.

The simulations of the thermal shield aim at verifying the temperature of the thermal shield during cooling down and the mechanical deformation depending on the material (copper and aluminium).

Mechanical Design

The thermal shield is hung inside the vacuum vessel thanks to eight rods attached between the top part of the thermal shield and the top plate. These rods are made of titanium alloy for mechanical issues and in order to reduce the thermal losses, as the thermal conductivity is lower than the one of stainless steel. They are about 50 mm long. The deflection of top part of the thermal shield has to be under 5mm considering the space between the magnetic shield and the thermal shield covered by multi-layer insulator (about 25 mm between the magnetic shield and the thermal shield without the MLI) and the manufacturing and assembly errors. In order to ease the manufacturing of the shield made of plates, the same thickness for

ISBN: 978-3-95450-191-5 doi:10.18429/JACoW-SRF2017-MOPB012

STATUS OF THE IFMIF LIPAc SRF LINAC

N. Bazin†, G. Devanz, H. Jenhani, O. Piquet, S. Chel, A. Bruniquel, A. Riquelme, P. Charon, G. Disset, P. Contrepois, P. Hardy, J. Chambrillon, J. Relland, B. Renard, J. Plouin, C. Boulch, D. Roudier, P. Carbonnier, L. Maurice, F. Eozenou, C. Servouin,
Irfu, CEA, Université Paris-Saclay, Gif-sur-Yvette F-91191, France
F. Toral, D. Regidor, CIEMAT, Madrid, Spain

Abstract

The IFMIF accelerator aims to provide an accelerator-based D-Li neutron source to produce high intensity high energy neutron flux to test samples as possible candidate materials to a full lifetime of fusion energy reactors. A prototype of the low energy part of the accelerator is under construction at Rokkasho Fusion Institute in Japan. It includes one cryomodule containing 8 half-wave resonators (HWR) operating at 175 MHz and eight focusing solenoids. This paper presents the status of the IFMIF SRF Linac.

THE IFMIF LIPAC SRF LINAC

The IFMIF LIPAc SRF Linac mostly consists of one cryomodule designed to be as short as possible along the beam axis to meet the beam dynamic requirements. As depicted in Figure 1, it is made of a rectangular section vacuum vessel, a warm magnetic shield, a thermal shield cooled with helium gas. A titanium frame supports the cold mass made of a cylindrical phase separator with cryogenic piping, the cavities and the solenoids.

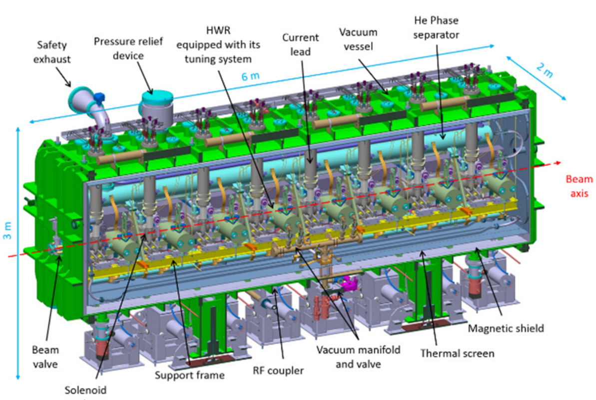

Figure 1: The IFMIF LIPAc cryomodule.

More details on the design of the cryomodule as well as the development plan and the actions taken to mitigate some risks are detailed in [1]. The next sections will present the manufacturing status of the main components of the cryomodule.

CAVITY STRING COMPONENTS

Cavities

The manufacturing of a series of 8 HWRs is in progress. An additional pre-serial cavity has been completed and tested during the production of the subcomponents of the series. A series of intermediate and qualification tests have been carried out for this HWR, between each major steps of manufacturing, and for all configurations:

- A vertical test (VT) of the niobium resonator be-fore heat treatment, after an average removal of 180 micrometers with BCP,
- A qualification VT after 650°C heat treatment and tank integration. The measured Q_0 was at $1.2x10^9$ at the nominal E_{acc} of 4.5 MV/m, and the quench field at 8.7 MV/m,
- An horizontal test in SaTHoRI using the same close-to-critical coupling RF feeding antenna,
- The horizontal test of the complete accelerating unit configuration, with the power coupler (Q_{ext}=$6.8x10^4$) and cold tuning system. The maximum accelerating field obtained was 5.5 MV/m in this configuration (administrative limit for high power test) (Figure 2).

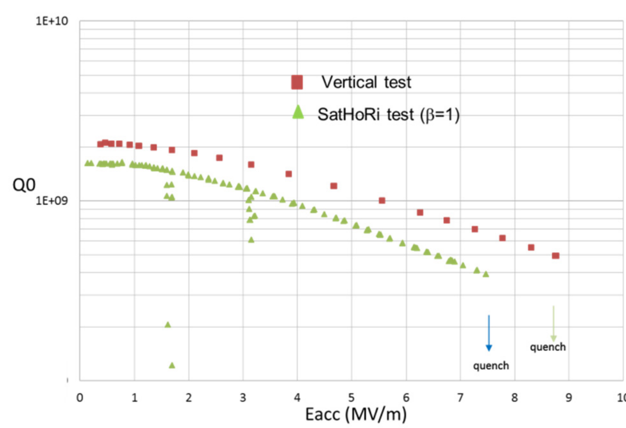

Figure 2: Horizontal test compared to vertical test for the pre-series cavity.

The first series HWR has been completed. The manufacturing has been completed following the licensing requirements, in terms of materials and weld qualifications, non-destructive testing on the cavity itself (radiography of welds) and titanium vessel (dye penetrant test) and final pressure testing of the helium space at 1.9 bar above atmospheric pressure.

The first vertical test of the bare resonator has been performed earlier this year. Although the cavity was not yet heat treated and had undergone several runs of static BCP etching to adjust its frequency, the Q_0 at nominal field was slightly above the specification of $5x10^8$. The next step is the preparation of the completed cavity and the qualification test.

†Contact: nicolas.bazin@cea.fr

Content from this work may be used under the terms of the CC BY 3.0 licence (© 2017). Any distribution of this work must maintain attribution to the author(s), title of the work, publisher, and DOI.

ISBN: 978-3-95450-191-5 doi:10.18429/JACoW-SRF2017-MOPB013

EUROPEAN XFEL INPUT COUPLER EXPERIENCES AND CHALLENGES IN A TEST FIELD

F. Hoffmann, D. Kostin, W.-D. Moeller, D. Reschke, M. Wiencek, DESY, Hamburg, Germany

Abstract

101 European XFEL accelerating modules with 808 superconducting cavities and input RF power couplers were assembled and then tested at DESY prior to installation in the European XFEL tunnel. In the Accelerating Module Test Facility (AMTF) warm and cold RF tests were done. The test results went directly to the operational setup for the LINAC. Input couplers did present several problems during the tests, resulting in some minor coupler design changes as well as in a few repair actions. The experience got from the said testing operation is worth to be shared and is presented here together with a discussion.

INTRODUCTION

When we started the European XFEL accelerating modules testing [1, 2] we faced the problem, that some of the modules were not okay for installing and needed a repair [3]. At the beginning we found a lot of not tightened screws. Mostly the warm part inner conductor to the cold part antenna fixing screw was not tightened with the right torque, or even loose (Figure 1). Another problem was once a left over rubber seal on top of a normal copper CF100 gasket which caused a burning of the rubber when high power RF was switched on (see Figure 7). This needed major repairs. During the cold tests on the module test benches in AMTF we faced occasionally some burnt (leaky) bellows of pushrods [4]. So some of them had to be exchanged. Also at module test stands (Figure 3) we discovered some warm parts from the last coupler productions with a lot of activities (discharge) inside or over heating during conditioning. These warm parts also had to be exchanged (Figure 2).

FUNDAMENTAL POWER COUPLERS

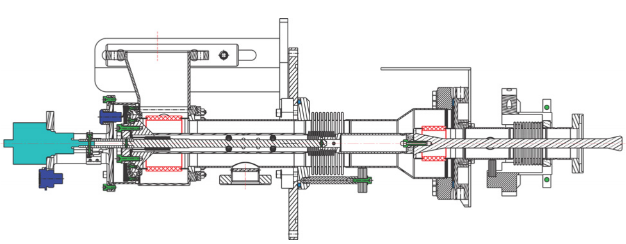

Figure 1: Drawing of XFEL-Input coupler.

Beginning with 3 so called PXFEL (prototype) modules and 3 pre-series modules, which were partly used for assembly training, we assembled at the end 101 XFEL-Modules for the linac and all of them are installed or foreseen to be installed.

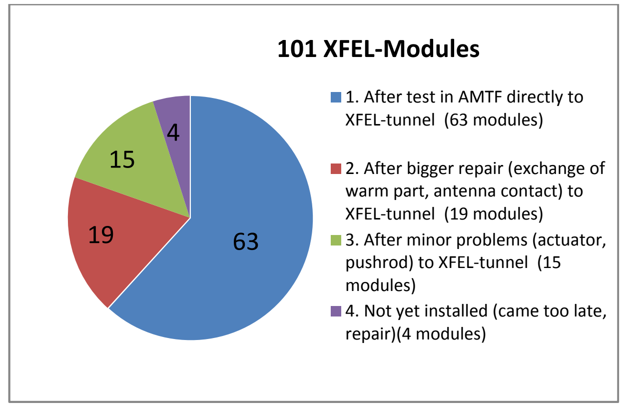

Figure 2: Diagram of module repair and installation.

In the 3 module test stands at DESY we tested all modules under the cold conditions before installation in the European XFEL tunnel (XTL).

Figure 3: One of three test stands in AMTF.

REPAIR OF RF POWER-COUPLERS

During the module tests in AMTF 13 warm parts (WP) were replaced because of contact problems of inner conductor of warm part to antenna of cold part. The reason of that was, that the screw of inner conductor was loose or not tightened with the right torque. The problem was, that we could recognize it only after switching on high RF power and with a low power everything seemed to be ok. The next problem was, that for repair we had to disconnect all connections (also cryogenics and vacuum) and put the damaged module to extra repair places not to handicap the tests of other modules and to have the required time for repair. All the power couplers with the defect connection of inner conductor showed nearly the same behavior and damage picture.

Content from this work may be used under the terms of the CC BY 3.0 licence (© 2017). Any distribution of this work must maintain attribution to the author(s), title of the work, publisher, and DOI.

ISBN: 978-3-95450-191-5 doi:10.18429/JACoW-SRF2017-MOPB015

ACCELERATOR MODULE REPAIR FOR THE EUROPEAN XFEL INSTALLATION

E. Vogel, S. Barbanotti, F. Hoffmann, K. Jensch, D. Kostin, L. Lilje,
W.-D. Moeller, M. Schmoekel, H. Weise, DESY, Hamburg, Germany
S. Berry, O. Napoly, CEA, Irfu, DACM, Centre de Saclay, France
M. Sienkiewicz, J. Swierblewski, M. Wiencek, IFJ PAN, Krakow, Poland

Abstract

Repair actions of different extent have been performed at 61 of the 100 accelerating series modules for the European XFEL to qualify them for tunnel installation. Four modules could not be repaired in time. CEA Saclay managed to perform three major repairs in parallel to the series module integration, the residual repair actions took place at DESY Hamburg. In this paper we will give an overview on the various technical problems which required being fixed before the tunnel installation and on the repair actions performed.

INTRODUCTION

The 100 superconducting accelerating series modules for the European XFEL [1,2] have been integrated and tested from September 2013 until August 2016 after the three pre-series modules whose integration started one year before. Institutes from six different countries (France, Germany, Italy, Poland, Russia and Spain), organized in 12 different work packages contributed with parts, capacity for work and facilities to the production and the testing of the modules [3].

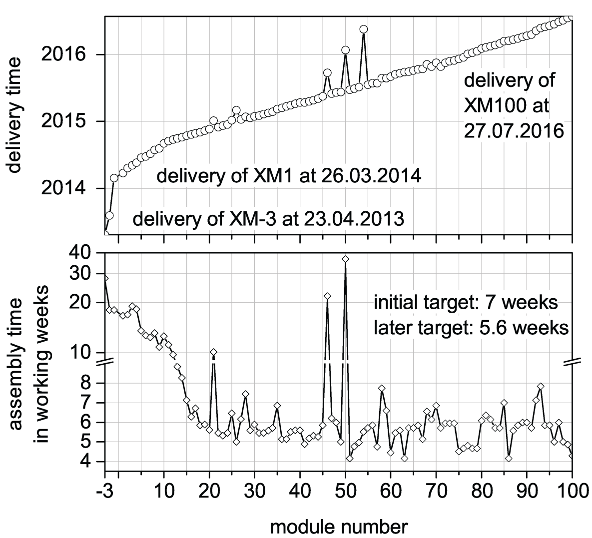

Figure 1: Delivery and assembly times of the modules.

An assembly infrastructure, called the ‘XFEL Village’, at CEA was used by the industrial contractor Alsyom for the integration of the modules under CEA supervision [4,5]. At two lines of seven workstations the components of the modules where integrated. The very challenging goal to produce one module per week has been achieved after the ramp-up phase lasting until module XM15 (Fig. 1). The improvement of the assembly quality and the otimization of the processes was an ongoing effort. Significant gradient degradation from XM6 to XM23, while CEA and Alsyom put all their effort in achieving the one module per week throughput, was overcome by an audit of string and module assembly conducted by CEA on XM26. A simplification of the clean room procedures was introduced at XM54. Thanks to organisational efforts, a 4-day throughput was reached in January 2015 with XM25 and maintained until the end of the production [6].

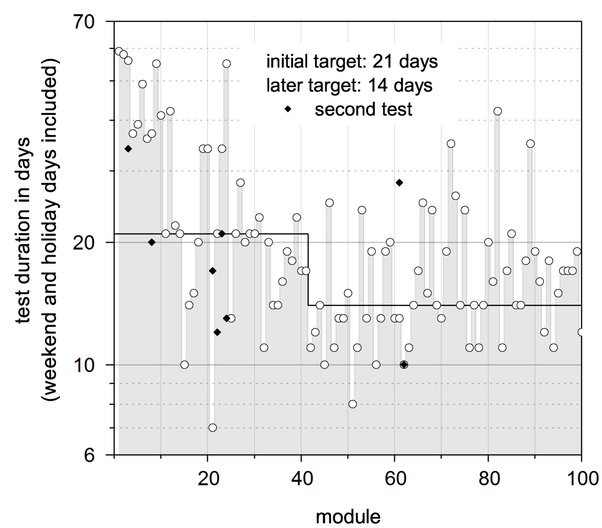

Figure 2: Module testing time.

After transportation from CEA to DESY, the modules have been received at the accelerator module test facility (AMTF) by a Polish team from IFJ PAN, Kraków. The team performed the complete test cycle including incoming inspection, installation to one of the three test stands, cool down, measurements of the cryogenic losses, rf operation of all cavities to determine the maximum cavity gradients and the levels where field emission starts. The initial target of 21 days per test was achieved in the ramp up phase. At the beginning, testing was handicapped by process line leaks, leaks at the connections of the gas return pipe (GRP) of the modules to the test stands, coupler push rod leaks and until about half-time the space for storing modules. Towards the end of the production overheating warm coupler parts became an issue. Performing a process optimization with

Content from this work may be used under the terms of the CC BY 3.0 licence (© 2017). Any distribution of this work must maintain attribution to the author(s), title of the work, publisher, and DOI.

ISBN: 978-3-95450-191-5 doi:10.18429/JACoW-SRF2017-MOPB016

OPERATION OF DIAMOND SUPERCONDUCTING RF CAVITIES

P. Gu†, C. Christou, P. Marten, S. Pande, A. Rankin, D. Spink, Diamond Light Source Ltd, Harwell Science and Innovation Campus, OX11 0DE, UK

Abstract

The Diamond Light Source (DLS) storage ring has been in operation using superconducting RF (SRF) cavities since 2007. Diamond has four superconducting cavity modules with two usually installed at any one time. The four cavities perform differently in many aspects such as reliable operating parameters and time in service, with the longest in continuous service for 7 years without failure and the shortest failing after only 8 months. All Diamond superconducting RF cavities suffered many fast vacuum trips in their early years, but after many years of efforts, the performance of the cavities have now been effectively managed by cavity voltage level control, weekly conditioning and partial warm-up during shut downs . We will discuss our experience with superconducting RF cavities and our future plan.

INTRODUCTION

The RF straight of Diamond storage ring is designed to allow three CESR type SRF cavities to be installed. In practice, only 2 cavities were in operation at the same time over the years. DLS has bought four cavities. For the moment, two cavities are in service, one is kept as spare and one is waiting for repair. A timeline of the four cavities installed in the three positions is shown in Fig. 1, with each cavity represented by a different colour. The stored beam current in the storage ring is also shown in the figure.

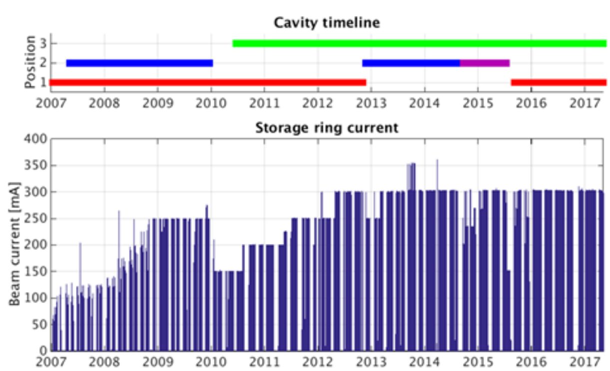

Figure 1: Cavity in service timeline and stored beam current.

The performance of the DLS SRF cavities varies hugely. It can be seen in Figure 1 that both cavity A (red) and cavity C (green) have been in operation for over 7 years while cavity D (purple) failed just 8 months after installation. Cavity B (blue) developed a leak in the indium seals during a cool-down after a warm-up to room temperature in 2014, but cavity C has survived many thermal cycles. The cavities suffered from fast vacuum trips in the early days of DLS. We have seen no cavity fast vacuum trips since September 2015 in our normal operating conditions but the avoidance of fast vacuum trips is the limiting factor of the cavity working voltage. General speaking, the performances of the cavities are not consistent with each cavity having a different safe operating voltage below which fast cavity trips do not occur.

CAVITY TRIPS

According to their signatures [1], cavity trips are mainly classified into fast vacuum trips, RF window vacuum trips, cavity quench, cavity arc and other trips. The fast vacuum trips and trips on RF window vacuum are two major types of cavity trip in DLS.

Fast Vacuum Trips and RF Window Vacuum Trips

During a fast vacuum trip, the cavity field collapses within several microseconds. A spike on the e- pickup in the waveguide near the coupling tongue can be observed before the trip. There are vacuum spikes on every gauge around the cavity. While in a trip on RF window vacuum, there is only vacuum spike on the pump-out box. The decay curve of the cavity field for a trip at the window is consistent with a high Q cavity.

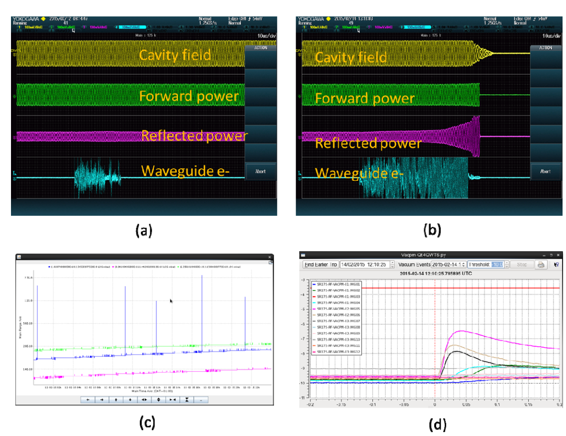

Figure 2: Activities on waveguide e- pickup and associated vacuum spikes.

Figure 2 shows the signals on cavity D waveguide e-pickup and vacuum gauges around the cavity. Figure 2 (a) shows an event on the waveguide e- pickup which didn't lead to a beam trip. Figure 2 (c) shows the vacuum signals of that day. There was only vacuum spike near the RF window. Every vacuum spike happened with a corresponding activity on the waveguide e- pickup at the same time. Figure 2 (b) shows an event on the waveguide elec-

† Pengda.gu@diamond.ac.uk

Content from this work may be used under the terms of the CC BY 3.0 licence (© 2017). Any distribution of this work must maintain attribution to the author(s), title of the work, publisher, and DOI.

ISBN: 978-3-95450-191-5 doi:10.18429/JACoW-SRF2017-MOPB017

Content from this work may be used under the terms of the CC BY 3.0 licence (© 2017). Any distribution of this work must maintain attribution to the author(s), title of the work, publisher, and DOI.

MULTIPHYSICS SIMULATIONS OF THE WIDE OPENED WAVEGUIDE CRAB-CAVITY

K. Papke*, A. Amorim Carvalho, A. Grudiev, and C. Zanoni
CERN, Geneva, Switzerland

Abstract

In the frame of a FCC study, a first prototype of a compact superconducting crab-cavity, using Nb-on-Cu-coating technique is being manufactured and investigated. The design, which is based on the ridged waveguide resonator, is subjected to multipacting and pressure sensitivity simulations. First results of these simulations are presented and compared to those of other SRF cavities. Furthermore, several aspects related to the design of the fundamental mode coupler and HOM dampers are presented.

INTRODUCTION

The study about a compact superconducting crab-cavity for LHC using Nb-on-Cu-coating techniques [1], launched in 2014 has been recently accepted for a FCC work package at CERN . In contrast to the Double Quarter Wave (DQW), Four-Road, and RF Dipole [2], the design of the cavity which we denote as Wide Opened Waveguide Crab Cavity (WOWCC) is based on a ridged waveguide resonator with wide open apertures to allow direct access to the interior for the surface preparation and coating (Fig. 1). Noteworthy, that due to the large apertures, the number of trapped higher order modes (HOMs) is comparably low which eventually facilitates their damping. Likewise, the longitudinal and transverse impedances are lower than those of the other three crab cavities. It should be mentioned that a similar design called Quasi-waveguide Multicell Resonator (QMiR) is being studied and developed at FermiLab for the Advanced Photon Source's Short Pulse X-ray project [3]. However, the QMiR is machined out of bulk niobium. We omit the motivation of thin-film against bulk niobium superconducting cavities since it has been addressed in [1].

The WOWCC will be operated with a frequency of 400 MHz at 4.5 K, providing a deflecting voltage of 3 MV over an effective length of 1 m with a total RF power loss of approximately 60 W. The main parameter are listed in Table 1.

In this paper, we follow up the studies presented in [1]. These involve the power loss and Q factor calculations incorporating a field dependent localized surface resistance and the frequency sensitivity against pressure fluctuations by means of coupled 3D RF and structural mechanics simulations. Further detailed calculations of the longitudinal and transverse impedances are compared to those of the DQW and the RF Dipole crab cavity. Moreover, the fundamental mode coupler and HOM antennas are addressed as well as the multipacting in the bare cavity.

* kai.papke@cern.ch

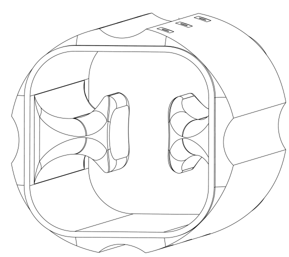

(a)

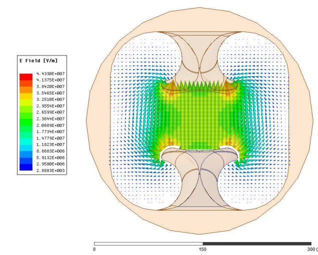

(b)

Figure 1: (a) Center part of the Wide Opened Waveguide Crab Cavity (WOWCC). (b) The electric field between the two mushroom-shaped ridges in the cavity center.

Table 1: Main Parameters of the WOWCC

Parameter	Unit	Value
dimensions (W×H×L)	[mm]	250×250×1400
smallest aperture	[mm]	42
frequency	[MHz]	400
geometry factor G	[Ω]	108.9
deflecting voltage V_{x0}	[MV]	3.0
R_x/Q	[Ω]	343.5
E_{pk} at V_{x0}	[MV/m]	45.3
B_{pk} at V_{x0}	[mT]	78.3
Q_0 at V_{x0}		4.0×10^8

RF DESIGN

The design process has been subjected to the following requirements exhaustively discussed in [1]:

- Facilitate the access for sputtering cathodes.
- The Frequency is fixed to 400 MHz.
- Minimum aperture is 42 mm.
- Minimize surface peak fields with respect to V_{x0}.
- Minimize sextupolar component b_3/V_{x0} [4].

In the following, we asses further RF characteristics of the optimized design or complete earlier studies, respectively.

RF Power Loss Calculation at 4.5 K

We further refined the procedure outlined in [1] to evaluate the dissipating power in the cavity wall P_{diss} as follows: (i) Calculate the RF field and surface loss density assuming a homogenous surface resistance of copper at 300 K[1]. (ii) Rescale locally the surface resistance taking into account the magnetic field B_s (Fig. 2) to obtain the total power loss

[1] The calculations are done using HFSS [5].

ISBN: 978-3-95450-191-5 doi:10.18429/JACoW-SRF2017-MOPB018

TESTING OF SRF CAVITIES AND CRYOMODULES FOR THE EUROPEAN SPALLATION SOURCE

N. Elias†, E. Asensi, C. Darve, F. Håkansson, W. Hees, C. G. Maiano, F. Schlander,
European Spallation Source ERIC, Lund, Sweden

ABSTRACT

The European Spallation Source (ESS) is currently under construction in Lund, Sweden. The ESS linear accelerator aims to deliver a 62.5 mA, 2.86 ms long proton beam pulse onto a rotating tungsten target, at 14 Hz repetition rate, thus achieving an energy of 2 GeV and 5 MW power. Most of the beam acceleration happens in the superconducting fraction of the linac, which is composed of three sectors of cryomodules named after the cavities housed within. The first sector of the SRF linac is composed of 13 Spoke cryomodules containing 2 double spoke cavities with a geometric beta of 0.5, the second is composed of 9 medium beta cryomodules each housing four elliptical cavities (β=0.67) and finally 21 high beta cryomodules enclosing four elliptical cavities (β=0.86). ESS has strategically built up a SRF collaboration with other European institutions, these partners will deliver through in-kind agreements cavities and cryomodules performing within the ESS specification. This article describes the process leading to the acceptance of cavities and cryomodules received from the different partners and the necessary tests required prior to the final installation in the ESS tunnel.

INTRODUCTION

The European Spallation Source

The European Spallation Source (ESS) [1] is an accelerator based neutron source and aims at becoming the worlds most powerful by colliding a 2 GeV pulsed proton beam onto a rotating helium cooled tungsten target where neutrons are produced by spallation process.

The project is funded by a collaboration of 17 European countries and is currently under construction in Lund, Sweden.

The ESS Superconducting Linac

The linac will deliver 62.5 mA, 2.86 ms long proton beam pulses at 4 % duty cycle with a repetition rate of 14 Hz and 5 MW average beam power [2].

The superconducting part of the linac [3] is composed of different families of cryomodules organized in three sectors containing:

- 13 spoke cryomodules,
- 9 elliptical medium-β cryomodules,
- 21 elliptical high-β cryomodules.

Each of the aforementioned cryomodules will contain superconducting cavities with similar name.

A summary of the ESS specifications of the superconducting linac is given in Table 1:

Table 1: ESS Specifications for Each Sector of The ESS Superconducting Linac

	Spoke	Medium-β	High-β
Proton energy range, MeV	90 to 216	216 to 571	571 to 2000
Cryomodules/Sector	13	9	21
Cavities/Cryomodule	2	4	4
Cavities/Sector	26	36	84
Sector length, m	55.9	76.7	178.9
Operating freq., MHz	352.21	704.42	704.42
Operating temp., K	2	2	2
Cavities optimum β	0.5		
Cavities geometric β		0.67	0.86
E_{acc}, $MV{\cdot}m^{-1}$	9	16.7	19.9

The ESS SRF Collaboration

A large fraction of the ESS construction budget will be realised by means of in-kind contributions from European partners. On this basis, a strategic ESS SRF collaboration [4] is taking place to design, manufacture and test cavities and cryomodules [5] in agreement with the ESS specification.

The spoke cavities will be manufactured and tested as part of the IPN Orsay contribution, as well as the cryomodule design and production, furthermore the testing of the cryomodules will take place at FREIA laboratory as a contribution of the Uppsala University.

The medium-β cavities will be manufactured and tested as part of the INFN/LASA contribution, while the high-β cavities manufacturing and testing is part of the STFC/ASTeC contribution, moreover the cryomodule production is under CEA-Saclay responsibility.

The testing of the first 3 pre-series cryomodules for both medium-β and high-β sections is done at CEA to validate the assembly procedures. The final site acceptance test for all the elliptical cryomodules is done at the ESS Lund Test Stand 2 (TS2).

From production until final acceptance for installation, the ESS cavities and cryomodules will undergo a series of inspections and acceptance tests to assure conformance to the requirements. In the subsequent sections we will focus on the processes that take place during the lifecycle of the cavities and cryomodules in respect to testing.

† nuno.elias@esss.se

Content from this work may be used under the terms of the CC BY 3.0 licence (© 2017). Any distribution of this work must maintain attribution to the author(s), title of the work, publisher, and DOI.

ISBN: 978-3-95450-191-5 doi:10.18429/JACoW-SRF2017-MOPB019

INTERFACE CHALLENGES FOR THE SRF CRYOMODULES FOR THE EUROPEAN SPALLATION SOURCE

F. Schlander*, C. Darve, N. Elias, C. G. Maiano
European Spallation Source ERIC, Lund, Sweden
P. Bosland, CEA/DRF/IRFU, Gif-sur-Yvette, France
G. Olry, Institut de Physique Nucléaire, CNRS/IN2P3, Université Paris Sud, Orsay Cedex, France

Abstract

The European Spallation Source is currently under construction in Lund in southern Sweden. The main part of the accelerator will consist of two different types of cryomodules housing three different types of cavities - double spoke cavities and two different elliptical cavities. The spoke cavities, as well as the cryomodules, will be provided by IPN Orsay, thus the external interfaces to the other accelerator systems have to be verified. While the procurement and assembly of the elliptical cryomodules will be performed by CEA Saclay, the cavities will be provided by INFN Milano and STFC Daresbury. Thus, in addition to the external cryomodule interfaces, also the internal interfaces between cavities and cryomodules have to be taken care of. This contribution presents the challenges related to this work.

INTRODUCTION

The proton accelerator of the European Spallation Source (ESS) [1] is composed of a warm section consisting of the proton source, low energy beam transport, radio frequency quadrupole, medium energy beam transport as well as the drift tube linac. The cold section will contain two types of SRF cryomodules, which will be described briefly in the following, and the main requirements of the cavities can be found in Table 1.

Table 1: Requirements on Superconducting Cavities

Requirement	**Spoke**	**medium-β**	**high-β**
Frequency / MHz	352.21	704.42	704.42
Optimum β	0.5		
Geometric β		0.67	0.86
E_{acc} / MV m^{-1}	9.0	16.7	19.9
E_{Pk} / MV m^{-1}	39	45	45
$B_{\mathrm{Pk}}/E_{\mathrm{Acc}}$ / mT/(MV/m)	6.80	4.79	4.3
$E_{\mathrm{Pk}}/E_{\mathrm{Acc}}$	4.28	2.36	2.2
Iris diameter / mm	56	94	120
RF peak power / kW	335	1100	1100
G / Ω	130	196.63	241
maximum R/Q / Ω	425	394	477
Q_{ext} / 10^5	1.75-2.85	7.5	7.6
min $Q_0(E_{\mathrm{acc}})$ / 10^9	1.5	5	5

The 13 spoke cryomodules contain two double spoke cavities each with an operating frequency of 352.21 MHz. A picture of the cryomodule is shown in Fig. 1.

Figure 1: Picture of ESS prototype spoke cryomodule with its valve box, installed in the test pit at IPN-Orsay.

As the cavities and the cryomodules are provided by IPN Orsay, the internal interfaces between cavities and cryomodule are in the hand of one partner. The same holds for the helium supply for the operation of the cryomodule.

The 30 elliptical cryomodules, which will be provided by CEA Saclay, contain four elliptical cavities each with an operating frequency of 704.42 MHz. ESS requires 9 cryomodules containing medium-beta ($\beta = 0.67$) cavities, and 21 cryomodules housing high-beta ($\beta = 0.86$) cavities. It is to be noted that the cavities will be provided by different partner laboratories, in particular INFN Milano (medium-beta) and STFC Daresbury (high-beta). Thus, in comparison to the spokes, already the internal interfaces between cavities and cryomodule have to be well defined with a special attention to mechanical clashes that may occur during the assembly phase of the cryomodule. A model of an elliptical cryomodule is shown in Fig. 2.

As SRF cryomodules are complex systems, they have to rely on various auxiliary systems to allow appropriate operation. For example, the cavities have to be under vacuum, then are cooled down to cryogenic temperatures with the means of liquid helium before acceleration of the particle beam is possible. In order to define the interfaces between

* felix.schlander@esss.se

Content from this work may be used under the terms of the CC BY 3.0 licence (© 2017). Any distribution of this work must maintain attribution to the author(s), title of the work, publisher, and DOI.

ISBN: 978-3-95450-191-5 doi:10.18429/JACoW-SRF2017-MOPB020

AN OPTIMAL PROCEDURE FOR COUPLER CONDITIONING FOR ESS SUPERCONDUCTING LINAC

H. Li, Uppsala University, Sweden
C. Maiano, E. Conejero, R. Zeng, European Spallation Source ERIC

Abstract

An optimal procedure for coupler and cavity conditioning is proposed for the ESS superconducting cavities, which is applicable for different test stands and following installation in the ESS tunnel. A preliminary procedure has been developed and successfully tested at FREIA facility, Uppsala. The preliminary procedure will now be improved by integrating it into LLRF and EPICS control. This will be a joint effort between FREIA and ESS and will be used at the test stands in Lund and on the couplers installed in the tunnel. Developing the conditioning procedures on a common platform offers ESS significant advantages by allowing the procedures to be reused at different sites and by recording data in a consistent format. The details of the procedure, its development and testing will be reported and the future activities will be described.

INTRODUCTION

The European Spallation Source (ESS) will use a total of 26 double-spoke cavities in the medium energy region, at 352.21 MHz, 36 medium beta elliptical cavities at 704.42 MHz and 84 high beta elliptical cavities also at 704.42 MHz [1]. ESS spoke cavity is designed and fabricated by IPNO, while series spoke cryomodule testing will be carried out in the Facility for Research Instrumentation and Accelerator development (FREIA), Sweden[2]. Production of series elliptical cavities is undertaken by INFN-LASA and STFC and series cryomodule assembling will be done by CEA, while final elliptical cryomodule testing will be performed in Test Stand 2 (TS2) at ESS site in Lund, Sweden.

As variety of RF tests carried out in different test stands all over European and very limited time is foreseen for commissioning cavities in ESS tunnel, it is crucial to develop optimal cavity commissioning/test procedures based on common hardware and software platform, aiming to reuse the procedures in different test stand and ESS tunnel. Based on common platforms, it will be also easier to share the knowledge and data between different test stands and ESS tunnel.

While typical coupler conditioning procedures in test stand focus mainly on reaching the required power level at required mode, the “optimal” procedures emphasize procedures reusing, knowledge accumulation and consistent result interpretation over different stages of cavity and cryomodule life cycle (test, commissioning, operation and maintenance).

During power coupler/cavity conditioning stage, a wide variety of RF modes (in term of RF pulse length, RF pulse peak power, and repetition rates) will be employed. Detailed and valuable information will be obtained and would benefit much for characterizing RF/Cavity dynamics. This will be critical when it comes to fault tolerance strategies and high efficiency operation strategies. It is thus equally important, if not more, during the stage of optimal procedure development, to identify and find ‘smart’ solutions to obtained adequate information to understand better cavity system and to get to know its limitations, thereby testing, controlling and operating the cavity system efficiently and effectively.

This paper thus discusses and proposes an optimal procedure for power coupler/cavity conditioning, in the purpose of reusing the procedure in different test stands and ESS tunnel, reducing the time and effort of overall power coupler/cavity conditioning, and finding a smart way to commissioning and operating RF/cavity system efficiently.

WORKFLOW CHALLENGE TO DEVELOP OPTIMAL PROCEDURES

Workflow Challenge with Multi-Stakeholders Collaboration

In theory, it is probably true that maximum benefit would achieve if the same procedure based on the same hardware and software platform can be applied in all test stands and ESS tunnel, however, it is always not operational in practice. We have to focus on what is concretely possible in short term to achieve in test stands with existing infrastructure, preferable software/hardware platform by technical experts, and available resources. It is then easier to work together to address concrete problem faced in development process, by exploring new ideas from all participants and by making best use of technologies already in place. In such context, a more practical workflow for procedure development shown in Fig. 1 is considered at ESS. This workflow is not only valid for coupler/cavity conditioning, but also can be applied for other cavity/RF test and commissioning procedures.

The challenge of this workflow with multiple stakeholders collaboration lies in the fact that, due to different stakeholders are undertaking different tasks and are in different development stages, it is inevitable that different version of procedures based on different platforms will exist. As a result, it becomes challenging and complex to reuse the procedure, to share data and result, and to accumulate knowledge in different test stands and ESS tunnel.

Content from this work may be used under the terms of the CC BY 3.0 licence (© 2017). Any distribution of this work must maintain attribution to the author(s), title of the work, publisher, and DOI.

ISBN: 978-3-95450-191-5 doi:10.18429/JACoW-SRF2017-MOPB023

FURTHER LAYOUT INVESTIGATIONS FOR A SUPERCONDUCTING CW-LINAC FOR HEAVY IONS AT GSI

W. Barth[1,2,5], K. Aulenbacher[2,4], M. Basten[3], F. Dziuba[2], ·V. Gettmann[2], M. Heilmann[1], T. Kürzeder[2], M. Miski-Oglu[2], H. Podlech[3], M. Schwarz[3] and S. Yaramyshev[1,5]
[1]GSI Helmholtzzentrum, 64291 Darmstadt, Germany
[2]HIM, Helmholtzinstitut, 55128 Mainz, Germany
[3]IAP, Goethe University, 60438 Frankfurt, Germany
[4]KPH, Johannes Gutenberg-University, 55099 Mainz, Germany
[5]MEPHI, National Research Nuclear University, 115409 Moscow, Russia

Abstract

Very compact accelerating-focusing structures, as well as short focusing periods, high accelerating gradients and very short drift spaces are strongly required for superconducting (sc) accelerator sections operating at low and medium beam energies. To keep the GSI-Super Heavy Element program competitive on a high level and even beyond, a standalone sc continuous wave Linac in combination with the GSI High Charge State injector (HLI), upgraded for CW-operation, is envisaged. The first Linac section (financed by HIM and GSI) as a demonstration of the capability of 217 MHz multi gap Crossbar H-structures (CH) is still in the beam commissioning phase, while an accelerating gradient of 9.6 MV/m (4 K) at a sufficient quality factor has been already reached. Recently the overall Linac design, based on a standard cryomodule, comprising three CH cavities, a rebuncher section and two 9.3 T-solenoidal lenses, has to be fixed. This paper presents the status of the Linac layout studies as well as the integration in the GSI accelerator facility.

INTRODUCTION

An UNILAC upgrade program is ongoing, designated to prepare for high intensity high current synchrotron injector operation for Facility of Antiproton and Ion Research (FAIR) [1-3]. As a result high duty factor beam time availability for SHE-research at GSI UNILAC will be strongly diminished due to the duty factor limitation for FAIR injector operation. Besides, an upgrade program of the HLI was already initialized comprising a new 18 GHz Electron Cyclotron Resonance in source (ECR), a CW capable RFQ and an IH-DTL [4], keeping the SHE program at GSI competitive [5]. An additional standalone sc CW-Linac [6] is assumed to meet the demands of the experimental program at its best. With significantly higher beam intensity the SHE production rate will be increased as well.

The design and construction of CW high intensity Linacs is a crucial goal of worldwide accelerator technology development [7-10]. Above all, compactness of a particle accelerator is a beneficial demand for the development of high intensity CW proton and ion Linacs [11-13]. In the low- and medium-energy range CW-Linacs can be used for several applications, as boron-neutron capture therapy, high productivity isotope generation and material science. A high-energy Linac is an integrated and essential part of several large scale research facilities, as spallation neutron sources or accelerator driven systems. Thus the study and investigation of the design, operation and optimization of a CW-Linac, as well as progress in elaboration of the superconducting technology (Fig. 1), is of high relevance.

Figure 1: CW-Linac demonstrator cavity@new clean room.

CW-LINAC LAYOUT AND R&D

Nine superconducting CH cavities operated at 217 MHz provide for ion acceleration to beam energies between 3.5 MeV/u and 7.3 MeV/u, while the energy spread should be kept smaller than ±3 keV/u. A conceptual layout [6] of this sc CW-Linac was worked out eight years ago. It allows the acceleration of highly charged ions with a mass to charge ratio of up to 6. For proper beam focusing superconducting solenoids have to be mounted between CH cavities. The general parameters are listed in Table 1.

Table 1: Design Parameters of the CW-Linac

Mass/Charge		6
Frequency	MHz	216.816
Max. beam current	mA	1
Injection Energy	MeV/u	1.4
Output energy	MeV/u	3.5 – 7.3
Output energy spread	keV/u	±3
Length of acceleration	m	12.7
Sc CH-cavities	#	9
Sc solenoids	#	7

R&D and prototyping (demonstrator project) [14, 15] in preparation of the proposed CW-Linac is assigned to a collaboration of GSI, HIM and IAP. The demonstrator

Content from this work may be used under the terms of the CC BY 3.0 licence (© 2017). Any distribution of this work must maintain attribution to the author(s), title of the work, publisher, and DOI.

ISBN: 978-3-95450-191-5 doi:10.18429/JACoW-SRF2017-MOPB024

Content from this work may be used under the terms of the CC BY 3.0 licence (© 2017). Any distribution of this work must maintain attribution to the author(s), title of the work, publisher, and DOI.

STEPS TOWARDS A SUPERCONDUCTING CW-LINAC FOR HEAVY IONS AT GSI

M. Miski-Oglu*[1], M. Amberg[1], K. Aulenbacher[5], W. Barth[1,2,3], F. Dziuba[1], V. Gettmann[1], M. Heilmann[2], S. Mickat[2], S. Yaramyshev[2,3], M. Basten[4], D. Bänsch[4], H. Podlech[4], U. Ratzinger[4]
[1]HIM, Mainz, Germany
[2]GSI Helmholtzzentrum, Darmstadt, Germany
[3]MEPHI, National Research Nuclear University, Moscow, Russia
[4]IAP Goethe University, Frankfurt, Germany
[5]KPH, Johanes Gutenberg-University, Mainz, Germany

Abstract

A superconducting (sc) cw-Linac at GSI should ensure competitive production of Super Heavies in the future. Further R&D for this cw-Linac, a so called "Advanced cw-demonstrator", with maximal energy of 3.5 MeV/u is ongoing. As a first step, the demonstrator project with one sc CH-cavity is completed, the beam tests are performed mid-summer 2017. The completion of the "Advanced CW-Demonstrator" includes successive construction of at least one new cryogenic modules comprising three CH-cavities and two solenoids each. In this contribution the layout of the cryo module and the Helium distribution system are presented.

ORIGINAL LAYUOT

Providing heavy ion beams for the ambitious experiment program at GSI, the Universal Linear Accelerator (UNILAC) serves as a powerful high duty factor (25%) accelerator. Beam time availability for SHE-research will be decreased due to the limitation of the UNILAC providing a proper high intensity beam for FAIR simultaneously. To keep the GSI-SHE program [1] competitive on a high level, a standalone sc cw-linac in combination with the upgraded GSI High Charge State Injector (HLI) is planned to build. The Figure 1 shows a conceptual layout of cw-linac. This design, proposed more then eight years ago [2], contains nine superconducting (sc) Crossbar H-mode (CH) cavities.

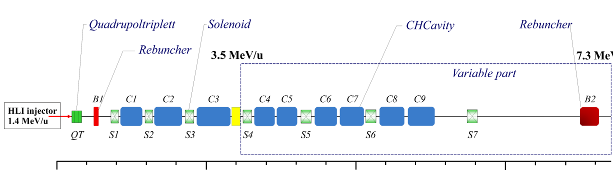

Figure 1: Original layout of cw-linac.

The beam with an energy of 1.4 MeV/u from HLI operating at 108.408 MHz, is transported through the line comprising of quadrupole lenses for transversal matching and rebuncher cavities for longitudinal matching to cw-linac. The multigap CH-cavities operate at double frequency of HLI and provide an effective accelerating gradient of 5.1 MV/m each. Seven sc solenoids with free beam aperture of 30 mm and magnetic field strength up to 9.3 T providing beam focusing. The first part of linac comprising of three CH multigap cavities accelerates ions up to 3.5 MeV/u, the second part provides for continuous variation of energies up to 7.3 MeV/u demanding by the experiments.

DEMONSTRATOR ENVIRONMENT AT GSI

The cw demonstrator project [3] (started in 2010) is aiming to show the capability of sc 15 gap CH cavities to accelerate ion beams. The schematic view of the testing environment is shown in Fig. 2.

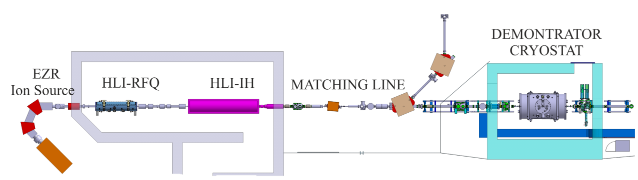

Figure 2: Testing environment for the demonstrator project at GSI.

The beam line before and behind the demonstrator cryostat is equipped with various beam diagnostic devices. Beam current transformers, Faraday cups, SEM-profile grids, a dedicated emittance meter [4], a bunch structure monitor [5] and phase probe pickups [6] (beam energy measurements applying time of flight) provides for proper beam characterization. At a beam time in 2015 the transverse emittance of Ar^{7+} and Ar^{10+} beams from HLI injector has been measured. These measurements [7] were used to calculate emittance backwards to the output of IH-DTL. The results are validated by comparison of measured emittance for various excitation of quadrupoles with calculated ones.

The liquid He cryostat maintains the cavity and two sc solenoids [3, 8] is placed within the radiation protection shelter. The cryostat is connected by flexible transfer line to liquid Helium reservoir with a capacity of 3000 liters, sufficient for one week of test operation. The used helium is collected by a 25 m^3 recovery balloon and then bottled by a compressor. The demands of the demonstrator project on liquid Helium is covered by an in house liquefier.

* m.miskioglu@gsi.de

ISBN: 978-3-95450-191-5 doi:10.18429/JACoW-SRF2017-MOPB028

HOM COUPLER DESIGN FOR CEPC CAVITIES*

H. J. Zheng†, F. B. Meng, J. Y. Zhai
Key Laboratory of Particle Acceleration Physics and Technology, Institute of High Energy Physics, CAS, Beijing 100049, China

Abstract

In this paper，it will be presented the higher order mode (HOM) coupler design for the Circular Electron-Positron Collider (CEPC) 650 MHz 2-cell cavity. The higher order modes excited by the intense beam bunches must be damped to avoid additional cryogenic loss and multi-bunch instabilities. To keep the beam stable, the impedance budget and the HOM damping requirement are given. A double notch coaxial HOM coupler, which will be mounted on the beam pipe, is planned to extract the HOM power below the cut-off frequency of the beam pipe. This paper summarizes the RF design of the HOM coupler, tolerance analysis, thermal analysis as well as mechanical structures.

INTRODUCTION

With the discovery of the Higgs boson at the LHC in 2012, the world's high energy physics (HEP) community is interested in future large circular colliders to study the Higgs boson. Because the Higgs mass is low (126 GeV), a circular e+e- collider can serve as a Higgs factory. The Institute of High Energy Physics (IHEP) in Beijing, in collaboration with a number of other institutes, has launched a study of a 50-100 km ring collider [1]. It will serve as an e+e- collider for a Higgs factory with the name of Circular Electron-Positron Collider (CEPC). A Preliminary Conceptual Design Report (Pre-CDR) was published in March, 2015 [2]. The e+e- beams are in the same beam pipe with a pretzel orbit, which is not suitable for a high luminosity Z factory. To solve the problem, a double ring scheme was raised, and the machine circumference was increased to 100 km [3]. The baseline SRF system layout and parameters are chosen to meet the minimum luminosity requirement for each operating energy, and with possible higher luminosity [4].

DAMPING REQUIREMENT

The baseline of the collider is a double-ring with 650 MHz 2-cell cavities shared between the two collider rings [4, 5]. In a storage ring, the beam instabilities in both the longitudinal and transverse directions caused by the RF system are mainly from the cavities themselves. To keep the beam stable, the radiation damping time should be less than the rise time of the multi-bunch instability. The HOMs of the cavities must be damped sufficiently to prevent coupled bunch instabilities and to limit parasitic mode losses. To damp different polarization HOMs, at least two HOM couplers per cavity are needed. The couplers need to damp the HOMs at frequencies from 780 to1471 MHz as shown in Fig. 1.

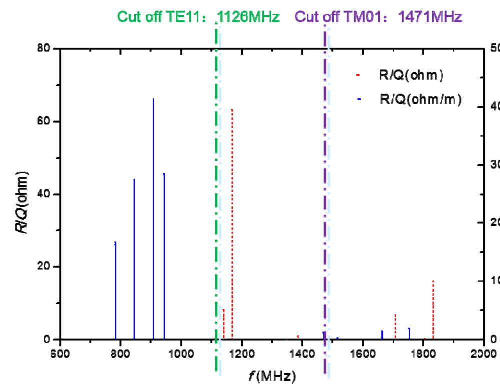

Figure 1: 650 MHz 2-cell cavity mode spectrum and the beam pipe cut-off frequency.

The average power losses can be calculated as single pass excitation. As shown in Fig. 2, HOM power damping of 0.47 kW for each 650 MHz 2-cell cavity is required for the CEPC collider. Resonant excitation should be considered especially for the low frequency modes below cut-off. The cut-off frequency of the waveguide modes for the beam pipe are 1.471 GHz (TM01) and 1.126 GHz (TE11). All the HOM power below the cut-off frequency should be coupled by the HOM coupler which mounted on the beam pipe and the propagating modes will be absorbed by two HOM absorbers at room temperature outside the cryomodule.

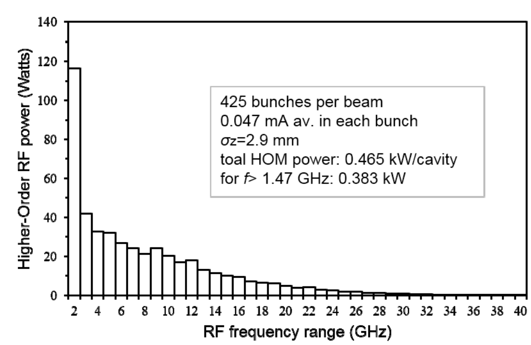

Figure 2: Frequency distribution of HOM power (H design).

HOM COUPLER DESIGN SCHEME

The HOM coupler design must be optimized for the operating frequency (high damping) and the HOM spectrum (low damping) of the cavities. A loop type

* This study was supported by National Key Programme for S&T Research and Development (Grant NO.: 2016YFA0400400).
† E-mail: zhenghj@ihep.ac.cn

Content from this work may be used under the terms of the CC BY 3.0 licence (© 2017). Any distribution of this work must maintain attribution to the author(s), title of the work, publisher, and DOI.

ISBN: 978-3-95450-191-5 doi:10.18429/JACoW-SRF2017-MOPB031

Content from this work may be used under the terms of the CC BY 3.0 licence (© 2017). Any distribution of this work must maintain attribution to the author(s), title of the work, publisher, and DOI.

FABRICATION AND COLD TEST RESULT OF FRIB BETA=0.53 PRE-PRODUCTION CRYOMODULE*

H. Ao†, J. Asciutto, B. Bird, N. Bultman, E. Burkhardt, F. Casagrande, C. Compton, K. Davidson, K. Elliott, A. Ganshyn, I. Grender, W. Hartung, L. Hodges, I. Malloch, S. Miller, D. Morris, P. Ostroumov, J. Popielarski, L. Popielarski, M. Reaume, K. Saito, M. Shuptar, S. Stark, J. Wenstrom, M. Xu, T. Xu, Z. Zheng
Facility for Rare Isotope Beams, Michigan State University, East Lansing, MI 48824, USA
A. Facco, INFN - Laboratori Nazionali di Legnaro, Legnaro (Padova), Italy

Abstract

The Facility for Rare Isotope Beams (FRIB) project fully utilizes superconducting cavities from a low energy: β=0.041 and 0.085 quarter-wave resonators (QWRs) and β=0.29 and 0.53 half-wave resonators (HWRs). Following the QWR, a β=0.53 pre-production cryomodule was assembled and cold tested as the first FRIB HWR cryomodule. The HWR cryomodule includes many different design features compared to the QWR. However, all cavities achieved and locked at the design field of 7.4 MV/m within phase and amplitude specifications. A total dynamic load of 33 W was sufficiently smaller than the specification of 63 W, and no Q_0 degradation was observed. An 8-T superconducting solenoid functioned as designed, and the degaussing procedure worked properly. This successful cold test allows for the start of production of HWR cryomodules for the next step.

INTRODUCTION

FRIB is a new joint project for a nuclear science facility funded by the DOE Office of Science, Michigan State University, and the State of Michigan [1, 2]. The FRIB driver linac accelerates stable ion beams (from protons to uranium) to energies more than 200 MeV/u, and at continuous wave beam power up to 400 kW, requiring full utilization of four types of superconducting cavities after an RFQ [3, 4].

The superconducting cavities consist of 80.5-MHz β=0.041 and 0.085 quarter-wave resonators (QWRs) and 322-MHz β=0.29 and 0.53 half-wave resonators (HWRs). Six different designed cryomodules contain four to eight of these resonators (see Fig. 1 and Table 1).

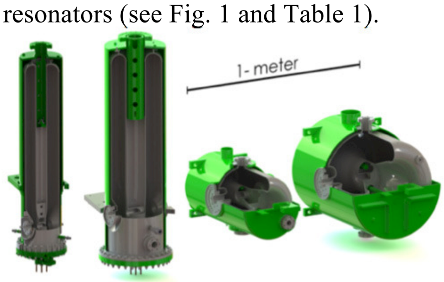

Figure 1: FRIB SRF cavities, from left, β=0.041, 0.085, 0.29, and 0.53.

*Work supported by the U.S. Department of Energy Office of Science under Cooperative Agreement DE-SC0000661
†ao@frib.msu.edu

Assembly of the FRIB cryomodules began with a pre-production QWR (β=0.085) cryomodule in 2015. Completed at the end of 2015, the pre-production QWR cryomodule was cold tested and its performances were validated successfully. Production of QWR cryomodules is in progress [5].

Following the QWR, a β=0.53 pre-production cryomodule was assembled as the first FRIB HWR cryomodule. Since the HWRs make up two-thirds of the FRIB cryomodules, the production of the HWR cryomodules are critical for the project. Compared to the QWR, the HWR cryomodule incudes different design features (e.g. RF couplers, pneumatic frequency tuners, magnetic shields, etc.). Due to these different features, a cold test of the HWR cryomodule is a significant milestone to validate the FRIB HWR cryomodule design.

This paper will review and discuss the assembly of the β=0.53 pre-production cryomodule and mainly the cold test results.

Table 1: FRIB Cryomodules and Configuration

Type	Quantity		
	Cryomodule	Resonator	Solenoid
β=0.041	3	12	6
β=0.085	11	88	33
β=0.29	12	72	12
β=0.53	18	144	18
β=0.085M*	1	4	0
β=0.53M*	1	4	0
Total	46	324	69

*Matching module

CRYOMODULE ASSEMBLY

Figure 2 shows the assembly sequence of the β=0.53 pre-production cryomodule. In the beginning, a cold mass and a baseplate are prepared as subassemblies (see from C1 to C3 in Fig. 2), then the cold mass is lifted onto the baseplate in the mid-sequence.

All beam line elements, resonators, solenoids, RF couplers, and beam line bellows, are assembled as the cold mass in an ISO 5 (class 100) clean room. All resonators are vertical tested and certified in advance of the clean room assembly, in addition to RF coupler conditioning.

ISBN: 978-3-95450-191-5 doi:10.18429/JACoW-SRF2017-MOPB034

SELECTION OF THE TYPE OF ACCELERATING STRUCTURES FOR THE SECOND GROUP OF CAVITY SC LINAC NUCLOTRON-NICA

M.A. Gusarova[1], D.V. Surkov, K.V.Taletskiy, A.A. Gorchakov, M.V.Lalayan, National Research Nuclear University – MEPhI, Moscow, Russia
D.A. Shparla, Physical-Technical Institute, National Academy of Sciences of Belarus, Minsk, Belarus
A.V. Butenko, G.V. Trubnikov, O.A. Sidorin, Joint Institute for Nuclear Research, Dubna, Russia
[1]also at National Research Center (Kurchatov Institute) - ITEP, Moscow, Russia

Abstract

The paper summarises the research results aimed on the choice of superconducting accelerating cavities for the second section of the SC linac Nuclotron-NICA injector project. This choice was based on comparative analysis of accelerating structures electrodynamic characteristics taking into account technological challenges of bulk niobium cavities production.

INTRODUCTION

The collaboration of JINR, NRNU MEPhI, INP BSU, PTI NASB, BSUIR and SPMRC NASB started in 2015 the project of SC linac-injector design. The possibility of LU-20 replacement by the new superconducting (SC) linac of 30 MeV energy for protons and ≥7.5 MeV/nucleon for deuterium beam is discussed now [1-4]. The development of the SRF technologies is the key task of new Russian - Belarusian collaboration.

The New Injector Linac for Nuclotron-Nica is the proposed replacement for LU-20 accelerator. This linac SC part general layout is showed on Fig. 1 [5]. Quarter-wave resonators (QWR) will be used for the first group of the cold part of the accelerator [6].

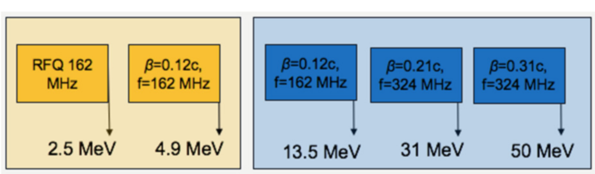

Figure 1: Proposed NICA injector layout of normal (left) and superconducting (right) structures.

According to the concept of the SC Linac Nuclotron-NICA [5] the second group of cold cavity resonators operates on 324 MHz, has phase velocity 0.21 and 7.7 MV/m accelerating gradient. Modern designs of CH, Spoke and HWR cavities allow one to reach this accelerating gradient. However, it is necessary to take into account the production possibilities and the lack of experience in superconducting accelerating resonators manufacturing. These factors are important for successful performance of the project.

At the frequency and phase velocity mentioned above CH, Spoke or Half-wave (HWR) resonators can be used. Table 1 presents the main advantages and disadvantages of these structures [7-10].

Table 1: Advantage and Disadvantage Different Types of Accelerating Structures for Medium β

cavity type, frequency and velocity range	Advantages	Disadvantages
HWR 80…500 MHz $0.1 \le \beta \le 0.5$	No dipole steering; High performance; Lower surface electric field; Wide β range	Not easy access; Difficult to tune than QWR
Spoke 325…805 MHz $0.15 \le \beta \le 0.6$	No dipole steering; High performance; Lower R_{sh} than HWRs; Wide β range	Not easy access; Difficult to tune than QWR; Larger size the HWRs; More expensive than HWRs; Quadrupole steering
CH above 170 MHz $0.07 \le \beta \le 0.45$,	Possibility of coupled structure at low β; Higher RF efficiency for $\beta \le 0.2$	Very long lens-free section for $\beta \ge 0.25$

At the stage of QWR prototypes production technological problems of manufacturing processes will be solved and the final decision on the type of accelerating structure for the second cold part cavity group will be made. Different structures of CH, Spoke and HWR type cavities were considered and simulated.

CH-TYPE CAVITY

Five-gap CH cavity is considered as one of the possible candidates. Figure 2 shows this cavity design studied. Dimensions and RF parameters of the structure are presented

---
* This project is supported in part by the FAIR-Russia Research Center

Content from this work may be used under the terms of the CC BY 3.0 licence (© 2017). Any distribution of this work must maintain attribution to the author(s), title of the work, publisher, and DOI.

ISBN: 978-3-95450-191-5 doi:10.18429/JACoW-SRF2017-MOPB035

Content from this work may be used under the terms of the CC BY 3.0 licence (© 2017). Any distribution of this work must maintain attribution to the author(s), title of the work, publisher, and DOI.

CRYOGENIC PROBE STATION AT OLD DOMINION UNIVERSITY CENTER FOR ACCELERATOR SCIENCE*

J. Makita†, J. R. Delayen, A. Gurevich, Old Dominion University, Norfolk, USA
G. Ciovati, Thomas Jefferson National Accelerator Facility, Newport News, USA

Abstract

With a growing effort in research and development of an alternative material to bulk Nb for a superconducting radiofrequency (SRF) cavity, it is important to have a cost effective method to benchmark new materials of choice. At Old Dominion University's Center for Accelerator Science, a cryogenic probe station (CPS) will be used to measure the response of superconductor samples under RF fields. The setup consists of a closed-cycle refrigerator for cooling a sample wafer to the cryogenic temperature, a superconducting magnet providing a field parallel to the sample, and DC probes in addition to RF probes. The RF probes will extract a quality factor from a sample patterned in a coplanar waveguide resonator structure on a 2in wafer. From the measured quality factor, the surface resistance and the penetration depth as a function of temperature and magnetic field will be calculated. This paper will discuss the design and measurement procedures of the current CPS setup.

INTRODUCTION

Over the decades of developmental efforts, there have been reported instances of Nb cavities operating at their theoretical limits. In order to meet the increasing demands of future accelerator performance and cost requirements, significant efforts have been made into research and development of new materials alternative to a bulk Nb. Some of the new innovations include nitrogen doped and infused niobium cavities [1–3], multi-layer coatings consisting of thin dielectric layers sandwiched between superconducting layers [4], a thin film niobium over copper [5], and cavities made with other materials such as MgB_2 and Nb_3Sn [6, 7].

This paper will discuss a closed-cycle cryogenic probe station at Old Dominion University that will be used as part of an R&D effort for benchmarking such new SRF materials. A sample will be fabricated into a planar transmission line resonator, and the CPS will be used to extract superconducting surface resistance and penetration depth under an RF field with varying DC parallel magnetic field. The obtained information would give insight into how the SRF cavities would perform using those new materials.

EXPERIMENTAL SETUP

Sample

A sample that will be prepared for the measurements are a series of superconducting half-wavelength coplanar waveguide (CPW) resonators designed on top of a dielectric substrate as shown in Fig 1. Because it is only necessary to deposit the superconducting film on one side of the substrate, the CPW structure provides an affordable method for a sample fabrication compared to other transmission line structures which requires a ground plane and a conducting strip on both sides of the substrate. The CPW resonators are patterned by photolithography after a film is deposited onto a dielectric substrate. A single 2in wafer can contain multiple resonators given that they are spread enough so that any cross coupling of power between adjacent resonators is negligible.

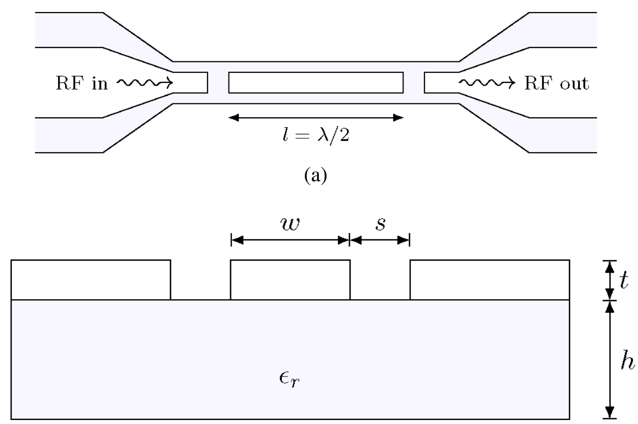

(a)

(b)

Figure 1: (a) A schematic diagram showing the top view of half-wave CPW resonator capacitively coupled to the RF input and output and (b) the side view with the center conductor width w, gap s, and a substrate with a dielectric constant ϵ_r and thickness h.

The design of the CPW resonator is chosen to achieve desirable resonant frequencies and also to minimize losses. Main components of the CPW resonator consist of a center conductor, ground planes separated by a gap S, coupling capacitors and contact pads where the RF probes make contacts. The ratio between the center conductor width W and the gap S are determined such that the characteristic impedance of the transmission line is approximately 50 Ω for maximum power transfer. A first sample that will be measured here will contain Nb resonators with two different center width: W = 10 µm and 15 µm and the gaps S = 6.15 µm and 8.77 µm in order to experiment with different geometric factors. The thickness of the film will be 200 nm or approximately five times the penetration depth λ. The lengths of the straight resonators are l = 17 mm, 20 mm, and 24 mm corresponding to the resonant frequencies of 2.5 GHz, 3.0 GHz, and 3.5 GHz respectively. Due to the space limitation, the lowest frequency achievable using a straight resonator is 2.5 GHz;

* Work supported by NSF Award PHY-1416051
† jmaki002@odu.edu

ISBN: 978-3-95450-191-5 doi:10.18429/JACoW-SRF2017-MOPB036

THE STUDY OF DEPOSITION METHOD OF Nb_3Sn FILM ON Cu SUBSTRATE*

Li Xiao†, Xiangyang Lu, Datao Xie, Weiwei Tan, Ziqin Yang, Jifei Zhao, Deyu Yang, Yujia Yang, Peking University, Beijing, China

Abstract

Our work is mainly focused on the fabrication methods of Nb_3Sn films on Cu substrates and film's properties. There are diffraction peaks of Nb_3Sn in the X-ray diffraction patterns in which without diffraction peaks of copper compounds. Scanning electron microstructures of Nb_3Sn film reflect its nice compactness and binding force between film and substrate.

INTRODUCTION

Niobium is extremely useful in superconducting radiofrequency (SRF) cavities because of its properties, so that it is by far the material of choice for modern SRF accelerators, but now cavities are being produced that reach close to the fundamental limits of this material. To continue to increase the reach of particle accelerators for frontier scientific research and to open new industrial applications for accelerators, researchers are examining the potential of alternatives to niobium with superior SRF properties [1].

An overview of the different materials being considered for SRF applications is given in [2], but one especially promising material is Nb_3Sn. It offers both a large critical temperature (Tc as high as 18 K) and large predicted H_{sh}, both of which are approximately twice those of niobium [3,4] And to avoid that the poor thermal conductivity of Nb_3Sn causes the cavity to quench, we choose Oxygen-free cooper substrate which has higher thermal conductivity. At the same time, the cost of copper is lower.

So it is significant in the SRF accelerator filed to deposit Nb_3Sn film on Cu substrate. Programs to produce Nb_3Sn coatings by methods have made continuing progress throughout the current decade, such as multilayer sputtering, vapor diffusion, chemical vapor deposition, liquid tin dipping, mechanical plating, electron beam co-evaporation, bronze processing, and electrodeposition [5-15]. Compared with all the other deposition methods of Nb_3Sn films, multilayer sputtering can increase the diffusion efficiency of the atoms in the process of annealing so it is easy to form Nb_3Sn film.

EXPERIMENT

Magnetron sputtering method and vacuum annealing technology were used to deposit the Nb-Sn multi-layer on copper substrate in this paper. After that, we analyze the thin films by such as X-ray diffraction (XRD) and high resolution field emission scanning electron microscopy (SEM), and continuously explore the preparation process and conditions of Nb_3Sn film based on copper substrate.

* This work has been supported by Major Research Plan of National Natural Science Foundation of China (No. 91026001) and National Major Scientific Instrument and Equipment Development projects (2011YQ130018).
† email address: 1601110262@pku.edu.cn

Films Preparation and Heat Treatment

At first, we deal with the copper substrate to get Smooth and clean surface. We polish copper substrate with 1200#,2000#,3000# sandpaper and abradant. After ultrasonic cleaning for more than three times, we wiped it with anhydrous ethanol and dry it by nitrogen, then installed it on the substrate holder in vacuum chamber of DC Magnetron sputtering device.

DC Magnetron sputtering device like Fig. 1 was used to deposit precursor film which included niobium and tin. The targets of Nb and Sn are detached, they take turns to deposit the film.

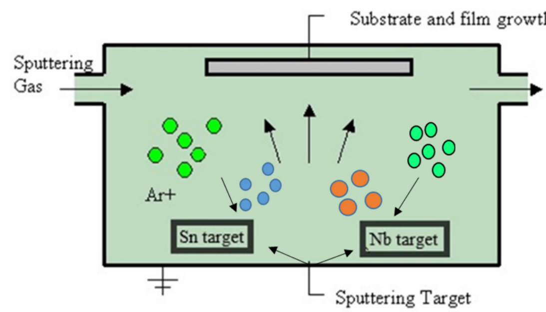

Figure 1: Schematic diagram of the principle of magnetron sputtering.

The base pressure of the chamber is 5×10^{-4} Pa. The working air pressure maintains at 0.5 Pa. The parameters of coating procedure are listed in Table 1. In order to avoid the reaction between copper and tin, and importing unnecessary impurities, we decide to deposit Nb on the copper substrate at first as the isolating layer [16]. After 6 minutes, Nb and Sn take turn to deposit on the substrate to get multilayer. in the end, we deposit Nb as the outermost shell of the precursor to prevent the loss of Sn during annealing.

Table 1: The Parameters of Coating Procedure

Project		electric current /A	voltage /V	Deposit time /min
Nb isolating layer		1	310	6
multi-layer	Sn	0.11	295	60
	Nb	1	307	60
Nb cover film		1	306	6

Then the precursor was put in the vacuum tube furnace whose air pressure is 1×10^{-4}Pa, The annealing curve is given in Fig. 2. The terraced heating and heat preservation

Content from this work may be used under the terms of the CC BY 3.0 licence (© 2017). Any distribution of this work must maintain attribution to the author(s), title of the work, publisher, and DOI.

ISBN: 978-3-95450-191-5 doi:10.18429/JACoW-SRF2017-MOPB037

PROGRESS OF THE 2x4-CELL SUPERCONDUCTING ACCELERATOR FOR THE CAEP THz-FEL FACILITY*

K. Zhou, X. Luo†, C. L. Lao, L. J. Shan, T. H. He
X. M. Shen, L. D. Yang, H. B. Wang, X. F. Yang, M. Li
Institution of Applied Electronics, CAEP, Mianyang, China
X. Y. Lu Peking University, Beijing, China

Abstract

The high average power THz radiation facility is now under construction in China Academy of Engineering Physics. The superconducting accelerator is one of the most important components for this facility, including two 4-Cell TESLA superconducting radio frequency cavities. The designed effective field gradients for both cavities are 10-12 MV/m. This paper will present the progress of the 2x4-cell superconducting accelerator, mainly including its construction and cryogenic test in Chengdu. At 2 K state, the cryomodule works smoothly and stably. The effective field gradients of both cavities have achieved 10 MV/m. Further beam loading experiments are now in progress.

INTRODUCTION

At present, China Academy of Engineering Physics (CAEP) is developing a THz radiation facility (THz-FEL) with Peking university and Tsinghua university. This is the first high average power THz user facility based on superconducting radio frequency (SRF) technology in China [1]. The THz-FEL facility consists of a high-brilliance electron gun, a superconducting accelerator, a high-performance undulator and so on, as shown in Fig. 1. The designed frequency of the THz radiation is 1-3 THz with the average output power beyond 10 W. Correspondingly, the electron energy after acceleration is 6-8 MeV and the effective field gradient should be 10-12 MV/m.

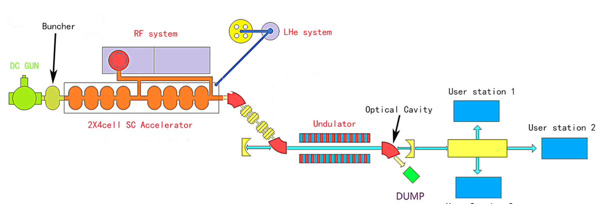

Figure 1: General layout of the CAEP FEL-THz facility.

The superconducting accelerator is one of the most important components for this facility, which contains the following subsystems: a cryostat, double 4-cell TESLA SRF cavities, double tuners, double main couplers and some auxiliary systems, including the microwave system, the cryogenic system and the low level RF control system, as shown in Fig. 2. The design and fabrication of these subsystems have been finished [2]. This paper presents the construction and cryogenic test of the 2x4-cell superconducting accelerator.

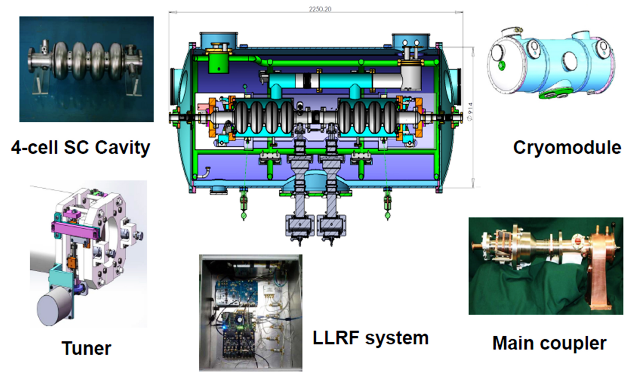

Figure 2: The cross-section and components of the superconducting accelerator [2].

CONSTRUCTION

The operation of the superconducting accelerator asks for extremely strict conditions: free of contamination, high vacuum, cryogenic temperature and low magnetic field. So, the assembly process is especially important for the superconducting accelerator to achieve good performances. The first step is the conditioning of the main couplers, which is operated in Chengdu. The microwave power from an induced output tube (IOT) has run up to about 25 kW in both pulse mode and CW mode.

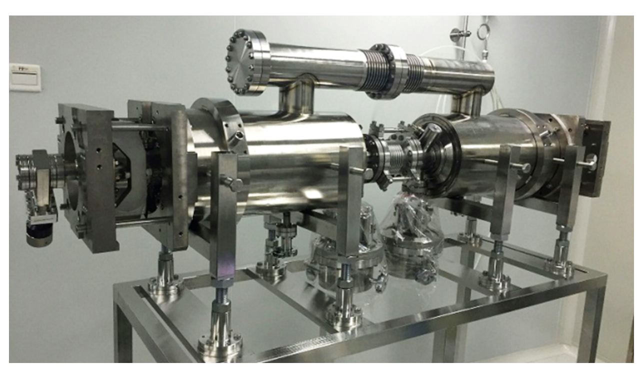

Figure 3: The axis part of the SC accelerator after assembly.

Since there is no 100-class clean room in our laboratory temporarily, we did the axis part assembling at Peking University after the conditioning of the main couplers. The cold

* Work supported by China National Key Scientific Instrument and Equipment Development Project (2011YQ130018), National Natural Science Foundation of China with grant (11475159, 11505173, 11576254 and 11605190).
† Email address: luox8688@163.com

Content from this work may be used under the terms of the CC BY 3.0 licence (© 2017). Any distribution of this work must maintain attribution to the author(s), title of the work, publisher, and DOI.

ISBN: 978-3-95450-191-5 doi:10.18429/JACoW-SRF2017-MOPB040

ESS HIGH-BETA CAVITY TEST PREPARATIONS AT DARESBURY LABORATORY

P.A. Smith†, L. Bizel-Bizellot, K. Dumbell, M. Ellis, P.Goudket, A.J. Moss, E. F. Palade, S. Pattalwar, M. Pendleton, and A. E. Wheelhouse, STFC, Daresbury, UK

Abstract

Science and Technology Facility Council (STFC) is responsible for supplying, and testing 88 high-beta elliptical SRF cavities, as part of the UK In Kind Contribution (IKC) to the European Spallation Source (ESS). The high-beta=0.86, cavities have been designed by CEA- Saclay and are a five cell Niobium cavity operating at 704.42 MHz. They are required to provide an accelerating gradient of 19.9 MV/m at an unloaded Q of $5x10^9$. Preparations are underway to upgrade the cryogenic and RF facilities at Daresbury laboratory prior to the arrival of the first cavities. As part of these arrangements, a niobium coaxial resonator has been manufactured, to validate the test facility. The design considerations, for the coaxial resonator are presented, along with preliminary results. The RF measurement system to perform the cavity conditioning and testing is also presented.

INTRODUCTION

As part of the UK IKC to the ESS project [1], STFC are undertaking the procurement, qualification, testing, and delivery to CEA Saclay. The latter, for the cryomodule integration of 88 high-beta dressed cavities. These cavities are five cell superconducting Niobium cavities operating at 704.42 MHz and with a beta of 0.86 (see Fig. 1). The desired operating gradient in the ESS linac is 19.9 MV/m with an unloaded Q of $5x10^9$. For qualification testing purposes the target gradient is 22.9 MV/m.

Figure 1: High beta 704.42 MHz undressed cavity.

The technical requirements for the high beta cavity are displayed in Table 1. As part of the programme STFC will undertake the procurement of fine-grain niobium material and the fabrication of SRF dressed cavities through recognised specialist manufacturers, to ensure that timescales can be met, and the quality is maintained. The qualification testing of the cavities is to be performed at Daresbury laboratory.

† Paul.a.smith@stfc.ac.uk

Table 1: Requirements on High-beta Cavities

Requirement	High-beta
Frequency (MHz)	704.42
Beta	0.86
E_{acc} (MV/m)	19.9
E_{pk} (MV/m)	45
B_{pk}/E_{acc} (mT MV/m)	4.3
E_{pk}/E_{acc}	2.2
Iris diameter (mm)	120
RF peak power (kW)	1100
G/Omega	241
Maximum R/Q (Ohms)	477
Q_{ext}	$7.6x10^5$
Minimum Q_u	$5x10^9$

To meet the demands for the qualification of the cavities, the RF and cryogenic facilities at Daresbury STFC are being upgraded to facilitate the measurement of the ESS high-beta cavities. This includes: new helium liquefaction and recovery systems; new digital Low Level RF (LLRF) systems, new RF racking and instrumentation; shielding, clean room, and High Pressure Rinse (HPR) facility. Further information about the cryogenic and liquefaction facilities can be found in [2], in these proceedings. Therefore this work will concentrate on the RF systems such as the RF measurement system, the LLRF and also several coaxial resonators used to test and validate the systems. The test system has been designed so that three cavities can be tested separately during a single cooldown. Later it will be seen that this has implications for the test system as a high power switching network is required to switch power between cavities.

Low Level RF (LLRF)

An FPGA system has been developed in-house; based on a Self-Excited Loop (SEL) algorithm, see Fig. 2. This is essential, since with a Q of approximately $5x10^9$, the standard 3dB bandwidth in transmission is on the order of 0.1 Hz. In order to test and verify the digital LLRF, at room temperature, a simple compact resonator was required to provide reliable validation. The ESS cavities are ellipsoidal with an outer diameter of approximately 400mm. Even a single cell cavity of this type would be expensive to manufacture, as well as quite bulky, so instead, compact coaxial resonators were designed, that operated around 704 MHz. These had an outer diameter of approximately 50mm and an ID of 14mm. They were supported in the middle by a disc of PTFE, where the electric field is a minimum.

Content from this work may be used under the terms of the CC BY 3.0 licence (© 2017). Any distribution of this work must maintain attribution to the author(s), title of the work, publisher, and DOI.

ISBN: 978-3-95450-191-5 doi:10.18429/JACoW-SRF2017-MOPB041

STATUS OF THE SOLEIL SUPERCONDUCTING RF SYSTEM

M. Diop, J.P. Baete, R. Cuoq, H. Dias, J. Labelle, R. Lopes, M. Louvet, C. Monnot, P. Marchand, S. Petit, F. Ribeiro, T. Ruan, R. Sreedharan, K. Tavakoli
Synchrotron SOLEIL, Gif-Sur-Yvette, France

Abstract

The 352 MHz SOLEIL SRF system consists in two cryomodules, each containing a pair of SC Nb/Cu cavities, cooled with LHe at 4K from a single 350 W cryoge-nic plant. In order to store 500 mA, a power of 575 kW and an accelerating voltage of 3-4 MV are required. The RF power is provided by 4 SSPA's, each delivering up to 180 kW. The original cavity input power couplers, which are LEP-type antennas, designed to handle up to 200 kW, were replaced by upgraded versions, able to transmit up to 300 kW CW. This opens the possibility to operate at full beam current with only one active cryomodule. The SRF system operational experience over the past ten years as well as the different upgrades are reported here.

INTRODUCTION

In the SOLEIL storage ring (SR), two cryomodules (CM's) provide the 352 MHz voltage of 3 - 4 MV and power of 575 kW, required at the nominal energy of 2.75 GeV with the full beam current of 500 mA and all the insertion devices. As shown in Figures 1 and 2, each CM contains two 352 MHz SC single-cell cavities, made of copper with niobium coating and cooled with liquid helium (LHe) at 4.5 K. Each cavity has its own frequency tuning, a mechanism driven by a stepping motor, which changes the cavity length. The HOM impedances are strongly damped thanks to four couplers of coaxial type, terminated with a loop (two for the monopole modes, two for the dipole modes) and located on the central tube that connects the two cavities. On the central tube, stand also the input power couplers (IPC's), CERN-LEP2 type antennas, which can transmit up to 200 kW CW. Recent R&D's led us to implement a new version, able to handle up to 300 kW CW.

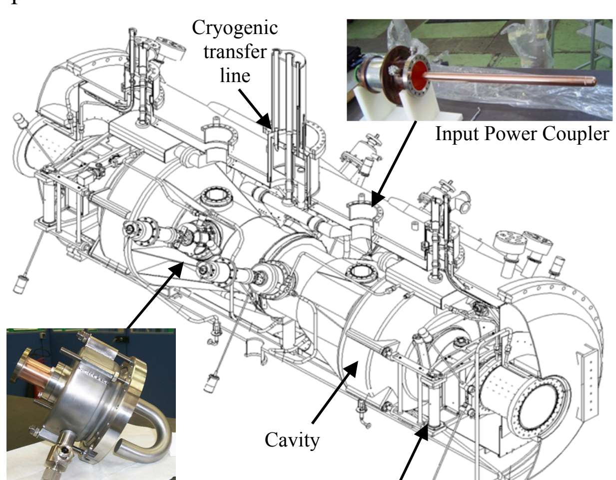

Figure 1: 3D-layout of the SOLEIL cryomodule.

Each of the four SR cavities is powered by a 180 kW SSPA, developed in house [1], which is a combination of four 45 kW towers; the tower itself consists in a combina-tion of 180 amplifier modules of 300 W with LDMOS transistors and integrated circulators.

A single cryogenic plant supplies both CM's in LHe and LN_2. It is based on a HELIAL 2000 unit from Air Liquide, operated in a dual liquefier/refrigerator mode [2].

One fully analogue low level RF system is dedicated to each cavity [3]. It comprises three relatively slow loops, which control the cavity resonant frequency and its acce-lerating field in amplitude and phase; besides a fast direct RF feedback copes with the Robinson instability at high current. This system can ensure a cavity voltage stability of ± 0.1% in amplitude and 0.03 degree in phase.

More detailed descriptions of the equipment, as well as reporting about the commissioning and phase 1 operation using a single CM can be found in references [4, 5].

Figure 2: CM1 in the SR.

OPERATIONAL EXPERIENCE AND UPGRADES

CM Frequency Tuner Issues and Cures

The SOLEIL SR RF system is in operation since 2006. Considering the difficulties encountered on the Super-3HC cavities at ELETTRA with a similar tuning system, which happened to get stuck after roughly fifty millions of motor steps [6], we were early aware of possible issues and therefore we came to operate at constant tuning and variable voltage during the injections [5]. Nevertheless, difficulties started after about two years of operation from repetitive jamming of the tuning mechanism. Fortunately, the impact on the user runs remained quite marginal.

Each cavity has its own tuner, aimed at changing its length. It consists in a double lever and a screw-nut as-sembly, driven by a stepper motor with a gear box. It is fully housed inside the CM, where it works under vacuum

Content from this work may be used under the terms of the CC BY 3.0 licence (© 2017). Any distribution of this work must maintain attribution to the author(s), title of the work, publisher, and DOI.

ISBN: 978-3-95450-191-5 doi:10.18429/JACoW-SRF2017-MOPB042

THE TRIUMF/VECC INJECTOR CRYOMODULE PERFORMANCE

Yanyun Ma†, K. Fong, T. Junginger, D. Kishi, A. Koveshnikov, R.E. Laxdal, N. Muller, R. Nagimov, D.W. Storey, E. Thoeng, Z.Y. Yao, V. Zvyagintsev,
TRIUMF, Vancouver, Canada

U. Bhunia, A. Chakrabarti, S. Dechoudhury, V. Naik, VECC, Kolkata, India

Abstract

The collaboration on superconducting electron Linac for rare ion beam facilities ARIEL (Advanced Rare IsotopE Laboratory) [1-4] and ANURIB [5] (Advanced National facility for Unstable and Rare Isotope Beams) has resulted in production of a superconducting Injector Cryomodule (VECC ICM) at TRIUMF for VECC. The cryomodule design utilizes a unique box cryomodule with a top-loading cold mass. The hermetic unit consists of a niobium cavity which operating at 1.3GHz and connected with two symmetrically opposed couplers which can deliver 100kW RF power to the beam. Liquid helium supplied at 4.4 K is converted to superfluid helium-II through a cryogenic insert on board which includes 4 K phase separator, 4K/2K heat exchanger and Joule-Thompson valve. In 2016, the VECC ICM has been tested at TRIUMF and demonstrated 10.5 MeV acceleration. A summary of the VECC ICM commissioning are presented.

INTRODUCTION

TRIUMF and VECC are developing high intensity electron linac driver to produce RIBs through photo-fission. Final design goals are 50MeV and 10mA/3mA at TRIUMF/VECC respectively [1, 5]. TRIUMF and VECC jointly designed the ICM (termed EINJ in ARIEL). Two injector cryomodules have been fabricated and beam tested at TRIUMF.

A first phase of ARIEL consisting of an ICM, and an accelerating cryomodule with just one accelerating cavity on board plus a `dummy' cavity that occupies the second cavity space in the cryomodule (ACMuno) was installed for initial technical and beam tests up to 23 MeV in 2014 [6]. A completed ACM with two cavities has been installed and is under testing to meet the operational goal of 3mA at 30MeV for first science application from ARIEL ISOL targets (Fig. 1) [3,4]. The 2nd ICM as part of a collaborative agreement with the ANURIB project at VECC [4] has been swapped with the 1st ICM and tested during ACM cryomodule offline. The 2nd phase of ARIEL will add ACM2 module and a ramp up in beam intensity to the full 50 MeV, 0.5 MW capability.

† mayanyun@triumf.ca

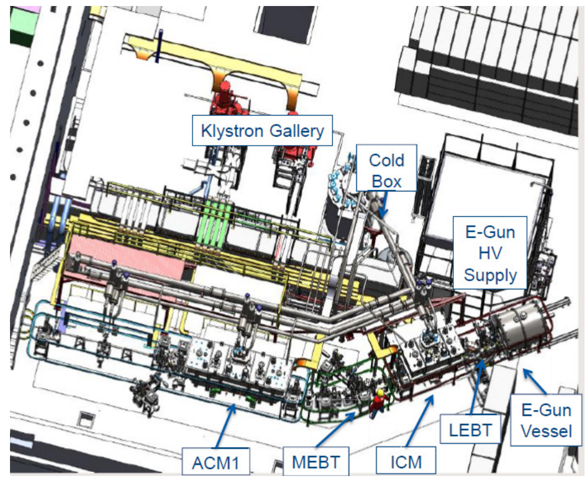

Figure 1: e-Linac layout at TRIUMF.

CRYOMODULE DESIGN

The injector cryomodule design [2], shown in Fig. 2, borrows significantly from the ISAC-II cryomodules.

In brief the module is a top-loading box-like structure with a stainless steel vacuum chamber. The cold mass is suspended from the lid and includes a stainless steel strongback, a 2 K phase separator, cavity support posts and the cavity hermetic unit. The hermetic unit consists of a niobium cavity, the end assemblies, an inter-cavity transition (ICT) with a stainless steel HOM damper, the fundamental power couplers (FPC) and an RF pick-up. The end assemblies include the warm-cold transition (WCT), HOM damping tubes and beam-line isolation valves.

A scissor jack tuner is attached to cavity's LHe jacket. The custom warm drive system utilizing a servo motor and a resolver placed on top of the cryomodule at atmosphere. The cold mass is surrounded by LN2 cooled thermal isolation box. There are two layers of mu metal, a warm layer just inside the vacuum box and a cold layer surrounding the cavity. A Wire Position Monitor (WPM) alignment monitoring system is installed with the hermetic unit.

In order to be self-reliant to convert 4 K atmospheric LHe into 2 K He-II, the box cryomodule design has sufficient head room that makes possible the addition of a dedicated 4 K/2 K cryo-insert on each module [7].

Content from this work may be used under the terms of the CC BY 3.0 licence (© 2017). Any distribution of this work must maintain attribution to the author(s), title of the work, publisher, and DOI.

ISBN: 978-3-95450-191-5 doi:10.18429/JACoW-SRF2017-MOPB043

Content from this work may be used under the terms of the CC BY 3.0 licence (© 2017). Any distribution of this work must maintain attribution to the author(s), title of the work, publisher, and DOI.

PANSOPHY, A JLAB SRF ENGINEERING DATA MANAGEMENT SYSTEM, SUPPORTING DATA COLLECTION, RETRIEVAL AND ANALYSIS UTILIZED BY LCLS-II

V. Bookwalter, M. Dickey, A. McEwen, M. Salvador
Thomas Jefferson National Accelerator Facility, Newport News, VA USA

Abstract

Pansophy is an engineering data management system composed of a collection of technologies that together provide a comprehensive solution for managing information in the production and testing of cavities and cryomodules. It is especially suited to support the Data & Quality Management Systems for large projects, including LCLS-II and the Jefferson Lab (JLab) 12 GEV upgrade, in addition to ongoing CEBAF Upgrade projects. With the extensive amounts of data collected for an individual project, data retrieval to facilitate feedback and enhancement of production and processing activities is a high priority. The priority shares importance with the needs of managing the project, including production status, Non-Conformance Reports (NCR), and Quality Management reports. Pansophy was introduced and first utilized in 2002. Since then, many enhancements have taken place. More recently, the focus has shifted to Data and Quality Management reports and statistical analysis. Such enhancements include a database driven menu system, extended MSWord macro pre-processing of travelers, and an extensive reporting system. The reporting system allows managers and group leaders to respond quickly to the needs of the project in areas of cavity and cryomodule production, data collection, NCR, Quality Management and schedule. Extensions include integration with the inventory system, allowing traceability from the receiving of manufactured parts to the final cryomodule product.

BACKGROUND

Pansophy was first introduced in 2002 as a system for the collection of production and test data of cryomodules for Jefferson Lab. The first large scale project that utilized Pansophy was the Spallation Neutron Source (SNS) at Oak Ridge National Laboratory in 2004, with the initial focus being on travelers and the collection of data. Since then, the focus has turned to quality management and data mining and analysis (Figure 1).

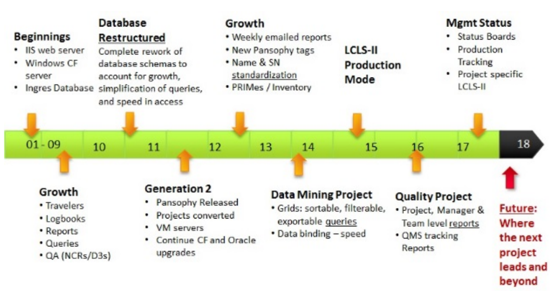

Figure 1: Pansophy Timeline.

Pansophy is a web-based engineering data management system (EDMS). The initial concept was to create a series of programs that would collect data produced during the manufacturing and testing of cavities and cryomodules. This includes such parameters as serial numbers, measurements, alignment, leak tests, cavity and cryomodule performance measurements and date of assembly. The system is a custom integration of several commercial software utilities, including DocuShare™, ColdFusion™, Oracle™, as well as, some common desktop programs, such as MSWord™ and MSExcel™. Users range from process managers, shop-floor technicians, and test engineers to after-the-fact data miners. Important quality assurance elements include procedural control, automated data accumulation into a secured central database, prompt and reliable data query and retrieval, and online analysis tools, all accessed by users via their platform-independent web browsers.[1]

The basic vehicle used for data collection in Pansophy is the traveler. Travelers are used to define and control a process and to gather data particular to the fabrication, assembly, or performance verification of components and completed cryomodules. Travelers are version controlled and tie directly to procedures, safety documents and drawings to give the user a complete picture and data set of the process of manufacturing and testing.

WHY EDMS?

During the production and testing of a cryomodule, over 13000 data points are collected. Multiply that by the 18 cryomodules as in the LCLS-II project and the data becomes unmanageable, especially if collected in spreadsheet format. To manipulate and analyse data across cryomodules within a project or to compare between projects would be impossible without additional functionality. Therefore, collecting data systematically into an online database with a cohesive user interface becomes a necessity for today's production environment (Figure 2).

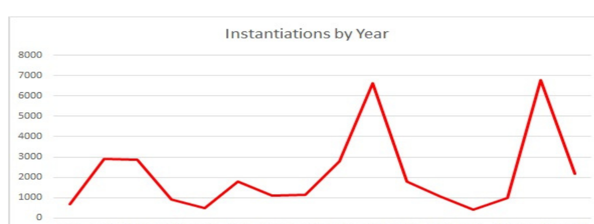

Figure 2: Number of Travelers by Year.

* Authored by Jefferson Science Associates, LLC under U.S. DOE Contract No. DE-AC05-06OR23177.

ISBN: 978-3-95450-191-5 doi:10.18429/JACoW-SRF2017-MOPB044

MAGNETIC HYGIENE CONTROL ON LCLS-II CRYOMODULES FABRICATED AT JLAB*

G. Cheng†, E. Daly, K. Davis, J. Fischer, N. Huque, B. Legg, H. Park, K. M. Wilson, L. Zhao,
Thomas Jefferson National Accelerator Facility, Newport News, U.S.A.

Abstract

Jefferson Lab (JLab) is in collaboration with Fermi National Accelerator Laboratory (Fermilab) to build 18 cryomodules to install at the SLAC National Accelerator Laboratory's tunnel as part of the Linac Coherent Light Source upgrade project (LCLS-II). Each LCLS-II cryomodule hosts 8 superconducting niobium cavities that adopt the nitrogen doping technique, which aims to enhance the cavity quality factor Qo to reduce the consumption of liquid helium used to cool down the cavities. It is known that the Qo of niobium cavities is affected by cavity surface magnetic field. Traditionally, magnetic shields made of high magnetic permeability mu-metals are employed as a passive shielding of the ambient magnetic fluxes. During the LCLS-II cryomodule development, magnetic hygiene control that includes magnetic shielding and demagnetization of parts and the whole-machine is implemented. JLab and Fermilab worked closely on developing magnetic hygiene control procedures, identifying relevant tools, investigating causes of magnetization, magnetic field monitoring, etc. This paper focuses on JLab's experiences with LCLS-II cryomodule magnetic hygiene control during its fabrication.

INTRODUCTION

The LCLS-II project adopts nitrogen-doped superconducting niobium cavities [1-2] for its potential to yield high Q_o, hence less heat load into the refrigeration system. Research has shown [2] that the doped cavities are more sensitive to surface magnetic field which causes surface resistance increase, compared to non-doped cavities. Hence, magnetic hygiene [3] control becomes necessary to preserve the high Q_o offered by doped cavities.

The LCLS-II specification [4-6] for the ambient magnetic field at cavity surface is < 5 milligauss (mG) or 0.5 µT. Fermi Lab and JLab are tasked to build thirty-five1.3 GHz cryomodules (CMs). An increase in the number of modules to build is in planning. The two labs collaborate on magnetic hygiene control by implementing the same or equivalent procedures. Fermi's magnetic hygiene management has been summarized in the past [7]. This paper introduces JLab's practical experiences on implementing magnetic hygiene control.

MAGNETIC SHIELDING

LCLS-II cryomodule's vacuum vessels (VV) are made of ASTM A516 Grade 60 carbon steel that has the capability to attenuate geomagnetic field if the vessel is demagnetized [8-9]. JLab performs demagnetization on all LCLS-II VVs by use of a demagnetization system developed by Fermi Lab for LCLS-II. Figure 1 shows a typical attenuation from a demagnetized LCLS-II VV for a production CM. It is seen that in the majority of the VV's length, the magnetic field is lower than 50 mG. The production CM's VVs are heat treated at 500 °C at the factory after welding and machining. The VV for prototype CMs (pCM) are not heat treated. JLab LCLS-II pCM VV after demagnetization shows higher than 50 mG magnetic field.

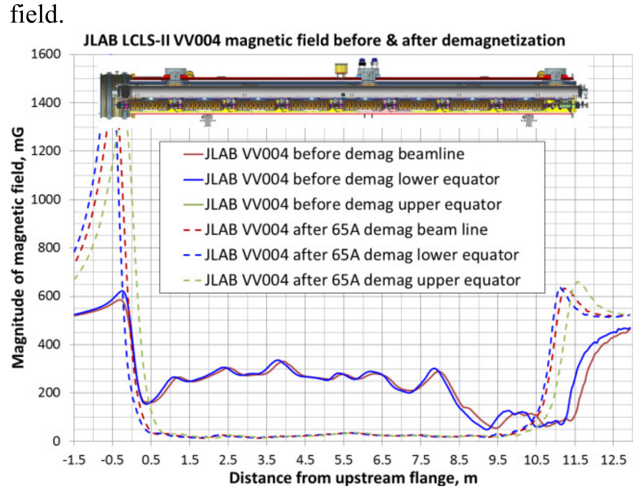

Figure 1: Magnetic field inside a LCLS-II VV post demagnetization.

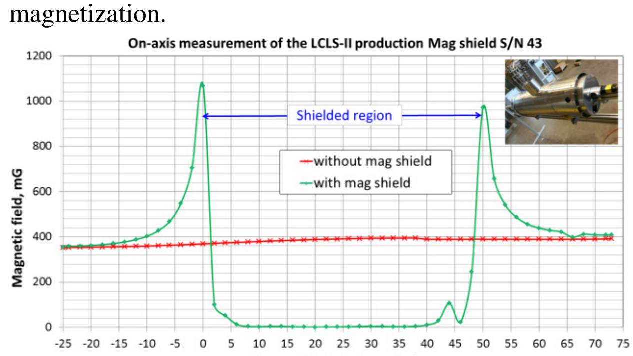

Figure 2: Mapped magnetic field inside a LCLS-II magnetic shield.

The LCLS-II CM adopts double-layer 1-mm thick Cryoperm 10® capped cylindrical magnetic shields [7] for each cavity. It has been discovered that such magnetic shields may have remnant magnetic field that may compromise their shielding performance. It is also well know that heat treatment can affect the permeability of magnetic shield materials. Therefore, an essential quality control step on the as-received magnetic shield is to perform field

* Authored by Jefferson Science Associates, LLC under U.S. DOE Contract No. DE-AC05-06OR23177. The U.S. Government retains a non-exclusive, paid-up, irrevocable, world-wide license to publish or reproduce this manuscript for U.S. Government purposes. The work is supported by the LCLS-II project.
† cheng@jlab.org

Content from this work may be used under the terms of the CC BY 3.0 licence (© 2017). Any distribution of this work must maintain attribution to the author(s), title of the work, publisher, and DOI.

ISBN: 978-3-95450-191-5 doi:10.18429/JACoW-SRF2017-MOPB045

Content from this work may be used under the terms of the CC BY 3.0 licence (© 2017). Any distribution of this work must maintain attribution to the author(s), title of the work, publisher, and DOI.

JLAB NEW INJECTOR CRYOMODULE DESIGN, FABRICATION AND TESTING*

G. Cheng†, M. Drury, J. Fischer, R. Kazimi, K. Macha, H. Wang, Thomas Jefferson National Accelerator Facility, Newport News, U.S.A.

Abstract

A new Injector Cryomodule (INJ CM) aimed to replace the existing Quarter Cryomodule in the CEBAF tunnel has been developed at Jefferson Lab (JLab). It is scheduled to be first tested in the Cryomodule Test Facility (CMTF) for module performance then the Upgraded Injector Test Facility (UITF) with electron beam. This new cryomodule, hosting a 2-cell and 7-cell cavity, is designed to boost the electron energy from 200 keV to 5 MeV and permit 380 μA – 1.0 mA of beam current. The 2-cell cavity is a new design whereas the 7-cell cavity is refurbished from a low loss cavity from the retired JLab Renascence Cryomodule. The INJ CM adopts quite a few designs from the JLab 12 GeV Upgrade Cryomodule (C100). Examples of this include having the cold mass hung from a spaceframe structure by use of axial and transverse Nitronic rods, cavities to be tuned by scissor-jack style tuners and the end cans are actually modified from C100 style end cans. However, this new INJ CM is not a quarter of the C100 Cryomodule. This paper focuses on the major design features, fabrication and alignment process and testing of the module and its components.

INTRODUCTION

Since its installation back in the early 1990s, the quarter cryomodule (QCM) presently in CEBAF injector section has been in service for 24+ years. JLab was granted to start its accelerator energy upgrade from 6 GeV to 12 GeV in 2004 [1]. Upgrade of the injector section is part of the 12 GeV project [1-3]. Although not part of the 12 GeV project, the QCM having a pair of 5-cell cavities and serving as the booster is aimed to be replaced by a new Injector Cryomodule (INJ CM) that also accommodates two RF cavities. The INJ CM's cavity string layout was optimized by conducting beam dynamics simulation [4] and determined to consist a 2-cell and a 7-cell cavity. Basing on operation experience, the QCM has a couple known issues [2, 4]: transverse deflecting field, or transverse "kick", and x/y coupling. Cavity RF design [5] then focused on optimizing the 2-cell cavity shape and minimizing the transverse kick due to power couplers to be less than 1 mrad in theory. The 12GeV upgrade cryomodule, also known as the C100 cryomodule, has eight 7-cell cavities, which adopt fundamental power couplers (FPC) and cavity end groups that bear up/down symmetry [6]. This symmetry is the remedy to cancel the x/y coupling that the original CEBAF cryomodule cavities, known as C50 cavities, have. The INJ CM 2-cell and 7-cell cavities are built with C100-style FPC and end group configuration so x/y coupling shall not exist in theory. In fact, the C100-style FPC's stub length was not optimized to minimize the transverse kick, but its 100mm length is deemed to be acceptable since the kick angle generated meets specification [5].

Mechanical design of the INJ CM cavities [7] and cryomodule commenced in 2011. The 2-cell cavity is a new design whereas the 7-cell cavity is refurbished from a low loss cavity used in JLab's Renascence cryomodule [8-9]. The INJ CM project experienced multiple halts due to funding issues. INJ CM design work finished in the Fall of 2015 and the machine is fully assembled by September 2016. It was then tested in JLab's CMTF. Before it is delivered to CEBAF tunnel injector section, the INJ CM needs to make a stop at the UITF to be commissioned and tested in a mimicked injector section that is equipped with a 200 kV DC gun to generate electron beam.

CRYOMODULE DESIGN

The QCM presently in service in CEBAF injector section is somewhat "a quarter" of a standard C50 cryomodule in that two 5-cell cavities are identical to C50 cavities and the supply & return end cans are duplicates of those for a C50 cryomodule. However, the new INJ CM is not really a quarter of any existing cryomodules at JLab. Its design largely mimicked C100 cryomodule but the core of the module, i. e. the cavity string, is unique. Things built around the cavity string are C100-style with modifications when necessary. The following paragraphs will go through the subsystems of the INJ CM with some details.

Cavity String

The 2-cell cavity [5, 7] is designed to be a $\beta = 0.6$, f = 1497 MHz elliptical cavity. Its location in the cryomodule with respect to upstream interface flange is dictated by beam dynamics studies. This cavity is built with 4-mm thick fine grain high RRR niobium and stiffening rings are added to raise the vibrational natural frequency and resistance to pressure induced stress [7]. The cavity is hosted in a stainless steel helium vessel that has one bellows permitting cavity tuning and a round helium inlet and an oval shape outlet for increased heat transfer capacity. To attenuate the geomagnetic field, a layer of 1-mm thick Cryoperm 10® magnetic shield is wrapped around the 2-cell cavity helium vessel. The 2-cell magnetic shield's openings take up a large percentage of the shield area so a thicker material is used than that of the 7-cell cavity's magnetic shield.

* Authored by Jefferson Science Associates, LLC under U.S. DOE Contract No. DE-AC05-06OR23177. The U.S. Government retains a non-exclusive, paid-up, irrevocable, world-wide license to publish or reproduce this manuscript for U.S. Government purposes.
† cheng@jlab.org

ISBN: 978-3-95450-191-5 doi:10.18429/JACoW-SRF2017-MOPB046

LCLS-II CRYOMODULE PRODUCTION AT JLAB*

R.Legg†, G. Cheng, E. Daly, K. Davis, M. Drury, J. Fischer, N. Huque, T. Hiatt, L. King, J. Preble, A. Reilly, M. Stirbet, K. M. Wilson, Jefferson Lab, Newport News, VA, USA

Abstract

The LCLS-II cryomodule construction program leverages the mature XFEL cryomodule design to produce technologically sophisticated cryomodules with a minimum of R&D according to an accelerated manufacturing schedule. JLab, as one of the partner labs, is producing 18 cryomodules for LCLS-II. To meet the quality and schedule demands of LCLS-II, many upgrades to the JLab cryomodule assembly infrastructure and techniques have been made. JLab reconfigured our clean room to provide a dedicated area for LCLS-II string assembly and instituted new protocols to minimize particulate transfer into the cavities during the cryomodule construction process. JLab has also instituted a set of magnetic hygiene protocols to be used during the assembly process to minimize magnetic field impingement on the finished cavity structure. The goal has been to have gradients, both maximum and field emission onset, that do not degrade between the cavity vertical test and final cryomodule qualification, while maximizing the Q_0 of each finished cavity. Results from the prototype cryomodule assembly are presented.

CRYOMODULE PRODUCTION AT JLAB

Jefferson Lab has a long standing core competency in cryogenics and superconducting radio frequency (SRF) systems. It is one of the underlying technologies that enabled CEBAF to provide unprecedented, high quality continuous wave (CW) beams initially at 4 GeV, then 6 GeV and now, with the recent upgrade, 12 GeV.

The primary mission of JLab's SRF enterprise is to maintain and improve the capability of the lab's accelerators for nuclear physics experiments, including developing the next generation of systems for a future electron ion collider (EIC).

A partial list of large cryomodule construction projects to date at Jefferson Lab include:

- Original CEBAF construction 42.25 cryomodules 1987-1993
  - 40 cryomodules plus Injector (2 cryomodules + two cryo-units), totalling 338 five (5) cell cavities
  - During peak production, 2 cryomodules were assembled per month
- SNS cryomodule, fabrication and test of 23 cryomodules built at JLab between 2001-2005
  - 11 Medium Beta , and 12 High Beta
- JLab FEL Project, 3 cryomodules started in 2003
- C50 refurbishment program started in 2006 (12 cryomodules as of 2016)
- 12 GeV, 10 cryomodules built from 2010-2012 using a new 7-cell "Low Loss" cavity design, new tuner, HOM couplers and probe feedthrough, new RF window design, and new cavity processing methods

Jefferson Lab has been in almost continuous cryomodule production for more than 25 years.

LCLS-II CRYOMODULE PRODUCTION

In the fall of 2013 the SLAC National Accelerator Laboratory approached Jefferson Lab to manufacture cryomodules for the LCLS-II free electron laser project being built at SLAC[1]. The schedule for the project is very aggressive and to meet it, the project decided to leverage the existing DESY and XFEL design [2] to produce technologically sophisticated cryomodules while minimizing the initial schedule risk and cost. Further, to reduce the time required to produce the large number of 1.3 GHz cryomodules required for the project, SLAC split the production between Fermi National Accelerator Laboratory (FNAL) and Jefferson Lab. The plan was to produce two identical prototype cryomodules utilizing as much existing hardware as possible to reduce schedule risk and overall cost while verifying the production design and processes [3]. Jefferson Lab and FNAL would share the procurement processes and use identical parts for the production modules, Figure 1. Each will build 17 production cryomodules with the plan that equivalent processes will yield equivalent performance. The goal is for each lab to ship a cryomodule to SLAC every five weeks.

Figure 1: LCLS-II Cryomodule.

The LCLS-II cryomodule also has a very demanding set of specifications [4]. The Q_0 and average gradient without field emission are much greater than previous cryomodules and required JLab to make a careful assessment of our procedures and facilities. As a result of that evaluation and the schedule constraints, several upgrades were made to improve cryomodule construction at JLab.

CRYOMODULE ASSEMBLY PROCESS

The assembly process begins with cavities arriving from industrial vendors and being inspected. After cavity inspection, each cavity is individually tested in the

* This work was supported by the LCLS-II Project and the U.S. Department of Energy, Contract DE-AC02-76SF00515
† rlegg@JLab.org

Content from this work may be used under the terms of the CC BY 3.0 licence (© 2017). Any distribution of this work must maintain attribution to the author(s), title of the work, publisher, and DOI.

ISBN: 978-3-95450-191-5 doi:10.18429/JACoW-SRF2017-MOPB049

Content from this work may be used under the terms of the CC BY 3.0 licence (© 2017). Any distribution of this work must maintain attribution to the author(s), title of the work, publisher, and DOI.

UPGRADED CAVITIES FOR THE CEBAF CRYOMODULE REWORK PROGRAM*

R. Rimmer†, G. Cheng, G. Ciovati, W. Clemens, E. Daly, K. Davis, J. Follkie, D. Forehand, F. Fors, J. Guo, J. Henry, K. Macha, F. Marhauser, L. Turlington, G. R. Myneni
Thomas Jefferson National Accelerator Facility, Newport News, VA 23606 USA

Abstract

The CEBAF cryomodule rework program has been a successful tool to recover and maintain the energy reach of the original baseline 6 GeV accelerator. The weakest original modules with eight five-cell cavities assembled in four "pairs", with a specification when new of 20 MV per cryomodule (5 MV/m), are disassembled, re-cleaned with modern techniques and re-qualified to at least 50 MV (12.5 MV/m), (leading to the acronym "C50"). The cost per recovered MV is much less than building new modules. However over time the stock of weak modules is being used up and the voltage gain per rework cycle is diminishing. In an attempt to increase the gain per cycle it is proposed to rework the cavities by replacing the original accelerating cells with new ones of an improved shape and better material. The original CEBAF HOM and FPC end groups are retained. The goal is to achieve up to 75 MV (19 MV/m) for the reworked module ("C75"). Three C75 5-cell prototype cavities have been fabricated, processed and tested as part of an R&D program aiming at providing cavities to be installed during the refurbishment of some of the original CEBAF cryomodules. We report on the fabrication experience and test results of the first trial pair, containing two such reworked cavities.

INTRODUCTION

In order to improve the energy gain of refurbished original CEBAF cryomodules with minimal cost, it was proposed to replace the cavity cells with newer ones of a new shape and material, which would allow achieving both higher accelerating gradient and quality factor than the original cavities. The end groups would be cut from existing cavities and welded to the new multi-cell structure to save as much of the existing cavity components as practically possible. The cell shape was chosen to be the 'high current' shape designed for a proposed high power FEL at JLab [1]. The material was chosen to be ingot Nb, a cavity material technology pioneered at Jefferson Lab since 2004 [2]. The performance specification is an accelerating gradient, E_{acc}, of 19 MV/m with a quality factor, Q_0, greater than 8×10^9 at 2.07 K. Three prototype cavities were built and the two with the best RF performance were assembled into a cavity pair to be installed in the cryomodule currently being refurbished, which is planned to be installed in CEBAF in August 2017.

*Authored by Jefferson Science Associates, LLC under U.S. DOE Contract No. DE-AC05-06OR23177. The U.S. Government retains a non-exclusive, paid-up, irrevocable, world-wide license to publish or reproduce this manuscript for U.S. Government purposes.
† rarimmer@jlab.org

CAVITY DESIGN

The cell shape adopted for the C75 cavity has the advantage of a ~14% lower E_p/E_{acc}, ~10% lower B_p/E_{acc} and ~10% higher R/Q·G compared to those of the Original Cornell (OC) shape, while having the same cell-to-cell coupling. Therefore the C75 cell shape has a more efficient design without compromising the HOM damping. The 5-cell cavity is designed to be field-flat by trimming each end half-cell by ~4 mm at the flat equator region, made from the same cup shape as used as for mid-cells. For the condition of maximum beam loading (460 µA beam current) and for the peak detuning by microphonics of ~20 Hz [3], the minimum RF power to operate the C75 cavities would be achieved for a Q_{ext} of ~2.5×10^7, compared to the Q_{ext} ~6.6×10^6 for the original CEBAF cavities. In order to achieve higher Q_{ext}-values, the distance between the end-cell and the fundamental power-coupler was increased by adding a Nb beam-tube ~40 mm long.

A draw-back of the C75 cell shape is that it has flat walls, which makes it less stiff compared to the OC shape. To mitigate this, stiffening rings are added between inner cells and between the end-cells and the end-groups. The position of the stiffening rings was determined by finite element analysis and verified experimentally [4] such that the C75 cavity would have the same stiffness as that of the OC CEBAF cavity, since the same cold tuner will be used.

CAVITY MATERIAL

Two Nb ingots produced by CBMM, Brazil, as part of the company's R&D program and sent to Jefferson Lab for evaluation and testing, were used for the fabrication of cavities *5C75-001* and *5C75-002*. A center hole was cut by wire electro-discharge machining and the ingots were sliced into 3.175 mm thick discs with a multi-wire slicing machine at Slicing Tech, Inc. The thickness tolerance achieved was ±0.1 mm and the average surface roughness was better than 1.6 µm. Additional ingot Nb discs to build *5C75-003* were purchased from Tokyo-Denkai (TD), Japan. Table 1 summarizes the material and its properties for each cavity. The use of a material with lower residual resistivity ratio (RRR) can be advantageous to achieve a higher quality factor, which is very beneficial for CW accelerators [5]. Medium purity (RRR = 100-200) ingot Nb material is an ideal combination to achieve good performance at lower cost than standard fine-grain, high-purity (RRR > 250) Nb.

ISBN: 978-3-95450-191-5 doi:10.18429/JACoW-SRF2017-MOPB050

CAVITY PROCESSING AND TESTING ACTIVITIES AT JEFFERSON LAB FOR LCLS-II PRODUCTION *

L. Zhao†, K. Davis, T. Reilly, A. Palczewski, K. Macha, J. Follkie, D. Forehand
Thomas Jefferson National Accelerator Facility, Newport News, USA

Abstract

Cryomodule production for LCLS-II is well underway at Jefferson Lab. This paper explains the process flow for production cavities, from being received at the Test Lab to being assembled onto cavity strings. Taking our facility and infrastructure into consideration, process optimization and process control are implemented to ensure high quality products.

BACKGROUND

LCLS-II as a pioneering X-ray free electron laser facility [1] aiming for unprecedented scientific opportunities [2], is an intellectual collaboration between US laboratories, university, and European research institutes. It demonstrates existing SRF technology [3, 4] as well as exploring cavity performance potential [5]. SRF cavities are provided by two vendors: Research Instruments, GmbH (Germany) and Ettor Zanon, S.p.A. (Italy) [6]. The fabrication of cryomodules (CMs) are shared between Fermi Lab and Jefferson Lab (JLAB), with each lab providing 18 CMs. Production related activities at Jefferson Lab include: qualification testing of SRF cavities, limited re-processing of cavities, cavity string assembly, CM assembly, CM testing, and eventually shipping CMs to SLAC. Jefferson Lab is currently at full production stage for the project and has been making the best use of the SRF knowledge developed over the years in the community.

CAVITY PROCESS FLOW

Helium vessel dressed cavities come from vendors under vacuum, ready to be tested. After registered into JLAB inventory system, the critical dimensions and passband frequencies of the cavities are measured. The exterior surface of the cavities is cleaned prior entering the cleanroom, where the cavities are connected to test stands and leak checked at the vertical attachment area (VAA). Once cavities pass leak check, they are moved to vertical staging area (VSA) and prepared for loading into the dewar. Depending on the background of the cavity, RF testing at 2K or multiple lower temperatures is performed at the vertical testing area (VTA). Cavities qualified for a string will be transferred back to the cleanroom, disassembled of both beam line flanges and testing fundamental power coupler (FPC), receive final high pressure rinse (HPR), and assembled onto a string. If a cavity does not meet qualification at the first vertical test due to field emission early onset, an HPR is performed as a remedy attempt. Fig. 1 shows the process flow of a cavity at JLAB after arriving from the vendors. Fig. 2 shows the path of a cavity through work centers at JLAB.

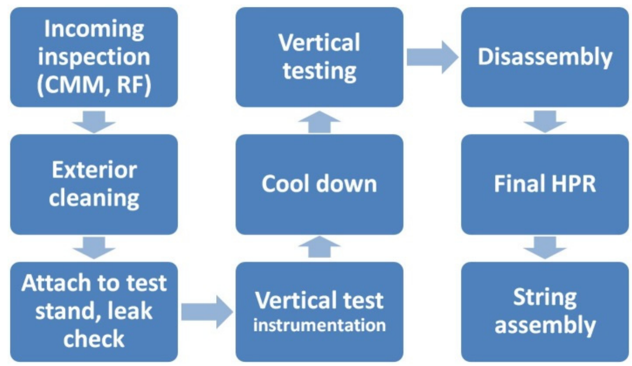

Figure 1: Process flow for LCLS-II cavities after arriving at JLAB from the vendors.

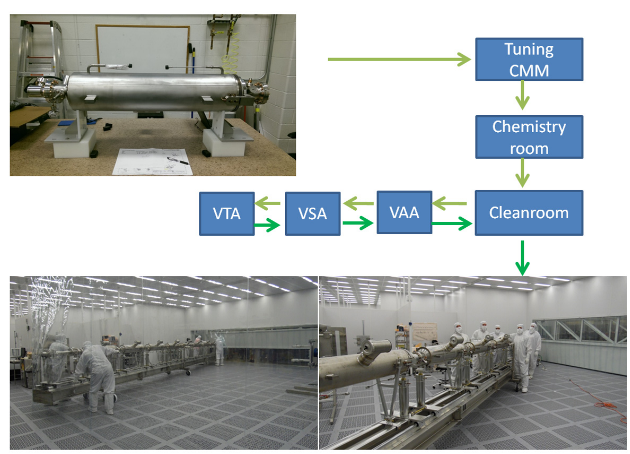

Figure 2: The path of LCLS-II cavities through JLAB work centers, from receiving inspection to an LCLS-II string.

CAVITY PROCESS TRACKING

Cavity process tracking is achieved by Pansophy system [7]. Each process has a traveler, which is a list of actions extracted from the procedure designated to the specific task. Travelers allow users to input critical information of the processes. The data entered could be searched within the network and used for statistics.

* Work supported by Jefferson Science Associates, LLC under U.S. DOE Contracts DE-AC05-06OR23177 and DE-AC02-76SF00515 for the LCLS-II Project.
† lzhao@jlab.org

Content from this work may be used under the terms of the CC BY 3.0 licence (© 2017). Any distribution of this work must maintain attribution to the author(s), title of the work, publisher, and DOI.

18th International Conference on RF Superconductivity SRF2017, Lanzhou, China JACoW Publishing
ISBN: 978-3-95450-191-5 doi:10.18429/JACoW-SRF2017-MOPB052

DUAL-RIDGE WAVEGUIDE LOAD DESIGN FOR eRHIC*

P. Kolb†1, Y. Gao[1,2], C. Pai[1], R. Porqueddu[1], K. Smith[1], and W. Xu[1]
[1]Collider-Accelerator Department, Brookhaven National Laborarory, Upton, NY 11973, USA
[2]Institute of Heavy Ion Physics, School of Physics, Peking University, Beijing 100871, China

Abstract

To increase the real estate gradient in the eRHIC electron accelerator waveguide HOM couplers are being considered. These significantly reduce the length of individual cavities and address inter-cavity trapped modes, allowing for an increased number of cavities per cryomodule, which would increase the real estate gradient. The choice of waveguide went to a dual ridge waveguide due to a smaller size compared to rectangular waveguides.

The waveguide termination, to convert the RF energy into thermal energy, is a custom designed load based on a silicon carbide dielectric that is already being used in beamline absorbers. Simulations of the RF properties of the load are presented as well as first measurements on a prototype.

INTRODUCTION

The eRHIC LINAC-Ring design [1] consists of one of the already existing ion-rings and a new electron accelerator based on the energy recovery LINAC (ERL) principle. In multiple turns the electron beam is accelerated to 18 Gev and after collision with the ion beam decelerated in the RF cavities to transfer the beam energy into electromagnetic field energy inside the cavity to accelerate further bunches. A limitation for the electron accelerator is the overall accelerator length as straight sections in the existing RHIC tunnel are limited to 200 m. As accelerating cavity, a five cell 647 MHz cavity operating at 16.2 MV/m is under consideration. To keep the real estate gradient high and keep the accelerator short enough to fit into the tunnel, waveguide higher order mode (HOM) couplers are proposed to take care of most of the HOM power generated by the beam. Beam line absorbers will take care of HOMs traveling between cryomodules. The current cavity design has six HOM waveguide ports as shown in Fig. 1, three on each side of the cavity at 120deg rotated to each other. The two sides are rotated by 30deg with respect to each other. For compactness, dual ridge waveguides (DRWG) will be used. This waveguide geometry is more compact than a rectangular waveguide at the same cut-off frequency. This will not only help with shortening the cavity length, but also reduce the thermal load to the cryogenic system. The waveguide geometry is chosen for a cut-off frequency for the fundametal waveguide mode of 770 MHz: significantly above the operating frequency but low enough for the HOMs to propagate into it. A cross section with dimensions is shown in Fig. 2.

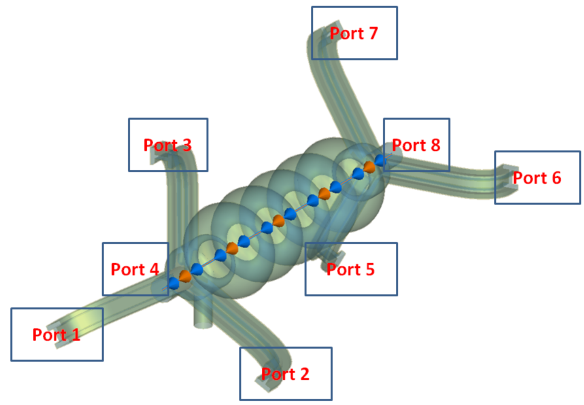

Figure 1: Simulation model of the 650 MHz cavity with six dual ridge waveguides for eRHIC.

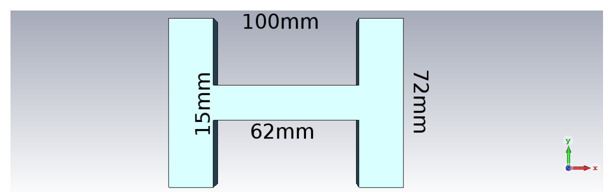

Figure 2: Cross-section view with dimensions of the DRWG with a cut-off frequency of 770 MHz.

These waveguides will terminate at loads at room temperature with water cooling. Due to multiple kW of HOM power on each load, cryogenic cooling would be unfeasible.

HOM POWER

To determine the generated HOM power it is necessary to estimate the cavity impedance. Since the electron bunches are short with σ_z=3 mm, the impedance spectrum needs to be considered up to 40 GHz. The termination of the waveguide has to accommodate this broadband requirement. At low frequencies, up to 2 GHz, the impedance is calculated by eigenmode simulations. At higher frequencies wakefield simulations are used to calculate the cavity impedance. Another part to calculating the HOM power is the beam spectrum. This is dominated by the bunch train repetition frequency of 9.38 MHz but can be tuned with the bunch spacing and the timing between the accelerating and decelerating bunch train. Calculations on different combinations of bunch spacing showed some impact on the overall HOM power. Details of the HOM calculations can be found in [2]. In total, about 10 kW of HOM power per cavity is estimated based on the calculated eigenmode frequencies and impedance.

* Work supported by LDRD program of Brookhaven Science Associates, LLC under Contract No. DE-AC02-98CH10886 with the U.S. DOE.
† pkolb@bnl.gov

Content from this work may be used under the terms of the CC BY 3.0 licence (© 2017). Any distribution of this work must maintain attribution to the author(s), title of the work, publisher, and DOI.

ISBN: 978-3-95450-191-5 doi:10.18429/JACoW-SRF2017-MOPB053

RF ENERGY HARVESTING OF HOM POWER *

Chen Xu[1], Ilan Ben-Zvi[1,2], Tianmu Xin[1], Qiong Wu[1]
[1] Brookhaven National Laboratory, Upton, New York 11973-5000, USA
[2] Stony Brook University, Stony Brook, New York 11794, USA

Abstract

In an accelerator cavity, Higher Order Modes (HOM) are generated by the current of the beam. The HOM power can reach tens of kilowatts per cavity in a high current accelerator, depending on the details of the beam and cavity design. In this report, we propose a novel RF harvesting system to convert the HOM power into DC power. The removal of this DC power from the cryogenic system is very efficient, and furthermore it may be used for various purposes such as driving RF amplifiers, charge batteries etc. We show that the efficiency of the harvesting system is very high. The proposed HOM power recycling system contains a multiple band harmonic RF coupler, broadband RF antenna system, a high power rectifier diode circuit and a DC load.

INTRODUCTION

High current linear accelerators (linacs) are becoming common. The higher the current, the higher is the HOMs' power. The HOM power spectrum is concentrated at harmonics of the bunch repetition frequency. When the accelerator operates as an Energy Recovery Linac (ERL), the required fundamental power required to operate the cavities is relatively very low. Yet, the HOM power can account for a significant fraction of the input RF power. In the ERL, the HOM power spectrum peaks at even harmonics of the bunch repetition frequency [1]. We propose an antenna system beaming the HOM RF power in a highly collimated pattern, followed by collection and conversion the RF power into DC power by arrays of diodes. A schematic HOM power collection and harvesting system is shown in Figure 1.

As a specific example, we will design a power removal and recycling system using a dual band RF horn antenna system and matched diode collection for a particular example of an ERL operating at 650 MHz.

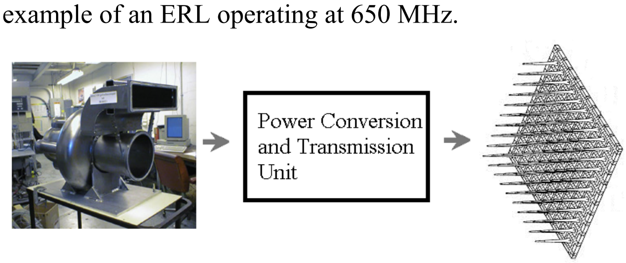

Figure 1: Schematic of an HOM power collection and conversion system. A CESR style cavity represents the HOM source on the left, a mode-converter and horn antenna is in the center and a diode array on the right.

This work is supported by Brookhaven Science Associates, LLC under Contract No. DE-AC02-98CH10886 with the U.S. DOE.
#chenxu@bnl.gov

This specific system will be operating at two frequency ranges: 1.3 and 2.6 GHz. We will explain why these two frequencies in the later sections in detail.

THE TRANSMISSION SYSTEM

The most common HOM out-coupling in accelerating cavities is a rectangular waveguide in TE10 mode. The field pattern of TE10 and TE11 in a rectangular waveguide, and the TE20 and TE11 in a circular waveguide are shown in Figure 2. From this figure, it is easy to see that the TE10 mode in rectangular waveguide can be easily converted to a TE11 in a circular waveguide. In addition, the TE11 mode in rectangular waveguide can be converted to a TE21 in a circular waveguide. In the circular horn, the energy densities of the TE11 and TE21 modes are distributed differently: The power of the TE11 is concentrated mainly about the axis center, while the TE21 has a null in the center. With an additional propagation distance, the power from these modes (which have different frequencies) are redistributed differently. The far field patterns of those modes form a circle enclosed by a ring. All simulations in this study are conducted in CST. [2]

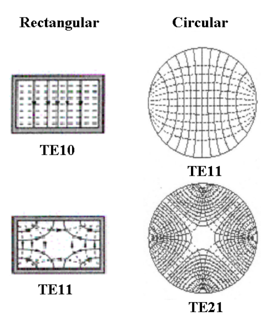

Figure 2: The field pattern of TE10 and TE10 in a rectangular waveguide, and the TE20 and TE11 in a circular waveguide.

To obtain a good directivity we use a conical horn antenna to launch the HOMs from a rectangular waveguide on a cavity. The far-fields of the horn antenna is the Fourier Transform of the fields at the opening of the horn. In addition, the radiation system is large enough for high power handling capacity, and experimental research is planned for the next step to study the ultimate power handling capacity. The HOM power generation in our example will be mostly at 1.3 and 2.6GHz, due to the ERL operation mode. We want to divide the 1.3GHz and 2.6GHz towards different destinations on the diode arrays, to optimize the harvesting unit energy conversion

Content from this work may be used under the terms of the CC BY 3.0 licence (© 2017). Any distribution of this work must maintain attribution to the author(s), title of the work, publisher, and DOI.

ISBN: 978-3-95450-191-5 doi:10.18429/JACoW-SRF2017-MOPB054

DESIGN OF FUNDAMENTAL POWER COUPLER FOR HIGH INTENSITY HEAVY-ION ACCELERATOR

Feng Bing[1,2], Weimin Pan[1], Tong-Ming Huang[1], Qiang Ma[1], Fanbo Meng[1] , Kuixiang Gu[1,2]
[1] Institute of High Energy Physics, Chinese Academy of Sciences, Beijing, China
[2] University of Chinese Academy of Sciences, Beijing, China

Abstract

A single-window coaxial coupler at warm has been designed for high intensity heavy-ion accelerator. The coupler is designed to handle 100kW CW power of 325 MHz and is currently being fabricated. T-bend transition and doorknob have been taken into account. The length of the T-bend short circuit is sensitive to S parameters and contributes to the online adjustment of VSWR in RF conditioning. The doorknob type is adopted to realize the transition from a half-height WR2300 waveguide to a coaxial line ended with a coupling antenna. This paper describes the RF design, thermal stress and heat load analysis of the coupler as well as multipacting simulations.

INTRODUCTION

Increasingly higher beam current and improved cavity gradient placed demanding requirements on fundamental power couplers. High reliability, bridging ambient and liquid helium temperatures, low cryogenic heat leak, reasonable cost, and preserving extreme cavity cleanliness are the main challenges for fundamental power couplers in continuous wave mode [1].

The ceramic window is a fragile component, and the cause of coupler failures is summarized as follows：

1）Cracked windows due to mechanical stresses

2）Cracked windows due to thermal stresses

3）Punctured windows due to electron activities

In addition, brazes and welds caused leakage is also one of the factors leading to damage.

The ADS proton linac adopted β=0.12 and β=0.21 superconducting Spoke cavities. Seven couplers for 325 MHz Spoke-012 SCC for Injector-I have been high power tested up to the nominal power levels in both TW (Spke-012: 10 kW) and SW modes (Spke-012: 5 kW) [2].

This coupler is designed for experimental purpose to deliver high RF power (100 kW). Its main parameters are summarized in Table 1.

Table 1: Main Parameters of the Coupler

Parameter	Value
Frequency	325 MHz
Input power	100 kW CW
Type	Coaxial, Antenna E-coupling, Fixed
Window	Single, coaxial disk

CALCULATIONS

The basic design of doorknob type is based on BEPCII 500MHz coupler, including a 50 Ω coaxial line, a planar window and a doorknob transition [3]. The T-bend type shares mutual window and outer conductor with doorknob type. Figure 1 shows the electromagnetic model.

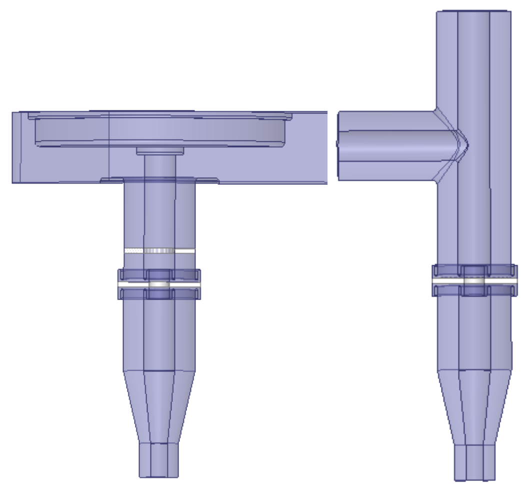

（a） (b)

Figure 1: The electromagnetic model (a) doorknob type (b) T-bend type.

RF window works as a vacuum barrier for the cavity and delivers power. The ceramic window(97.6% Al2O3 Morgan Φ=170mm) adopts a choke structure to avoid the high electrical field at ceramic braze joints and adds vacuum, electron flow, ARC probes in the vacuum side. The S11 of original design of the ceramic window is -27dB at 325MHz.

Figure 2 shows the calculated S11 curve of the whole coupler. The S11 reads -49dB at 325MHz, and the bandwidth is approximately 13MHz at -25dB for doorknob coupler. The geometry of the T-bend transition is a crucial part to satisfy the matching condition as it is very sensitive to S parameters and nominal frequency.

Content from this work may be used under the terms of the CC BY 3.0 licence (© 2017). Any distribution of this work must maintain attribution to the author(s), title of the work, publisher, and DOI.

ISBN: 978-3-95450-191-5 doi:10.18429/JACoW-SRF2017-MOPB061

Content from this work may be used under the terms of the CC BY 3.0 licence (© 2017). Any distribution of this work must maintain attribution to the author(s), title of the work, publisher, and DOI.

QUALITY CONTROL OF COPPER PLATING IN STF-2 INPUT POWER COUPLERS

E. Kako[1, 2] †, R. Ueki[1], H. Kutsuna[3], J. Taguchi[3], K. Okihira[4], K. Sennyu[4], H. Umezawa[5], F. Saito[5], K. Tetsuka[6] and O. Yushiro[6]
[1] KEK, High Energy Accelerator Research Organization, Tsukuba, Ibaraki, Japan
[2] SOKENDAI, The Graduate University for Advanced Studies, Hayama, Kanagawa, Japan
[3] Nomura Plating Co. Ltd., Osaka, Japan
[4] Mitsubishi Heavy Industries Mechatronics Systems Ltd., Kobe, Japan
[5] Tokyo Denkai Co. Ltd., Tokyo, Japan
[6] Toshiba Electron Tubes and devises Co. Ltd., Ohtawara, Japan

Abstract

Purity of thin copper plating used for input power couplers in a superconducting cavity system is one of important characteristics for considering thermal losses at low temperature. Various samples of thin copper plating on stainless sheets were fabricated by four venders with their own plating techniques. The RRR values of the samples with different thickness of copper plating were compared in the condition before and after heat treatment at 800ºC in a brazing furnace. Deterioration of the RRR was observed in all of samples after heat treatment. The results of the RRR measurements and sample analysis of impurities are reported in this paper.

INTRODUCTION

The primary role of a high power input coupler is to transfer RF power from a generator to a cavity and beams. High power input couplers are one of the most critical components of a superconducting RF cavity system and includes varieties of key technologies in design, fabrication, conditioning and operation. Many types of high power couplers for CW and pulsed operation were fabricated, and the RF conditioning was carried out at KEK, [1, 2]. Reduction of both thermal loads, which consists of a dynamic loss due to RF losses and a static loss due to heat leak from outside, is an important consideration in input couplers. In this view point, quality control of Cu-plating of input couplers has a significant role for supressing thermal losses. Purity and thickness of Cu-plating are essential parameters for the fabrication process of input couplers. Heat treatment at 800ºC for brazing gives a remarkable influence in property of Cu-plating. Investigation for quality control of Cu-plating is discussed in this paper.

DYNAMIC LOAD OF INPUT COUPLER

International cryomodule test named S-1 Global [3] in 2010 was aimed to compare each performance of different components included in a cavity package. One of the purposes in S-1 Global was to compare the performance of input couplers between TTF-III couplers [4] developed by DESY and STF-2 couplers [5] developed by KEK.

† eiji.kako@kek.jp

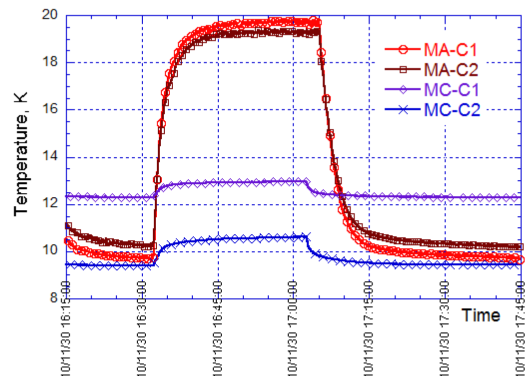

Figure 1: Temperature rises at connection flanges of input couplers at the condition of detuned 32 MV/m: MA-C1 and MA-C2 show the temperature at STF-2 couplers (red lines). MC-C1 and MC-C2 show the temperature at TTF-III couplers (blue lines) [6].

Table 1: Measured dynamic heat loads in a single cavity operation; a total dynamic heat load of a cavity and a coupler ($P_{loss-(Total)}$), a dynamic heat load of a coupler under a detuned condition ($P_{loss-(Detune)}$) and a net dynamic heat load of a cavity ($P_{loss-(Cavity)} = P_{loss-(Total)} - P_{loss-(Detune)}$) [6].

Cavity	Z-109	AES-004	MHI-07	MHI-06
Coupler	TTF-III	TTF-III	STF-2	STF-2
Eacc [MV/m]	28	25	32	32
$P_{loss-(Total)}$ [W]	0.8	1.4	2.8	2.6
$P_{loss-(Detune)}$ [W]	0.1	0.2	0.7	1.2
$P_{loss-(Cavity)}$ [W]	0.7	1.2	2.1	1.4
Q_0	8.8 x 10^9	4.3 x 10^9	4.3x 10^9	6.5 x 10^9

Figure 1 shows a comparison of temperature rises due to dynamic RF losses of TTF-III and STF-2 couplers [6]. The temperature rise was less than 1 degree in the TTF-III couplers and around 10 degrees in the STF-2 couplers. Measured results of the dynamic heat loads in the cavity equipped with each coupler are summarized in Table 1. The dynamic heat load of a coupler is shown by

ISBN: 978-3-95450-191-5 doi:10.18429/JACoW-SRF2017-MOPB062

DEVELOPMENT OF HOM ABSORBERS FOR CW SUPERCONDUCTING CAVITIES IN ENERGY RECOVERY LINAC

T. Ota†, M. Takasaki, M. Yamada, A. Miyamoto, K. Sato,
Toshiba Corporation, Yokohama, Japan
T. Konomi, K. Umemori, H. Sakai, E. Kako,
High Energy Accelerator Research Organization, Tsukuba, Japan

Abstract

Higher Order Modes (HOM) absorbers for Superconducting cavities in energy recovery linac (ERL) have been developing at TOSHIBA in collaboration with High Energy Accelerator Research Organization (KEK) since 2015. A prototype HOM absorber for 1.3 GHz 9-cell superconducting cavity was fabricated. An aluminum nitride based lossy dielectrics (AlN) cylinder was brazed in a copper cylinder. Stainless steel flanges were joined on either end of the copper cylinder by electron beam welding to fabricate a whole prototype HOM absorber. AlN/Cu brazing tests and Cu/SUS welding tests were carried out before fabricating the prototype. Fabrication process of the prototype HOM absorber will be presented in this paper.

INTRODUCTION

KEK has been designing the 10 mA class ERL-FEL light source accelerator. The main linac uses 9-cell cavities with beam line type HOM absorbers. The target accelerating gradient is 12.5 MV/m. The 9-cell cavity is designed from experience of the KEK compact ERL (cERL) main linac [1]. HOM absorbers are one of the key components to determine the ERL cavity performance to reduce the HOM problem for the high current operation. The absorption heat of HOM absorber is estimated to about 10 W. The use of the AlN is planned as HOM absorber material because it has high RF absorption at 80 K. Permittivities and Permeabilities of AlN were measured at room temperature and 80K. It was confirmed that 80 K data keep high value at high frequency [2]. Shape of HOM absorber has been designed [3].

TESTS BEFORE FABRICATING A PROTOTYPE HOM ABSORBER

Brazing Tests

Brazing tests between AlN and Cu were carried out before fabricating a prototype HOM absorber. An AlN cylinder was brazed in a copper cylinder, which has lattice-like slots on the inner surface. The size of an AlN cylinder and a copper cylinder used for the tests are shown in Table 1. The outer surface of an AlN cylinder was Mo-Mn metalized and Ni plated. Brazing conditions are shown in Table 2. Figure 1 shows a test piece after brazing. Ultrasonic testing of the test piece in the water bath was carried out to check their good adhesions. It was found that the AlN cylinder was partially touched the copper cylinder. To confirm the mechanical properties of the brazed connection during thermal cycling, the test piece was cooled down to 80 K with nitrogen gas. After cooling, cracks occurred in the AlN cylinder (see Fig. 2). The test piece was cooled in one hour from room temperature to 80 K. It was too fast to cool the test piece uniformly.

†tomoko.ota@toshiba.co.jp

Table 1: Test Pieces for Brazing

Material	Inner Diameter	Thickness	Length
AlN	100 mm	10 mm	20 mm
Copper	120 mm	6.5 mm	69 mm

Table 2: Brazing Conditions

Brazing material	Silver
Process temperature	750 ºC
Furnace atmosphere	Hydrogen

Figure 1: Test piece of brazing.

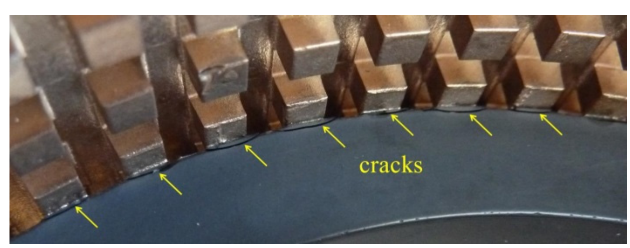

Figure 2: Cracks occurred in AlN cylinder.

Welding Tests

Welding tests between Cu and SUS were carried out. Stainless steel flanges were joined on both ends of a copper cylinder by electron beam welding (EBW). The size of a copper cylinder and stainless steel flanges used for the tests are shown in Table 3. They are the same size as the prototype. Conditions of EBW are shown in Table 4. Figure 3 shows the test piece after welding. Back side of the flange and the copper cylinder was welded to

Content from this work may be used under the terms of the CC BY 3.0 licence (© 2017). Any distribution of this work must maintain attribution to the author(s), title of the work, publisher, and DOI.

ISBN: 978-3-95450-191-5 doi:10.18429/JACoW-SRF2017-MOPB063

Content from this work may be used under the terms of the CC BY 3.0 licence (© 2017). Any distribution of this work must maintain attribution to the author(s), title of the work, publisher, and DOI.

FUNDAMENTAL STUDIES FOR THE STF-TYPE POWER COUPLER FOR ILC

Y. Yamamoto†, E. Kako, T. Matsumoto, S. Michizono, A. Yamamoto, KEK, Tsukuba, Japan
M. Irikura, H. Yasutake, M. Ishibashi, TETD, Otawara, Japan

Abstract

From the view point of mass-production for the power coupler in ILC (International Linear Collider), the fundamental studies for the STF-type power coupler are under progress by the collaboration between KEK and TETD. At present, there are various rinsing procedures for power coupler in the world-wide laboratories. In this R&D, the main topic is to investigate the various rinsing effects in the copper plating and the ceramic through the high power test. In this paper, the first results will be presented.

INTRODUCTION

In recent years, the SRF accelerator with several hundreds of superconducting cavities becomes standard in the real world. For example, ~800 cavities are used for European X-ray Free Electron Laser (E-XFEL) [1], ~300 cavities for Linac Coherent Light Source II (LCLS-II) [2], and ~100 for European Spallation Source (ESS) [3]. Naturally, the number of cavity is same as that of power coupler. The quality control in the mass-production of the power coupler is significantly important, similar to the cavity. Actually, the quality control of the power coupler was significant in E-XFEL [4]. The points in the quality control are the copper plating, the ceramic quality, the Titanium-Nitride (TiN) coating procedure, the rinsing procedure, and so on. As the first milestone, this R&D started from the quality check of the copper plating, and the rinsing effect by the different method in the power coupler.

FABRICATION OF TEST PIECES

At first, the 20 test pieces were fabricated for the copper plating, and the ceramic as shown in Figure 1. Each specification is described in the following:

Copper Plating Sample

The specification of the copper plating is as follows:

- Substrate: SUS316L
- Size: 50 mm x 100 mm x 5 mm
- Thickness of copper plating: 25 µm
- Base plating: Gold strike
- Copper plating: Pyrophosphate

During the process of copper plating from test piece #7 to #9, the quality was suddenly changed due to the malfunctioning in the pre-cleaning process, and then another process line was used after grinding the “No good” copper plating, and consequently, it was successfully done from test piece #7.

Ceramic Sample

The specification of the ceramic sample is as follows:

- Purity: 95%
- Size: 19 mm (diameter) x 3mm (thickness)
- Relative permittivity: 8.8 @10GHz
- Dielectric loss tangent: 6 x 10^{-4} @10GHz
- Resistivity: >10^{12} Ω·m

This type of ceramic has been used for the STF-2 power couplers installed into the S1-Global, the capture, and the STF-2 cryomodules [5].

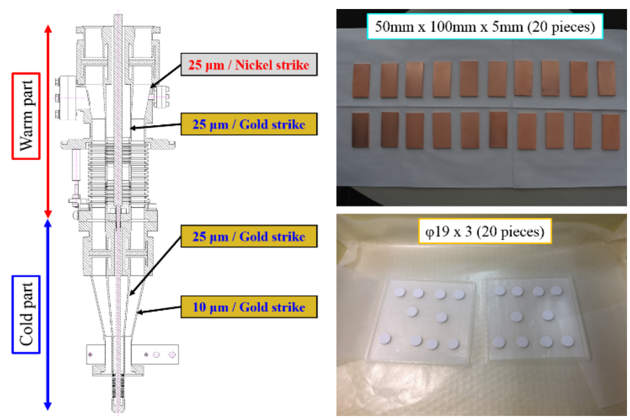

Figure 1: Plug-compatible STF-type power coupler (left), and the test pieces for the copper plating and the ceramic (right).

STUDY FOR COPPER PLATING

The first goal is the investigation for the various rinsing procedures carried out in the various laboratories in the world. Specifically, the rinsing effect was investigated by the following three methods:

- Ultrapure water rinsing; used in STF
- Ultrasonic rinsing; used in E-XFEL, ESS
- Ozonized water rinsing; used in Super-KEKB

Heat Treatment

After the copper plating process, the test pieces were heat-treated for about 30mins at 800℃, and after that, two pieces had many blisters on the edge region as shown in Figure 2. These blisters are quite similar to that observed at the cold part #1 for the plug-compatible STF-type power coupler [6]. Presumably, the hydrogen gas remained inside the copper plating layer after the copper plating process, then, it swelled during the heat treatment, and the copper plating also had many blisters. However, it is difficult to spot the quality of copper plating as “No good” at the incoming inspection after the copper plating process. In the mass-production, it is crucial to keep checking the quality

† yasuchika.yamamoto@kek.jp

ISBN: 978-3-95450-191-5 doi:10.18429/JACoW-SRF2017-MOPB064

HIGH POWER TEST FOR PLUG-COMPATIBLE STF-TYPE POWER COUPLER FOR ILC

Y. Yamamoto†, E. Kako, T. Matsumoto, S. Michizono, A. Yamamoto, KEK, Tsukuba, Japan
E. Montesinos, C. Julie, CERN, Geneva, Switzerland

Abstract

From the view point of plug-compatibility for the power coupler in the International Linear Collider (ILC), recommended by Linear Collider Collaboration (LCC) in 2013, new STF-type power couplers with 40mm of input port diameter were re-designed, fabricated and successfully high-power-tested. Moreover, from the view point of the cost reduction for the ILC, another type of power couplers with Titanium-Nitride (TiN) coating-free ceramic were also fabricated and high-power-tested by the collaboration between CERN and KEK. In this paper, the detailed results for the both power couplers will be presented.

INTRODUCTION

Following the recommendation by the LCC [1] in 2013, the STF-type power couplers with the plug-compatible design were re-designed and fabricated to meet the specification in the Technical Design Report (TDR) [2] for ILC [3]. Additionally, two cold parts with ceramic window without TiN coating were also fabricated for lower cost study. Therefore, there are two warm and cold parts with the TiN-coated ceramic window, and two cold parts with the coating-free ceramic window, fabricated in 2014, as shown in Table 1. For the test of each type of ceramic, the two warm parts are common, and only cold parts were exchanged each other.

Table 1: Summary of the Plug-compatible STF-type Power Couplers Fabricated in 2014

Coupler	Ceramic vendor	Ceramic colour	Coating
Warm #1, #2	A	White	TiN
Cold #1, #2	A	White	TiN
Cold #3, #4	B	Gray	Free

Table 2 shows the R&D history of the plug-compatible STF-type power coupler. The RF design by HFSS [4] and the mechanical design were simultaneously done. The fabrication for all components of power couplers were completed on November in 2014, delivered to KEK, and the incoming inspection was done there on March in 2015. After the assembly work for the test bench in the clean room, the low power measurement using the network analyser was done, and adjusted the coupling to the waveguide system by changing the insertion length of the inner conductor. The test bench was connected to the high power test area. As for the power coupler with coating-free ceramic, the same thing was done. In the following sections, each item is described in detail.

† yasuchika.yamamoto@kek.jp

RF DESIGN BY SIMULATION

The RF simulation by HFSS was done for the various models as described later. The main changed points from the STF-2 power coupler [5] are the power coupler port of 40 mm, and the wider range of the external Q. In the following sub-sections, the result is described in detail.

Coupling to Cavity

To fix the range of external Q, the coupling to the cavity (the cavity shape is TESLA) was estimated for two models:

- Real end-cell model (for two different diameter)
- Symmetric end-cell model

These two models are shown in the top two figures of Figure 1. For the real end-cell model, the input antenna with two different diameters was tested. The result for external Q is given in the bottom-left figure. From this plot, it is clear that the insertion length ranges within 24 to 36 mm to meet the range of $10^{6\text{-}7}$ for Q_{ext}.

Table 2: R&D History of Plug-compatible STF-type Power Coupler

Date	Content
Nov/2013	Recommendation for plug-compatible design from LCC in LCWS2013 [6]
Feb/2014	Completion of mechanical design
Jun/2014	Completion of RF design by simulation
Nov/2014	Completion of prototype coupler fabrication
Mar/2015	Incoming inspection in KEK
Aug/2015	Assembly work in clean room (Warm #1, #2 + Cold #1, #2)
Dec/2015	Low power test at bench
Jan/2016	High power test at bench
Feb/2016	Dis-assembly, and re-assembly work in clean room (Warm #1, #2 + Cold #3, #4)
Feb/2016	Low power test at bench
Mar/2016	High power test at bench

Full Test Bench Model

After the calculation for the coupling to the cavity, the simulation was done for the full test bench model connected with two power couplers including the bellows to check the RF matching, as shown in the bottom-right figure in Figure 1. It typically took several hours per run to do this simulation. At this time, the waveguide system and the doorknob are the previous type, not optimized for this plug-compatible STF-type power coupler. This might generate the unexpected phenomena with some risks in the both of low and high power tests.

Content from this work may be used under the terms of the CC BY 3.0 licence (© 2017). Any distribution of this work must maintain attribution to the author(s), title of the work, publisher, and DOI.

ISBN: 978-3-95450-191-5 doi:10.18429/JACoW-SRF2017-MOPB065

DEVELOPMENT OF HYBRID SUPERCONDUCTING PHOTOCATHODES ON NIOBIUM USING HIGH QE COATINGS

M. Warren†, Z. Yusof, L. Spentzouris, N. Samuelson, A. Denchfield, J. Zasadzinski,
Physics Department, Illinois Institute of Technology, Chicago, IL 60616, USA
W. Gai, E. Wisniewski, J. Shao, AWA, Argonne National Lab, Argonne, IL 60439, USA

Abstract

The quantum efficiencies (QE) and other relevant properties of photocathodes consisting of bulk Nb substrates coated with thin films of Cs_2Te and Mg are reported. Using the standard recipe for Cs_2Te deposition developed for Mo substrates (220 Å Te thickness), a QE ~11% - 13% at light wavelength of 248 nm is achieved for the Nb substrates, consistent with that found on Mo. Systematic reduction of the Te thickness for both Mo and Nb substrates reveals a surprisingly high residual QE ~ 6% for a Te layer as thin as 15 Å. A theoretical investigation based on the Spicer 3-Step model along with a solution of the Fresnel equations for reflectance, *R*, leads to a reasonable fit of the thickness dependence of QE and suggests that layers thinner than 15 Å may still have reasonably high QE. Such an ultra-thin, semiconducting Cs_2Te layer may be expected to produce sharp electron bunches with minimal ohmic losses for RF frequencies ~ 1 GHz.

For Nb/Mg bilayers dark current measurements up to 60 MV/m were obtained at the Argonne Wakefield Accelerator test station and fitted using Fowler-Nordheim theory. Enhanced field emission is likely due to surface roughness of the Nb substrate. The Mg layer appears to be robust down to 10 nm with no serious damage in high fields. A factor of 10 increase in QE over the bare Nb is found without any surface treatment of the Mg.

INTRODUCTION

Future free-electron-laser (FEL)-based light sources will require low emittance, high brightness and high average-current electron beams, necessitating high duty cycle (> 1 MHz) or effectively CW operation [1]. Superconducting radiofrequency (SRF) photoinjectors made of pure Nb are currently a favored choice for producing such beams as they dissipate significantly less power than normal RF guns [2]. The photocathode is an integral component of the photoinjector, contributing to the surface RF impedance, and therefore ideally it should be superconducting as well. A replaceable, superconducting plug cathode would be particularly attractive for a compact SRF linac as it has a simple design [2,3]. Recent advances in Nb-based SRF cavities, including record high Q values at 15-20 MV/m via a nitrogen doping process [4], as well as the successful in-situ growth of higher T_C Nb_3Sn on the inside surface [5, 6] suggests that a compact electron linac operating at 4.2 K is feasible in the future. The limiting factor is that the current choices of superconducting photocathode have relatively low quantum efficiencies (QE), e.g., for Nb QE < 0.01% and for Pb QE < 0.1% at 248 nm wavelength [3].

A potential way out of this difficulty is to consider hybrid structures whereby a thin film coating of a high QE material is deposited onto a bulk superconductor such as Nb or Nb_3Sn. For metallic overlayers, there is the phenomenon of the superconducting proximity effect which allows a thin, non-superconducting surface layer to acquire a Cooper pair condensate (zero dc resistance), and energy gap, via coupling to the underlying superconducting substrate [7,8]. Such an approach seems particularly attractive for thin films of Mg on Nb where earlier proximity effect studies have shown promising results [9]. Also, Mg has one of the highest QE values of any metallic element, ~ 0.1% at 248 nm. More detailed results on such Nb/Mg hybrid structures will be reported elsewhere [10].

High peak current is more easily obtained with semiconductor cathodes such as cesium telluride (Cs_2Te) [11,12]. It has a QE as high as 20% and has consistently produced a QE > 1% during normal accelerator operations over a period of at least a year, providing a relatively large bunch charge per laser pulse, and has been shown to be robust in a photoinjector environment. It has been used as an electron source in SRF photoinjectors, but only as a normal-state photocathode[13]. This requires a more complex engineering design to isolate the cathode from the rest of the superconducting cavity. It typically consists of an SRF cavity injector with a hole so that a high-QE normal photocathode can be introduced through a long rod, requiring an additional choke to minimize RF losses through the hole. Separate cooling and vacuum loading systems are also required. While this allows an electron pulse with high peak current, it is not clear if this method will meet the future needs of CW operation and, furthermore, may not be suitable for a compact linac.

Here we consider the use of Cs_2Te for a hybrid superconducting photocathode. Given that it is a semiconductor, the proximity effect might be weak or nonexistent. [7,8,9] However, even in the absence of any induced superconductivity, a very thin semiconducting surface layer may be highly transparent to the applied RF and contribute minimally to the surface impedance, which will still be determined predominantly by the underlying Nb substrate, while still providing the advantage of a higher QE than a metallic superconductor. Thus our study focuses on ultra-thin films of Cs_2Te on Nb substrates with thicknesses significantly less than the typical Te layer thickness (210Å) of Cs_2Te used in the standard "recipe" grown on a Mo substrate. The results thus far are reproducible and very encouraging. We find that the QE of Cs_2Te on Nb is nearly

† email: mwarren3@hawk.iit.edu

Content from this work may be used under the terms of the CC BY 3.0 licence (© 2017). Any distribution of this work must maintain attribution to the author(s), title of the work, publisher, and DOI.

ISBN: 978-3-95450-191-5 doi:10.18429/JACoW-SRF2017-MOPB066

DEVELOPMENT OF 81.25 MHz 20 kW SSPA FOR RAON ACCELERATOR

Ohryong Choi†, Hyojae Jang, Kitaek Son, Doyoon Lee, and Hoechun Jung,
Rare Isotope Science Project, Institute for Basic Science, Daejeon, Korea

Abstract

A heavy ion accelerator, RAON is under development in Daejeon, Korea by Rare Isotope Science Project (RISP).In this accelerator, 81.25 MHz Radio Frequency Quadrupole (RFQ) will be used for the acceleration of various ions from several tens of keV/u to about half MeV/u [1]. For this system two 80 kW RF power sources are planned and RISP will develop them with a solid state power amplifier (SSPA) architecture. As a first step, a 20 kW SSPA was developed and the performance was tested. In this presentation the current status of developed SSPA and the test results will be presented.

INTRODUCTION

A SSPA system is used to supply RF to RFQ cavity in RAON. It consists of PSU, drive unit, final unit (4EA), circulator, combiner, and directional coupler. The power supply unit (PSU) is a device that supplies power to the drive and final amp. The purpose of the drive amplifier is to deliver power to the final amplifiers. Also, in the drive amplifier, the output of the same phase is divided into four and transmitted to each of the final amplifier inputs. The final amplifier is a device that can obtain high power by using LDMOS transistor [2]. And in order to cool the heat generated from the LDMOS transistor, a water cooling system is necessary. Circulator is a protective device for the SSPA by blocking the flow of the reflected RF to the SSPA and dumping it to the water cooled dummy load. The combiner is a device used to synthesize the power of final amplifiers in order to obtain the high power. The dual directional coupler is a device to monitor the forward power and reflected power of the SSPA. Fig. 1 shows the structure of the HPRF system for RFQ cavity in RAON.

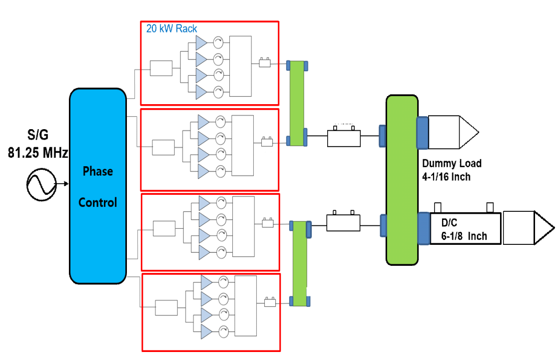

Figure 1: HPRF system for RFQ cavity in RAON.

The HPRF system of RFQ was to generate 20kW power per one rack. Inside the Rack, there are of 4 final amplifiers, and Fig. 2 is the internal structure of the final amplifier.

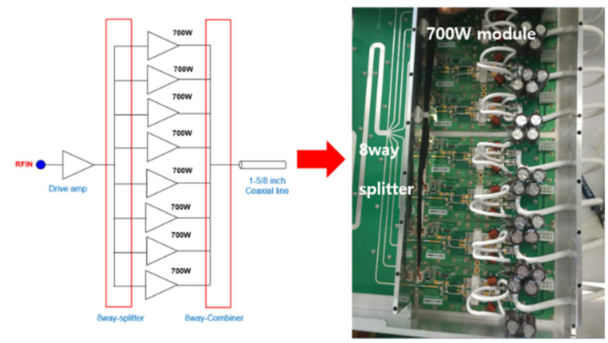

Figure 2: Block diagram of the final amplifier in 20kW rack.

We used 8-way splitter and combiner based on PCB. Internal transistor adopts LDMOS technology, and it has advantages such as the high efficiency, and the operation with mismatched power well. Each final amplifier is equipped with a circulator for protection from reflected power. We also install a high power combiner for synthesizing high power from four final amplifiers.

FULL POWER TEST OF 5 kW UNIT

In the 19-inch rack, a 5 kW final amplifier was mounted with a circulator and a full power test was performed. Fig. 3 shows 5 kW full power test bench.

Figure 3: 5 kW Full power test bench.

†cor@ibs.re.kr

Content from this work may be used under the terms of the CC BY 3.0 licence (© 2017). Any distribution of this work must maintain attribution to the author(s), title of the work, publisher, and DOI.

ISBN: 978-3-95450-191-5 doi:10.18429/JACoW-SRF2017-MOPB068

DEVELOPMENT OF 4-WAY 81.25 MHz 20 kW HIGH POWER COMBINER USING PARALLEL PLATE STRUCTURE *

Kitaek Son†, Hyojae Jang, Ohryong Choi, Doyoon Lee and Hoechun Jung
Rare Isotope Science Project, Institute for Basic Science, Daejeon, Korea

Abstract

The recent development of semiconductor technology has proved that solid-state RF amplifier is a quite effective alternative high power RF source for numerous accelerator applications. To develop a high power SSPA system, high power combiner is required to combine the RF power from a lot of solid-state RF module [1]. The parallel plate RF power combiner, which is designed to combine various high power modules, is developed for RAON (Rare the rare isotope accelerator complex for on-line experiment). In this presentation, the status of developed 81.25 MHz 20 kW power combiner will be described.

INTRODUCTION

The RAON adopts solid state power amplifier as a power source for providing RF fields in RF cavity. Until now, the source of the HPRF (high power RF) system is mainly using klystrons to supply E-field in the cavity at the accelerator. However, in recent years, performance of SSPA (solid state power amplifiers) has been improved, and it is good enough to replace klystrons as the main system. Semiconductor Transistor using LDMOS (laterally diffused metal oxide semiconductor) technology currently has more than power of 1 kW [2]. In addition, it is developed to prevent the reflecting power effectively generated from impedance mismatching. SSPA devices used for RFQ cavity in RAON are equipped with four units in the 19-inch rack. In order to provide RF power of 10 kW or more in 19-inch rack, combiner that can integrates multiple SSPA devices is required to synthesize high power. Power combiners of less than 5 kW can be fabricated on a conventional PCB. But the high power combiner more than 5 kW has limitations in fabrication based on conventional a PCB. Therefore, RF group working for RAON project designed the combiner that can synthesize more than 20 kW RF power by using two thick silver-plated plates separated by 1~2mm.

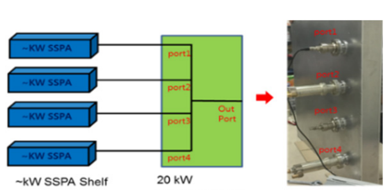

Figure 1 : Structure of 4way combiner to integrate SSPA(solid state power amplifier) unit.

†skt1385@ibs.re.kr

We performed drawing work by using 3D inventor tool. The combiner was fabricated based on the 3D drawings and the result is obtained by using VNA (vector network analyzer). Figure 1 shows a combiner structure to integrate four SSPA devices. In order to combine SSPA devices for RFQ cavity, the high power combiner that can withstand more than RF power of 20 kW is required [3]. Generally, n-way RF combiners are designed with two types; Wilkinson-type or Gysel-type. The structure of combiner was designed with the Gysel method to synthesize high power over 20 kW. The Gysel structure has the advantage that a ballast resistance over 1kW can be connected to an external ground. In addition, the two silver-plated plates inside the combiner are designed to be in a stable quasi-TEM mode by keeping the spacing in parallel. Figure 2 shows the Wilkinson and Gysel structure.

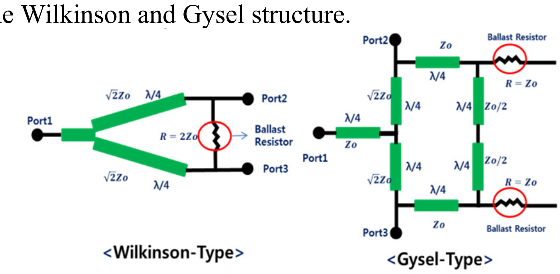

Figure 2 : Two structures to fabricate high power RF combiners.

SIMULATION OF THE GYSEL COMBINER

The HPRF SSPA used in the RFQ cavity consists of the 20 kW power systems in a 19-inch rack. There are four SSPA (solid state power amplifier) units in the rack and the 4-way high power combiner to synthesize the power of the four SSPA units. The thickness of the silver-plated plate inside the combiner is designed to withstand a high power more than 20 kW.

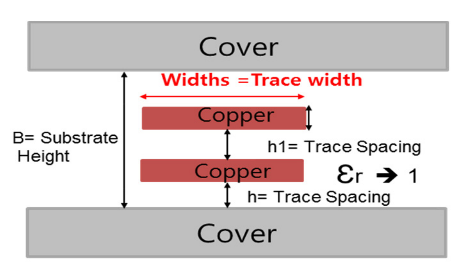

Figure 3: Structure of parallel plate.

Content from this work may be used under the terms of the CC BY 3.0 licence (© 2017). Any distribution of this work must maintain attribution to the author(s), title of the work, publisher, and DOI.

ISBN: 978-3-95450-191-5 doi:10.18429/JACoW-SRF2017-MOPB069

DESIGN OF THE HIGH POWER INPUT COUPLER FOR CEPC MAIN RING CAVITY

T. Huang, Q. Ma, K. Gu, J. Zhai, Institute of High Energy Physics (IHEP), Beijing, China

Abstract

The main ring cavities of CEPC project are two-cell elliptical superconducting cavities operating at 650 MHz in CW mode. Each cavity equips with one high power input coupler and each coupler has to deliver at least 300 kW of CW RF power to the beam. A variable coupling from 1E5 to 2E6 is required to meet different operation modes. Considering the cavities working with high quality factor up to 2E10, the coupler assembled with cavity in class 10 clean room is strongly recommended to protect the cavity from contamination. Also, low cryogenic heat loss is one of the important issues for a large scale CW operation machine. Some of the above requirements should be compromise. Therefore, it's a big challenge to design a high power input coupler fulfilling the above requirements simultaneously. A new coupler that employs 75 Ohm coaxial line sections, a planar ceramic disk window, a coaxial to waveguide transition and a coupling adjusting actuator has been designed. In this paper, the RF design, thermal stress analysis and preliminary mechanical design of the coupler are presented.

INTRODUCTION

CEPC is a 100 km circular electron positron collider operating at 90-240 GeV center-of-mass energy of Z, W and Higgs bosons. The SRF system parameters of the CEPC Main Ring is in reference [1]. Each cavity equips with one power coupler and each coupler has to deliver at least 300 kW of CW RF power to the beam. The different requirements at Z, W and H operation have imposed the use of a variable power coupler with a coupling value varying from 1E5 to 2E6. In the meanwhile, considering the large scale and high performance requirement of CEPC, clean assembly, low cryogenic heat loss, high reliability and low cost are also important issues of the coupler design. The main requirements of power coupler are summarized in Table 1.

The main design challenges are:

• High average RF power: more than 300 kW, CW, TW;

• Wide range of variable coupling: factor of 20;

• Clean assembly: coupler and cavity assembled in class 10 clean room;

• Low cryogenic heat loss: 2 K dynamic heat loss less than 1 W at 300 kW, CW, TW.

Table 1: The Main Requirements of the Power Coupler

Parameters	Value
Frequency	650 MHz
Power	300 kW, CW, TW
Q_e	1E5 to 2E6
2 K heat loss	1 W (dynamic, 300 kW, CW, TW)
Assembly	Coupler and cavity assembled in class 10 clean room

RF DESIGN

The power coupler of BEPCII 500MHz SCC has been proved excellent high power handling capability and mechanical reliability [2]. Therefore, we take into account the experience during the CEPC main ring coupler design. The general layout of the coupler assembly is shown in Fig. 1. Like BEPCII coupler, this coupler consists of three sub-assemblies: 1) doorknob to realize the transition from waveguide to coaxial line; 2) RF window to provide RF-transparent vacuum barrier; 3) coaxial line to transfer and feed RF power into the cavity. The outer diameter of the disk ceramic is of the same size as that in the BEPCII coupler; the doorknob dimensions are scaled to adapt 650MHz.

Too meet the special requirements of CEPC main SCC, the structure modifications based on BEPCII coupler are the follow:

• A larger profiled antenna tip is designed to provide a strong coupling;

• Two sections of bellows are adopted on the outer conductor to realize a coupling adjusting;

• The length of the vacuum part reduced greatly to assure the coupler assembled with cavity in class 10 clean room;

• The impedance of the coaxial line changed from 50 Ohms to 75 Ohm to achieve a low dynamic heat loss and increase the multipacting power level above 300 kW.

Content from this work may be used under the terms of the CC BY 3.0 licence (© 2017). Any distribution of this work must maintain attribution to the author(s), title of the work, publisher, and DOI.

18th International Conference on RF Superconductivity SRF2017, Lanzhou, China JACoW Publishing
ISBN: 978-3-95450-191-5 doi:10.18429/JACoW-SRF2017-MOPB070

THE IMPROVEMENT OF THE POWER COUPLER FOR CADS SC SPOKE CAVITIES*

T.Huang†, Q.Ma, H.Lin, X.Chen, G.Wang, W.Pan, Z.Li, K.Gu, F.Meng, F.Bing,
Institute of High Energy Physics (IHEP), Beijing, China

Abstract

Twenty superconducting spoke cavities mounted in three cryomodules (CM1, CM2 and CM4) were installed in the CADS, a test facility of 10 mA, 25 MeV CW proton linac. Each cavity was equipped with one coaxial type fundamental power coupler (FPC). Fatal window crack was observed during the test cryomodule (TCM) commissioning. A series of experiments were subsequently implemented and eventually attributed the window crack to the electron bombardment from cavity field emission (FE). Improvements covering the coupler cleaning and assembly procedure, the structure and position modifications were thus implemented, aiming to reduce the cavity contamination and avoid the window damaged by cavity FE electrons.

This paper will describe how the coupler window damaged by cavity field emission and the improvements for cure. In addition, the performances of FPCs for CM1, CM2 and CM4 were compared.

INTRODUCTION

Accelerator Driven sub-critical System (ADS) is a proton accelerator-based facility to produce energy and to destroy nuclear waste efficiently. The China ADS (CADS) project, started in 2011, aiming to construct a 15 MW continuous wave (CW) proton linac of 1.5 GeV and 10 mA from 2011 to 2030s. As a pilot project, the goal of the R&D phase is to build a 25 MeV proton linac by 2016 and to solve some critical technical problems. Figure 1 shows the schematic of the R&D phase of CADS. Two different Injector schemes are proposed: IHEP (Institute of High Energy Physics) is responsible for Injector-I and IMP (Institute of Modern Physic) is responsible for Injector-II [1]. Fourteen beta=0.12 superconducting spoke cavities mounted in two cryomodules (CM1 and CM2) were installed in the CADS Injector-I; and each cavity was equipped with one 10 kW fundamental power coupler (FPC). The main linac section consists of two cryomodules (CM3 and CM4). Six beta=0.21 superconducting spoke cavities were adopted in CM4; and each cavity was fed by one 20 kW FPC.

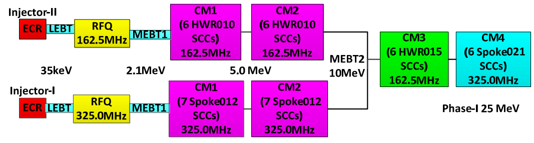

Figure 1: The schematic of the R&D phase of CADS.

* Work supported by the "Strategic Priority Research Program" of the Chinese Academy of Sciences, Grant No. XDA030209
† huangtm@ihep.ac.cn

In accordance to the progress of construction and technical difficulties, the commissioning of Injector-I was carried out in several steps. Firstly, two spoke cavities with two FPCs were installed in a test cryomodule (TCM). Fatal window crack was observed during the TCM commissioning. A series of experiments were subsequently implemented and eventually attributed the window crack to the electron bombardment from cavity field emission. The assembly procedure of the FPCs for CM1 cavities was thus optimized to avoid the cavity contamination; along with the coupler clean procedure, the structure and position modifications for CM2 and CM4 cavities. This paper will describe how the coupler window damaged by cavity field emission and the improvements for cure. In addition, the performances of FPCs for CM1, CM2 and CM4 were compared.

WINDOW DAMAGE BY CAVITY FIELD EMISSION

The RF processing of the TCM housing two cavities and two FPCs started in January, 2015. While unexpected fatal window crack were encountered during the RF processing. The following characteristics were observed based on further inspection and experiments:

- The ceramic crack usually happened at a RF power level of less than 1 kW, even with very tight vacuum interlock of 1E-6 Pa;
- Power can easily reach to 3 kW when the cavity detuned; however, once cavity tuned, ceramic cracked after several times of periodically triggered arc events. So we deduce that the fatal crack might have something to do with the cavity performance;
- Large X-ray dose was measured near the window when cavity gradient above 3 MV/m, which indicated serious field emission (FE) happened within the cavity;
- There is no electron or iron bombarding trace on the RF surface of the coupler, which indicated no serious Multipacting and discharging inside the coupler.

Based on above characteristics, we speculate the reason of the ceramic crack is as follows: first, serious FE happened in the cavity, then electrons flied out from the coupling port and impacted directly on the vacuum side of the ceramic, which made the ceramic charged; and then electrostatic discharging happened once exceeding the ceramic breakdown voltage; Finally, the strong energy released from the discharging made the ceramic punctured along the thickness direction and resulted in fatal vacuum leak.

Content from this work may be used under the terms of the CC BY 3.0 licence (© 2017). Any distribution of this work must maintain attribution to the author(s), title of the work, publisher, and DOI.

ISBN: 978-3-95450-191-5 doi:10.18429/JACoW-SRF2017-MOPB071

THE RECENT RESEARCH OF HOM DAMPER FOR SUPERCONDUCTING CAVITY IN IHEP

F. Meng †, H. Zheng, P. Zhang, W. Pan, T. Huang, Q. Ma, H. Lin, J. Zhai
Institute of High Energy Physics (IHEP), Beijing, China

Abstract

For high current accelerator, the efficient higher-order mode (HOM) damping is always an important issue. HOM damper with microwave absorbing material is a key component for high power and broadband HOM damping application. To pursue the high damping efficiency, some ideal material with good microwave absorbing capacity is essential during the RF design and fabrication phase. Sometimes the selection and test of material is the first step and also a long step. This paper will present the recent work on HOM dampers for BEPCII 500MHz cavity and CEPC 650MHz cavity in IHEP.

INTRODUCTION

High Energy Photon Source (HEPS) has been initiated by IHEP in Beijing, which is a 6GeV kilometre-scale light source [1]. In the planned on-axis beam injection scheme, the 499.8MHz ellipsoidal SC cavity will be used as the third-harmonic cavity, which will work with the fundamental 166.6MHz quarter-wave SC cavity [2]. For the high current requirement of HEPS, the HOM damper located on the beam pipe is essential in the 499.8MHz SRF system. Since the same frequency, the design and experience of BEPCII 500MHz SRF system will be used in this project. The research on 500MHz HOM damper (the HOM damper used for 500MHz cavity) has been developed for the 500MHz spare cavity in IHEP several years ago. Based on this successful experience, this paper will describe the recent work on 500MHz HOM damper, about RF design optimization to lower the fabrication cost and absorbing capacity research of ferrite, and so on.

To explore the magic Higgs Boson for high energy physics, the R&D of Circular Electron-Positron Collider (CEPC) has been promoted by IHEP in the collaboration with some other institutes and university. CEPC will be a 120GeV 100 km ring collider with high luminosity. The 650MHz 2cell ellipsoidal SC cavity is adopted as the main accelerating cell in the storage ring [3]. Due to the short bunch length, the HOM spectrum is extremely wide. The beam pipe HOM damper will be used to suppress the HOM power from 1.5GHz to 20GHz, which is above the cut-off frequency of beam pipe [4]. For the broadband absorbing requirement, some new materials need to be explored. At the latter part of this paper, the recent design and exploration of 650MHz HOM damper will be reported.

* The work of CEPC 650MHz cavity HOM damper described in this paper was supported by National Key Programme for S&T Research and Development (Grant NO.: 2016YFA0400400).
† E-mail: mengfb@ihep.ac.cn

500MHz DAMPER OPTIMIZATION

The research on 500MHz HOM damper has a long history, since the typical design of Cornell CESR type and KEKB type [5]. Years ago, the 500MHz damper has been developed successfully for the spare cavity in IHEP, the prototype is shown in Fig. 1. This IHEP type damper used ferrite as its RF absorbing material. The ferrite on the inner surface of damper is arc-shaped, which can fit the cylinder shape with 8 pieces. This damper had an excellent absorbing efficiency, which is higher than 50% around 1GHz.

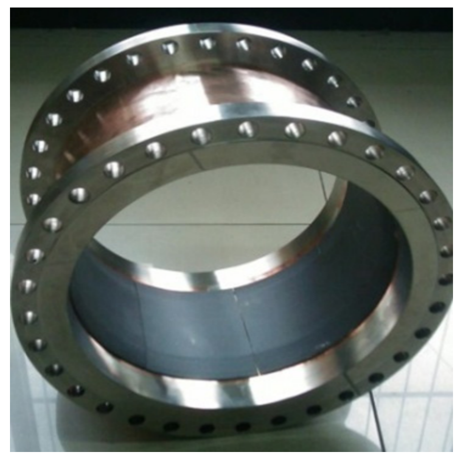

Figure 1: IHEP 500MHz HOM damper for spare cavity.

Due to the arc-shaped ferrite, the material preparation and the brazing technology is too difficult to lower the yield of damper. As a consequence, the development cost is expensive. For the economic consideration, it is an attractive job to optimize the RF design of damper to make a balance between the absorbing efficiency and fabrication cost.

The direction of optimization is to make the shape of ferrite more convenient for processing. Naturally, the first choice is ferrite sheet. As we know, it will increase the reflection of RF power on the contact section, that using the polygon to fit the circle. So the ferrite size and some other feature should be optimized to realize impedance matching, in order to decrease the reflection coefficient. As a result, the absorbing efficiency of damper will not change too much, sometimes even better. The optimized RF structure of damper is shown in Fig. 2.

Content from this work may be used under the terms of the CC BY 3.0 licence (© 2017). Any distribution of this work must maintain attribution to the author(s), title of the work, publisher, and DOI.

ISBN: 978-3-95450-191-5 doi:10.18429/JACoW-SRF2017-MOPB072

THE DEVELOPMENT OF THE LLRF CONTROL SYSTEM FOR THE NEW HIGH POWER TEST STAND OF COUPLERS *

L. Chen†, W.Chang, Y.M. Li, C.L. Li, T.C. Jiang, R.X. Wang, S.h. Zhang, IMP, Lanzhou, China

Abstract

The procedure of room-temperature high power test or condition for couplers is very import, which can hardly be circumvented before they are assembled on the accelerating cavities [1]. A new high-power test stand of fundamental mode power coupler is under development at IMP. The design, assembly and test of the RF control system has been finished up to date. This paper introduces the major functions of the LLRF control system. The test results of the arc interlock, RF test and the test of the system as a whole have been present.

INTRODUCTION

RF control system is crucial for the development of the new test stand. There are a few disadvantages for the precedent LLRF control system:

- Control devices are not compact enough.
- Remote control is not available.
- Real-time test power can't be displayed.
- The output of source signal is not precise especially in amplitude sweeping mode.

In view these shortcomings, the precedent control system can hardly meet our demand. The new control system is aimed to solve the problems just mentioned above. In addition to the conditioning modes in the old control system, including amplitude sweeping conditioning mode, pulse conditioning mode, we've embed the system with auto-conditioning mode and we've also altered the amplitude sweeping mode by adding a plateau between the "gonging up" and "gonging down" of the output power, forming trapezoid-wave in order to improve the efficiency of conditioning. Fig. 1 shows the functions we aim to accomplish in the new LLRF control system.

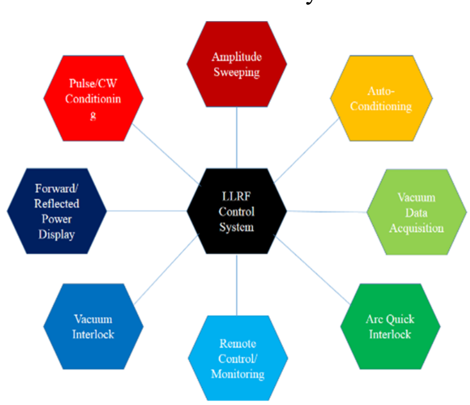

Figure 1: Layout of the functions of the new LLRF control system.

* Work supported by the Youth Innovation Promotion Association CAS and special fund on equipment from CAS.
† chenlong15@impcas.ac.cn

To accomplish the desired functions, data sampling, input and output of digital and analogue signals, and fast and reliable timing are all involved. We take the product of myrio-1900(left picture in Fig. 2) produced by NI company as the core of the LLRF control system. And the whole system is developed with Labview2016. The right picture in Fig. 2 shows the new compact LLRF system.

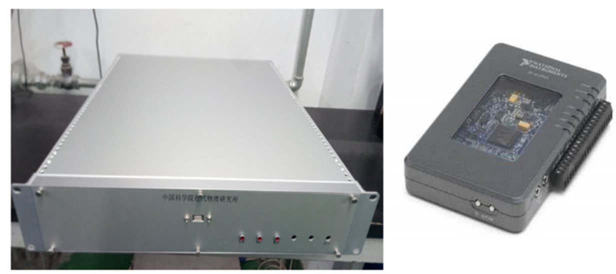

Figure 2: LLRF control system (Left) and Myrio 1900 (Right).

THE ACCOMPLISMENT OF SUNDRY CONDITIONING MODES

Pulse/CW Conditioning Mode

Practical conditioning experience has shown that conditioning in pulse mode is the most demanding step through the whole progress [2]. It's majorly because outgassing caused by multipacting is extremely serious at the beginning. Conditioning can hardly be continuous due to frequent vacuum interlocks and arc interlocks. Pulse mode in certain duty factor can make conditioning sustainable by reducing the period that multipacting lasts in the couplers, which brings less intensive outgassing. To obtain pulse signal in flexible pulse length and repetition, we utilize a fast rise (6ns) RF switch (ZYSWA-2-50DR) in Fig. 3, which has 50Ω matching resistance and is driven by TTL voltage. The pulse length can be calculated out by the PC with the input repetition frequency and duty factor, according to which the FPGA control the time that the driven TTL lasts. Because of the excellent timing of FPGA, the pulse short to 1μs can be produced.

Amplitude-Sweeping Modes

Sweeping RF amplitude is also an effective and non-dispensable way to condition couplers because of the possible recurrence of multipacting at some RF power points [2]. The precedent system can only provide triangle-wave amplitude sweeping and due to the impreciseness of timing in PC machine, amplitude-sweeping can hardly be controlled perfectly. The consequence of it is that the power nay rush

Content from this work may be used under the terms of the CC BY 3.0 licence (© 2017). Any distribution of this work must maintain attribution to the author(s), title of the work, publisher, and DOI.

ISBN: 978-3-95450-191-5 doi:10.18429/JACoW-SRF2017-MOPB074

ANALYSIS OF HIGHER ORDER MODES OF THE SUPERCONDUCTING CAVITIES FOR THE CHINA-ADS INJECTOR-II IN IMP*

C. Zhang†, Y. He, S. H. Zhang, W.M. Yue, A. D. Wu, S. X. Zhang, R. X. Wang, Y. M. Li, T. C. Jiang, Y.L. Huang, S. C. Huang, F. Pan, L. Chen, Q. J. Wu
Institute of Modern Physics, Lanzhou, China

Abstract

The influence of the higher order modes on the beam dynamics and the cryogenic losses has been studied for the superconducting half wave resonators of the China ADS in this paper. In addition, the necessity of HOM dampers in the Superconducting (SC) cavities is discussed.

INTRODUCTION

The Accelerator Driven System for nuclear waste transmutation of China (China ADS) is a high intensity CW proton beam facility which is based on the superconducting accelerating structure with the design specifications of 10 mA beam current and 25 MeV based on the half wave resonator (developed by Institute of Modern Physics) and spoke cavities (developed by Institute of High Energy Physics) [1]. In this work, two types of half wave resonator cavities (f=162.5MHz, β_{opt}=0.10, 0.15 [2]) of IMP have been investigated for their possible dangerous HOMs.

STUDY OF HOMS

For the high current CW acceleration, the higher order modes should be considered, as they may lead to extra heating loads to the superconducting cavity. In the paper, according to the beam parameters of the China ADS as beam current 10 mA and repetition frequency of 162.5 MHz, HOMs have been discussed.

Calculation Methods and Simulation Results

- Monopoles:

When bunches travel along the beam axis, the monopole will be excited, and the equilibrium voltage can be derived for the CW operation at n-order of monopole [3,4,5]:

$$V_{CW,n} = \Delta V_{q,n} \sum_{m=0}^{\infty} exp\left(-m\frac{T_b}{T_{d,n}} + im\omega_n T_b\right) = \frac{\Delta V_{q,n}}{1-exp(-\frac{T_b}{T_{d,n}}+i\omega_n T_b)}. \quad (1)$$

In which, $\Delta V_{q,n}$ =-q*(ω_n/2)*(R/Q)$_n$(β) is voltage excited by the point-like treated bunch, $T_{d,n}=2Q_{L,n}/\omega_n$ is the decay time constant with $Q_{L,n}=1/(Q_0^{-1}+Q_{ext}^{-1})$ the loaded quality factor. The dissipated power can be calculated by:

$$P_{C,n} = \frac{V_{CW,n}^2}{(\frac{R}{Q})_n * Q_{0,n}}. \quad (2)$$

- Dipoles:

The off axis bunch can excite dipole modes, the transverse voltage excited can be expressed [4,5]:

$$\Delta V_{\perp,n} = \frac{1}{2} ixq \frac{\omega_n^2}{c} \left(\frac{R}{Q}\right)_{\perp,n} (\beta). \quad (3)$$

The transverse R/Q can be given as:

$$\left(\frac{R}{Q}\right)_{n,\perp}(\beta) = \frac{\left|\int_{-\infty}^{\infty} E_{n,z}(\rho=a) exp\left(i\omega_n \frac{z}{\beta c}\right) dz\right|^2}{(k_n a)^2 \omega_n U_n}. \quad (4)$$

where $k_n=\omega_n/c$. And the dissipated power of dipole modes can be calculated in the same way as the monopole modes.

The HOM calculations have been done with MWS of CST [6] as presented in Table 1 and Table 2.

Table 1: RF Parameters of HOMs for HWR-0.10

Modes	Frequency (MHz)	V_c (*10^5V)	V^*_c (*10^5V)	R_a/Q_0 (Ω)	$(R_a/Q_0)_l$ (Ω/m²)
M1	162.5	4.8		113.2	/
M2	346.77	0.005	2.5	~0	1360
M3	500	4.4		30	/
M4	676.6	0.009	5	~0	734
M5	767.4	3		38	/
M6	816.4	0.033	1.4	~0	32
M7	820.4	0.03	1	~0	16.4
M8	832.3	0.064	0.07	~0	0.086
M9	848.2	4.2		17	/
M10	898.8	6		32	/
M11	954.6	0.035	3.2	~0	107
M12	1004	~0	1.18	~0	12.5
M13	1005	0.02	3.14	~0	88
M14	1040	0.16	0.15	0.02	0.18
M15	1130	5.72		23	/

*V_c^*: for some modes with very weak longitudinal electric field along the beam axis, voltage was calculated along the axis off the beam axis 20mm.

Table 2: RF Parameters of HOMs for HWR-0.15

Modes	Frequency (MHz)	V_c (*10^5V)	V^*_c (*10^5V)	R_a/Q_0 (Ω)	$(R_a/Q_0)_l$ (Ω/m²)
M1	162.5	6.2	/	192	/
M2	317	0.003	0.5	~0	71.3
M3	418	5.6	/	60	/
M4	458	8.6	/	126	/
M5	519	0.006	0.84	~0	45.9
M6	543	0.02	0.05	~0	0.14
M7	544	0.009	0.6	~0	20
M8	589	5.8	/	46	/
M9	630	0.013	1.2	~0	52
M10	650	0.008	1.7	~0	95
M11	712	5	/	28	/
M12	768	0.0009	1.7	~0	58
M13	773	0.006	0.05	~0	0.05
M14	826	5	/	24	/

The effective impedance distribution for monopole and dipole are shown in Figure 1 and Figure 2.

* Work supported by Natural Science Foundation of China, No.11505253
† email address: zhangcong@impcas.ac.cn

Content from this work may be used under the terms of the CC BY 3.0 licence (© 2017). Any distribution of this work must maintain attribution to the author(s), title of the work, publisher, and DOI.

ISBN: 978-3-95450-191-5 doi:10.18429/JACoW-SRF2017-MOPB075

QUENCH PROTECTION IN DIGITAL POWER SUPPLIES FOR SUPER-CONDUCNTING MAGNETS IN ADS

J. Zhao, S. Zhang, Z. Z. Zhou, Institute of Modern Physics,Chinese Academy of Sciences, Lanzhou, China

Abstract

The front-end demo superconducting Linac for Chinese ADS (Accelerator Driven Sub-critical System) project is under construction at institute of modern physics (IMP) in Lanzhou. It will demonstrate the key technologies and the feasibility of a high power beam for the future national project "the Chinese Initiative Accelerator Driven Subcritical System (CIADS)". In this system, there are about 60 superconducting magnets, including solenoids, vertical corrector and horizontal corrector. They are utilized to focus and correct the proton beam. Quench protection of the superconducting magnets is key to reliability of the facility. A full digital power supply is developed and employed as excitation source for all of these superconducting magnets. In this paper, an FPGA-based Quench protection scheme implemented in the power supplies is mainly described. The commissioning results show that it is feasible.

INTRODUNCTION

The front-end demo for Chinese ADS project is constructing at the Institute of Modern Physics (IMP) in Lanzhou. It is one of the major tasks of the China accelerator driven sub-critical system (China ADS) proposed by Chinese Acadamy of Sciences (CAS) is one of "Stratage Tecnology Pilot Project" started in 2011. The 25 MeV, 10mA, continuous-wave (CW) superconducting proton Linac will to the key technologies and the feasibility of a high power beam for the future national project "the Chinese Initiative Accelerator Driven Subcritical System (CIADS)".

There are about 60 superconducting solenoids in this in this facility. The objective of the superconducting solenoid is to focus and correct proton beam. The effective length of a superconducting solenoid is 200 mm. And each solenoid has one vertical correction and one horizontal correction. The quench of the magnets is an important question for this project, so it is necessary to talk about implementation of quench. In this project, A quench protection scheme which is carried out inside power supplies for the superconducting magnets was adopted.

POWER SUPPLIES FOR SUPER-CONDUNCTION MAGNET

Main Circuit

The power supplies for the superconducting magnets are a full digital power supply [1]. They are specially developed for the superconducting magnets in Chinese ADS project. The rated value of power supplies for the superconducting solenoids is ±180A/5V, and the rated value of the power supplies for their corrector is ± 25A/5V. A schematic diagram of main circuit structure is show in Figure 1. The C1 is energy-storage capacitor, the K1~K4 means H bridge structure. The discharge circuit consists of the K5, K6, R1, R2 and L (R2 and L are parameters of load). The inductance of the superconducting solenoid is about 1.4 H. And the inductance of their corrector is about 0.036H. The discharge circuit is controlled by the quench signal from the superconducting magnets. The discharge circuit has two state: normal state and quench state. In normal state，the two switcher (K5 and K6) keep open; in quench state, the K5 is closed and K6 is open if current is positive. In quench state, the K6 is closed and K5 is open if current is negative. The state transition of all the switchers is in charge of the FPGA-based digital controller.

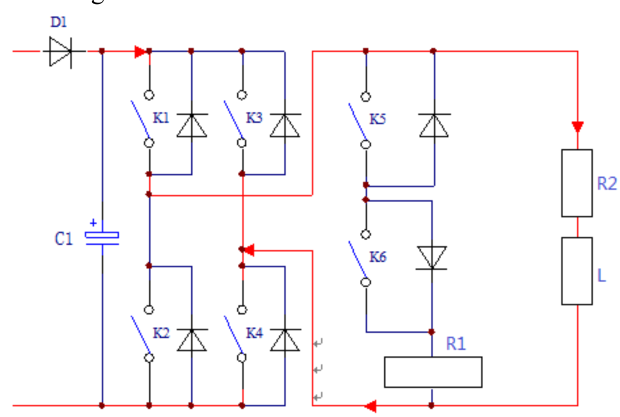

Figure 1: A schematic diagram of main circuit structure.

FPGA-based Digital Controller

The digital controller is a key component for the power supplies [2]. Figure 2 shows the structure of the digital controller of the power supplies. Its core unit is an FPGA (Cyclone II, Altera company). And there are two CPUs (NIOSII) in the FPGA. The CPU1 is used to transmit control data, the CPU2 controls the regulator to generator current. All control data and parameter is saved in the SDRAM. The ETHERNET is main communication interface between the controller and the accelerator control system. And the quench protection module is designed for quench protect of the superconducting magnets. For the fast protection and high reliability purpose, the module is implemented by VHDL. VHDL (VHSIC Hardware Description Language) is a hardware description language used in electronic design automation to describe digital and mixed-signal systems such as field-programmable gate arrays and integrated circuits. VHDL can also be used as a general purpose parallel programming language.

Content from this work may be used under the terms of the CC BY 3.0 licence (© 2017). Any distribution of this work must maintain attribution to the author(s), title of the work, publisher, and DOI.

ISBN: 978-3-95450-191-5 doi:10.18429/JACoW-SRF2017-MOPB076

ANALYSIS OF THE PRODUCTION, INSTALLATION AND COMMISSIONING OF THE EUROPEAN-XFEL FREQUENCY TUNERS

R. Paparella†, A. Bosotti, D. Sertore, INFN/LASA Segrate (MI), Italy
C. Cloué, C. Madec, T. Trublet, CEA/IRFU, Gif-sur-Yvette, France
C. Albrecht, A. Bellandi, S. Barbanotti, J. Branlard, K. Jensch, L. Lilje, DESY, Hamburg, Germany

Abstract

In the European-XFEL superconducting linac, mechanical frequency tuners equipped with stepper motors and piezoelectric actuators provide cold tuning of each of the 768 1.3 GHz cavities. More than 820 complete tuning systems were fabricated and pre-assembled in industry, tested at several stages before and after assembly and successfully commissioned during cryo-module cold tests at AMTF (DESY). Quality control strategy adopted to preserve the well-assessed tuner reliability through such a large-scale industrial production is critically reviewed and the lessons learned are presented in this paper. The statistical analysis of the large set of data acquired up to the recent commissioning of the entire linac is then summarized.

THE E-XFEL TUNING SYSTEMS

Cold tuning systems for the main linac cavities at 1.3 GHz has a largely assessed design and has been extensively tested at DESY from TTF to the currently operating FLASH linac [1]. It features a double asymmetric leverage mechanics and its stretching action on the cavity is actuated by a stepper-motor driven unit working at cold. Two piezoelectric ceramic stacks are installed in a single preloading frame to counteract dynamic tune disturbances (Fig. 1).

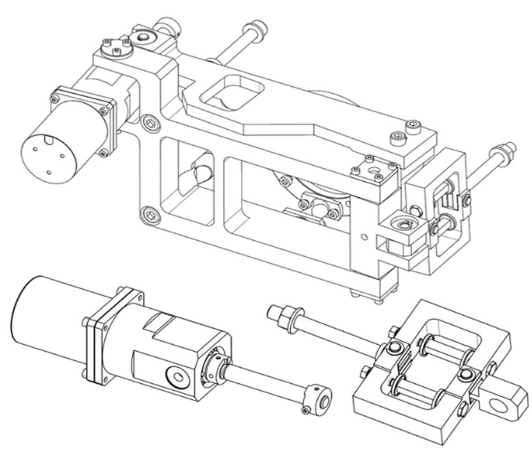

Figure 1: E-XFEL tuner with drive unit and piezo subsets.

QUALIFICATION OF VENDORS

Given the assessed design and performances, focus since the initial stage has been on the preservation of manufacturing and assembling quality going to industrialization phase. Key choices at this stage have been:

- Minimize the number of parts to be procured. The whole system has been divided into three subsets: mechanics (leverage, joints), drive unit (motor, gearbox, shaft and nut), piezo system (actuators, frame).
- Get the most out of industrial partner know-how. Both actuators (piezo and motors) were installed into their respective units by the manufacturer themselves, units were then delivered as "ready-to-use" at the cryomodule installation stage at CEA (France).
- Competition between vendors. Prototypes from any possible provider were tested at labs and at least two vendors were qualified by DESY for each subset.
- Introduce and additional quality control stage upon tuner assembly on string at CEA. This check should be performed by non-expert personnel.

All the several in-house developments through the years at DESY as well as at partner labs were gathered and transferred to interested companies in order to avoid a sole-supplier dependency scenario and evaluate different technical alternatives.

Qualification of Motor Drive Vendors

Support was provided to companies to apply the dry-lubricant coating recipe developed at DESY and to provide a cryogenic test of each produced unit.

Two technical options were evaluated for both stepper motor and gearbox components against the expected workload of 14 MSteps: Sanyo Denki and Phytron for the former, Harmonic Drive and Phytron planetary gear for the latter case.

Qualification of Piezo Vendors

Assembly and pre-loading of piezo stacks is the crucial stage of any piezo-actuated systems and for any cold tuning system before E-XFEL these operations have been usually "hand-crafted" by lab experts.

Several companies were, at the time, already qualified for the production of cryogenic proof multi-layer piezo stacks but the E-XFEL requirements set a further step. In order to benefit from a scenario where the piezo manufacturer itself integrates the actuators, the ability to assemble the whole mechanical fixture was then asked to companies.

Qualification of Mechanics Vendors

Drawings and tolerances of E-XFEL tuner mechanical components, initially supplied by CEA and adapted to a local supplier in France, underwent a significant simplifications and relaxation through the interaction with contacted large-scale, high precision machining companies.

† E-mail: rocco.paparella@mi.infn.it

Content from this work may be used under the terms of the CC BY 3.0 licence (© 2017). Any distribution of this work must maintain attribution to the author(s), title of the work, publisher, and DOI.

ISBN: 978-3-95450-191-5 doi:10.18429/JACoW-SRF2017-MOPB077

Content from this work may be used under the terms of the CC BY 3.0 licence (© 2017). Any distribution of this work must maintain attribution to the author(s), title of the work, publisher, and DOI.

OPERATIONAL EXPERIENCE OF THE EUROPEAN-XFEL 3.9 GHz COAXIAL TUNERS

R. Paparella†, A. Bellandi[1], A. Bignami, A. Bosotti, D. Sertore, INFN/LASA, Segrate, Italy
C. Maiano, ESS, Lund, Sweden
P. Pierini[2], INFN/LASA, Segrate, Italy and DESY, Hamburg, Germany

Abstract

The European-XFEL injector hosts a third-harmonic section composed by a module with eight 3.9 GHz cavities equipped with a coaxial frequency tuner inspired by INFN-LASA Blade Tuner design. The 3.9 GHz tuning system met specifications during all the injector runs in 2016 up to the recent commissioning of the entire linac; it matched the required tuning range and frequency sensitivity although higher than expected cavity detuning was experienced during pressure transients in the cryogenic system. An analysis of all collected experimental data is reported in this paper together with the strategy developed to provide a sound and effective retuning routine to the control room operator.

INTRODUCTION

The 3rd harmonic 3.9 GHz section at the European XFEL (E-XFEL) injector provides linearization of the longitudinal beam phase space after the first accelerating section. To compensate the effect of the space charge, a long bunch is generated in the RF gun. The subsequent RF acceleration in the first 1.3 GHz module produces cosine sinusoidal curvature in the longitudinal phase space of the incoming bunch. To remove this effect, a 3.9 GHz module is placed afterwards to linearize the longitudinal phase space and prepare the beam for the following compression and acceleration stages.

The E-XFEL third harmonic module is an 8-cavity module that provides a maximum voltage of 40 MV, corresponding to an accelerating field higher than 15 MV/m per cavity. All the cavities are operated close to 180° phase with respect to the incoming beam.

INFN Milano–LASA has provided, as in-kind contribution, the main components of the 3rd harmonic module now in operation in the E-XFEL tunnel [1].

The coaxial tuner used on the FNAL ACC39 module was scaled from the INFN blade tuner design originally proposed for the TESLA collider. Progresses at INFN on the blade tuner concept for ILC led to the development of a simpler, lighter and cheaper device (the "slim" tuner), that has been extensively characterized.

TUNER DESIGN

Assuming as a reference the slow-tuning mechanics geometry of the ILC Blade Tuner, a baseline 3.9 GHz cavity tuner model has been designed. The prototype design has been extensively characterized through different levels of simulation up to a 3D FE (Finite Element) model of the whole tuner; this allowed carefully estimating and understanding global kinematics and safety factors. Resulting layout is showed in Fig. 1, where the FE mesh (0.6 M elements, 0.16 M knots) is presented together with an example of longitudinal strain distribution along the tuner.

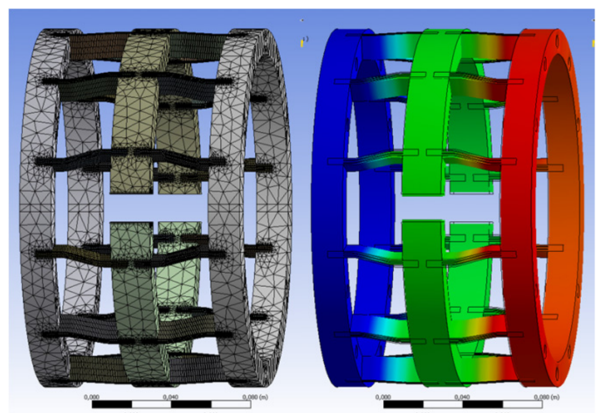

Figure 1: 3.9 GHz cavity tuner FE model developed for kinematics and stress analyses: mesh matrix (left), longitudinal strain distribution (right).

Full-body FE model results (“Full Tuner” case) were evaluated against selected reference cases:

- Case 1 - Single blade 3D FE “cartesian” model, were torsional effect is assumed to be negligible.
- Case 2 - Free single blade 3D FE model, including blade torsion.
- Analytical model - blade geometry is simplified down to a straight plate connecting the two rings.

An overview of analyses results is shown here below in Fig. 2 for what concerns the evaluation of tuner stroke and corresponding safety margin, defined as the ratio between the highest nodal stress in simulation over the material (titanium gr. 5) tensile yield.

The discrepancy in absolute strain visible between FE models and analytical case, about 0.3 mm, corresponds to the difference in length between the simplified blade used in the model compared to the actual shape at the maximum stretching.

† Email address: ROCCO.PAPARELLA@MI.INFN.IT
1 Currently at DESY, Hamburg, Germany
2 Currently at ESS, Lund, Sweden

ISBN: 978-3-95450-191-5 doi:10.18429/JACoW-SRF2017-MOPB078

POWER COUPLER DESIGN FOR THE LUCRECE PROJECT

H. Guler, O. Bouras, W. Kaabi, M. El Khaldi , D. Auguste, J. Bonis,
Laboratoire de l'Accélérateur Linéaire CNRS/IN2P3 Université Paris-Saclay, Orsay, France

Abstract

The LUCRECE project aims at developing an elementary RF system (cavity, power source, LLRF and controls) suitable for continuous (CW) operation at 1.3 GHz. This effort is made in the framework of the advanced and compact FEL project LUNEX5 (free electron Laser Using a New accelerator for the Exploitation of X-ray radiation of 5th generation), using superconducting linac technology for high repetition rate and multi-user operation (http://www.lunex5.com). In this context, based on its large experience on coupler design and RF conditioning, LAL Laboratory is in charge of the design and the fabrication of RF couplers that could operate at up to 15-20 kW in CW mode. For this purpose, couplers based on Cornell 75kW CW couplers (RF power couplers for the CBETA ERL injector) are under consideration and will be adapted to the LUCRECE needs. Electromagnetic simulations and associated thermal heating will be discussed.

INTRODUCTION

The CBETA injector coupler was the first 1.3 GHz input power coupler to operate at relatively high power in CW mode (75 kW). It was designed starting from TTF III double window coupler model [1]. However, it has been significantly modified to fulfil the ERL injector requirements [2]:

- The cold part was completely redesigned using a 62 mm, 60Ω coaxial line (instead of a 40 mm, 70Ω line) for a better power handling, more efficient heat load dissipation and to avoid multipacting.
- The antenna tip was enlarged and shaped for stronger coupling.
- The outer conductor bellows design (both in warm and cold coaxial lines) was improved for better cooling (Heat intercepts were added).
- Forced air-cooling of the warm inner conductor bellows and "warm" ceramic window was added.

The Cornell coupler design was then used in several CW machine like ARIEL at TRIUMF (20kW) [3] or BESSY VSR at HZB (10kW) [4]. The following study aims to adapt the Cornell coupler design to our need in the framework of coupler prototyping for LUNEX5 machine project (20kW in CW mode). RF studies and thermal simulations results for different design configurations will be presented and discussed.

ELECTROMAGNETIC SIMULATIONS

The coupler electromagnetic (EM) behaviour has been simulated using the ANSYS/HFSS software. The mechanical geometry has been simplified, by removing all the unnecessary parts like the screw holes, and all the different sharp edges, that will not contribute to the simulation of EM wave propagation inside the coupler. The outer geometry complications are also neglected in the simulation since the wave propagation in the conductor is not influenced by the coupler external part. All unnecessary geometric complication would increase the mesh amount and therefore the simulation time. Regarding the coupler design, the simulated electromagnetic RF wave is not symmetric which forbids using axial symmetry to increase the simulation speed. The 3D simulation is then necessary. The wave propagation inside the coupler has been simulated as showed on Fig. 1.

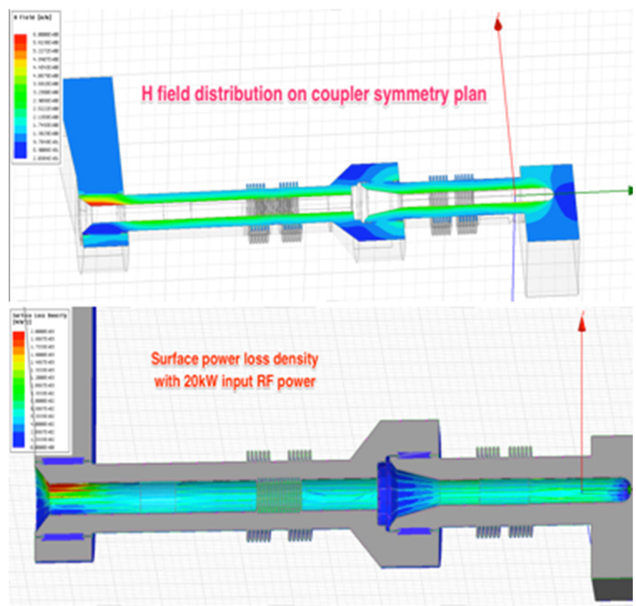

Figure 1: HFSS simulations with the Cornell coupler geometry: H field distribution on the coupler symmetry plan (top) and the surface power loss density on the inner conductor surface (down).

The field distributions shown its highest value in the warm inner conductor in the warm ceramic side where the RF power input is delivered. Deposited RF power has been simulated on the different copper surfaces of the inner conductor, including the bellows that are the area that needed the most accurate meshing. The propagation of RF wave in the coupler generates losses with joule effect in the Inner (CI)/Outer (CX) conductor and dielectric losses in the ceramic windows, as a result, each of these elements will heat up.

The heating in the ceramics has been induced by the EM wave that deposited power inside the ceramics and can be calculated via the following formula:

$$P_{vol} = \epsilon \iint E^2 dV \qquad (1)$$

With $\epsilon = tan(\beta) \simeq 1.0x10^{-4}$ for the ceramics. Concerning the ceramics and at 10 kW input power in CW mode,

Content from this work may be used under the terms of the CC BY 3.0 licence (© 2017). Any distribution of this work must maintain attribution to the author(s), title of the work, publisher, and DOI.

ISBN: 978-3-95450-191-5 doi:10.18429/JACoW-SRF2017-MOPB079

HOM COUPLER ALTERATIONS FOR THE LHC DQW CRAB CAVITY*

J. A. Mitchell†[1, 2], G. Burt[2], N. Shipman[1, 2], Lancaster University, Lancaster, UK
B. Xiao, S.Verdú-Andrés, Q. Wu, BNL, Upton, NY 11973, USA
R. Calaga, CERN, Geneva, Switzerland
[1]also at CERN, Geneva, Switzerland
[2]also at the Cockcroft Institute, Daresbury, UK

Abstract

As part of the High Luminosity Large Hadron Collider (HL-LHC) project, 16 crab cavities are to be installed in the LHC in 2025. The two crab cavity designs are the Double Quarter Wave (DQW) and Radio Frequency Dipole (RFD). Preliminary beam tests in the Super Proton Synchrotron (SPS) are planned for both cavity types, with the DQW scheduled for testing in 2018. In reference to to Higher Order Mode (HOM) damping, the DQW has three identical on-cell HOM couplers. These HOM couplers provide a band-stop response at the frequency of the fundamental mode and act as a transmission path for the cavity HOMs. For the SPS cavity design, several geometric constraints exist. These give rise to dimensional limitations which in-turn impose limitations on the RF performance of the HOM couplers. As such, for the LHC assembly, the HOM coupler design is re-visited to take into account the relaxed geometric limitations, hence allowing the feasibility of an increased RF performance to be investigated. In addition to the RF performance, several geometric alterations were incorporated to ease manufacturing processes, tolerances and costs.

DQW CRAB CAVITY INTRODUCTION

The purpose of the DQW crab cavity [1] is to provide a transverse electromagnetic kick to a proton bunch, allowing bunch rotation which leads to an increase in luminosity [2]. The effect is applied to both beams prior to collision and a kick of equal magnitude in the opposite direction is then applied after the collisions.

To provide a transverse kick capable of meeting the specified voltage of 3.4 MV [3] whilst fitting in the restricted space available in the LHC, an initial Proof-of-Principle (PoP) DQW was designed. Cavity design alterations were then made primarily to reduce the magnetic field seen at the HOM coupler port areas. Two ports were also removed from the design [4]. The cavity design for the SPS is shown in Fig. 1.

In addition to the fundamental mode at ∼ 400 MHz there also exist several Higher Order Modes (HOMs). Figure 2 shows the on-axis impedance spectrum for the bare cavity up to the beam-pipe cut-off of ~2 GHz (84 mm beam-pipe) [5]. The simulation was done using CST Microwave Studio [6] with 7.57×10^6 mesh cells and with a wake length of 1 km. In

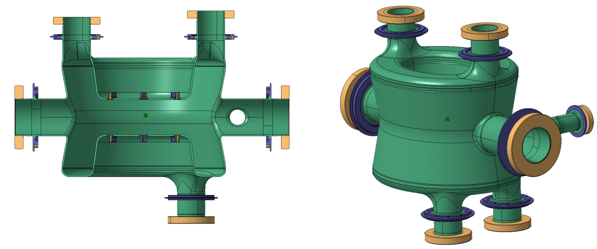

Figure 1: Geometry of the SPS DQW crab cavity.

this paper, the z-direction refers to the longitudinal direction and y to the direction orthogonal to the capacitive plates.

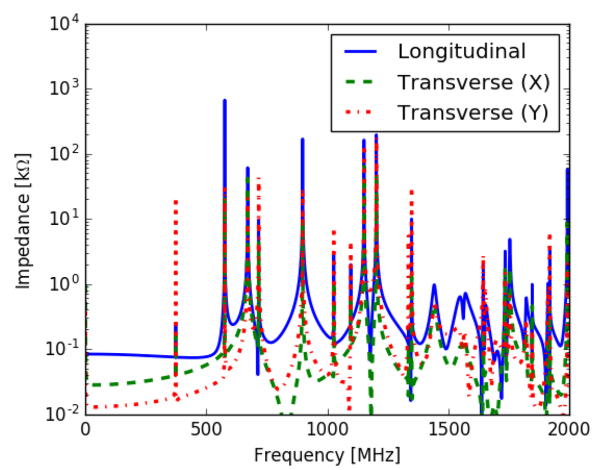

Figure 2: Bare cavity on-axis impedance from wakefield simulations in x, y and z.

HOM couplers are used to damp the HOMs, minimising their effect on beam stability and HOM power. The couplers act as a transmission path to the HOMs but as a band-stop filter to the fundamental mode. The fully dressed cavity is displayed in Fig. 3.

SPS HOM COUPLER

For the SPS crab cavity, geometric limitations meant an angled HOM coupler was designed. A schematic of the coupler is shown in Fig. 4. Although the coupler length restriction imposes restrictions on the RF performance, the right angled coupler gives an advantage in that the ceramic is perpendicular to the direction of field emission. The coupler is made from Niobium and internally cooled with superfluid helium, allowing operation in the superconducting regime.

* This work is supported by the HL-LHC project, Lancaster University and the Cockcroft core grant.
† j.a.mitchell@lancaster.ac.uk

Content from this work may be used under the terms of the CC BY 3.0 licence (© 2017). Any distribution of this work must maintain attribution to the author(s), title of the work, publisher, and DOI.

ISBN: 978-3-95450-191-5 doi:10.18429/JACoW-SRF2017-MOPB080
Content from this work may be used under the terms of the CC BY 3.0 licence (© 2017). Any distribution of this work must maintain attribution to the author(s), title of the work, publisher, and DOI.

THE STABLE OPERATION OF MPG AND MEASUREMENT OF OUTPUT

B. T. Li, D. Y. Yang, L. Xiao, J. F. Zhao, X. Y. Lu†, Y. J. Yang, Z. Q. Yang,
State Key Laboratory of Nuclear Physics and Technology, Beijing , China

Abstract

This paper presents the energy spread measurement result of electron beam produced by MPG. The operation parameters and the experimental result are reported. The average current density of 1.8 mA was obtained at 2.856 GHz. The energy spread of the electron beam is also measured, in which the energy of the most electrons is less than 50 eV and the FHWM is less than 15 eV. The fifth order operation mode is obtained.

INTRODUCTION

The development of electron sources with high current, short pulse, low emittance, good stability has been a challenging topic in the field of accelerators. RF-gun uses microwave electric field to generate electrons, which can provide high quality beam.

The concept of micro-pulse electron gun was put forward in 1969[1]. It was thought to be a very promising electron source with wide range of application. Tsinghua University [2,3], University of Science and Technology of China [4,5], China Academy of Engineering Physics [6], Shanghai Institute of Applied Physics [7] and Peking University have done some research on MPG [8,9]. But after many years of research, it is still not put into practical application because of the unstable operating state and the unknown beam qualities.

In this paper, the design and operation results of a novel MPG are reported. Its stability has been greatly improved. The electron energy spread of the beams was measured by a retarding field energy analyzer.

THEORETICAL ANALYSIS

For MPG with negative feedback mechanism, it is necessary to meet two requirements to guarantee its stable operation: self-bunching requirements and material characteristics. To meet the above requirements, the MPG has to work at a suitable peak cavity voltage, which should be between the characteristic peak cavity voltage and the minimum peak cavity voltage [8,9].

According to the simulation in Ref. [9] and the primary experimental result, the energy of the electrons is about 30eV and the length of the bunch is about 10ps. Based on the conditions above, the energy spread of the beam is measured by a retarding field energy analyzer as shown in Figure1 which utilizes a retarding field to decelerate the electrons.

Assume that the energy spectrum of a given energy E is

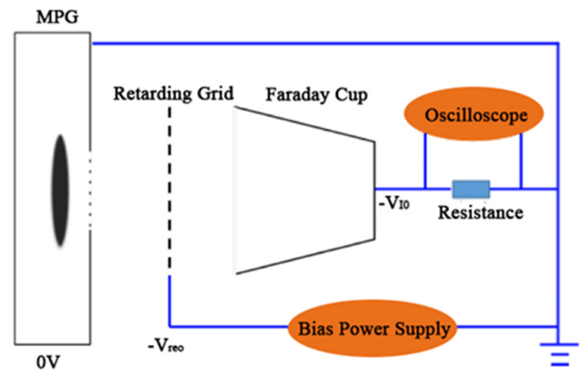

Figure 1: The layout of the energy spread measurement system.

$$S(E_0,T,f,E,k)=\frac{I_s(E)}{I_0} \quad (1)$$

in which E_0 is a specific field intensity of the MPG cavity, T is the transmittance of the grid, f is the frequency, k is the material's secondary electron multiplication parameter, $I_s(E)$ is the beam density composed of electrons that reached the collector overcoming the retarding field, I_0 is the beam density without the retarding field. So the energy spectrum can be expressed as

$$\frac{d\delta}{dE}=\frac{\partial S(E_0,T,f,E,k)}{\partial E} \quad (2)$$

The minus ensures that the result is positive.

$$\frac{d\delta}{dE}=-\frac{1}{I_0}\frac{\partial I_s}{\partial E} \quad (3)$$

SOFTWARE SIMULATION RESULTS

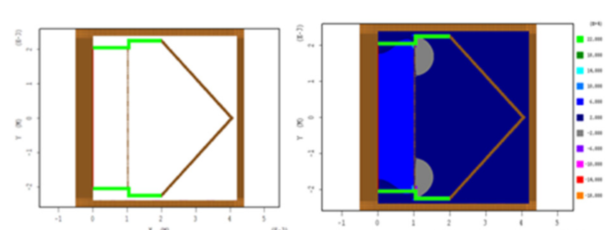

Figure 2: Simulation diagram and X-direction electric field distribution.

We use MAGIC to simulate the electron beam motion during the operation of the retarding field energy analyzer, the simulation results are as shown in Figure 2. The distance between electron emission surface and cathode is 1mm, the simulation time is 3.5ns. The beam size is

---
† email address: xylu@pku.edu.cn

ISBN: 978-3-95450-191-5 doi:10.18429/JACoW-SRF2017-MOPB082

A PRELIMINARY SCHEME FOR X-RAY EMISSION BASED ON MICRO-PULSE ELECTRON GUN

Yujia Yang†, Xiangyang Lu, Jifei Zhao, Deyu Yang, Ziqin Yang, Weiwei Tan, Li Xiao, Boting Li
†Institute of Heavy Ion Physics, Peking University, China

Abstract

X-ray is now widely used in many areas of physics, biology, chemistry and materials. And how to achieve emission, monochrome, and focusing of x-ray is of great significance to study. Micro-pulse electron gun (MPG) is a new type of electron source, with characteristics of high repetition frequency, short-pulse and low cost. Generating x-ray with better monochromaticity is one of the potential applications of MPG. And a preliminary scheme of X-ray based on MPG is proposed in this paper. The scheme is designed by comparing different anode materials and the thickness of filters. The simulation results based on the software MCNP5 show that the proposed scheme can effectively improve the monotonicity of the generated X-rays.

INTRODUCTION

The emission of characteristic radiation is a type of x-ray that is widely-used because of its low power, easy to obtain and characteristic of elements. Miniature transmission x-ray tube generates x-ray with smaller spot dimension. Compared with traditional reflective x-ray tube, it benefits of its low cost and limiting the scattering of incident electron beam. Basically, the key component of miniature transmission x-ray tube is the transmission anode [1], which is a target film (~μm) with metallic elements deposited onto the inner surface of Beryllium (Be) foil (0.3 mm) (Fig. 1).

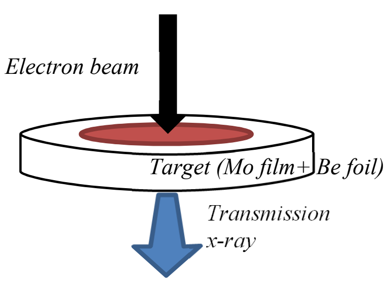

Figure 1: Electron bombardment of Mo target.

The element Argentum (Ag) is widely chosen as the target film, because miniaturization of transmission x-ray tube gives the limitation of electron energy about 30keV. It means characteristic x-ray of Ag excited by injected electrons with low energy has the highest yield than W. Mo, etc. However, by increasing the electron energy the element Molybdenum (Mo) also has a good performance on the emission spectrum. What's more, the melting point of Mo is 2617°C much higher than Ag which is 961.78°C. For MPG, Mo is a better choice for target film for electron beams with higher energy. MPG (Micro-pulse Electron Gun) is a kind of electron gun that provides electron beams with advantages of short pulse, high current, high tolerance and low cost. In Peking university, MPG-MTBMS and MPG-BMAS have been established and can operate steady for more than 10 hours. The energy of electron beams extracted from MPG-BMAS is adjustable ranging form 0-100keV, the spot diameter is about 4mm, and the emittance $\varepsilon_x/\mathrm{mm} = 1.47 \pm 0.06\ \mathrm{mm\cdot mrad/mm}, \varepsilon_y/\mathrm{mm} = 1.51 \pm 0.06\ \mathrm{mm\cdot mrad/mm}$. According to these measured parameters, MPG-BMAS already have the initial conditions for x-ray experiments now. It is urgent to solve the design of x-ray tube.

To analyse the performance of x-ray tube, two main methods are numerical analysis and Monte Carlo simulations. Numerical analysis gives the evaluation of intensity for characteristic radiation and bremsstrahlung, while Monte Carlo simulation such as MCNP5 code gives the spectrum, and enables us to improve the applicability of analytical techniques based on emission of characteristic radiation [2-3]. The MCNP5 code is a Monte Carlo transport code for photons, neutrons, and electrons [4]. In x-ray tube electrons interact with the target material, the resulting x-ray is absorbed and scattered by the target and filter atoms, making the emission spectrum further complex. The Monte Carlo method can greatly simplify the calculation of these processes.

THEORETICAL BACKGROUND

The principle behind miniature transmission x-ray tube is the excitation of atomic shells by primary radiation, resulting in the emission of characteristic x-rays. The energy and intensity depend on the elements of target and the quality of incident electrons.

Miniature transmission x-ray tube with MPG as the electron source, the exiting electrons focused through the collimator directly interact with target. The initial diameter of the electron beam is 4mm and incident area would be submicron scale. The anode target uses a thin film structure, and the thickness of the film is determined by the range of electrons in the material.

The electrons lose energy in the material by collision and radiation. The mass collision stopping power and the mass radiation stopping power depend on the material and the energy of electrons. The greater the initial energy of the electron have, the greater the loss of energy in the unit thickness, and the electron energy loss occurs mainly on the anode surface (~μm). The range of electrons in the material can be derived from the Tabata, Ito and Okabe empirical formula [5]:

$$R(m) = a_1\left(\frac{ln[1+a_2(r-1)]}{a_2} + \frac{a_3(r-1)}{1+a_4(r-1)^{a_5}}\right)\rho \quad (1)$$

*Supported by Major Research Plan of National Natural Science Foundation of China (No. 91026001) and National Major Scientific Instrument and Equipment Development projects (2011YQ130018).
† email address: yangyujia@pku.edu.cn

Content from this work may be used under the terms of the CC BY 3.0 licence (© 2017). Any distribution of this work must maintain attribution to the author(s), title of the work, publisher, and DOI.

ISBN: 978-3-95450-191-5 doi:10.18429/JACoW-SRF2017-MOPB086

FIRST RESULTS OF THE IFMIF/EVEDA-SaTHoRI TESTS

O. Piquet, N. Bazin, P. Carbonnier, J. Chambrillon, J.-F. Denis, M. Desmons, G. Devanz, F. Eozénou, P. Hardy, E. Jacques, H. Jenhani, Y. Lussignol, L. Maurice, J. Relland, P. Sahuquet, C. Servouin, Irfu, CEA, Université Paris-Saclay, Gif-sur-Yvette F-91191, France
I. Moya, D. Gex, A. Jokinen, G. Phillips, P. Cara, F4E, Garching, Germany
P. Mendez, CIEMAT, Madrid, Spain

Abstract

The SaTHoRI test stand (Satellite de Tests HOrizontal des Résonateurs IFMIF) aims at characterizing a jacketed and fully dressed cavity with its RF coupler and frequency tuner. A dedicated test cryostat has been manufactured and connected to an existing horizontal test cryostat which provides the cryogenic coolant. A RF source – provided by the IFMIF/EVEDA project - has been installed and commissioned at CEA-Saclay. This paper describes the test stand and presents the first results.

INTRODUCTION

The first phase of the IFMIF project aims at validating the technical options for the construction of an accelerator prototype, called LIPAc (Linear IFMIF Prototype Accelerator). The superconducting cryomodule components are under construction [1] and will be assembled under the responsibility of F4E (Fusion for Energy) with CEA assistance at Rokkasho Fusion Institute in Japan, where a cleanroom will be built by QST. [2, 3]. In addition to the vertical test for individual HWR qualification, the validation test of an accelerating unit (HWR [4] equipped with its tuner and power coupler [5]), which is part of a mitigation pan explained in [6], took place in a dedicated horizontal cryostat SaTHoRI before the delivery of the components for assembly. These tests will provide benchmark data for the cavity behaviour (RF, mechanical, field probe, tuner calibration…) and will allow to perform preliminary testing of some components of the SRF Linac: RF source, LCS components and instrumentation.

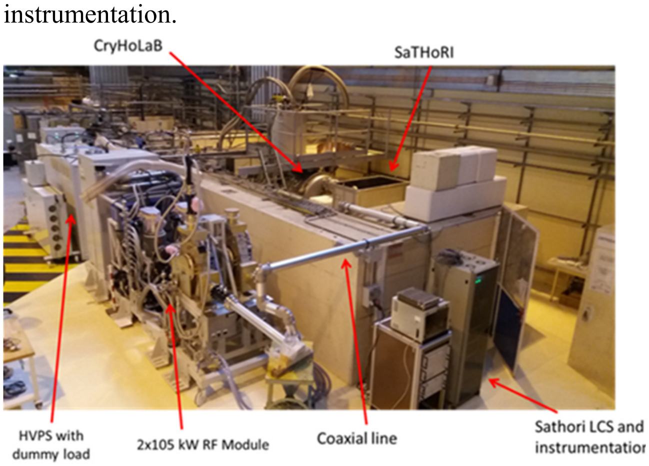

Figure 1: Test stand at CEA-Saclay.

TEST STAND AT CEA-SACLAY

For the SaTHoRI test, a dedicated test stand has been installed at CEA-Saclay. It is made of a 175 MHz CW RF source with a coaxial line, a cryostat, a biological protection and cubicles for the local control system and instrumentation (Figure 1).

SaTHoRI Cryostat

CEA is equipped with a horizontal cryostat called CryHoLab (Large horizontal cryostat) to test jacketed cavity equipped with tuning system and power coupler [7, 8]. Unfortunately, this cryostat was too small to receive an equipped HWR-cavity, a new cryostat called SaTHoRI has been developed. It is connected to CryHoLab in order to benefit from the already existing cryogenic distribution and the pumping system (Figure 2).

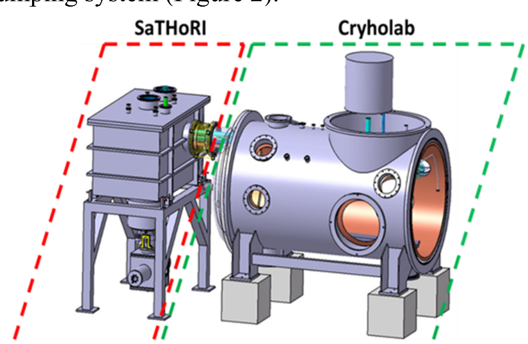

Figure 2: Principle of the SaTHoRI cryostat connected to CryHoLaB.

This new cryostat (Figure 3) mainly consists of:

- A vacuum vessel which supports the cavity / coupler assembly and insulates the cold parts from room temperature. The cavity is hung on the top lid of the vessel using four titanium alloy rods to limit the heat load on the cold parts.
- A thermal shield which limits the radiation heat flux on the cold parts. It is cooled with liquid nitrogen which is derived from the cooling circuit of the thermal shield of the CryHoLab.
- A magnetic shield made of mu-metal sheets fixed on the inner surface of the vacuum vessel to protect the cavity from the earth magnetic field. The design of this shield allows a goal of 2 µT at the HWR surface by using 2 mm thick mu-metal sheets.

Content from this work may be used under the terms of the CC BY 3.0 licence (© 2017). Any distribution of this work must maintain attribution to the author(s), title of the work, publisher, and DOI.

ISBN: 978-3-95450-191-5 doi:10.18429/JACoW-SRF2017-MOPB087

FREQUENCY TUNER DEVELOPMENT AND TESTING AT CORNELL FOR THE RAON HALF-WAVE-RESONATOR*

M. Ge†, F. Furuta, J. E. Gillette, T. Gruber, S. Hartman, M. Liepe, T. O'Connell, P. Pamel, P. Quigley, J. Sears, V. Veshcherevich, CLASSE, Cornell University, Ithaca, New York, USA
B. H. Choi, J. Joo, J.W. Kim, W.K. Kim, J. Lee, I. Shin, Institute for Basic Science, Daejeon, Korea

Abstract

The half-wave-resonators (HWRs) for the RAON project require a slow frequency tuner that can provide >80 kHz tuning range. Cornell University is currently in the process of designing, prototyping, and testing this HWR tuner. In this paper, we present the optimized tuner design, prototype fabrication, test insert preparation, and cryogenic test results. The performance of the tuner is analysed in detail.

INTRODUCTION

A RAON HWR cryomodule [1-3] houses two HWR cavities, each of which requires an individual slow frequency tuner. Cornell University is developing the prototype HWR tuner, which is based on the pneumatic tuner developed by Argonne National Laboratory (ANL) [4]. The pneumatic tuner requires a pressure regulation system to control tuning amounts; as an alternative way, we adopted a scissor section mounted with a cryogenic step-motor to replace the bellow section of the pneumatic tuner. In this way, the HWR tuner will be merely driven by electrical signals. The main concern of this design is that the scissor section could bind or not move smoothly at low temperatures (2K – 4.2 K). In this paper, we prove the scissor-section scenario can work for the HWR tuner.

TUNER DESIGN AND FABRICATION

The preliminary design of the HWR tuner has been reported in Ref. [5]. In this section, we briefly review the design. The target frequency of the HWR (geometrical $\beta = 0.12$) is 162.5MHz at 2K. The slow frequency tuner ought to provide at least 80 kHz tuning range. We designed the maximum tuning amount up to 200 kHz, which will give an adequate margin for the HWR frequency control.

Mechanical Design

The 3D model, shown in Fig. 1, illustrates the HWR tuner structure: two tuning bars are mounted on each beam-pipe flange; four strings link the two pairs of tuning bars. The scissor-section driven by the cryogenic stepper-motor is attached on the strings by its frames.

When the motor is turning, the scissor-section will move the frames ① and ② in the reverse directions, as is shown in Fig. 2 (a). The frames ① and ② are attached on the strings via their hooks by which the frames can push the strings ④ in the middle and squeeze the cavity beam-pipe flanges by the tuning bars ③, depicted in Fig. 2 (b).

* Work supported by the Ministry of Science, ICT, MSIP and NRF. Contract number: 2013M7A1A1075764.
† mg574@cornell.edu

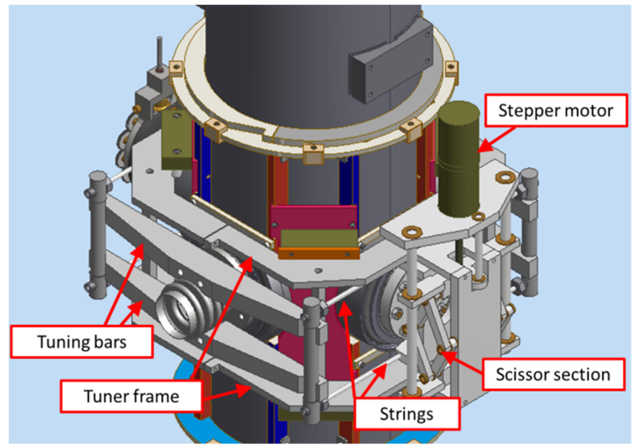

Figure 1: 3D model of the tuner installed on a HWR.

The material for the tuning bars is 316 stainless steel (SS) to avoid thermal stress between the tuning bar and beam-pipe flange which is made of SS as well. The ideal material for the strings is titanium (Ti) which has similar thermal expansion coefficient to niobium (Nb); thus a Ti string gives very small thermal stress cross the tuner and does not change the cavity frequency much during cooldown. Since a Ti string is not easy to obtain, we explore SS strings and control the thermal stress by adjusting the tension of the string. The scissor-section is made of Ti for reducing the total weight of the tuner. Table 1 summarizes the thermal expansion rate of Ti, Nb, and SS.

Table 1: Material Shrinkage Rate from 300K to 2K [6, 7]

Material	$\frac{\Delta L}{L}$ (%)
Ti (grade-2)	0.172
Nb	0.146
SS (316L)	0.319

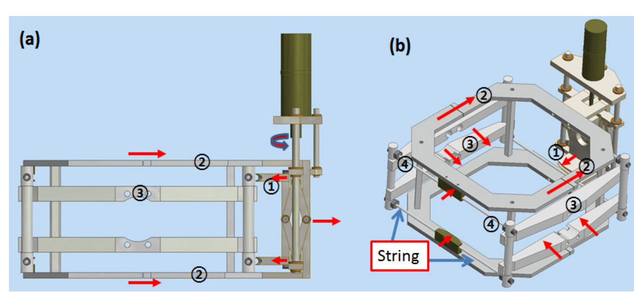

Figure 2: Illustration of the moving mechanism of the tuner.

All the tuner parts have been fabricated at Cornell University. Fig. 3 shows the tuning bars, the tuner frame, and the strings.

Content from this work may be used under the terms of the CC BY 3.0 licence (© 2017). Any distribution of this work must maintain attribution to the author(s), title of the work, publisher, and DOI.

ISBN: 978-3-95450-191-5 doi:10.18429/JACoW-SRF2017-MOPB088

EXPERIENCE ON IN-SITU MODULE REPAIR AND SET UP OF NON XFEL CAVITY STRINGS AT DESY

M.Schmökel, A.Daniel, N. Krupka, A. Matheisen, S.Saegebarth, M.Schalwat, P.Schilling,
DESY, Hamburg, Germany

Abstract

All components installed to the European XFEL cavity string modules underwent an intensive inspection and quality control before acceptance for installation to cavi-ties or modules. Even though some RF feed throughs for HOM coupler- and Pick Up antennas showed leaks at the ceramic insulation after module test at 2 K. Due to time restriction and continuity of production the exchange of these parts needed to be done without reentering the cleanroom. Successful repair of these modules took place by setting up a local cleanroom onto the cavity string.

In collaboration with Helmholtz-Zentrum Dresden-Rossendorf (HZDR), a cavity string for the ELBE project [1] [2] was assembled at DESY and transported to HZDR for installation to the vacuum vessel.

A spare module with 3.9 GHz resonators for the European XFEL was set up at DESY and will be tested and qualified for the European XFEL. Due to delay in delivery of the power couplers, four power couplers were installed after string assembly.

INTRODUCTION

DESY and the European XFEL had contracted that modules, which failed in the final tests, would be repaired by DESY. For three modules, where the repair could be done by exchange of just one feed through, this repair was done with a local cleanroom on the cantilever system for module assembly.

The cavity string for HZDR was assembled in January 2017 in the DESY cleanroom and afterwards transported to HZDR for the complete installation.

The 3.9 GHz spare module X3M2 was assembled in collaboration between INFN Milano and DESY, comparable to the 3.9 GHz module X3M1 for the European XFEL [3].

REPAIR SEQUENCES

Composition and Qualification of the Clean Room

For the repair of the modules outside the cleanroom, a local cleanroom was needed (Fig. 1). To achieve a sufficient air flow and air quality at the HOM coupler- and Pick Up antennas, the magnetic shielding and the tuners had to be disassembled. For the composition of the local cleanroom a filter fan unit (FFU) was installed and the assembly position was encased with foil. The assembly area in the local cleanroom had to be cleaned with ethanol and lint free tissues.

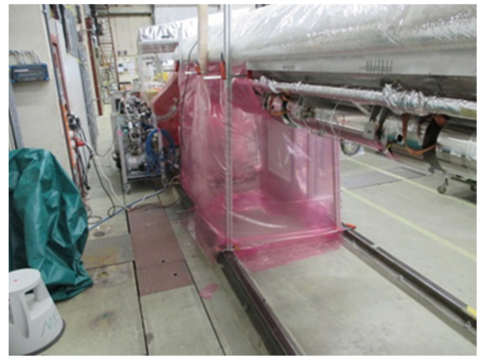

Figure 1: Local cleanroom on the string.

The local cleanroom was reviewed with an anemometer for the air flow speed and a particle counter. The air flow speed was between 0.48 m/s and 0.66 m/s (Fig. 2). The particle counts at the assembly position were better than specified in ISO 4 norm (Fig. 3).

Figure 2: The control of the air flow speed.

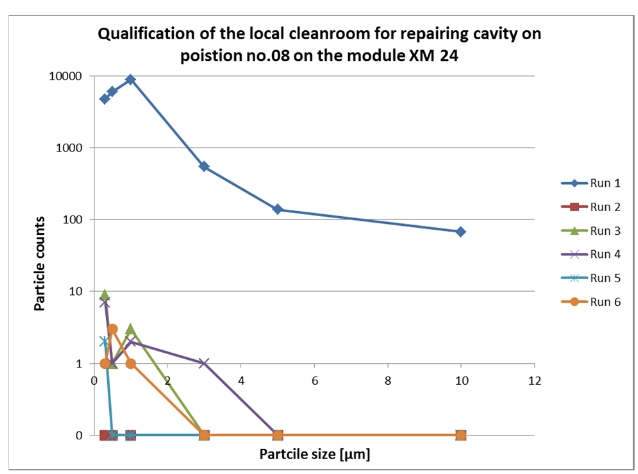

Figure 3: Example of the particle qualification of the local cleanroom for XM24.

Content from this work may be used under the terms of the CC BY 3.0 licence (© 2017). Any distribution of this work must maintain attribution to the author(s), title of the work, publisher, and DOI.

ISBN: 978-3-95450-191-5 doi:10.18429/JACoW-SRF2017-MOPB089

CHARACTERISATION OF MAGNETIC SHIELDING MATERIAL FOR HL-LHC CRAB CAVITIES*

K. Eiler†, A. Parrella[1,2], P. Arpaia[2], M. Buzio, O. Capatina, S.A.E. Langeslag,
CERN, Geneva, Switzerland
N.J. Templeton, STFC Daresbury Laboratory, Warrington, UK
[1]also at University of Lisbon, Portugal
[2]also at University of Naples Federico II, Italy

Abstract

In order to guarantee optimum performance, the crab cavities for the high-luminosity upgrade of CERN's LHC need to be shielded from external magnetic fields. Consequently, they will be enclosed by two layers of magnetic shielding, of which the inner is immersed in superfluid helium at 2 K. A Ni-based high-permeability material with a tailored composition and a designated heat treatment is applied. Its magnetic properties at cryogenic temperatures are however not yet fully assessed. Especially the effect of deformation on magnetic properties has not been thoroughly investigated, however strain effects may have severe consequences.

A magnetic measurement set-up has been developed, and the magnetic permeability at room temperature and at cryogenic temperatures is evaluated, showing that the maximum relative permeability at 4 K exceeds the design criteria of 100 000. Measurements of the magnetic permeability after introduction of uniaxial plastic deformation between 0% and 3% are conducted by means of an Epstein frame. Results show that deformation induces significant decrease of the magnetic performance, underlining that particular care must be taken during all stages of handling and operation.

INTRODUCTION

The High Luminosity upgrade of the LHC at CERN includes the installation of bulk niobium crab cavities, which are SRF cavities intended to tilt proton bunches for compensation of their crossing angle at the interaction points. The prototypes of the crab cavities will be tested with a proton beam in the Super Proton Synchrotron (SPS) at CERN in 2018 [1]. As for other bulk niobium cavities, magnetic shields are used to cancel the initial magnetic field on the cavities' radio frequency (RF) surfaces to guarantee optimum performance and a high quality factor. Cryophy, a high Ni-content alloy, has a very high maximum relative permeability, and is used as the inner of two layers of passive magnetic shielding, immersed in liquid helium. Its composition and heat treatment are designed to achieve maximum permeability at 2 K.

The magnetic layer operating at cryogenic temperature, hence the cold magnetic shield, is designed to be assembled from various parts and bolted, to avoid any plastic deformation that adversely affects its magnetic permeability. However, not least due to the low shield thickness of 1 µm, there is a certain risk of introducing plastic deformation. The effects of such a deformation are not entirely understood and little literature exists on this topic, but it is evident that mechanical strain already at low deformation can have a serious impact on the magnetic properties [2].

The magnetic shields have been designed to obtain no more than 1 µT of initial magnetic field on the cavity surface with an external field of 200 µT [3]. Therefore, the requirement for the cold magnetic shield is a relative magnetic permeability of more than 100 000 at liquid helium temperature [4].

EXPERIMENTAL

Cryophy is a ferromagnetic material developed to reach maximum magnetic permeability at cryogenic temperature. Its composition and heat treatment are adjusted to this purpose.

The following sets of samples were made for the tests conducted at CERN:

- 15 sample rings for direct current (DC) measurements of the magnetic permeability at room temperature (RT) as well as cryogenic temperatures (77 K and 4 K) with inner and outer diameters of 76 mm and 114 mm, respectively
- 32 rectangular samples (320 mm by 40 mm) for alternating current (AC) measurements of the magnetic permeability in an Epstein frame to assess the influence of unidirectional mechanical strain

The samples, as well as all parts of the magnetic shields for the SPS test, have been annealed by the supplier, Magnetic Shields Ltd, in their final geometry in order to avoid loss of magnetic permeability during cutting. The parts for the magnetic shield are bolted together during assembly of the shield around the cavity, so that no major plastic deformation is introduced.

To be as close as possible to the actual conditions of the application, the sample thickness of 1 mm is the thickness of the magnetic shield prototypes.

* Research supported by the High Luminosity LHC project
† konrad.eiler@cern.ch

Content from this work may be used under the terms of the CC BY 3.0 licence (© 2017). Any distribution of this work must maintain attribution to the author(s), title of the work, publisher, and DOI.

ISBN: 978-3-95450-191-5 doi:10.18429/JACoW-SRF2017-MOPB090

Content from this work may be used under the terms of the CC BY 3.0 licence (© 2017). Any distribution of this work must maintain attribution to the author(s), title of the work, publisher, and DOI.

SUB-MICRO-TESLA MAGNETIC SHIELDING DESIGN FOR CRYOMODULES IN THE HIGH-GRADIENT PROGRAM AT CERN

S. Papadopoulos*, L. Dassa, J. P. Dequaire, F. Gerigk,
F. Pillon, S. Ramberger, P. Yilmazer
CERN, Geneva, Switzerland

Abstract

In the framework of the High-Gradient R&D program at CERN a cryomodule, consisting of four superconducting 5-cell cavities, has been designed. In order to reduce flux trapping in the surface of the superconductor and to minimize Q degradation during a quench, highly effective magnetic shielding is needed. The solution proposed includes cold and warm passive shielding enhanced by four compensating coils. In this paper the magneto-static simulation results are presented illustrating different design considerations that led to a final design. Finally the shielding ability of the vacuum vessel is investigated experimentally through ambient magnetic field measurements.

INTRODUCTION

The High-Gradient (HG) test cryomodule contains four 5-cell bulk Nb $RRR = 300$ superconducting cavities operating at 704.4 MHz. The design Q-factor of 10^{10} will allow an operation with 25 MV/m accelerating gradient. For reaching this value the average surface resistance needs to be $R_s \leq 27\,\text{n}\Omega$.

Trapped Flux Surface Resistance

The overall surface resistance R_s is given by the sum of the different loss mechanisms (Eq. (1)):

$$R_s = R_{BCS} + R_{TF} + R_{res} \tag{1}$$

where R_{BCS} is the BCS surface resistance, R_{TF} is the resistance due to trapped magnetic flux and R_{res} is any other residual resistance due to impurities and lattice disruptions. For the HG cavities $R_{BCS} = 6\,\text{n}\Omega$ [1] and the expected $R_{res} = 10\,\text{n}\Omega$. These values allow an $R_{TF} \leq 11\,\text{n}\Omega$. With a trapped-flux sensitivity of around 2.2 nΩ/μT [2] the maximum ambient magnetic field on the cavity surface needs to be $B_{amb} \leq 5\,\mu\text{T}$.

Nevertheless, recent studies [3] illustrate the strong relation between trapped magnetic flux and quenching while full recovery of the Q-factor after quenching is possible only in absence of ambient magnetic field. This motivates the investigation and design of a sub-μT magnetic shielding solution that will ensure stability and high-performance during operation.

Magnetic Shielding Factor

The *magnetic shielding factor* S of a magnetic shield is defined as the ratio of the external magnetic field over the magnetic field at the center of the shield: $S = B_{ext}/B_{center}$. Analytical expressions exist for the calculation of the shielding factor for the simple case of a cylindrical shield. The shielding factor of a magnetic shield depends on the orientation of the magnetic field. The parallel shielding factor $S_\parallel$ refers to the case of a magnetic field parallel to the central axis of the shield. The perpendicular shielding factor $S_\perp$ refers to the case of a magnetic field perpendicular to the central axis of the shield. The $S_\parallel$ is different for cylinders with open and closed ends. The relevant formulas are given in Eqs. (2), (3), and (4).

$$S_\perp = \frac{\mu \cdot d}{D}, \tag{2}$$

$$S_\parallel^{open} = 4NS_\perp + 1 \tag{3}$$

$$S_\parallel^{closed} = \frac{S_\parallel^{open}}{1 + D/2L} \tag{4}$$

where μ is the magnetic permeability of the material, d is the thickness of the shield, D is the diameter of the cylinder, L is the length and N is the demagnetization factor [4]. The demagnitization factor N is a function of the ratio L/D. Measurements and calculations concerning the demagnetization factor of cylinders can be found in [5–7]. The equations assume linear magnetic material and give a good idea for the initial parameters of the needed shield. Nevertheless, the impact of saturation due to material non-linearities, the high complexity of the shield to fit the mechanical design of the cryomodule and the need for extensive shielding optimisation, not only at the center of the shield but in the whole area of the cavity surface require detailed magnetostatic simulations.

MAGNETIC SHIELDING DESIGN

Magnetic Shielding Materials

The design proposed includes a warm magnetic shield close to the interior side of the vacuum vessel and four cold shields around the helium vessel of the cavities. For the manufacturing of the cold shield cryophy® material has been chosen as it is specifically developed for reaching a high relative magnetic permeability value at cryogenic temperatures [8]. The highly permeable mu-metal material can be used for the warm shield. For the magneto-static simulations, manufacturers of mu-metal and cryophy® suggest the use of the following values: $\mu_r^{mumetal} = 50000$ and $\mu_r^{cryophy} = 15000$ [9, 10]. The shielding system is shown in Figure 1.

* sotirios.papadopoulos@cern.ch

ISBN: 978-3-95450-191-5 doi:10.18429/JACoW-SRF2017-MOPB094

COMMISSIONING OF DEMONSTRATOR MODULE FOR CW HEAVY ION LINAC@GSI

V. Gettmann*[,2], M. Miski-Oglu[2], W. Barth[1,2,5], K. Aulenbacher[2,4], M. Heilmann[1], T.Kürzeder[2]
S. Yaramyshev[1,5], M. Basten[3], F. Dziuba[2], M. Schwarz[3], H. Podlech[3]
[1]GSI Helmholtzzentrum, 64291 Darmstadt, Germany
[2]HIM, Helmholtzinstitut, 55099 Mainz, Germany
[3]IAP, Goethe University, 60438 Frankfurt, Germany
[4]KPH, Johannes Gutenberg-University, 5099 Mainz, Germany
[5]MEPHI, National Research Nuclear University, 115409 Moscow, Russia

Abstract

The cw – Linac – demonstrator is a prototype of the first section of the proposed cw-LINAC@GSI, comprising a superconducting CH-cavity embedded by two superconducting solenoids. The sc CH-structure is the key component and offers a variety of research and development. The beam focusing solenoids provide maximum fields of 9.3 T at an overall length of 380 mm and a free beam aperture of 30 mm. The magnetic induction at the fringe is minimized to 50 mT at the inner NbTi-surface of the neighboring cavity. The fabrication of the key components is finished, as well as the cold performance testing of the RF cavity. The cryostat is ready for assembling and the test environment is completely prepared. After successful testing of the RF-Power coupler, the components have been assembled to the suspended frame under cleanroom conditions. Alignment, assembly, under cleanroom condition issues will be presented.

CW LINAC DEMONSTRATOR

Table 1: Main Parameters

CH-Cavity		
β		0.059
max A/Q		6
Resonance Frequency	MHz	217
Gap number		15
Total length	mm	690
Cavity Diameter	mm	409
Aperture	mm	20
Effective gap voltage	kV	225
Accelerating gradient	MV/m	5.1
Cryostat		
Inner length	mm	2200
Inner diameter	mm	1120
Material		Al
Operating temperature	°K	4.4
Operating pressure above atmosphere	bar	< 1
Solenoids		
Aperture	mm	30
Total length	mm	380
Max. field	T	9.3
Nominal current	A	110

*v.gettmann@gsi.de

The demonstrator project kick-off at GSI was in 2010, which was followed by design studies for the key components as the 217 MHz CH cavity, two sc solenoids, and the cryostat itself. Meanwhile the fabrication is completed. The main parameters are listed in Table1.

The concept of a suspended support frame, which carries the cavity embedded by two sc solenoids, is followed (Fig.1) [1]. The support frame as well the accelerator components are suspended by eight tie rods each in a cross-like configuration (nuclotron suspension) balancing the mechanical stress during the cooling-down and warm up (Fig.2). This way the components will always stay within the tolerance limits related to the beam axis (long. ±2mm, trans. ±0.2mm).

The cryostat has been loaded at the RF and cold test in summer 2016. The cryogenic systems as well as all mechanical tasks were solved for the final beam test.

Figure 1: The cw demonstrator comprising a CH-cavity embedded by two solenoids on a support frame, which hang into the cryostat.

Content from this work may be used under the terms of the CC BY 3.0 licence (© 2017). Any distribution of this work must maintain attribution to the author(s), title of the work, publisher, and DOI.

ISBN: 978-3-95450-191-5 doi:10.18429/JACoW-SRF2017-MOPB096

ESTIMATION OF ALIGNMENT ERROR BY MEASURING HIGHER-ORDER-MODE OF INJECTOR SUPERCONDUCTING CAVITY AT KEK-cERL

Y. Honda*, E. Kako, T. Konomi, T. Miyajima, T. Obina, H. Sakai, K. Umemori
KEK, Ibaraki, Japan

Abstract

cERL is a test accelerator of an energy recovery linac scheme which can realize a high quality beam in a high averaged current. In order to realize a low emittance beam, beam position control in the superconducting accelerating cavity is important. By measuring higher-order-modes (HOM) excited in the cavities, the electrical center of the cavity can be detected. Comparing the HOM signals of the three independent cavities in the injector cryo-module, we estimated the relative alignment errors of the three cavities. The relative positioning errors were found to be 2.5 mm and 0.3 mm in the horizontal and vertical planes, respectively.

INTRODUCTION

The energy recovery linac (ERL) is the unique scheme to realize a low emittance and short bunch beam of linac quality at a high averaged current. A test ERL accelerator (cERL [1]) has been constructed in KEK for demonstrating the feasibility of future ERL facilities.

In order to realize the low emittance, precise tuning of the beam trajectory in the accelerator cavities is important. The beam trajectory should be aligned on the field center of all the cavities. In the case of SRF accelerator of the cERL injector, three independent 2-cell cavities are installed in the cryo-module. If the three cavities are not aligned on a straight line, the beam has to have finite offsets with respect to each cavity even if one tryed to tune the incoming beam trajectory. The requirement of the alignment precision was estimated to be better than 0.4 mm for keeping the emittance degradation less than 10 %.

It is difficult to directly check the alignment of the cavities by an mechanical method once they were installed and cooled in the cryo-module. One promising and most effective method is to measure the beam signal. We have developed a setup to detect the higher-order-modes (HOM) of the cavities excited by the beam passage. By measuring the dipole mode signal of each cavity while scanning the beam trajectory, the field center of each cavity can be estimated.

PRINCIPLE

Excitation of rf modes in a cavity structure by a beam passage is a well established phenomenon. When a bunch of charge q passes a cavity, the output power from an extraction port of the cavity is given as

$$P_{out} = \frac{\omega q^2}{4Q_{ext}}(R/Q) \quad , \tag{1}$$

where ω is the angular frequency of the mode, Q_{ext} is the external quality factor of the port. The R/Q is the integration of the electric field of the mode along the beam trajectory normalized by the total energy of the mode U, given as

$$R/Q = \frac{|\int \vec{E}\cdot\vec{ds}|^2}{\omega U} \quad . \tag{2}$$

Since a dipole mode (TM110) has a node at the cavity center, the excited amplitude of the dipole mode is proportional to the beam offset with respect to the field center. When the beam passes at the electrical center of the cavity, the dipole modes are not excited.

SETUP

Injector Accelerator Cavity

The injector accelerator consists of three 2-cell 1.3 GHz SRF cavities installed in a cryo-module [2]. Figure 1 shows a drawing of the cavity. In order to remove various HOM excited by the beam passage, 5 HOM couplers are attached for each cavity, 3 in the upstream side and 2 in the downstream side. The parameters related to HOM has been reported in elsewhere [3]. Table 1 summarizes the important parameters of the dipole mode used in this study.

Table 1: Parameters of the TM110 Mode

Parameter	value	comment
Frequency	1800 MHz	
Q_{ext}	~3000	for 5 port
R/Q	0.04 Ω	for 1 mm offset

Figure 2 shows the beam line layout around the injector module. The electron beam from a DC-gun, the beam energy was 390 keV in this experiment, is accelerated up to 6 MeV by this injector accelerator. There are steering magnets, namely ZH4 for the horizontal and ZV4 for the vertical plane, at the upstream of the cryo-module. We used these magnets for scanning the beam trajectory in this experiment. The screen monitor, MS3, located at the downstream was used to calibrate the steering kick. The signal from HOM pick-up ports are transferred to the detection electronics located at the outside of the accelerator shield.

* yosuke@post.kek.jp

Content from this work may be used under the terms of the CC BY 3.0 licence (© 2017). Any distribution of this work must maintain attribution to the author(s), title of the work, publisher, and DOI.

ISBN: 978-3-95450-191-5 doi:10.18429/JACoW-SRF2017-MOPB097

DEGRADATION AND RECOVERY OF CAVITY PERFORMANCES IN COMPACT-ERL INJECTOR CRYOMODULE

E. Kako†, T. Konomi, T. Miura, H. Sakai and K. Umemori
KEK, High Energy Accelerator Research Organization, Tsukuba, Ibaraki, Japan
SOKENDAI, The Graduate University for Advanced Studies, Hayama, Kanagawa, Japan

Abstract

After cryomodule assembly and first cool-down tests in 2012, the cERL injector cryomodule has been stably operated with beam for five years. However, gradual increases of x-ray radiation levels due to field emission were observed during long term beam operation. High power pulsed RF conditioning as a cure method was applied in the cool-down period in 2016 and 2017, so that degraded cavity performances have almost recovered up to the previous levels. Performance recovery status in three 2-cell cavities is reported in this paper.

INTRODUCTION

In order to demonstrate an excellent performance for a future project in ERL (Energy Recovery Linac), beam commissioning in compact-ERL (cERL) at KEK has been steadily in progress [1]. The target values of a beam current and beam energy in the cERL are 10 mA and 35 MeV, respectively. Operational beam currents at a beam energy of 20 MeV have increased step by step, up to 10 μA in 2014, 100 μA in 2015 and 1.0 mA in 2016 [2]. Beam operation with high bunch charges of 60 pC was successfully performed in 2017 [3]. An injector cryomodule is required to accelerate CW electron beams of 10 mA from the beam energy of 500 keV to 5.0 MeV [4]. Assembly of the injector cryomodule was started in April, 2012, and the completed cryomodule was installed in the accelerator hall in July, 2012 [5]. After this, cool-down cycles of 11 times have been carried out for 6 years. Increase of x-ray radiation level has been gradually observed during long term beam operation. High power pulsed RF conditioning was applied in order to supress field emission and reduce the x-ray radiation level. Performance degradation and recovery in the cERL injector cryomodule are described in this paper.

INJECTOR CRYOMODULE

Schematic drawing of an inside structure in the cERL injector cryomodule is shown in Figure 1. Each cavity was driven by two input couplers to reduce the required RF power handling capacity and to balance transverse momentum kicks owing to input couplers. Each 2-cell cavity was dressed with a helium (He) jacket, which was made of titanium and maintained the temperature at 2 K. Magnetic shields were put inside the He jackets. For damping higher-order-modes (HOMs), an HOM coupler scheme was chosen. Five loop-type HOM couplers were attached on both beam pipes of each cavity [6]. As a frequency tuning system, a slide-jack tuner equipped with a pair of piezo elements was attached at thick titanium base-plates. An RF input coupler is the most critical component in high power applications of superconducting cavities. A coaxial coupler, equipped with a warm (room temperature) single disk-type ceramic RF window with cooling water channels was used for the CW input couplers. After assembly of the injector cryomodule, the completed cryomodule was installed in the beamline, as seen in Figure 2. The No.1 cavity is driven by a 30 kW klystron, and the No.2 and No.3 cavities are driven by a 300 kW klystron. Then, cool-down tests for low and high RF power measurements were successfully performed before starting the beam commissioning. It was demonstrated that each coupler can transmit RF power of 40 kW in CW [7].

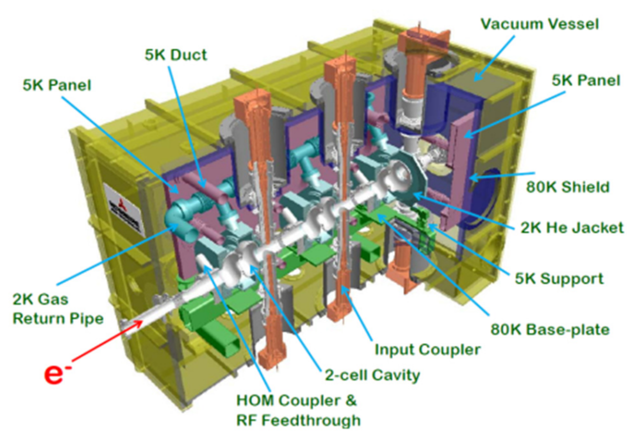

Figure 1: Injector cryomodule for cERL.

Figure 2: Injector cryomodule installed in beam line.

† eiji.kako@kek.jp

Content from this work may be used under the terms of the CC BY 3.0 licence (© 2017). Any distribution of this work must maintain attribution to the author(s), title of the work, publisher, and DOI.

ISBN: 978-3-95450-191-5 doi:10.18429/JACoW-SRF2017-MOPB099

DESIGN OF C-ADS INJECTOR-I CRYOMODULE FOR 325MHz CAVITIES

RuiXiong Han, Rui Ge, ShaoPeng Li, LiangRui Sun, MinJing Sang, Rui Ye,
Lin Bian, XiangZhen Zhang, JieHao Zhang, Zhuo Zhang, JianQin Zhang, MiaoFu Xu,
Institute of High Energy Physics, CAS, Beijing, China

Abstract

The Chinese Accelerator Driven Sub-critical system (C-ADS) uses a high energy proton beam to bombard the metal target and generate neutrons to deal with the nuclear waste. The Chinese ADS proton linear has two 0~10 MeV injectors and one 10~1500 MeV superconducting linac. Injector-I is studied by the Institute of High Energy Physics (IHEP) under construction in the Beijing, China. The linear accelerator consists of two accelerating cryomodules operating at the temperature of 2 Kelvin. This paper describes the structure and thermal performances analysis of the cryomodule. The analysis takes into account all the main contributors (support posts, multilayer insulation, current leads, power couplers, and cavities) to the static and dynamic heat load at various cryogenic temperature levels. The thermal simulation analysis of the cryomodule is important theory foundation of optimization and commissioning.

INTRODUCTION

The Chinese Accelerator Driven Sub-critical system (C-ADS) project is based on a proton Linac that provides a10mA, 1.5 GeV CW proton beam for nuclear waste transmutation. The C-ADS linac includes two major sections: the injector section and the main linac section. [1]. The general layout of the linac is shown in Fig. 1. To satisfy the restricted stability and reliability command of the C-ADS driver linac in the lower energy part, there will be two identical Injectors operating in parallel, backing each other up. One of them, Injector I is under design and construction at Institute of High Energy Physics (IHEP), Chinese Academy of Sciences(CAS) [2]. The injector I consists of two accelerating cryomodules (CM1 and CM2), which accelerates proton beam up to 10MeV. One C-ADS cryomodule houses 7 325 MHz Spoke（β =0.12）superconducting cavities, 7 high power couplers, 7 superconducting solenoids, 7Beam Position Monitors(BPM), et al, and the cavities and solenoids will be immersed in a 2K liquid helium bath .

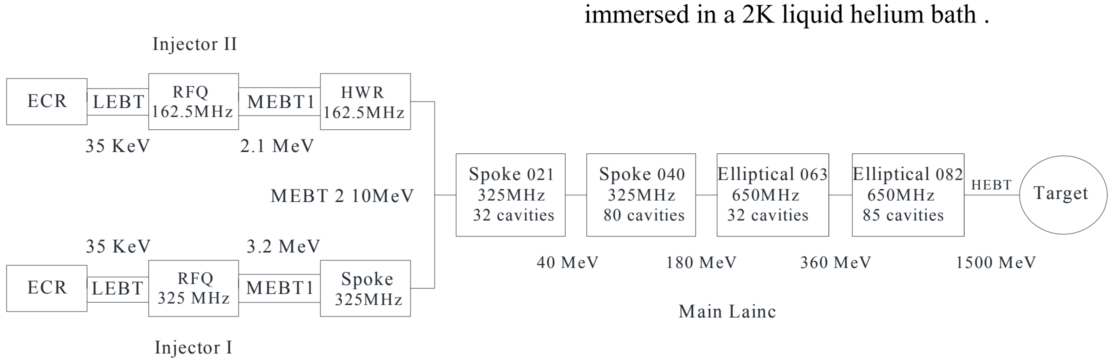

Figure 1: Schematic layout of the C-ADS driver linac.

STRUCTURE OF THE C-ADS INJECTOR-I CRYOMODULE

The C-ADS Injector-I system includes two cyomodules: CM1 cyomodule and CM2 cyomodule. The C-ADS Injector-I cryomodules are based on a modular bottom-supported, the cavities string and cold mass are supported by composite posts, and put them on a strongback at room temperature.

The cryomodule can be separated into three parts, the outer vacuum vessel; the cavities string assembly which comprises of the seven spoke cavities and their associated auxiliary components (high-power input coupler, helium tank, mechanical tuner etc.), the seven superconducting solenoids package including their current leads; the so-called cold-mass of the cryostat, which includes the cryogenic pips, support fixtures (for the cavity string), thermal shields, etc. Transverse and Longitudinal section of the cryomodule are shown in Figs. 2-3.

The design of the accelerator module described as following. A stainless steel vacuum vessel with a

standard diameter about 1400 mm, strongback at the room temperature acting as a support structure, together with 14 posts on top of the strongback, a 2 K two phase pipe connected to the cavity Helium vessels, a 5K forward and return line, a 80 K forward and return line, and a warm-up/cool-down line with capillaries to the bottom of each cavity and solenoid helium vessel. Two Aluminum thermal shields that 5 K helium shield and 80 K nitrogen shield attached to the support structure, and 10 layers of upper insulation (MLI) for 5 K and 30 layers for 80 K.

Content from this work may be used under the terms of the CC BY 3.0 licence (© 2017). Any distribution of this work must maintain attribution to the author(s), title of the work, publisher, and DOI.

ISBN: 978-3-95450-191-5 doi:10.18429/JACoW-SRF2017-MOPB101

CRYOMODULE FABRICATION AND MODIFICATION FOR HIGH CURRENT OPERATION AT THE MAINZ ENERGY RECOVERING SUPERCONDUCTING ACCELERATOR MESA*

T. Stengler†[1], K. Aulenbacher[12], F. Hug[1], T. Kürzeder[2], D. Simon[1]
[1] Johannes Gutenberg-Universität Mainz, Germany
[2] Helmholtz-Institute Mainz, Germany

Abstract

At Johannes Gutenberg-Universität Mainz, the Institute for Nuclear Physics is currently building the multiturn ERL 'Mainz Energy-Recovering Superconducting Accelerator' MESA. The 1.3 GHz cryomodules are based on the ELBE modules at Helmholtz Center Dresden-Rossendorf (HZDR) but are modified to suit the high current, energy recovering purposes of MESA. With two 9-cell TESLA cavities each, they shall provide 50 MeV energy gain per turn. The design and fabrication was done by Research Instruments GmbH, Bergisch Gladbach, Germany. The current status of the cryomodules, the test set up at the Helmholtz-Institute Mainz, the cavity properties and their tests will be discussed.

INTRODUCTION

At the Institute for Nuclear Physics of Johannes Gutenberg-Universität Mainz, Germany, a new Energy-Recovering Superconducting Accelerator is under construction. This accelerator will be the first superconducting accelerator at Mainz and will complement the existing, multiturn electron accelerator MAMI [1]. MESA will run at 1.3 GHz and serve two main experiments: P2 and MAGIX.

P2 will investigate the Weinberg angle with high precision [2,3], while MAGIX is planned as a multi purpose high resolution spectrometer [4] to measure the form factor of the proton and search for the dark photon [5].

To provide the required beam energy for the experiments, two cryomodules will be installed. The design is based on the ELBE cryomodules, which are in use at the Helmholtz Center Dresden-Rossendorf (HZDR), Germany [6]. Modifications had to be done, to satisfy the demands of a high current c. w. beam with a duty cycle of 100 %. The modules are currently in production at RI Research Instruments GmbH, Bergisch Gladbach, Germany and will be delivered soon (fourth quarter of 2017). The cavities are already manufactured by RI, and SRF tested at DESY, Germany [7]. This paper will show the results of the vertical SRF tests, the power coupler conditioning at HZDR and the cryomodule test set up at the Helmholtz-Institute Mainz.

* Work supported by the German Research Foundation (DFG) under the Cluster of Excellence "PRISMA" EXC 1098/2014
† stengler@kph.uni-mainz.de

MAINZ ENERGY-RECOVERING SUPERCONDUCTING ACCELERATOR

MESA is an multiturn electron accelerator with two different modes of operation to be conform with the different requirements of the experiments. It can be operated as a normal multiturn linac (external beam "EB" mode) or as an energy-recovery linac (energy recovery "ER" mode). An overview can be found in Fig. 1.

Two different kind of sources are currently under development to provide a polarized beam by photo emission (STEAM) [8] or a high intensity beam (SPOCK) [9]. Behind the low energy beam transportation, a normal conducting pre-accelerator (MAMBO) [10] pre-accelerates the electrons to 5 MeV. The main accelerator contains two cryomodules for acceleration and deceleration. One turn provides an energy gain of 50 MeV. The number of turns depends on the mode of operation.

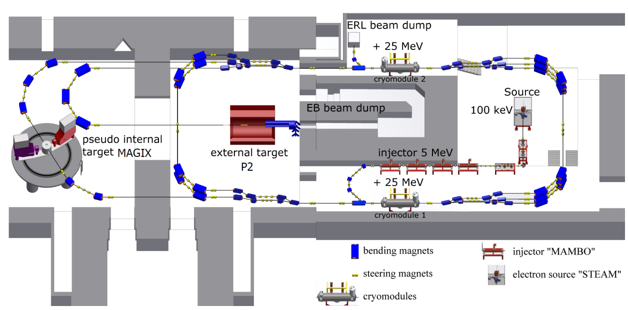

Figure 1: Current design of the MESA lattice. The accelerator is centred around the external beam (EB) mode beam dump. The fixed target experiment P2 is located in the accelerator hall, while the pseudo-internal target MAGIX is located in a separated hall.

At external beam (EB) mode, an energy of 155 MeV at a beam current of 150 µA [11] for polarized electrons is needed. Therefore the beam passes the cryomodules three times.

At energy-recovery (ER) mode, MESA accelerates a non-polarized 105 MeV beam with high currents between 1 mA up to 10 mA. After two turns through the main accelerator, the beam will interact with the pseudo-internal target MAGIX. In current simulations, 0.16 % of the beam is lost in the experiment [12]. The non-interacting part of the beam will be guided back into the accelerator with a phase shift of 180° and will be decelerated down to 5 MeV.

Content from this work may be used under the terms of the CC BY 3.0 licence (© 2017). Any distribution of this work must maintain attribution to the author(s), title of the work, publisher, and DOI.

ISBN: 978-3-95450-191-5 doi:10.18429/JACoW-SRF2017-MOPB102

PRELIMINARY DESIGN ON THE CRYOMODULE OF THE HWR FOR THE SECONDARY PARTICLE GENERATION AT KOMAC*

Hyeok-Jung Kwon†, Han-Sung Kim, Seung-Hyun Lee, Jeong-Jeung Dang, Kyung-Hyun Kim, Young-Gi Song, Yong-Sub Cho
KOMAC, KAERI, Gyeongju, Korea

Abstract

A 100-MeV proton linac based on the radio frequency quadrupole (RFQ) and conventional drift tube linac (DTL) has been operating for user service at KOMAC (Korea Multi-purpose Accelerator Complex). A superconducting linac based on the half-wave resonator (HWR) is studied in order to increase the proton energy from 100 MeV to 160 MeV for the secondary particle generation such as neutron. A cryomodule for the HWR was designed. The operating temperature of the HWR is 2 K. One cryomodule contains four HWR cavities and it didn't have superconducting solenoid because a doublet lattice using normal conducting magnet was considered as focusing elements. A thermal design was conducted and the structure was designed based on the existing well proven technologies. In this paper, the results of the design on the cryomodule for KOMAC HWR are summarized.

INTRODUCTION

A 100-MeV proton linac has been operating for user beam service since 2013. There were 2 beam lines to supply proton to users at 2013, one for 20 MeV beam users and the other for 100 MeV beam users. Both beam lines were general purpose beam line. The third beam line, whose purpose is to produce radioisotope (RI) by using high power proton beam, was constructed in 2015 and is under operation. The fourth beam line, whose purpose is to supply low flux beam to users from the space radiation study and detector development, was constructed in 2016 and is under commissioning [1].

Until now, the major application field of the proton beam is to use the proton beam itself. But it is well-known that energetic proton beam on target can be used to generate secondary particles which have a variety of application fields too. Two kinds of secondary particle are considered to develop secondary particle research platform at KOMAC, one is a Li-8 beam and the other is a neutron. The proposed layout of the secondary particle research facility is shown in Fig. 1. A Li-8 is a beta-emitting radioisotope of which lifetime is 0.8 s. Due to its asymmetry of the angular distribution of the emitting beta-particle, it is used for beta-NMR (Nuclear Magnetic Resonance) as a probe beam. A pulsed neutron generated from the target bombardment by proton beam is a major application field of the high power proton accelerator. KOMAC is going to start a research on the pulsed neutron source based on the proton accelerator by using 100 MeV linac. The research fields include a neutron production target, a short pulse proton beam generation technology, a pulsed neutron beam line. In addition, we considered the development of the superconducting accelerator technology to increase the existing 100 MeV linac. As a first step, we are going to develop a half-wave resonator (HWR) to increase the proton energy from 100 MeV to 180 MeV in the empty space of the KOMAC linac tunnel [2].

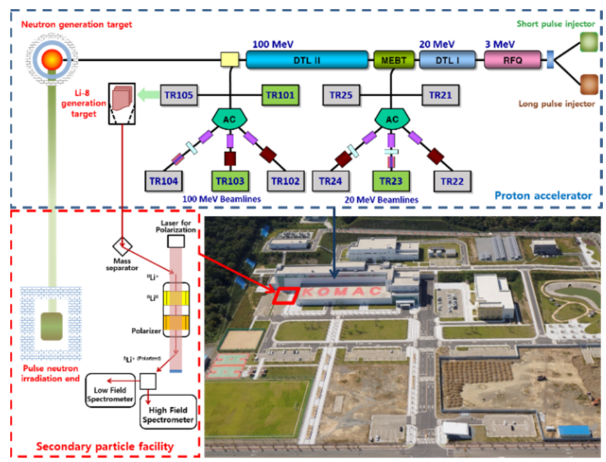

Figure 1: Layout of Secondary Particle Facility.

HALF-WAVE RESONATOR

The operating frequency is 350 MHz which is the same with the RFQ and DTL. The maximum values of the peak electric field and peak magnetic field were limited under 35 MV/m and 70 mT respectively in electromagnetic design stage. One feature of the KOMAC HWR is that the geometrical beta of the cavity is 0.58 which means the height of the HWR is nearly the same with the diameter. The designed HWR is shown in Fig. 2 and the design parameters are summarized in Table 1.

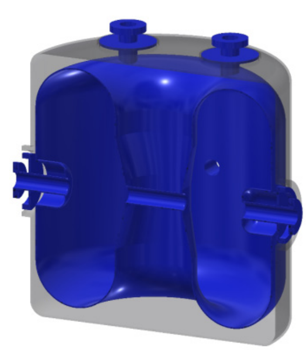

Figure 2: 350 MHz Superconducting half wave resonator for KOMAC proton linac.

* Work supported by Ministry of Science, ICT & Future Planning of the Korean Government.
† hjkwon@kaeri.re.kr

Content from this work may be used under the terms of the CC BY 3.0 licence (© 2017). Any distribution of this work must maintain attribution to the author(s), title of the work, publisher, and DOI.

ISBN: 978-3-95450-191-5 doi:10.18429/JACoW-SRF2017-MOPB104

DEVELOPMENT OF A NOVEL SUPPORTING SYSTEM FOR HIGH LUMINOSITY LHC SRF CRAB CAVITIES

T. Jones[1], STFC Daresbury Laboratory, Warrington, UK
G. Burt, University of Lancaster, Lancaster, UK
K. Artoos, R. Calaga, O. Capatina, T. Capelli, M. Sosin, J. Swieszek, C. Zanoni, CERN, Geneva, Switzerland
[1]also at University of Lancaster, Lancaster, UK

Abstract

Compact SRF Crab Cavities are integral to the HL-LHC upgrade. This paper details the design of support structures within the SPS (Super Proton Synchrotron) Crab Cavity Cryomodule. For ease of alignment each cavity is supported with the mechanical tuner and RF Fundamental Power Coupler (FPC) via a common support plate. To reduce heat leak and remove bellows in the FPC it was determined that this would be the fixed support for the cavity. In addition, novel flexural blades were designed to give increased stiffness yet allow for thermal contraction of the cavity towards the fixed point of the FPC. This approach was superior when compared via simulation to several alternative techniques. A detailed simulation model was used for optimisation of directional stiffness, identification of vibration modes and minimising thermal stresses. A transmission matrix was developed to assess modal deflection for given ground vibration conditions. The spreadsheet gives an instantaneous yet comparable result to time consuming random vibration FE Analyses. The final engineering design of the supporting system is now complete and will also be described in this paper.

INTRODUCTION

There are currently 2 crab cavity designs envisaged for the HL-LHC upgrade. These are the Double Quarter Wave Resonator (DQW) and the RF Dipole (RFD), the designs for which are shown in Fig. 1. The design of the DQW RF structure has been led by Brookhaven National Laboratory, the RFD by Old Dominion University. Each cavity type has a different deflecting plane, the DQW rotates bunches vertically, whereas the RFD deflects bunches horizontally. The cavities sit within a Grade 2 Titanium liquid helium tank. This material was chosen as it has an almost identical co-efficient of thermal expansion to the Niobium cavity. There are mechanical interfaces on the cavity for connection to the Cavity Tuner. The SRF Compact Crab Cavities designed for HL-LHC have never been tested with beam. The risk of installing unqualified cavities into the LHC was deemed unacceptable; therefore a test of 2 DQW cavities in the Super Proton Synchrotron is planned for 2018.

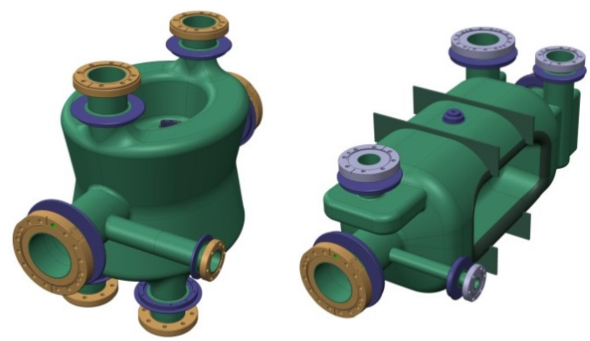

Figure 1: DQW (left) and RFD (right) prototype crab cavity models.

The cryomodule designed to house the cavities during testing on the SPS is shown in Fig. 2. This paper describes the process by which the cavity support structures were designed and integrated into the cryomodule. The cavity support system is to be capable of supporting the ~250 Kg dressed cavity, yet with low cross section in order to minimise conductive heat losses into the 2 Kelvin cryogenic system. The support system should allow for thermal contraction of the 2 K components so that there are no stresses above the respective material yield, and the cavity should not be deformed during cool down. In addition, cavity RF detuning due to vibration (microphonics) is to be minimised to <5.5 Hz [1]. The choice of operating below the lambda point of helium, i.e. the operation at 2 K is partially driven by this desire to minimise microphonics as in this superfluid state helium should not boil [2]. Microphonics can be compensated by the use of a fast acting Piezo tuner, however, it is believed that through careful design of the cryomodule this should not be required for the HL-LHC Crab Cavities.

Content from this work may be used under the terms of the CC BY 3.0 licence (© 2017). Any distribution of this work must maintain attribution to the author(s), title of the work, publisher, and DOI.

ISBN: 978-3-95450-191-5 doi:10.18429/JACoW-SRF2017-MOPB105

THERMOSIPHON COOLING LOOPS FOR ARIEL CRYOMODULES

Yanyun Ma†, A. Koveshnikov, R.E. Laxdal, D. Lang, N. Muller,
TRIUMF, Vancouver, Canada

Abstract

Thermosiphon cooling loops have been used in ARIE [1,2] cryomodules for 1.3GHz superconducting cavities cooling. It can deliver 4K liquid Helium from 4K phase separator to cavity thermal intercepts and return the vaporized liquid to the 4K phase separator as a refrigerator load. The design and test results are presented in this paper.

INTRODUCTION

The ARIEL is an on-going project at TRIUMF which will triple TRIUMF's capability of rare isotope production over the next ten years for the needs of the international scientific community [3]. ARIEL uses a 50 MeV, 10 mA continuous-wave (CW) electron linear accelerator (e-Linac) as a driver accelerator utilizing superconducting bulk niobium technology at 1.3 GHz. The accelerator is divided into three cryomodules including a single cavity injector cryomodule (ICM) and two accelerating cryomodules (ACM) with two cavities each as shown in Fig. 1.

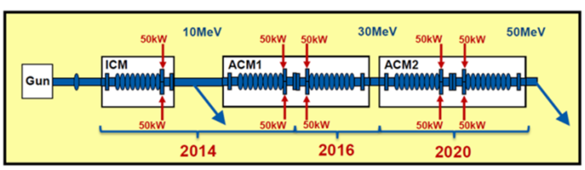

Figure 1: A schematic of the e-Linac showing the installation stages.

A first phase consisting of an ICM, and an accelerating cryomodule with just one accelerating cavity on board plus a `dummy' cavity that occupies the second cavity space in the cryomodule (ACMuno) was installed for initial technical and beam tests to 23 MeV in 2014 [4]. An upgrade that added a second 1.3 GHz nine-cell cavity to ACM1 is under testing [5,6]. The 2nd phase will add ACM2 module and a ramp up in beam intensity to the full 50 MeV, 0.5 MW capability.

The ARIEL cryomodule design, shown in Fig. 2, borrows significantly from the ISAC-II cryomodules. Each cryomodule is outfitted with an on-board 4K to 2K cryogenics insert [2,7]. The insert consists of a 4K phase separator, a 2.5gm/sec heat exchanger, a JT expansion valve and a 4K cooldown valve.

The 300 K to 4 K connections of cavities at the beam pipes and at the power couplers are intercepted at both 77 K and 4K. Piping within the cryomodule delivers the 4.2K Helium from phase separator to a number of 4K thermal intercepts and then returns the two phase He back to the 4K phase separator. Depending on the thermal load, the density mismatch between the liquid side (supply side) and the two-phase side (return side) can overcome the head pressure difference between supply and return pipes. In this case a mass flow will be initiated in the siphon loops and convective heat transfer will occur from the load to the helium.

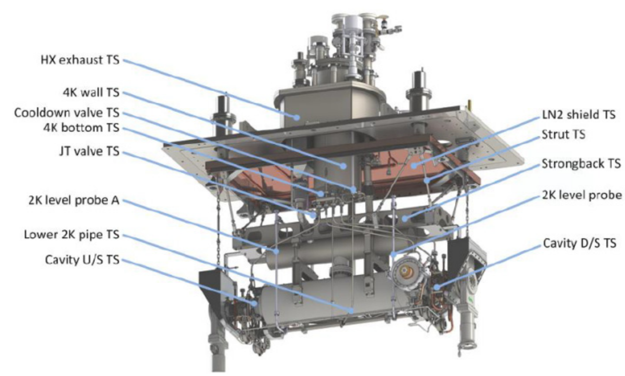

Figure 2: ICM assembly.

Thermosiphon loops were designed, tested and optimized at TRIUMF during the development of the 4 K/2 K cryogenic insert and the commissioning of cryomodule.

THERMOSIPHON DESIGN

The simple structure and higher cooling capacity make thermosiphon an attractive cooling method as shown in Fig. 3. The 4K thermal intercept circuit in Fig. 3 (a) is replaced by a supply line from the 4K reservoir to the heat loads with returning vapour returning to the upper part of the phase separator which shown in Fig. 3 (b). It is attractive since it reduces the liquefaction load on the refrigerator system and reduces the external piping, heaters and control valves as well. The thermosiphon supply pipe is started from the bottom of the 4K phase separator and divided to several pipes underneath the cold mass. There are four thermal intercepts for each cavity: two of them on the beam pipe flanges and the other two on the couplers. The 4K thermal intercepts are isolated with 77K thermal intercepts by bellows. The return pipes deliver the liquid Helium to the thermal intercepts. All the return pipes are connected together through a manifold and then connected to 4K phase separator.

† mayanyun@triumf.ca

Content from this work may be used under the terms of the CC BY 3.0 licence (© 2017). Any distribution of this work must maintain attribution to the author(s), title of the work, publisher, and DOI.

ISBN: 978-3-95450-191-5 doi:10.18429/JACoW-SRF2017-MOPB106

TEST RESULTS OF THE EUROPEAN XFEL SERIAL-PRODUCTION ACCELERATOR MODULES

K. Kasprzak*, M. Wiencek, A. Zwozniak, IFJ PAN, Krakow, Poland
D. Kostin, D. Reschke, N. Walker , DESY, Hamburg, Germany

Abstract

The serial-production tests of 100 cryomodules for the European XFEL have been finished. In this paper the statistics of the cold RF measurements in the AMTF (Accelerator Module Test Facility) are reported for all the modules. In addition comparison between the cavity vertical test results and module test results are presented.

INTRODUCTION

In August 2016 measurements of serial-production accelerating components for the European XFEL project was finished. The main element of the accelerator (linac) is called the cryomodule and it consists of 8 SRF TESLA type cavities. Each one was examined in the dedicated test infrastructure called AMTF at DESY during the 4 year production period. Tests were performed on two shifts by the team of the engineers from the IFJ PAN, Krakow, Poland [1]. The measurements resulted in information about operating parameters, namely: maximum gradient, quality factor of the RF cavities, as well as cryo-losses and control parameters. After testing, 97 modules have been installed in the European XFEL tunnel. Finally, since April 2017 the accelerator has been successfully commissioned [2].

In this paper an analysis of the final measurement results for serial production cryomodules (from XM1 to XM100) is presented. Based on the AMTF test results there are several ways, in which to quantify the production [3]. Here the emphasis is put on the difference between cryomodule and the vertical test results taking into account the production order and cavity position in the cryomodule. Investigated are data obtained during the pulsed high power RF test and heat-loads measurements. The aim of the pulsed high power RF measurement is to study operating gradients and cavity limits. The data are also compared to those obtained during the vertical measurements. An analysis of the heat-load measurements, which aim to quantify the thermal cryogenic load during operation, is also presented.

CAVITIES PULSED HIGH POWER RF TEST: PERFORMANCE MEASUREMENT OF THE CAVITIES INSTALLED IN THE CRYOMODULES

In order to measure the performance of the European XFEL cavities, the pulsed high power RF test was performed [4]. The maximum and operating accelerating gradients [MV/m] were obtained.

* karol.kasprzak@ifj.edu.pl

The operational limits on the cavity gradients were chosen as the minimum value of:

- (X-RAY) the gradient when radiation exceeds 10^{-2} mGy/min one or other end of the module,
- (BD) the gradient before the quench limit (0.5 MV less),
- (PWR) limit of the ATMF infrastructure (31 MV/m),
- (CPL) cavity operation limit caused by a fundamental power coupler having not conditionable RF discharge or strong overheating (overtemperature) problem.

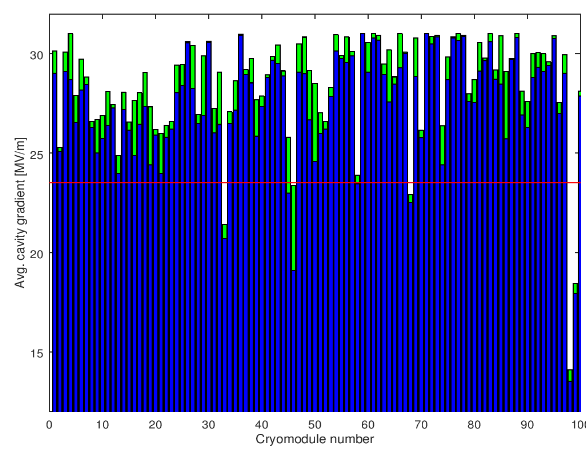

Figure 1: Average of the operating (blue) and maximum (green) gradient for cavities in each serial-production cryomodule. European XFEL Specification is marked by a red line.

The maximum gradient was defined as the highest of the above, taking into account a radiation safety limit of 10 mGy/min for the X-ray measurements.

The European XFEL design operating gradient [5] for a single cavity is specified as 23.6 MV/m, sufficient to achieve the design energy goal of 17.5 GeV with some margin.

Content from this work may be used under the terms of the CC BY 3.0 licence (© 2017). Any distribution of this work must maintain attribution to the author(s), title of the work, publisher, and DOI.

ISBN: 978-3-95450-191-5 doi:10.18429/JACoW-SRF2017-MOPB109

LCLS-II CRYOMODULE TRANSPORT SYSTEM TESTING

N. Huque, E.F. Daly, Jefferson Lab, Newport News, VA 23606, USA
M. McGee, Fermi National Accelerator Laboratory, Batavia, IL 60510, USA

Abstract

The Cryomodules (CM) for the Linear Coherent Light Source II (LCLS-II) will be shipped to SLAC (Menlo Park, California) from JLab (Newport News, Virginia) and FNAL (Batavia, Illinois). A transportation system has been designed and built to transport the CMs over the road in a safe manner. It uses an array of helical isolator springs to attenuate shocks on the CM to below 1.5g in all directions. The system rides on trailers equipped with Air-Ride suspension, which attenuates vibration loads. The prototype LCLS-II CM (pCM) was driven 750 miles to test the transport system; shock loggers recorded the shock attenuation on the pCM, and vacuum gauges were used to detect any compromises in beamline vacuum. Alignment measurements were taken before and after the trip to check for deformation of CM components. Passband frequencies and cavity gradients were measured at 2K at the Cryomodule Test Facility (CMTF) at JLab to identify any degradation of CM performance after transportation. The transport system was found to have safely carried the CM and is cleared to begin shipments from JLab and FNAL to SLAC.

INTRODUCTION

The transportation of a CM over the road poses many opportunities for absorbing damage. While there is always the risk of a catastrophic incident on the road that can destroy the CM, there is also the danger of damage caused by shocks and vibrations that are part of the regular journey. Road transport can often see shock loads as high as 3g – 4g [1], which can deform and misalign cavities and damage other sensitive components and piping. The transport system minimizes the effects of such shocks by attenuating them to acceptable levels.

The CM transportation system is based on that designed by the Deutsches Elektronen-Synchrotron (DESY) used to transport European X-ray Free Electron Laser (XFEL) CMs from Paris, France to Hamburg, Germany. Over one hundred CMs were successfully transported the ~500 miles between the two.

To gauge the types of shock loads that may be experienced during a trip, the JLab pCM was transported over the first leg of its planned route from JLab to SLAC. A study on XFEL CMs found that the maximum allowable load on a CM is 1.5g [2]. The following criteria determined whether the CMs may be safely transported during the remainder of the project:

- Shock attenuation from the transportation system.
- Physical deformation of CM components.
- Uncompromised beamline and insulating vacuums.
- Degradation of CM performance.

TRANSPORT SYSTEM DESIGN

The Shipping System consists of four main elements (Fig. 1): The CM itself, Shipping Frame, Shipping Caps and a flatbed trailer equipped with Air-Ride Suspension.

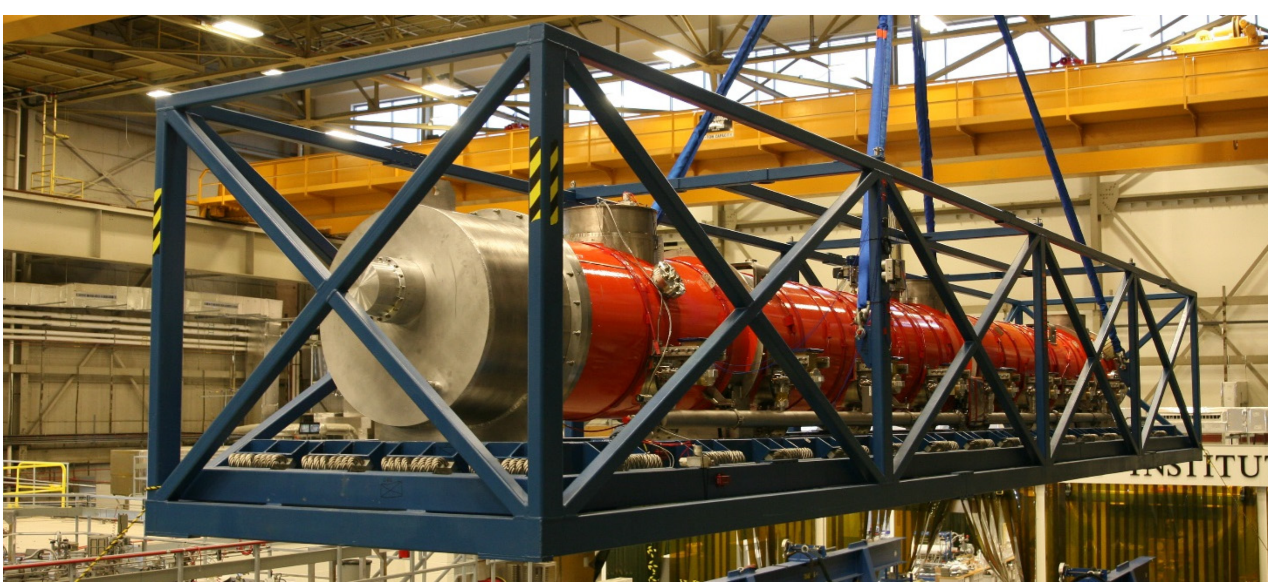

Figure 1: The LCLS-II CM installed in the shipping frame.

Content from this work may be used under the terms of the CC BY 3.0 licence (© 2017). Any distribution of this work must maintain attribution to the author(s), title of the work, publisher, and DOI.

ISBN: 978-3-95450-191-5 doi:10.18429/JACoW-SRF2017-MOPB110

RESULTS OF ACCELERATED LIFE TESTING OF LCLS-II CAVITY TUNER MOTOR

N. Huque, E. F. Daly, Jefferson Lab, Newport News, VA 23606, USA
Y. Pischalnikov, Fermi National Accelerator Laboratory, Batavia, IL 60510, USA

Abstract

An Accelerated Life Test (ALT) of the Phytron stepper motor used in the Linear Coherent Light Source – II (LCLS-II) cryomodule cavity tuner has been carried out at Jefferson Lab (JLab). Since the motor will reside inside the cryomodule, any failure would lead to a very costly and arduous repair. As such, the motor was tested for the equivalent of 9 lifetimes before being approved for use in the production cryomodules. The 9-cell LCLS-II cavity is simulated by disc springs with an equivalent spring constant. Degradation in performance is measured with hysteresis plots of the motor position vs. tuner position – measured via an installed linear variable differential transformer (LVDT). The titanium spindle and traveling nut have been inspected for damage and loss of lubrication. The Phytron motor passed the ALT and is currently being installed in LCLS-II cryomodules.

INTRODUCTION

The LCLS-II Cavity Tuner is a lever-style tuner, consisting of the frame, two piezo actuators, and a Phytron stepper motor - the LVA 52-LCLS II-UHVC-X1 (Fig. 1). In the current testing setup, the piezo actuators are not present and replaced by solid cylinders. Table 1 describes the working parameters of the tuner and motor [1].

The motor itself consists of four main components: the stepper motor, gearbox, titanium spindle and traveling nut. A copper heat sink is located at the edge of the motor section to attach to a thermal strap. The planetary gearbox has a ratio of 1:50. The spindle is a titanium M12x1 thread with a diamond-like carbon (DLC) coating, which attaches to a similarly sized stainless steel traveling nut. The traveling nut has a TECASINT 1041 insert which mates to the M12x1 thread [2].

The motor manufacturer Phytron has the capability to test motors in vacuum at 77K. A test in vacuum at 4K as done here is a more realistic simulation of the motor's operating environment.

TESTING SETUP

The cavity is simulated via two sets of disc springs, designed to imitate the cavity's stiffness of 3kN/mm [3]. The tuner frame and springs are attached to an Aluminium base plate (Fig. 2), which is positioned inside the Tuner Test Can [1].

The can is evacuated and lowered into a vertical test area (VTA) dewar for cold testing at ~4K. Unlike the cryomodule, there is no active pumping on the test can.

An LVDT is positioned between the main lever arm of the tuner and the Aluminium base plate. The LVDT is the primary means of recording and measuring the tuner arm's movement, and the motor's operation. The feedback voltage of the LVDT is used to define the tuner arm displacement. In the provided graphs, the zero-position of the LVDT is at a value of 0.016V [1].

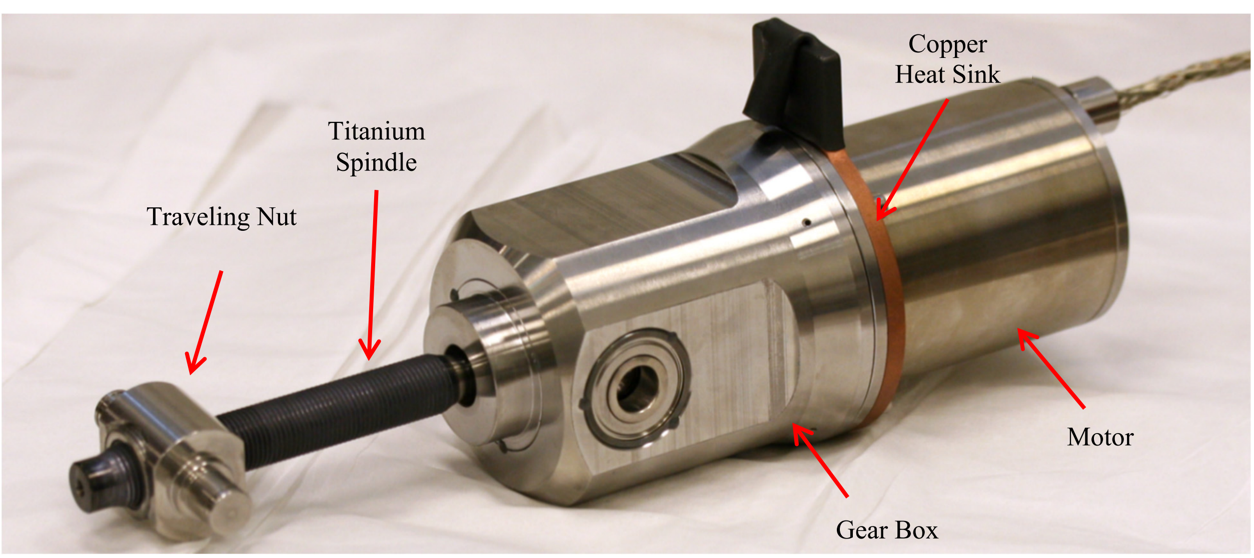

Figure 1: Phytron motor assembly, showing the main components.

Content from this work may be used under the terms of the CC BY 3.0 licence (© 2017). Any distribution of this work must maintain attribution to the author(s), title of the work, publisher, and DOI.

ISBN: 978-3-95450-191-5 doi:10.18429/JACoW-SRF2017-MOPB111

Content from this work may be used under the terms of the CC BY 3.0 licence (© 2017). Any distribution of this work must maintain attribution to the author(s), title of the work, publisher, and DOI.

EUROPEAN XFEL LINAC RF SYSTEM CONDITIONING AND OPERATING TEST

D. Kostin, J. Branlard, A. Gössel, O. Hensler, M. Omet, D. Reschke, A. Sulimov, N. Walker, M. Wiencek, DESY, Notkestrasse 85, 22603 Hamburg, Germany.

Abstract

96 accelerating modules with 768 TESLA / European XFEL type superconducting cavities were installed in the European XFEL ([1] – [3]) LINAC tunnel (XTL) in fall 2016. Warm conditioning of the RF system - High/Low Level RF System and main input couplers - begun even before finishing the accelerator installation works. All modules were conditioned and tested prior to the installation in the tunnel in the AMTF test stand at DESY. Nevertheless, due to some repair activities on warm input coupler parts, warm conditioning was needed on a few modules/couplers. Cooling down to 2K begun in December 2016 and was finished in January 2017. Since then cold conditioning and tests are running. A few input couplers did have problems with conditioning and were disconnected, limiting otherwise the system performance. Some cavities in the modules showed multipacting (MP) effects, mostly because the cavity vacuum was vented with dry nitrogen gas because of mentioned repairs on couplers in some modules. Such MP effects did appear in AMTF as well. All MP effects were successfully conditioned until now.

INTRODUCTION

The European XFEL layout is described in ([1] – [3]). Prior to Linac accelerating modules installation in the tunnel SRF cavities and modules were tested, their performance and limits evaluated and documented ([3] – [7]). Tunnel installation is almost finished now. High power RF system (HPRF, klystrons) are commissioned, low lever RF (LLRF) system is being commissioned [8]. Parallel to LLRF commissioning fundamental power couplers (FPC) conditioning is done, followed by SRF accelerating cavities conditioning and operating test.

FUNDAMENTAL POWER COUPLERS

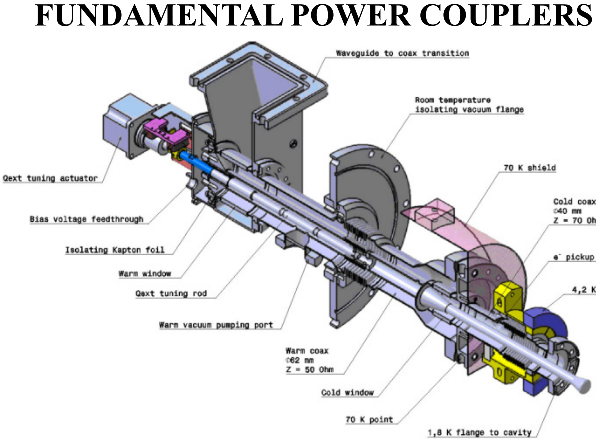

Figure 1: European-XFEL FPC layout.

Last developments for the European XFEL FPC are described for example in [9].

Solving Push-Rod Vacuum Leak Problem

During the module tests in AMTF 35 warm parts (WP) were replaced because of inner screw contact problems and problems with the conditioning, cold 70K window overheating and not conditionable discharges. Another recurrent problem were the tuning push-rod bellow (inside the FPC warm window, Fig. 1) vacuum leaks – 30 push-rods were replaced until the problem was understood and solved finally in the tunnel.

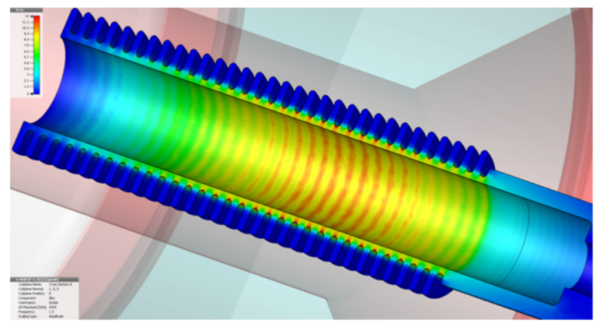

Figure 2: CST MWS FPC simulation: push-rod bellow.

Figure 3: FPC push-rod bellow vacuum leak spot cut-out.

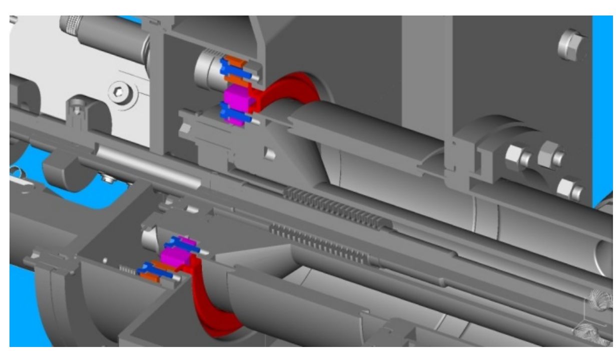

Figure 4: FPC copper coax-gasket (red).

ISBN: 978-3-95450-191-5 doi:10.18429/JACoW-SRF2017-TUXAA01

CEPC SRF SYSTEM DESIGN AND CHALLENGES*

J.Y. Zhai†, Y. Chi, J. Dai, J. Gao, R. Ge, D. Gong, R. Han, T. Huang, S. Jin, Z. Li, B. Liu, Z. Liu
Q. Ma, F. Meng, Z. Mi, G. Pei, Q. Qin, P. Sha, Q. Wang, T. Zhao, H. Zheng, IHEP, Beijing, China
Carlo Pagani, University of Milan and INFN-LASA, Milan, Italy

Abstract

CEPC is a 100 km circular electron positron collider operating at 90-240 GeV center-of-mass energy of Z, W and Higgs bosons. CEPC and its successor SPPC, a 100 TeV center-of-mass super proton-proton collider, will ensure the elementary particle physics a vibrant field for decades to come. The conceptual design report (CDR) of CEPC will be completed in the end of 2017 as an important step to move the project forward. In this contribution, CEPC SRF system CDR design and challenges will be introduced, including the system layout and parameter choices, configuration at different operation energies, transient beam loading and its compensation, cavity fundamental mode (FM) and higher order mode (HOM) induced coupled bunch instabilities (CBI) and the beam feedback requirement, etc. The SRF technology R&D plan and progress as well as the SRF infrastructure and industrialization plan are discussed at last.

INTRODUCTION

The discovery of the low mass Higgs boson in 2012 triggered renewed interest in a large circular e+e- collider served as a Higgs factory. The ring must have a large circumference in order to combat the synchrotron radiation from the high energy electron and positron beams. If such a large size ring were to exist, the tunnel would be ideal for housing a pp collider with an energy much higher than that of the LHC. In this context, the CEPC-SPPC project - a 240 GeV centre-of-mass energy Circular Electron Positron Collider (CEPC) and its successor in the same tunnel a 100 TeV centre-of-mass energy Super Proton Proton Collider (SPPC) - was proposed in October 2012 and officially given the name in June 2013 by the Chinese high energy physics (HEP) community. The CEPC experiment at the Higgs resonance is planned to start in 2030. Experiments at the Z-pole and the WW production threshold will be also conducted. The luminosity goal for Higgs is 2×10^{34} $cm^{-2}s^{-1}$ and higher than 1×10^{34} $cm^{-2}s^{-1}$ for Z-pole.

The CEPC-SPPC preliminary conceptual design (Pre-CDR) (white book) was published in March 2015 [1]. At that time, a 54 km single ring with pretzel scheme was chosen as the baseline for a low project cost. However, due to the difficulty of the pretzel scheme and low luminosity of Z-pole, a partial double ring (PDR) with crab-waist scheme was proposed instead in May 2015. The advantages of PDR are: 1) PDR can avoid pretzel separation by collision with two bunch trains (1+1). 2) PDR in the two collision regions allow the use of the crab-waist scheme to enhance the luminosity and reduce the RF voltage due to longer bunch length. 3) More bunches can be accommodated in the long bunch trains to have higher luminosity for Z-pole. While the disadvantages are also obvious mainly due to transient beam loading of the large bunch gaps and the saw-tooth effect. In order to alleviate the problems, the scheme of advanced partial double ring (APDR) was proposed in May 2016. Eight partial double rings with 4+4 short bunch trains can reduce the RF transient. But the dynamic aperture as well as the saw-tooth effect of such a scheme is still problematic and needs further investigation. Finally, in November 2016, the 100 km double ring (Fig. 1) was chosen as the baseline scheme for the CEPC conceptual design report (CDR), which is to be published in the end of 2017. The APDR scheme is the alternative design for CDR. As the intermediate step towards CDR, a CEPC-SPPC progress report (yellow book) [2] was published in April 2017 to summarize the latest design and R&D progress since 2015.

Figure 1: CEPC Main Ring layout.

As a result of the continuous evolution of the collision scheme, ring type and circumference and other machine top parameters in these four years, the design of the CEPC superconducting RF (SRF) system also changed a lot. The main differences of the SRF system between CEPC Pre-CDR and CDR are: 1) Ring circumference changed from 54 km to 100 km, thus lower RF voltage; 2) Ring type from single ring to double ring, thus more bunches, lower bunch charge and HOM power; 3) W and Z mode design included. In this paper, we will only focus on the latest design especially the double ring scheme, while the Pre-CDR design was described in detail in reference [3].

* Work supported by National Key Programme for S&T Research and Development of China (Grant NO.: 2016YFA0400400)
†zhaijy@ihep.ac.cn

Content from this work may be used under the terms of the CC BY 3.0 licence (© 2017). Any distribution of this work must maintain attribution to the author(s), title of the work, publisher, and DOI.

ISBN: 978-3-95450-191-5 doi:10.18429/JACoW-SRF2017-TUXAA02

LESSONS LEARNED FROM THE HIE-ISOLDE CAVITY PRODUCTION AND CRYOMODULE COMMISSIONING

W. Venturini Delsolaro†, K. Artoos, O. Capatina, Y. Kadi, Y. Leclercq, E. Montesinos, A. Miyazaki, V. Parma, G. Rosaz, K Schirm, A. Sublet, S. Teixeira Lopez, M. Therasse, L. Williams
CERN, Geneva, Switzerland

Abstract

The HIE-ISOLDE superconducting linac started operations at CERN in 2015 with a first cryomodule hosting five superconducting quarter wave resonators (QWR). These cavities are based on the Nb/Cu technology. In time, two more cryomodules have been assembled, installed and commissioned on line, bringing the energy reach for the heaviest ions (A/q=4.5) up to 7.5 MeV/u. In 2017, while the first three cryomodules were prepared for the physics run, six more cavities were produced of which five will be installed in a fourth cryomodule. With this, the high beta section of the linac will be complete and the energy will reach 10 MeV/u for A/q=4.5. In this paper we review the experience and lessons learned during the construction of HIE-ISOLDE, along with some still open questions.

INTRODUCTION

The High Intensity and Energy ISOLDE (HIE-ISOLDE) project [1] is a major upgrade of the ISOLDE facility at CERN, aiming at increasing the intensity and the energy of the post accelerated radioactive ion beams (RIB) up to 10 MeV/u for the heaviest species available at ISOLDE. The layout of the post accelerator in 2017 is shown in Fig. 1.

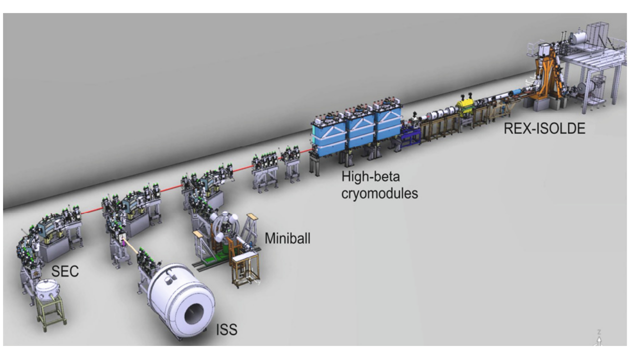

Figure 1: Layout of the HIE ISOLDE linac in 2017.

The principal technology choice, of a superconducting linac based on Nb/Cu quarter wave resonators (QWR), was made in 2007. One year later, R/D on cavity development and design work started. In 2009 the project was formally approved by CERN. Cavity series production started in 2014, and the first beam acceleration with one cryomodule was achieved in October 2015. Since then, one new cryomodule was added every year. A second physics campaign, with two cryomodules, was carried out in 2016, and in 2017 the linac is delivering beam to the users using three cryomodules hosting a total of fifteen high beta QWR and three superconducting solenoids. The cryomodules are of the common vacuum concept following the examples of TRIUMF and INFN Legnaro. A fourth cryomodule is under assembly and will be installed in the winter stop 2017-2018. So far, the performance of the cavities in the linac has been satisfactory, as shown in Fig. 2.

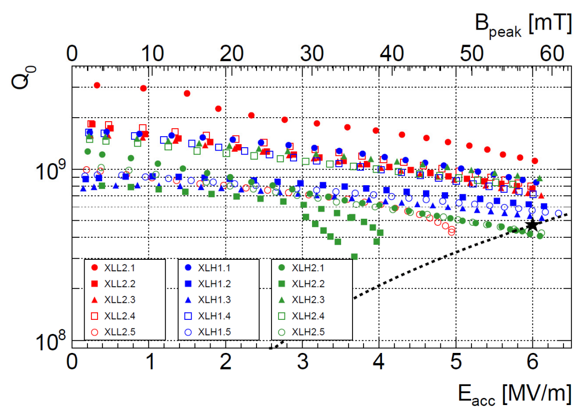

Figure 2: on line performance of the first 15 cavities. The dotted line corresponds to 10 W cavity power dissipation.

ORGANIZATIONAL CHALLENGES

The SRF systems of the HIE ISOLDE linac were entirely designed and for a large part manufactured and assembled at CERN. Only a few key elements were subcontracted to external companies. The complexity and delicacy of the tasks and the diversity of disciplines involved to fulfil them in an environment characterized by multiple projects, sharing infrastructures and resources, posed remarkable organizational challenges.

Project Organisation and Technical Coordination

As it is common in large organizations having to manage multiple activities, CERN has a matrix type organizational model, whereby specialists are pooled in organic units, each delivering their services to different projects. The advantages and disadvantages of such structures for the Organization and for the single projects are well known [2]. In this context the HIE-ISOLDE project was structured in thematic working groups, gathering experts from different organic units to make-as much as possible-consensual decisions and coordinate the work, while maintaining their multiple reporting lines. Since initially little staff was assigned to the project, fellows and students were at the

† Walter.Venturini@cern.ch

Content from this work may be used under the terms of the CC BY 3.0 licence (© 2017). Any distribution of this work must maintain attribution to the author(s), title of the work, publisher, and DOI.

ISBN: 978-3-95450-191-5 doi:10.18429/JACoW-SRF2017-TUXAA03

PROGRESS OF FRIB SRF PRODUCTION*

T. Xu†, K. Saito, H. Ao, B. Bird, N.K. Bultman, F. Casagrande, C. Compton, K.D. Davidson, K. Elliott, V. Ganni, A. Ganshyn, W. Hartung, M. Ikegami, P. Knudsen, S.M. Lidia, E.S. Metzgar, S.J. Miller, D.G. Morris, P.N. Ostroumov, J.T. Popielarski, L. Popielarski, M.A. Reaume, S. Shanab, M. Shuptar, S. Stark, D.R. Victory, J. Wei, J.D. Wenstrom, M. Xu, T. Xu, Y. Xu, Y. Yamazaki, FRIB, Michigan State University, East Lansing, Michigan, USA
A. Facco, INFN/LNL, Legnaro (PD), Italy
K. Hosoyama, KEK, Ibaraki, Japan
M.P. Kelly, ANL, Argonne, Illinois, USA
R.E. Laxdal, TRIUMF, Vancouver, Canada
M. Wiseman, JLab, Newport News, Virginia, USA

Abstract

The Facility for Rare Isotope Beams (FRIB), under construction at Michigan State University, will utilize a driver linac to accelerate stable ion beams from protons to uranium up to energies of > 200 MeV per nucleon with a beam power of up to 400 kW. The FRIB linac consists of 46 cryomodules containing a total of 324 superconducting radiofrequency (SRF) resonators and 69 superconducting solenoids. The design of all six types of cryomodules has been completed. The critical SRF components have been tested as subsystems and validated in production cryomodules. The mass production of SRF cryomodules is underway. Here we report on the progress of the technical construction of the FRIB superconducting linac.

INTRODUCTION

FRIB is a new facility for cutting-edge nuclear physics research with rare isotopes. It is being constructed at Michigan State University (MSU), sponsored by the US Department of Energy (DOE). The FRIB driver linac will accelerate stable ion species to energies of no less than 200 MeV/u, providing up to 400 kW on the target to produce rare isotopes [1]. FRIB conventional construction started in March 2014, and the accelerator system construction began in October 2014. The FRIB accelerator building was completed in 2016 (Figure 1, right). Installation of the liquid helium distribution lines in the tunnel is nearly complete; cryomodule installation started in 2017 (Figure 1, right). Considerable progress has been made since the last SRF conference report two years ago [2]. Linac commissioning will be staged, starting with the Front End in Fall 2017. FRIB project completion will be in 2022 and nearly 1,400 users are anticipated.

FRIB DRIVER LINAC

As described in Table 1, the FRIB driver linac has four families of SRF cavities: 2 types of quarter wave resonators (QWRs) at 80.5 MHz, and 2 types of half wave resonators

Table 1: FRIB Cavities and Cryomodules.

β	Type	Component Counts (baseline + spares)		
		Cryomodules	Cavities	Solenoids
Quarter Wave Cryomodule				
0.041	accelerating	3 + 1	12 + 4	6 + 2
0.085	accelerating	11 + 1	88 + 8	33 + 3
	matching	1 + 1	4 + 4	-
Half Wave Cryomodule				
0.29	accelerating	12	72	12
0.53	accelerating	18	144	18
	matching	1	4	-
TOTALS		46 + 3	324 + 16	69 + 5

Figure 1: Left: aerial view of the FRIB accelerator building. Right: cryogenic distribution lines and cryomodules.

* Work supported by the U.S. Department of Energy Office of Science under Cooperative Agreement DE-SC0000661
† XuTi@frib.mes.edu

Content from this work may be used under the terms of the CC BY 3.0 licence (© 2017). Any distribution of this work must maintain attribution to the author(s), title of the work, publisher, and DOI.

ISBN: 978-3-95450-191-5 doi:10.18429/JACoW-SRF2017-TUXBA01

LOW TEMPERATURE DOPING OF NIOBIUM CAVITIES: WHAT IS REALLY GOING ON?*

P. N. Koufalis†, J. T. Maniscalco, M. Liepe, Cornell University, Ithaca, NY, USA

Abstract

It was first discovered at Fermilab, and subsequently replicated at Cornell, that low temperature heat treatments (120 – 160 °C) of niobium cavities in a low pressure atmosphere (20 – 60 mTorr) of nitrogen can lead to the so-called 'Q-rise' and high Q_0 similar to that of cavities nitrogen-doped at high temperatures (~800 °C). It was suggested by Fermilab that the low temperature baking effect observed (i.e. Q-rise and high Q_0) was a result of nitrogen 'infusion' in the first ~5 nm of the niobium surface. We conducted a systematic study of the low temperature baking effect using RF measurements of a cavity prepared with a low temperature treatment as well as detailed secondary ion mass spectroscopy measurements of single-crystal niobium samples treated with various temperatures, durations, and gas mixtures. We demonstrate that the low-temperature baking is, in fact, drastically lowering the electron mean free path in the RF penetration layer, and that this is not primarily due to nitrogen 'infusion'. Instead, it is shown that the diffusion and presence of other interstitial impurities (specifically carbon and oxygen) at high concentrations are the cause of the reduction in mean free path and, therefore, of the observed Q-rise and high Q_0 values.

INTRODUCTION

Many previous experiments have shown that niobium cavities doped with nitrogen at high temperature (~800 °C) leads to higher quality factors, Q_0, and an increase of Q_0 with increasing gradients, E_{acc} [1, 2]. This effect is often to referred to as 'anti-Q-slope' or 'Q-rise' [1]. Both effects result in lower cryogenic power loads reducing operating costs.

More recently it was discovered that cavities treated in a low temperature (~160 °C), low pressure (~40 mTorr) nitrogen atmosphere exhibited the same effects as cavities doped at high temperatures [3]. In this temperature regime, nitrogen only diffuses a few nm into the niobium surface over the course of a day whereas at higher temperatures (~800 °C) nitrogen is able to diffuse several μm into the surface within minutes. The observed effects in low temperature doped cavities were attributed to the presence of nitrogen in the first ~2 nm [4] and came to be called nitrogen 'infusion' [5]. However, it has been shown that nitrogen is not present in sufficient quantities to account for the observed Q-rise [6]. We demonstrate that it is other interstitial impurities (i.e. carbon and oxygen) that is responsible for the reduction of the mean free path and, therefore, of the observed effects.

Four TESLA-shaped [7] 1.3 GHz cavities received surface treatments summarized in Table 1 with Q_0 vs. E_{acc} measurements shown in Fig. 1. Each cavity received electropolishing (EP) and high pressure rinsing (HPR) with deionized water before heat treatment.

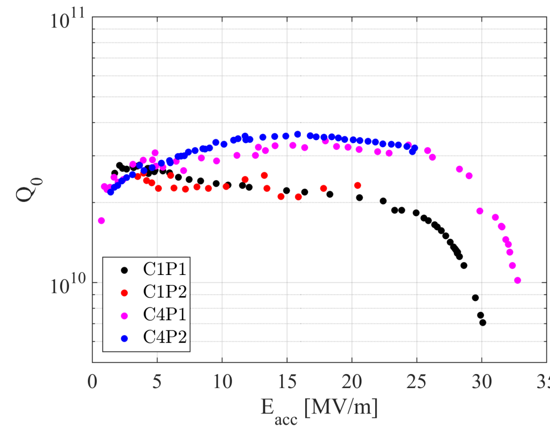

Figure 1: RF cavity performance for TESLA-shaped 1.3 GHz cavities at T = 2.0 K for a high temperature nitrogen doped cavity, a low temperature doped cavity, and two standard-treatment bulk-niobium cavities. Q-rise is observed for both the low temperature and high temperature doped cavities.

HIGH TEMPERATURE NITROGEN DOPING

By introducing interstitial nitrogen to the niobium lattice the density of potential scattering sites increases and consequently the electron mean free path, ℓ, is reduced [2]. It has been experimentally observed that higher concentrations of nitrogen correspond to shorter mean free paths. The 'strength' of the Q-rise correlates strongly with the decrease in mean free path thus making ℓ a useful material parameter for quantifying the doping level [2]. Recent theoretical work by Gurevich [8] and experimental work by Maniscalco [9] provide a promising insight into the physical mechanism that leads to the observed effects in doped cavities.

In the high-temperature nitrogen-doping process the niobium cavity is heated treated in a low-pressure (~40 mTorr) nitrogen atmosphere at temperatures from 600-1000 °C. Niobium nitrides form on the surface of the cavity at these temperatures, allowing nitrogen to diffuse from the nitride into the bulk preferentially occupying octahedral interstitial sites [1,2,10]. Treatments may or may not include an annealing step in ultra-high vacuum after doping. Following heat treatment, the cavity receives an EP to remove the lossy nitride layer. We will see that low temperature doped cavities do not require post-doping EP.

* Work supported by NSF Award PHYS-1416318.
† pnk9@cornell.edu

Content from this work may be used under the terms of the CC BY 3.0 licence (© 2017). Any distribution of this work must maintain attribution to the author(s), title of the work, publisher, and DOI.

ISBN: 978-3-95450-191-5 doi:10.18429/JACoW-SRF2017-TUYAA01

THE IMPORTANCE OF THE ELECTRON MEAN FREE PATH FOR SUPERCONDUCTING RF CAVITIES*

J. T. Maniscalco†, P. N. Koufalis, and M. Liepe
CLASSE, Cornell University, Ithaca, NY, 14853, USA

Abstract

Theoretical results offer a potential explanation for the anti-Q-slope, the phenomenon of decreasing microwave surface resistance with increasing radio-frequency electromagnetic field strength. This effect has been observed in niobium doped with impurities, chiefly nitrogen, and has been put to use in the Linac Coherent Light Source II (LCLS-II) accelerator currently under construction. Our work, presented here, finds a strong link between the electron mean free path, the main measure of impurity doping, to the overheating of quasiparticles in the RF penetration layer. This is an important effect that adjusts the magnitude of the theoretical anti-Q-slope by providing a mechanism to counteract it and introduce a surface resistance that increases with field strength. We discuss our findings in a study of niobium cavities doped at high temperature (800-990 °C) as well as new analysis of low-temperature-doped cavities.

INTRODUCTION

This work is a continuation of research previously published in Ref. [1]; some of the earlier results are summarized here for completeness.

A classic observation in the field of SRF is the dependence of the BCS surface resistance on the electron mean free path ℓ. This resistance reaches a minimum when $\ell \approx \xi_0/2$, where ξ_0 is the clean coherence length [2]. In 2013, researchers at Fermilab and Jefferson Lab discovered an additional effect linked to the mean free path, namely that niobium SRF cavities doped with impurities (and thus with shorter mean free paths than clean niobium) under certain conditions exhibit a microwave surface resistance that decreases as the strength of the RF magnetic field in the cavity increases [3,4]. This phenomenon, now commonly referred to as the “anti-Q-slope”, has been studied at length in nitrogen-doped niobium cavities, and has been employed in the ongoing LCLS-II project [5–8]. In general, nitrogen-doped SRF cavities reach peak quality factors two to four times higher than their undoped brethren, due to the combination of the above two effects. Figure 1 shows characteristic RF performance of a nitrogen-doped cavity in comparison with an undoped electropolished cavity.

Recent theoretical work by A. Gurevich (ODU) offers a mechanism to explain the reduction in surface resistance that manifests as the anti-Q-slope [9]. Magnetic fields parallel to the surface of a superconductor excite screening currents on the surface which prevent magnetic flux from entering the superconducting bulk. These currents can be strong enough to significantly modify the density of states of the quasiparticles (unpaired, normal-conducting electrons). For materials with sufficiently sharp energy gap peaks, this modification smears out the peak, both lowering the effective energy gap and decreasing the total number of available states near the gap. Under the right conditions, this increases the pair-breaking energy, which decreases the density of normal-conducting electrons and thus decreases the microwave surface resistance.

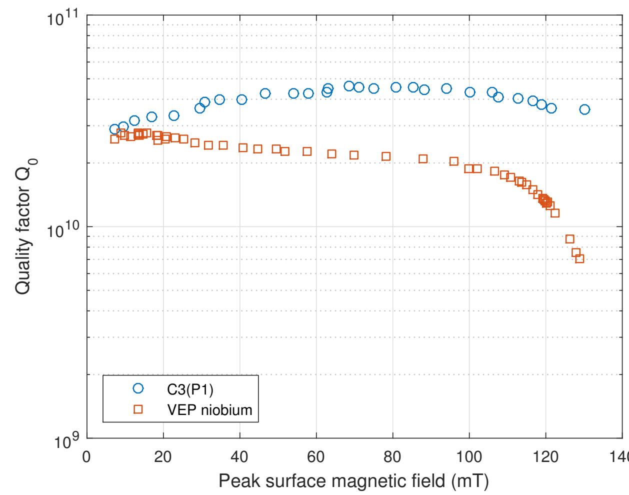

Figure 1: Comparison of intrinsic quality factor Q_0 as a function of surface magnetic field B_{pk} for a nitrogen-doped cavity (blue circles) and an electropolished niobium cavity (red squares).

This decrease in resistance is counteracted by a field-dependent increase in resistance due to the overheating of quasiparticles in the RF surface. The electromagnetic field oscillating in the cavity dissipates power into the surface due to the surface resistance; inefficiencies in transporting this thermal energy out to the cryogenic bath cooling the cavity result in an increase of the temperature of the electrons on the surface. This then results in a feedback effect, where the increasing power dissipated at higher fields leads to an increasing surface resistance. The magnitude of this overheating effect is controlled by the “overheating parameter” α', with contributions from the electron-phonon energy transfer rate Y, the thermal conductivity κ, and the Kapitza resistance h_K. In the linear approximation of low overheating, α' has the following definition:

* This work was supported in part by the U.S. National Science Foundation under Award No. PHY-1549132, the Center for Bright Beams, and under NSF Award No. PHY-1416318.
† jtm288@cornell.edu

Content from this work may be used under the terms of the CC BY 3.0 licence (© 2017). Any distribution of this work must maintain attribution to the author(s), title of the work, publisher, and DOI.

ISBN: 978-3-95450-191-5 doi:10.18429/JACoW-SRF2017-TUYAA02

ADVANCEMENT IN THE UNDERSTANDING OF THE FIELD AND FREQUENCY DEPENDENT MICROWAVE SURFACE RESISTANCE OF NIOBIUM

M. Martinello*, S. Aderhold, S. K. Chandrasekaran, M. Checchin, A. Grassellino, O. Melnychuk, S. Posen, A. Romanenko, D.A. Sergatskov
Fermi National Accelerator Laboratory, Batavia, IL 60510, USA

Abstract

The radio-frequency surface resistance of niobium resonators is incredibly reduced when nitrogen impurities are dissolved as interstitial in the material, conferring ultra-high Q-factors at medium values of accelerating field. This effect has been observed in both high and low temperature nitrogen treatments. As a matter of fact, the peculiar anti Q-slope observed in nitrogen doped cavities, i.e. the decreasing of the Q-factor with the increasing of the radio-frequency field, come from the decreasing of the BCS surface resistance component as a function of the field. Such peculiar behavior has been considered consequence of the interstitial nitrogen present in the niobium lattice after the doping treatment. The study here presented show the field dependence of the BCS surface resistance surface of cavities with different resonant frequencies, such as: 650 MHz, 1.3 GHz, 2.6 GHz and 3.9 GHz, and processed with different state-of-the-art surface treatments. These findings show for the first time that the anti Q-slope might be seen at high frequency even for clean Niobium cavities, revealing useful suggestion on the physics underneath the anti Q-slope effect.

INTRODUCTION

Superconducting Radio-Frequency (SRF) cavities are key components of modern particle accelerators. For continuous wave (CW) accelerators it is extremely important to maximize the cavity Q-factor in order to lower the power dissipated in the cavity walls and, therefore, the cryogenic cost. The so-called Nitrogen-doping is a surface treatment capable to dramatically improve the SRF performance, increasing the Q-factor by a factor of three at medium values of accelerating field, i.e. around E_{acc} = 16 MV/m [1]. Peculiar signature of such a treatment is the increasing of the quality factor as a function of the accelerating field, called anti Q-slope to underline that the trend is opposite to the usual Q-slope observed at medium accelerating field, in standard treated niobium cavities.

The R&D of SRF cavities in the last decades has been particularly focused in studying 1.3 GHz cavities, as of major importance for large accelerator project such as the International Linear Collider (ILC), the European X-ray Free Electron Laser (EXFEL) and the Linear Coherence Ligth Source II (LCLS-II). This is especially true for the N-doping treatment that, right after its discovery in 2013, has been implemented for the LCLS-II cryomodule production. This paper show the first systematic study of the field dependent micro-wave surface resistance variation as a function of different resonant frequencies.

The micro-wave surface resistance R_s is intimately related with the cavity Q-factor, being $Q_0 = G/R_s$, where $G = 270\,\Omega$ is the geometrical factor, independent on material properties. In agreement with common convention, the RF surface resistance is defined as sum of two contributions, the BCS surface resistance (R_{BCS}), and the residual resistance (R_{res}). Mattis and Bardeen [2] defined for the first time the BCS surface resistance contribution, which takes into account dissipation coming from thermally excited quasiparticles, in agreement with the Bardeen-Cooper-Schrieffer theory of superconductivity [3]. R_{BCS} decays exponentially with the temperature and depends on several material parameters, such as: London penetration depth λ_L, coherence length ξ_0, energy gap Δ, critical temperature T_c and mean free path ℓ.

Decomposing the surface resistance contribution [4], it has been shown that the anti Q-slope of N-doped cavities is consequence of the decreasing of the BCS surface resistance components as a function of the accelerating field. Recent studies has also suggested that this enhancement of the superconductivity at medium field, may be due to non-equilibrium distribution of quasi-particles [5]. Findings reported later on in this paper will corroborate further such a hypothesis.

EXPERIMENTAL PROCEDURE

The different surface resistance contributions (R_{BCS} and R_{res}) has been calculated as a function of the accelerating field, for elliptical niobium cavities resonating at 650 MHz, 1.3, 2.6 and 3.9 GHz. A summary table of the surface treatment studied for each resonant frequency is shown in Table 1.

As previously mentioned, the BCS surface resistance exponentially decreases as a function of the temperature. Therefore, in case of low frequencies cavities, such as 650 MHz and 1.3 GHz, the R_{BCS} contribution at T = 1.5 K becomes negligible compared with the residual resistance R_{res}, therefore $R_S(1.5\,K) \simeq R_{res}$ and:

$$R_{BCS}(2K) = R_s(2K) - R_{res}\,. \tag{1}$$

In case of high frequency cavities R_{BCS} at T = 1.5 is not negligible instead, and in this case R_{res} has to be calculated from $R_S(T)$ data interpolation. Since the residual resistance is independent on temperature, by fitting $R_S(T)$ acquired during the cavity cooldown, in a data range between 2 K

* mmartine@fnal.gov

Content from this work may be used under the terms of the CC BY 3.0 licence (© 2017). Any distribution of this work must maintain attribution to the author(s), title of the work, publisher, and DOI.

ISBN: 978-3-95450-191-5 doi:10.18429/JACoW-SRF2017-TUYBA01

PROGRESS ON CHARACTERIZATION AND OPTIMIZATION OF MULTILAYERS

C. Z. Antoine, M. Aburas, A. Four, Irfu, CEA, Université Paris-Saclay,
F-91191 Gif-sur-Yvette, France
H Hayano, S Kato, T Kubo, T Saeki, KEK, High Energy Accelerator Research Organization,
1-1 Oho, Tsukuba, Ibaraki 305-0801 Japan
Y Iwashita, Kyoto ICR, Kyoto University, Uji, Kyoto 611-0011 Japan

Abstract

We present a complete study of a Multilayers Nb/MgO/NbN series with several thicknesses in order to determine the optimum thickness of the NbN layer and to compare experiments and recent theoretical advances proposed by A. Gurevich or T. Kubo. The structure and composition of the samples have been characterized structural point of view (SEM- EDX, XPS), and from the superconducting point of view (Tc, local magnetic penetration field, PCT…).

An optimum thickness has indeed been measured (close from the theoretical predictions), and the protective effect of the dielectric interlayer against avalanche vortex penetration has been evidenced.

INTRODUCTION

Although the multilayer idea was proposed for SRF applications in 2006 [1], more than 10 years later only a few group have been involved in the development of these new metamaterials. The main issue is to master a deposition technique able to produce some 10 nm films inside a cavity, and a second issue is to optimize the proposed structures with the actual superconducting parameters from these thin films which may actually differ a lot from the bulk ideal values.

From the material point of view, it is more convenient to optimize the structures on small samples, but one requires the development of specific tools to measure their performances. Systematic classical characterizations are also mandatory in hope to develop a predictive model able on the role of the particular crystalline defects present with one or another technique, and find out which one are desirable and which one should be prevented.

International Context

Up to now most of the work has been conducted on NbN, even if on paper it is not the most favourable candidate for SRF applications. Indeed NbN has proven to be a material of choice for the fabrication of Josephson junctions in superconducting electronics based on RSFQ [2]. Its fabrication on flat sample by classical techniques (e.g. reactive DC or magnetron sputtering) is well mastered.

Work on Samples: Characterization on NbN or NbTiN samples has initially been conducted at Saclay and collaborators [3-9], and at Jlab and collaborators (see e.g. [10-15]).

Early DC Squid magnetometry have shown indeed an H_{C1} increase on multilayers compared to bulk Nb, but interrogation remains to know if those results are relevant for SRF applications, since the sample is immersed in a DC field with some orientation and edge effects due to demagnetization parameter.

Similar improvement was measured on MgB_2, by LANL and collaborators [11, 16-18], thanks to an hybrid physical chemical vapor deposition technique developed by X.X. Xi at Penn State University [19]. Further work is being done at Temple university [18, 20]

Characterization tools are being developed to overcome the drawbacks of DC magnetometry.

A local magnetometer was developed at Saclay (See below and M. Aburas, [21]), where the magnetic field is applied with a coil which size is much smaller than the sample size. As the field decays quickly away from the coil, the sample can be considered as an infinite plane and no demagnetization effects occur. The same type of magnetometer is now under development at Kyoto University.

For instance in ref [18], the MgB_2 films are deposited on ellipsoids niobium substrates, so that iso-field lines lie parallel to the surface and no demagnetization effect occurs. In ref [22, 23] the same techniques is used along with µSR. µSR is a very powerful technique since it can probe the existence of a magnetic volume (i.e. field penetration) at various thicknesses, but as it is quite heavy, the turnover is slow. More detail can be found in [24]

Fast turnover techniques are being (re)developed, For instance STFC Darresbury is building a system where the sample is a tube surrounded by a coil. A magnetic probe inserted inside the tube allow to determine the field at which the whole tube transit to the mixed state (note that in this configuration, one is insensitive to vortices trapped close to the external surface) [25].

All these set-ups are dedicated to evaluate the maximum field before vortex penetration. On the other hand, it is also mandatory to evaluate the surface resistance.

Although several "sample" cavities exist or are under development ([26] and Fig. 1), they still exhibit severe drawbacks: most of them are operating at relatively high frequency to accommodate small samples. Thus they are limited by the BCS part of the surface resistance of the cavity body (usually Nb) that mask the only parameter that cannot be predicted yet: the residual surface resistance. Getting faster turnovers is also necessary.

Content from this work may be used under the terms of the CC BY 3.0 licence (© 2017). Any distribution of this work must maintain attribution to the author(s), title of the work, publisher, and DOI.

ISBN: 978-3-95450-191-5 doi:10.18429/JACoW-SRF2017-TUYBA02

THERMAL BOUNDARY RESISTANCE MODEL AND DEFECT STATISTICAL DISTRIBUTION IN Nb/Cu CAVITIES*

R Vaglio†, Dipartimento di Fisica, Università di Napoli Federico II, CNR SPIN and INFN, Napoli, Italy
V Palmieri, Legnaro National Laboratories—Istituto Nazionale di Fisica Nucleare (INFN), Legnaro, Italy

Abstract

The 'Q-slope' problem has so far strongly limited the application of niobium thin film sputtered copper cavities in high field accelerators.

In our work, we consider the hypothesis that the Q-slope is related to local enhancement of the thermal boundary resistance at the Nb/Cu interface, due to poor thermal contact between film and substrate. We introduce a simple model that directly connects the Q versus E_{acc} curves to the distribution function $f(R_{Nb/Cu})$ of the $R_{Nb/Cu}$ thermal contact values at the Nb/Cu interface over the cavity surface. Starting from the experimental curves, using inverse problem methods, we deduce the distribution functions generating those curves.

The technique has been applied to different cavity typologies, and by different groups, including LNL-INFN and CERN (ISOLDE and TQR cavities). In all the examined cases to fit the data it is sufficient to assume that only a small fraction of the film over the cavity surface is in poor thermal contact with the substrate. The distribution functions typically follow a simple power-law statistical distribution, and are temperature and frequency independent.

The whole body of information and data reported seems to be consistent with the hypothesis that the main origin of the Q-slope in thin film cavities is indeed related to bad adhesion at the Nb/Cu interface.

INTRODUCTION

As well known to the SRF community, the 'Q-slope' problem has so far strongly limited the application of niobium thin film Nb/Cu sputtered copper cavities [1]. Indeed, though in principle, sputtered Nb/Cu RF superconducting cavities should present many relevant advantages over bulk Nb cavities, in practice, the large Q-solpe, typically observed in these cavities, limits their use in high field accelerators. A comparison of the accelerating field dependence of bulk and film cavities is schematically reported in Fig.1.

Since the early nineties researchers tried to understand and fight the Q-slope problem in thin films. Among others, the following effects were considered [2-6]:

-hydrogen or oxygen diffusion from the bulk Cu substrate
-grain-boundary losses due to film polycristallinity
-enhanced field dependence of the gap or of the fluxon dissipation mechanisms

Though all these mechanism can indeed be active, no convincing experimental proof of their relevance has been given and all attempts to fight the problem where not fully successful.

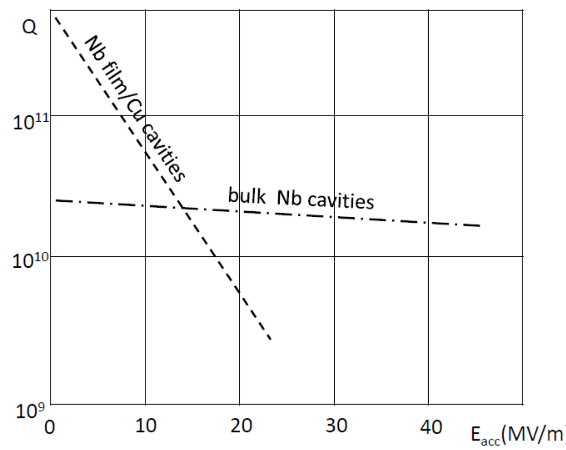

Figure 1 : Q-factor versus the accelerating field for Nb film sputtered cavities compared to bulk niobium cavities. Typical behavior is schematically reported for 1.3 – 1.5 GHz CERN cavities at low temperatures (1.7-1.8K).

In our recent works [7,8], we considered the hypothesis that the Q-slope is related to local enhancement of the thermal boundary resistance at the Nb/Cu interface, due to poor thermal contact between film and substrate. We introduced a simple model that directly connects the Q versus E_{acc} curves to the distribution function $f(R_{Nb/Cu})$ of the $R_{Nb/Cu}$ thermal contact values at the Nb/Cu interface over the cavity surface. Starting from the experimental curves, using inverse problem methods, we deduce the distribution functions generating those curves.

Here we will show and discuss new data taken in our laboratory and we will show how the extracted statistical distributions does not depend, for thin film cavities, on temperature, proving the robustness of the model. Similar results obtained at CERN will be finally discussed

THE THERMAL FEEDBACK MODEL

The thermal feedback model assumes that, in the presence of rf power P_{rf} at the cavity inner surface, the surface resistance R_s can be calculated by iteration through the following equations:

$$R_s(T) = \frac{A\omega^2}{T}\exp\left[-\frac{\Delta(T)}{K_B T}\right] + R_{so}\ ;\ T = T_o + \Delta T$$
$$\Delta T = R_B P_{rf} = \frac{1}{2}R_B R_s(T) H_{rf}^2 = \frac{1}{2}R_B R_s(T)\left(\frac{k}{\mu_o}\right)^2 E_{acc}^2 \qquad (1)$$

* Work supported by INFN ISIDE Project and CNR-SPIN
† email address vaglio@na.infn.it

Content from this work may be used under the terms of the CC BY 3.0 licence (© 2017). Any distribution of this work must maintain attribution to the author(s), title of the work, publisher, and DOI.

ISBN: 978-3-95450-191-5 doi:10.18429/JACoW-SRF2017-TUYBA03

THE WAY OF THICK FILMS TOWARD A FLAT Q-CURVE IN SPUTTERED CAVITIES *

V. Palmieri†, G. Caldarola, S. Cisternino, D.A. Franco-Lespinasse, C. Pira, H. Skliarova, F. Stivanello, Legnaro National Laboratories - ISTITUTO NAZIONALE DI FISICA NUCLEARE (INFN), Legnaro, Italy
R. Vaglio, Dip. di Fisica, Università di Napoli Federico II, CNR SPIN and INFN, Napoli, Italy

Abstract

Thick films have bulk like properties. In this paper it is explored the possibility to sputter 70 micron thick films in order to get rid of the Q-slope in Niobium sputtered Copper Cavities. An innovative method based on the multilayer deposition of zero-stress single layers is reported. The deposition of zero-stress thick films into 6 GHz Copper seamless cavities, has shown the possibility to obtain straight curves for the Q-factor versus accelerating fields.

INTRODUCTION

This work will describe how the approach of thick films could be useful in order to solve the notorious problem of the Q-slope of Niobium thin films sputtered Copper cavities. At the actual point of technology, if the problem will be not solved, the film sputtering technology risks to be discarded from being adopted for next projects of accelerating machines.

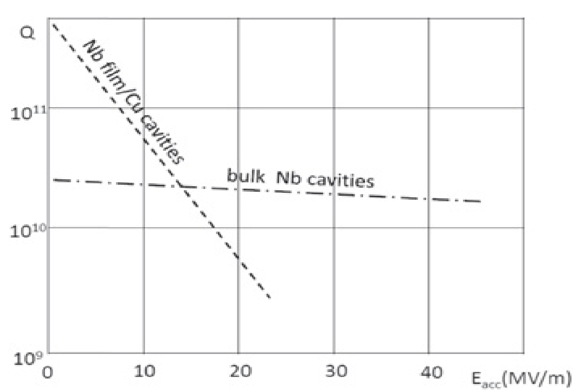

Figure 1: Classical behavior at 1.5 GHz and 1.8K of Nb thin film sputtered Cu cavities compared to Niobium bulk cavities [1].

However, it must be remarked that the slope of the Q-Factor versus the accelerating field, E_{acc} will certainly depend from the film deposition and not from the Niobium-Copper system. There is indeed experimental evidence that Niobium-clad Copper Cavities display a flat Q-factor and they reach accelerating fields up to 40 MV/m [2].

Niobium-clad cavities and Niobium sputtered cavities differ mainly for two factors: the Niobium thickness and the Niobium interface. For clad cavities indeed the thickness is normally hundreds of times higher than for films. Also the interface is incommensurably better for clad Cavities, since the explosive bonding makes the Niobium physically interdiffusing into Copper with almost a perfect joining at the interface.

So, how a high thickness of the Niobium film deposited onto Copper could affect cavity RF performances? One possibility is connected to the fact that a thick film has a value of the Residual Resistivity Ratio (RRR) higher than that of a thin film. The reason for that is at least twofold: The most evident reason is that a Niobium thick film will have larger grains than a thin film, so that the electron mean free path will be not limited by the thin thickness. Another possible reason is that if there is any impurity diffusing from the substrate, the inter-grain percolative path up to the film top surface is much larger in a thick film rather than in thin films.

Bulk Niobium sheets and also Niobium clad Copper sheets, can be purchased with RRR values in the range from 250 to 300, while thin films have often RRR values mainly around 30. Now a lower value of RRR could directly affect the Superconducting gap, and, in turn, the Rs value [3].

A further possible mechanism by which a thick film could perform better than a thin film, is the following: for a defect located at the Nb/Cu interface, in case of a thin film the produced heat flow will be transmitted unidimensionally from the film to the Cu substrate. In thick films instead the heat transmission occurs three-dimensionally, and the heat flux can easily shunt the defect at the interface [4].

Niobium Copper interface is by sure a crucial element in determining cavity performances and Q-slopes, and this has been first proposed in a previous paper by some of the authors [5]. A defected thermal contact at the Nb-Cu interface is by sure responsible of a Q-slope. And the quality of the interface depends from the film stress, that directly acts on the film adhesion to the substrate. The quality of interface is even more jeopardized in case of Niobium and Copper, because these two metals have no miscibility below 1080°C in any range of the phase diagram. Now, a thick film will be adherent to the substrate, only if it will be absolutely not stressed.

Therefore, a higher purity and a better Nb-Cu interface would push to explore thick Niobium films rather than thin Niobium films for the coating of Copper cavities.

* Work supported by the INFN V group experiment ISIDE and performed under the CERN-INFN-FTSC Agreement N. KE2722/BE/FCC
† email address palmieri@lnl.infn.it

Content from this work may be used under the terms of the CC BY 3.0 licence (© 2017). Any distribution of this work must maintain attribution to the author(s), title of the work, publisher, and DOI.

ISBN: 978-3-95450-191-5 doi:10.18429/JACoW-SRF2017-TUPB001

338 MHz CRAB CAVITY DESIGN FOR THE eRHIC HADRON BEAM*

S. Verdú-Andrés†, I. Ben-Zvi[1], Q. Wu, B. P. Xiao, Brookhaven National Laboratory, Upton, USA
[1]also at Stony Brook University, Stony Brook, USA

Abstract

Crab crossing is an essential mechanism to restore high luminosity in the electron-hadron collider eRHIC. The current ring-ring eRHIC design envisages a set of crab cavities operating at 338 MHz. This set of cavities will provide the crabbing kick to the hadron beam of eRHIC. Double-Quarter Wave (DQW) cavities are compact, superconducting RF deflecting cavities appropriate for crab crossing. This paper summarizes the main design requirements and presents an optimized RF design of a DQW cavity for the crabbing system of the ring-ring eRHIC hadron beam.

INTRODUCTION

Crab crossing is an essential mechanism to restore high luminosity in the electron-hadron collider eRHIC. The current eRHIC design envisages the collision of 7 cm-long proton bunches with 0.43 cm-long electron bunches. Both proton and electron bunches have a nominal transverse size of 0.123 mm at the Interaction Point (IP). With a full crossing angle of 22 mrad, the Piwinski angle is 6.26 rad for the proton beam and 0.38 rad for the electron beam. This translates into a significant luminosity reduction with respect to head-on collisions unless crab crossing is implemented.

The crabbing system of the ring-ring eRHIC shall provide a 13 MV kick to the 275 GeV proton beam. The main requirements for such crabbing system are listed in Table 1 [1]. The required kick will be delivered by 3 cavities operating at 338 MHz. This frequency is close to the crabbing system of HL-LHC [2]. The crabbing system for eRHIC will use DQW cavities, like the HL-LHC.

Table 1: Main Requirements for Crabbing System of Ring-ring eRHIC Proton Beam

Parameter	Magnitude	Unit
RF frequency	338	MHz
Full crossing angle	22	mrad
Beta function at cavity location	1200	m
Beta function at IP	0.94	m
Transverse beam size at IP	0.123	mm
Bunch length	7	cm
Piwinski angle	6.26	rad
Cavity aperture	100	mm
Beam energy	275	GeV
Total voltage per IP per side	13	MV
Number of cavities	3	

* Work supported by the US Department of Energy via Brookhaven Science Associates LLC under contract no. DE-AC02-98CH10886.
† sverdu@bnl.gov

THE DOUBLE QUARTER WAVE CAVITY

Quarter Wave Resonator (QWR) cavities are coaxial devices operating in the TEM mode and offering a compact solution for acceleration or deflection of particle beams. In a QWR, with length of $\lambda/4$, the inductance in the shorted end fully transforms into a capacitance in the opened end. A QWR is sketched in Fig. 1.

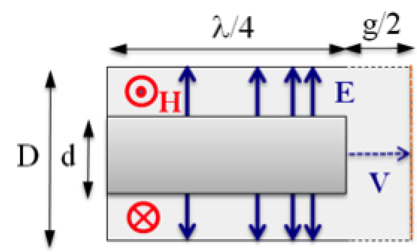

Figure 1: Quarter Wave Resonator (QWR).

The TEM mode operation of the coaxial line is characterized by a radial electric field and an azimuthal magnetic field which amplitude is inversely proportional to the radial coordinate. The peak surface magnetic field H_{peak} in a QWR is located in the inner conductor of the coaxial line, in the shorted end, taking the following value:

$$H_{peak} = \frac{V}{60\pi d \ln(D/d)}, \tag{1}$$

where V is the voltage in the opened end, d is the inner conductor diameter and D is the outer conductor diameter.

A QWR provides a deflecting voltage if the particle beam crosses the cavity in the transverse direction (that is, along the orange line indicated in Fig. 1), but also provides a residual accelerating voltage. The DQW – a symmetrized version of a QWR – does not provide an accelerating voltage to the beam. The deflecting voltage V_t in a DQW cavity is proportional to the voltage V and to the plate length (that is, d) as follows:

$$V_t \approx \frac{d}{g} V, \tag{2}$$

where g is the gap or distance between the two plates. Eq. (2) provides the maximum values that V_t can take, due to the curvature of the field along the beam path [3]. Combining Eq. (1) and Eq. (2), the peak surface magnetic field in a QWR can be written in terms of the required deflecting voltage as:

$$H_{peak} \approx \frac{g}{d^2 \ln(D/d)} V_t. \tag{3}$$

Content from this work may be used under the terms of the CC BY 3.0 licence (© 2017). Any distribution of this work must maintain attribution to the work, publisher, and DOI.

ISBN: 978-3-95450-191-5 doi:10.18429/JACoW-SRF2017-TUPB002

NOVEL HOM DAMPER DESIGN FOR HIGH CURRENT SRF CAVITIES*

Wencan Xu[1], I. Ben-Zvi[1,2], M. Blaskiewicz[1], Y. Gao[1], D. Holmes[1], P. Kolb[1], G. McIntyre[1], R. Porqueddu[1], K. Smith[1], R. Than[1], F. Willeke[1], B. Xiao[1], T. Xin[1], C. Xu[1], A. Zaltsman[1]
[1] Collider-Accelerator Department, Brookhaven National Laboratory, Upton, NY, 11790, USA
[2] Physics&Astronomy Department, Stony Brook University, Stony Brook, NY, 11794, USA

Abstract

The ERL-Ring eRHIC design incorporates a new high current (50 mA), multi-pass (6 passes) ERL, generating 5-18 GeV electron beams to collide with the ion beams of the existing RHIC. One critical challenge for eRHIC is to damp HOMs. The average HOM power is up to 8 kW per cavity, potentially much more if the electron beam spectrum overlaps with cavity HOM spectrum. We present a novel HOM damping scheme, employing ridge waveguides, which is able to well damp both longitudinal and transversal modes. This paper will describe the design of the HOM damping scheme, including RF design, HOM damping results, progress of prototyping.

INTRODUCTION

An Electron-Ion Collider, eRHIC, is proposed at Collider-Accelerator Department at BNL. There are two technologies are under evaluating: one is ERL-Ring [1] technology, which uses ERL technology to provide CW high current, high energy electron beams to collide with proton beams, the other one is Ring-Ring [2], which is to use pulse recirculating linac as an injector to inject electron beams into a storage ring and then collide with proton beams. The SRF requirement for ERL-Ring eRHIC and Ring-Ring eRHIC is significantly different. For ERL-ring, it requires the cavity operating CW at 16 MV/m with Q0 > 3e10, and well HOM damping for the high BBU threshold and HOM power; however, the recirculating-linac requires high gradient operation at 26 MV/m with Q0>1e10, and limited HOM damping requirement.

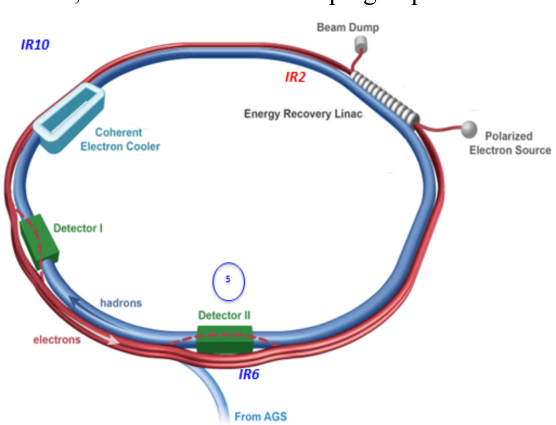

Figure 1: Layout eRHIC. Existing "Blue" hadron ring (center); Electron ring and SRF linac at IP2.

This paper is to study the HOM damping scheme for the ERL-Ring eRHIC SRF linac. As shown in Figure 1, the ERL is realized by two FFAG ring to accelerate the electron beams up to 20 GeV. The high current SRF linac is located at 2 o'clock inside the existing RHIC tunnel, where only 200 m straight section is available. The required energy gain for the linac is 1.67 GeV, so that the electron beam energy can reach 20 GeV by passing through the SRF lianc 12 times. This is the reason that a compact, igh efficient HOM damping is demanded.

This paper describes the layout of the linac and HOM damping scheme for the linac, then focuses on the high current HOM damping schemes.

ERL-RING ERHIC SRF LIANC

SRF Linac Layout

ERL-Ring eRHIC SRF linac is a high current, up to 50 mA, and mulitpasses, up to 12 passes, ERL. Depending on the number of passes, it can provide electron beams with energy of 5 to 20 GeV. The SRF linac for the ERL-Ring eRHIC contains eighty eight 647 MHz 5-cell cavities in 22 cryomodules (four cavities per cryomodule). The total length of the linac is 189 meter, which fits into the straight section of the RHIC tunnel (200 m). The main linac parameters are listed in Table 1.

Table 1: ERL-Ring eRHIC SRF Linac

Parameters	Number	Unit
Energy Gain	1.67	GeV
Beam current	50	mA
Bunch charge	5.3	nC
No. of passes	12	
Linac length	189	m
No. of cavities	88	
No. of cryomodule	22	
Real-estate gradient	8.83	MV/m

ERL Bunch Pattern

The revolution frequency of the RHIC is 78 kHz, and there are 120 RF buckets (110 proton bunches and 10 RF bucket's abort gap), so the collision repetition rate is 9.38 MHz. This is also the repetition rate of the electron bunches from the source. However, there are 5 accelerat-

* Work supported by LDRD program of Brookhaven Science Associates, LLC under Contract No. DE-AC02-98CH10886 with the U.S. DOE.
† email: wxu@bnl.gov

Content from this work may be used under the terms of the CC BY 3.0 licence (© 2017). Any distribution of this work must maintain attribution to the author(s), title of the work, publisher, and DOI.

ISBN: 978-3-95450-191-5 doi:10.18429/JACoW-SRF2017-TUPB004

HOM DAMPING WITH AN ENLARGED BEAM TUBE FOR HEPS 166.6 MHz SC CAVITIES

X. Hao*, Z. Li, F. Meng, P. Zhang, X. Zhang
Institute of High Energy Physics(IHEP),Chinese Academy of Sciences(CAS),Beijing, China

Abstract

The 166.6 MHz superconducting cavities have been proposed for the High Energy Photon Source (HEPS) storage ring, which is initiated by the Institute of High Energy Physics in Beijing. Their higher order modes (HOMs) have to be damped sufficiently in order to limit coupled-bunch instabilities and parasitic mode losses. In order to keep the beam stable, the impedance budget and the HOM damping requirement are given. As one HOM damping option, an enlarged beam tube allows HOMs to propagate and subsequently be absorbed by downstream HOM dampers installed on the inner surface of the beam tube. And the conventional coaxial HOM coupler, which will be mounted on the big beam tube, is planned to extract the HOM power below the cut-off frequency of the beam pipe.

INTRODUCTION

High Energy Photon Source (HEPS) is a 6 GeV kilometer-scale light source [1], and the main beam parameters are listed in Table 1. Prior to its official construction, a test facility namely HEPS-TF has been approved in 2016 to R&D and prototype key technologies and components [2].

Table 1: Beam Parameters of the HEPS Storage Ring

Parameter	**Value**
Circumference	1300 m
Beam energy(E_0)	6 GeV
Beam current(Ib)	200 mA
Total energy loss per turn	2.5 MV
Beam power	500 kW

A 166.6 MHz RF system has been chosen to be the fundamental RF system for the HEPS storage ring to accommodate the newly proposed novel injection scheme [2]. The current R& D has been focused on the 166.6 MHz superconducting (SC) cavity [3]. Due to the low RF frequency and high beam current, higher order modes (HOM) damping becomes one of the key challenges of the 166.6 MHz SC cavities. This paper will focus on the HOM damping requirements and present a preliminary design of a HOM coupler.

THE HOMS AND THEIR DAMPING REQUIREMENTS

In a storage ring, the beam instabilities in both the longitudinal and transverse directions caused by the RF system are mainly from the cavities. To keep the beam stable, the radiation damping time should be less than the rise time of the multi-bunch instability. Thus HOMs of the cavities must be sufficiently damped to prevent coupled bunch instabilities and to limit parasitic mode losses. To damp different HOMs with different polarizations, at least two HOM couplers per cavity are needed. In this paper, only one HOM coupler has been use for the cavity to extracting monopole mode and one dipole polarization.

Figure 1 shows the RF model of the recently designed 166.6 MHz cavity namely proof-of-principle (PoP) cavity [2, 3]. This cavity serves as a starting point for the following HOM studies.

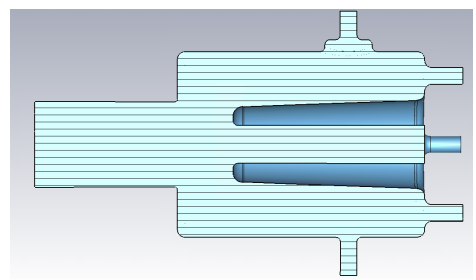

Figure 1: The 166.6 MHz PoP cavity.

The Monopole and Dipole Modes

HOMs in the cavity are calculated by using CST MWS [4]. The frequency convergence is below 10 kHz for every mode. The results are listed in Table 2 for monopole modes, Table 3 for dipole modes. The R/Q for monopole and dipole mode is calculated by [5].

Table 2: The List of Monopole Modes

Mode	**Freq [MHz]**	**R/Q [Ω]**
M1	166.860	135.8
M2	464.623	70.1
M3	700.789	46.5
M4	921.376	7
M5	1195.580	3.3
M6	1347.644	13
M7	1483.832	8
M8	1556.6	13
M9	1744.500	5
M10	1819.567	12.6
M11	2011.997	8.2

$$\frac{R}{Q}[\Omega] = \frac{|V|^2}{\omega U} \tag{1}$$

* haoxr@ihep.ac.cn

Content from this work may be used under the terms of the CC BY 3.0 licence (© 2017). Any distribution of this work must maintain attribution to the author(s), title of the work, publisher, and DOI.

ISBN: 978-3-95450-191-5 doi:10.18429/JACoW-SRF2017-TUPB005

EVELOPMENT OF SPOKE CAVITY FOR MAIN LINAC OF CHINA ADS

Zhongquan Li*, Weimin Pan, Yunlong Chi, Jianshe Cao, Shaopeng Li, Feisi He, Haiying Lin, Qiang Ma, Peng Sha, Xinying Zhang, Zhenghui Mi, Bo Xu and Jiyuan Zhai
Institute of High Energy Physics (IHEP), Chinese Academy of Sciences (CAS)
19B Yuquanlu Road, Shijingshan district, Beijing, China

Abstract

During past six years, two kinds of single spoke resonators with beta equal to 0.21 (SSR021) and 0.40 (SSR040) were developed at IHEP CAS, the SSR021 was adopted to accelerate proton from 10 to 36MeV, and 36 to 160MeV for SSR040. Up to now, two kinds of naked spoke cavities have been test in vertical, also the module of SSR021, which equipped with the liquid helium jacket, magnetic shield layer and frequency tuner, has been fulfilled and test, the performance of all of components reach the design requirements. Recently a cryogenic module with six SSR021, six solenoid coil and six BPM, which we call it fourth cryogenic module (CM4) in main linac of ADS, assembled and commissioned with proton beam.

INTRODUCTION

After two injector had commissioned successfully at the Institute of High Energy Physics (IHEP) in Beijing and the Institute of Morden Physics (IMP) in Lanzhou, separately in 2016, all of ADS member were dedicated to fulfil main linac assembly in IMP, the main linac, which connect to injector II, are composed by CM3 and CM4 (see Fig. 1) [1]. On the 5th June 2017, Main linac had successfully accelerated 12.6mA pulse beam from 10 to 26MeV, also accumulated CW 170μA beam to 25MeV, here CM3 is assembled by five 162.5MHz, beta equal to 0.15 half wave resonator (HWR015), and CM4 is assembled by six 325MHz SSR021 [2], all of HWR015 and SSR021 themselves work well during all commissioning period. For future plan, four prototype SSR040 had been fabricated and two of them already had been tested, measuring results shown a good consistency with pioneer cavities.

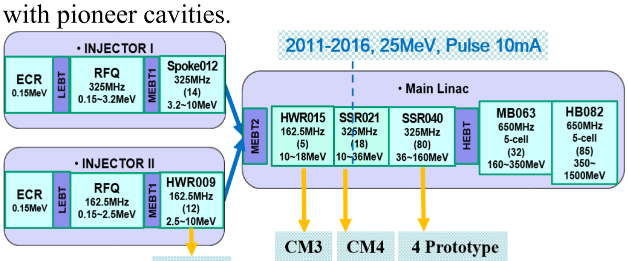

Figure 1: Roadmap of China ADS.

FABRICATION ART OF SPOKE CAVITY

With the efforts to improve the manufacturing technique of spoke cavity through several successive year, we have changed initial design scheme many time, such as the changing of flange from blank hole to through hole, increasing the elliptical blend radius of side plate, especially simplifying the structure of enhance ring, the latest design as shown in Fig. 2, a significant difference comparing to traditional type spoke cavity is that there is a big hole on the side plate, and pasted again by another bowl-like part (green part in Fig.2, we call it nose cone part), the purpose is aimed to welding the seam between cylinder and side plate from inside to avoiding a critical back-forming welding procedure, if we do so, another convenient aspect is that the welding seam can be polished by hand through the big centre hole, the final welding seam between side plate and nose cone is handled by back-forming welding, in this case, this final welding seam can been well-polished by hand with a long handle polishing tools. According the manufacturing process mentioned above, the total welding seam number is reduced dramatically to 25 from traditional one's more than sixties, it benefits by the simple design of enhance ring, another essential benefit is lying on that all of welding seam can be polished by hand with polishing tools, it is verified by the facts that test performance of all of spoke cavities fabricated according this procedure, including prototype ones, reach the design target.

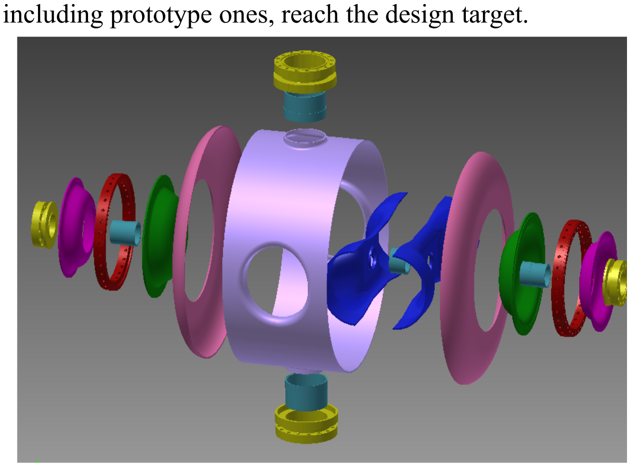

Figure 2: Explosive structure of SSR040.

* Supported by the "strategic Priority Research Program" of the Chinese Academy of Sciences (Grant NO.: XDA03020000, CAS).
# lizq@ihep.ac.cn

Content from this work may be used under the terms of the CC BY 3.0 licence (© 2017). Any distribution of this work must maintain attribution to the author(s), title of the work, publisher, and DOI.

18th International Conference on RF Superconductivity SRF2017, Lanzhou, China JACoW Publishing
ISBN: 978-3-95450-191-5 doi:10.18429/JACoW-SRF2017-TUPB008

PERFORMANCE OF SRF HALF-WAVE-RESONATORS TESTED AT CORNELL FOR THE RAON PROJECT*

M. Ge†, F. Furuta, J. E. Gillette, T. Gruber, S. Hartman, M. Liepe, T. O'Connell, P. Pamel, J. Sears, V. Veshcherevich, CLASSE, Cornell University, Ithaca, New York, USA
B. H. Choi, J. Joo, J.W. Kim, W.K. Kim, J. Lee, I. Shin, Institute for Basic Science, Daejeon, Korea

Abstract

Two prototype half-wave-resonators (HWR; 162.5MHz and β=0.12) for the RAON project were tested at Cornell University. In this paper, we report and analyse detailed results from vertical tests, including tests of the HWRs without and with helium tank. Surface preparation at Research Instruments is discussed, as well as the development of new HWR preparation and test infrastructure at Cornell.

INTRODUCTION

Two prototype HWRs (162.5MHz, β=0.12) for the RAON project [1, 2] are being developed by the Institute for Basic Science (IBS), Research Instruments (RI), and Cornell University. Fabrication and surface treatments of the prototype cavities (HWR-1 and 2) were completed by RI. The cavities were shipped to Cornell for the vertical tests to evaluate their RF performance. After fabrication, the bare HWR-1 received Buffer-Chemical-Polishing (BCP) of 150μm, then was baked in a high-vacuum furnace at 625°C for 10 hours, followed by a light BCP (5-10μm), High-Pressure-Water-Rinsing (HPR), and clean assembly. After the vertical test at Cornell, the bare cavity was sent back to RI for helium tank welding and re-cleaning. The dressed HWR-1 was shipped to Cornell again for a second vertical test. The HWR-2 bare cavity followed an identical procedure as the HWR-1, but the helium tank welding has not been completed yet. In this paper, we report on the tests of 1) the HWR-1 bare and dressed cavity; 2) the HWR-2 bare cavity.

DEVELOPMENT OF TEST INFRASTRUCTURE

The new HWR infrastructure utilizes the existing SRF facilities at Cornell. We built two sets of input and pick-up couplers, HWR handling frames for both a bare and dressed cavity, and modified a 9-cell cavity vertical test insert for this project [3, 4].

Input and Pick-up Couplers

The HWR tests are done at temperatures of 2 – 4.2 K, and the input coupler should match the intrinsic quality factor of the cavity (Q_0) to keep the coupling factor (β) close to 1. If multipacting occurs during test, RF processing of the cavity is required. In this case, the input coupler needs to be set at a strong coupling, i.e. $\beta \approx 100$. Therefore, we built a variable coupler which has a straight antenna and can be mounted in the middle section of the cavity. The input coupler (Fig. 1 (a)) can travel 50 mm, and tune the external quality factor (Q_e) from $\sim 1\times10^7$ to $\sim 1\times10^{11}$. The pick-up coupler (Fig. 1 (b)) is a fix coupler with $Q_e \sim 1\times10^{13}$ to match the required power level of the LLRF system.

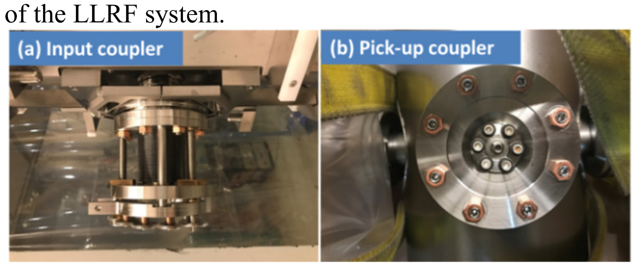

Figure 1: (a) Photograph of the input coupler; (b) Photograph of the pick-up coupler.

HWR Handling Frames and RF Insert

The photographs of the HWR cavity without and with helium tank are depicted in Fig. 2 (a) and (b) respectively. The bare-cavity weight is about 80 lbs; the dressed cavity is about 130 lbs with the helium tank. A handling frame is needed to hold the cavity on the RF insert for the cold tests. The frame for the bare cavity holds the cavity flanges instead of the cavity body, which will not deform the cavity; thus it will not shift the cavity frequency. The frame for the dressed cavity is attached on the helium tank without touching the cavity body as well.

Figure 2: Photograph of (a) the bare HWR cavity (b) the dressed HWR cavity. Both cavities are installed with the handling frames.

* Work supported by the Ministry of Science, ICT, MSIP and NRF. Contract number: 2013M7A1A1075764.
† mg574@cornell.edu

Content from this work may be used under the terms of the CC BY 3.0 licence (© 2017). Any distribution of this work must maintain attribution to the author(s), title of the work, publisher, and DOI.

ISBN: 978-3-95450-191-5 doi:10.18429/JACoW-SRF2017-TUPB009

Content from this work may be used under the terms of the CC BY 3.0 licence (© 2017). Any distribution of this work must maintain attribution to the author(s), title of the work, publisher, and DOI.

HIGH-FREQUENCY SRF CAVITIES*

T. Oseroff†, D. L. Hall, M. Liepe, and J. T. Maniscalco
CLASSE, Cornell University, Ithaca, NY, 14853, USA

Abstract

Historically, the frequency of superconducting RF cavities has been limited by cryogenic power dissipation increasing rapidly with frequency, due to the BCS surface resistance having a quadratic dependence on frequency. Now, new SRF surfaces using doped niobium and compound superconductors like Nb3Sn can drastically reduce the BCS part of the surface resistance. The temperature independent part of the surface resistance (residual resistance) can therefore become dominant, and has its own, different frequency dependence. We have developed a model to analyze cryogenic cooling power requirements for SRF cavities as function of operating frequency, temperature, and trapped flux to evaluate the impact of the novel low-loss SRF surfaces on the questions of optimal operating frequency and frequency limit. We show that high-frequency SRF cavities now become a realistic option for future SRF driven accelerators. As the transverse cavity size decreases inversely with respect to its resonant frequency, such high-frequency SRF cavities could greatly reduce cost.

INTRODUCTION

SRF cavity dimensions scale inversely with resonant frequency. Thus if cavity designs were increased beyond the standard 0.5 - 1.3 GHz range, it could potentially decrease the power dissipated in the surface because of the smaller surface area. However, the power dissipated in the cavity wall also scales with the total surface resistance of the cavity. The surface resistance of the classic SRF material choice, Niobium, is dominated by BCS component which has a quadratic dependence on frequency. This means that going to higher frequencies offers no benefits for Nb. New candidates for SRF materials, Nb_3Sn and N-doped Nb, have a much smaller BCS resistance allowing for the residual resistance to have a significant contribution. If the residual resistance is large enough compared to the BCS resistance and has a small enough dependence on frequency then it is possible the total power dissipated could decrease at higher frequencies. For this reason it is worth investigating the potential benefits of N-doped Nb and Nb_3Sn at frequencies beyond the standard range.

POWER

The power dissipated in a cavity of length L can be put in terms of the shunt impedance R_a and the accelerating voltage V_c.

$$\begin{aligned} P_{diss} &= \frac{V_c^2}{R_a} \\ &= \frac{V_c^2}{\left(\frac{R_a}{Q}\right)_{total} Q} \\ &= \frac{E_{acc}^2 L^2}{\left(\frac{R_a}{Q}\right)_{cell} \left(\frac{L}{\lambda/2}\right) \left(\frac{G}{R_s}\right)} \\ &= \frac{E_{acc}^2 L^2 R_s}{\left(\frac{R_a}{Q}\right)_{cell} \left(\frac{2Lf}{c}\right) G} \end{aligned}$$

In the third line E_{acc} is the accelerating field, the ratio of shunt impedance to quality factor (R_a/Q) in a cell is independent of surface resistance and can be calculated for a given geometry, $L = N\lambda/2$ (where N is the number of cells in the structure) for π-mode operation, and the quality factor is $Q = \frac{G}{R_s}$ where G is the geometry factor of the cavity and R_s is the surface resistance. Thus the ratio of power dissipated to length of the structure is

$$\frac{P_{diss}}{L} = \frac{E_{acc}^2 c}{2\left(\frac{R_a}{Q}\right)_{cell} G} \left(\frac{R_{BCS}}{f} + \frac{R_0}{f}\right) \quad (1)$$

Where the total resistance has been split into its BCS and residual components. From Eq. (1) it is clear that the term resulting from $R_{BCS} \propto f^2$ can only increase the dissipated power with frequency. The residual term, however, could serve to decrease with frequency if $R_0 \propto f^\alpha$ where $\alpha < 1$.

The cryogenic power required to maintain the bath temperature is found by

$$P_{cryo} = P_{diss} \times \text{Efficiency}$$

The efficiency used is shown in Fig. 1. There is an optimal temperature, where the balance between R_{BCS} increasing with temperature and the efficiency decreasing with temperature is satisfied.

RESISTANCE

There has been little experimental work with N-doped and Nb_3Sn cavities at frequencies above 1.3 GHz. As seen in Eq. (1) the frequency dependence of the surface resistance plays a critical role in determining the viability of cavities at higher frequencies. This means that to more accurately estimate the performance of these cavities at high frequencies it is necessary to call upon untested theoretical predictions.

* This work was supported by the U.S. National Science Foundation under Award PHY-1549132, the Center for Bright Beams
† teo26@cornell.edu

ISBN: 978-3-95450-191-5 doi:10.18429/JACoW-SRF2017-TUPB010

MULTIPACTOR STUDY IN THE COUPLER REGION OF THE DIAMOND SCRF CAVITIES

S. A. Pande[1]†, C. Christou, P. Gu, Diamond Light Source, Oxfordshire, UK
G. Burt , [1]Lancaster University, Lancaster, UK

Abstract

The Diamond storage ring operates with two CESR-B type Superconducting RF cavities. The cavities suffer from trips with a sudden loss of accelerating field if operated above a certain voltage. Consequently the cavities are operated between 0.8 and 1.4 MV for better reliability. These cavities are iris coupled and have fixed Qext. At these lower operating voltages, the optimum condition for beam loading is satisfied at powers around 100 kW. For operation at 300 mA with two cavities, the power needed per system exceeds 200 kW. Consequently, 3 stub tuners are used to lower the Qext to move the optimum condition close to 200kW. Additionally, the difference in the height of the coupling waveguide on the cavity and that of the vacuum side waveguide on the window assembly results in a step transition. This step results in a standing wave between the cavity and window even at matched operation. The 3 stub tuner further modifies this standing wave. Numerical simulation reveals that the standing wave field from the cavity penetrates into the coupling waveguide increasing the probability of multipactor in this region. The results of multipactor simulations with CST Studio are discussed.

INTRODUCTION

The Diamond cavities suffer from fast vacuum trips if operated above a threshold voltage which lies between 0.8 to 1.4 MV [1]. A very sharp rise in pressure is recorded on the beam pipe gauges and also in the Pump Out Box (POB), which is a small section of the reduced height waveguide equipped with the ports for vacuum pumping connecting the RF window. For some of the trips, the pressure rise occurs only in the POB. Typically the cavity field collapses in few µs, a fraction of the cavity filling time appropriate for the Q_{ext} of the cavity. A fast data acquisition system based on NI PXI-5105 has been installed in the RF Hall to study the nature of these trips.

Figure 1 shows layout of the RF straight with cavities in positions 2 and 3. The numbers in blue show the gauge numbers. The gauge numbers 01, 21, 04, 06, 07, 09 and 10 are mounted on the beam pipe whereas gauge numbers 05 and 08 are mounted on the POBs of cavity-2 and cavity-3 respectively. Figure 2 shows the CST [2] model of the Diamond CESR Cavity with the RBT (Round Beam Tube) taper, the coupling waveguide, the RF window, the rest of the waveguide WR1800 and the 3-stub tuner. |The HOM loads are shown as cyan cylinders. Note the locations of various pickups. The HF pickup which has highest coupling is used for frequency and voltage control of the cavity. The WaveGuide e$^-$ (referred to as WGe$^-$ in the following) pickup is located just under the coupling tongue, (a specially shaped iris) to pick any electronic activity in this region. There are 2 HOM pickups located on the RBT and 4 on the FBT thermal transitions on the cavity. However, there are extra pickups included in the model to make the structure symmetric to reduce the size of the model. A pair of very weakly coupled pickups is located on the taper as shown.

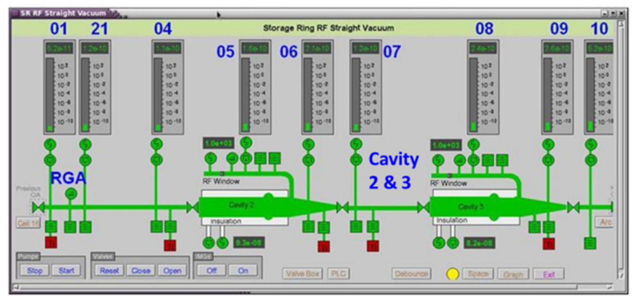

Figure 1: Layout of the RF straight with cavity 2 and 3 in place. The numbers in blue show the vacuum gauge numbers starting from cavity 1 (not shown) side.

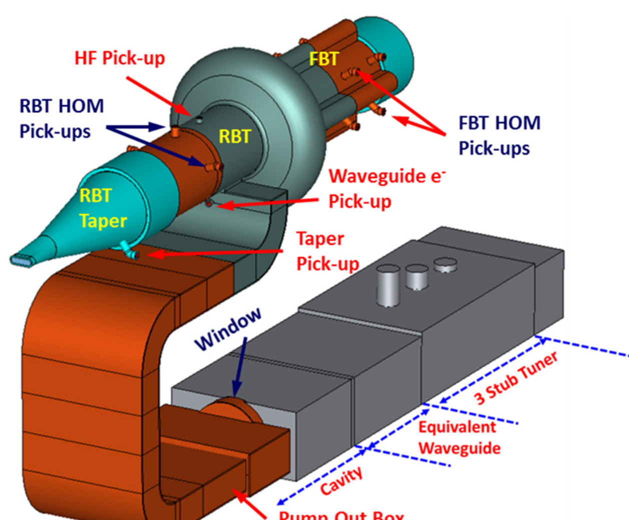

Figure 2: CST model of the Diamond CESR cavity with RBT taper, the coupling waveguide and different pickups.

The data recorded on the NI TDMS system shows the cavity field collapses typically in few µs, which is a fraction of the cavity filling time corresponding to the Q_{ext} of the cavity. These trips are characterised by a sharp signal recorded on the WGe$^-$ pickup. Figure 3 shows the signals recorded during such a fast trip on Cavity-3. The plot on the right shows from top, the Cavity-3 LLRF probe, FBT

†shivaji.pande@diamond.ac.uk

Content from this work may be used under the terms of the CC BY 3.0 licence (© 2017). Any distribution of this work must maintain attribution to the author(s), title of the work, publisher, and DOI.

ISBN: 978-3-95450-191-5 doi:10.18429/JACoW-SRF2017-TUPB013

ADVANCED MANUFACTURING TECHNIQUES FOR THE FABRICATION OF HL-LHC CRAB CAVITIES AT CERN

M. Garlaschè*
CERN, Geneva, Switzerland

Abstract

RF Crab Cavities are an essential part of the HL-LHC upgrade at CERN. Two concepts of such systems are being developed: the Double Quarter Wave (DQW) and the RF Dipole (RFD). The following paper describes the advanced manufacturing techniques developed for the fabrication of the DQW cavity prototype with an outlook on the upcoming RFD prototype production.

INTRODUCTION

In the framework of the High Luminosity upgrade project for the LHC (HL-LHC) at CERN, large sections of the accelerator will be modified [1]. One of the core enhancements are the so called crab cavities. These are novel RF cavities, aimed at reducing the crossing angle at the interaction points via the drift motion they impose to the beam bunches.

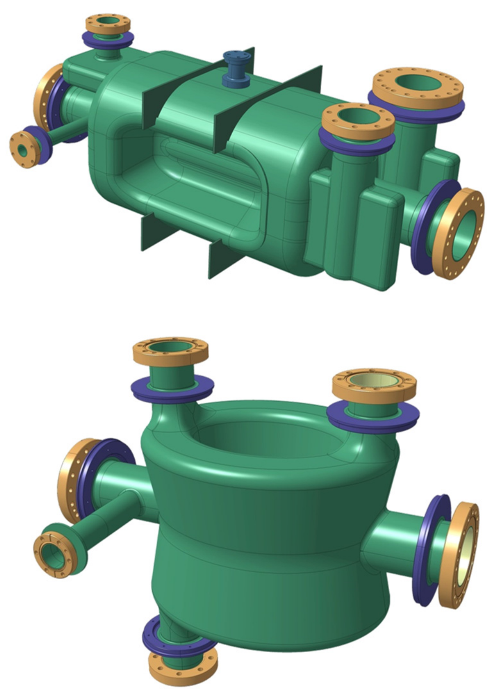

Figure 1: (Top) RFD Cavity; (Bottom) DQW Cavity.

Two different cavity designs are foreseen (see Fig.1) - one for horizontal (RF Dipole, RFD) and one for vertical (Double Quarter Wave, DQW) interaction – resulting in 16 crab cavities to be installed, two per each beam, on each side of both the ATLAS and CMS experiments [1].

In order to validate the correct operating principle, design and manufacturing of each cavity type, specific tests are foreseen in the SPS accelerator at CERN [2].

For such tests, two units of the DQW cavity have been successfully produced at the CERN Main Workshop between beginning of 2016 and first quarter of 2017; while manufacturing of two RFD units is to be launched in the second quarter of 2017.

This paper describes the manufacturing approach and advanced techniques implemented for the challenging DQW fabrication.

DQW MANUFACTURING

DQW Cut-out

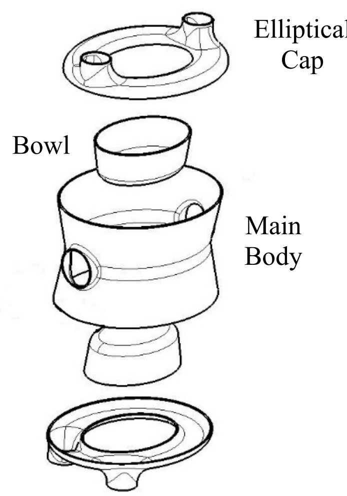

Figure 2: Scheme of exploded subcomponents.

Figure 2 shows the exploded scheme of subcomponents opted for the manufacturing of the DQW cavity. The three main subcomponents (SbC) are the Main Body, the Elliptical Caps, and the Bowls. Missing from the image are the extremities of the cavity, which connect the latter to the beam line on the main body, and to its power coupling systems on the top and bottom elliptical caps.

The rationale behind the cut-out can be resumed in the following points:

- Electron Beam (EB) welds need to comply with stringent RF, tightness and pressure equipment specifications; this leads to tight requirements on maximum acceptable weld defects (e.g. shrinkage, sagging, excessive penetration ranging in the few tenths of mm). Moreover the last joining welds are performed on components pertaining high added value and cannot be easily repaired. Cavity subdivision must thus firstly aim at allowing for the easiest weld configurations. Furthermore, wherever possible, welds must be kept away from high-field regions.

* marco.garlasche@cern.ch

Content from this work may be used under the terms of the CC BY 3.0 licence (© 2017). Any distribution of this work must maintain attribution to the author(s), title of the work, publisher, and DOI.

ISBN: 978-3-95450-191-5 doi:10.18429/JACoW-SRF2017-TUPB014

IN-SITU BULK RESIDUAL RESISTIVITY RATIO MEASUREMENT ON DOUBLE QUARTER WAVE CRAB CAVITIES

N. Shipman[1,2]*, G. Burt, J. Mitchell[1,2], Lancaster University, Lancaster, UK
A. Castilla, K. Chahín[3], A. MacPherson, CERN, Geneva, Switzerland
I. Ben-Zvi, Brookhaven National Laboratory, Upton, USA
[1]also at Cockroft Institute, Daresbury, UK
[2]also at CERN, Geneva, Switzerland
[3]also at DCI-UG, Guanajuato, Mexico

Abstract

A four wire measurement was used to measure the bulk RRR on two DQW Crab Cavities. The measurement procedure is explained and the values obtained for each cavity are compared together with the values obtained from Niobium samples of the same stock from which the cavities were manufactured. Measurement errors are carefully analysed and further improvements to the measurement procedure are suggested.

INTRODUCTION

Introduction to HL-LHC and Crab Cavities

High-Luminosity-LHC [1], HL-LHC, is a project to upgrade the Large Hadron Colider [2], LHC, by increasing the luminosity by a factor of 10. This will allow more accurate measurements of newly discovered particles and allow the discovery of rare processes which are below the current sensitivity level of the LHC.

In order to achieve the requisite increase in luminosity it is necessary to utilise crab cavities. Crab cavities rotate the particle bunches about an axis perpendicular to the plane containing both beam axes in such a way as to almost completely counteract the geometric luminosity reduction which would otherwise occur as a result of the non-perfect overlap of the colliding bunches [3] as shown in Fig.1.

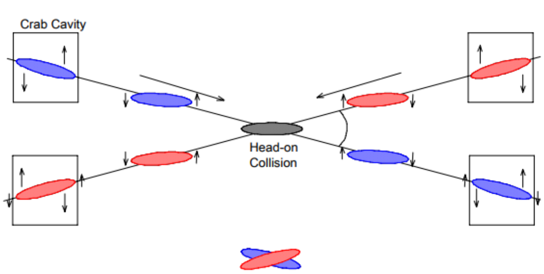

Figure 1: For each beam crab cavities upstream and downstream of the interaction point rotate the bunches to reduce the luminosity loss due to the non-perfect overlap that would otherwise be caused by the crossing angle.

Three prototype designs of crab cavities for the HL-LHC project were built. The double quarter wave crab cavity,

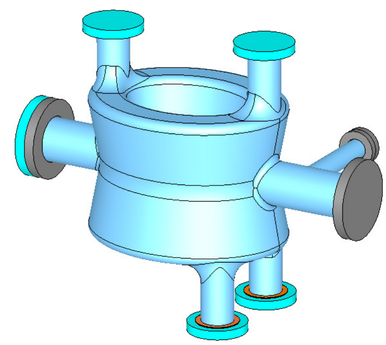

(a) A 3D model of the DQW SPS crab cavity.

(b) Photograph of the DQW SPS crab cavity without helium tank.

Figure 2: DQW SPS crab cavity.

DQW [4], the radio frequency dipole crab cavity [5], RFD and the UK four rod cavity [6], UK4R. For HL-LHC, the DQW and RFD were selected to be installed in the LHC and the DQW cavity will also first be tested in the super proton synchrotron, SPS. Two "DQW SPS" cavities have been constructed for this purpose and prior to testing in the SPS they have undergone cold testing both at JLAB [7] and at CERN [8]. Figure 2 shows both a 3D representation in Sub-Fig.2a and a photograph of a completed DQW SPS cavity in Sub-Fig.2b, before the helium tank was installed.

Introduction to RRR

The residual resistivity ratio, RRR, of a metal is defined as the ratio of the resistivity at 300K to the resistivity at a low temperature just above the superconducting transition. [9]

* nicholas.shipman@cern.ch

Content from this work may be used under the terms of the CC BY 3.0 licence (© 2017). Any distribution of this work must maintain attribution to the author(s), title of the work, publisher, and DOI.

ISBN: 978-3-95450-191-5 doi:10.18429/JACoW-SRF2017-TUPB016

Content from this work may be used under the terms of the CC BY 3.0 licence (© 2017). Any distribution of this work must maintain attribution to the author(s), title of the work, publisher, and DOI.

REDESIGN OF CERN'S QUADRUPOLE RESONATOR FOR TESTING OF SUPERCONDUCTING SAMPLES

V. del Pozo Romano*[1], F. Gerigk, R. Betemps, R. Illan Fiastre and T. P. Mikkola
CERN, Geneva, Switzerland
[1]also at Ciemat, Madrid, Spain

Abstract

The quadrupole resonator (QPR) was constructed in 1997 to measure the surface resistance of niobium samples at 400 MHz, the technology and RF frequency chosen for the LHC. It allows measurement of the RF properties of superconducting films deposited on disk-shaped metallic substrates. The samples are used to study different coatings which is much faster than the coating, stripping and recoating of sample cavities. An electromagnetic and mechanical re-design of the existing QPR has been done with the goal of doubling the magnetic peak fields on the samples.

Electromagnetic simulations were carried out on a completely parametrized model, using the actual CERN's QPR as baseline and modifying its dimensions. The aim was to optimize the measurement range and resolution by increasing the ratio between the magnetic peak fields on the sample and in the cavity. Increasing the average magnetic field on the sample leads to a more homogenous field distribution over the sample, which in turn gives a better resolution. Some of the modifications were based on the work already done by Helmholtz-Zentrum-Berlin for their upgraded version of the QPR.

DESCRIPTION

The QPR consists of a screening cavity made by two separate cans and four vertical rods supported from the top-plate that are bent at the end into half ring pole shoes (see Fig. 1) [1]. The loop formed by the two pole shows is placed 0.7 mm above the sample disk and focusses the RF field to its surface. The resonance inside the cavity occurs because the length of the rods plus the gap between them and the sample is λ /2 of the operation frequency of 400 MHz, although it was also refurbished in 2009 for operation at 800 MHz and 1.2 GHz [2]. The sample is welded to a niobium cylinder that is inserted from below into the resonator, leaving a gap between them. This can be compared to a coaxial line where the inner cylinder is thermally decoupled from the resonator and also higher modes than the quadrupole mode are in cut off within the gap.

The measurement of the surface resistance is done by a calorimetric method. The advantages of this technique is the high sensitivity and the independence from a reference sample. The resonator is immersed in an helium bath that also flows inside the hollow rods. As the fields decay on the gap, the cylinder is only heated on the sample's surface. Below the sample's disk a heater is attached and used to change its temperature, also four temperature sensors are placed under the regions of high magnetic field. Once the temperature is stabilized with the DC heater, the RF is turned on and the power of the heater is lowered until reaching the initial temperature. The power dissipated by RF is the difference

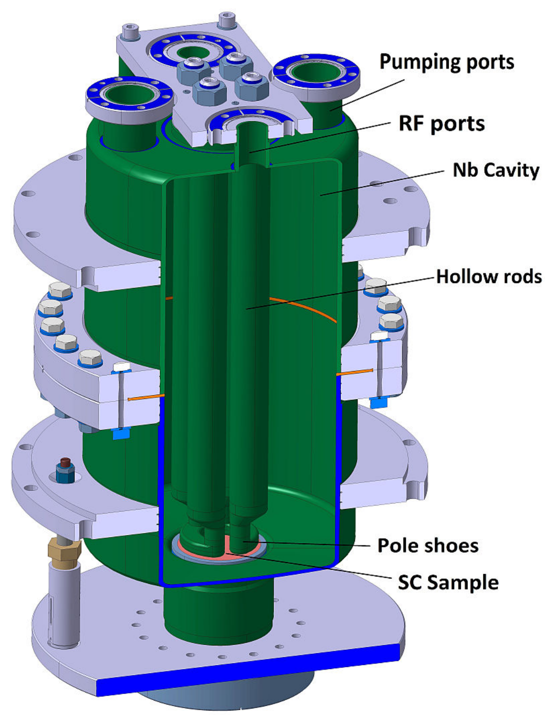

Figure 1: 3D view of the quadrupole resonator as prepared for fabrication.

between the DC power applied without RF, P_{DC1} and the DC power applied with RF P_{DC2}. Assuming the surface resistance R_S to be constant over the sample surface area and independent of the magnetic field, the surface resistance can be calculated as the power dissipated divided by the integrated magnetic field over the sample surface [3, 4].

$$R_S = \frac{2 \cdot (P_{DC1} - P_{DC2})}{\int_{Sample} |\vec{H}|^2} \tag{1}$$

RF OPTIMIZATION

The aim of this study was to optimize the size and parameters of the Quadrupole Resonator (QPR) at CERN, in order to maximize some figures that define the performance of the QPR as they are related to thermal quenchs that limit the peak magnetic field on the sample to 60 mT, field emission, multipacting and microphonics when operated at 800 and 1200 MHz [5].

* veronica.del.pozo.romano@cern.ch

ISBN: 978-3-95450-191-5 doi:10.18429/JACoW-SRF2017-TUPB020

MICROPHONICS PASSIVE DAMPING

E. Zaplatin, Forschungszentrum Juelich, Germany
A. Kanareykin, Euclid TechLabs, Ohio, USA
V. Yakovlev, FNAL, Geneva, IL, USA

Abstract

Different types of external loads on the resonator walls predetermine the main working conditions of the SRF cavities. The most important of them are very high electromagnetic fields that result in strong Lorentz forces and the pressure on cavity walls from the helium tank. For pulsed operation, the Lorentz forces usually play the decisive role for the cavity design. For CW operation, the liquid helium vessel pressure instability even for 2K operations is the source of large microphonics. All deformations resulting from any type of external loads on cavity walls lead to shifts in the working RF frequency in the range of hundreds of kHz. Taking into account high Q-factor of SC cavities such a large frequency shift takes the cavity out of operation.

Here we present and discuss the achievements and problems of microphonics passive damping in different type SRF cavities.

INTRODUCTION

One of the critical issues for new SC accelerators with modest beam current is small beam loading. Optimum coupling to the planned beam current would require relatively narrow cavity bandwidths. The thin walls of the SC RF cavities, and the narrow operating bandwidths, make them susceptible to detuning due to variations of the helium bath pressure, Lorentz pressure or to mechanical vibrations (microphonics). As the cavities detune, additional RF power is required to maintain the accelerating gradient. Sufficient reserve RF power has to be provided to compensate for the peak detuning levels that are expected, and not just for the average detuning. For narrow bandwidth cavities, providing sufficient reserve RF power can significantly increase both the acquisition cost and the operational cost of the machine. To mitigate the level of microphonics all possible passive measures must be employed in combination with other approaches. Under microphonics passive damping (MPD) we understand the common resonator-helium vessel structure design satisfying the ultimate requirements on low dependence of the resonance frequency shift on the cavity wall loading with a simple tuning procedure.

TECHNICAL APPROACH

For better understanding of the SC RF cavity behavior under vacuum load, different elliptical cavity middle cell shapes (Cornel reentrant [1], ICHIRO "low-loss" [2], MSU half-reentrant (HR) [3]) were investigated, in comparison with the well-developed TESLA-shape [4] cavity (Fig. 1).

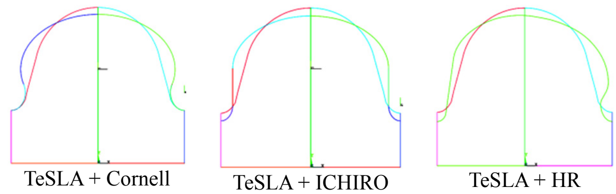

Figure 1: Mid-cell geometries.

The response of the cavities to a pressure differential was calculated with vacuum inside the resonator and ambient pressure is outside. The simulations were done with the cell-to-cell junction constrained by symmetry. The pressure differential changes the cavity shape and shifts the RF frequency of the accelerating mode. Inward deformation near the iris (the region of high electric field) increases the capacitance and hence reduces the frequency. Inward deformation near the equator (high magnetic field region) reduces the inductance and hence increases the frequency. Thus, the effects tend to cancel one another.

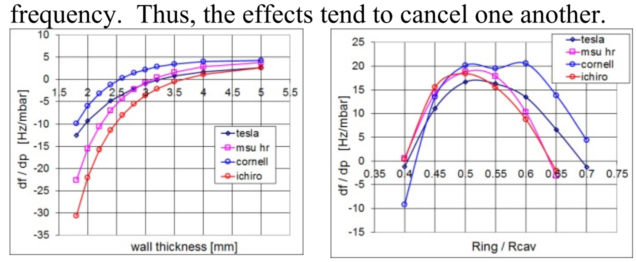

Figure 2: Middle cell frequency shift response to external pressure (left - R_{ing}/R_{cav} = 0.55, right - *wall thickness = 2.8 mm*).

The cavity rigidity depends on thickness of the cavity wall (Fig. 2, left). The frequency shift is approximately zero for a non-stiffened cavity with a wall thickness of about 3 mm. The frequency shift is different for each of the investigated geometries because of their different shape rigidity. A stiffening ring can be used to change the cell rigidity, thus varying the ratio between frequency shift from cavity capacitance and inductance change to produce a substantial reduction in df/dp. There are two places for the ring position where the frequency shifts reaches zero (Fig. 2, right). However, the higher ring position also results in an overall too high cavity rigidity, which causes in a large increase in the tuning force.

The response of an elliptical cavity middle cell to the external pressure differential was also investigated for a lower resonant frequency (650 MHz), in the framework of Project X (now PIP-II) [5], for two cavity types with β=0.91 and β=0.61.

Content from this work may be used under the terms of the CC BY 3.0 licence (© 2017). Any distribution of this work must maintain attribution to the author(s), title of the work, publisher, and DOI.

ISBN: 978-3-95450-191-5 doi:10.18429/JACoW-SRF2017-TUPB021

Content from this work may be used under the terms of the CC BY 3.0 licence (© 2017). Any distribution of this work must maintain attribution to the author(s), title of the work, publisher, and DOI.

FIRST CONSIDERATIONS ON HZB HIGH FREQUENCY ELLIPTICAL RESONATOR STIFFENING

E. Zaplatin, Forschungszentrum Juelich, Germany
H-W. Glock, J. Knobloch, A. Neumann, A. Velez, Helmholtz-Zentrum Berlin, Germany

Abstract

There are two projects that currently are under development and construction at HZB which utilize high frequency elliptical resonators – Energy Recovery Linac Prototype (bERLinPro, 7-cell, 1300 MHz, β=1) and BESSY Variable pulse-length Storage Ring (VSR, 5-cell, 1500/1750 MHz, β=1). A critical issue of both projects is small effective beam loading in cavities operating at high CW fields (Eacc of 20 MV/m) with a narrow bandwidth. This necessitates precise tuning and therefore good compensation of microphonics and coupled Lorentz-force detuning driven instabilities. Motivated by this we present a conceptual study of an integrated SRF resonator and helium vessel structure design to ensure a reduced resonance frequency dependence on pressure and Lorentz forces to minimize their impact on the accelerating field profile.

PRESSURE RESPONSE OF MID-CELL

In the accelerator facilities (such as Cornell ERL, the KEK ERL and bERLinPro) that plan to use SRF cavities in the continuous wave (cw) operation with low effective beam loading and thus a narrow band width, the Lorentz force detuning becomes the factor that should be taken into account during structural design. Additionally, the peak fluctuations in the helium bath pressure are the source of the cavity resonance frequency shift.

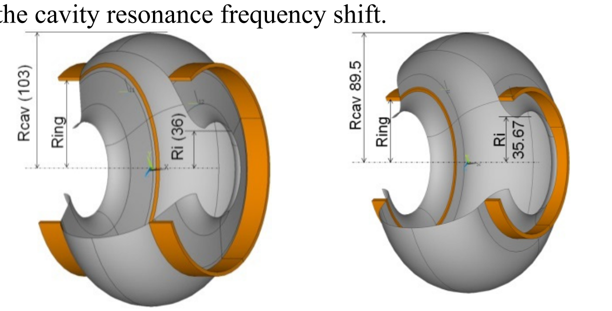

Figure 1: HZB bERLinPro (1300 MHz, β =1) and BESSY VSR (1500 MHz, β =1) mid-cell simulation models.

The bERLinPro elliptical 7-cell cavity and the original BESSY VSR 5-cell cavity RF designs were reported elsewhere [1-2]. (Note that the latest BESSY VSR resonator design is 4-cell cavity). Initial investigations of the cavity mechanical properties were performed on middle cell geometries (Fig. 1). The simulations were made with the cell-to-cell junction constrained by symmetry. The procedure of middle cell stiffening optimization was similar like used in [3]. The main goal was to find the stiffening ring positions to balance resonator frequency shifts caused by the change of the magnetic and electric stored energies. The summaries of numerical simulations are presented on Figs. 2-3.

The best stiffening ring positions in terms of df/dp minimization are the large ring radius (R_{ing}/R_{cav}=0.77) or no rings at all (R_{ing}/R_{cav}=0.35 corresponds to no rings case) for both resonators. The last case of results without rings repeats the similar investigations for other 1300 MHz, β=1 elliptical structures like TeSLA, Cornell re-entrant, ICHIRO "low-loss" and MSU half re-entrant cavities [4].

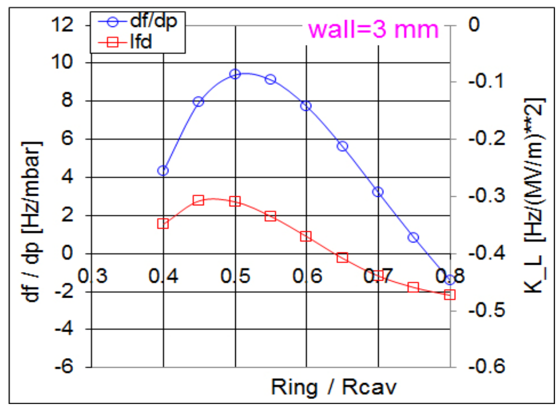

Figure 2: bERLinPro 1300 MHz, β =1 middle cell simulation summary (red curve – Lorentz force sensitivity, blue curve – pressure sensitivity).

The main deformations caused by the Lorentz force pressure occur at the iris section of the cell geometry. Hence, the main part of the frequency shift resulted by electrical field region deformations that in turn always results in the negative frequency shift.

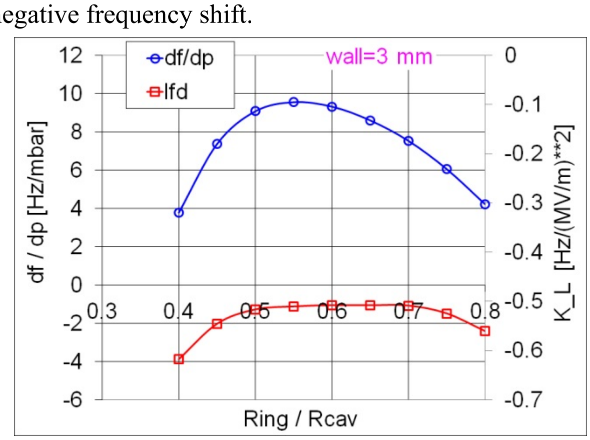

Figure 3: BESSY VSR 1500 MHz, β =1 middle cell simulation summary.

Small BESSY VSR cavity dimensions resulted in higher Lorentz force frequency sensitivity dependence on resonator wall deformations with low dependence on ring positions.

ISBN: 978-3-95450-191-5 doi:10.18429/JACoW-SRF2017-TUPB022

FIRST MEASUREMENTS OF THE NEXT SC CH-CAVITIES FOR THE NEW SUPERCONDUCTING CW HEAVY ION LINAC@GSI

M. Basten[1,*], K. Aulenbacher[3,4], W. Barth[2,3,5], M. Busch[1], F. Dziuba[3], V. Gettmann[3], M. Heilmann[2], Th. Kürzeder[3], M. Miski-Oglu[3], H. Podlech[1], M. Schwarz[1], S. Yaramyshev[2,5]
[1]IAP University of Frankfurt, 60438 Frankfurt am Main, Germany
[2]GSI Helmholtz-Centre, 64291 Darmstadt, Germany
[3]HIM Helmholtz-Institute Mainz, 55099 Mainz, Germany
[4]KPH Mainz University, 55128 Mainz, Germany
[5]MEPhI National Research Nuclear University, 115409 Moscow, Russia

Abstract

In the future the existing GSI-UNILAC (Universal Linear Accelerator) will primarily be used to provide high power heavy ion beams at a low repetition rate for the FAIR project (Facility for Antiproton and Ion Research). To keep the ambitious Super Heavy Element (SHE) physics program at GSI competitive a superconducting (sc) continuous wave (cw) high intensity heavy ion Linac is highly desirable to provide ion beams at or above the coulomb barrier [1]. The fundamental Linac design composes a high performance ion source, a new low energy beam transport line, the High Charge State Injector (HLI) upgraded for cw, and a matching line (1.4 MeV/u) followed by the new sc-DTL Linac based on CH-cavities [2] for acceleration up to 7.3 MeV/u. The construction of the first demonstrator section has been finished in the 3rd quarter of 2016. It comprises the first crossbar-H-mode (CH) cavity with two sc 9.3 T solenoids and has been successfully tested at the end of 2016 [3]. Currently the next two sc 8 gap CH-cavities are under construction at Research Instruments (RI). First intermediate measurements during the fabrication process as well as the latest status of the construction phase will be presented.

LAYOUT OF THE CAVITY

Since December 2016 the next two sc 217 MHz CH-cavities for the new sc cw-Linac are under construction at Research Instruments, Bergisch Gladbach, Germany. They are the next milestone after the successful RF test of the demonstrator cavity at GSI [3] and the first successful beam operation at GSI-High Charge Injector (HLI) [4]. Both subsequent cavities have the same constant beta, as well as the same geometry. The revised design (see Fig. 1) without girders and with stiffening brackets potentially reduces the pressure sensitivity and expedites the fabrication process. The design gradient is about 6 MV/m, which has to be achieved by 8 accelerating cells. Its resonant frequency is the second harmonic of the HLI at GSI, Darmstadt. In Table 1 the main parameters of the first two 217 MHz CH-cavities are depicted.

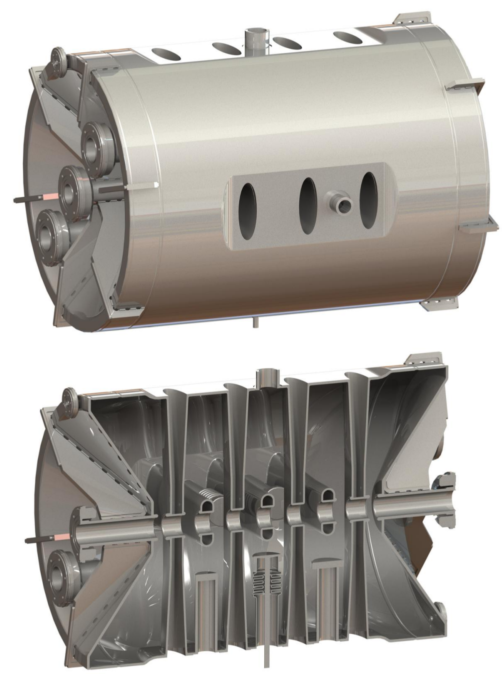

Figure 1: Layout of the sc 217 MHz CH-cavity 2 and 3.

Table 1: Main Parameters of CH-Cavity 2 and 3

Parameter	Unit	
β		0.069
Frequency	MHz	216.816
Accelerating cells		8
Length ($\beta\lambda$-definition)	mm	381.6
Cavity diameter (inner)	mm	400
Cell length	mm	47.7
Aperture diameter	mm	30
Static tuner		3
Dynamic bellow tuner		2
Wall thickness	mm	3-4
Accelerating gradient	MV/m	6
E_p/E_a		5.2
B_p/E_a	mT/(MV/m)	<10
G	Ω	50
R_a/Q_0	Ω	1070

* Basten@iap.uni-frankfurt.de

Content from this work may be used under the terms of the CC BY 3.0 licence (© 2017). Any distribution of this work must maintain attribution to the author(s), title of the work, publisher, and DOI.

ISBN: 978-3-95450-191-5 doi:10.18429/JACoW-SRF2017-TUPB023

FURTHER TESTS ON THE SC 325 MHz CH-CAVITY AND POWER COUPLER TEST SETUP*

M. Busch[†,1], W.A. Barth[2,3,4], M. Basten[1], F. Dziuba[3]
V. Gettmann[3], H. Podlech[1], U. Ratzinger[1], M. Schwarz[1]
[1]IAP, Frankfurt University, Frankfurt am Main, Germany
[2]GSI Helmholtzzentrum, Darmstadt, Germany
[3]HIM, Helmholtz-Institut Mainz, Mainz, Germany
[4]MEPhI, National Research Nuclear University, Moscow, Russia

Abstract

The 325 MHz CH-cavity which has been developed and successfully vertically tested at the Institute of Applied Physics, Frankfurt, has reached the final production stage. After the repair of the leaky membrane flange further tests in a vertical and horizontal environment are in preparation. The corresponding 325 MHz power couplers have been conditioned and tested at a dedicated test stand up to the power level of 40 kW (pulsed) for the targeted beam operation. Furthermore a new developed test stand for the 217 MHz power couplers has been designed and elaborated for the cavities of the sc cw-LINAC project at GSI.

PRESENT STATUS OF THE 325 MHz CH-CAVITY

After successful tests with gradients up to 14.1 MV/m at 2 K [1] the 325 MHz CH-cavity was sent back to Research Instruments for final weldings of the helium vessel and surface treatment. However, the final leak tests discovered a small leak inside the membrane bellow within the port for the power coupler.

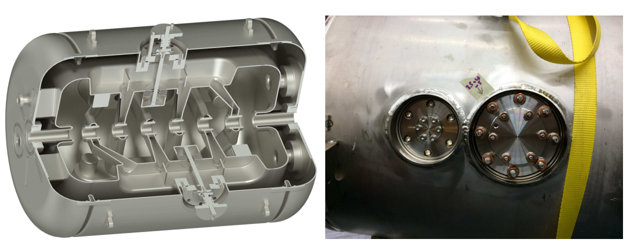

Figure 1: Left: Cross section of the 325 MHz CH-Cavity. Right: Position of the leak (power coupler port).

Due to the complex and sensitive position of the leak it was decided to cut out a race track profile around the coupler and pick-up port, respectively, including the membrane bellows (s. Fig. 1). Meanwhile a replacement "trough" has been fabricated and welded to the helium vessel (s. Fig. 2). The cavity is now being prepared for vertical tests and a horizontal test environment is under development.

* Work supported by GSI, BMBF Contr. No. 05P15RFRBA
† busch@iap.uni-frankfurt.de

Figure 2: Left: Separated helium vessel (cut out profile including membrane bellows). Right: Replacement trough welded into the helium vessel.

325 MHz POWER COUPLER TEST SETUP

The tests of the FPCs for the 325 MHz CH-cavity were performed at a dedicated test stand [2].

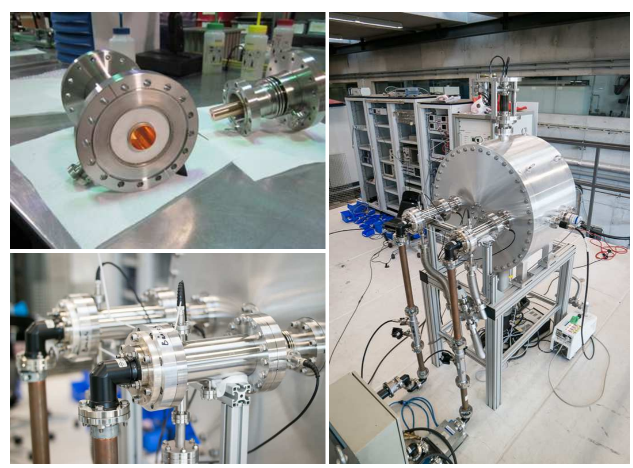

Figure 3: Pictures of the coupler's cold and warm parts (top left) and the assembly with the pill box cavity.

This setup consisted of a tuneable pillbox cavity made of aluminum and enabled two power couplers to be conditioned up to 40 kW pulsed power (s. Fig. 3). The couplers were equipped with two Langmuir probes biased with a voltage of 50 V, four Pt100 probes for temperature measurement and a pumping port for the volume between the ceramic windows. Besides the measurement of P_f and P_r the current of the Langmuir probes as well as the pressure between the alumina windows have been recorded to detect Multipacting events. In a first step the couplers were preconditioned

Content from this work may be used under the terms of the CC BY 3.0 licence (© 2017). Any distribution of this work must maintain attribution to the author(s), title of the work, publisher, and DOI.

ISBN: 978-3-95450-191-5 doi:10.18429/JACoW-SRF2017-TUPB024

PERFORMANCE TESTS OF THE SUPERCONDUCTING 217 MHz CH CAVITY FOR THE CW DEMONSTRATOR

F. Dziuba[1,*], M. Amberg[1,3,†], K. Aulenbacher[1,4], W. Barth[1,2,5], M. Basten[3], M. Busch[3], V. Gettmann[1], M. Heilmann[2], M. Miski-Oglu[1], H. Podlech[3], A. Schnase[2], M. Schwarz[3], S. Yaramyshev[2,5]

[1]HIM Helmholtz Institute Mainz, 55099 Mainz, Germany
[2]GSI Helmholtzzentrum für Schwerionenforschung GmbH, 64291 Darmstadt, Germany
[3]IAP Goethe University Frankfurt, 60438 Frankfurt am Main, Germany
[4]KPH Johannes Gutenberg University Mainz, 55128 Mainz, Germany
[5]MEPhI National Research Nuclear University, 115409 Moscow, Russia

Abstract

Regarding the future research program of super heavy element (SHE) synthesis at GSI, high intense heavy ion beams above the coulomb barrier and high average particle currents are highly demanded. The associated beam requirements exceed the capabilities of the existing Universal Linear Accelerator (UNILAC). Besides the existing GSI accelerator chain will be exclusively used as an injector for FAIR (Facility for Antiproton and Ion Research) providing high power heavy ion beams at a low repetition rate. As a consequence a new dedicated superconducting (sc) continuous wave (CW) linac is highly demanded to keep the SHE research program at GSI competitive on a high level. In this context the construction of the first linac section, which serves simultaneously as a prototype to demonstrate its reliable operability has been finished at the end of 2016. The so called demonstrator cryomodule comprises two sc 9.3 T solenoids and a sc 217 MHz Crossbar-H-mode (CH) cavity with 15 equidistant accelerating gaps. Furthermore, the performance of the cavity has been successfully tested at cryogenic temperatures.

INTRODUCTION

Regarding the future construction of a sc CW linac at GSI an R&D program has been initiated. It is intended to build and test the first linac section with beam at the GSI High Charge State injector (HLI) [1,2]. Regarding this, a sc 217 MHz multigap CH cavity [3] with 15 accelerating cells was built (see Fig. 1 and Table 1). The beam dynamics concept of the cavity is based on the special EQUidistant mUlti-gap Structure (EQUUS) [4]. Three dynamic bellow tuners inside the cavity allow frequency adjustment during operation [5]. For future beam tests a 5 kW power coupler is available. After final surface preparation steps the new cavity has been extensively tested with low level RF power at 4.2 K.

CAVITY RF TESTS

At the beginning of 2016 a first RF test of the sc 217 MHz CH cavity (without helium vessel) at the Institute of Applied Physics (IAP) of Goethe University Frankfurt has been performed [6]. The performance of the cavity was limited by field emission caused by insufficient surface preparation at that time. Nevertheless, a maximum accelerating gradient of $E_a = 6.9$ MV/m at $Q_0 = 2.19 \times 10^8$ has been reached (see Fig. 2).

Figure 1: Sectional view of the sc 217 MHz CH cavity [6].

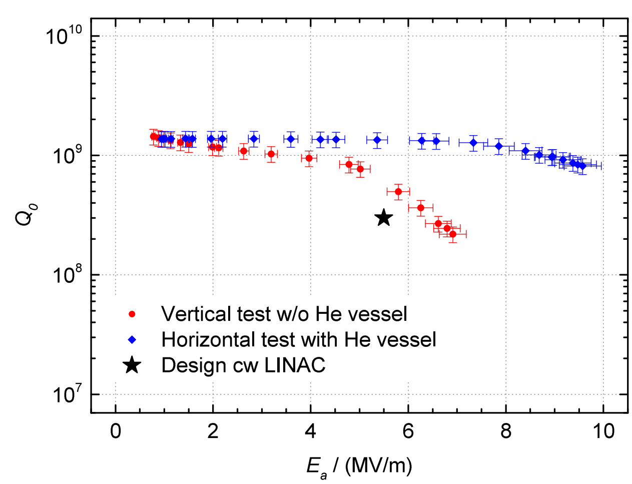

Figure 2: Measured Q_0 vs. E_a curves at 4.2 K for two different RF tests [7].

* f.dziuba@gsi.de
† on leave

Content from this work may be used under the terms of the CC BY 3.0 licence (© 2017). Any distribution of this work must maintain attribution to the author(s), title of the work, publisher, and DOI.

18th International Conference on RF Superconductivity SRF2017, Lanzhou, China JACoW Publishing
ISBN: 978-3-95450-191-5 doi:10.18429/JACoW-SRF2017-TUPB028

IMPROVEMENT OF MAGNETIC CONDITION FOR KEK-STF VERTICAL TEST FACILITY TOWRD HIGH-Q STUDY

K. Umemori#, T. Dohmae, E. Kako, T. Konomi, T. Kubo, A. Terashima, K. Tsuchiya, M. Masuzawa, G. T. Park, R. Ueki, KEK, Ibaraki, Japan
T. Okada, SOKENDAI, Japan

Abstract

Improvement of unloaded Q-values of SRF cavities are important to reduce surface loss of cavity and heat loads of He refrigerators. R&D activities have been developed worldwide. We also started work toward high-Q, but soon realized that magnetic condition of KEK-STF vertical test facility was not good enough to carry out high-Q measurements. First, magnetized components were searched. Shafts to move variable coupler were found to be most magnetized one and exceed more than 1 Gauss. Magnetized components were exchanged to non-magnetized one. In order to further reduce remnant magnetic field, a solenoid coil was prepared and used to cancel it. To suppress flux trapping, a heater was located around an upper beampipe of cavity and made thermal gradient. Owing to these efforts, Q-value of more than 1×10^{11} can be measured with a condition of residual resistance of ~3 nΩ. Clear flux expulsion signal can be also observed. In this presentation, we report about efforts to reduce ambient magnetic field and to realize high-Q measurements. Results of vertical tests, including flux expulsion measurements, are also presented.

INTRODUCTION

Realization of high-Q for SRF cavity is desirable to reduce cryogenic loss of accelerator system. Recently high-Q studies, such as N-doping, N-infusion, flux expulsion and optimized cooling procedure, are often carried out at world-wide [1]. However, to perform such measurements, control of magnetic field is essential. It is known that remnant magnetic field around cavity surface can be trapped during cool-down process and trapped magnetic flux become source of residual resistance [2].

Magneti field of KEK-STF vertical test facility was not well controlled and measurement of high-Q was difficult. We tried to de-magnetize vertical test components and cancel remnant magnetic field using a solenoid coil.

HISTORY OF VERTICAL TEST RESULTS

Several single cell cavities were fabricated at KEK-CFF (cavity fabrication facility) and carried out vertical test at KEK-STF vertical test area [3,4].

Left of Fig. 1 shows history of residual resistance for single-cell vertical test measurements at KEK-STF from 2014 to 2015. Data for large grain, fine grain and seamless cavities are plotted. It shows that measured residual resistance tend to gradually increase with time. Right of Figure 1 shows Q-E curve for large grain single-cell cavity at low temperature, less than or around 1.5 K. It was measured at 2014/February, 2014/April and 2015/May. At first measurement, very high-Q value around 1×10^{11} was observed. After that, we tried to reproduce this high-Q results, but Q-values rather degraded measurement by measurement. It was difficult to get high-Q results at KEK-STF vertical test system.

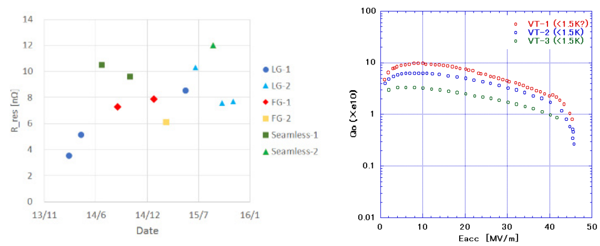

Figure 1: (Left) Residual resistance for vertical test of single-cell cavities. (right) History of Q-E curve for large grain single-cell cavity for three times vertical tests.

KEK-STF vertical test dewar has single magnetic shield inside. After cool-down by liquid He, its shielding characteristics degraded. As a result, around 10mG of remnant magnetic field remain inside vertical test dewar [5]. Cancelling of this remnant field is one important issue.

Components, such as flanges, which are directly touching to Nb are made by SUS316, but some of others are made by SUS304, for which magnetization was suspected. De-magnetization of vertical test components is also essential.

MAGNETIZED MEASUREMENT FOR VT COMPONENTS

Magnetization of each of vertical test components were surveyed by using a three axes flux gate sensor, Bartington Mag-03MS100, inside the magnetic shield whose size is 300 mm diameter and 1 m long, as shown in Fig. 2.

It was found that relatively large number of components were magnetized. Table 1 and Fig. 3 show a list and pictures of highly magnetized components. The numbers shown in Table 1 is absolute of measured magnetic field. One of metal valve and SUS304 long-nuts showed large magnetization of 430 and 300 mG, respectively. Some SUS304 bolts and washers were also magnetized around 100 mG. These are components magnetized more than 100 mG. Table 2 also shows a list of magnetized components. But this time magnetized less than 100 mG. D-sub connectors, bolts, nuts, washers etc. are magnetized. Even value is not large, but sometimes we use many of them. Then we need to care about these components too.

kensei.umemori@kek.jp

Content from this work may be used under the terms of the CC BY 3.0 licence (© 2017). Any distribution of this work must maintain attribution to the author(s), title of the work, publisher, and DOI.

ISBN: 978-3-95450-191-5 doi:10.18429/JACoW-SRF2017-TUPB032

STUDY ON 650MHz 5-CELL PROTOTYPE CAVITIES AT IHEP*

S. Jin†, J. Gao, D.J. Gong, Z.C. Liu, P. Sha, J.Y. Zhai, T.X. Zhao, and H.J. Zheng,
Key Laboratory of Particle Acceleration Physics & Technology, Institute of High Energy Physics, Chinese Academy of Sciences, Beijing 100049, China

Abstract

CEPC Pre CDR pointed that the 650 MHz 5-cell SRF cavity could be a candidate for the main ring of the single-ring pretzel scheme at the Higgs energy in 2015. Then EM design of 5-cell cavities were published later. So, the study on the fabrication of a 5-cell prototype cavity with waveguide HOM couplers were carried on at IHEP. In the paper, we will mainly report the mechanical design and fabrication progress of the 5-cell prototype. Besides, fabrication of a bare 2-cell prototype cavity was also carried on according to the further study after Pre-CDR. Challenges and possible solutions for the prototypes development will also be discussed.

INTRODUCTION

After the discovery of Higgs boson in 2012, a Circular Electron Positron Collider (CEPC) was proposed. In 2015, the CEPC Preliminary Conceptual Design Report was published and pointed that the 650 MHz 5-cell SRF cavity could be a candidate for the main ring of the single-ring pretzel scheme at the Higgs energy. On the other hand, further studies showed that a 650 MHz 2-cell cavity would be a better choice for the double ring or partial double ring with the crab waist scheme at the Higgs, W and Z energy, and 5-cell cavity could be used at the possible higher energy upgrade [1].

The electromagnetic (EM) design of 5-cell and 2-cell cavities were published respectively later [2,3]. So, study on the fabrication of a 5-cell with waveguide (WG) HOM couplers for higher HOM power and a bare 2-cell prototype cavities were carried on at IHEP. In the paper, we will mainly report the mechanical design and fabrication progress of the two prototypes. Challenges and possible solutions for the prototypes development will also be discussed.

STRUCTURE AND CHALLENGE OF 5-CELL CAVITY EM DESIGN

Figure 1 shows the EM design model of 5-cell prototype. As we can see, besides a cylinder input coupler, there are also totally five WG couplers in two beam tubes. EM design shows that it has good RF characteristics for the absorption of high power HOM [2].

However, if we directly transfer the EM model to a real cavity for fabrication, there will be several challenges hard to resolve:

1) Whole cavity very large: the length of each WG is near 1m; and beam tubes are about 0.4m;
2) Great cost for both material and fabrication;
3) Almost hard to finish if consider post-treatments for the cavity by existing facilities, such as ultrasonic cleaning, HRP, BCP, heat treatment.
4) A lot problems in the processes of real fabrication, RF test, and usual travel, assembly and so on.

So, structure modification has to be done from EM model to real cavity which is suitable for real fabrication.

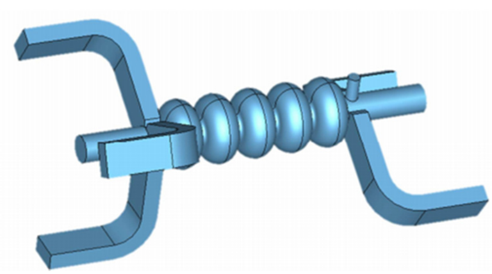

Figure 1: EM design of 5-cell prototype cavity [2].

STRUCTURE MODIFICATION FOR 5-CELL CAVITY PROTOTYPE

According to the challenges discussed above, consideration were made for the modification as following:

1) Post-treatment of cavity: ultrasonic cleaning, HRP, BCP, heat treatment;
2) Cold RF test requirement on the dimension;
3) Cavity performance: Quality factor.

Figure 2 shows the structure after modification. As shown, modification mainly focus on two parts: one is we cut the length of WG; the other is that we add an extension beam tube instead of original beam tube.

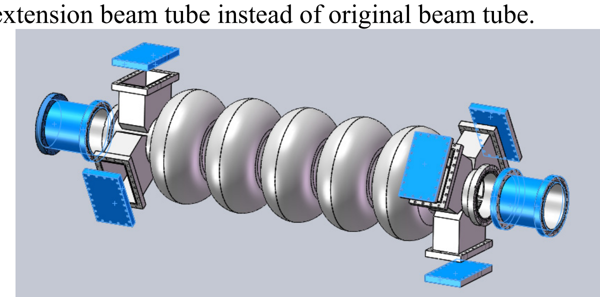

Figure 2: Modified structure for fabrication.

After above two modification, there are also some problems. First is the seal of the WG. Although the cut of WG can make the structure more simple, if a normal stainless steel flanges, a lot of power will be dissipated on it to lower the quality factor of the cavity . Table 1 shows

* Work supported by Research Programme for Beijing Municipal S&T Commission; National Key Programme for S&T Research and Development (Grant NO.: 2016YFA0400400); in part by the CAS Center for Excellence in Particle Physics (CCEPP).
† Corresponding author email: jinsong@ihep.ac.cn

Content from this work may be used under the terms of the CC BY 3.0 licence (© 2017). Any distribution of this work must maintain attribution to the author(s), title of the work, publisher, and DOI.

ISBN: 978-3-95450-191-5 doi:10.18429/JACoW-SRF2017-TUPB033

TESTS OF THE HIGH CURRENT SLOTTED SUPERCONDUCTING CAVITY WITH EXTREMELY LOW IMPEDANCE

Zhenchao Liu*, Jie Gao, Feisi He, Song Jin, Zhenghui Mi, TongXian Zhao, Hongjuan Zheng, IHEP, Beijing, China
Fang Wang, Dehao Zhuang, PKU, Beijing, China

Abstract

Slotted superconducting cavity is a novel structure with extremely low impedance and high BBU threshold. It can be used in various high current applications. A 1.3 GHz 3-cell slotted superconducting cavity was designed and tested. The room temperature test results show the cavity has an extremely low impedance. The vertical test results show the cavity gradient can reach several MV/m, but it was limited by the test end group made of steel.

INTRODUCTION

Various methods are adopted to efficiently damp the HOMs of the cavity in order to increase the Beam Break-Up (BBU) threshold of the cavity and reach the desired current intensity. Since the circular collider needs to deliver a bunch with a large number of electrons or positrons, the HOMs power in the cavity can reach several kW. Both the ERL and the circular collider require superconducting cavities with heavy HOM damping and efficient HOM extracting. We have proposed a high HOM damping cavity which can fulfil such an application. Ampere class BBU threshold can be achieved for the slotted cavity as the external Q of the HOMs is extremely low. The power of HOMs can be efficiently extracted from the cavity by means of a waveguide which runs around the cavity body. To demonstrate this idea, we have built a 1.3 GHz 3-cell slotted cavity.

In order to deliver a high current beam, these cavities are designed according to the following principles: low cell numbers, large iris and large beam pipe, optimized cell shape, efficient HOMs damping and extracting structure. The common objective of all these designs can be found in the need to increase the HOMs damping.

Compared with the ERL application, the superconducting cavity used in the circular collider delivers a lower beam current; however, the HOMs power of the cavity is much higher than the ones used in the ERL since the charge of each bunch is very large. A low impedance superconducting cavity with high HOM extracting efficiency constitutes a key goal for both the ERL and the circular collider.

BBU THRESHOLD

The beam current in a cavity is limited by its BBU threshold. For a single high order mode, the BBU threshold is given by [1]

$$I_{th} = \frac{2c^2}{e\left(\frac{R}{Q}\right)_\lambda Q_\lambda \omega_\lambda} \frac{1}{T_{12}^* \sin \omega_\lambda t_r} \tag{1}$$

and

$$T_{12}^* = T_{12}\cos^2\theta_\lambda + \frac{T_{14}+T_{32}}{2}\sin 2\theta_\lambda + T_{34}\sin^2\theta_\lambda \tag{2}$$

Here, c is the speed of light, e is the elementary charge, λ is the mode number, $(R/Q)_\lambda$ is the shunt impedance (in Ω), Q_λ is the quality factor, ω_λ is the HOM frequency, θ_λ is the polarization angle with respect to the x direction, t_r is the bunch return time, and the matrix T describes how a transverse momentum is transported to a transverse displacement after one turn.

From equation (1), we know that the BBU threshold is inversely proportional to the cavity intrinsic parameter $(R/Q)_\lambda \cdot Q_\lambda$. Thus, in order to increase the BBU threshold, it is necessary to decrease the impedance item $(R/Q)_\lambda \cdot Q_\lambda$.

The HOMs power of the cavity is $P_{HOM}=k_{||}IQ$, here $k_{||}$ is the cavity loss factor, I is the average beam current and Q is the quantity of electric charge of one bunch. For the circular collider, the bunch charge is about several nC which results in several kW HOMs power per cavity. For the ERL application, the HOMs power per cavity is about 1 kW or less.

CAVITY PARAMETERS

The slotted cavity was put three waveguide wings 120 degree separated around the cavity body to absorb the high order mode of the cavity. This structure shows extremely high damping of dipole and quadrupole modes which can give an ampere class beam current [2]. Table 1 shows the cavity main parameters. Table 2 shows the cavity shape parameters.

Table 1: Parameters of the 1.3 GHz Slotted Superconducting Cavity

Type	**Elliptical**
Operating frequency (MHz)	1300
Working gradient(MV/m)	15
Q_0	1×10^{10}
Beta	1
No. of cell	3
Dia. of iris (mm)	41.152
Dia. of beampipe (mm)	48.733
R/Q (Ω)	268.9
G (Ω)	265
E_{pk}/E_{acc}	3.57
B_{pk}/E_{acc} (mT/(MV/m))	5.72
Field flatness (%)	>97

* email address: zcliu@ihep.ac.cn

Content from this work may be used under the terms of the CC BY 3.0 licence (© 2017). Any distribution of this work must maintain attribution to the author(s), title of the work, publisher, and DOI.

ISBN: 978-3-95450-191-5 doi:10.18429/JACoW-SRF2017-TUPB034

THE 166.6 MHZ PROOF-OF-PRINCIPLE SRF CAVITY FOR HEPS-TF

P. Zhang*, J. Dai, X. Hao, T. Huang, Z. Li, H. Lin, Q. Ma, F. Meng, Z. Mi, W. Pan, Y. Sun, G. Wang, Q. Wang, X. Zhang, Institute of High Energy Physics (IHEP), Beijing, China

Abstract

The 166.6 MHz superconducting RF cavities have been proposed for the High Energy Photon Source (HEPS), a 6 GeV kilometer-scale light source. The cavity is of quarter-wave type made of bulk niobium with β=1. Each cavity will be operated at 4.2 K providing 1.2 MV accelerating voltage and 145 kW of power to the electron beam. During the HEPS-Test Facility (HEPS-TF) phase, a proof-of-principle cavity has been designed in IHEP and manufactured in Beijing. The subsequent BCP was conducted in Ningxia, while HPR, cleanroom assembly and 120 degree bake was done in IHEP. The cavity was finally vertical tested at both 4.2 K and 2 K in IHEP. The cavity Q_0 at designed gradient (when V_c=1.5 MV) at 4.2 K was measured to be 2.4×10^9 with E_{peak} of 42 MV/m and B_{peak} of 65 mT. The maximum E_{peak} and B_{peak} reached 86 MV/m and 131 mT respectively at both 4.2 K and 2 K, and the corresponding Q_0 was measured to be 5.1×10^8 (4.2 K) and 3.3×10^9 (2 K). The residual surface resistance was measured to be 2.3 nΩ.

INTRODUCTION

High Energy Photon Source (HEPS) is a 6 GeV storage ring light source with kilometer-scale circumference and ultra-low emittance [1]. It has been proposed by IHEP and is planned to be built in Beijing suburb. The electron beam is firstly accelerated to 300 MeV by a linac and subsequently injected into a ~400 m booster ring to further ramp its energy to 6 GeV prior to its final injection into the ~1300 m storage ring. Its main beam parameters are listed in Table 1. Prior to its official construction, a test facility namely HEPS-TF has been approved in 2016 to R&D and prototype key technologies and key components.

Table 1: Beam Parameters of the HEPS Storage Ring

Parameter	Value
Energy	6 GeV
Circumference	~1300 m
Current	200 mA
Energy loss w/ IDs	2.5 MeV/turn
Total SR power	500 kW

A double-frequency RF system has been conceived to realize the recently proposed on-axis injection scheme [2]. The fundamental RF frequency has been chosen to be 166.6 MHz while the third harmonic RF is 499.8 MHz [3]. This scheme will make two stable RF buckets to enable the merging of the injected bunch into the circulating beam. The high harmonic RF system needs to be active rather than passive.

The choice of the fundamental RF frequency is made by compromising competing demands of the kicker and the RF system. The state-of-art kicker has a total width of a few nano-seconds and favors a larger separation of the RF buckets, in other words, a lower RF frequency. On the other hand, a higher frequency will make the RF system more compact. Furthermore, in order to use as much as possible the mature technology of 500 MHz superconducting cavities, the main RF frequency has thus been chosen to be 166.6 MHz, one third of 499.8 MHz. Therefore the 166.6 MHz RF system naturally becomes the focus of the R&D during HEPS-TF phase.

Given the relatively low RF frequency (166.6 MHz), both normal conducting (NC) and superconducting (SC) options have been considered. A detailed comparison of these two options are given in [3]. This paper will focus on the 166.6 MHz SC cavity, in particular, the newly designed proof-of-principle cavity.

THE RF DESIGN

The Proof-of-Principle (PoP) cavity has been planned as the first cavity to be built in order to maximize learning on cavity manufacturing techniques, surface treatment and higher order mode (HOM) characterization. The cavity shall capture as many as possible the features which will be used in the final cavity design to ensure the experiences obtained are most relevant.

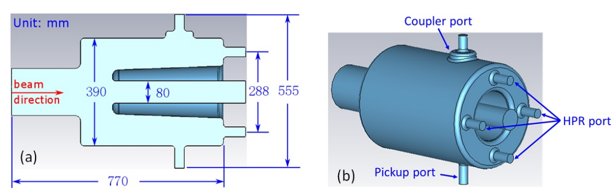

Figure 1: The 166.6 MHz PoP cavity.

Due to a low RF frequency and β=1, the popular elliptical shape will make the cavity geometry excessively large ($\beta \cdot \lambda/2$) thus unpractical for manufacturing. The quarter-wave cavity has then been chosen. The RF design and optimization were conducted within the following boundaries: firstly, the outer conductor radius is preferably to be less than 250 mm while keeping the inner conductor as big as possible, this is to ensure a manageable cavity size, larger beam aperture and larger helium volume inside the inner conductor; secondly, the peak electric field (E_{peak}) and peak magnetic field (B_{peak}) at design gradient (V_c=1.5 MV) needs to be less than ~40 MV/m and ~65 mT respectively, and this reserves 20% margin in peak fields when operating at nominal gradient (V_c=1.2 MV); thirdly, the frequency of the first dipole mode needs to be higher than 400 MHz to ensure

* zhangpei@ihep.ac.cn

Content from this work may be used under the terms of the CC BY 3.0 licence (© 2017). Any distribution of this work must maintain attribution to the author(s), title of the work, publisher, and DOI.

ISBN: 978-3-95450-191-5 doi:10.18429/JACoW-SRF2017-TUPB035

FREQUENCY PRE-TUNING OF THE 166.6 MHz PROOF-OF-PRINCIPLE SRF CAVITY FOR HEPS-TF

P. Zhang*, X. Hao, Z. Li, X. Zhang
Institute of High Energy Physics (IHEP), Beijing, China

Abstract

A 166.6 MHz proof-of-principle SRF cavity has been designed for the High Energy Photon Source-Test Facility (HEPS-TF). The cavity is a β=1 quarter-wave resonator made of bulk niobium operating at 4.2 K. A pre-tuning scheme was made to accommodate the cavity frequency shift mainly due to manufacturing tolerances, the subsequent surface treatment and finally the cooldown process. To this end, the length of the cavity outer conductor was chosen as a free parameter for the pre-tuning. The cavity frequency was carefully monitored during the production, cavity treatment and vertical test. The measurement results agree well with our calculations. It is worth noticing that the pre-tuning method only involves one-time measurement of the cavity resonant frequency and its outer conductor length.

INTRODUCTION

High Energy Photon Source (HEPS) has been planned by IHEP to be built in Beijing suburb in the next few years. It is a 6 GeV, 200 mA light source with a kilometer-scale storage ring aiming for ultra-low emittance [1]. The fundamental RF frequency is 166.6 MHz while the high harmonic cavity is of 499.8 MHz [2]. Prior to its official construction, a test facility (HEPS-TF) was approved in 2016 to R&D key technologies. The current focus of the RF system is the 166.6 MHz superconducting cavity. A proof-of-principle (PoP) cavity has been subsequently designed, fabricated and vertical tested this year and reported in [2, 3].

The production of a 166.6 MHz PoP cavity requires several process steps: cavity fabrication, surface treatment and cavity cooldown to 4.2 K. The cavity resonant frequency evolves after each process and this needs to be characterized. By analytical calculation, electromagnetic simulation and RF measurements, the frequency shift can be well determined, while the frequency uncertainties can be estimated [4]. Possessing a good knowledge of the frequency variation, a pre-tuning step was determined and described in this paper. The length of the cavity outer conductor is used as a free parameter to recover the frequency shift.

THE TARGET FREQUENCY

The target frequency of the cavity is 166.6 MHz at 4.2 K with the cavity immersed in a 1 bar of Liquid Helium bath while having vacuum inside. According to simulations, 19 kHz from the cavity frequency will be lost by pumping the cavity volume from air to vacuum maintaining the ambient pressure of 1 bar. Figure 1 shows the step-by-step scaling of the cavity frequency. Warming up the cavity from 4.2 K to 293 K will thermally expand the cavity volume and thus bring down the cavity frequency by 220 kHz. The last contribution to the frequency shift is the permittivity of the ambient air. This will contribute -53 kHz to the cavity measured in air. Finally the cavity measured in ambient environment with 20°C, 50% relative humidity and normal pressure shall have a resonant frequency of 166.446 MHz in order to ensure a correct frequency at 4.2 K. This will serve as a guide during the following cavity process step. The exact number of the frequency shift will only be determined by measurements as described in the following sections.

f_0(MHz)	Δf	Temp.	Cav. inner volume	Cav. outer volume
166.600		4.2K	Vacuum	1bar LHe
	0 kHz	Tuning force→0kgf		
166.600		4.2K	Vacuum	1bar LHe
	+19 kHz	Pressure differ. between inside/outside (with supports)		
166.619		4.2K	Vacuum	Vacuum
	-220 kHz	4.2K→293K (with supports)		
166.399		293K	Vacuum	Vacuum
	-53 kHz	Vacuum → air		
166.346		293K	Ambient air	Ambient air
	+100 kHz	After BCP&Annealing → before BCP&Annealing (remove 200μm) (+39kHz, if uniformly remove 200μm)		
166.446		293K	Ambient air	Ambient air

Figure 1: The step-wise frequency scaling from simulation.

The cavity has been supported by 4 titanium rods and 2 backplanes as shown in Fig. 2 to ensure a proper mechanical rigidity during pumping to vacuum and cooldown to 4.2 K. The exploded view of the cavity is shown in Fig. 3 noted with components' name. The following study was based on the supported cavity with LBP flange fixed [5].

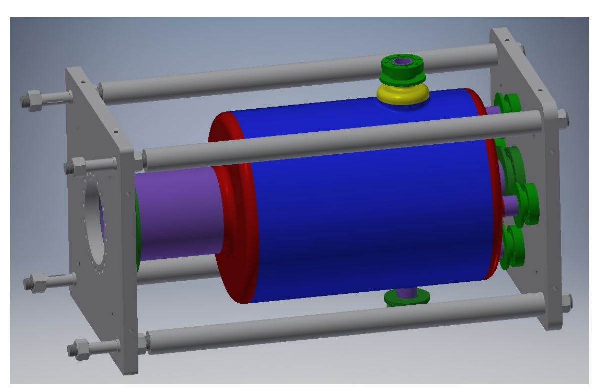

Figure 2: The cavity with supporting frame.

* zhangpei@ihep.ac.cn

Content from this work may be used under the terms of the CC BY 3.0 licence (© 2017). Any distribution of this work must maintain attribution to the author(s), title of the work, publisher, and DOI.

ISBN: 978-3-95450-191-5 doi:10.18429/JACoW-SRF2017-TUPB036

R&D OF CEPC CAVITY*

P. Sha†, B. Q. Liu, X. Y. Zhang, Z. H. Mi, H. J. Zheng, J. Y. Zhai
Key Laboratory of Particle Acceleration Physics and Technology, Institute of High Energy Physics, CAS, Beijing 100049, China

Abstract

CEPC will use 650 MHz cavities for the collider (Main Ring) and 1.3 GHz cavities for the Booster. Each booster cryomodule contains eight 1.3 GHz 9-cell cavities, which is similar as LCLS-II, E-XFEL and ILC. Each collider cryomodule contains six 650 MHz 2-cell cavities, which is totally new. So our R&D of CEPC cavity mainly focuses on the 650 MHz 2-cell cavity. A cryomodule which consists of two 650 MHz 2-cell cavities has began in early 2017. In this thesis, the RF and mechanical design is displayed with Helium vessel. Besides, multipacting is analyzed. In order to achieve high Q, N-doping is also studied [1, 2].

INTRODUCTION

Baseline layout and parameters for CEPC Main Ring SRF system have been public [3]. There're two SRF sections in total, and each one has two SRF stations. There're 14 cryomodules per station, which consist of six 650MHz 2-cell cavities each. So there're 336 650MHz 2-cell cavities in total. RF and Mechanical design of these cavities have been completed. And fabrication of prototype cavities would start soon. The vertical test goal is 4E10@22 MV/m, while the horizontal one is 2E10@16 MV/m. Both these targets are extremely high to reach, so N-doping would be adopted. In recent years, it has been proposed and proven to increase *Q* of superconducting cavity obviously, which lowers the BCS surface resistance. It was discovered in 2012 at FNAL, which has been promoted by FNAL, JLAB and Cornell together. Since 2013, there have been over 60 cavities nitrogen doped in USA laboratories. After N-doping, *Q* of 650 MHz single-cell cavities for PIP-II increased to $7{*}10^{10}$ at E_{acc}=17 MV/m, which doubled from no N-doping, as Figure 1 [4].

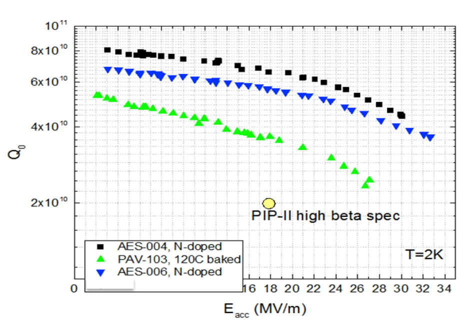

Figure 1: Vertical test results of 650 MHz high beta single-cell cavities for PIP-II.

RF DESIGN OF 650 MHz 2-CELL CAVITY

The goal of RF design is to minimize B_{peak}/E_{acc} and E_{peak}/E_{acc}, maximize R/Q and k (cell to cell coupling). Elliptical cavity is characterized by different geometrical parameters, as Figure 2. The values of Riris, b/a and alpha have been optimized to achieve this goal.

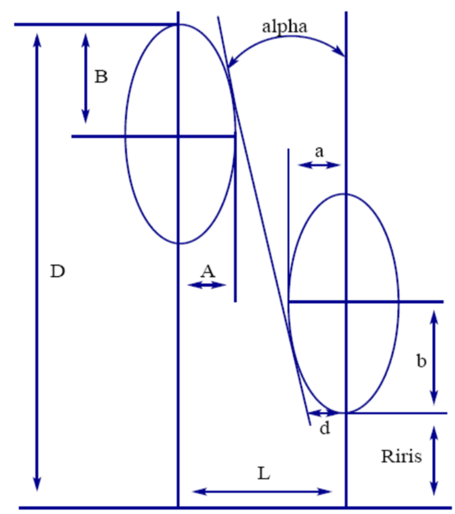

Figure 2: Profile of cell shape.

Larger Riris results to larger k and easier HOM damping, but increases B_{peak}/E_{acc} and E_{peak}/E_{acc}, as Figure 3.

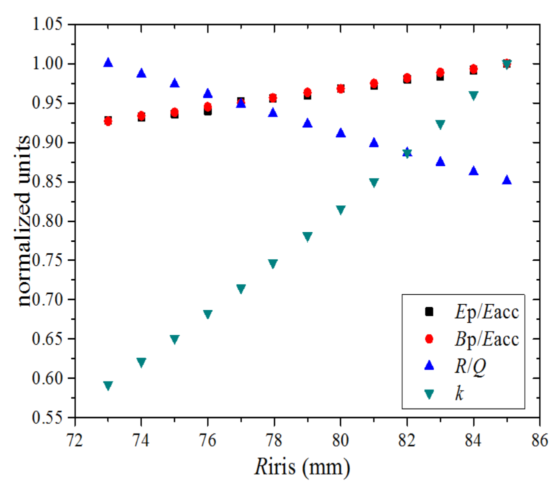

Figure 3: Optimization of Riris.

The iris ellipse ratio (b/a) is determined by the local optimization of the peak electric field, as Figure 4.

* This study was supported by National Key Programme for S&T Research and Development (Grant NO.: 2016YFA0400400) and National Natural Science Foundation of China (Grant NO.:11505197).
† shapeng@ihep.ac.cn

Content from this work may be used under the terms of the CC BY 3.0 licence (© 2017). Any distribution of this work must maintain attribution to the author(s), title of the work, publisher, and DOI.

ISBN: 978-3-95450-191-5 doi:10.18429/JACoW-SRF2017-TUPB037

A 166.6 MHZ PROOF-OF-PRINCIPLE SRF CAVITY FOR HEPS-TF: MECHANICAL DESIGN AND FABRICATION

X. Zhang*, Z. Li, P. Zhang, H. Lin, Y. Sun, Institute of High Energy Physics (IHEP), Beijing, China
X. R. Hao[1], Institute of High Energy Physics, Beijing, China
[1]University of Chinese Academy of Sciences, Beijing, China

Abstract

166.6 MHz superconducting RF cavities operating at 4.2 K have been proposed by IHEP for the High Energy Photon Source - Test Facility (HEPS-TF). The cavity is a quarter wave resonator with beam going through the cavity inner conductor. The cavity and its stiffness were designed and optimized to meet pressure safety requirement and to reduce frequency sensitivity due to helium pressure fluctuations. Tuning sensitivity, Lorentz force detuning and microphonics were also simulated. Most calculations have been validated by experiments. This paper reports the mechanical design and fabrication details of the first proof-of-principle cavity.

INTRODUCTION

The High Energy Photon Source (HEPS), a 6 GeV kilometre-scale, ultralow-emittance storage ring light source, is to be built in the suburb of Beijing, China [1]. As the R&D project for HEPS, a test facility namely HEPS-TF has been approved to prototype key technologies and components. The new injection scheme [2] requires two RF frequencies for the storage ring, meanwhile limited by the development of the fast kicker system, 166.6 MHz has been chosen as the main RF frequency and the 499.8 MHz for the third harmonic cavity respectively. The main parameters of the double-frequency RF system [3] are listed in Table 1. Extensive efforts have been made on the 166.6 MHz superconducting (SC) cavity and relevant studies of the RF system.

Table 1: Main Parameters of the RF System

Parameter	Fundamental cavity	Harmonic cavity
Frequency	166.6 MHz	499.8 MHz
RF voltage	3.5 MV	3.2 MV
Number of cavities	4	2
RF voltage / cavity	1.2 MV	1.7 MV
Peak power / cavity	150 kW	200 kW

Due to the low operating frequency (166.6 MHz) and $\beta = 1$, a quarter wave shape was adopted, which makes the cavity geometry suitable for manufacturing. A proof-of-principle (PoP) cavity has been designed and optimized [4]. The RF model is shown in Fig. 1.

This paper describes the mechanical design with a focus on the pressure sensitivity, cavity rigidity, Lorentz force

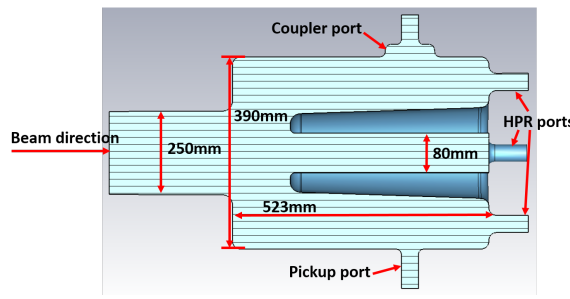

Figure 1: The 166.6MHz PoP cavity.

detuning (LFD), stress analysis and microphonics. The fabrication details of the PoP cavity will also be mentioned.

THE MECHANICAL DESIGN

The mechanical design of the 166.6 MHz PoP cavity was optimized using SolidWorks CAD [5] and ANSYS simulation codes [6]. The measurement results show good agreement with the calculations.

Model

The mechanical model for study is shown in Fig. 2. To simplify the simulation, some features of the model are removed, such as the coupler and pickup ports. The wall thickness of some cavity parts is increased to reinforce its strength. Since the beam tube in the inner conductor is too long, a stiffening ring was added. Two stiffeners were designed, and the bowl shaped one was finally chosen due to better performance.

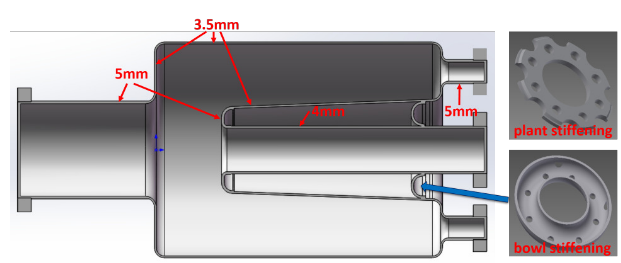

Figure 2: The mechanical model.

The cavity is made of RRR300 niobium and Ti-45Nb alloy. The maximum allowable stress (S) is determined by [7]

$$S = \min(\frac{\text{Ultimate strength}}{3.5}, \text{Yield strength} \times \frac{2}{3}). \qquad (1)$$

* zhangxinying@ihep.ac.cn

Content from this work may be used under the terms of the CC BY 3.0 licence (© 2017). Any distribution of this work must maintain attribution to the author(s), title of the work, publisher, and DOI.

ISBN: 978-3-95450-191-5 doi:10.18429/JACoW-SRF2017-TUPB038

MECHANICAL DESIGN OF A 650 MHZ SUPERCONDUCTING RF CAVITY FOR CEPC*

X. Zhang †, Z. Mi, P. Sha, J. Zhai, F. He, Q. Ma, Institute of High Energy Physics (IHEP), Beijing, China

Abstract

A 650 MHz superconducting RF cavities have been proposed by IHEP for the Circular Electron-Positron Collider (CEPC). The major components are a 2-cell elliptical cavity, end groups, stiffness and helium vessel, which have been optimized to meet the design requirement. The minimization of the Lorentz force detuning and the sensitivity of resonance frequency to Helium pressure variations was the main goal of the optimization. Also detailed stress analysis, tuning and microphonics performance of dresses cavity will be presented in this paper.

INTRODUCTION

As the Higgs boson has been discovered in 2012, some proposals are being raised building a Higgs factory for further fine measurement of the new particle. Circular Electron-Positron Collider (CEPC) has been launched by IHEP to study of a 50-100 km ring collider [1], and now is under extensive design. The CEPC baseline accelerator [2] is a fully partial double ring configuration with a circumference of 100 km and the RF system for Higgs, W and Z operation [3] in each beam line of electron and positron as shown in Fig. 1. The layout and parameters of SRF system [4] are chosen to meet the minimum luminosity requirement for each operating energy, and with possible higher luminosity.

For CEPC collider, 650 MHz 2-cell superconducting RF cavities shared between the two collider rings has been proposed to operate in CW mode at 2 K. The main RF parameters of the 650 MHz 2-cell cavity [5] are listed in Table 1. There are 56 cryomodules in the main ring, and each of the 10 m-long collider cryomodule contains six 650 MHz cavities [2], as shown in Fig. 2. So the number of 650 MHz 2-cell cavities needed in the main ring is 336.

Table 1: Parameters of 650 MHz 2-cell Cavity

Parameters	value
R/Q	212.7 Ω
G	284.1 Ω
E_p/E_{acc}	2.38
B_p/E_{acc}	4.17 mT/(MV/m)
length	1060 mm
equator diameter	410 mm

This paper reports the mechanical design and optimization of the 650MHz 2-cell elliptical cavity. The pressure sensitivity, cavity rigidity, Lorentz force detuning (LFD), stress analysis and Microphonics have been studied to improve the mechanical stability.

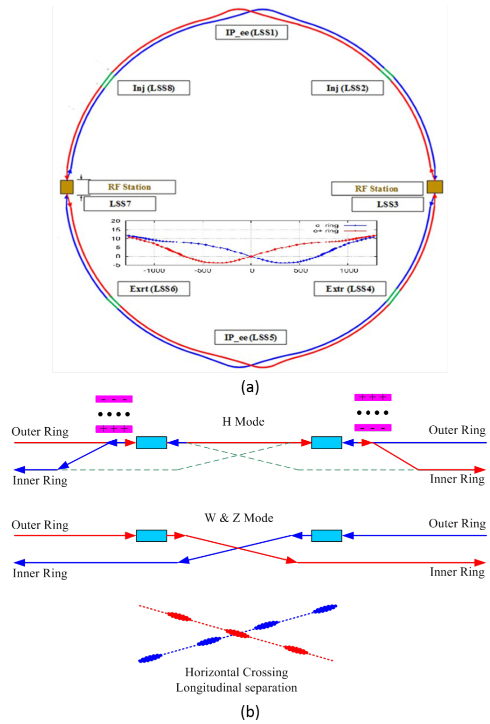

Figure 1: The CEPC baseline design (a) and one section of RF station layout (b).

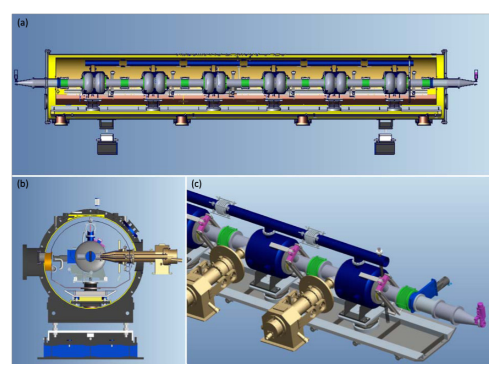

Figure 2: The layout of 650MHz 2-cell cavities in cryomodule.

THE MODEL

The mechanical model includes the cavity, stiffness, endgroups and liquid helium (LHe) vessel, and the material of them are niobium with RRR300, niobium, Ti-45Nb alloy and titanium respectively, as shown in Fig. 3. The maximum allowable stress (S) at room temperature of Niobium,

* Work supported by National Key Programme for S&T Research and Development (Grant NO.: 2016YFA0400400)
† zhangxinying@ihep.ac.cn

Content from this work may be used under the terms of the CC BY 3.0 licence (© 2017). Any distribution of this work must maintain attribution to the author(s), title of the work, publisher, and DOI.

ISBN: 978-3-95450-191-5 doi:10.18429/JACoW-SRF2017-TUPB039

ELECTROPOLISHING OF NIOBIUM FROM DEEP EUTECTIC SOLVENTS BASED ON CHOLINE CHLORIDE *

Qingwei Chu, Yuan He, Shenghu Zhang, Zhiming You, Hao Guo, Pingran Xiong, Lu Li,
Institute of Modern Physics, Chinese Academy of Sciences, Lanzhou, P. R. China

Abstract

Niobium (Nb) was electropolished from choline chloride-based deep eutectic solvent (DES). The purpose of this paper was to systematically investigate the influence of various electropolishing parameters, including electropolishing time, electrolyte temperature and voltage, on the electropolishing rate, surface roughness and microstructure of Nb. The result showed that the electropolishing parameters had a significant impact on the performance of Nb. Prolonging electropolishing time and negatively shifting voltage, the electropolishing rate of Nb increased first and then decreased, and the roughness decreased first and then increased. With the electrolyte temperature increased, the electropolishing rate increased and surface roughness decreased. Based on surface analysis by scanning electron microscope (SEM), smoother Nb can be achieved under properly controlled conditions.

INTRODUCTIONS

The inner surface of niobium cavity plays a most important role in determining the efficiency and maximum accelerating gradient, various surface treatments are employed to get a smooth and clean surface. The electropolishing (EP) and buffered chemical polishing (BCP) processes have been used to polish the Nb surface of SRF cavities to eliminate the unevenness of the material's surface and to achieve possibly the highest surface smoothening effect. During the standard EP process, the electrolyte used for Nb surface is composed of HF and H_2SO_4 in a volume ratio of 1:9. BCP solution is a mixed acid solution of HF, HNO_3 and H_3PO_4 by volume ratio of 1:1:1 or 1:1:2. The mixed acid solution has huge potential hazards for operating personnel and environment. And some researches believed that only with the use of HF can breakdown of the strong passive film on the Nb surface. Due to the hazard of HF, HF-free electrolyte for the electropolishing of Nb is an important research direction. As an alternative, some non-aqueous solvents, for example, ionic liquid, provide an alternative to replace hazardous acidic mixtures for the electropolishing of Nb.

In recent decades, ionic liquids are of great interest for electrochemical purposes due to wide potential windows, thermal stability, high solubility of metal salts, avoidance of water and metal/water chemistry and high conductivity compared to non-aqueous solvents [1, 2]. Abbott and co-workers [3] introduced a relatively new class of ionic liquid, deep eutectic solvent (DES), based on eutectic mixtures of choline chloride (ChCl) with a hydrogen bond donor species. DES is a powerful and potential media for the electropolishing of metals due to its low cost, environmental friendliness and high purity, and so on. To date, there are very few studies on the electropolishing of Nb from DES. Tarek M. Abdel-Fattah et al. [4, 5] used VB4 ionic liquid by mixing choline chloride, ethylene glycol and ammonium fluoride, in a 1:2:1 molar ratio. It was found that the VB4 polishing is capable of producing smooth Nb surfaces, and this ionic liquid is a viable replacement for acid-based methods for preparation of SRF cavities. However, the performance of Nb is affected by several experimental factors, such as the electropolishing time, voltage, current density, temperature, stirring process and so on. However, there was almost no paper reported the influence of electropolishing parameters on Nb.

Based on previous work, in the present study, we explored the electropolishing of Nb from a 1:2 ChCl -based ionic liquid. The effect of various electropolishing parameters, such as electropolishing time, temperature and voltage, on the electropolishing rate, surface roughness and microstructure of Nb was examined. The microstructure of Nb surfaces was investigated using scanning electron microscopy (SEM).

EXPERIMENTAL DETAILS

Choline chloride (ChCl), urea and ammonium fluoride (AF) were used as obtained. The ChCl-based ionic liquid was formed by stirring the mixture of the two components in a mol ratio of 1ChCl: 2urea in a beaker at 80°C until a homogeneous, colorless liquid formed. Then NH_4F was added to the mixture with gentle stirring to give the final ratio of 1ChCl: 2urea: 1AF.

The electropolishing of Nb samples was performed through a RST5200 electrochemical workstation with a three-electrode system, where a Cu plate (7 mm×20 mm) was used as working electrode, a Nb plate (20 mm×17 mm×3 mm) as counter electrode and a glassy carbon disk (1.0 mm diameter) as reference electrode. Before each set of experiments, the electrodes were cleaned in an ultrasonic acetone bath, rinsed with distilled water and dried. The set of parameters has been selected according to the most important factors established in preliminary trials, as follows: (1) duration time: from 10 to 30 min; (2) temperature: changed from 50 to 80 °C; (3) negative voltages: ranged from -3 V to -6 V, respectively. The stirring rate was approximate 100 rpm. After electropolishing, the sample was thoroughly cleaned with distilled water and ethanol, and then dried. Each sample repeated twice under the same condition before characterization. The electropolishing rate is: $v=m / (t * s)$,

*chuqingwei@impcas.ac.cn

Content from this work may be used under the terms of the CC BY 3.0 licence (© 2017). Any distribution of this work must maintain attribution to the author(s), title of the work, publisher, and DOI.

ISBN: 978-3-95450-191-5 doi:10.18429/JACoW-SRF2017-TUPB040

DESIGN AND OPTIMIZATION OF MEDIUM AND HIGH BETA SUPERCONDUCTING ELLIPTICAL CAVITIES FOR THE CW LINAC IN CIADS*

Y. Huang†, L. Chen, Y. Li, S. Zhang, Y. He, IMP, CAS, Lanzhou, China

Abstract

Superconducting technology is adopted in the main accelerating section of the CW Linac in China Initiative Accelerator Driven Sub-critical System (CIADS) to accelerate the 10 mA proton beam from 2.1 MeV up to 1.5 GeV. The medium to high energy section of the superconducting linac is composed of two families of SC elliptical cavities with optimum beta 0.62 and 0.82 for the acceleration of proton beam from 158 MeV to 1.5 GeV. In this paper, the design and optimization of the 650 MHz medium and high beta elliptical cavities are discussed, including the RF design, high order modes (HOMs) analysis, and the multipacting analysis.

INTRODUCTION

China is now developing an Accelerator Driven Sub-critical System, which is composed of a CW superconducting linac, a spallation target and a nuclear reactor operating in the sub-critical mode, to dispose the nuclear waste and solve the problems of nuclear fuel shortage. Superconducting technology is adopted in the main accelerating section of the CW Linac, including the 162.5 MHz half wavelength resonators (HWR), 325 MHz spoke cavities, and 650 MHz elliptical cavities. Two families of SC elliptical cavities are adopted with optimum beta 0.62 to accelerate the proton beam from 158 MeV to 250 MeV and 0.82 cavities for the acceleration from 250 MeV to 1.5 GeV.

RF DESIGN

The elliptical cavity can be parameterized with the geometrical parameters shown in Fig. 1. The main parameters in the elliptical cavities are the half-cell length L/2, the equator radius D, the iris radius radius r, the equator axis parameters B and A, the iris axis parameters b and a, and the wall angle alpha. Once the cavity frequency and the optimum beta (or the geometry beta) is determined, the half-cell length is also confirmed. The cavity structure can then be optimized with B, A, b, a and alpha. Here alpha is depending on A and a.

The iris radius r is mainly related to the cell-to-cell coupling. A larger r is helpful to achieve good inter cell coupling and field flatness, but will also come with the reduction of the R/Q and the increase of the Epk/Eacc and Bpk/Eacc, which will decrease the cavity properties.

The equator radius D is manly related to the cavity frequency, which can be used to tune the cavity during the optimization.

The equator axis parameters B and A will mainly change the magnetic field enhance factor Bpk/Eacc while the iris axis parameters b and a will mainly affect the electric field enhance factor Epk/Eacc.

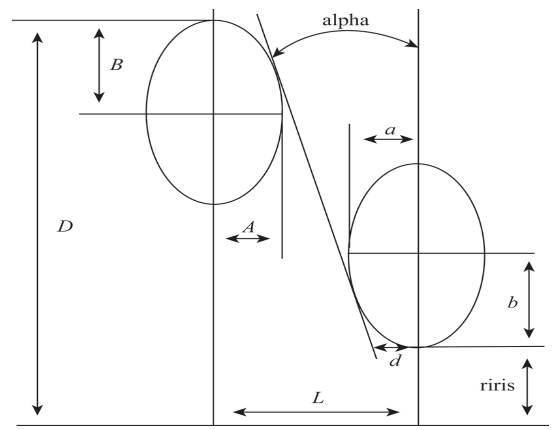

Figure 1: Geometry parameters of the elliptical cavity.

The cavity cell number is a balance of the acceleration efficiency, the cavity acceptance and the extraction of the HOM modes. Here 5 cell is adopted for the medium beta 062 cavity and 6 cell is adopted for the 082 cavity, as shown in Fig. 2 and Fig. 3. The geometry parameters and the electromagnetic parameters are list in Table 1 and Table 2.

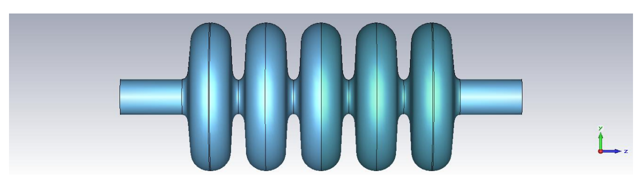

Figure 2: Cavity model of the 5 cell 062 cavity.

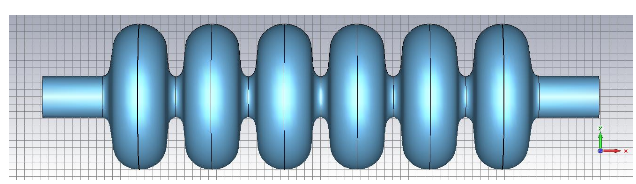

Figure 3: Cavity model of the 6 cell 082 cavity.

HOM ANALYSIS

Beam passing through the cavity, HOMs will be excited. Some of the HOMs can be efficiently been damped from the beam pipe or the HOM couplers on the beam pipe, while the others are difficult to damp since the electromagnetic fields of these modes are very weak in the beam pipe, which were called the “Trapped modes”. These trapped HOMs will have effect on the beam qualities both in the longitudinal and transverse directions, and will also result to additional cryogenic loss.

* Work supported by National Natural Science Foundation of China (91426303, 11505255)
† email address: huangyulu@impcas.ac.cn

Content from this work may be used under the terms of the CC BY 3.0 licence (© 2017). Any distribution of this work must maintain attribution to the author(s), title of the work, publisher, and DOI.

ISBN: 978-3-95450-191-5 doi:10.18429/JACoW-SRF2017-TUPB041

DESIGN OF A TRIPLE SPOKE CAVITY FOR THE HIF DEMO INJECTOR*

W. Ma [1, 2, †], T. He [1, 2], L. Yang [1, 2], L. Lu [1]
[1] Institute of Modern Physics, Chinese Academy of Science, Lanzhou 730000, China
[2] University of Chinese Academy of Sciences, Beijing 100049, China

Abstract

A 325 MHz triple spoke type superconducting cavity for lead beams with beta=0.3 is designed for the heavy ion inertial fusion (HIF) Demo facility. The design and simulations of the triple spoke will be reported in this paper, including the electromagnetic (EM) design and mechanical study using CST microwave studio (MWS) and ANSYS workbench.

INTRODUCTION

In the 1970s, the accelerator scientists proposed several HIF projects to solve the energy problem, such as HIBALL[1] in USA, HIDIF[2-3] in Germany and HIBLIC [4] in Japan. As shown in Fig. 1 [4], the heavy-ion beams were used to irradiate the deuterium-tritium (D-T) target and to increase the plasma temperature and density to reach the Lawson criterion. All above proposed HIFs were large scale facilities and were too large to be built.

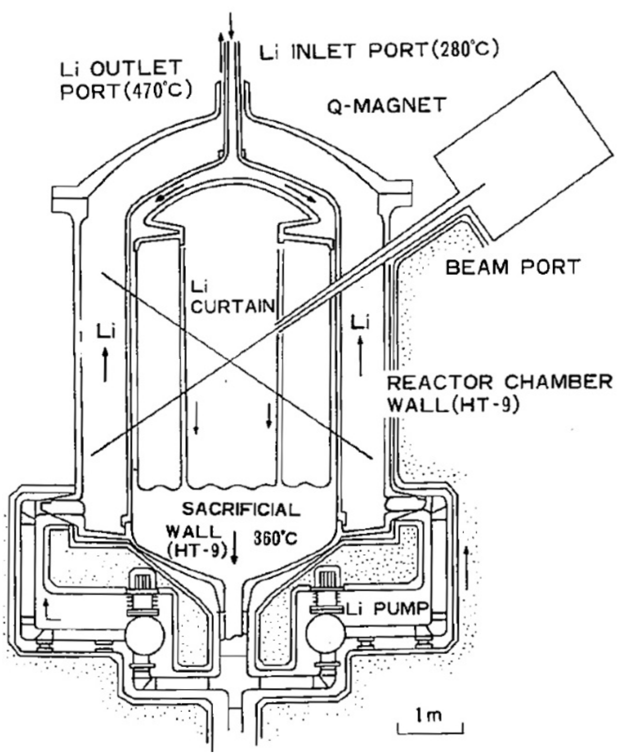

Figure 1: The principle of the heavy-ion inertial fusion. This image is designed for the HIBLIC reactor.

We propose a demo facility shown in Fig. 2 for these researches. In this demo facility, a 240 mA heavy ions beam will be accelerated up to 10 MeV/u and 50 MeV/u by a 600-meter-long linac driver and downstream heavy-ion synchrotron systems. There is a four-times storage ring where RF storage, electron cooling and stochastic cooling technologies can be developed. After bunch compressors, the bunched heavy ions will be injected into four induction bunches for recompressing and strengthening. Finally, the recompressed beams will be delivered to the experimental fusion facilities. The width of the final bunch is 10~20 ns, which requires superconducting focusing technologies for target heating.

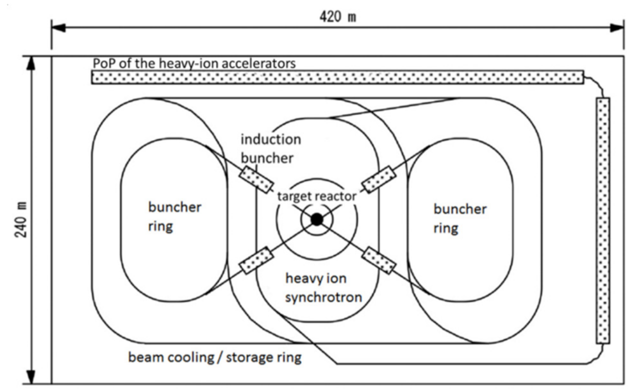

Figure 2: DEMO facilities of a multi-beam cavity type linac-based HIF system.

We are trying to design a new HIF driver linac, using the direct plasma injection scheme (DPIS) technologies and multi-beam acceleration [5]. A simple layout of HIF driver system is shown in Fig. 3. In this system, a powerful laser will split to four and produce four high-intensity Pb+ ion beams (115 mA/channel), which will be directly injected to a four-beam type Interdigital H-mode (IH) RFQ [6], where four 125 mA beams will be accelerated to 300 keV/u from 3 keV/u at an operation frequency of 40.625MHz. Two beams funneling system will be adopted to funnel the accelerated ion beams from the RFQ. The beam intensity will be enhanced to 220 mA/channel before injecting to a two-beam type drift tube IH (DT-IH) linac system. The two-beam type IH-DTLs will accelerate 220 mA/channel ions up to 1.2 MeV/u at an operation frequency of 81.25 MHz. The system could also offer one-beam type DT-IH linacs, which will accelerate 410 mA/channel ions up to 4.7 MeV/u at an operation frequency of 162.5 MHz. Finally, superconducting (SC) linacs will offer high accelerating field to accelerate 400 mA ions up to the 50 MeV/u at the operation frequency of 162.5MHz and 325 MHz. Comparing with the initial proposed HIF driver, the total length of the new HIF injector based on the multi-beam linac is only about 2.5 km, which is constructible.

* Work supported by NSFC of China under Grant No. 11475232 and No. 11535016.
† email address: w_ma@impcas.ac.cn

Content from this work may be used under the terms of the CC BY 3.0 licence (© 2017). Any distribution of this work must maintain attribution to the author(s), title of the work, publisher, and DOI.

ISBN: 978-3-95450-191-5 doi:10.18429/JACoW-SRF2017-TUPB046

Content from this work may be used under the terms of the CC BY 3.0 licence (© 2017). Any distribution of this work must maintain attribution to the author(s), title of the work, publisher, and DOI.

EXPERIENCE ON DESIGN, FABRICATION AND TESTING OF A LARGE GRAIN ESS MEDIUM BETA PROTOTYPE CAVITY

M. Bertucci†, A. Bignami, A. Bosotti, J.F. Chen, P. Michelato, L. Monaco, R. Paparella, D. Sertore, INFN–LASA, Segrate (MI), Italy
C. Pagani, University of Milano & INFN-LASA, Milano, Italy
S. Pirani*, ESS, Lund, Sweden and on leave at INFN-LASA, Segrate (MI), Italy

Abstract

INFN-LASA built a complete Medium Beta cavity, based on the ESS prototype design, with novel large-grain material sliced in sheets from an ingot provided by CBMM manufacturing experience. Design and fabrication are reported as well as results on the physical and chemical analyses performed on samples at different cavity production stages. Results from the cold tests performed are also summarized and critically discussed in view of future R&D activities.

INTRODUCTION

In the framework of the ESS activity in progress at INFN - LASA, we have designed a 704.42 MHz Medium (β=0.67) beta prototype cavity plug compatible [1] with the ESS cryomodule design [2]. Two prototypes of these cavities have been built and treated at Ettore Zanon S.p.A. under the supervision of INFN-LASA, following a "build-to-print" scheme, namely the same successful strategy adopted for the production of the 800 1.3 GHz and of the 20 3.9 GHz series cavities of the European XFEL [3, 4]. To validate the cavity design and the production process, one cavity (MB001) was built using Fine Grain niobium (i.e. the standard technology), as foreseen for the series. A second prototype (MBLG002) has been produced using Large Grain niobium with the aim of exploring the possibilities and potentialities of this material, exploiting the same production procedure: thanks to this it will be possible to compare the two material performances and then highlight the large grain material features. Among them, the potential benefits due to higher achievable thermal stability coming from the phonon peak around 2 K in thermal conductivity and the cost benefit due to lower bare material prices and simplified Nb fabrication process [5].

In this article, we present our experience on the material preparation, fabrication, treatments and testing of the LG niobium cavity based on our design for ESS Medium Beta cavities and some considerations about cavity performance.

MATERIAL PREPARATION

CBMM (Brazil) produced a high RRR (≈ 300) Large Grain Nb ingot with a diameter compatible with the Medium Beta and High Beta ESS Superconducting cavities (about 480 mm), by using a special crucible and metallurgic techniques. This is nowadays the biggest LG Nb ingot ever produced. From this, two shorter and lighter ingots (about 200 kg) have been then obtained. Figure 1 shows the two ingots at Heraeus in preparation for the slicing process, just after their arrival from CBMM.

Figure 1: CBMM Large Grain ingots at Heraeus in preparation for the slicing process.

Heraeus GmbH in Hanau sliced then the ingot into disks with a 4.65 mm thickness using a multi-wire sawing machine adapted to our large ingot diameter. The "oxygen protection" technique has been employed so to avoid permanent degradation of RRR, by reducing O_2 diffusion and gettering. In Fig. 2 the LG disks after slicing process are shown.

Figure 2: Large Grain ingots after slicing at Heraus.

After the slicing process, the Nb sheets have been chemically etched by Buffered Chemical Polishing (BCP 1:1:2) to remove about 30 µm of mechanically damaged surface layer.

In order to reduce the hydrogen content, which is expected to increase during the wire-saw and BCP opera-

† Michele.bertucci@mi.infn.it
* now at ESS, Lund

18th International Conference on RF Superconductivity SRF2017, Lanzhou, China JACoW Publishing
ISBN: 978-3-95450-191-5 doi:10.18429/JACoW-SRF2017-TUPB047

PASSBAND MODES EXCITATION TRIGGERED BY FIELD EMISSION IN ESS MEDIUM BETA CAVITY PROTOTYPE

J.F. Chen†, M. Bertucci, A. Bosotti, P. Michelato, L. Monaco, R. Paparella, D. Sertore, INFN-LASA, Segrate (MI), Italy
S. Pirani[1], T.P.Å Åkesson, M. Eshraqui, M. Lindroos, ESS, Lund, Sweden
[1]on leave at INFN-LASA, Segrate (MI), Italy
C. Pagani, Università degli Studi di Milano & INFN Milano - LASA, Segrate (MI), Italy

Abstract

During the first vertical test of ESS Medium-Beta large-grain prototype cavity in INFN-LASA, a phenomenon of coexisting two passband-modes was observed: 4/6 π mode was excited spontaneously during the power rise of 3/6 π mode. This phenomenon, probably the first time seeing a passband mode excited from non-accelerating mode, is most likely due to the field-emission electrons that transfer their energy gained from the 3/6 π mode to the 4/6 π mode. In this paper, we present the experimental results, the excitation mechanism and the related simulation results.

INTRODUCTION

As an in-kind contribution to the ESS project, INFN-LASA is in charge of the development and of the industrial production of the whole set of 36 medium-beta (MB) resonators. Two cavity prototypes, with same geometry but different materials, have been realized: one is in Fine Grain (FG) niobium, i.e. the standard technology for SC cavities and the other in Large Grain (LG) niobium.

Among their vertical tests at LASA, the two cold tests of FG cavity prototype, before and after tank welding, respectively, show excellent performance with low field emission (FE) [1].

Also, the LG cavity was cold tested two times and in both cases, it quenched at about 10 MV/m. In the first test, the quench was accompanied by strong field emission and Multipacting measured via x-ray radiation detectors [2, 3]. Moreover, the simultaneous presence of two passband-modes was observed: 4/6 π mode was excited spontaneously during the power rise of 3/6 π mode. After the 1st test, the cavity was treated with an additional flash BCP and a long 24-hour HPR to cure the strong field emission observed [2]. In the 2nd test, the cavity quenched at same field level but with very low field emission, and the phenomenon of passband-mode excitation was not observed anymore.

This passband-mode excitation is most likely due to field-emitted electrons that transfer their energy, gained from the main mode, to the secondary mode. With a similarity to the phenomenon observed in the TESLA cavities in which the 7/9 π mode is excited during the power rise of π mode [4], the passband mode excitation in ESS MB cavity is observed, probably the first time in an elliptical cavity triggered by a non-accelerating mode. Therefore, it is of interest to study the electrons' behaviour and the triggering condition of this passband mode excitation in the ESS MB cavity.

EXPERIMENTAL OBSERVATION

In order to study the location of field emitters, the cavity has been tested in all the other five-passband modes during its first test at cold. During the power rise of 3/6 π mode, another mode with higher frequency but lower transmitted power, -28 dB, was observed on the screen of the spectrum analyzer, as shown in Figure 1. According to the frequencies distribution of the 1st monopole band in ESS MB cavity [5], this mode is confirmed as 4/6 π mode.

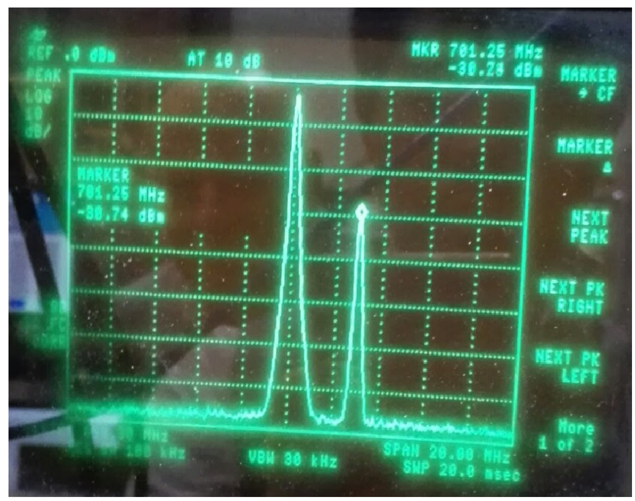

Figure 1: Passband excitation was observed in the 1st test at cold of our ESS MB prototype LG cavity (high peak: 3/6 π mode; low peak: 4/6 π mode).

This phenomenon occurred close to the quench field level in 3/6 π mode, accompanied by strong FE. Figure 2 shows the Q_0 vs E_{acc} result of LG cavity in 3/6 π mode, where the reported accelerating field value is scaled to represent the maximum accelerating field in this mode. According to the test result, the maximum equivalent accelerating field is about 10 MV/m, corresponding to a maximum on-axis field about 20 MV/m. The field relationship of the modes can be calculated by

$$E_2/E_1 = \sqrt{P_2/P_1} \approx 0.04$$

where P_1 and P_2 are transmitted power of 3/6 π mode and 4/6 π mode, respectively, measured by the spectrum in dBm. Given the field of triggering mode and the difference of two transmitted powers, the maximum on axis field of excited mode can be estimated at about 1 MV/m.

†jinfang.chen@mi.infn.it

Content from this work may be used under the terms of the CC BY 3.0 licence (© 2017). Any distribution of this work must maintain attribution to the author(s), title of the work, publisher, and DOI.

ISBN: 978-3-95450-191-5 doi:10.18429/JACoW-SRF2017-TUPB048

Content from this work may be used under the terms of the CC BY 3.0 licence (© 2017). Any distribution of this work must maintain attribution to the author(s), title of the work, publisher, and DOI.

INFN- LASA MEDIUM BETA CAVITY PROTOTYPES FOR ESS LINAC

D. Sertore†, M. Bertucci, A. Bignami, A. Bosotti, J. Chen, P. Michelato, L. Monaco, R. Paparella, INFN Milano - LASA, Segrate (MI), Italy
S. Pirani, ESS, Lund, Sweden and on leave at INFN-LASA, Segrate (MI), Italy
C. Pagani, Università degli Studi di Milano & INFN Milano - LASA, Segrate (MI), Italy

Abstract

INFN-LASA, in the framework of INFN contribution to the European Spallation Source, has developed, produced and tested 704.42 MHz Medium Beta (β = 0.67) cavities. Mode separation and avoidance of HOM excitation by machine line frequencies have driven the cavity design. The production at the industry, also in view of the INFN in-kind contribution of series cavities, has been done "build-to-print" and we have implemented our own quality control process, based on our XFEL experience, from raw material to cavity ready for test. The cavities have been then cold tested in our upgraded Vertical Test Facility. In this paper, we report on our experience on the different phases of the cavity production and test processes.

INTRODUCTION

The Medium Beta (MB) section of the European Spallation Source (ESS) Linac is composed of 36 six-cell elliptical superconducting (SC) cavities (β = 0.67) [1]. As a part to the in-kind contribution of Italy to the ESS project, INFN-LASA is in charge of the development and of the industrial production of the whole set of 36 resonators [2]. Two cavity prototypes, with same geometry but different materials, have been produced in order to verify and optimize all the fabrication and treatment processes for the 36 series Medium beta cavities. One cavity is made by Fine Grain niobium (FG, MB001), i.e. the standard technology for SC cavities and the other is built using Large Grain (LG, MBLG002) niobium. The main motivation to build cavities based on LG niobium is to explore both the physical potential benefit due to higher achievable thermal stability coming from the "phonon peak" in the thermal conductivity and the cost benefit due to lower bare material prices. The Medium beta cavity prototypes have been completely designed by INFN LASA team and built by Ettore Zanon S.p.A, a qualified (XFEL, FRIB, LCLSII, etc.) superconducting cavity vendor in Schio (Italy), under our constant supervision. Indeed, a quality control protocol has been issued to follow every step of the cavity fabrication with tests to be fulfilled and passed before accessing to the successive construction phase. Once the subcomponents were ready and passed the quality controls, they were assembled vertically on a dedicated frame in preparation for the final Electron Beam Welding (EBW) equatorial operation.

After the welding procedure, the cavities underwent the following main production steps:

- Dimensional control and data record with the CMM (Coordinate Measuring Machine), inner and outer visual inspections (surfaces, weld beads).
- Frequency tuning (pre-tuning) before treatments.
- Dimensional control and data record with the CMM machine after pre-tuning.
- Bulk Buffered Chemical Polishing (BCP) (~ 200 µm surface removal), divided in three steps.
- 600° annealing to eliminate material internal stresses and degassing the cavity.
- Final frequency tuning and field flatness correction up to at least 95% of field profile uniformity.
- Dimensional control and data record with the CMM, inner and outer visual inspections (surfaces, weld beads).
- Final (Flash) BCP treatment (~ 20 µm surface removal), 12 h HPR, assembly of accessories and final checks (leak tightness and vacuum quality, RF spectrum).

Between each Bulk BCPs a High Pressure Rinsing (HPR) procedure of two hours was made. This procedure consists in washing the cavity surface with high pressure jets (100 bar) of Ultra Pure Water (UPW) to assure both the full removal of chemicals residuals and the cleanliness of the cavity itself. After the Final BCP and before making the vacuum inside the cavity, the High Q and the pick-up antennas, for the RF cavity vertical tests, were assembled in clean room and a long HPR of 12 hours was made.

Both prototypes (FG and LG cavities) were delivered, under vacuum condition and ready for the test at cold, to LASA within the end of 2016 and they were tested at the LASA Vertical Test Facility. As a consequence of the FG cavity good results, well above the ESS requirements, and in view of its assembly in the prototype ESS Medium Beta section cryomodule (M-ECCTD), in 2017 this cavity was equipped with its He-tank and prepared at the industry for a new cold RF test at LASA. Finally, this second test showed no performance degradation, validating the full integration process.

CAVITY CONSTRUCTION

The MB cavities are fabricated using INFN design and are plug-compatible with CEA design boundary conditions, including helium tank, fundamental coupler, flanges and tuner connections.

From Subcomponents to Cavities

The base cavity components are the Half Cells with three different geometries, labelled respectively as Inner Cell (IC), Pen Cell (PC) and End Cell (EC). HCs are used to produce the Dumb Bells (Inner Dumbbell (ID) and two terminal Dumb Bells respectively PD and CD and the End Groups (EGT and EGC). Main quality control steps for

† daniele.sertore@mi.infn.it

ISBN: 978-3-95450-191-5 doi:10.18429/JACoW-SRF2017-TUPB049

DESIGN STUDY ON THE SUPERCONDUCTING HWR FOR SECONDARY PARTICLE GENERATION AT KOMAC*

Han-Sung Kim†, Hyeok-Jung Kwon, Seung-Hyun Lee, Jeong-Jeung Dang, Hae-Seong Jeong, Yong-Sub Cho, Korea Multi-purpose Accelerator Complex of KAERI, Gyeongju, Korea

Abstract

A 100-MeV proton linac has been operated since 2013 at KOMAC (Korea Multi-purpose Accelerator Complex) and provides the accelerated proton beam to various users from the research institutes, universities and industries. To expand the utilization fields of the accelerator, we have a plan to develop a secondary particle utilization facility including a pulsed neutron source and radio-isotope beam based on the 100-MeV linac. According to the preliminary analysis, the neutron yields can be increased by about 2.5 times if the incident proton beam energy increases from 100 MeV to 160 MeV. Therefore, we carried out design study on the SRF linac based on half-wave resonator to increase the proton beam energy. Baseline design parameters include 350 MHz operating frequency, 2 K operation temperature, and peak electric field and magnetic field less than 35 MV/m and 70 mT, respectively. The available space at existing accelerator tunnel was also taken into consideration. Details on the design study on the SRF linac based on HWR cavity for the secondary particle utilization facility at KOMAC will be given in this presentation.

INTRODUCTION

A 100-MeV proton linac at KOMAC is being used for various application fields including bio/medical research, material test, basic science and space technology [1]. The utilization of the l00-MeV linac, however, is limited mainly to the direct proton beam irradiation on various specimen. It is well-known that energetic proton beam on target can be used to generate secondary particles.

Secondary particle utilization facility based on 100-MeV proton linac is under consideration at KOMAC. Currently, a pulsed neutron for neutron science and application and Li-8 beam for beta-NMR application are good candidates for such facility as shown in Fig. 1.

In addition, slight energy upgrade from 100 MeV can improve the yield of the secondary particle generation greatly. For example, pulsed neutron yield is more than doubled if the proton beam energy is increased to 160 MeV. The technology of choice for beam energy upgrade is SRF (Superconducting Radio-Frequency). The existing accelerator tunnel has room for linac extension up to roughly 180 MeV based on 350 MHz superconducting accelerator.

Several types of SRF cavity structure are currently used for acceleration of the low-beta proton beam such as quarter-wave resonator (QWR), half-wave resonator (HWR), spoke cavity, and so on. For example, two-gap spoke structure is chosen as a baseline design for European Spallation Source (ESS). Though spoke structure has some advantages over HWR and intensive study has been given to that structure, there is no operating accelerator based on spoke structure mainly due to its technological difficulty. In this study, we chose HWR structure as shown in Fig. 2 and performed preliminary design study on the HWR suitable for accelerating proton beam from 100 MeV to 180 MeV. Once the proton energy is increased up to about 180 MeV, a well-developed elliptical structures can be used thereafter.

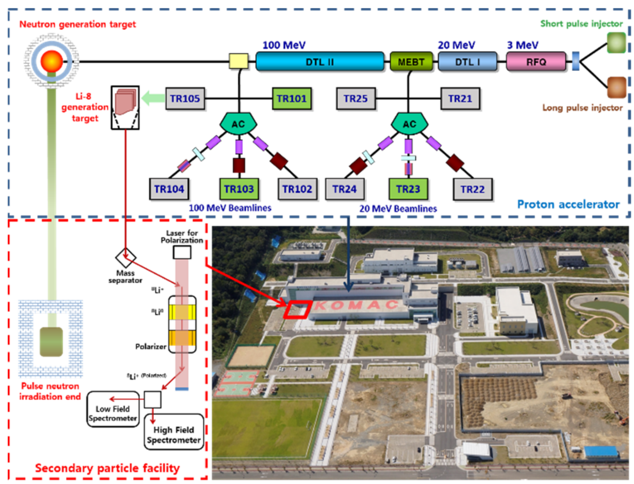

Figure 1: Layout of secondary particle facility.

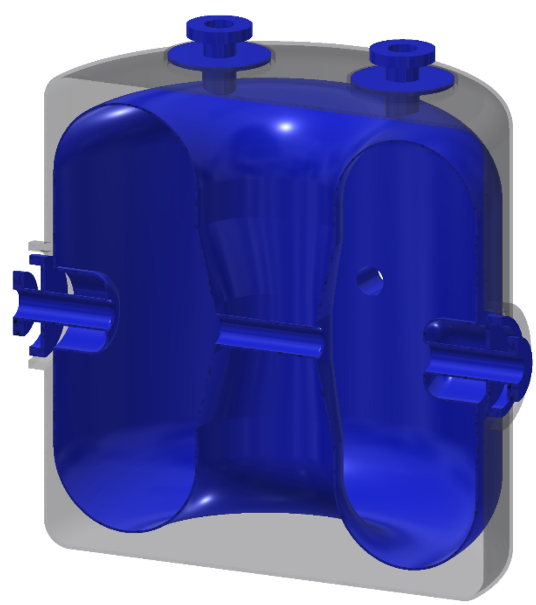

Figure 2: 350 MHz Superconducting half wave resonator for KOMAC proton linac.

* Work supported by KOMAC operation fund of KAERI by MSIP
† kimhs@kaeri.re.kr

Content from this work may be used under the terms of the CC BY 3.0 licence (© 2017). Any distribution of this work must maintain attribution to the author(s), title of the work, publisher, and DOI.

ISBN: 978-3-95450-191-5 doi:10.18429/JACoW-SRF2017-TUPB052

HIGHER ORDER MODES DAMPING IN 9-CELL SUPERCONDUCTING CAVITY WITH GROOVED BEAM PIPE*

A. M. Bulygin, R. Donetskiy, Ya.V. Shashkov
National Research Nuclear University MEPhI (Moscow Engineering Physics Institute), Moscow, Russia

Abstract

This paper is focused on higher order modes (HOM) damping efficiency analysis in 9-cell superconducting cavities with HOM couplers and with grooved beam pipe. Comparison of two methods of HOM damping is presented. In order to increase efficiency of damping of trapped modes the end cells of the structure were modified.

HIGHER ORDER MODES

A large number of modes in a broad frequency range are induced by the beam passing through the structure [1]. The on-axis movement of the bunch leads to the appearance of monopole modes, off-axis bunch also excites multipole HOM (dipole, quadrupole, etc).

HOM leads to a number of negative factors: energy losses, beam deflection from axis, additional heat load on cryogenics, beam break up etc.

Electrodynamic characteristics (EDC), such as external Q-factor (Q_{ext}) and shunt impedance R_{sh} are used to evaluate the HOMs impact on bunch. Transverse shunt impedance to the Q-factor ratio can be calculated either through Panofsky-Wenzel theorem:

$$\frac{R_{sh\perp}}{Q} = \frac{\left|\int_0^l \frac{1}{k_z}\frac{\partial E_z}{\partial r} e^{ik_z z} dz\right|^2}{\omega W} \quad (1)$$

where W-stored energy, k_z-wave number; or using direct integration of transverse magnetic H and electric fields:

$$\frac{R_{sh\perp}}{Q} = \frac{\left|\int_0^l \left(i \cdot c \cdot \mu_0 \cdot H_\perp(z) + E_\perp(z)\right) e^{ik_z z} dz\right|^2}{\omega W} \quad (2)$$

For axially symmetric structures longitudinal field derivative in (1) can be replaced by the difference, and given that the longitudinal field dipole waves on the structure axis are zero, the resulting expression will look like this:

$$\frac{R_{sh\perp}}{Q} = \frac{\left|\int_0^l \frac{1}{k_z}\frac{E_Z(r = l)(z)}{\Delta r} e^{ik_z z} dz\right|^2}{\omega W} \quad (3)$$

In order to decrease their influence on the travelling bunch it is necessary to decrease the HOM Q-factor values. The most common method for HOM damping in accelerating structure involves the coaxial couplers which extracts HOM power to the external load. Despite the fact that couplers provide a reasonable HOM damping they are often of complicated design and could be subject to multipacting discharge. Their presence also leads to break of accelerating structure axial symmetry. Kick momentum to the beam could be crucial for electron linear colliders, energy recovery linacs and particle accelerators with high beam current.

The resent progress allows applying complex geometries of superconducting cavities to minimize the effect of the HOMs [1-3]. Despite the very low achieved Q-values of HOM their complex geometry can increase the cost of cavity production. Several modifications of simple structure with grooved beam pipe were investigated in order to achieve the lowest values of HOM Q-factor.

9-CELL CAVITIES WITH CYLLINDRICAL BEAM PIPES

In order to increase the HOM damping efficiency of trapped modes in [4] the different radiuses of end cells were used (Fig. 1(a)). This allowed increasing beam's energy to 80-100 MeV. For the 9-cell cavity with cylindrical beam pipes the field distribution for operational mode at 1300 MHz was flattened by the modification of the end-cells (Fig. 1(b)).

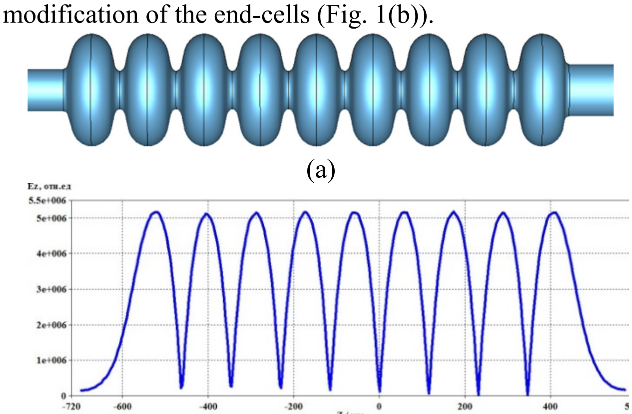

Figure 1: (a) Model of 9-cell cavity with cylindrical beam pipes and (b) electric field distribution for operational mode.

HOM EDCs were calculated for the 9-cell cavity with cylindrical beam pipes in frequency range up to 3 GHz. Dispersion curves (Fig. 2) helped to determine the most dangerous HOMs.

The monopole mode TM_{011}, dipole modes TE_{111}, TM_{110} and quadrupole modes TE_{211} and TM_{210} (Fig. 3) are of the most concern for this structure. The EH_{111} mode is the most "dangerous", because its frequency (2576 MHz) is nearly the double accelerating frequency (1300 MHz). It means that EH_{111} can greatly impact on beam.

* This project is supported in part by the MEPhI 5/100 Program of the Russian Academic Excellence Project

Content from this work may be used under the terms of the CC BY 3.0 licence (© 2017). Any distribution of this work must maintain attribution to the author(s), title of the work, publisher, and DOI.

ISBN: 978-3-95450-191-5 doi:10.18429/JACoW-SRF2017-TUPB053

Content from this work may be used under the terms of the CC BY 3.0 licence (© 2017). Any distribution of this work must maintain attribution to the author(s), title of the work, publisher, and DOI.

LESSONS LEARNED FROM RF-DIPOLE PROTOTYPE CAVITIES FOR LHC HIGH LUMINOSITY UPGRADE*

S. U. De Silva[1#], H. Park[2], J. R. Delayen[1], Z. Li[3]
[1]Old Dominion University, Norfolk, VA 23529, USA
[2]Thomas Jefferson National Accelerator Facility, Newport News, VA 23606, USA
[3]Stanford Linear Accelerator National Laboratory, Menlo Park, CA 94025, USA

Abstract

The rf-dipole cavity has successfully demonstrated the principles of using a compact cavity operating in TE_{11}-like mode in generating a transverse kick. Several proof-of-principle rf-dipole cavities have been fabricated and the rf tests have demonstrated high transverse gradients. The rf-dipole geometry has been adapted into a square-shaped geometry designed to meet the dimensional constraints for the LHC also maintaining crabbing in both horizontal and vertical planes. Recently, two prototype rf-dipole cavities intended for the test at SPS for have been completed that is designed to accommodate the FPC and HOM dampers. The performance during the rf tests have shown excellent results on achieving the design requirements of operation for the crab cavities for SPS. This paper presents the experiences and lessons learned during the cavity preparation and testing, including process validation, frequency tracking.

INTRODUCTION

A prototype rf-dipole cavity have been designed for the LHC High Luminosity Upgrade [1] to crab the proton beam in horizontal plane. Set of two crabbing cavities will be installed in a single cryomodule to be tested in SPS prior to installation in LHC. Two prototype cavities of SPS-style have been completed successfully with the performance of the bare cavity cryogenic tests exceeding design specifications [2]. The fully fabricated cavity is shown in Fig. 1. The rf tests of both the cavities have achieved transverse kicks of 4.4 MV and 5.8 MV well above the design requirement of 3.4 MV. The corresponding intrinsic quality factors at nominal voltage of 3.4 MV are 8.5×10^{9} and 1.2×10^{10} that corresponds to power dissipations of 3.2 W and 2.3 W respectively.

Figure 1: 400 MHz prototype rf-dipole cavity.

*Work supported by DOE via US LARP Program and by the High Luminosity LHC Project. Work was also supported by DOE Contract No. DE-AC02-76SF00515
#sdesilva@jlab.org

CAVITY FABRICATION

The two cavities were fabricated by Niowave Inc. under DOE SBIR/STTR program and completed at Jefferson Lab under US LARP. The cavity center body and end plates were formed with 4 mm high RRR Nb sheets. The FPC, HHOM, VHOM and beam pipes were formed with 3 mm Nb sheets. The stamped parts are shown in Fig. 2. The formed parts are welded in to 3 sub-assemblies consisting of center body, end group with FPC and HHOM couplers and end group with VHOM coupler and pick up port as shown in Fig. 3.

Figure 2: Formed parts of the two rf-dipole cavities.

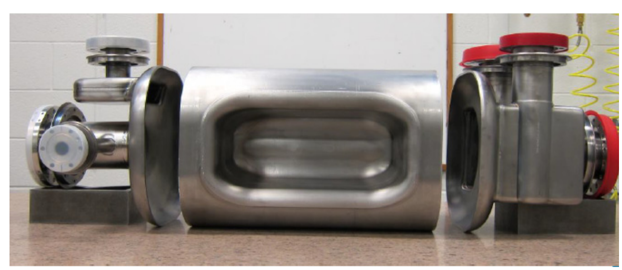

Figure 3: Sub-assemblies of the rf-dipole cavity.

The 3 sub-assemblies of both the cavities were thoroughly investigated for any pits or protrusions on the inner surface. All the uneven welds were grinded as shown in Fig. 4 especially near the poles where peak magnetic field is high.

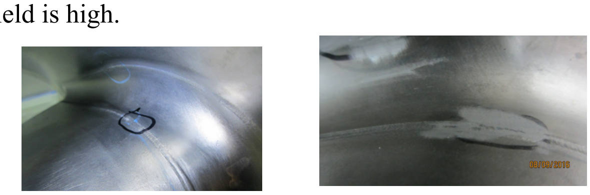

Figure 4: Surface polishing of the rf-dipole cavity.

ISBN: 978-3-95450-191-5 doi:10.18429/JACoW-SRF2017-TUPB054

RF TESTS OF RF-DIPOLE PROTOTYPE CRABBING CAVITIES FOR LHC HIGH LUMINOSITY UPGRADE*

S. U. De Silva[1, †], H. Park[2], J. R. Delayen[1], Z. Li[3]
[1]Old Dominion University, Norfolk, VA, USA
[2]Thomas Jefferson National Accelerator Facility, Newport News, VA 23606, USA
[3]Stanford Linear Accelerator National Laboratory, Menlo Park, CA 94025, USA

Abstract

The superconducting rf-dipole crabbing cavity is one of the two crabbing cavity designs proposed for the LHC high luminosity upgrade. The proof-of-principle (P-o-P) rf-dipole cavity operating at 400 MHz has demonstrated performance exceeding the design specifications. The prototype cavity for SPS beam test has been designed to include the fundamental power coupler, HOM couplers, and all the ancillary components intended to meet the design requirements. The crab cavities will be installed in the SPS beam line prior to the installation in LHC; this will be the first crabbing cavity operation on a proton beam. The fabrication of two prototype rf-dipole cavities is currently being completed at Jefferson Lab. This paper presents the details on cavity processing and cryogenic test results of the rf-dipole cavities.

INTRODUCTION

The LHC High Luminosity Upgrade consists of an upgrade in the magnet system and installation of crabbing cavities in the LHC ring [1]. The crabbing cavities allow the head-on collision of bunches at the interaction point, hence increasing the luminosity up to 5×10^{34} cm^{-2}s^{-1} with an integrated luminosity of 250 fb^{-1} per year. Crabbing systems will be installed at both ATLAS and CMS interaction points. These crabbing cavities also reduce the pile up of colliding bunches at the interaction point. Each crabbing system includes eight crabbing cavities per interaction point and bunches are crabbed in vertical plane at ATLAS and in horizontal plane at CMS. The vertical crabbing of bunches will be carried out by the double quarter wave cavity and rf-dipole cavities will crab bunches in the horizontal plane.

Two prototype cavities of each type were fabricated by Niowave Inc. and completed at Jefferson Lab under US-LARP. The full prototype rf-dipole cavity design is shown in Fig. 1.

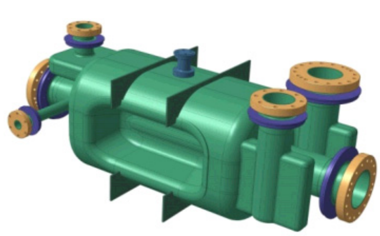

Figure 1: 400 MHz prototype rf-dipole cavity.

*Work supported by DOE via US LARP Program and by the High Luminosity LHC Project. Work was also supported by DOE Contract No. DE-AC02-76SF00515
†sdesilva@jlab.org

RF-DIPOLE DESIGN

The rf-dipole cavity has been designed to operate in a TE_{11}-like mode where the primary contribution to the kick is given by the transverse electric field [2]. A square shaped design in adapted in the prototype design to meet the dimensional constraints [3]. The rf properties of both P-o-P and prototype cavities are listed in Table 1.

Table 1: RF Properties of Cylindrical Shaped P-o-P and Square Shaped Prototype RF-dipole Cavities

Parameter	P-o-P Cavity	Prototype Cavity	Units
Nearest HOM	590	633.5	MHz
Peak electric field (E_p*)	4.02	3.6	MV/m
Peak magnetic field (B_p*)	7.06	6.2	mT
Geometrical factor	120	107	Ω
$[R/Q]_t$	287	430	Ω
$R_t R_s$	3.4×10^4	4.6×10^4	Ω^2
At E_t* = 1 MV/m			
V_t	3.4		MV
E_p	36.5	33	MV/m
B_p	64	56	mT

The prototype cavity will operate at peak fields of 33 MV/m and 56 mT at nominal operating voltage of 3.4 MV.

MULTIPACTING ANALYSIS

The multipacting analysis of the bare cavity was completed using the Track3P code from SLAC ACE3P suite [4]. The bare cavity doesn't include any FPC or HOM couplers.

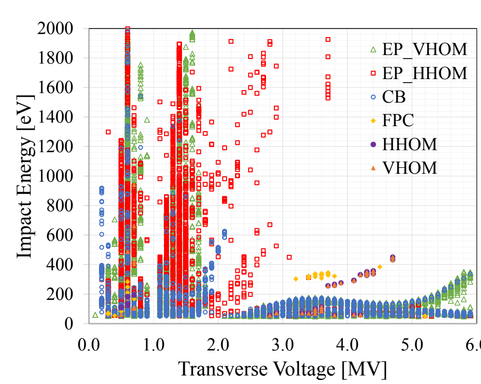

Figure 2: Impact energy of resonant particles as a function of transverse voltage.

Content from this work may be used under the terms of the CC BY 3.0 licence (© 2017). Any distribution of this work must maintain attribution to the author(s), title of the work, publisher, and DOI.

ISBN: 978-3-95450-191-5 doi:10.18429/JACoW-SRF2017-TUPB055

Nb_3Sn THIN FILM DEPOSITION ON COPPER BY DC MAGNETRON SPUTTERING*

Weiwei Tan†, Xiangyang Lu, Datao Xie, Li Xiao, Ziqin Yang, Jifei Zhao, Deyu Yang, Yujia Yang, Boting Li, Peking University, Beijing, China

Abstract

Nb_3Sn for SRF cavities has been coated on copper samples by DC magnetron Sputtering. Pure Nb and Sn target were installed separately in the magnetron sputtering device. Nb_3Sn precursor was coated on copper in the Ar atmosphere of 0.5 Pa. The Nb_3Sn precursor was annealed in the vacuum furnace whose pressure is 10^{-4} Pa. The XRD results demonstrate the exist of Nb_3Sn crystal, and MPMS results show superconductivity of Nb_3Sn. The highest critical temperature obtained is 15 K.

INTRODUCTION

Nb_3Sn is a promising alternative SRF material to bulk niobium. Its highest critical temperature reported is 18.3 K [1] and superheating field is 400 mT [2]. These two features are beneficial to SRF accelerator, including the high Q_0 of cavities, higher theoretical maximal accelerating field, comparing with bulk niobium cavity.

Copper cavities has several advantages, including better thermal stability (resistance to "quench") owing to the much higher thermal conductivity of OFE copper substrate and reduced material cost [3]. All of these advantage is compared with bulk niobium cavity.

Some researchers have demonstrated the feasibility of coating Nb_3Sn by magnetron sputtering. Rossi [4] deposited multiplayer Nb_3Sn on niobium samples and cavities by UHV magnetron sputtering technique. Rosaz [5] condensed Nb_3Sn film on copper sample by using a stoichiometric Nb-Sn target. Guitron [6] deposited Nb_3Sn films on sapphire, whose SRF properties has been characterized by SIC system.

To take advantage of the merits of Nb_3Sn and copper, Nb_3Sn thin film deposition on copper by dc magnetron sputtering is conducted in Peking University. Separated Nb and Sn target is used in magnetron sputtering device.

EXPERIMENT DETAILS

The Nb_3Sn films on copper coating is carried out on a DC magnetron sputtering device, which is shown in Fig. 1. Nb target and Sn target were installed in the vacuum chamber. The RRR of Niobium is above 300. The purity of Sn target is 99.99%. The sample holder is placed between two target. The chamber base pressure is 5×10^{-4} Pa. As the sample holder rotate, the Nb particle and Sn particle condense on the OFE copper substrate.

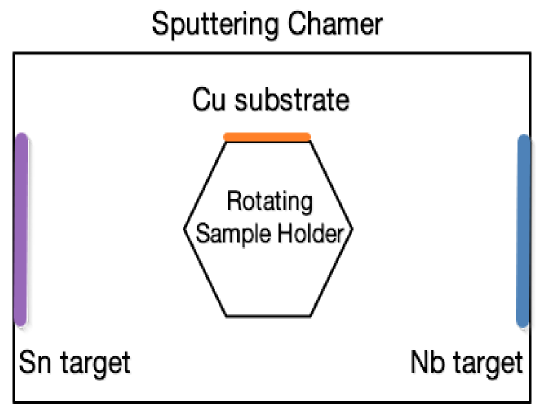

Figure 1: schematic picture of sputtering chamber. The Sn and Nb target were placed separately and Cu substrate is rotating.

The size of OFE Copper substrate is 25 mm ×50 mm. After mechanical polishing with 300# 600#, 1200#, 2000# sandpaper, chemical polishing is used. The polishing agent is SUBU solution [7] and working temperature is 72 °C. The SUBU is preceded for 30 minutes and followed by 10 minutes passivation with a dilute solution of sulfamic acid [8]. After mechanical and chemical polishing, the copper substrate is cleaned in ultrapure water by ultrasonic cleaning. The polished copper substrate is shown in Fig.2.

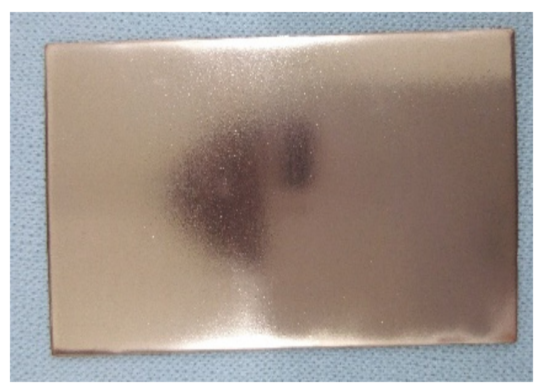

Figure 2: the copper substrate polished by SUBU solution.

The parameters of coating procedure are listed in Table 1. Isolating layer over the copper in used to avoid the reaction between Sn and Cu. In order to reduce contamination of other elements, the element Nb is chosen for isolating layer. After 6 min coating of isolating layer, the power of tin target is turn on and the sample begin to rotate. About 1 um Nb_3Sn precursor film on copper is obtained after the 240 min coating of mixing layer including Nb and Sn element. Sputtering process gas is Ar and the pressure maintains 0.5 Pa. The bias voltage added in copper substrate maintains -100 V.

* This work has been supported by Major Research Plan of National Natural Science Foundation of China (No. 91026001) and National Major Scientific Instrument and Equipment Development projects (2011YQ130018).
† email address: tanweiwei@pku.edu.cn

Content from this work may be used under the terms of the CC BY 3.0 licence (© 2017). Any distribution of this work must maintain attribution to the author(s), title of the work, publisher, and DOI.

ISBN: 978-3-95450-191-5 doi:10.18429/JACoW-SRF2017-TUPB056

STUDY ON A LOW BETA HIGH CURRENT TAPER TYPE SUPERCONDUCTING HALF WAVE RESONATOR FOR BISOL*

Feng Zhu#, Hutianxiang Zhong, Shengwen Quan, Fang Wang, Liwen Feng, Meng Chen
Institute of Heavy Ion Physics & State Key Laboratory of Nuclear Physics and Technology, Peking University, Beijing, 100871, China

Abstract

Beijing Isotope-Separation-On-Line Neutron-rich Beam Facility (BISOL) for both basic science and applications is a project proposed by China Institute of Atomic Energy and Peking University. Deuteron driver accelerator of BISOL would adopt superconducting half wave resonator (HWR) with low beta and high current. For pre-research of BISOL, a β=0.09 162.5 MHz taper type HWR cavity has been designed for accelerating deuteron beam with several tens of mA. The Design, fabrication, post-processing and room temperature RF measurement of the HWR cavity are presented here.

INTRODUCTION

Many projects based on high current proton and deuteron linear accelerators have been proposed to better support various fields of science. Beijing Isotope-Separation-On-Line Neutron-rich Beam Facility (BISOL) was recently proposed by the union of Peking University (PKU) and China Institute of Atomic Energy (CIAE) [1]. A high current deuteron accelerator is one of two drivers for BISOL. It can also run as an intense neutron beam source. High current deuteron beams will be accelerated by a RF superconducting (SRF) linear accelerator after RFQ to 40 MeV. The deuteron accelerator adopts half wave resonator (HWR) as the SRF accelerating structure because of its good properties. A β=0.09 162.5 MHz HWR cavity has been designed to accelerate several tens of mA deuteron beam after RFQ. We will present the details of design fabrication, post-processing and RF measurement of the β=0.09 HWR cavity in this paper.

DESIGN

Compared to the cylindrical or squeezed HWR cavity, taper type HWR cavity which has conical inner and outer conductors has better mechanical properties, much higher shunt impedance r/Q and lower surface fields [2]. Compared to the race-track shaped center conductor, the ring-shaped "Donut" center conductor has much lower peak magnetic field and thus higher accelerating gradient and much higher shunt impedance meaning same energy gain less power [3]. With this "Donut" shape, there is better symmetric field in radial direction along the beam pipe and can eliminate the quadrupole effect to the beam. In order to accelerate several tens of mA deuteron beams, the HWR cavity has a larger beam pipe diameter of 40 mm. The electromagnetic design was done by CST code [5]. Figure 1 shows the β=0.09 162.5 MHz HWR cavity.

*Work supported by National Basic Research Project (No. 2014CB845504)
#zhufeng7726@pku.edu.cn

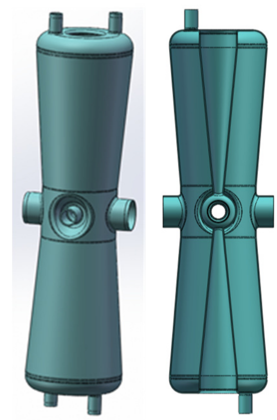

Figure 1: The 162.5 MHz, high current β=0.09 HWR cavity designed by Peking University.

CST particle tracking mode is used to simulate multipacting (MP) in this low β HWR cavity. The simulation result gives that MP in the HWR cavity mainly locates at the dome of the short plate, which is two-point first order MP. Figure 2 shows the MP intensity comparison between the cavity HWR1 with round short plate and cavity HWR2 which has flat short plate with r1 = 5 mm and r2 =35 mm. HWR1 might have strong MP when the accelerating gradient is between 3~8 MV/m. We changed the blending radii of the short plate with the inner and outer conductors and made the short plate flatter to suppress MP. The shape of the short plate is shown in Fig. 3. Simulation results give that smaller r1 and larger r2 has better effect on suppressing MP. When r1 = 5 mm and r2 =35 mm, MP growth rate is less than one in a very big gradient range. The MP intensity is quite low when the gradient is higher than 4 MV/m, which is safe for the cavity operation. Calculation from CST shows that the RF parameters are similar for the two HWR cavities.

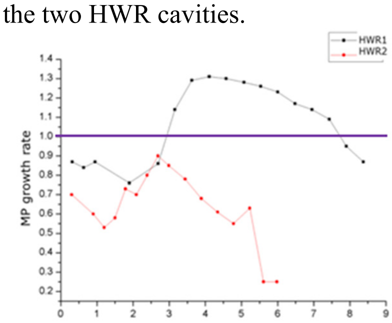

Figure 2: MP intensity v.s. gradient for two different HWR cavities (HWR1 and HWR2).

Content from this work may be used under the terms of the CC BY 3.0 licence (© 2017). Any distribution of this work must maintain attribution to the author(s), title of the work, publisher, and DOI.

ISBN: 978-3-95450-191-5 doi:10.18429/JACoW-SRF2017-TUPB060

Content from this work may be used under the terms of the CC BY 3.0 licence (© 2017). Any distribution of this work must maintain attribution to the author(s), title of the work, publisher, and DOI.

INNOVATIVE CRYOGENIC TEST FACILITY FOR TESTING SRF CAVITY SERIES PRODUCTION

L. Bizel-Bizellot†, M. Ellis, S. Pattalwar, M. Pendleton, P. Smith, A. Wheelhouse, STFC, Daresbury, United-Kingdom

Abstract

Testing SRF cavities in a vertical cryostat is the first step in qualifying the performance of SRF cavities before being integrated into a cryo-module. The European Spallation Source (ESS) requires 84 + 4 high-beta 5 cells, 704 MHz cavities (HβC) which will be manufactured and qualified for their RF performance in a vertical cryostat at Science and Technology Facility Council (STFC) Daresbury Laboratory (DL) in the United-Kingdom. Taking a conventional approach each vertical test would require a large cryostat demanding more than 8500 litres of liquid helium for testing 3 cavities simultaneously. In order to reduce the overall operating time / cost, an alternative method has been developed to divide the liquid helium consumption by 5 by filling liquid helium only in each individual helium vessels enclosing each cavity placed horizontally in the cryostat (see Table 1).

Therefore the test is performed in more realistic conditions such as in a cryo-module and reduces the operating time / cost. This also reduces the mass flow-rate to be handled by a factor of 10, leading to 2 g/s, thus reducing the size of the associated components such as the 2 K pumps, safety devices, valves and transfer lines.

INTRODUCTION

This paper presents all cryogenic aspects of the new test facility at STFC DL for testing the high-beta SRF cavity production for the ESS [1] accelerator. The test facility shows some peculiarities regarding the conventional way to perform SRF tests. First, the cryostat tests cavities with their jacket (their helium tank). This allows a significant reduction of the helium consumption in comparison to a big bath of LHe where cavities are soaked. The second main difference compared to other large-scale facilities is the orientation in which the cryostat holds cavities: horizontally. This enables the configuration to be close as possible to the final assembly in the cryo-module. Therefore, the main topic presented in this contribution is the cryogenic process, and the different modes of the facility operation. At the end, test rate estimation for the production is given. Figure 1 presents a schematic of the overall facility with a focus on the cryogenics systems.

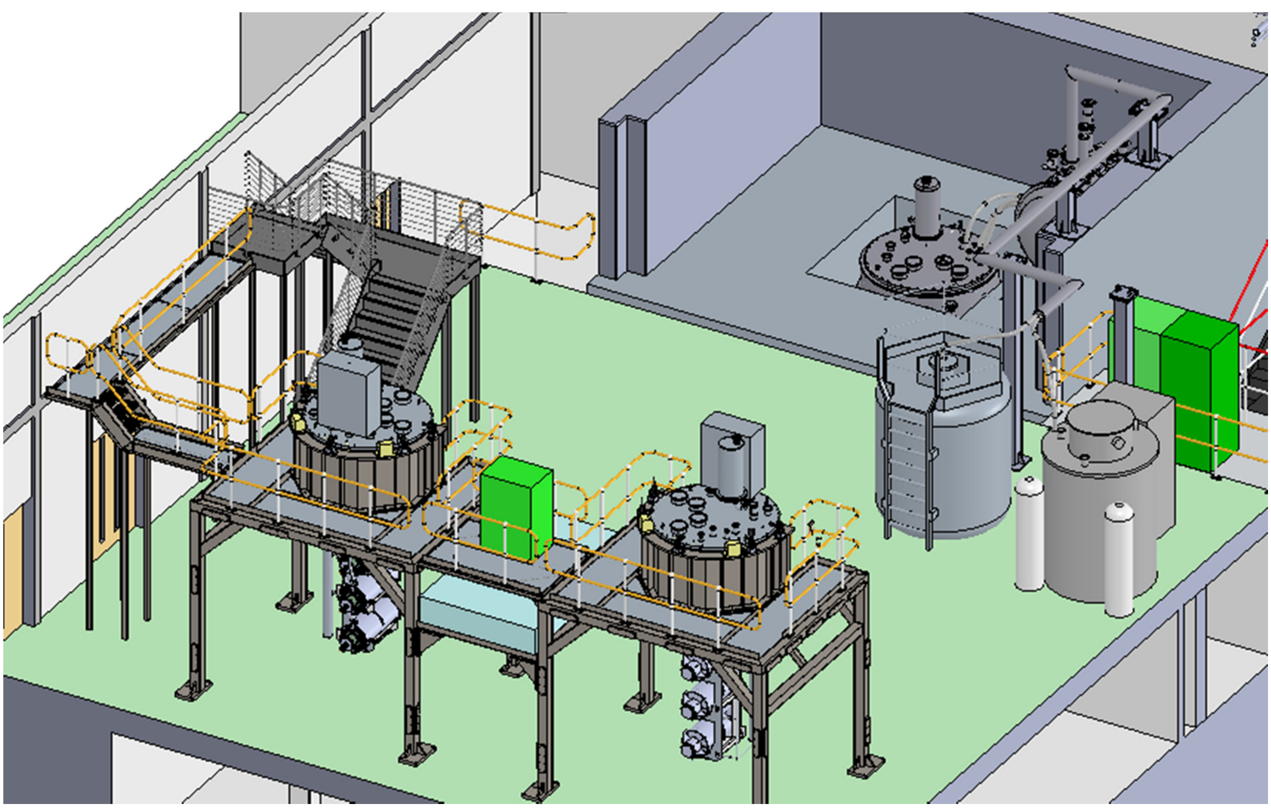

Figure 1: Overall Daresbury test facility CAD view.

† louis.bizel-bizellot@stfc.ac.uk

ISBN: 978-3-95450-191-5 doi:10.18429/JACoW-SRF2017-TUPB063

FABRICATION OF A SRF DEFLECTING CAVITY FOR THE ARIEL -LINAC

Douglas W. Storey[†,1,2], Robert E. Laxdal[2], Ben Matheson[2], Norman Muller[2]
[1]University of Victoria, Victoria, Canada
[2]TRIUMF, Vancouver, Canada

Abstract

A superconducting RF deflecting cavity has been designed and is being fabricated at TRIUMF to allow simultaneous beam delivery to both rare isotope production and an energy recovery linac. The 650 MHz cavity will operate in a TE-like mode in CW. The design has been optimised for high shunt impedance and minimal longitudinal footprint, reaching roughly 50% higher shunt impedance with 50% less length than comparable non-TM mode cavity geometries. Due to low power dissipation at 4K at the maximum required deflecting voltage of 0.6 MV, low cost manufacturing techniques have been employed in the construction of the cavity. These include the use of reactor grade Niobium and TIG welding in an inert atmosphere. Development of the manufacturing processes will be presented along with the status of fabrication.

INTRODUCTION

The ARIEL electron linac (e-Linac) is a 0.3 MW continuous wave (CW) accelerator, extensible to 0.5 MW. It will provide up to 10 mA of 30-50 MeV electron beam to TRIUMF's new ARIEL facility to drive the production of rare isotopes [1]. Acceleration is provided by three to five nine-cell TESLA style 1.3 GHz SRF cavities, each providing 10 MV/m accelerating gradient. An upgrade path is planned that would add a recirculation loop to the e-Linac that would allow the electron beam to make a second pass through the accelerating cavities. This could be operated either as a recirculating linac – doubling the electron energy through a second accelerating pass, or as an Energy Recovery Linac (ERL) – decelerating the electrons on the second pass. Operation in ERL mode would provide beam to an infrared or THz band Free Electron Laser in the back leg of the loop.

Rare isotope production is performed using the CW beam with 650 MHz bunch spacing, populating every second RF bucket of the 1.3 GHz accelerating fields. This allows for simultaneous operation of the ERL/FEL by populating the in-between buckets with bunches bound for the ERL loop. RF separation of the bunches is then required after the first pass of the accelerating cavities to direct the bunches bound for either ARIEL or the ERL down the appropriate beamline.

A 650 MHz deflecting mode cavity has been designed to provide opposite transverse momentum to adjacent bunches to initiate their separation. To achieve the required deflection of several mrad, the nominal deflecting voltage of the cavity is 0.3 MV, with up to 0.6 MV being considered. The design of the cavity is based off the RF Dipole geometry developed for the LHC Hi-Lumi upgrade crab cavities [2]. The geometry was optimized for higher shunt impedance, resulting in a so-called "Post-and-Ridge" geometry (Fig. 1), where undercuts to the ridge decrease the on-axis magnetic field component which opposes the deflection imparted by the electric field. This change increases the peak electric and magnetic fields from the RF Dipole design. This however is not a concern in this application as relatively low deflecting voltages are required. The RF performance parameters are listed in Table 1.

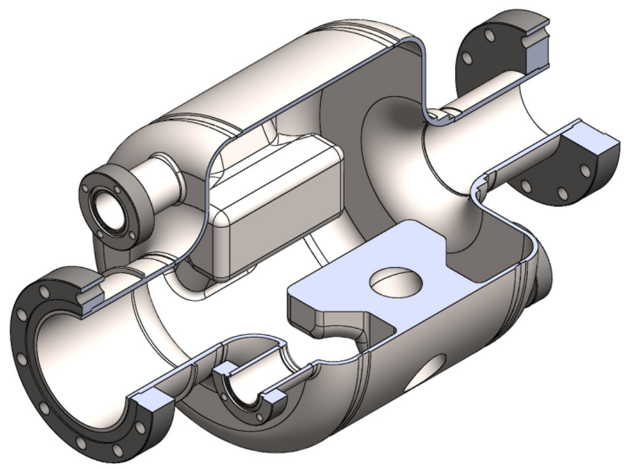

Figure 1: The cavity geometry showing the modified ridge shape. The "undercuts" allow the magnetic field to circulate around the ridges, decreasing the on axis magnetic field component.

Table 1: Cavity Performance Parameters

Parameter	Value	Unit
Resonant frequency	650	MHz
Inner Diameter	204	mm
Inner Length	175	mm
Aperture	50	mm
Deflecting voltage	0.3 – 0.6	MV
Shunt impedance, $R_{\perp}/Q$	625	Ω
Geometry Factor	99	Ω
Peak electric field	9.5 – 19	MV/m
Peak magnetic field	12 – 24	mT
RF power dissipation at 4.2 K	0.35 – 1.4	W

The resulting cavity design provides the required deflecting voltage within a compact cavity with high shunt impedance and low RF power dissipation. The cavity will operate at 4.2 K, simplifying the cryomodule design and making use of the liquid helium services supplying the e-Linac accelerating cavities. Additionally, due to the low fields on the cavity walls, non-standard fabrication

† dstorey@triumf.ca

Content from this work may be used under the terms of the CC BY 3.0 licence (© 2017). Any distribution of this work must maintain attribution to the author(s), title of the work, publisher, and DOI.

ISBN: 978-3-95450-191-5 doi:10.18429/JACoW-SRF2017-TUPB064

OPERATING EXPERIENCE ON CAVITY PERFORMANCE OF ISAC-II SUPERCONDUCTING HEAVY ION LINAC

Z. Yao†, T. Junginger, A.N. Koveshnikov, R. E. Laxdal, Y. Ma, D.W. Storey, E. Thoeng, B. S. Waraich, V. Zvyagintsev, TRIUMF, Vancouver, Canada

Abstract

ISAC-II is a superconducting heavy ion linac with 40 quarter wave resonators (QWRs) as an extension of ISAC facility for ISOL based on radioactive ion beam production and acceleration. Phase-I with twenty 106 MHz cavities has been operating since 2006. The design spec was achieved with the completion of Phase-II with another twenty 141 MHz cavities in 2010. The cavity performance statistics and operating experience have been accumulated over years. This paper will summarize the operating experience on cavity performance of ISAC-II.

INTRODUCTION

SRF at TRIUMF began in 2000 with cavity and infrastructure development in support of the ISAC-II heavy ion linac as an extension of ISAC facility for ISOL based on radioactive ion beam production and acceleration. The specification of ISAC-II is to accelerate heavy ions to and above the Coulomb barrier, specifically the goal is to reach an energy of E > 6.5 MeV/u for A/q = 6. This is equivalent to a minimum effective accelerating voltage of 30 MV [1]. In 2006 Phase-I with acceleration voltage of 20 MV was commissioned for operation [2]. Phase-II upgrade was completed in 2010 with achievement of additional 20 MV of acceleration voltage [3]. ISAC became a leading ISOL facility supporting a full physics program with both stable and radioactive beams being delivered.

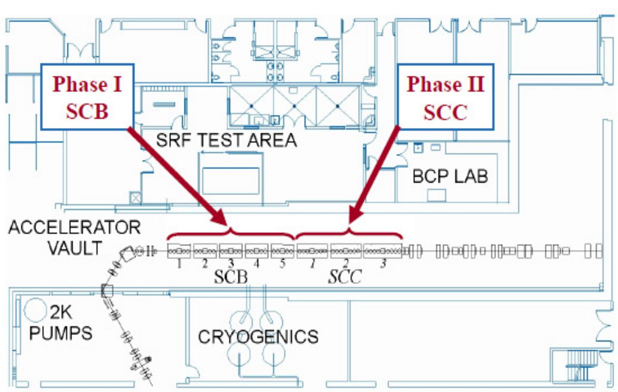

Figure 1: Layout of ISAC-II linac and SRF infrastructure.

The Phase-I (SCB) consists of twenty 106 MHz QWRs housed in five cryomodules with four cavities per cryomodule. The first eight cavities have a geometric beta of 0.057 and the remainder a geometric beta of 0.071. The Phase-II (SCC) also consists of twenty QWRs housed in three cryomodules, six cavities in each module for SCC1 and SCC2 and eight cavities in SCC3. These bulk niobium cavities have a geometric beta of 0.110 and are resonating at 141 MHz. Both Phase-I and Phase-II cryomodules have one 9 T superconducting solenoid symmetrically placed in the cryomodule. The layout of ISAC-II linac is shown in Fig. 1.

ISAC-II CAVITIES

The ISAC-II cavities are QWRs, shown in Fig. 2, patterned after structures built for the low beta section of the INFN-Legnaro heavy ion linac. The cavities have a simple construction with a cylindrical shape, a rigid upper flange and an annular lower flange designed for mounting a removable tuning plate. The helium jacket is a cylinder of reactor grade niobium formed from two sheets and welded to the upper and lower flanges. A common outer conductor diameter of 180 mm is used for all cavities. The chief difference between the Phase-I and Phase-II cavities besides the frequency (and therefore the height) is that in Phase-II cavities the inner conductor beam port region is outfitted with a donut style drift tube to improve transient time factor. The cavities are specified to operate at an effective acceleration of 1.1 MV for a cavity power of 7 W at 4.2 K and corresponding peak surface fields of 30 MV/m and 60 mT [4]. The Phase-I cavities were produced by Zanon and the Phase-II cavities by PAVAC Industries.

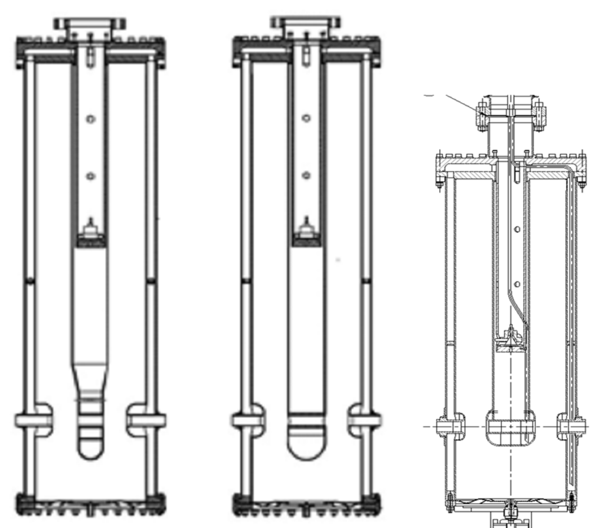

Figure 2: ISAC-II cavities for the geometry betas of 0.057, 0.071 and 0.11.

The RF parameters of Phase-I and Phase-II cavities are listed in the Table 1.

† zyyao@triumf.ca

Content from this work may be used under the terms of the CC BY 3.0 licence (© 2017). Any distribution of this work must maintain attribution to the author(s), title of the work, publisher, and DOI.

ISBN: 978-3-95450-191-5 doi:10.18429/JACoW-SRF2017-TUPB065

DESIGN OF MULTI-FREQUENCY COAXIAL TEST RESONATORS

Z. Yao†, T. Junginger, R. E. Laxdal, B. Matheson, B. S. Waraich, V. Zvyagintsev,
TRIUMF, Vancouver, Canada

Abstract

A significant issue in low beta resonators is medium field Q-slope (MFQS) at 4 K. To study the MFQS and the field dependence of surface resistance in low beta resonators, a quarter-wave resonator (QWR) and a half-wave resonator (HWR) were designed to be tested at integer harmonic frequencies of 200 MHz, and up to 1.2 GHz. A series of chemistry and heat treatments will be applied to these cavities so that a systemic study on the surface resistance of the coaxial resonators associating with post-processing, RF field, and frequency can be done. The detail design of these cavities is reported in this paper.

INTRODUCTION

The resonant frequency of low beta cavities, operating in TEM mode, of proton or heavy ions linac applications are normally in the range of 80 MHz to 350 MHz. [1 - 4] These frequencies provide opportunity of 4 K operation to reduce the cost of cryogenics system. However, at 4 K strong Q-slope in the medium field regime, which is in general the operational field level, reduces cavity performance. Presently the large facilities under construction or in design stage are choosing to operate at 2 K even at low frequency to avoid this performance degradation. [5]

A preliminary study on MFQS and field dependent surface resistance was reported based on vertical tests of an 81 MHz QWR and a 162 MHz HWR. [6] 48 hours 120 ˚C baking takes the edge off MFQS and improve operational quality factor at 4 K for both QWR and HWR. The low temperature bake reduces BCS resistance and weaken field dependence of BCS component simultaneously. Further investigation on QWRs demonstrates the energy gap is increased by 120 ˚C bake and the field dependence of that is eliminated, shown in Fig. 1.

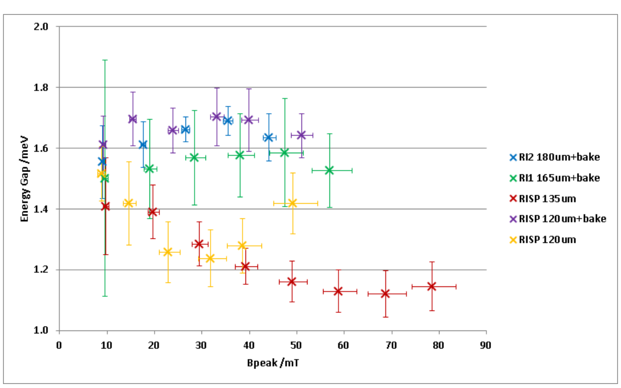

Figure 1: The comparison of the field dependent energy gaps of baked and unbaked 81 MHz beta=0.047 QWRs.

For the purpose of developing systemic study tools for MFQS of low beta resonators, two delegated QWR and HWR cavities are designed and being fabricated at TRIUMF, shown in Fig. 2. The coaxial structure is chosen to represent the common geometry of low beta resonators. They are proposed to be the low beta style 'single cell' cavities to investigate field dependent surface resistance as functions of surface treatment, heat treatment, and RF frequency. Doping of the low beta resonators could be further explored on them combining with the development of RF induction furnace in house.

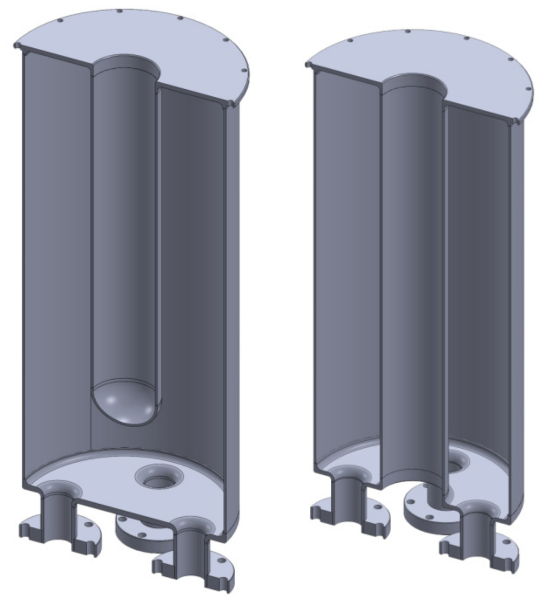

Figure 2: The cross section views of multi-mode QWR and HWR cavities.

CAVITIES SPECIFICATIONS

The cavities are designed as 'single cell' purpose resonators for the fundamental SRF R&D programs. They will be tested in cryostat at various electromagnetic field levels, temperatures, and resonant frequencies, to study the field dependent surface resistance in low beta resonators correlated to the different surface treatments or heat treatments. To be distinct from acceleration purpose superconducting cavities, the high shunt impendence and the low peak field ratio (E_{peak}/E_{acc} and B_{peak}/E_{acc}) for fundamental mode (accelerating mode) is not critical. Some common features, such as beam ports and helium jacket, are eliminated to simplify the cavity design. However, in accordance with research proposal, some specific requirements are requested for the design.

- The cavities are required to be tested at various frequencies in TEM modes. The resonant frequency window should cover the common operational fre-

† zyyao@triumf.ca

Content from this work may be used under the terms of the CC BY 3.0 licence (© 2017). Any distribution of this work must maintain attribution to the author(s), title of the work, publisher, and DOI.

ISBN: 978-3-95450-191-5 doi:10.18429/JACoW-SRF2017-TUPB066

RF RESULTS OF Nb COATED SRF ACCELERATOR CAVITIES VIA HiPIMS

M. Burton, M. Beebe, R. A. Lukaszew, The College of William & Mary, Williamsburg, VA, USA
A. Palczewski, L. Phillips, C. E. Reece, Thomas Jefferson National Accelerator Facility, Newport News, VA, USA

Abstract

Bulk Niobium (Nb) SRF (superconducting radio frequency) cavities are currently the preferred method for acceleration of charged particles at accelerator facilities around the world. However, bulk Nb cavities have poor thermal conductance and impose material and design restrictions on other components of a particle accelerator. Since the SRF phenomena occurs at surfaces within a shallow depth of ~ 1 mm, a proposed solution to this problem has been to deposit a superconducting Nb thin film on the interior of a cavity made of a suitable alternative material such as copper or aluminum. While this approach has been attempted in the past using DC magnetron sputtering (DCMS), such cavities have never performed at the bulk Nb level. However, new energetic condensation techniques for film deposition offer the opportunity to create suitably thick Nb films with improved density, microstructure and adhesion compared to traditional DCMS. One such technique that has been developed somewhat recently is "High Power Impulse Magnetron Sputtering" (HiPIMS). Here we report early results from various thin film coatings carried out on a 1.5GHz Nb cavity and small coupon samples coated at Jefferson Lab using HiPIMS.

INTRODUCTION

Superconducting radio frequency (SRF) cavities have been used for decades in particle accelerators around the world. SRF allows a particle accelerator to operate in a high duty cycle, or CW mode, due to the significantly reduced heat generation in the superconducting material, as well as low beam impedance and high efficiency of RF power transfer to the beam [1]. Throughout the history of SRF, cavities have been made from bulk Nb shaped and welded into adequate resonant cavity designs. However, bulk Nb imposes several drawbacks. First, Nb can exhibit significantly varied RF properties based upon how the Nb material was originally processed, pertaining the cavity construction and conditioning. In particular, due to its refractory metal nature, Nb can be notoriously difficult to machine and weld into the required resonant cavity shapes. Second, since some heat is still generated by a superconductor in the RF mode and the system must be operated at 2K, the poor thermal conductance of Nb can lead to high cryogenic cooling costs. Lastly, niobium itself is a costly material compared to copper or aluminum. As mentioned earlier, one alternative proposed is to take advantage of the shallow, ~1μm, depth of the SRF phenomena by using an alternative suitable material for the resonant cavity shape and coating the interior active surface with an appropriate superconducting thin film, such as Nb. Thin films offer many advantages over bulk materials due to the possibility of engineering the resulting film, and thereby surface, properties using the various processing parameters available during the film growth and coating the interior of materials with more favorable bulk properties, such as Cu, thereby reducing the production as well as operating costs of SRF accelerating structures.

Thin film SRF cavities have been attempted in the past with limited success. The first time thin film Nb cavities were attempted in earnest was in the 1980's at CERN for the LEP accelerator [2]. CERN deposited Nb thin films on the interior of Cu cavities using DC magnetron sputtering (DCMS) and DC biased diode sputtering. While the CERN films exhibited good low field Q-values, they had a major downside, which was the observed strong dependence of the Q-value on RF field. That is, as the accelerator was driven to higher power the efficiency of the cavity strongly decreased. This behavior was termed the "Q-slope". Even with this problem, CERN used Nb/Cu cavities in the LEP and LHC facilities since the cavities still met the operating criteria and exhibited enhanced magnetic properties allowing reduction of shielding in the system. To this day, the cause of the Q-slope has not been fully understood and no Nb thin film cavities have overcome this defect. Many explanations have been proposed as the cause of the Q-slope such as poor film-substrate interface, poor Nb thin film quality and even microscopic film delamination leading to a feedback system of heating; but none have been unequivocally demonstrated [3,4,5].

Of the many causes proposed for the Q-slope, many can be associated with the film deposition methods utilized. DC sputtering is a low energy deposition method and, even though it is still quite good for many other applications, it has been shown to yield films with properties below their bulk counterparts for the case of superconducting materials. Therefore, one proposed solution is to explore more energetic condensation methods, such as: high power impulse magnetron sputtering (HiPIMS) or electron-cyclotron resonance (ECR), to create films with enhanced properties more suitable for SRF application [6]. However, due to the geometric challenges of coating the interior of SRF cavities some techniques are more easily adapted than others. HiPIMS is one such technique which offers the ability to coat the interior of an SRF accelerating cavity using existing DCMS systems. HiPIMS works on the principle of pulsing the magnetron to extremely high power densities thereby increasing the plasma density by several orders of magnitude over DCMS plasma resulting

Content from this work may be used under the terms of the CC BY 3.0 licence (© 2017). Any distribution of this work must maintain attribution to the author(s), title of the work, publisher, and DOI.

ISBN: 978-3-95450-191-5 doi:10.18429/JACoW-SRF2017-TUPB067

INSIGHTS INTO FORMATION OF Nb_3Sn FILM DURING THE VAPOR DIFFUSION PROCESS*

Uttar Pudasaini[1], G. Eremeev[2], Charles E. Reece[2], J. Tuggle[3], and M. J. Kelley[1,2,3]
[1]Applied Science Department, The College of William and Mary, Williamsburg, VA 23185, USA
[2]Thomas Jefferson National Accelerator Facility, Newport News, VA 23606, USA
[3]Virginia Polytechnic Institute and State University, Blacksburg, VA 24061, USA

Abstract

The potential of Nb_3Sn for superconducting radio frequency (SRF) cavities is widely recognized and renewed R&D efforts continue to bring new insights about the material's structure and properties. We have systematically coated niobium with Nb_3Sn using the vapor diffusion technique under varying coating conditions to elucidate the reaction of tin with niobium at the temperatures of interest. The analysis of the coated samples is revealing new understanding about the two-stage nucleation/deposition ("vapor diffusion") process that allows us to form a hypothesis regarding Nb_3Sn formation mechanism. The essential aspect of nucleation is the deposition of a high coverage, nanoscale-thin tin film with particle assemblage by decomposition of tin chloride on the niobium surface at temperatures sufficient for reduction of the thick niobium oxide film, usually at about 500 °C. The deposition is followed by the reaction of tin from tin vapor with the niobium surface to form Nb_3Sn at about 1200 °C, where the surface and grain boundaries start to play key role in the formation process initiation and progression. These findings improve understanding of the Nb_3Sn growth in the typical vapor diffusion process used for accelerator cavity coatings

INTRODUCTION

Since the performance of niobium SRF cavities is now approaching the fundamental limit, SRF technology based on alternate superconducting materials is gaining more attention for better performance and cost reduction. The alternative SRF cavity material demands higher values of both the critical temperature and superheating field because they determine the RF performance and accelerating gradient of SRF cavity. The intermetallic compound Nb_3Sn pledges better performance and significant reduction of production and operational cost of SRF cavities, because both the critical temperature and superheating field of Nb_3Sn are nearly twice that of niobium [1]. At the present time, it is the front running alternative material to substitute niobium in SRF cavities. Because of the brittleness and lower thermal conductivity of bulk material, Nb_3Sn cavities should be prepared by depositing a thin layer of Nb_3Sn coating inside a prefabricated cavity structure. Tin vapor diffusion is the leading technique for coating the interior surface of a niobium cavity with a Nb_3Sn layer of few-micron thickness.

The tin vapor diffusion technique is comprised of two steps–nucleation and deposition. The nucleation step involves tin chloride evaporation at a lower temperature of about 500 °C. Deposition follows nucleation, and involves evaporation of tin at a higher temperature of 1100 - 1200 °C, a temperature favorable to form Nb_3Sn phase on substrate niobium. Since the performance of a Nb_3Sn-coated cavity prepared by this technique is very promising, it is necessary to better understand the mechanism of Nb_3Sn formation and its growth kinetics to optimize the coating parameters for further improvement. This contribution discusses the results from recent experiments that could shed some new light on the formation and kinetics of Nb_3Sn coating during the coating process.

Nb_3Sn COATING EVOLUTION

The typical coating process at Jefferson Lab consists of a 1-hour nucleation step at 500 °C followed by a 3-hour deposition step at 1200 °C [2]. A set of scanning electron microscopy (SEM) images is shown in Figure 1 to elucidate the evolution of a Nb_3Sn coating.

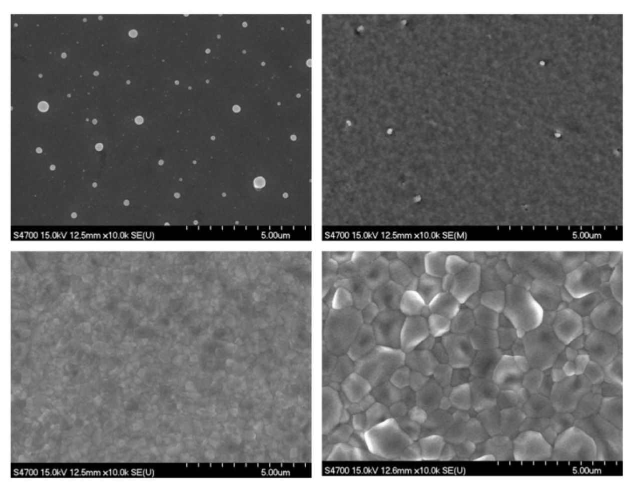

Figure 1: SEM images obtained after interrupting the coating process after one hour at 500 °C (top left), one minute at 1200 °C (bottom left), one hour at 1200 °C and 3 hours at 1200 °C (bottom right). Note that similar amounts of Sn and $SnCl_2$ were used in each experiment.

Energy dispersive X-ray spectroscopy (EDS) examination of bright features observed after 1 hour at 500 °C confirm the distribution of tin particles at the Nb

*Partially authored by Jefferson Science Associates under contract no. DEAC0506OR23177. Work at College of William & Mary supported by Office of High Energy Physics under grant SC0014475. This material is based upon work supported by the U.S. Department of Energy, Office of Science, Office of Nuclear Physics.

Content from this work may be used under the terms of the CC BY 3.0 licence (© 2017). Any distribution of this work must maintain attribution to the author(s), title of the work, publisher, and DOI.

ISBN: 978-3-95450-191-5 doi:10.18429/JACoW-SRF2017-TUPB069

RIGOROUS DATA PROCESSING AND AUTOMATIC DOCUMENTATION OF SRF COLD TESTS*

K. G. Hernández-Chahín[1]†, S. Aull, N. Stapley, P. Fernandez Lopez, N. Schwerg
CERN, Geneva, Switzerland
[1]also at DCI-UG, Guanajuato, Mexico

Abstract

Performance curves for SRF cavities are derived from primary quantities which are processed by software. Commonly, the mathematical implementation of this analysis is hidden in software such as Excel or LabVIEW, making it difficult to verify or to trace, while text-based programming like Python and MATLAB require some programming skills for review and use. As part of an initiative to consolidate and standardise SRF data analysis tools, we present a Python program converting a module containing the collection of all commonly used functions into a LaTeX(PDF) document carrying all features of the implementation and allowing for a review by SRF experts, not programmers. The resulting document is the reference for non-experts, beginners and test stand operators. The module is imported in any subsequent processing and analysis steps like the symbolic analysis of the measurement uncertainties or the study of sensitivities. As an additional layer of protection the functions can be further wrapped including assertions, type and sanity checks. This process maximises function reuse, reduces the risk of human errors and guarantees automatically validated and documented cold test results.

INTRODUCTION

During cold tests of SRF cavities a great number of different signals are measured and automatically recorded. The acquisition and storage is done by test programs often written in LabVIEW [1,2] or INSPECTOR [3]. From these primary quantities we derive figures of merit such as the unloaded quality factor Q_0 and the accelerating gradient E_{acc}. The first processing and derivation of these quantities is done immediately using the data acquisition software, where the routines for the calculations are implemented using the programing language provided by the software manufacture. The final analysis of the data is conducted during the post-processing using Excel [4], MATLAB [5] or Python [6, 7] where the analysis routines are custom libraries of the user.

Over the last year we came across the following problems and pitfalls of this approach:

- In LabVIEW and Excel the implementation of the analysis function is somehow hidden from the operator and difficult to verify by the user.
- The functions have to be implemented twice, once for the test software and once for post-processing hence doubling the effort for maintenance.
- Although it is instructive and recommended for any beginner in the field of SRF to implement their own set of analysis functions, for routine operation a single reviewed and protected set is needed.
- In general the implementation of mathematical expressions in any programming language (graphical or text) is cumbersome or unpleasant to read.

In order to overcome these problems the cold-test software system should meet the following requirements:

- Single point of function definition
- Built-in documentation
- Version control
- Nesting and re-use of the core implementation
- Simple and reliable review process
- Automatic tests and sanity checks

In this paper we present an approach consisting of two core components: 1) a central python implementation (`srf_functions`) of all analysis functions as e.g. provided in Padamsee's book [8] and 2) an automatic documentation tool (`dokator`) converting the functions and especially the underlying code into a type-set representation for review by SRF experts and practitioners and not programmers.

SRF_FUNCTIONS

Figure 1 shows the approach with the central element the `srf_functions`. This module or library contains all mathematical expressions used for the evaluation of the measurements and used in the construction of more complex analysis routines. These functions are used for all computations from the data taken with the measurement software (INSPECTOR or LabVIEW) during the cold test to the post processing of the final results.

Single Point of Function Definition

We base our approach on one single Python [6, 7] module, `srf_functions`, which contains the implementation of all computations. We chose Python due to its wide spread use, flexibility and various freely available packages. The implementation is kept to a minimum of complexity while placing the effort in clean definitions and documentation.

Un-typed Function Definition

In the core module we define all functions un-typed. This means that the implementation does not rely on any specific features as long as the used objects support standard math operation such as `+ - * / **` with the latter being the power operator in Python. Special symbols or functions like

* Work supported by the Beam Project (CONACYT, Mexico).
† karim.gibran.hernandez.chahin@cern.ch

Content from this work may be used under the terms of the CC BY 3.0 licence (© 2017). Any distribution of this work must maintain attribution to the author(s), title of the work, publisher, and DOI.

ISBN: 978-3-95450-191-5 doi:10.18429/JACoW-SRF2017-TUPB070

INFN-LASA CAVITY DESIGN FOR PIP-II LB650 CAVITY

C. Pagani[1], J.F. Chen[†], M. Bertucci, A. Bignami, A. Bosotti, P. Michelato
L. Monaco, R. Paparella, D. Sertore, INFN-LASA, Segrate (MI), Italy
S. Pirani, ESS, Lund, Sweden
[1]also at University of Milan, Milan, Italy

Abstract

INFN-LASA is going to join the international partnership for Fermilab PIP-II project and to provide a novel design for the 650 MHz cavity of the 0.61 beta linac section, plug compatible with the Fermilab Cryomodule design. This paper reports the cavity design features both from the ElectroMagnetic and mechanical aspects, with focus on the rationales at the basis of the choice of main parameters. Furthermore, the current plans for the future R&D activity are here reported, including the ongoing production of three single cells and two complete cavities with our LB650 prototype design.

INTRODUCTION

The Fermilab PIP-II Linac is designed to deliver an average proton beam current of 2 mA at an energy of 800 MeV, to be fully compatible with Continuous Wave (CW) operation [1]. One main section of the Linac is the 650 MHz superconducting part of $\beta_G = 0.61$ that contains 33 five-cell cavities, accelerating proton beam from 185 MeV to 500 MeV.

INFN-LASA is going to join the international partnership to provide a novel design for the LB650 cavities, fully plug compatible with the Fermilab Cryomodule design, i.e. beam pipes, couplers, Helium tank, tuners and so on.

This paper describes the INFN-LASA design of LB650 cavity, including both ElectroMagnetic (EM) and mechanical designs with detailed reasons for the choice of geometric parameters. Based on this choices, three single-cell prototypes are being fabricated to validate the design, and to explore the road for the development of five-cell cavities in near future, being two complete cavities already planned.

CAVITY DESIGN

PIP-II cavities are required to be compatible with CW operation. Since in this CW operational mode, the RF duty factor is not a knob for tuning the dynamic heat load, a high accelerating efficiency in terms of R/Q is instead necessary. A high R/Q of cavity principally requires small iris aperture and small wall-angle; this may lead to difficulties in Field Flatness tuning, cavity surface treatment and cleaning. In addition, the relatively small beam current of PIP-II results in high external Q (Q_{ex}) of the cavity that implies a narrow bandwidth of the accelerating mode. In order to have a stable beam acceleration, a strict control of the Lorentz Force Detuning and microphonic is required, not only with stiffening rings but also by a proper shape of the cells. Our cavity design considers all these effects and aims to have an optimal balance between the multiple geometric parameters.

Our goal in designing the cavity is to achieve as high as possible accelerating efficiency with acceptable cell-to-cell coupling, and as low as possible pressure sensitivity and Lorentz Force Detuning (LFD) coefficient with modest cavity stiffness, to allow cavity tuning.

Firstly, we will describe the process to reach the minimum acceptable cell-to-cell coupling while maximizing the R/Q. Secondly, we explain the relationship between LFD and geometric parameters. At last, we adjust the radius of the stiffening ring to achieve a relatively low-pressure sensitivity.

Rationales

The cavity parameter R/Q is mainly determined by aperture sizes. A smaller aperture is preferred for high R/Q, even if this choice decreases significantly the cell-to-cell coupling, k_{cc}. The k_{cc} obviously affects the sensitivity of the field profile of the π-mode to frequency error of individual cells. This field flatness sensitivity is measured by the ratio [2, 3]:

$$N^2/(\beta k_{cc})$$

where N is the number of cells, β is the relative velocity and k_{cc} is the cell-to-cell coupling.

It is favourable to keep this ratio low. A list of some successful cavities is used for comparison, as shown in Table 1. Taking TESLA ratio as reference, the PIP-II LB650 cavity shall have $k_{cc} \geq 0.95\%$.

Table 1: Comparison of Cell-to-Cell Coupling

Cav	**N**	**β**	**k_{cc} (%)**	**$N^2/(\beta k_{cc})$**
TESLA	9	1	1.87	4331
SNS MB	6	0.61	1.52	3883
ESS MB	6	0.67	1.55	3467
PIP-II LB650	5	0.61	**0.95**	4331

The Buildcavity [4] and Superfish [5] codes are used for the cavity design. In Buildcavity, seven parameters are used to determinate a half-cell: R_{iris}, D, alpha, R, r, d and L, corresponding to iris radius, equator diameter, side wall angle, equator elliptical ratio (B/A), iris elliptical ratio (b/a) and length, as shown in Figure 1.

The half-cell shape is designed iteratively. Starting from an initial half-cell shape with Riris =48.0 mm, D=196.0 mm , alpha= 2°, R=1, r=1.7, d= 14 mm and L =70.4 mm, we change only the iris radius to find the relationship between k_{cc} and R/Q. Figure 2 shows both the k_{cc} and R/Q versus R_{iris}. As we can see, the cell-to-cell coupling monotonically decreases with the rising R/Q. Due to this reason, the k_{cc} = 0.95% is chosen to obtain the maximum R/Q. Meanwhile, the iris diameter of 88 mm can be fixed.

† email address: jinfang.chen@mi.infn.it

Content from this work may be used under the terms of the CC BY 3.0 licence (© 2017). Any distribution of this work must maintain attribution to the author(s), title of the work, publisher, and DOI.

ISBN: 978-3-95450-191-5 doi:10.18429/JACoW-SRF2017-TUPB071

TEST RESULT OF 650 MHz, BETA0.61, SINGLE CELL NIOBIUM CAVITY

Sudeshna Seth[1*], Sumit Som[1], Surajit Ghosh[1], Pranab Bhattacharyya[1], Aditya Mandal[1], Sundeep Ghosh[1], Anjan Dutta Gupta[1], P. Prakash[2], Kishore Kumar Mistri[2], Thomas H. Nicol[3], Allan Rowe[3], Anna Grassellino[3], Timergali N. Khabiboulline[3],Dmitri A. Sergatskov[3], Oleksandr Stepanovych Melnychuk[3], Shekhar Mishra[3], Michael Kelly[4], Thomas Reid[4]
[1] Variable Energy Cyclotron Centre (VECC), Kolkata, India
[2] Inter University Accelerator Centre (IUAC), New Delhi, India
[3] Fermi National Accelerator Laboratory, Illinois, USA
[4]Argonne National Accelerator Laboratory, Illinois, USA

Abstract

VECC has been involved in the design, analysis and development of 650 MHz, beta 0.61 (LB650), elliptical Superconducting RF linac cavity, as part of research and development activities on SRF cavities and associated technologies under Indian Institutions Fermilab Collaboration (IIFC). A single-cell niobium cavity has been indigenously designed and developed at VECC, with the help of Electron Beam Welding (EBW) facility at IUAC, New Delhi. Various measurements, processing and testing at 2K in Vertical Test Stand (VTS) of the single-cell cavity were carried out at ANL and Fermilab, USA, with active participation of VECC engineers. It achieved a maximum accelerating gradient (Eacc) of 34.5 MV/m with Quality Factor of 2E+09 and 30 MV/m with Q_0 of 1.5E+10. This is the highest accelerating gradient achieved so far in the world for LB650 cavities. This paper describes the design, fabrication and measurement of the single cell niobium cavity. Cavity processing and test results of Vertical Test of the single-cell niobium cavity are also presented.

CAVITY DESIGN

A 650 MHz 5-cell elliptical cavities with geometric β_G = 0.61 has been designed to optimize acceleration efficiency to operate in superfluid helium at a temperature2.0K, with gradient (Eacc) of 17 MV/m.The cell shape has been designed to minimize the peak surface magnetic and electric fields, Hpeak and Epeak, to achieve the required gradient and minimize field emission, and to minimize multipacting and to maximize R/Q and G to have less RF power dissipation in cavity wall and smaller heat load on the cryogenic system [1]. RF design of the 5-cell cavity has been carried out using 2-D Superfish and 3-D CST Microwave Studio [2]. EM design parameters of the optimized geometry of 5 cell, LB650 cavity are summarized in Table 1 [1] and electric field lines for accelerating mode (π-mode) of the cavity have been shown in Figure 1. Geometry of end cell of the cavity is optimized to have good field flatness over the five cells. Also a single cell elliptical cavity, which has the same dimensions as that of the mid-cell of 5-cell LB650 cavity, has been simulated in both Superfish and CST Microwave Studio. Frequency of single-cell niobium cavity with beampipe is found to be 645.2 MHz. Electric field lines in single cell niobium cavity have been shown in Figure 2.

* sseth@vecc.gov.in

Table 1: Cavity EM Parameters of 5-Cell Cavity

	Values
Frequency	650MHz
Shape, No of Cells	Elliptical, 5
Geometric beta(β_G)	0.61
Effective Length = 5*(βgλ/2)	703.4mm
Iris Aperture	96mm
Wall angle for midcell	2.4◦
Wall angle for endcell	4.5◦
Epeak /E_{acc}	3
Bpeak /E_{acc}	4.84
R/Q	296
G	200
Cell to cell coupling K_{cc}	1.24%

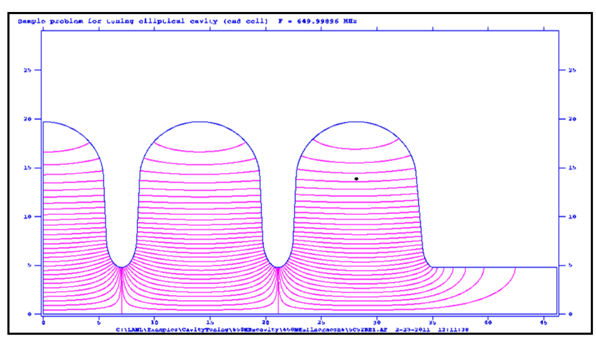

Figure 1: Accelerating mode at 649.99896MHz.

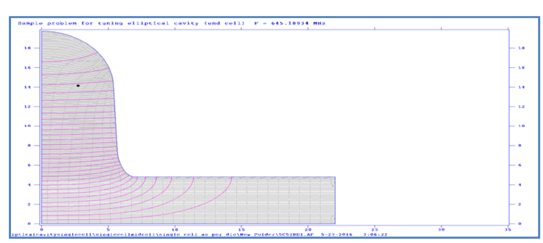

Figure 2: Fundamental mode of the Single-cell at 645.19 MHz.

Content from this work may be used under the terms of the CC BY 3.0 licence (© 2017). Any distribution of this work must maintain attribution to the author(s), title of the work, publisher, and DOI.

ISBN: 978-3-95450-191-5 doi:10.18429/JACoW-SRF2017-TUPB072

Content from this work may be used under the terms of the CC BY 3.0 licence (© 2017). Any distribution of this work must maintain attribution to the author(s), title of the work, publisher, and DOI.

INVESTIGATION OF BCP PARAMETERS FOR MASTERY OF SRF CAVITY TREATMENT

F. Éozénou, E. Cenni, G. Devanz, T. Percerou, T. Proslier, C. Servouin, M.L.L. Nghiem*
Irfu, CEA, Université Paris-Saclay, F- 91191 Gif-sur-Yvette, France
*Université Pierre et Marie Curie, 4 place Jussieu, F- 75252 Paris, France

Abstract

Mastery of Standard Buffered Chemical Polishing (with mixture of hydrofluoric, nitric and phosphoric acids) is of paramount importance for the treatment of SRF resonators with complex geometry as IFMIF half-wave resonators, in order to control accurately their frequency evolution. Furthermore, strong and unexpected asymmetry in removals has recently been observed after BCP treatment of ESS-medium beta resonators.

The goal of this study is to investigate accurately influence of parameters such as surface geometry and orientation, acid temperature, agitation and their coupling on the removal rate. We will also focus on the influence of by-products such has NOx on kinetics. The mixture used is HF(40%)-HNO_3(65%)-H_3PO_4(85%) with ratio 1-1-2.4.

INTRODUCTION

Electropolishing has become the reference surface treatment process for high-gradient elliptical cavities. However, standard chemical process with mixtures of hydrofluoric, nitric and phosphoric acids, also known as Buffered Chemical Polishing (BCP) remains the reference process for the preparation of low-beta resonators.

The main and simplified chemical reactions occurring at the niobium surface are:

Niobium oxidation with nitric acid:

$$6\,Nb + 10\,HNO_3 \rightarrow 3\,Nb_2O_5 + 10\,NO + 5\,H_2O \quad (1)$$

Dissolution of niobium oxide with HF:

$$Nb_2O_5 + 10\,HF \rightarrow 2\,NbF_5 + 5\,H_2O \quad (2)$$

The main by-products are fluorinated salts and NO molecules (more generally NOx with x<3) which is a yellowish toxic gas. Both might be observed during experiments on samples (see later).Applied to the treatment of niobium SRF resonators, this process generates removal rates between 0.5 and 1 µm/min.

We propose in this paper simple experiments on niobium samples to guide the BCP treatments of structures with complex geometries. It is of paramount importance to anticipate the treatment in order to:

- Achieve the required removal all over the surface of the cavity
- Avoid local heating during the cavity treatment
- Control the frequency to maintain it in the tuning range

For example, assuming a uniform removal, the theoretical frequency variation for half-wave IFMIF resonators is -200 Hz/µm. After BCP treatment, we reproducibly achieve -500 Hz/µm because of non-uniform removal.

Furthermore, BCP is useful for this kind of structures to tune the frequency by etching at relevant locations [1].

The goal of the work presented here is to precisely quantify the influence of parameter such as:

- Temperature
- Fluid velocity
- Surface orientation
- Influence of NOx gases (by-product of the chemical treatment)

Some researchers have modeled chemical treatment with Computational Fluid dynamics (CFD) [2-4]. An accurate knowledge of parameters involved in BCP would make it possible to enrich such codes with relevant data.

The mixture used for experiments on samples was home made. The proportions are 1-1-2.4 in HF-HNO_3-H_3PO_4. This bath composition used at CEA Saclay makes it possible to have HF concentration in mass below 7%, which is required for safety considerations. The higher H_3PO_4 concentration, which acts as buffer, results in a lower removal rate compared to 1-1-2 composition.

MOTIVATION: DIFFERENT REMOVAL RATE FOR SIMILAR CAVITIES

BCP chemical treatments have been recently carried out on 704MHz elliptical ESS resonators, of two different types: β = 0.67 (6 cells) [5] and β = 0.86 (5 cells). The cavities were polished in vertical position, with continuous acid circulation. The cavities are similar (see details in Table 1) and similar parameters were used (T = 15°C, acid flow of 20 L/min) for the chemical treatment (Fig. 1). However, the achieved removal rates differ significantly. The achieved removal rate is 0.5 µm/min for the high beta cavity, where as it is as high as 1 µm/min in the medium-β case.

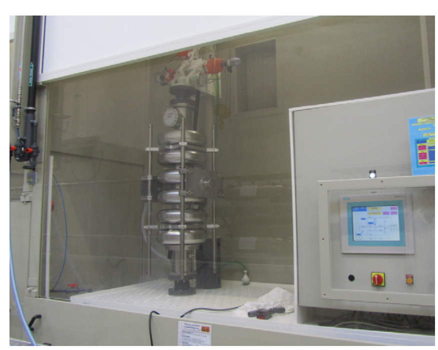

Figure 1: ESS medium-beta cavity during BCP treatment.

ISBN: 978-3-95450-191-5 doi:10.18429/JACoW-SRF2017-TUPB073

VERTICAL ELECTRO-POLISHING COLLABORATION BETWEEN CORNELL, KEK, AND MARUI GALVANIZING CO. LTD.*

F. Furuta†, M. Ge, T. Gruber, J. Kaufman, J. Sears, M. Liepe, CLASSE, Cornell University, U.S.A.
H. Hayano, S. Kato, T. Saeki, High Energy Accelerator Research Organization, KEK, Japan
V. Chouhan, Y. Ida, K. Nii, T. Yamaguchi, Marui Galvanizing Co., Ltd., Japan

Abstract

Cornell's SRF group, KEK, and Marui Galvanizing Co. Ltd (MGI) are collaborating since 2014 on Vertical Electro-Polishing (VEP) R&D as a part of a US/Japan Program for Cooperation in High Energy Physics. We have focused on an improvement of removal uniformity during the VEP process. MGI and KEK have developed their original VEP cathode named i-cathode Ninja®, which has four retractable wing-shape parts per cell. Cornell processed one single cell cavity with VEP using this cathode and performed a vertical test. KEK also provided one 9-cell cavity to Cornell. Cornell then performed surface treatments including Cornell VEP and RF test on this 9-cell cavity. The progress by the VEP collaboration and RF test results are presented in this paper.

INTRODUCTION

Cornell's SRF group has led the development of Vertical Electro-Polishing (VEP), which requires a much simpler setup and is less expensive compared with the conventional Horizontal EP [1]. After the successes of the Cornell VEP on the high gradient cavities for the ILC (>35MV/m with Q>0.8×10^{10}) [2] and High-Q cavities for LCLS-II (Q>2.7×10^{10} at 16MV/m) [3], Cornell's VEP R&D focus has shifted to more advanced topics. One topic is a new EP cathode development in collaboration with KEK and Marui. The EP process in vertical direction can be affected by gravity, resulting in a removal difference between the upper and lower half cells. To compensate for removal un-uniformity, a cavity typically needs to be flipped over after half of the target removal. Marui has been developing a new cathode named "i-cathode Ninja" to improve the removal uniformity during its VEP R&D with KEK [4, 5]. Marui's work coincides with Cornell's interest in removal R&D, and collaboration between Cornell and KEK-Marui was started in 2014. As a part of this collaboration, KEK provided Cornell one brand-new 9-cell cavity, MHI-02, which was fabricated in house at KEK, for the future development of a 9-cell scale Ninja cathode. In this paper, we report the progress on these projects with detailed cavity test results.

NEW VEP CATHODE R&D AT CORNELL

Figure 1 shows a 1.3GHz TESLA shape single-cell cavity installed into Cornell VEP system with the Ninja-cathode. Two types of the Ninja cathode and top and bottom EP sleeves were shipped from Marui to Cornell. Cornell's VEP system was upgraded to allow for acid circulation during the VEP process with the Ninja cathode.

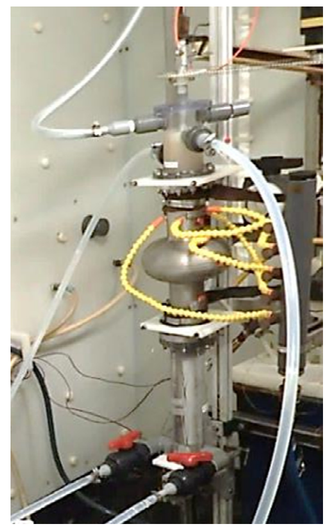

Figure 1: Cornell VEP system with the Ninja cathode.

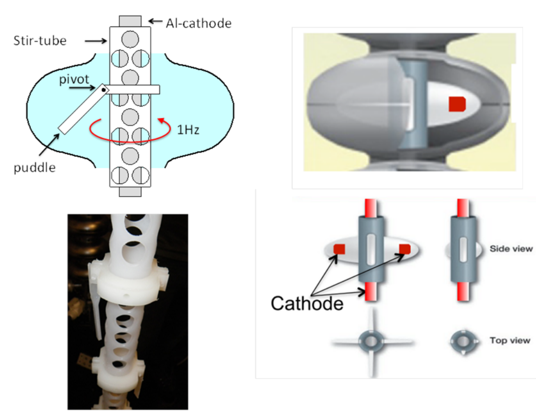

Figure 2: Images of Cornell VEP cathode (left); Marui's i-cathode Ninja type-I (right).

Cornell's and Marui's VEP Cathodes

Cornell VEP cathode (Fig. 2, left) consists out of an aluminium rod and a stirring tube with paddles (one paddle per cell). Teflon mesh lapped around the stirring tube (not shown in the figure) guides the hydrogen bubbles produced on the cathode during the EP process to prevent them from attacking the niobium surface. Marui's Ninja cathode (Fig. 2, right) consists out of an aluminium cathode rod, polyvinyl chloride (PVC) tube, and retractable Teflon wings (four wings per cell). PVC is an acid resistance material, and inexpensive. It is therefore suitable

* Work is supported by JFY2015 US/Japan Program for Cooperation in High Energy Physics
#ff97@cornell.edu

Content from this work may be used under the terms of the CC BY 3.0 licence (© 2017). Any distribution of this work must maintain attribution to the author(s), title of the work, publisher, and DOI.

ISBN: 978-3-95450-191-5 doi:10.18429/JACoW-SRF2017-TUPB074

RF PERFORMANCE OF MULTI-CELL SCALE NIOBIUM SRF CAVITIES PREPARED WITH HF FREE BIPOLAR ELECTRO-POLISHING AT FARADAY TECHNOLOGY*

F. Furuta†, M. Ge, T. Gruber, J. Kaufman, J. Sears, M. Liepe, CLASSE, Cornell University, U.S.A.
T. Hall, M. Inman, E. J. Taylor, R. Radhakrishnan, S. Snyder, Faraday Technology, Inc., Englewood, OH, U.S.A.

Abstract

Cornell's SRF group and Faraday Technology, Inc. have been collaborating on two phase-II SBIR projects. One of them is the development and commissioning of a 9-cell scale HF free Bipolar Electro-Polishing (BEP) system. Faraday Technology had completed the proof of principle of BEP on the single cell scale prior to the work reported here, and has now developed a new 9-cell scale BEP system. Cornell has fabricated three single cell cavities and has assembled them together as a 9-cell scale test string. The 9-cell scale test string has received BEP at Faraday Technology and RF testing has been performed on the three single cell cavities one-by-one at Cornell. Here we give a status update on the new 9-cell scale BEP system commissioning and on results from RF tests of the BEP cavities.

INTRODUCTION

Cornell's SRF group has led the development of Vertical Electro-Polishing (VEP), which requires a much simpler setup and is less expensive compared with the conventional Horizontal EP [1]. After the successes of the Cornell VEP on the high gradient cavities for the ILC (>35 MV/m with Q>0.8x10^{10}) [2] and High-Q cavities for LCLS-II (Q>2.7x10^{10} at 16 MV/m) [3], Cornell's VEP R&D focus has now shifted to more advanced topics. One topic is HF free VEP protocols in collaboration with Faraday Technology Inc. Currently hydrofluoric (HF) acid based electrolyte is used in EP. As the SRF projects become larger, the environmental impact of large usage of hazardous HF based acid on niobium cavities becomes not negligible. Therefore, R&D on a less hazardous or more eco-friendly niobium surface process has been performed and has made good progress [4, 5]. As part of recent progress on this eco-friendlier advanced EP work, Faraday Technology Inc. has established pulse forward/pulse reverse EP (Bipolar-EP) with an HF free electrolyte, and demonstrated high gradient performance with a single cell cavity in collaboration with FNAL [6, 7]. Now Cornell's SRF group and Faraday Technology Inc. have started collaboration on Bipolar, HF free EP for multi-cell cavities. This collaboration is supported by the Department of Energy's (DOE) phase-II Small Business Innovation Research (SBIR) program. In this paper, we report on the progresses of this project with detailed cavity test results.

* Work is supported by SBIR DOE award DE-SC0011235 (1002).
† ff97@cornell.edu

NEW 9-CELL SCALE BIPOLAR-EP SYSTEM AT FARADAY TECHNOLOGY, INC.

Bipolar-EP

Figure 1 shows a general representation of the Bipolar EP anodic/cathodic pulse waveform. The waveform consists of 1) an anodic forward pulse to grow an oxide layer on the niobium surface, 2) voltage time off to dissipate the heat, remove reaction products, and replenishes reacting species, and 3) a cathodic pulse with reversed voltage to remove the oxide layer on the niobium surface, thus eliminating the need for HF. More detail descriptions of the bipolar EP techniques are published and can be found elsewhere [6, 8, 9].

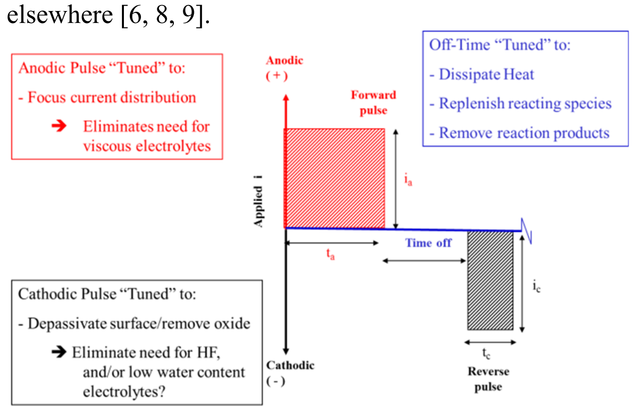

Figure 1: General bipolar EP process representation [6].

9-cell Scale Bipolar-EP

One of the project goals was scaling up the Bipolar-EP system from single cell scale to 9-cell cavity scale, and demonstration of the multi-cell scale Bipolar-EP process. While Faraday Technology Inc. upgraded the system to 9-cell scale, Cornell completed fabrication of three 1.3 GHz TESLA shape single cell cavities. Cavity IDs are LTE1-13, -14, and -15 (LTE: L-band TESLA shape Elliptical cavity). The three single cells were then connected via Teflon spacer rings and treated together as a 9-cell scale cavity equivalent string (TESLA 9-cell: 1250 mm; three 1-cell string: 1200 mm). Figure 2 shows the three single cell string (top; LTE1-14, middle; LTE1-15, bottom; LTE1-13) on the 9-cell scale Bipolar EP system at Faraday Technology Inc.

Content from this work may be used under the terms of the CC BY 3.0 licence (© 2017). Any distribution of this work must maintain attribution to the author(s), title of the work, publisher, and DOI.

ISBN: 978-3-95450-191-5 doi:10.18429/JACoW-SRF2017-TUPB075

VERTICAL ELECTRO POLISHING OF SUPERCONDUCTING SINGLE- AND MULTI CELL GUN RESONATORS

N. Steinhau Kühl, R. Bandelmann, A. Matheisen, M. Schmökel, S. Saegebarth,
DESY Hamburg Germany,
A. Arnold HZDR, Dresden, Germany

Abstract

At DESY activities on surface treatment of superconducting RF gun cavity resonators at 1.3 GHz are ongoing. Due to the small opening on the endplate for insertion of cathodes, no reasonable acid flow can be realized with the existing set up for horizontal electro polishing. To benefit from electro polishing of Niobium surfaces, an adapter to the existing horizontal electro polishing bench at DESY was set up and is in operation now. Vertical EP was applied on 1.3 GHz SRF gun resonators with 1.6 and 3.5 cell geometry. Work flow, process conditions as well as test results of gun cavities treated so far at DESY are described.

INTRODUCTION

The development of superconducting RF gun cavities for CW application is still ongoing. The DESY set up for vertical EP was modified to treat different types of 1.3 GHz SRF gun and normal cavities up to a length of 3.5 cells. In 2003 the Rossendorf 3.5 cells SRF gun was prepared at DESY by using buffered chemical polishing (BCP) in the chemical etching stand of the DESY cleanroom [1,2]. In a new approach, a Rossendorf 3.5 cell SRF gun was prepared by using the vertical EP set up for rinsing with HF and for an EP procedure in 2016.

EP SET UP FOR DIFFERENT RF GUN CAVITIES

The first setup of the vertical EP for 1.6 cell SRF gun resonators (Fig. 1) was built on the DESY system [3], which is designed for horizontal electro polishing of single and 9 cell 1.3 GHz resonators of Tesla /XFEL type [4]. The gun 16G2 is made from one standard TESLA type end cell with beam tube with HOM coupler, power coupler port and a 0.6 cell of middle cell geometry. The 0.6 cell ends with a welded on back plate, made from RRR 300 Niobium. A center hole of 5 mm ID in this back plate allows inserting plugs with different surface coating for study (Fig. 2).

The second RF gun cavity which was installed to the DESY set up was the Rossendorf 3.5 cells SRF gun with a center hole of 14 mm ID at the end of the cavity (Fig. 3). The hydrodynamic resistivity of the 14 millimeter ID hole for the acid flow prevents any nearly homogenous flow distribution in horizontal position like for the single- and nine cell geometries polished so far at DESY. Only in vertical position a well-defined acid flow and polishing of the SRF gun cavity during the EP treatment could be realized for this application.

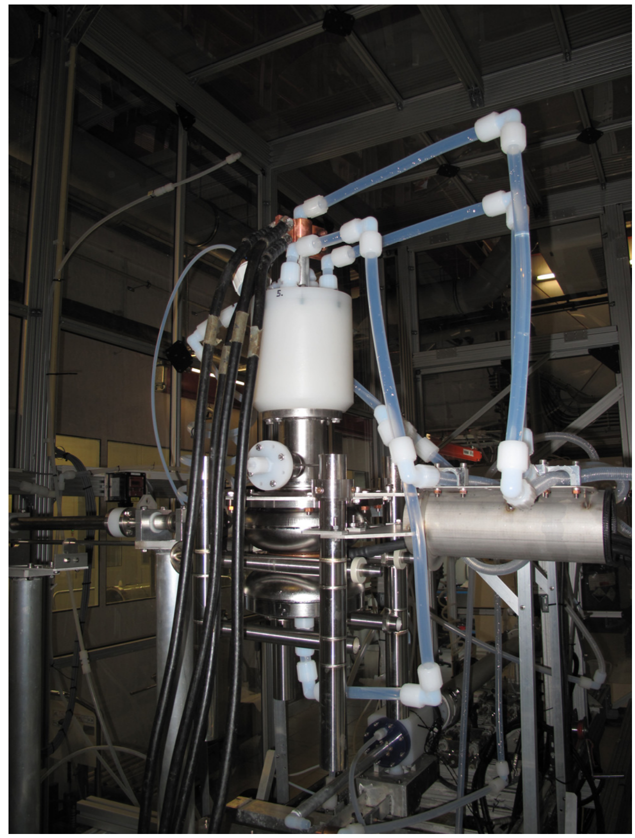

Figure 1: 1.6 cells SRF gun installed in the DESY EP set up.

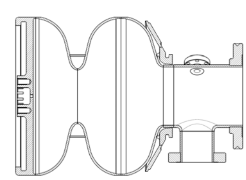

Figure 2: 1.6 cells SRF gun.

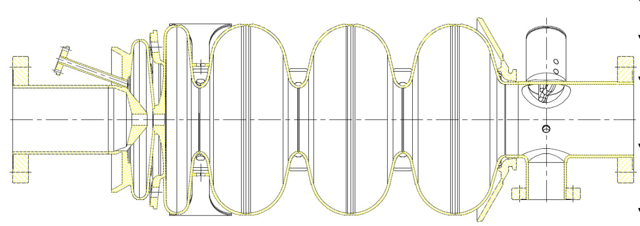

Figure 3: 3.5 cells SRF Rossendorf gun.

To use this vertical EP set up for different types of TESLA shaped SRF gun cavities the DESY set up had to be adapted.

Content from this work may be used under the terms of the CC BY 3.0 licence (© 2017). Any distribution of this work must maintain attribution to the author(s), title of the work, publisher, and DOI.

ISBN: 978-3-95450-191-5 doi:10.18429/JACoW-SRF2017-TUPB078

SUBU CHARACTERISATION: BATH FLUID DYNAMICS VS ETCHING RATE

A. Pérez Rodríguez, L. Marques Antunes Ferreira, A. Sublet,
CERN, Geneva, Switzerland

Abstract

The chemical polishing bath SUBU is widely used at CERN to prepare copper RF cavities surfaces before niobium thin film coating; examples are HIE-ISOLDE, LHC and future FCC accelerating cavities. The performance of the polishing process is affected by bath temperature and fluid dynamics. As part of on-going activities to characterise SUBU, the actual study was done to identify a correlation between the etching rate and physical parameters linked to the bath fluid dynamics. A first approach was made using experimental data from a simplified model setup, transposing them via numerical simulation to a real cavity geometry and verifying the agreement with an experiment in a real size (HIE-ISOLDE) mock-up. In a second approach to improve the accuracy of the calculation, the relation of the measured local etching rates, extracted from the mock-up, to flow dynamics quantities extracted from simulation was investigated. As a result, a relation between the local etching rate and the turbulence kinetic energy was obtained. This relation can be exploited to improve the polishing tools and so optimise the current process, as well as to predict the etching rate in other cavity geometries.

INTRODUCTION

The chemical polishing SUBU (mixture of sulfamic acid, hydrogen peroxide, n-butanol and ammonium citrate) is a surface treatment carried out at CERN to ensure the optimal performance of accelerating RF cavities based on niobium thin film on copper. The SUBU treatment is used to remove the damaged layer of the copper substrate originated during the cavity fabrication and to smooth the inner surface to hinder the electron emission induced by the high electric field. This copper surface treatment is widely used as it is relatively easy to setup, independently of the cavity geometry. In the specific case of the HIE-ISOLDE quarter wave cavities, the polishing bath SUBU flows into the cavity, which is kept in vertical position, through four tubes and it flows out through the top and the beam apertures, as shown in Fig. 1.

The two variables that have a major impact on the polishing process are temperature and bath fluid dynamics (FD); the first is easily kept constant across the entire surface, but constant FD conditions along the whole cavity's structure is much harder to achieve.

In a previous experimental study, the impact of the SUBU bath fluid dynamics on the etching rate was assessed; samples were exposed to controlled bath agitation and characterised in terms of etching rate and resulting surface roughness.

This investigation was conducted in a laboratory set-up consisting of a rotating cylinder electrode (RCE) that enabled to impose a known angular velocity on a sample.

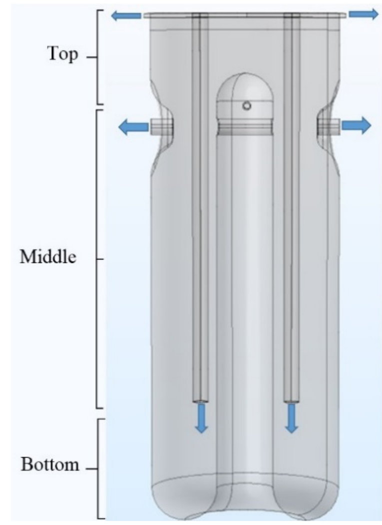

Figure 1: Scheme with the SUBU bath inlets and outlets during the polishing process.

The outcome of this work was that fluid dynamics plays indeed a fundamental role on the etching rate distribution, and on the achieved roughness; as expected, the removal of material is proportional to the bath FD values neighbouring the sample wall.

RATIONALE OF THE APPROACH

The experimental work mentioned previously justifies the study of the impact of the FD on the etching rate. This would allow to analyse the homogeneity of the polishing and to study its impact on the RF performance.

Therefore, the objective of the present study is to identify, through modelling, a possible correlation between the etching rate and variables linked to the bath fluid dynamics. Two different approaches were made; they are described hereafter.

First Approach

In the first approach, the etching rates measured in a laboratory setup at different agitation conditions were correlated to two FD variables (shear rate and turbulence kinetic energy (TKE)). These two variables were obtained with the help of a simulation software using as model the configuration of a laboratory setup and, finally, tested in a real cavity geometry.

The laboratory setup was composed of a sample holder RCE immersed in a defined volume of the SUBU bath, as shown in Fig. 2.

Content from this work may be used under the terms of the CC BY 3.0 licence (© 2017). Any distribution of this work must maintain attribution to the author(s), title of the work, publisher, and DOI.

18th International Conference on RF Superconductivity SRF2017, Lanzhou, China JACoW Publishing
ISBN: 978-3-95450-191-5 doi:10.18429/JACoW-SRF2017-TUPB082

Content from this work may be used under the terms of the CC BY 3.0 licence (© 2017). Any distribution of this work must maintain attribution to the author(s), title of the work, publisher, and DOI.

SETUP OF A SPATIALLY RESOLVING VECTOR MAGNETOMETRY SYSTEM FOR THE INVESTIGATION OF FLUX TRAPPING IN SUPERCONDUCTING CAVITIES

B. Schmitz*, K. Alomari, J. Köszegi, O. Kugeler, Y. Tamashevich, J. Knobloch
Helmholtz-Zentrum Berlin, Germany

Abstract

Flux trapping is the major contribution to the residual resistance of superconducting cavities. In order to gain a better understanding of the mechanisms involved and aiming at an eventual minimization of trapped flux, a measurement setup based on AMR sensors was devised that allows for monitoring the magnetic field vector at various positions near the cavity surface. First results of the efforts are presented.

INTRODUCTION

The precise investigation of loss mechanisms in SRF cavities is the key to a comprehensive understanding of their limitations in both the quality factor and the accelerating gradient. To minimise these mechanisms it became evident [1], that the trapped magnetic flux needs to be examined more closely.

This has been done by placing fluxgate magnetometers in the cryostat [2] or next to the cavity [3] or even inside the cavity [4] and measuring the magnetic field before, during and after the phase transition directly. However, fluxgate measurements inhibit certain disadvantages: They are limited to one dimension, they average the field over a typical length of 20 mm, and they are quite costly with >1k€ per sensor. The usage of AMR sensors is a more favourable alternative at ~ 1€/sensor, as the usability has been demonstrated [5].

A magnetic mapping system was designed using many of these AMR sensors which allows a spatial vectorial measurement around the whole cavity. The general set up and the first results of the commissioning run are presented.

EXPERIMENTAL SETUP

For the mapping of the magnetic field around a cavity, arrays of AMRs have been created. These arrays are distributed on different PCB boards to allow a variable and flexible placement around a cavity or any other sample that needs to be evaluated. At each position 3 sensors are installed, one for each spatial direction.

The connection toward the outside of the cryostat is done via 41 pin military vacuum feed-throughs. For data acquisition an imc spartan device without any additional operational amplifiers or analogue to digital converters was used. imc spartan itself provides an analogue to digital converter as well as an amplifier for each of its 128 channels. We were able to measure voltage drops in the region of few µV which corresponds to a few µT. The control of the whole setup was done by an integrated LabView routine.

* benedikt.schmitz@helmholtz-berlin.de

The arrays were placed around a cavity during a vertical test as depicted in Fig. 1.

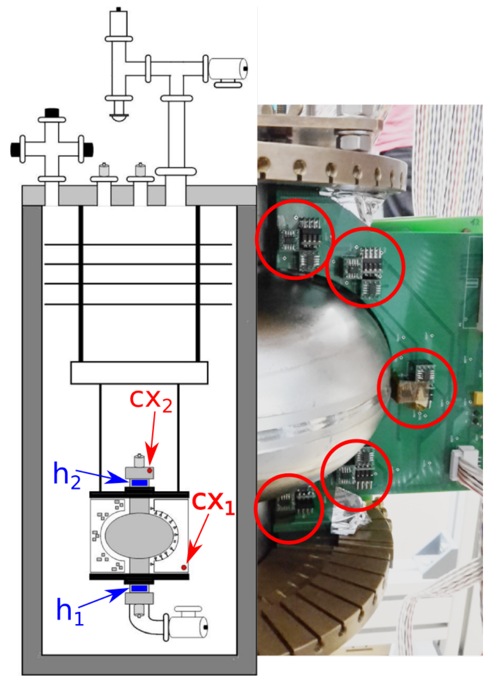

Figure 1: The left side shows an overall view including the position of two cernox sensors (red dots). *Cernox 1* (short: cx_1) measured the Helium bath temperature at the lower edge of one magnetic board. *Cernox 2* (short: cx_2) measured the temperature at the top flange of the cavity's beam pipe. The blue positions show where the two heaters of the cavity are fixed. Heater 1 (short: h_1) on the lower beam pipe and Heater 2 (short: h_2) on the upper beam pipe. The magnetic mapping has also been coupled with a thermometry system, which can be seen on the right side of the setup sketch. The right side shows a picture of the setup. The magnetic boards are fixed around the cavity, so that the sensors get as close as possible to the cavity surface. Each red circle includes one three dimensional measurement point.

Setup of Array

The whole setup consists of a specific number of PCB boards. Here we used four boards arranged around the cavity in 90° steps. Each PCB has a shape similar to boards used in thermometry [6] that allows to place sensors on the cavity surface. All boards are attached to the cavity with a holder, every board had its own feedthrough, so that it is possible

ISBN: 978-3-95450-191-5 doi:10.18429/JACoW-SRF2017-TUPB083

POST PROCESSING OF A 166.6 MHz HEPS-TF CAVITY AT INSTITUTE OF HIGH ENERGY PHYSICS*

J. Dai†, Z.Q. Li, P. Zhang, Institue of High Energy Physics, Chinese Academy of Science, Beijing 100049, China

Abstract

A 166.6 MHz Proof-of-Principle (PoP) superconducting RF cavity has been fabricated by IHEP for the High Energy Photon Source Test Facility (HEPS-TF) [1]. After a series of post-processing including chemical etching (BCP), high temperature heat treatment, High Pressure water Rinsing (HPR) and 120℃ baking, the cavity was cold RF tested and reached $E_{peak} = 86.5$ MV/m and $B_{peak} = 132.1$ mT with $Q_0 = 5.1 \times 10^8$ at 4.2K. The cavity was RF tested again at 2K, and reached $E_{peak} = 85.5$ MV/m and $B_{peak} = 131.1$ mT with $Q_0 = 3.3 \times 10^9$.

INTRODUCTION

HEPS-TF mainly aims at the research and engineering verification of the key technologies needed for the construction and operation of High Energy Photon Source. The 166.6 MHz superconducting RF cavity is built to verify the key techniques of cavity parts in the program, mainly focus on cavity manufacturing and post-processing [2, 3]. The cavity was fabricated by Beijing HE-Racing Technology Co., Ltd. (HERT). After surface grinding, the cavity was sent to Ningxia Orient Superconducting Technology Co., Ltd (OSTEC) to proceed the chemical etching, 750℃ annealing and initial high pressure water rinsing. Then the cavity was sent back to IHEP in Beijing to perform the final HPR and 120 ℃ baking. The 4.2K cold RF test results suggest that cavity reaches $Q_0 = 2.4 \times 10^9$ when cavity voltage is 1.5MV, exceeding the design target 1.5MV, $Q_0 > 5 \times 10^8$ @ 4.2K.

CAVITY PROCESSING

The BCP facility is placed on a two storey house, with acid supply tank and acid circulating pipe on the first floor, and acid Storage Tank and pure water tank are placed on the second floor [4]. First, the acid solution is mixed in the acid supply tank according to the standard BCP recipe (Hydrofluoric HF (49%), Nitric (69.5%), and Orthophosphoric (85%)). The acid is mixed evenly by a blower inside the tank, meanwhile, is cooled to 12℃ through a cooling chiller.

The cavity structure is relatively complex for chemical etching. It has eight flanges, one for power coupler, one for pick-up, two for beam pipes and another four flanges for HPR. The acid flows through the larger beam pipe port and flows out of the other seven ports, allowing the flow of acid to be substantially uniform at each outlet, as shown in Fig. 1.

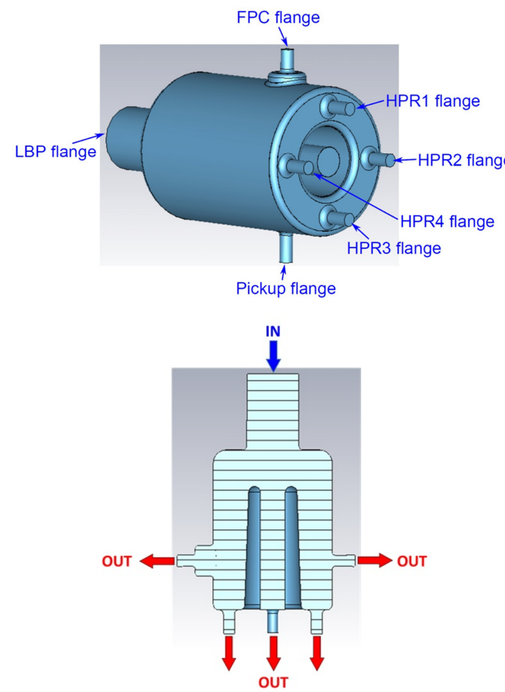

Figure 1: Acid path arrangement in cavity.

After the cavity is assembled in BCP system (see Fig. 2), the acid is pumped into the acid storage tank on the second floor, and then flowed into the circulation pipeline on the first floor by the action of gravity. In order to bring the heat generated by chemical action to cooling system, the acid is circulated in the system by a recirculation pump. This circulation and acid flow also help remove bubbles generated on the cavity surface so as to obtain a smooth cavity surface. During the acid circulation, two water chiller control the acid temperature ~15℃. After 75 minutes, ~70 μm etch is performed. The waste acid is dumped into an acid dump tank on the first floor and the DI water on the upstairs flows into the cavity and circulates about six circles to remove the residual acid on the cavity surface. Then the cavity is dismounted from the system and flipped vertically 180 degrees to perform another 50 μm chemical etching. During chemical etching, an ultrasonic gauge is placed on 28 locations on the outside surface of the cavity to monitor the etching amount. After 50 minutes etch and the following six cycles of DI water rinsing, the cavity is taken out of the pipe circulation system and sent to perform HPR to remove the residual chemicals on the surface.

*Work supported by High Energy Photon Source Test Facility (HEPS-TF) project
†daijin@ihep.ac.cn

Content from this work may be used under the terms of the CC BY 3.0 licence (© 2017). Any distribution of this work must maintain attribution to the author(s), title of the work, publisher, and DOI.

ISBN: 978-3-95450-191-5 doi:10.18429/JACoW-SRF2017-TUPB084

EP SYSTEM DEVELOPMENT AT IHEP*

Song Jin†, Jin Dai, Jie Gao, Dianjun Gong, Feisi He, Pei Zhang, Zhongquan Li, Zhenchao Liu, Peng Sha, Jiyuan Zhai, and Tongxian Zhao, Institute of High Energy Physics, Chinese Academy of Sciences, Beijing, China

Abstract

Electropolishing (EP) System is a critical facility for SRF cavity treatment, especially for high performance cavities which are necessary for several great projects like LCLS-II, CEPC, Shanghai XFEL, and so on. So, an EP system was under development at IHEP. At this stage, we would like a horizontal EP facility. Main purpose is for elliptical SRF Nb cavities like 500MHz single cell cavities. Besides, it should be compatible for other frequency cavities, such as 650MHz and 1.3GHz cavities. In this paper, we will mainly report the preliminary design for the EP system. Several key points in the design will be also discussed.

INTRODUCTION

EP as a critical technology for SRF cavity surface treatment was widely accepted and developed in the world [1]. In the beginning of EP development, it mainly shows advantages on the improvement of the cavity accelerating gradient. Taking, for example, it is proved that the application of EP could improve the accelerating gradient of ILC cavities from about 25MV/m by BCP treated to around 35MV/m. So, it became a standard procedure of ILC project. In recent years, EP also shows the importance in N-doping technology for High Q_0 studies, which was adopted by LCLS-II [2] and is also an important candidate for future projects like CEPC, Shanghai XFEL. Besides, for Future Circular Collider (FCC) project, a new EP facility is also under fabrication for copper surface treatment which will be used as substrate for Cu/Nb cavities [3]. So, we also would like to develop an EP system at IHEP for the R&D and projects on SRF cavities.

CAPABILITY GOAL OF THE EP SYSTEM

At present, there are two types of EP system. One is horizontal EP (HEP) system, and another is vertical EP (VEP) system. For VEP system, it is developed in recent years, and much later than HEP system. In VEP system, the cavity will not rotate along the axial direction. So, no rotation sleeves are needed. It will be more convenient for acid draining and compatible with DI water cleaning. So, it takes smaller space and lower cost comparing with the horizontal EP. However, at present, VEP still belong to state-of-the-art technology. Good results from VEP are still limited especially for project used cavities. So, as first step at IHEP, we will begin with HEP at this stage.

* Work supported by HEPS-TF project and Research Programme for Beijing Municipal S&T Commission
† Corresponding author email: jinsong@ihep.ac.cn

Taking account of possible projects in the future, such as HEPS, CEPC, Shanghai XFEL, and so on. We would like that the system can be compatibility for following cavities as shown in Fig. 1:

1) 500MHz single cell cavities;
2) 650MHz 2cell and 5-cell cavities;
3) 1.3GHz 9cell cavities.

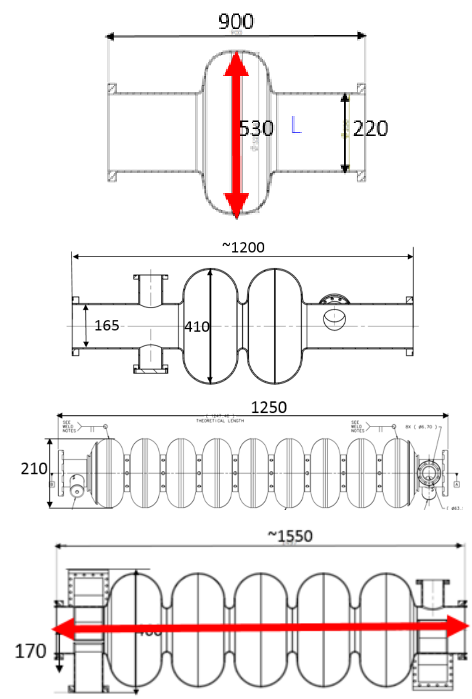

Figure 1: Sketches of four types of cavity prototypes which may need EP at IHEP. The frequencies of cavities from upper to lower are 500MHz, 650MHz, 1.3GHz, and 650MHz, respectively.

As we see in Fig. 1, although there are four types of the cavities, actually for EP system we only need to choose two types as consideration. One is 500MHz single cell cavity since it has a largest radial size. The other is 650MHz 5-cell cavity since it has a largest axial size and inside cavity volume.

SYSTEM DESIGN

Main Components of the System

Figure 2 shows main components for the whole system. It can be roughly divide into four parts:

1) Plumbing and Instruments;
2) Mechanical Structure;
3) Control and Data Logging;
4) Infrastructure;

Content from this work may be used under the terms of the CC BY 3.0 licence (© 2017). Any distribution of this work must maintain attribution to the author(s), title of the work, publisher, and DOI.

ISBN: 978-3-95450-191-5 doi:10.18429/JACoW-SRF2017-TUPB085

QUENCH DETECTION ON SUPERCONDUCTING CAVITY BY SECOND SOUND*

Zhenchao Liu†, Jie Gao, Feisi He, Haiying Lin, Pei Zhang, Institute of High Energy Physics, Chinese Academy of Sciences, Beijing, China

Abstract

High gradient is very important for superconducting cavity, however it may be limited by quench on the cavity high field region. Quench can be caused by various reasons. To locate the position is the key to reveal the mysteries of quench. OST sensor was widely used to locate the quench position. Now we are developing the quench position detection system by RTD sensors such as Cernox. In this paper, we will show the design of the second sound system and testing results on the QWR cavity.

INTRODUCTION

Second sound is an effective way to detect the quench position on superconducting cavity. It was first used to detect the quench position on the SC split-ring resonators at ANL by a germanium resistor sensor [1]. Oscillating Superleak Transducers (OST) were used to locate the quench site of the 1.3 GHz 9-cell cavity at Cornell University [2]. Later after that second sound quench site detection of SC cavity by OST was widely used on the world. Second sound detection was also used in standard dressed TESLA-Shape SRF cavity at DESY [3]. Other types of sensor were also developed to detect second sound. For example, transition edge sensors was used in second sound test [4, 5].

A second sound quench site detection system is in developing for the PAPS. We chose the highly sensitive thermometers such as germanium bare chip resistor or Cernox bare chip resistor as the second sound detection sensors. Tests with SC cavity and heater in liquid helium at 2K were taken.

A 166.7 MHz Quarter wave resonator (QWR) developed for the photon source was used for the quench site location. The detector was put close to the quench area with high magnetic field.

PRINCIPLE

The speed of second sound in He-II is proper to be used for position detection. It is about 17m/s at 2K.

The time duration (RF quench time and first second sound signal) times the speed of second sound is the distance between quench point and detector. The quench position can be calculated by three detectors with known positions. Figure 1 shows the second sound signal transporting from the quench point to the detectors. Figure 2 shows the speed of the second sound [6].

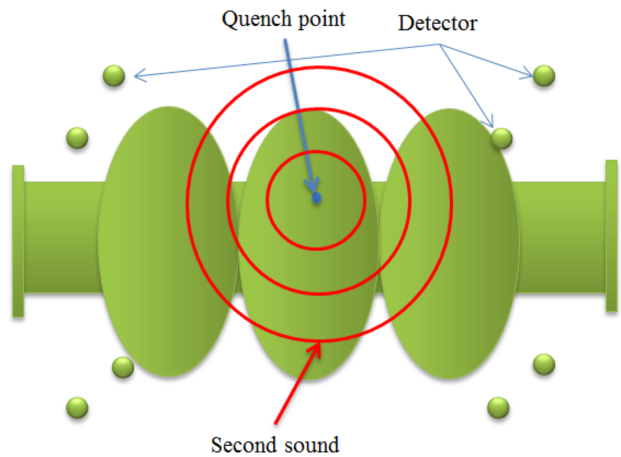

Figure 1: Principle of quench site detection by second sound.

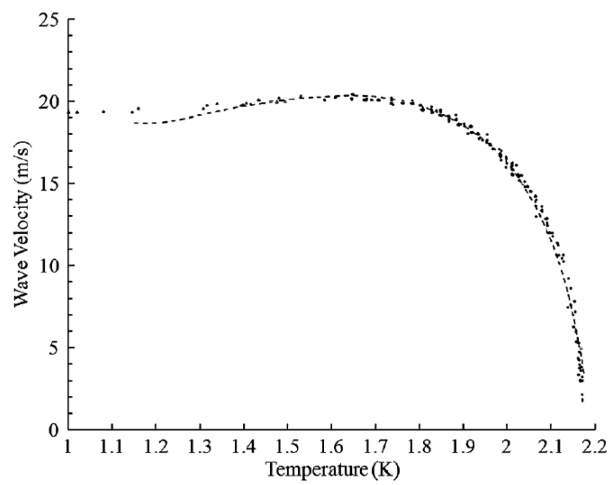

Figure 2: Velocity of second sound propagating in liquid helium.

EXPERIMENTS

There are several types of detectors can be used to detect the second sound signal. OST is a sensitive detector designed for second sound with a bias voltage. It was developed for detecting second sound only. Thermometer sensors can also be used to detect second sound signal such as Cernox bare chip sensors or germanium bare chip sensors. Transition edge sensors can also be used for such detections. Here we first tested the Cernox bare chip sensors and germanium bare chip sensors. We are also developing the OST sensor. It will be tested later and compared with the thermometry sensors.

* Work supported by PAPS
† zcliu@ihep.ac.cn

Content from this work may be used under the terms of the CC BY 3.0 licence (© 2017). Any distribution of this work must maintain attribution to the author(s), title of the work, publisher, and DOI.

18th International Conference on RF Superconductivity SRF2017, Lanzhou, China JACoW Publishing
ISBN: 978-3-95450-191-5 doi:10.18429/JACoW-SRF2017-TUPB086

Content from this work may be used under the terms of the CC BY 3.0 licence (© 2017). Any distribution of this work must maintain attribution to the author(s), title of the work, publisher, and DOI.

STUDY ON LOCAL CHEMICAL TREATMENT FOR RECOVERY FROM SURFACE OXIDATION BY HPR PROCESS ON SRF CAVITIES*

H. Guo†, P.R. Xiong, Z.X. Shi, Z.M. You, Y.K. Song, W.M. Yue, A.D. Wu, Y.M. Li, T. Tan, Y.He, S.H. Zhang, Institute of Modern Physics, Chinese Academy of Sciences, Lanzhou, China

Abstract

High pressure rinsing (HPR) with ultra-pure water (UPW) is the last step which is commonly used for SRF cavities cleaning. The serious surface damage will be caused due to the failure of the distance control between the nozzle and cavity surface or the breakdown of the wand rotation. The surface of taper HWR cavities which are used for CIADS project was damaged in HPR process. Two methods were used for surface recovery and the result will be presented in this paper.

INTRODUCTION

High pressure rinsing (HPR) is widely used as the final cleaning step in superconducting cavities post process. It could remove the residual acid and particles inside the cavity. An oxidation layer on niobium surface will be formed if the water jetted by high pressure impact on one spot and the distance between nozzle and niobium surface is very close [1]. A new HPR system is designed in IMP, which is used for HWR015 cavity cleaning. This kind of cavity is used for CIADS project [2]. Recently, the surface of HWR015 cavities was oxidized by this new HPR system. In this paper, we would show two methods which are used for surface recovery.

HPR SYSTEM

The new automated HPR system consisting of cavity fixture, a wand and nozzle has been designed and installed at IMP (see Fig. 1). It has 5 axles. The cavities can be moved and rotated, which make sure all ports of cavity can be cleaned without disassembly. The nozzle of HPR system have three fan jets, two side and one top (see Fig. 2).

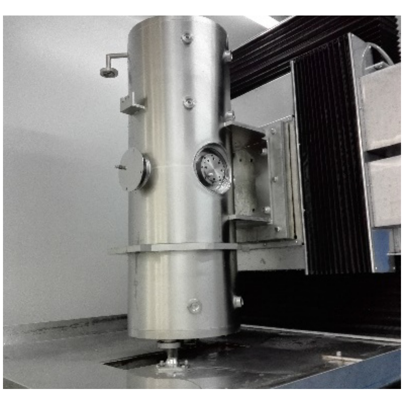

Figure 1: Automated HPR system.

* Work supported by the National Natural Science Foundation of China (91426303) and special fund on equipment from CAS.
† email address: guohao@impcas.ac.cn

Figure 2: The nozzle of HPR system.

SURFACE OXIDATION

During the HPR process of HWR015, the distance between nozzle and surface of inner conductor is too close (less than 50mm). The water sprayed from top jet impacted the surface for a long time. Then a bluish violet spot appeared on the centre of the surface (see Fig. 3). This spot is oxide layer caused by long time HPR, and it is certified by Tyagi and Sertore. [1,3,4] There were 4 cavities have oxide layer, and it is prepared for crymodule immediately. So a method should be found to solve this problem as soon as possible.

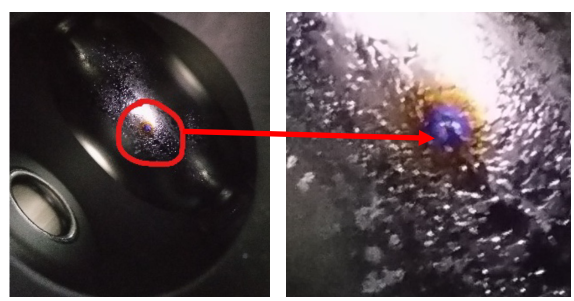

Figure 3: Bluish violet spot on the surface of inner conductor.

SURFACE RECOVRY

Local chemical treatment is the fastest method. It is use acid to etching the oxidized spot and remove the oxide layer. In order to test the result before and after local chemical treatment. Samples experiment have been done first.

Samples Experiment

At beginning, we prepared two samples of niobium which were impacted by HPR for 180 second. The surface of samples is oxidized obviously. (see Fig. 4 a and c). Two acids have been prepared for recovery experiments. The first acid is HF (40 wt%), the other one is BCP acid (HF: HNO_3 : H_3PO_4=1:1:2). The parameter of experiment see Table 1. After acid etching, the oxide layer disappeared obviously. Thus we can use these methods on cavities.

ISBN: 978-3-95450-191-5 doi:10.18429/JACoW-SRF2017-TUPB087

LOW TEMPERATURE AND LOW PRESSURE PLASMA FOR THE HWR SUPERCONDUCTING CAVITY IN-SITU CLEANING*

A.D. Wu†, L. Yang, C.L. Li, H. Guo, P.R. Xiong, W.M. Yue, W. Chang, Y.M. Li, S.H. Zhang, Y. He, H.W. Zhao, Institute of Modern Physics, CAS, Lanzhou, China
F.J. Gou, Sichuan University, Chengdu, China

Abstract

The glow discharge for low temperature and low pressures plasma were utilized for the half-wave resonator (HWR) superconducting cavity in-situ cleaning. The plasma was on ignition of the Argon/Oxygen mixture atmosphere, which was under the low pressure of 0.5 to 5.0 Pascal. Driven by the RF power with the frequency of the cavity fundamental mode, the plasma showed the typical characteristic of the typical RF glow discharge, which the temperature of the electrons about 1eV that diagnosed by the optical emission spectrum. The experimental parameters for the discharge were optimized to obtain the uniform plasma distribution on the HWR cavity, including the RF power, the atmospheric pressure and the oxygen proportion.

INTRODUCTION

Field emission in the superconducting radio frequency cavity is the major obstacle to operation at high accelerating gradients. The in-situ plasma processing developed at SNS has been proven to be an effective technology to solve the field emission issues for the elliptical cavities [1]. The low temperature and low pressure glow discharge, which was the chemically reactive oxygen plasma, was utilized to remove the contamination of hydrocarbons from the inner surface of the cavities at the room temperature.

The inert gas, as commonly using of argon and neon, mixed with few percent of oxygen as the working atmosphere was ignited by the RF power via the coupler. The plasma interaction with inner surface of cavity has two mechanisms: the ions bombarding the surface by physical sputtering progress, and the hydrocarbons chemically oxidized as the volatile substances desorption from the surface. The electric sheath between the plasma region and cavity surface with a bias voltage will accelerate the ions to bombard the surface. The bias voltage is determined by the electron temperature [2]:

$$V = -\alpha T_e . \tag{1}$$

Where, Te is the temperature of free electrons in scale of eV and the $\alpha = \ln(2\pi m_e/M_i)/2$ is a constant value. For Ar^+ and Ne^+ the α is 4.7 and 3.5 [2]. In addition, the electron number density is a significance parameter for rates of plasma-surface interaction.

To understanding of the plasma discharge property in the HWR type cavity and the plasma interaction with niobium surface during the in situ cleaning progress, the investigation on the characters of electron temperature and number density was studied on a half wave resonator which used in the CADS project. The plasma properties were diagnosed by the optical emission spectrum method.

EXPERIMENT SETUP

The experimental platform was consisted of radio frequency system, vacuum system and the optical emission spectrum (OES) system, as shown in Figure 1.

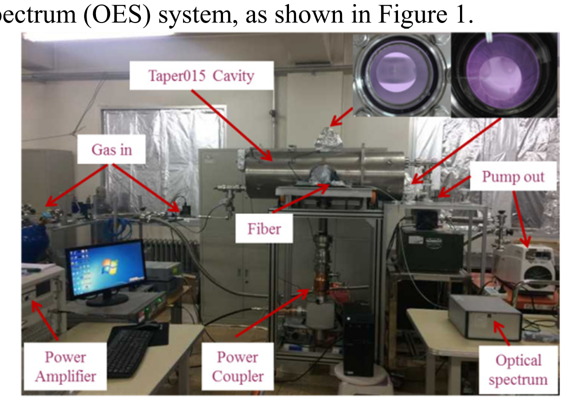

Figure 1: The plasma discharge experimental platform.

In order to be closer to the accelerator operation on the line, the type of Taper015 with the optimized beta of 0.15, which was used for CADS 25MeV linac, and a fundamental power coupler with the structure of dual ceramic windows were installed. However, the maxim of power amplify for this experiment was just 1kW, this value for operation on tunnel was 20kW. Thus the coupler antenna was adjusted for the coupling factor around 0.9.

The argon and oxygen were premixed with volume rate of 100: 3 under the control of two mass flowing controller (MFC). The premixed Ar/O_2 was fed to cavity through the third MFC. With help of pumping system, the gas pressure can be changed from 0.1 to 100 Pa on the cavity.

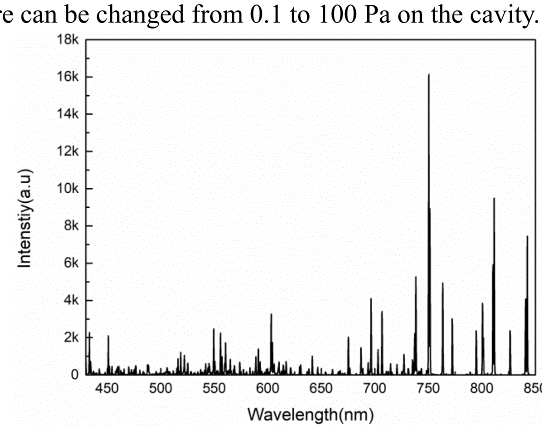

Figure 2: The OES spectrum of Ar/O_2 plasma discharge.

* Work supported by National Natural Science Foundation of China (91426303,11505255)
† Email address: antonwoo@impcas.ac.cn

Content from this work may be used under the terms of the CC BY 3.0 licence (© 2017). Any distribution of this work must maintain attribution to the author(s), title of the work, publisher, and DOI.

ISBN: 978-3-95450-191-5 doi:10.18429/JACoW-SRF2017-TUPB090

Content from this work may be used under the terms of the CC BY 3.0 licence (© 2017). Any distribution of this work must maintain attribution to the author(s), title of the work, publisher, and DOI.

INVESTIGATION OF HIGH TEMPERATURE BAKING OF JACKETED QUARTER WAVE RESONATORS

Abhishek Rai, Prakash N. Potukuchi, Somasundara Kumar Sonti, Padmanava Patra, Kishore Kumar Mistri and Dinakar Kanjilal

Inter-University Accelerator Centre (IUAC), Aruna Asaf Ali Marg, New Delhi 110067, India

Abstract

The Superconducting booster Linac at IUAC has been delivering accelerated ion beams for scheduled experiments since 2013 [1, 2]. It has three accelerating modules with eight Quarter Wave Resonators (QWR) (β_{opt}=0.08**)** in each module. The QWRs for the first module were built at Argonne National Laboratory while those for the second and third modules have been built in-house. During the electropolishing of one of the indigenously built resonators (QWR # I03) the RF surface got spoiled due to a wrong mixture of acid that was meant for etching. In subsequent cold tests of the cavity, its performance was poor (2.6 MV/m @ 4 W). There was evidence of Q disease also, as the performance deteriorated further (~20%) when the cavity was held at 100-120 K for ~8 hours .In an attempt to recover the cavity, it was baked at 650 °C for 10 hours along with its outer stainless steel jacket. A series of tests were conducted thereafter, wherein a substantial improvement (**A** factor of two) in the performance was observed. Encouraged by these results**,** another QWR designed for a lower beta (β_{opt}=0.05) was also heat treated identically. This improved its performance in a similar fashion. This paper presents the different treatments followed to enhance the cavity performance vis-à-vis the test results.

INTRODUCTION

The Superconducting Linac at IUAC, which serves as a booster to the 15 UD Pelletron accelerator [3], uses Niobium Quarter Wave Resonators (QWR) as the accelerating element. It has a total of 27 QWRs installed in 5 cryostats. These are, a Superbuncer cryostat housing one, three Linac cryostats each housing eight and a Rebuncher cryostat with two QWRs respectively. Figure 1 shows the schematic of the Pelletron-Linac system at IUAC.

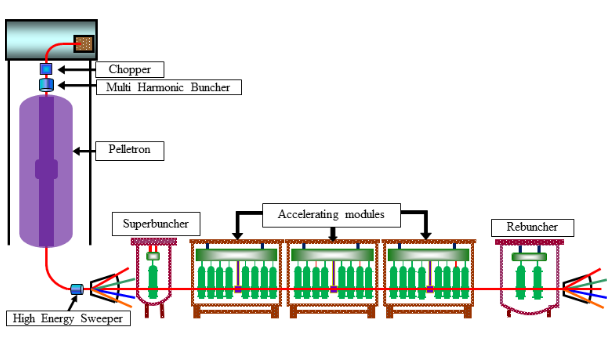

Figure 1: 15 UD Pelletron-Linac system.

The QWR was designed and developed in collaboration with Argonne National Laboratory (ANL) [4, 5]. The first batch of 12 QWRs were built at ANL. Resonator fabrication facilities [6] were thereafter setup at IUAC and the remaining QWRs for the Linac were built in-house. These facilities include an electron beam welding machine, a surface treatment lab and a high vacuum annealing furnace. The first indigenous QWR (QWR # I01) was fabricated using the Niobium sub-assemblies left over from the ANL project. This was completed in the year 2003. The resonator achieved an accelerating gradient of 5 MV/m at 6 W of input power at 4.2 K, surpassing the design goal of 4 MV/m @ 6 W. It was subsequently installed in the Linac. Two more cavities (QWR # I02 and I03) were thereafter fabricated to freeze the fabrication algorithm and develop confidence in the indigenous fabrication procedures. QWR #I02 was successfully tested offline and was installed in the Linac. QWR # I03 was also tested offline after a light Electropolishing (EP) and the results were promising. To further improve the cavity performance it was given another round of EP. During the process it suffered an accident which resulted in an uneven etching of the RF surface. In a subsequent test the cavity performance was very poor and there was significant frequency detuning. The resonator was henceforth used as a test piece for doing microphonics measurement and other developments at room temperature.

QWR # I03 HISTORY

QWR # I03 was one of the first cavities that could be termed as a complete indigenous fabrication in the sense that all the niobium sub-assemblies were built in-house. Post fabrication, the cavity was given a light EP (~20µm) (this was besides ~250 µm of EP done during fabrication). In the subsequent cold test it achieved a gradient of 3.1 MV/m @ 3.5 W (Q =1.8×10^8) @ 4.2 K. Q measurements could not be done at higher powers due to shortage of LHe supply. It was decided to EP the cavity to remove another ~50 µm from the surface before installing it in the Linac. During the second EP, as soon as the electrolyte was transferred into the cavity, the acid temperature shot up to ~ 55 °C and spontaneous uncontrolled etching of the surface started. This was accompanied with the emission of brown fumes (possibly NO_2). All these symptoms pointed towards the contamination of the EP electrolyte with HNO_3. The contaminated electrolyte was immediately pumped out but the damage had already been done. The RF surface became very rough (almost like scales of a fish), as shown in

ISBN: 978-3-95450-191-5 doi:10.18429/JACoW-SRF2017-TUPB091

STUDY ON VERTICAL ELECTROPOLISHING OF NINE-CELL NIOBIUM COUPON CAVITY

V. Chouhan†, Y. Ida, K. Nii, T. Yamaguchi, Marui Galvanizing Co., Ltd, Himeji, Japan
H. Hayano, S. Kato, H. Monjushiro, T. Saeki, M. Sawabe, High Energy Accelerator Research Organization (KEK), Tsukuba, Japan

Abstract

We report a study on vertical electropolishing (VEP) performed for a 1.3-GHz nine-cell niobium (Nb) coupon cavity using a unique cathode called Ninja Cathode. The design of the cathode for VEP of a nine-cell cavity was based on the Ninja cathode used for single-cell cavity since the Ninja cathode reduced longitudinal asymmetry in material removal and yielded smooth surface of the single-cell cavity. Moreover, single-cell Nb cavities after being treated in VEP using Ninja cathodes showed good performance in vertical RF tests. The nine-cell coupon cavity used in this study was designed to have totally nine coupons set on the iris and equator positions of the first, fifth and ninth cells. These three cells also contain viewports near the upper and lower iris positions. Measurement of currents for the individual coupons and in-situ observation are possible using the viewports to understand EP phenomenon at different locations of the cavity. VEP results, which include removal thicknesses at different positions of the cavity and surface study of the coupons, are discussed.

INTRODUCTION

Electropolishing (EP) process is adopted as the final surface treatment of niobium (Nb) superconducting RF cavities to achieve their good performance in terms of field gradient and quality factor. A cavity is currently electropolished (EPed) in a horizontal posture in the so-called horizontal EP process. A vertical EP (VEP) process, which supposed to be a cost effective method, is currently under research for optimization of EP parameters. Earlier we have introduced the issues, which appear in the VEP process, including longitudinal asymmetric removal and rough surface of a cavity [1]. In order to minimize the issues, a unique cathode called Ninja cathode with four retractable blades was developed and applied to single-cell cavities. The cathode minimized removal asymmetry and roughness of the entire surface inside the cavities [2–4].

This work describes application of the Ninja cathode on the nine-cell coupon cavity [5, 6] and its effect on the cavity surface and removal.

EXPERIMENT

Ninja Cathode

The Ninja cathode for a nine-cell cavity was prepared with the similar design that of the Ninja cathode applied to the single-cell cavity as reported elsewhere [4]. The Ninja cathode for a nine-cell cavity contained 3 insulating blades and covered with PTFE meshed sheet to reduce a number density of H_2 bubbles in the cavity cells.

Nine-cell Coupon Cavity

A nine-cell coupon cavity (9-CCC) was designed to have nine coupons set at different locations of the cavity. The first (top), fifth (center) and ninth (bottom) cells contain coupons at the equator and near upper, and lower iris positions. The coupons at the irises were set with viewports. Figure 1 shows schematic of cavity with positions of the coupons and viewports. The detail of the 9-CCC is given in Ref. [5]. EP currents from the individual coupons and cavity can be measured. The viewports were used to take movies and observe behaviour of gas bubbles and the effect of blades on the cavity surface.

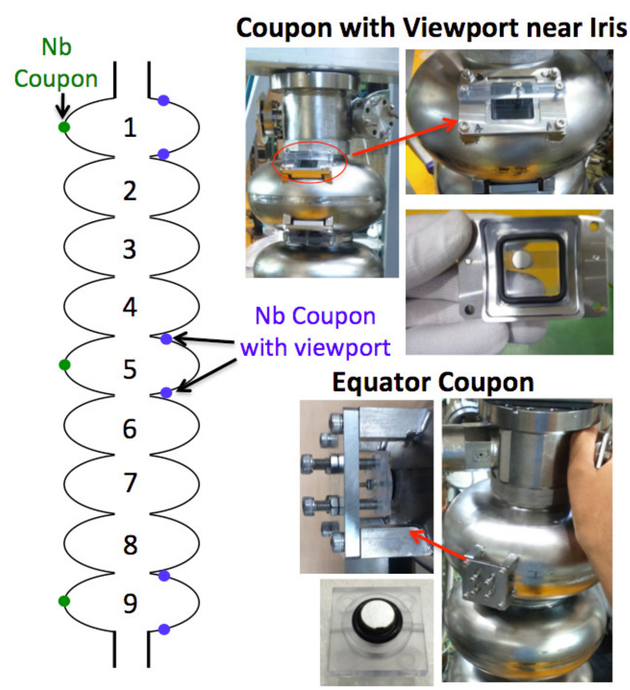

Figure 1: Photographs and schematic show coupons and viewports and their positions at irises and equator.

VEP Setup

A system was designed to perform VEP of nine-cell and single-cell cavities. The system is equipped with separate acid and water pipelines, flow meters, an acid reservoir, water spray facility for cooling of the cavity, a water reservoir for spray water, heat exchangers for the

† vchouhan@e-marui.jp

Content from this work may be used under the terms of the CC BY 3.0 licence (© 2017). Any distribution of this work must maintain attribution to the author(s), title of the work, publisher, and DOI.

ISBN: 978-3-95450-191-5 doi:10.18429/JACoW-SRF2017-TUPB092

ANALYSIS OF NIOBIUM SURFACE AND GENERATED PARTICLES IN VERTICAL ELECTROPOLISHING OF SINGLE-CELL COUPON CAVITY

V. Chouhan†, Y. Ida, K. Nii, T. Yamaguchi, Marui Galvanizing Co., Ltd, Himeji, Japan
H. Hayano, S. Kato, H. Monjushiro, T. Saeki, M. Sawabe, High Energy Accelerator Research Organization (KEK), Tsukuba, Japan

Abstract

In our previous studies, we have reported parameter investigation for vertical electropolishing (VEP) of one-cell niobium (Nb) Tesla/ILC type cavities using a Ninja cathode. A one-cell coupon cavity containing six Nb disk coupons at its different positions was found effective to reduce time and cost to establish an optimized VEP recipe. In this work, we present surface analyses of VEPed Nb coupon surfaces using scanning electron microscope (SEM), energy dispersive x-ray spectroscopy (EDX) and x-ray photoelectron spectroscopy (XPS). Surfaces contained micro- and nano-sized particles which were found with random distributions and different number densities on the beam pipe and iris coupons. Surfaces of equator coupons were found to have relatively less number of particles or almost clean. To analyze particles, a few particles were picked-up from a coupon surface using a tungsten tip under SEM and analyzed with EDX, while the coupon was moved out from the SEM chamber to avoid its effect in EDX spectra. The particles were confirmed as oxygen-rich niobium and contained fluorine and carbon also. XPS analysis of the coupon surfaces was also performed for further study of surface chemistry.

INTRODUCTION

Niobium (Nb) superconducting radio-frequency cavities are used in the accelerator facilities worldwide. Performance of the Nb cavities depends on the inner surface morphologies and the contaminants present at the cavity surface. The contaminants present on a cavity surface enhance the risk of field emission which limits the cavity performance. The surfaces of Nb samples after being treated with the electropolishing (EP) process, which is used as the final surface treatment of Nb cavities, were widely studied. The previous studies reported sulfur (S) and fluorine (F) contaminants on the EPed surfaces [1−3]. Some studies have found Nb particles on the cavity surface [2, 3]. However, generation mechanism of such Nb particles is still unclear and elemental information of such particles is not enough. Therefore, further study to ascertain the conditions in which such particles are formed and detailed elemental study of such particles should be performed. We have already reported a surface treatment process of single-cell cavities with the vertical electropolishing (VEP) performed using a unique cathode named Ninja cathode [4−7]. In this study, we present the particle distribution at different positions of the single-cell coupon cavity by analyzing the Nb coupons, which were set to the cavity in the VEP process. The study also shows surface analysis of Nb samples EPed in a beaker at laboratory scale, and was aimed to determine the process in which particle formation occurs on the EPed surface.

† Email address: vchouhan@e-marui.jp

EXPERIMENT

Vertical EP

VEP experiments of a single cell Nb coupon cavity were carried out using a setup as reported elsewhere [4]. The cavity was designed to have six Nb disk type coupons at beam pipe, iris and equator positions as illustrated in Ref. [4]. A VEP experiment was performed with a special cathode named Ninja cathode which contains retractable blades. The blades were made of insulator, whereas Al cathode parts were set on the insulating blades [5, 6]. VEP were performed with the standard electrolyte (98wt% sulfuric acid and 55wt% hydrofluoric acid in a volumetric ratio of 9:1) used for EP of Nb cavities. VEP was performed with Ninja cathode's rotation speed of 30 rpm, acid circulation in the cavity from the bottom to top direction with a flow rate of ~5 l/min, a cavity temperature below 25°C, and at an applied voltage of ~12 V. The VEP experiment lasted for 80 min to remove Nb with a thickness of ~50 µm. The EP acid was circulated in the cavity for ~15 min after the voltage was turned-off. The cavity was rinsed with pure water after the acid was drained-out.

Laboratory EP

Lab EP experiments were performed for Nb samples prepared in a size of 20 x 14 mm^2 from the same Nb sheet that was used to make Nb coupons for VEP experiments. Therefore, all the samples and coupons had the same initial surface with rolling marks and an average roughness Rz of ~4.5 µm. Nb samples used as an anode were set in an EP bath while an Al plate was set as a counter electrode. The EP of the samples were performed at stirring speeds of 0, 80 and 170 rpm for a removal thickness of ~50 µm. In each experiments, two samples were EPed at the same time. EP bath temperature was maintained at ~20°C.

Surface Analysis

The coupons and sample surfaces were observed with a scanning electron microscope (SEM). The SEM chamber maintained at ultrahigh vacuum was equipped with energy dispersive x-ray spectroscopy (EDX) and a field emission scanner (FES). The FES was designed with a scanning anode tungsten (W) needle with a sharp tip. The needle can be moved in xyz directions with a precision of

Content from this work may be used under the terms of the CC BY 3.0 licence (© 2017). Any distribution of this work must maintain attribution to the author(s), title of the work, publisher, and DOI.

ISBN: 978-3-95450-191-5 doi:10.18429/JACoW-SRF2017-TUPB093

Content from this work may be used under the terms of the CC BY 3.0 licence (© 2017). Any distribution of this work must maintain attribution to the author(s), title of the work, publisher, and DOI.

Nb SINGLE-CELL CAVITY VERTICAL ELECTRO-POLISHING WITH NINJA CATHODE AND EVALUATION OF ITS ACCELERATING GRADIENT

K. Nii#, V. Chouhan, Y. Ida, T. Yamaguchi, Marui Galvanizing Co., Ltd., Himeji, Japan
H. Hayano, S. Kato, H. Monjushiro, T. Saeki, M. Sawabe, KEK, Tsukuba, Japan
P. Carbonnier, F. Eozenou, Y. Gasser, L. Maurice, T. Proslier, C. Servouin, CEA-Saclay, Gif-Sur-Yvette, France

Abstract

Marui Galvanizing Co., Ltd. has been improving Vertical Electro-Polishing (VEP) technology for Nb superconducting RF cavity in collaboration with KEK. In this collaboration, we developed a unique cathode namely "Ninja cathode" for VEP treatment of Nb cavities. We have already reported that longitudinal symmetry in niobium removal and surface state of a single cell cavity were improved after VEP using the Ninja cathode. In this article, we report a result of accelerating gradient evaluation for 1.3 GHz single cell RF cavity after VEP with Ninja cathode.

INTRODUCTION

Marui Galvanizing Co., Ltd. has been developing Nb SRF cavity vertical electro-polishing (VEP) technologies for cavity mass production and manufacturing cost reduction in collaboration with KEK. Until now, construction and improvement of VEP facility and original structure cathode "i-cathode Ninja" (Ninja cathode) have been performed [1–9]. Using these items and a single cell coupon cavity whose coupon surface can be evaluated in detail after VEP, we performed VEP experiments many times and reported that surface status and removal thickness distribution were improved in comparison with conventional VEP [2, 6, 8].

Furthermore, in order to apply VEP for cavity mass production, evaluation of cavity's accelerating gradient after VEP with Ninja cathode is required. To approach this issue, single cell cavity VEP with Ninja cathode and accelerating gradient evaluation were performed in collaboration with Marui – KEK – CEA Saclay.

NINJA CATHODE AND VEP SETUP

In this experiment, CEA Saclay's single-cell cavity (C1-19, after buffered chemical polishing (BCP)) was VEPed with Marui's VEP facility and Ninja cathode. The Ninja cathode used in this experiment has 4 insulating wings and enhanced cathode area (Ninja-3). It was proved that polished surface and removal thickness distribution were improved by using this Ninja cathode for VEP. Figure 1 shows the schematic view of Ninja cathode (Ninja-3).

#keisuke_nii@e-maui.jp

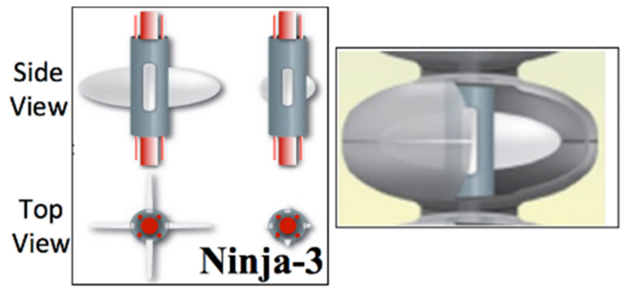

Figure 1: Schematic view of Ninja cathode (with 4 insulating wings and enhanced cathode area, Ninja-3).

The process of this experiment was bulk VEP1 (target removal 50 um) – status conformation – bulk VEP2 (target removal 50 um) – status conformation – HPR and anneal – final VEP (target removal 10 um) – HPR and vertical test (VT). HPR and anneal were performed in KEK, HPR and VT were performed in CEA Saclay. Before this VEP, inner surface was inspected with Kyoto camera and found defects were locally grinded in KEK. Figure 2 shows the VEP setup and the single-cell cavity.

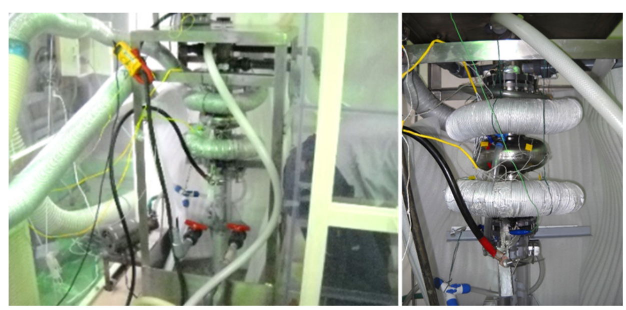

Figure 2: Photos of the VEP setup and the single-cell cavity.

VEP EXPERIMENT AND VERTICAL TEST RESULT

Table 1 shows conditions of bulk VEP1, bulk VEP2 and final VEP. The VEP parameters were selected according to previous VEP experiments that show good results. The anneal condition was 750°C, 3hours. Figure 3 shows the logged data of voltage and current density of each VEP.

ISBN: 978-3-95450-191-5 doi:10.18429/JACoW-SRF2017-TUPB095

Content from this work may be used under the terms of the CC BY 3.0 licence (© 2017). Any distribution of this work must maintain attribution to the author(s), title of the work, publisher, and DOI.

MODELING THE HYDROFORMING OF A LARGE GRAIN NIOBIUM TUBE WITH CRYSTAL PLASTICITY*

A. Mapar, T. R. Bieler†, Michigan State University, East Lansing, MI 48824, USA
F. Pourboghrat, The Ohio State University, Columbus, OH 43210, USA
J. E. Murphy, University of Nevada, Reno, NV 89557, USA

Abstract

Current SRF cavities are made from fine grained polycrystalline niobium half-cells welded together. Hot spots are commonly found in the heat-affected zone, making seamless hydroformed cavities attractive. Large grain cavities usually perform as well as fine grain cavities, often having a higher Q, presumably due to fewer grain boundaries. Large grain Nb forms non-uniformly, which introduces problems in manufacturing. A model that could realistically predict the deformation response of large grain Nb could facilitate the design of large grain hydroformed tubes.

To this end, a crystal plasticity model was developed and calibrated with tensile stress-strain data of Nb single crystals. A seamless large grain tube was made from rolling a fine grain sheet into a tube, welded, and heat treated to grow large grains. The heat treatment resulted in a large grain tube with a single grain orientation in the center. The tube was hydroformed until it cracked. The hydroforming process was simulated with the crystal plasticity model, which was able to predict the deformed shape of the tube, the location of the crack and other localized areas with heterogeneous strain.

INTRODUCTION

The International Linear Collider (ILC) project will require a very large amount of niobium (Nb) to fabricate cavities in a limited time. This large future demand has stimulated alternative cavity fabrication strategies such as directly slicing disks out of as-cast Nb ingots [1] which eliminates the costly Nb sheet rolling process [2] and reduces waste for axisymmetric parts. It has been shown that cavities manufactured from large grain (grains larger than 5-10 mm) sheets often have a better superconducting radio frequency (SRF) performance than the fine grain (grain size in range of 50 μm) sheets [2, 3]. This increase in performance is correlated with the presence of fewer grain boundaries in the material. Also, the sheet rolling process can introduce impurities to the material. Slices that are cut form from an ingot potentially have fewer defects per unit volume.

Nb ingots are manufactured by electron beam melting of a Nb feedstock. This molten Nb drips into a continuous casting mold. The ingot made with this process has a nearly columnar grain structure. As single crystal ingots are routinely fabricated in other materials, it may be possible to fabricate ingots with a preferred orientation [1]. However, the intrinsic plastic anisotropy of Nb single crystals [4, 5] will lead to non-uniform forming, which must be anticipated.

Particle accelerator cavities are traditionally made from deep drawing of a Nb sheet into bowl shapes having a hole in the center. Two bowls are welded together to make an elliptical cavity. Then a tube with the inner diameter equal to the diameter of the holes is welded to each end to make a single cell cavity.

The standard deep drawing process for manufacturing particle accelerator cavities, is not an optimal process. A manufacturing process like tube hydroforming has the potential to fabricate a cavity from a single piece of tube, and the lack of welding could lead to better reproducibility and improve the performance of the cavity while reducing the manufacturing costs. Tube hydroforming is a forming process in which an internal hydraulic pressure imposes the deformation force.

The goal of this research is to study the possibility of making a particle accelerator cavity from the large grain tube that was previously made [6]. The current study uses a crystal plasticity model with dynamic hardening rule that was presented in [7] to predict the hydroforming of a large grain Nb tube.

MAKING A LARGE GRAIN TUBE

To provide a means to examine effects of large grain material on hydroforming, a seamless large grain Nb tube with an outer diameter of 38 mm was made from a 2 mm-thick polycrystal Nb sheet. The tube was manufactured by Dr. Jim Murphy at University of Nevada, Reno.

A rectangular Nb sheet was bent into a 38 mm (1.5 inch) outer diameter tube and arc welded. To grow the crystals and convert the initial microstructure to a large grain structure, the tube was locally heated to a very high temperature (near the melting temperature) in a high vacuum (~5×10^{-6} torr) furnace. The vacuum reduced impurities that have a lower melting point and a higher vapor pressure. The hot zone was then moved along the length of the tube with a fixed velocity, which encouraged recrystallization and grain growth parallel to the tube axis. More details about the tube making process is given in [6].

CHARACTERIZATION OF THE TUBE

After the heat treatment, the orientation of the tube was examined with a Laue camera. Laue measurement is an X-ray diffraction based technique and does not need to be performed in a vacuum.

* Work supported by the U.S. Department of Energy, Office of High Energy Physics, through Grant No. DE-FG02-09ER41638.
† bieler@egr.msu.edu

ISBN: 978-3-95450-191-5 doi:10.18429/JACoW-SRF2017-TUPB096

SRF CAVITY ASSEMBLY IN CLEAN ROOM WITH HORIZONTAL LAMINAR FLOW

Akihiro Miyamoto†, Hiroshi Hara, Katsuya Sennyu, Takeshi Yanagisawa, Mitsubishi Heavy Industries Mechatronics Systems, Ltd, Kobe, Japan

Abstract

Mitsubishi Heavy Industries Mechatronics Systems, LTD. and our group company, hereinafter MHI group, have introduced a clean room for assembling superconducting RF cavity. Unlike a usual clean room with vertical laminar flow, this is a clean room with horizontal laminar flow. We have assembled SRF cavity in this clean room and obtained a good result in vertical test. SRF cavity assembly in clean room with horizontal laminar flow is rare in the world, but it has advantages in improving workability of cryomodule assembly. We report the case of applying clean room with horizontal laminar flow to SRF cavity assembly.

PROBLEM OF CONVENTIONAL CLEAN ROOM

In order to achieve high accelerating gradient, special attention is required so that the particulates do not contaminate inside of SRF cavity. Therefore, a work that needs to open the flange of the cavity must be performed in a clean room with ISO4 or ISO5 cleanliness.

Generally, in this class of clean room, the HEPA filter is installed on the ceiling, the porous floor is installed on the floor surface, and laminar flow from the ceiling to the floor surface purifies the air. This type of clean room with vertical laminar flow is widely used in the world, but has problems as follows.

- Construction cost of the clean room is expensive.
- Maintenance cost of the clean room is also expensive.
- Once the clean room is contaminated by particulates, it takes a long time to recover the cleanliness.
- It is difficult to handle heavy objects in the clean room because it is restricted to bring a general lifting tool that generates dust into the clean room. Therefore, special lifting tools which do not generate particulates must be designed, manufactured and used at a high cost.
- There are many procedures for the workers before they enter the clean room in order to minimize the contamination of particulates from the outside. The workability is not good.

FLOOR KOACH

Floor COACH Ez is an advanced clean room developed and manufactured by KOKEN Ltd. This clean room consists of fan filter units, guide screen and collision wall. Fan filter units are constructed by stacking multiple fan filter units, KOACH F 1050-F (See Figure 1). Filtered air has uniform velocity and direction. The air flows horizontally downstream along the guided screen. The space between the downstream end of the guide screen and the collision wall is open. The air flow hitting on the collision wall is discharged from this open part. The air flow can capture particulates in the air and discharged particulates from the clean room. And under ideal condition, ISO1 cleanliness is obtained in the area surrounded by fan filter unit, guide screen and collision wall. (See Figure 2 for outline of the Floor KOACH Ez). This clean room is not sealed at all and it is quite different from a normal clean room. But this characteristic gives us many advantages in SRF cavity assembly.

Figure 1:Fan filter unit KOACH F 1050-F, W1050 ×D627×H929mm, Source of drawing: Product catalogue of KOKEN LTD..

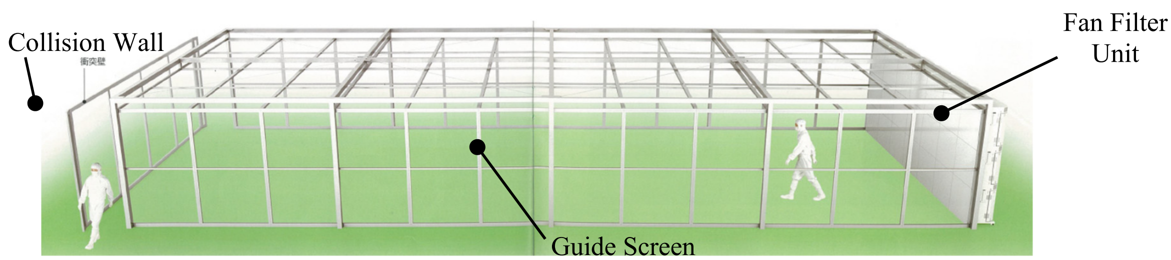

Figure 2: Floor KOACH Ez, source of drawing: product catalogue of KOKEN LTD..

† email address akihiro_miyamoto@mhims.co.jp

Content from this work may be used under the terms of the CC BY 3.0 licence (© 2017). Any distribution of this work must maintain attribution to the author(s), title of the work, publisher, and DOI.

ISBN: 978-3-95450-191-5 doi:10.18429/JACoW-SRF2017-TUPB097

R&D OF ELECTRO-POLISHING (EP) PROCESS WITH HF-FREE NEUTRAL ELECTROLYTE BY BIPOLAR-PULSE (BP) METHOD

Junji Taguchi, Kohei Ishida, Yasuhiro Mochida, Toshiyuki. Nakajima, Nomura plating Co., Ltd, Nishiyodogawa, Osaka Japan
Satoru Kakudo, Masanori Kunieda , The University of Tokyo, Tokyo, Japan
Hitoshi Hayano, Takayuki Saeki†, KEK / Soukendai, Tsukuba, Ibaraki, Japan

Abstract

Currently the Electro-Polishing (EP) process of Superconducting Radio-Frequency (SRF) accelerating niobium (Nb) cavity is performed with the electrolyte that is the mixture of hydrofluoric and sulfuric acids. However, the electrolyte is very dangerous and the environmental load in the disposal process of electrolyte is very heavy. This is the reason why the high cost is necessary in the safe design of facility and the safe operation of process in the conventional EP method. In such a situation, considering the reduction of cost and environmental load in the EP process, we performed the R&D of novel EP process with HF-free neutral electrolyte by Bipolar-Pulse (BP) method. In this presentation, we will report the removal rate, surface roughness and the results of surface analysis for the Nb-coupon samples that were processed by the BP-EP with HF-free neutral electrolyte.

INTRODUCTION

Final surface preparations of Superconducting Radio-Frequency (SRF) niobium (Nb) cavities play a critical role in order to achieve high performance of SRF accelerator. Electro-Polishing (EP) process with electrolyte that is the mixture of sulfuric acid (H_2SO_4) and fluoric acid (HF) is thought to be the best final surface preparation method to achieve higher gradient of SRF cavity and it has already been conventional technology around the world as the standard [1]. Development of Electro-Polishing (EP) method that does not use fluoric acid is desired in the mass-production of SRF cavities in the future project like ILC, because the electrolytic solution used in this method is very dangerous for the operator due to toxic gases (ex. HF, H_2S, SO_x) generated in the process and then the complex instrumentation and operation are required for the safety which increase the cost. In addition, it is reported that sulfur is produced as byproduct in the process and this causes degradation of cavity performance [2]. Equation (1) shows the chemical reaction which creates sulphur as by-product.

$$x\mathrm{H_2S} + \mathrm{SO}x \rightarrow x\mathrm{H_2O} + \mathrm{S} \qquad (1)$$

Then the development of Electro-Polishing (EP) method without sulfur is also desired. In such a situation, Faraday Inc. and FNAL have studied the Electro-Polishing (EP) by Bipolar-Pulse (BP) method with diluted H_2SO_4 electrolyte for the SRF cavity [3]. In the BP-EP method, the sign of applied voltage is periodically switched to positive and negative (Bipolar-Pulse) in the EP process. Typical Bipolar-Pulse (BP) current in BP-EP process is shown in Fig. 1. In the plating process, this method has been widely used and applied in industries in order to obtain uniform thickness of plating. We already performed series of experiments for the BP-EP process of Nb coupon samples with alkaline electrolyte, i.e. diluted NaOH solution, and achieved smooth surface of Nb-coupon sample [4-6]. Therefore, the diluted H_2SO_4 and/or NaOH electrolytes are already used in the HF-free BP-EP process of Nb surface. However, if we could perform the BP-EP with neutral electrolyte, we can achieve extremely safe BP-EP process and also extreme cost-reduction.

In this paper, we report the BP-EP method with neutral electrolyte. The advantages of neutral electrolyte are listed as followings. 1) Neutral solution is safer than acid and/or alkaline solutions. The BP-EP facility becomes much simpler and the cost of facility might be reduced more drastically. 2) The safety issues in the operation of BP-EP process become much simpler and the operation cost might be reduced more too. It means that the mass-production of SRF Nb cavities might become easier and the cost of cavity might become cheaper. 4) In general, the electrolytic removal processes typified by the micro electro-discharge machining process are based on the neutral electrolyte. Such technologies might give the hint to apply the neutral electrolyte to the BP-EP of Nb surface.

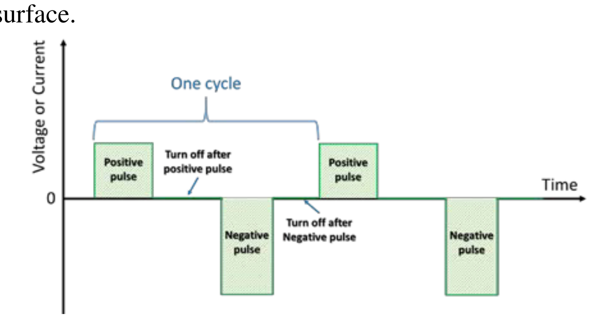

Figure 1: Typical wave form of periodic Bipolar-Pulse (BP) current.

We studied the BP-EP process with neutral electrolyte in the following three steps:

- We selected the best anion in the neutral electrolyte by using several acid solutions in the BP-EP process with Nb-coupon samples.

†takayuki.saeki@kek.jp

Content from this work may be used under the terms of the CC BY 3.0 licence (© 2017). Any distribution of this work must maintain attribution to the author(s), title of the work, publisher, and DOI.

ISBN: 978-3-95450-191-5 doi:10.18429/JACoW-SRF2017-TUPB098

THE EFFECT OF PROCESS PARAMETERS ON THE SURFACE PROPERTIES OF NIOBIUM DURING PLASMA ETCHING*

J. Peshl†, Old Dominion University, Norfolk, VA, USA
A.-M. Valente-Feliciano, Thomas Jefferson National Laboratory, Newport News, VA, USA
J. Upadhyay, Los Alamos National Laboratory, Los Alamos, NM, USA
S. Popovic, L. Vuskovic, Old Dominion University, Norfolk, VA, USA

Abstract

We have shown that plasma etching using an electronegative Ar/Cl_2 discharge can effectively remove surface oxide layers on Nb samples as well as bulk Nb from single cell SRF cavities [1]. With accelerating fields on the order of wet etching processes and a decrease in field emission the use of plasma assisted etching for bulk Nb processing is a worthwhile endeavor. We are presenting work on the surface properties of plasma etched Nb. Cavity grade Nb coupons were made by water jet cutting, and then polished to achieve surface properties equivalent to electropolishing (<1 micron). The coupons were plasma etched while process parameters (rf power, gas pressure, temperature and dc bias voltage) are varied. These samples are placed on the inner surface of the cylindrical cavity to be etched. The experimental setup is similar to the single cell cavity plasma etching setup [2]. Each sample is weighed and scanned before and after plasma processing with an AFM, SEM, and digital optical microscope that provide both atomic composition and surface roughness profiles. Comparing the scans allows us to make conclusions about the effect of each experimental parameter on the surface properties.

INTRODUCTION

Superconducting radio frequency (SRF) Niobium (Nb) cavities require sufficient surface preparation before they can be considered for use in high energy particle accelerators. Improving the cavity's surface smoothness, the removal of surface impurities, and dulling the effect of grain boundaries all have significant impacts on the cavity's performance. Currently, buffered chemical polishing (BCP) or electropolishing (EP) are the most common methods for achieving satisfactory surface characteristics [3]. These processes, while effective, require the use of hydrogen flouride liquid acid baths, of which pose great environmental and human safety concerns. The semiconductor industry has been successful for a number of years in using "dry" plasma etching for the processing of silicon wafers. Using this as inspiration, plasma etching of a 3-D asymmetric Nb surface has proven to be a promising alternative to wet etching techniques [1, 2, 4–6]. This plasma etching alternative has the opportunity to provide a more controllable, cost effective, and safer form of surface modification that can achieve accelerating fields and Q-factors on the order of it's wet etching counterparts. In addition, plasma etching seems to reduce the field emission of SRF Nb cavities significantly, making the endeavor all the more worthwhile [1].

We have shown that plasma etching using an electronegative Ar/Cl_2 discharge can effectively remove surface oxide layers on Nb samples as well as bulk Nb cavities [1, 2, 4–6]. During this work, relationships between experimental parameters and the etching rate of the plasma were explored. These parameters include the rf power, gas pressure, sample temperature, gas composition, electrode geometry, dc bias voltage, and frequency of the power source. While some of these parameters may play a larger role in the etch rate than others, all must be considered when attempting to attain an ideal figure of merit. The etch rate and amount of surface material that can be removed are obviously important when one considers the application of this technology to SRF cavities, but it is also important to address the other qualities that make a proper superconducting cavity, including the surface properties.

As it was important to find the relationship between experimental parameters and the etch rate, it is important to understand the relationship between certain parameters and the resulting surface properties of plasma etched Nb. The parameters of interest are 1) gas pressure, 2) rf power, 3) temperature, and 4) dc bias voltage. These parameters have a great deal of influence on the results, each for their own reasons. In particular, and the main emphasis of this paper, the dc bias on the inner electrode provides one of the mechanisms required for etching to occur at all. Normally, the smaller powered electrode is the etched surface since it naturally develops a large negative self-bias voltage due to current conservation and it's small surface area. This high negative voltage on the powered electrode attracts the free positive ions in the plasma more than the cavity surface, thus making etching of the cavity impossible, as is seen in Fig. 1 (left) [5]. However, if a positive voltage is forced onto the powered electrode, the cavity becomes the surface with the highest negative voltage, and becomes etched. The same effect can be seen if the surface area of the electrode is increased, since this changes the capacitive nature of the plasma. In order to remove surface impurities, the chlorine ions must be accelerated toward the cavity wall with enough kinetic energy to facilitate a chemical reaction. This is a combination of both physical and chemical etching that is called reactive ion etching. With enough kinetic energy when hitting the surface, the chlorine ions react with the surface to make niobium pentachloride; a volatile product

* This work is supported by the Department of Energy under grant No. DE-SC0014397.
† jpeshl@odu.edu

Content from this work may be used under the terms of the CC BY 3.0 licence (© 2017). Any distribution of this work must maintain attribution to the author(s), title of the work, publisher, and DOI.

ISBN: 978-3-95450-191-5 doi:10.18429/JACoW-SRF2017-TUPB099

VERTICAL TEST SYSTEM FOR SUPERCONDUCTING RF CAVITIES AT PEKING UNIVERSITY*

D. Zhou, S. Quan, J. Hao, L. Lin, L. Feng, F. Wang, F. Zhu,
H. Xie, D. Zhuang, W. Cheng, K. Liu, J. Chen
State Key Laboratory of Nuclear Physics and Technology & Institute of Heavy Ion Physics,
Peking University, Beijing 100871, China

Abstract

A new vertical test system (VTS) for superconducting RF cavities has been designed and constructed at Peking University. This facility is designed to operate at a temperature of 2 K and with pumping speed of 10 g/s for helium gas at 30 mbar. In this paper, we present the structure design, modification of 2 K system, ambient magnetic field and radiation shielding, LLRF and the test run of this VTS.

INTRODUCTION

The VTS facility is designed to test superconducting RF cavities ranging from 325 MHz low β cavities to 1.3 GHz high β cavities at 2 K. Most of the cryostat of VTS is assembled under the ground level in a well that was prepared for the facility. The upgraded cryogenic system can work at a pumping speed of 10 g/s for helium gas at 30 mbar to meet the requirement of vertical test. A 1 kW, 1.3 GHz RF system with its low level RF (LLRF) control system has been developed for the VTS. A two-layer structure to shield the magnetic field is installed in the VTS. A set of radiation shielding modules has been designed and constructed to ensure the ambient dose rate during the operations are below the prescribed level.

MAJOR SYSTEMS DESCRIPTION

The layout of VTS and its cryostat is shown in Fig. 1. Most of the cryostat is installed into a concrete well that has a diameter of 1.3 m and a depth of 5 m. The upgraded 2 K system is assemble in the building next to the cryostat. Multiple pipes connect the old and the upgraded 2 K system with the cryostat. They work together to provide competent conditions for measuring the cavities.

VTS Cryostat

The VTS cryostat consists of a vacuum vessel, a thermal shield and a helium vessel. The vacuum vessel has a 112 cm diameter and a depth of 430 cm. It is made of 304 stainless steel with the thickness of 1 cm. The thermal shield is installed within the vacuum vessel. It can significantly reduce the heat loss between the helium and room temperature. The thermal shield is made of 3 mm thick cooper with a cooper tube twining around it. The cooper tube has a diameter of 1 cm and is used to transport liquid nitrogen to maintain the temperature of thermal shield below 80 K.

* Work supported by National Key Program for S&T Research and Development (Grant No. 2016YFA0400400) and Major State Basic Research Development Program of China (Grant No. 2014CB845504)

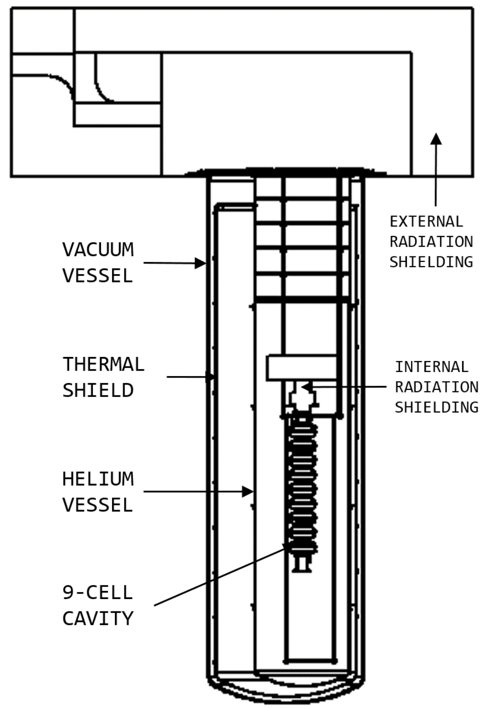

Figure 1: Layout of VTS and cryostat.

The picture of the helium vessel is shown in Fig 2. The helium vessel has an inner diameter of 70 cm and a depth of 366 cm, holding 2000 L liquid helium during the operations. In order to reduce the residual magnetism, which will have a negative effect on the performance of the cavities, the helium vessel is made of 316L stainless steel with the thickness of 2 mm.

Modification of 2K System

The schematic diagram of the 2 K system is shown in Fig. 3. Before the construction of VTS, Peking University already introduced a liquid helium system from the Linde Group. It contains a helium gas compressor, L410 helium liquefier and a 2000 L helium dewar. The modification of 2 K system includes a new 2 K valve box, upgrade of the 2 K pump unit and a new helium recovery and purification system.

The pictures of the old pump unit and the new pump unit is shown in Fig 4 and Fig 5. The old pump unit can work at the pumping speed of 3.2 g/s, and the speed of the new one is 6.8 g/s. During the test, the heated helium gas is extracted

Content from this work may be used under the terms of the CC BY 3.0 licence (© 2017). Any distribution of this work must maintain attribution to the author(s), title of the work, publisher, and DOI.

ISBN: 978-3-95450-191-5 doi:10.18429/JACoW-SRF2017-TUPB100

DETERMINING BCP ETCH RATE AND UNIFORMITY IN HIGH LUMINOSITY LHC CRAB CAVITIES

T. Jones[1], S. Pattalwar, STFC Daresbury Laboratory, Warrington, UK
G. Burt, J. Mitchell, University of Lancaster, Lancaster, UK
L. Marques Antunes Ferreira, R. Calaga, O. Capatina, R. Leuxe, CERN, Geneva, Switzerland
S. Verdu-Andres, B.Xiao, Brookhaven National Laboratory, Upton, USA
[1]also at University of Lancaster, Lancaster, UK

Abstract

The compact SRF Crab Cavities required for HL-LHC have complex geometries making prediction of average and local BCP etch rates a difficult task. This paper describes a series of experiments and simulations used to determine the etch uniformity and rate within these structures. An initial experiment was conducted to determine the correlation between etch rate and flow rate in a simple Nb tube. These results were then incorporated into Computational Fluid Dynamics simulations of acid flow in the Double Quarter Wave (DQW) cavity to predict etch rates across the surface and allow optimisation of the BCP setup. There were several important findings from the work; one of which is that the flow rate in the relatively large body of the cavity is predominantly driven by natural convection due to the exothermic reaction. During BCP processing of the DQW cavity a significant difference in etching was observed between upper and lower horizontal surfaces which was mitigated by etching in several orientations. Two DQW cavities manufactured by CERN have received a heavy BCP of 200 µm followed by 2 light BCPs of 20 µm each. Subsequent testing has shown performance exceeding required accelerating gradient and Q factor.

INTRODUCTION

There are several previous studies investigating the fluid flow of Buffered Chemical Polishing (BCP) acid within elliptical cavities [1, 2, 3]. In these studies it is common that a baffle be designed in order to give uniform flow speed within the cavities. Without baffles the etch rate at the iris of an elliptical cavity is typically twice that of the equator [4]. Another technique which has been proven to give good cavity performance is rotation of the cavity. This paper shows that this is most likely due to providing agitation of the acid in all areas of the cavity rather than providing uniform flow rate. For the complex shape of the Double Quarter Wave (DQW) SRF Crab Cavity (Fig. 1) the design of baffles to steer flow would be a time consuming process, and rotating the cavity would also require a significant hardware investment within the CERN BCP facility. It was therefore decided that the DQW prototype cavity would be etched in fixed positions, with varying orientations and flow ports to give an approximately uniform flow. Computational Fluid Dynamics (CFD) was used to identify the orientations with the most uniform (lowest standard deviation) flow condition. An experiment was performed to derive a correlation between etch rate and acid flow rate. This was used to predict the material removal rates at the surfaces of the cavity and to provide the average removal rate. The cavity was then etched and non-uniformities in etching were observed due to the low flow in the cavity.

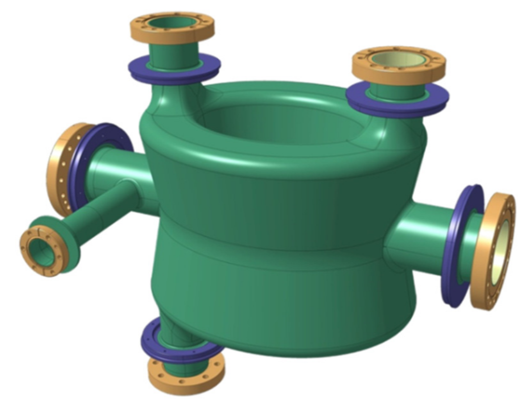

Figure 1: Double Quarter Wave SRF Crab Cavity.

DQW BCP CFD SIMULATION

CFD analysis was performed using ANSYS CFX [5] to identify the flow speed of acid throughout the volume of the DQW cavity in 8 different orientations, Fig. 2. Range (maximum minus minimum), standard deviation and mean average flow speed were evaluated across 21 monitor points distributed within the cavity volume. The boundary conditions for the analyses were as follows:

- The dynamic viscosity of acid used was 0.022 Ns/m^2 [1].
- A total flow of 6 litres per minute was distributed equally across the 3 inlets.
- The density of the acid used was 1458 kg/m^3.
- Buoyancy was turned on, with 9.81 m/s^2 applied in the direction shown in Fig. 2.
- Acid specific heat capacity 2090 J/kg/K [6].
- Tests were performed in each orientation with and without 1200 W/m^2 applied to all cavity surfaces to represent heat from the exothermic reaction [7].
- Results were obtained for a rotating cavity at 0.7 rev/min, one 50% (50) and one 90% full of acid (90), with 6 L/min flow through one beam port. For this a rotating mesh was used in a transient multi-phase analysis lasting 90 seconds (Fig. 3).

Content from this work may be used under the terms of the CC BY 3.0 licence (© 2017). Any distribution of this work must maintain attribution to the author(s), title of the work, publisher, and DOI.

ISBN: 978-3-95450-191-5 doi:10.18429/JACoW-SRF2017-TUPB103

DC MAGNETISM OF NIOBIUM THIN FILMS

S. Wilde[1,3], R. Valizadeh[1], O.B. Malyshev[1], G. B. G. Stenning[2], T.B. Sian[1,4], S. Pattalwar, N. Pattalwar, A. Hannah[1], and B. Chesca[3]
[1]ASTeC, STFC Daresbury Laboratory, Warrington, UK
[2] ISIS, STFC Rutherford Appleton Laboratory, Didcot, UK
[3] Department of Physics, Loughborough University, Loughborough, UK
[4] The University of Manchester, Manchester, UK

Abstract

Niobium thin films were deposited onto a-plane sapphire with varying kinetic energy and varying substrate temperature. There were no consistent trends which related the particle energy or substrate temperature to RRR. The sample which displayed the largest RRR of 229 was then compared to both a thin film deposited with similar conditions onto copper substrate and to bulk niobium. DC magnetometry measurements suggest that the mechanism of flux entry into thin film niobium and bulk niobium may vary due to differences in the volumes of both defects and impurities located within the grains. Results also suggest that magnetic flux may penetrate thin films at small fields due to the sample geometry.

INTRODUCTION

The RF cavities made of copper and coated with a thin layer of superconducting material are already widely used as an alternative to bulk Nb cavities. They are less expensive, copper has better thermal conductivity, and in theory they could perform even better than the bulk Nb cavities. However, in present their cavities do not provide the same quality of $Q_0(E)$ function yet. ASTeC continues its superconducting thin film programme of systematic study on correlation between the surface preparations, the deposition parameters, morphology, structure and chemistry, and superconducting properties of the films. This paper was devoted to deposit the film with the highest quality and compare its properties to bulk Nb and to check how significant could be the edge effect in SQUID magnetometer measurements in magnetic field.

FILM DEPOSITION

18 niobium thin film samples were deposited in ASTeC by either high impulse magnetron sputtering (HiPIMS), DC or Pulsed DC magnetron sputtering onto single crystal a-plane sapphire. Each substrate was cleaned in ultrasonic baths of acetone, then isopropanol, then deionised water before being inserted into the deposition chamber. The vacuum system was baked prior to deposition at 150 °C for 3 days to achieve a base pressure of 2 x 10^{-10} mbar. A three-inch planar magnetron was used to deposit the sample with a 99.95% purity niobium target. The magnetron was 150 mm from the substrate surface at an angle of 45°. The substrate was rotated at 4 rpm for the duration of the deposition. Krypton sputter gas was used during the deposition at a constant pressure of 7 x 10^{-3} mbar. For samples deposited by HiPIMS, the power supply was set to pulse at 200 Hz with a pulse length of 100 µs. The average plasma current was 600 mA whilst the peak current at the target surface was 40 A. When depositing with pulsed DC, the power supply was set to a power of 400 W with repetition rate of 350 kHz and 50 % duty cycle. DC sputtering was performed with a power of 400 W. Films were deposited with a substrate temperature ranging 500 to 1000 °C with either a grounded substrate or a DC bias voltage of -80 V. The deposition was monitored throughout by sampling small volumes of process gas with an RGA and by optical spectrometer. It has been assumed that HiPIMS provides the largest ionisation percentage of the sputtered material, followed by pulsed DC then finally DC [1]. The study intends to describe the changes in superconducting properties of niobium thin films which depend on substrate temperature and the energy of sputtered material. A-plane sapphire was chosen as substrate due to its high melting temperature of 2050 °C.

Samples were first measured for RRR. The sample with the largest RRR was later compared to a sample deposited with the same deposition conditions onto copper substrate which has a much lower melting temperature of 1085 °C. The comparable samples were also analysed by both SEM and DC magnetometer.

RESULTS

RRR Measurements

The deposited films were tested for RRR using a four-point probe with the resistance of the sample measured from room temperature down to below T_C. The RRR results for every deposited sample are shown in table 1. The results show that RRR varies from 10 to 229 for all samples however there was no consistent trend which connected RRR with either the power supply used, the deposition temperature or the applied bias. In some cases, very similar deposition conditions resulted in very different RRR.

The resistance versus temperature curve for the sample with the largest RRR of 229 is shown in Fig. 1. The sample was deposited by HiPIMS at 800 °C with a -80 V DC bias. A sample deposited with the same deposition conditions onto copper substrate, and with RRR of 52, is also shown for comparison. The sample deposited onto a-plane sapphire exhibited the smallest normal state resistance of all samples at 0.0006 mΩ just before the superconducting transition. The superconducting transition temperature of

Content from this work may be used under the terms of the CC BY 3.0 licence (© 2017). Any distribution of this work must maintain attribution to the author(s), title of the work, publisher, and DOI.

ISBN: 978-3-95450-191-5 doi:10.18429/JACoW-SRF2017-TUPB104

FIRST FULL CRYOGENIC TEST OF THE SRF THIN FILM TEST CAVITY

Philippe Goudket[2], Oleg B. Malyshev[2], Shrikant Pattalwar[2], Ninad Pattalwar, Lewis Gurran[1,2], Reza Valizadeh[2], Louis Bizel Bizellot
ASTeC, STFC Daresbury Laboratory,Warrington,Cheshire,UK
Graeme Burt[2], [1]Lancaster University, Lancaster, UK
[2]also at Cockcroft Institute, Warrington, Cheshire, UK

Abstract

A test cavity that uses RF chokes, rather than a physical seal, to contain the field is a promising method of SRF sample testing, especially in thin films research where the rate of sample production far outstrips that of full SRF characterisation. Having the sample and cavity physically separate reduces the complexity involved in changing samples - major causes of low throughput rate and high running costs for other test cavities - and also allows direct measurement of the RF power dissipated in the sample via power calorimetry. Choked test cavities operating at 7.8 GHz with three RF chokes have been designed and tested at Daresbury Laboratory. As part of the commissioning of this system, we performed the first full SRF test with a bulk Nb sample and we verified that the system would perform as required for future superconducting thin film sample tests.

INTRODUCTION

The ASTeC Thin Film SRF program consists of the following parts:

- Surface preparation and deposition of the samples using PVD and CVD methods [1, 2].
- Characterisation of the samples using various surface analysis techniques including SEM, XPS, XRD, EDX, etc. [1-4]
- Measuring superconducting properties in DC and AC conditions: RRR, magnetisation (SQUID), magnetic field penetration, etc. [1, 4-6].
- Testing of the various samples at RF frequencies using a dedicated cavity design [7, 8].

To achieve testing of planar samples, the cavity was designed, built, and commissioned at Daresbury Laboratory. The cavity was initially measured at room temperature as reported in [8], then at cryogenic temperature with a copper sample plate in order to ensure no radiation could be produced.

This paper reports on the first full cryogenic test of the thin film test cavity design which was carried out with a bulk niobium sample plate.

CAVITY DESIGN

A radiofrequency (RF) cavity and cryostat dedicated to the measurement of superconducting coatings at GHz frequencies was designed to evaluate surface resistive losses on a flat sample. The test cavity consists of two parts: a cylindrical half-cell made of bulk niobium (Nb) and a flat Nb disc. The two parts can be thermally and electrically isolated via a vacuum gap, whereas the electromagnetic fields are constrained through the use of RF chokes. Both parts are conduction cooled hence the cavity halves are suspended in vacuum during operation. The flat disc can be replaced with a sample, such as a Cu disc coated with a film of niobium or any other superconducting material. The RF test provides simple cavity Q-factor measurements and can also be set up for calorimetric measurements of the losses on the sample.

The test cavity itself is described in [8]. It is succinctly a cylindrical pillbox-type cavity, operated in the TM_{010} mode at 7.8 GHz (see Fig. 1). The resonance is induced through a straight RF probe connected to a micrometer allowing variable coupling to the cavity body. The cavity frequency choice is a primarily defined by the available sample size which dictates the maximum extent of the chokes. A lower frequency cavity which might be less affected by BCS resistance would require larger samples. The advantage of this method is the combination of a compact cavity with a simple planar sample.

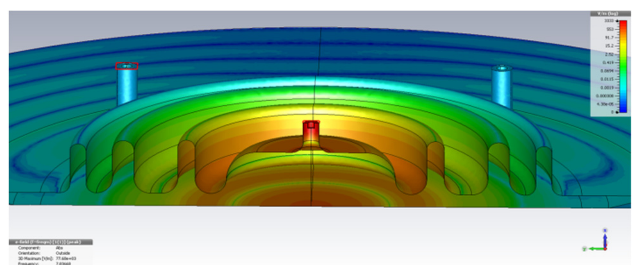

Figure 1: E-field distribution on the surface of the three choke cavity (top) and sample plate (bottom) simulated using CST.

CRYOGENIC FACILITY

The cryogenic set-up was reported on in previous papers [8] and shown in Fig. 2 for completeness. The steel sample chamber is constructed to have a long neck leading to warm ports for the RF cables and thermometry wiring. This is surrounded by concentric LHe and LN_2 chambers. The cradle assembly holding the test cavity and sample is bolted onto the bottom face of the LHe reservoir.

The outer insulation vacuum and sample chambers are pumped separately. By pumping He vapour from the LHe chamber, cavity and sample temperatures down to 2 K can be reached. As the sample is only weakly thermally coupled to the cold plate, cool-down is generally ensured by 3 mbar He gas convection in the sample chamber.

Content from this work may be used under the terms of the CC BY 3.0 licence (© 2017). Any distribution of this work must maintain attribution to the author(s), title of the work, publisher, and DOI.

ISBN: 978-3-95450-191-5 doi:10.18429/JACoW-SRF2017-TUPB106

STANDARDIZED BEAMLINE PARTICULATE CHARACTERIZATION ANALYSIS: INITIAL APPLICATION TO CEBAF AND LCLS-II CRYOMODULE COMPONENTS*

C. E. Reece†, J. Spradlin, O. Trofimova, and A.-M. Valente-Feliciano
Thomas Jefferson National Accelerator Facility, Newport News, VA 23606, USA

Abstract

Despite continuously evolving efforts to minimize and manage the occurrence of particulates in operational SRF accelerator systems, the presence of electron field emission from contaminating particulates on SRF surfaces with high surface electric fields remains a consistent challenge. Jefferson Lab has recently initiated a standardized particulate sampling and characterization practice in order to gain more specific and systematic knowledge of the particulates actually present. It is expected that patterns emerging from such sampling will strengthen source attribution and guide improvement efforts. Initial samples were gathered from a cryomodule and adjoining warm girders that were removed from the CEBAF tunnel for reprocessing. The collection and analysis techniques were also used to characterize particulates on the inside of LCLS-II string components. Samples are transferred to clean industry-standard forensic GSR carbon tape spindles and examined via automated cleanroom SEM scanning for particle localization trends and sizing. The particulates are subsequently analyzed with EDS for elemental composition. A catalogue of found particle types is being accumulated. The methods used and results obtained from these initial applications will be presented.

INTRODUCTION

That extrinsic particulates on the surface of high electric field regions of superconducting rf (SRF) cavities present performance-limiting effects via electron field emission has been very well established. Significant efforts are made to obtain clean "particulate-free" interior cavity surfaces. Effective cleaning processes have been developed by the community, largly using ultrasonic detergents and high pressure rinsing with ultra-pure water. See, for example references [1-5]. In addition, careful attention has been applied to development and control of assembly and handling techniques which attempt to minimize contamination of clean surfaces.[6-8]

Success with this contamination control is indicated by the absence of field-emission-induced x-radiation during high-field operation of the SRF cavities. Higher field applications require higher standards of maintained cleanliness to assure success. Field-emission free multi-cell cavity performance above 40 MV/m has been demonstrated at multiple labs. The very non-linear exponential field emission current response has been successfully modeled by Fowler-Nordeim theory.

Practical reality to date, however, is that all SRF accelerators exhibit more x-ray production and attendant extra heat load attributed to particulate-induced electron field emission than desired. Geometries that allow acceleration of emitted electrons significantly above 10 MeV also encounter activation and material degradation due to neutron production.[9]

Accelerator cleanliness standards have clearly evolved over the past 30 years. An effort has recently begun at Jefferson Lab to increase the systematic characterization of particulates on the CEBAF beamline, both in the older sections constructed in the early 1990's and in more recent assemblies. An important preliminary investigation on a cryomodule from the JLab FEL identified significant contamination.[10] We seek now to implement a standardized particulate collection and characterization protocol in order to provide better feedback to all potential contributors to the problem.

SAMPLE COLLECTION METHOD

We take as a working assumption that the subject particulate contamination has arrived at the surface after the sampled beamline surface was previously clean and free of such contaminants. So, the particulates are expected to be at least initially non-adhered to the surface. For the collection of each sample, we employ a section of fresh cleanroom wipe rated for ISO-4 use, wetted with reagent isopropyl alcohol. Approximately 2 cm^2 of the wipe is rubbed gently over the surface to be sampled. All other contact with the collecting wipe is avoided. The collection area of the wipe is then pressed against a freshly exposed clean carbon tape, with intent to transfer and adhere collected particulates to the carbon tape.

We take advantage of the commercial availability of standardized and serialized forensic gunshot residue (GSR) analysis spindles. These are guaranteed clean. Each spindle is topped by carbon tape. A standard holder accepts an array of these GSR spindles for examination under scanning electron microscope (SEM). At Jefferson Lab, we collect particulate samples onto GSR spindles under ISO-5 or better conditions, then transport the samples to our Tescan VEGA3 XMH SEM, located in the JLab cleanroom suite, for analysis. (See Fig. 1.)

SAMPLE ANALYSIS METHOD

In order to establish a sustainable, systematic, and rather high-volume analysis of samples collected from multiple sources, we aim to automate as much of the analytical work as possible. Once an array of spindles is

* Authored by Jefferson Science Associates under contract no. DEAC05-06OR23177 to the US DOE Office of Science, Office of Nuclear Physics.
† reece@jlab.org

Content from this work may be used under the terms of the CC BY 3.0 licence (© 2017). Any distribution of this work must maintain attribution to the author(s), title of the work, publisher, and DOI.

ISBN: 978-3-95450-191-5 doi:10.18429/JACoW-SRF2017-TUPB108

GENESIS OF TOPOGRAPHY IN BUFFERED CHEMICAL POLISHING OF NIOBIUM FOR APPLICATION TO SUPERCONDUCTING RADIOFREQUENCY ACCELERATOR CAVITIES*

L. Zhao[1,†], C. E. Reece[1], M. J. Kelley[1,2]
[1]Thomas Jefferson National Accelerator Facility, Newport News, VA 23606, USA
[2] Applied Science Department, The College of William and Mary, Williamsburg, VA 23187, USA

Abstract

Topography arising from the final etch step in preparing niobium superconducting radiofrequency (SRF) accelerator cavities is understood to significantly impact cavity performance at high field levels. This study investigated the effect of process temperature and time on the etch rate and topography arising from the widely-used buffered chemical polishing (BCP). This study aims to understand more thoroughly the genesis of topography in BCP of polycrystalline niobium, with the ultimate aim of finding a path to surface smoothness comparable to that obtained by electro-polishing (EP). It was found that the etch process is controlled by the surface reaction; and that the etch rate varies with crystallographic orientation. The familiar micron-scale roughening necessarily results. Gas evolution has an impact, but is secondary. The major outcome is that surface smoothness comparable to EP appears to be inherently unachievable for polycrystalline niobium using BCP, setting an upper limit to the gradient for which it is useful.

BACKGROUND

BCP is still an essential step in SRF cavity fabrication, from welding surface preparation, to bulk removal, to final surface "flash" polishing, despite the rapid development of alternative polishing methods. The attractive advantage of BCP lies in its simple setup and fast process. The disadvantage of BCP, however, is that the "polished" niobium surface displays a characteristic roughness. Instead of discarding BCP due to this roughness, it is more efficient to use it wisely where suitable [1-2], which will eventually optimize the cavity fabrication process. To achieve that, it is necessary to understand the forming mechanism of this characteristic topography. This study provides evidence to support that crystal orientation dependent etching plays a major role in the formation of BCP niobium topography. It adds to existing understanding about the niobium BCP reaction and resulting surfaces [3-6].

* Work supported by Office of High Energy Physics, U.S. Department of Energy, Grant SC0007907 to the College of William & Mary and by U.S. DOE Contract No. DE-AC05-06OR23177 to Jefferson Science Associates.
† lzhao@jlab.org

EXPERIMENT

Material and Preparation

The polycrystalline (fine grain) niobium samples were electric discharge machined (EDM) from high RRR sheet material used for cavity fabrication. The bi-crystal and single crystal samples were cut from a large grain sheet. The sample dimensions were all 10 mm × 10 mm × 3.2 mm. After EDM, the samples were etched in 1:1:2 BCP solution for 1 min to remove machining contaminants. They were then rinsed with de-ionized water and air dried.

For polishing rates and topography study, various polishing conditions were performed and they are summarized in Table 1.

Table 1: Niobium Sample Types and Polishing Conditions

Sample type	Temperature	Duration	Orientation
Fine grain	0-30°C	1-20minutes	Face up, down, and sideway
Bi-crystal	Room Temperature (20~22°C)	12minutes	Face up
Single crystal	Room Temperature (20~22°C)	Accumulated 90minutes	Face up

Polishing rates were determined using polycrystalline samples. Samples were immersed in fresh 1:1:2 BCP solution for designated duration from 1 to 10 minutes, taken out of solution, rinsed with de-ionized water, and air dried. No stirring was applied during polishing. Polishing rates were calculated from the weight difference before and after polishing divided by polishing time and polished surface area.

Characterization

The topography of the niobium samples was examined by scanning electron microscopy (SEM), optical microscopy, and atomic force microscopy (AFM). The crystal orientation of the niobium samples was examined by electron backscatter diffraction (EBSD).

Content from this work may be used under the terms of the CC BY 3.0 licence (© 2017). Any distribution of this work must maintain attribution to the author(s), title of the work, publisher, and DOI.

ISBN: 978-3-95450-191-5 doi:10.18429/JACoW-SRF2017-TUPB111

R&D ACTIVITIES ON CENTRIFUGAL BARREL POLISHING OF 1.3 GHZ NIOBIUM CAVITIES AT DESY/UNIVERSITY OF HAMBURG*

A. Prudnikava†, B. Foster[1], Y. Tamashevich[2], The University of Hamburg, Germany
A. Ermakov, DESY, Hamburg, Germany
[1]also at DESY and University of Oxford, UK
[2]presently at HZB, Berlin, Germany

Abstract

In this paper the status of research activities at ILC-HiGrade Lab (DESY/University of Hamburg) on Centrifugal Barrel Polishing (CBP) of 1.3 GHz Niobium Cavities is presented. We focus on CBP based on the polishing recipe reported by Fermi National Laboratory and Jefferson Lab [1]. The aim is to gain a better understanding of the limitations of this technique, detailed characterization of the treated surface after each polishing step using a "coupon" single cell cavity. Plastic deformations upon initial CBP steps, embedded polishing media and residual damage upon final polishing were investigated at different areas of the cavity.

INTRODUCTION

Current serial production technology of superconducting radio frequency (SRF) Nb cavities represents a complicated process which includes a number of technological steps starting from purification of raw niobium and production of plane sheets up to mechanical fabrication of cavities, chemical and thermal processing and finally testing.

Forming steps can cause mechanical damage of approximately 120 µm into the interior surface of the cavities. Electron-beam welding of the cavities can produce weld beads on the interior surface of the cavity [2]. Electropolishing (EP) is presently the preferred route for preparing the final cavity interior surface.

Despite rigorous control of technological steps according to the respective technical specification, some cavities quench at low gradients, particularly due to defects in the equator areas of the cells. Some of the defects, such as pits, welding sputters and inclusions of foreign material are difficult to remove by chemical polishing.

Centrifugal barrel polishing (CBP), a mechanical processing of the interior of the cavities has a high potential to revive such cavities. It can be used instead of "bulk" EP in a standard mass production to remove the damaged surface layer as it is not sensitive to material inclusions. At the same time, it can effectively remove protrusions and reduce the contour of the weld bead. A smooth surface provided by CBP is a good starting condition for the following EP. A moderate "final" EP treatment (10-40 µm) might be enough to reach high surface quality and, therefore, better cavity performance. In addition the usage of hazardous reagents would be significantly reduced. However, the processing recipe of CBP and the optimal amount of "final" EP are to be estimated. Here we continue this study by further exploring CBP process, in particular, the surface roughness and plastically deformed layer at the coupon surface using metallography technique. The attempts to reduce the damaged layer are also considered.

* Work supported by BMBF Project SRF_RandD
† alena.prudnikava@desy.de

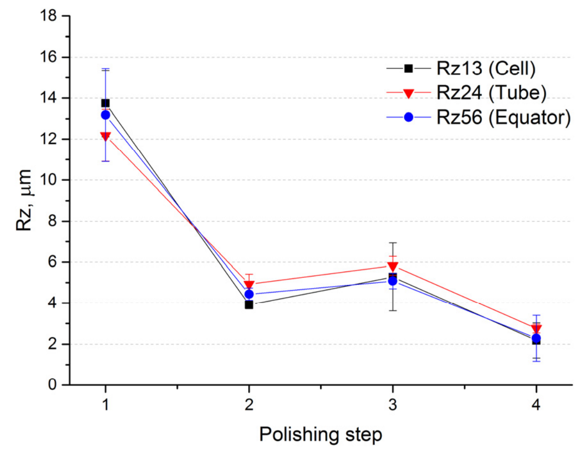

Figure 1: Roughness R_z (peak-to-valley height, µm) of Tube (red triangles), Cell (black squares), and Equator (blue circles) area coupons measured after 1-4 steps of CBP.

PREVIOUS WORK

We have investigated JLab/FermiLab four-step CBP recipe [1] in detail. A mirror-smooth surface has been achieved on single- and 9-cell cavities by applying CBP in a four-step process (here steps are numbered as CBP#1, CBP#2 and so on), firstly with ceramic triangles (Duramedia ACT), then plastic cones (VF-RG 22), alumina mesh (#600) and finally colloidal silica (40 nm) as abrasives. Earlier we reported some of the results at [3]. In particular, the surface of the coupons installed at irises, cells and equators after each polishing step was investigated with microscopic (SEM) and spectroscopic (EDX) techniques. Abrasion rate (the rate at which material is removed) and pollution with polishing media were analysed. The origin of large deep scratches left after the final polishing step was identified, and partially eliminated (by multiple changing of the polishing solution). Cross sectioning of some coupons after the final treatment by metallographic method revealed the presence of a thick (up to ~40 µm) damaged layer on the surface.

Content from this work may be used under the terms of the CC BY 3.0 licence (© 2017). Any distribution of this work must maintain attribution to the author(s), title of the work, publisher, and DOI.

ISBN: 978-3-95450-191-5 doi:10.18429/JACoW-SRF2017-TUPB112

FIRST TEST OF ELECTROPOLISHING SYSTEM AT IMPCAS

Lu Li †, Yuan He, Zhiming You, Hao Guo, Pingran Xiong, Xinlong Zhu,
Yongming Li, Ziqin Yang, Qinwei Chu, Shenghu Zhang, Bin Zhang,
Institute of Modern Physics, Chinese Academy of Sciences, Lanzhou, China

Abstract

IMP（Institution of Modern Physics） has designed, fabricated and installed the first SRF cavity electropolishing system of China. It is sized for 1.3GHz SRF cavities, and works for multiple cell cavities with further upgrade of structure.

INTRODUCTION

Producing high field and Q-values in superconducting RF cavities of niobium has required the removal of a substantial layer of the inner cavity surface, typically of the order of 100 microns in depth. Two methods have commonly been used: EP (electropolishing) or BCP (buffered chemical polish). EP of niobium cavities is proving to yield consistently better performance than BCP [1, 2]. To take advantage of high performance levels obtainable with EP technique, a completed EP system was installed and operated at IMP.

IMP EP SYSTEM

The electropolishing system, consists by a chiller, a heat exchanger, an acid sump, tilt-rotation tooling and instrumentation for process control and direct current power supply variable up to 160 amperes and 40 volts. Figure 1 and 2 shows the end groups of tilt-rotation tooling designed for assembly and disassembly of cavities and electrodes into and out.

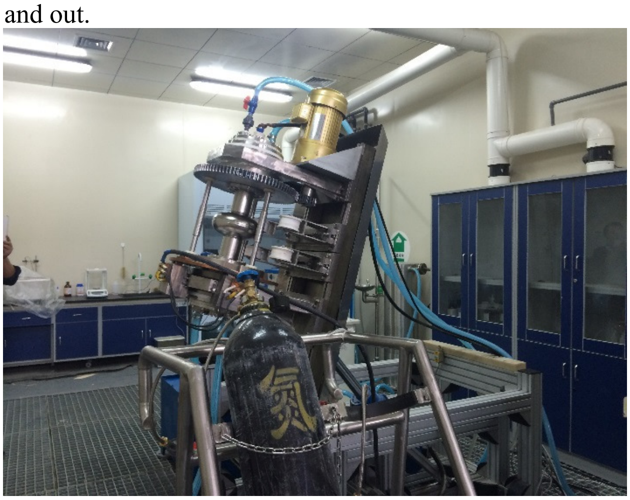

Figure 1: Tilt and rotation tooling on the vertical section.

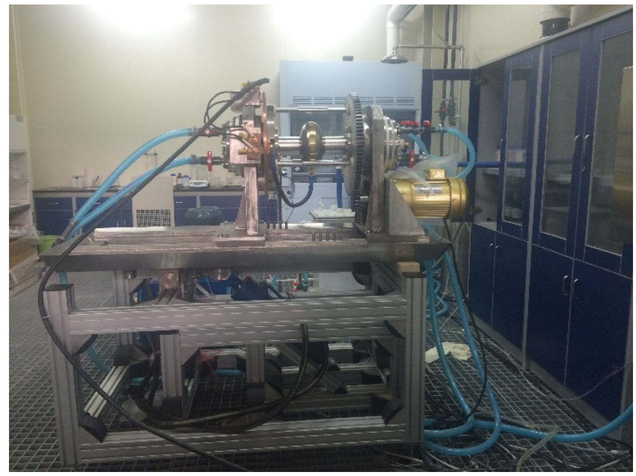

Figure 2: Tilt and rotation tooling on the horizontal section.

FIRST TEST OF EP SYSTEM

Our first 1.3GHz one-cell cavity test has been started. Figure 3 and 4 shows the typical Voltage-Current Density curves as a function of adjustments of the working parameters by use two different shapes of cathodes. Figure 3 shows the U-C curve of system run with a regular kind of cathode. It's a straight stick made up with pure aluminium. We control the acid temperature between 12 to 18 ˚C with heat exchanger and cavity outside cooling water spray. Figure 4 also shows the U-I curve of system run with a different kind of cathode. It's designed by our institute. It looks like a boot and also made up with pure aluminium. The flow acid temperature was controlled between 12 to 18 ˚C. We control the system run with different acid flow rate about 4 L/min, 6L/min and 8L/min. And under each flow rate, we try different rotation speed of 1rpm, 2rpm and 3 rpm. Here, we use different parameters of the shape of cathode, rotation speed and acid flow rate, to try to find out the optimal processing control. Compared Figure 3 and 4, the new shape of cathode working under 1rpm, 4L/min acid flow rate, power supply between 18 to 20 v is the optimal parameter of processing control for this EP system with one-cell cavity.

Figure 5 shows the comparison of inner surface performance of one-cell cavity after bulk BCP and EP (the surface removal of more than 100 μm).

† lilu@impcas.ac.cn

Content from this work may be used under the terms of the CC BY 3.0 licence (© 2017). Any distribution of this work must maintain attribution to the author(s), title of the work, publisher, and DOI.

ISBN: 978-3-95450-191-5 doi:10.18429/JACoW-SRF2017-TUPB113

SURFACE CHARACTERIZATION OF NITRIDED NIOBIUM SURFACES*

A. Prudnikava†, B. Foster[1], Y. Tamashevich[2], The University of Hamburg, Germany
[1]also at DESY and University of Oxford, UK
[2]presently at HZB, Berlin, Germany

Abstract

Thermal treatment of niobium radio frequency cavities in nitrogen atmosphere is employed in ILCLS-II Project in order to improve the quality factor of Nb cavities. A so called "N-infusion" thermal treatment is applied without any post processing [1, 2], whereas "N-doping" requires the removal of the upper layer of 5-30 um. For better understanding the mechanism of such an improvement, a detailed characterization of the nitrided surface is necessary. Our studies are focused on characterization of the niobium surface subjected to such treatments (surface morphology, nitrogen concentration profile, hardness, phase composition). The sample preparation technique for studying the hydride precipitation in N-Nb system is presented, and current activities on studying of N-infused Nb samples by SQUID and PPMS are briefly discussed.

INTRODUCTION

The SRF niobium cavities, a key component of current and future efficient particle accelerator, are made from high-purity niobium and undergo a complex multi-step production process to achieve a high accelerating gradient, E_{acc}, and a high quality factor, Q_0. These quantities, together with the manufacturing yield, drive cost and performance factors such as cryogenics plant size, beam energy, machine length etc. Recently new processing procedures including thermal treatments in nitrogen atmosphere demonstrated Q_0 values two times above the previous record [1, 2]. The possible mechanism of such improvement is the decrease of the superconducting surface resistance of niobium by lowering mean free path of "normal" electrons caused by interstitial nitrogen [3] as well as possible suppression of small hydride precipitates due to the trapping effect [4]. In order to contribute to understanding of the improved cavity performance we perform similar treatments of samples to gain knowledge about the surface state. Here we demonstrate a technique for sample preparation in order to study the N-H interaction in Nb with varied nitrogen content at the surface, as well as characterisation of such surface with X-ray Photoelectron Spectroscopy (XPS) and laser profilometry. We also present some data on our current studies of the samples subjected to same treatments as TESLA cavities (EXFEL, N-doping, N-infusion): magnetisation curves and complex magnetic susceptibility.

EXPERIMENTAL DETAILS

The experimental work was carried on at DESY site, ILC-HiGrade Lab within a common R&D Project. Investigations were carried out both on fine-grained (FG, Tokyo Denkai) and large-grained (LG, Heraeus) Nb samples cut by electro erosion from 2.8 mm-thick sheets followed by a few µm BCP. The sample heat treatments were performed in a furnace consisting of a ceramic tubular chamber (Ø7 cm, 1.5 m in length) with a three zone temperature control and water cooled flanges and operates at a maximal temperature of 1000 °C and working pressure of ~10^{-4} Pa. A titanium tube was placed in the middle of the furnace, as a sample holder, with an additional thermocouple close to the samples for more precise temperature control. The gas regulator provided partial gas pressures of a few Pa (30 mTorr) required to reproduce the treatment of cavities described in [1, 2].

The experiments were performed at various temperatures, nitridation times and drive-in diffusion steps ($T\_t_{nitridation}\_t_{drive-in}$). The typical p,T(t) plot of one of the treatments is presented in Fig. 1.

Thorough characterisation of LG Nb surface treated at 900_20N$_2$_30 and 800_20N$_2$_30 by GDOES, SEM/EDX,

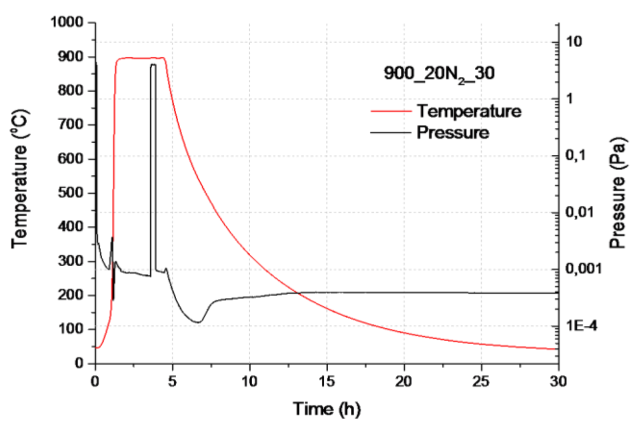

Figure 1: (p, T) vs. t plots during nitridation of Nb samples (900_20N$_2$_30).

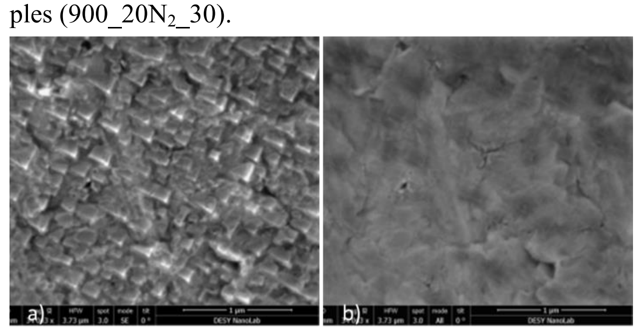

Figure 2: SEM images of the nitrided at 900_20N$_2$_30 surface obtained with: a – secondary electrons, b – backscattered electrons.

* Work supported by BMBF Project SRF_RandD
† alena.prudnikava@desy.de

Content from this work may be used under the terms of the CC BY 3.0 licence (© 2017). Any distribution of this work must maintain attribution to the author(s), title of the work, publisher, and DOI.

ISBN: 978-3-95450-191-5 doi:10.18429/JACoW-SRF2017-WEXA01

HIGH PERFORMANCE NB3SN CAVITIES*

D.L. Hall†, M. Liepe, R. D. Porter, T. Arias, P. Cueva,
D. B. Liarte, D. A. Muller, J. P. Sethna, N. Sitaraman
Cornell Laboratory for Accelerator-Based Sciences and Education (CLASSE),
Ithaca, NY 14853, USA

Abstract

In recent years, 1.3 GHz single-cell cavities coated with Nb_3Sn at Cornell University have repeatedly demonstrated quality factors of 10^{10} at 4.2 K and >15 MV/m. Ongoing research is currently focussed on the impact of intrinsic and extrinsic factors that limit the quality factor and quench field in these cavities. New single-cell cavities have been commissioned to enable further exploration of the coating parameter space. Experimental studies on both cavities and sample coupons have been supplemented by theoretical work done on layer growth, trapped vortex motion and flux entry. In this paper, we provide a comprehensive overview of the latest developments on Nb_3Sn cavities, including work conducted in collaboration with the new NSF Center for Bright Beams, with a brief summary on work being done in the field at large.

INTRODUCTION

Nb_3Sn is demonstrating itself to be a promising next-generation alternative to niobium for use in SRF cavities, outperforming the best niobium cavities at 4.2 K and 16 MV/m [1–3]. However, questions still remain on how to ensure high efficiency at high gradients.

COATING PROCEDURE

To date the best-performing Nb_3Sn cavities have been fabricated using the vapour diffusion process [4], in which a niobium substrate is exposed to tin vapour in an ultra-high vacuum (UHV) furnace at temperatures above 950°C. A diagram of the custom-built UHV furnace used for coating 1.3 GHz single-cell ILC cavities at Cornell University is shown in Fig. 1. The furnace consists of a niobium chamber inserted into the main furnace hotzone, at the base of which is a small alcove in which the tin source is placed. Surrounding this alcove is a secondary heater than allows the tin source to be held at a temperature higher than that of the cavity.

The coating process is described in detail in Ref. [5], but is briefly summarised here. High purity tin, in a tungsten crucible, is placed into the alcove at the base of the furnace. Just above it, a tungsten crucible containing the nucleation agent $SnCl_2$ is placed. The niobium substrate – cavity or coupon – to be coated is lowered into the furnace, and the furnace is sealed. After a 24-48 hour degas cycle at 180°C, the chamber and source together area taken to 500°C and held there for 5 hours to allow the nucleation agent to pre-seed the niobium substrate with tin. Following this, a temperature difference of 150°C is established between the tin source and the coating chamber. Together, they are raised to a temperature of approximately 1120°C in the chamber and 1250°C at the source. This stage, referred to as the *coating* stage, is held for the amount of time prescribed by the recipe. Often, the source heater is then turned off, and allowed to equilibrate to the temperature of the cavity, substantially reducing the rate of tin arriving at the surface. Following this *annealing* stage, the power to the furnace is cut and the entire structure is allowed to cool by radiation until 25°C , at which point the furnace is opened.

This coating process differs from that used at other labs, both historically and currently. Coating furnaces have been used at Siemens AG, the University of Wuppertal, Jefferson Lab and Fermi National Laboratory. A diagram demonstrating the differences between the different designs of coating furnace is shown in Fig. 2.

UNIFORMITY OF THE COATED LAYER

In the first coatings at Cornell there was significant difficulty with non-uniform coatings of a single-cell cavity, which led to poor performance and significant Q-slope. This was resolved by introducing a temperature gradient between the source and the chamber at the beginning of the ramp up to coating temperatures, which has contributed to the exceptional performance seen in these cavities.

In particular, the first cavity coated at Cornell, denoted ERL1-5, was found to exhibit significant heating on the half-

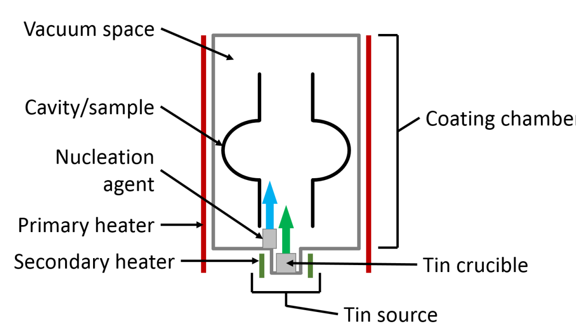

Figure 1: A simplified diagram of the Cornell UHV coating furnace. The cavity is located in a chamber placed inside the main hotzone. At the base of the chamber is the tin source, which is surrounded by a secondary hotzone that allows the source to be held at a temperature higher than that of the cavity.

* This work was primarily supported by U.S. DOE award DE-SC0008431. This work was supported in part by the U.S. National Science Foundation under Award PHY-1549132, the Center for Bright Beams.
† dlh269@cornell.edu

Content from this work may be used under the terms of the CC BY 3.0 licence (© 2017). Any distribution of this work must maintain attribution to the author(s), title of the work, publisher, and DOI.

ISBN: 978-3-95450-191-5 doi:10.18429/JACoW-SRF2017-WEXA03

Content from this work may be used under the terms of the CC BY 3.0 licence (© 2017). Any distribution of this work must maintain attribution to the author(s), title of the work, publisher, and DOI.

HIGH-PERFORMANCE THIN-FILM NIOBIUM PRODUCED VIA CHEMICAL VAPOR DEPOSITION (CVD)*

R. Porter†, D. L. Hall, M. Liepe, and J. T. Maniscalco
Cornell Laboratory for Accelerator-Based Sciences and Education (CLASSE), Ithaca, NY, USA
V. Arrieta, S. McNeal, and B. Williams, Ultramet, Pacoima, CA, USA

Abstract

Bulk niobium cavities have been the standard for superconducting particle accelerators for many years. However, the cost of high RRR niobium start materials makes them expensive. The use of Chemical Vapor Deposition (CVD) processing technologies to produce thin Nb films on low-cost substrates (e.g. copper) offers a method to significantly reduce the cost of accelerator cavity fabrication while increasing cavity performance capabilities. Recent optimization of CVD niobium processes for high RRR Nb films has led to RF performance approaching that of bulk Nb. In collaboration with Ultramet, Cornell continues to explore the potential of CVD techniques. This paper presents results from a detailed study of CVD thin film Nb materials produced by Ultramet on 5-inch diameter copper and molybdenum substrates, including RF performance results with T-mapping and detailed surface analysis of performance limiting regions. Our work shows that CVD-based cavity fabrication methods are a promising alternative to sheet-formed bulk cavities, and to other thin Nb film techniques, warranting further development. Additional results from the field will be discussed.

INTRODUCTION

High RRR bulk niobium cavities have been used in accelerators for decades and are nearing their theoretical performance limits [1,2]. The superconducting penetration depth is significantly less than 1 μm making it feasible to create a superconducting surface on accelerator cavities made from copper or other low-cost substrates via the application of a thin niobium film. A thin-film approach offers several advantages over traditional bulk niobium: Materials having thermal conductivities much higher than niobium, such as copper ($75\,\mathrm{W/m\cdot K}$ for niobium vs. $300-2000\,\mathrm{W/mv\cdot K}$ for copper), increase the thermal stability fo the cavity and decreases the sensitivity of the cavity to surface defects; copper is roughly one tenth the price of high RRR niobium sheet start materials, reducing the cost of manufacturing; thin films have been shown to have reduced flux trapping sensitivity (reduced by as much as 1%), reducing magnetic shielding requirements [3]; the techniques can avoid or substantially reduce the need for electron beam welding and mechanical manipulations such as pressing and rolling, reducing cost and likelihood of inclusions; and if the produced thin film is of sufficient quality, mechanical and chemical polishing may be avoidable, though some techniques still require mechanical or chemical treatments.

Chemical Vapor Deposition is used in industry to produce free-standing niobium components, and thin and thick films of niobium on substrates. The CVD-based technique has advantages over other thin-film niobium techniques. CVD techniques can rapidly grow niobium films. Ultramet, through several decades of CVD process development routinely achieves deposition rates exceeding 300 μm/hr. The CVD process forms a robust metallurgical diffusion bond between the niobium coating and the substrate for optimal thermal contact and is compatible with high pressure rinsing and mechanical polishing (e.g. centrifugal barrel polish).

In this paper we will summarize previous work towards the adaption of CVD niobium processing for SRF applications, with particular focus on work done in the past year by Cornell University in collaboration with industry partner Ultramet. Much of the work discussed here has been previously published by Cornell University [4–6], Ultramet [7], and P. Pizzol et al. [8–10]. Although a CVD technique, we will not discuss Atomic Layer Deposition (ALD) in this work.

CHEMICAL VAPOR DEPOSITION

In the CVD process one or more precursor and reactant gasses/vapors are exposed to the substrate (in a chamber called the reactor) and either react or (thermally) decompose, leaving behind the coating material. A diagram of a reactor used can be seen in Fig. 1. There are a variety of compounds, temperatures, pressures, and configurations for coating various materials. A common process for coating niobium is to vaporize $NbCl_5$ (the precursor) in a bubbler, carry it into the reactor using a gas (such as argon) while simultaneously pumping in hydrogen gas (the reactant gas). The reaction: $2\,NbCl_5 + 5\,H_2 \rightarrow 2\,Nb + 10\,HCl$ takes place, leaving niobium on the substrate while the remaining gasses are pumped out of the reactor. The substrate is heated (to, say, 700 C) so that the reaction primarily takes place on the substrate. This technique is used by P. Pizzol et al. to produce niobium thin films [8].

SAMPLE STUDIES

Initial work between Cornell and Ultramet began in the early 2000's [4]. In 2005 Cornell tested a CVD niobium coating on a molybdenum puck provided by Ultramet (with no coating process information provided). This sample had a slightly suppressed T_c of 8.88 K versus 9.26 K for bulk

* This work was supported under Department of Energy SBIR Phase 1 Award No. DE-SC0015727 to Ultramet. This work made use of the Cornell Center for Materials Research Shared Facilities which are supported through NSF MRSEC program, Award No. DMR-1120296
† rdp98@cornell.edu

ISBN: 978-3-95450-191-5 doi:10.18429/JACoW-SRF2017-WEYA02

CONSTRUCTION AND PERFORMANCE TESTS OF PROTOTYPE QUARTER-WAVE RESONATOR AND ITS CRYOMODULE AT RIKEN

N. Sakamoto*, O. Kamigaito, H. Okuno, K. Ozeki, K. Suda, Y. Watanabe, K. Yamada
RIKEN Nishina Center, Saitama, Japan
E. Kako, H. Nakai, K. Umemori, KEK, Ibaraki, Japan
H. Hara, K. Okihira, K. Sennyu, T. Yanagisawa
Mitsubishi Heavy Industries Mechatronics Systems, Ltd. (MHI-MS), Kobe, Japan

Abstract

This paper describes the development of a superconducting quarter-wave resonator for use in an intense low-β-ion linear accelerator [1]. The prototype cavity was fabricated from bulk Nb, inner cavity surface processing was performed, and vertical testing was carried out. In the vertical test, a Q-value of 8.7 $\times 10^8$ was obtained with an operating field gradient of 4.5 MV/m at a frequency of 75.5 MHz [2]. Here, we describe the results of the performance tests and various phenomena we experienced during the tests. After the vertical tests, the helium vessel was assembled and the prototype resonator was integrated into a cryomodule. Initial cooldown testing results are described. Performance testing of the cryomodule is continuing. The situation of upgrade of the RIKEN heavy-ion RIKEN Linac (RILAC) [3, 4] is also reported.

INTRODUCTION

Since 2015, the accelerator group of Nishina Center joined the ImPACT program, led by Dr. Fujita, to develop a system for processing so-called long-lived fission products (LLFPs) via nuclear reactions and transmutations induced by ion beams provided by a particle accelerator [5]. As a part of this program, a superconducting (SC) resonator and its cryostat were proposed and accepted, and we began to research its feasibility and manufacturability and design it for performance in a high-power continuous-wave linear accelerator (linac). Linac energy and ion species will be optimized by extensive simulations and new data for nuclear reactions conducted under the ImPACT program.

The developed superconducting cavity was based on the structure of a quarter-wave resonator (QWR) (Fig. 1) for optimum β as low as 0.08. The schematic of the prototype is shown in Fig. 1. The planned operating acceleration gradient is 4.5 MV/m with a Q-factor of 8.9 $\times 10^8$ estimated by using 3D simulation package Micro Wave Studio (MWS) [6]. The refrigeration capacity is set at 8 W for cavity wall loss.

Based on what we have learned with the development of the QWR, we are proceeding with the upgrade of the RILAC. Two cryomodules, each of which will hosts 4 QWRs with a frequency of 73 MHz.

* nsakamot@ribf.riken.jp

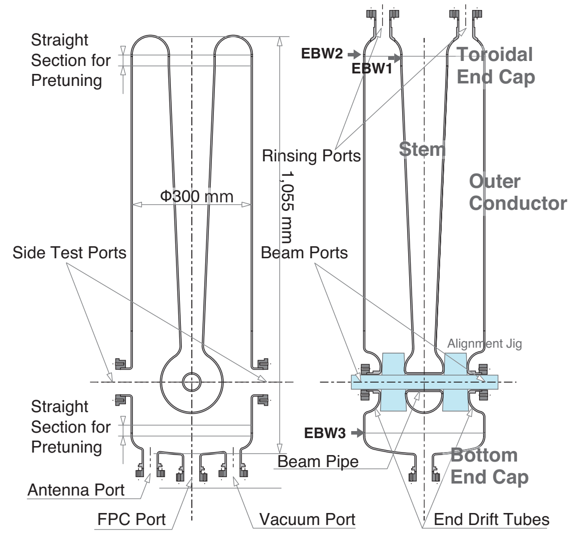

Figure 1: Schematic of the prototype QWR cavity (75.5 MHz).

MANUFACTURING OF PROTOTYPE Nb QWR CAVITY

Fabrication of Cavity

The prototype cavity is made of pure Nb sheets with a residual resistance ratio of 250 provided by Tokyo Denkai Co., Ltd. (TD), and hard Nb (so-called grade 2 Nb) provided by ULVAC is used for port flanges instead of NbTi. The pipes of the beam ports and the beam pipe were machined from bulk Nb (provided by TD). Frequency tuning during manufacturing and interior surface processing are major technical issues in the fabrication of a SC cavity. The main cavity components consist of a top toroidal end cap, an inner conductor (the so-called stem), an outer conductor with beam ports, and a bottom end cap. These parts have two straight sections near the top and bottom for frequency tuning. Note that the prototype cavity does not use a liquid He refrigerator, so it was not required to have a license from the High Pressure Gas Safety Institute of Japan. Before joining the parts by electron beam welding (EBW), the amount of material to cut from the straight sections was carefully determined from measurement of the resonance frequency by pre-assembling the cavity and accounting for shrinkage by the EBW process. Most of the difficulty in pre-tuning comes from the fact that the upper part (indicated as EBW1 and 2 in Fig. 1) must be

Content from this work may be used under the terms of the CC BY 3.0 licence (© 2017). Any distribution of this work must maintain attribution to the author(s), title of the work, publisher, and DOI.

18th International Conference on RF Superconductivity SRF2017, Lanzhou, China JACoW Publishing
ISBN: 978-3-95450-191-5 doi:10.18429/JACoW-SRF2017-WEYA03

A SEAMLESS QUARTER-WAVE RESONATOR FOR HIE-ISOLDE

S. Teixeira López*, M. A. Fraser, M. Garlasché, T. Mikkola,
A. Miyazaki, A. Sublet, W. Venturini Delsolaro
CERN, Geneva, Switzerland

Abstract

The superconducting linac booster for the HIE-ISOLDE project, in operation at CERN, is based on Nb/Cu coated Quarter Wave Resonators (QWR) [1]. The performance of the series cavities has been presumably limited by defects in the copper substrates close to the electron beam (EB) weld. A novel cavity design has been developed and prototyped in order to allow the manufacturing of the resonators by machining them from the bulk, without any weld. The RF design was optimized for the customary figures of merit and fully integrated in the HIE-ISOLDE cryomodule. Mechanical tolerances were assessed in relation to the available range of pre-tuning and demonstrated on a dummy prototype. Beam dynamics simulations were carried out to check the effects on the beam when the new cavities will be installed in the high energy end of the linac. This document covers the design and the experimental results of the first Nb/Cu seamless QWR for HIE-ISOLDE.

INTRODUCTION

In the context of the HIE-ISOLDE project, a post accelerator is being built at CERN for the radioactive ions beams produced at the ISOLDE facility. The linac relies on superconducting Quarter Wave Resonators, based on the Nb/Cu technology. In the baseline design of this RF cavity substrate [2] , the QWR is made out of two 3D forged OFE copper parts which are joined together by EB welding. The location of the EB weld is close to the shorting section of the QWR, i.e. on the high magnetic field region and the two parts have to be carefully prepared and matched by shrink fitting. The manufacturing process was developed and successfully tested at CERN (three prototypes were done prior to launching the series production, and two more recently). Regrettably, many cavities produced in industry were subject to defects, mostly located close to the EB weld (projections, inclusions, etc.). The most critical defects, shown in Figure 1, were in the form of cracks going deep into the material, predominantly along grain boundaries.

The origin of these imperfections was thoroughly investigated but a full understanding could not be reached. The relative degradation of the Q values in the series cavities as compared to the prototypes has been correlated to the amount of defects observed. This degradation can be observed in Figure 2.

The purpose of the work described in this document was to modify the design of the copper substrates with the aim of making it possible to machine them from a single copper billet, thus avoiding completely the EB weld. The inspiration came from the experience done with a smaller QWR for the ALPI linac in INFN [3]. The main modification required was to reduce the protuberances of the RF surface at the beam ports (cavity noses). This was considered possible and even favourable in the high energy section of the HIE ISOLDE Linac [4]. Removing the weld from the high magnetic field region would eliminate the main source of potential imperfections in the location where the sensitivity to RF losses is highest. The cross section for conduction cooling of the cavity is also very much increased in the new design. For these two reasons the final cavity performance was expected to improve.

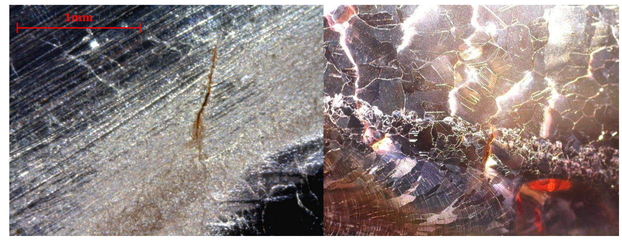

Figure 1: Defects on the welding area of the QS series cavities.

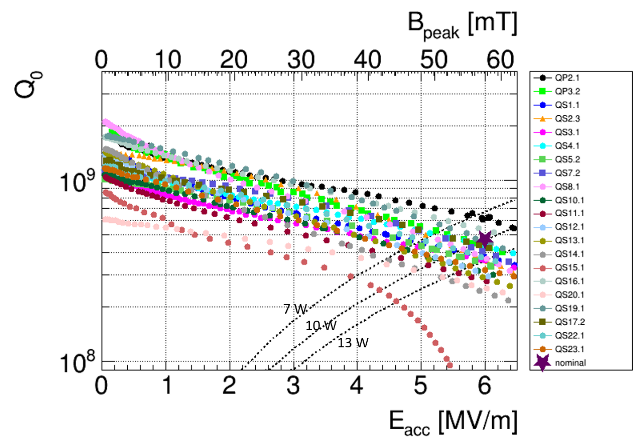

Figure 2: Performance of the QS cavities.

RF DESIGN

This study presents a comparison of a new seamless conical cavity (QSS) and the nominal design (QS) that is currently installed in the first, second and third cryomodules (CM1, CM2 and CM3). All the simulation results presented in this work have been performed with CST Microwave Studio 2016 [5] and bench-marked using ANSYS HFSS [6].

The new RF design started as a perturbative expansion of the already existing series production (QS) cavity, which

* silvia.teixeira@cern.ch

Content from this work may be used under the terms of the CC BY 3.0 licence (© 2017). Any distribution of this work must maintain attribution to the author(s), title of the work, publisher, and DOI.

ISBN: 978-3-95450-191-5 doi:10.18429/JACoW-SRF2017-WEYA05

PROGRESS TOWARD 2 K HIGH PERFORMANCE HALF-WAVE RESONATORS AND CRYOMODULE*

Z.A. Conway†, B.M. Guilfoyle, M.J. Kedzie, M.P. Kelly and T.C. Reid, Argonne National Laboratory, Argonne, IL 60439, U.S.A.
H. Guo, Institute of Modern Physics, Chinese Academy of Sciences, Lanzhou, China

Abstract

Argonne National Laboratory is implementing a novel 2.0 K superconducting cavity cryomodule operating at 162.5 MHz. This cryomodule is designed for the acceleration of 2 mA H$^-$/proton beams from 2.1 to 10.3 MeV as part of the Fermilab Proton Improvement Project-II (PIP-II). The 2.0 K cryomodule is comprised of 8 half-wave cavities operated in the continuous wave mode with 8 superconducting magnets, one in front of each cavity. In this paper we will review recent cavity results which demonstrate continuous-wave operated cavities with low-field residual resistances of 2.5 nΩ which achieve peak surface fields up to 134 MV/m and 144 mT, electric and magnetic respectively, with field emission onset fields greater than 70 MV/m in the production cavities following the prototyping effort.

INTRODUCTION

Argonne National Laboratory is building a superconducting half-wave accelerator cryomodule for the Proton Improvement Project-II (PIP-II) at Fermi National Accelerator Laboratory (FNAL). This cryomodule will accelerate a 2 mA H$^-$ beam from 2.1 to 10.3 MeV for a new 800 MeV linac which will replace the existing 400 MeV machine [1, 2]. The cryomodule houses 8 162.5 MHz half-wave resonators (HWRs) and 8 superconducting solenoids, one in front of each resonator. The entire cold-mass will operate at 2.0 K and each of the HWRs is designed to provide up to 2.0 MV of effective voltage gain for beta = 0.11 H$^-$ ions with less than 2 W of dynamic cryogenic load. In 2015 the cold test results of two prototype HWRs were presented showing low-field residual resistances of 2.5 nΩ with peak surface fields reaching 90 MV/m and 95 mT [3]. Since then the fabrication and processing of an additional 7 HWRs, referred to as production HWRs, ha been finished. 5 of the 7 production HWRs have been cold tested and 4 of those have exceeded the prototype HWR peak field performance. In this paper the production HWR RF performance parameters, results of cold testing and future plans will be discussed.

HALF-WAVE RESONATOR PROPERTIES

The need to couple 2 MV per resonator to an H$^-$ beam with β=0.11 resonators operating at 162.5 MHz while reducing the peak surface fields and cryogenic losses (< 2 W) simultaneously and maximizing the shunt impedance determined the HWR design [4]. This was accomplished with an advanced geometry based on conical inner and outer conductors. The conical shape increases the volume over which the magnetic energy is stored decreasing the peak surface magnetic field and increasing the shunt impedance in a manner analogous to re-entrant elliptical-cell resonators [5]. This design is electromagnetically similar to recently commissioned quarter-wave resonators which have excellent online performance [6]. Table 1 gives the RF performance parameters for the HWRs. Figure 1 shows a finished HWR with an integral 304L stainless steel helium jacket.

The RF design described above includes 2 ports on each end of the resonator. These ports ensure that the aluminium electropolishing cathodes remove material from the cavity surface as evenly as practical and also provide good drainage with sufficient high pressure water rinse wand access for thorough low-particulate cleaning.

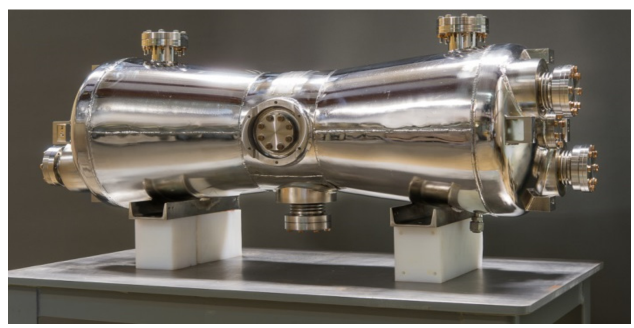

Figure 1: A 162.5 MHz, β = 0.11, niobium half-wave resonator enclosed in an integral stainless-steel helium vessel. The cavity is 125 cm end-to-end.

Table 1: HWR RF Parameters

Parameter	Value
Frequency	162.5 MHz
Beam Aperture	33 mm
β	0.112
Effective Length (βλ)	20.7 cm
E_{peak}/E_{acc}	4.68
B_{peak}/E_{acc}	5.02 mT/(MV/m)
$G = R_sQ$	48.2 Ω
R_{sh}/Q	271.7 Ω

*This material is based upon work supported by the U.S. Department of Energy, Office of Science, Office of Nuclear Physics, under contract number DE-AC02-06CH11357, and the Office of High Energy Physics, under contract number DE-AC02-76CH03000. This research used resources of ANL's ATLAS facility, which is a DOE Office of Science User Facility.
† zconway@anl.gov

Content from this work may be used under the terms of the CC BY 3.0 licence (© 2017). Any distribution of this work must maintain attribution to the author(s), title of the work, publisher, and DOI.

ISBN: 978-3-95450-191-5 doi:10.18429/JACoW-SRF2017-THXA03

CRAB CAVITIES FOR THE HIGH-LUMINOSITY LHC*

Rama Calaga, CERN, Geneva, Switzerland

Abstract

As a first step towards the realization of crab crossing for High-Luminosity LHC (HL-LHC), two superconducting crab cavities are foreseen to be tested for the first time in the SPS with protons. The progress on the cavity fabrication, RF test results, cryomodule development and integration into the SPS are presented. Some aspects of the beam tests with crab cavities in the SPS are outlined.

INTRODUCTION

A luminosity upgrade of the LHC is planned for 2024-25 to extend the lifetime and physics reach of the LHC into the next decade. This upgrade will increase the integrated luminosity potential by ten-fold to 300 fb^{-1}/yr from the present LHC [1]. Two key superconducting technologies are required to enable this upgrade high field large aperture quadrupoles and high field compact crab cavities. Fig 1 shows a schematic layout of the interaction region upgrade (to to scale).

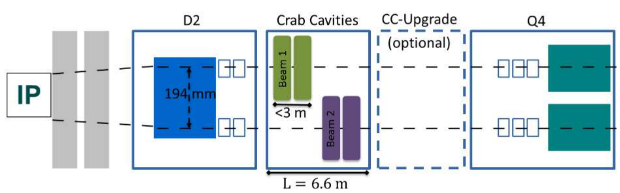

Figure 1: Schematic of the LHC interaction region and the respective magnetic and RF elements to be upgraded for HL-LHC.

Some relevant parameters for the LHC design and upgrade are listed in Table 2.

Table 1: Some relevant parameters for the LHC nominal and upgrade lattices.

	Unit	LHC	HL-LHC
Energy	[TeV]	7	7
p/bunch	[10^{11}]	1.15	2.2
Bunch Spacing	[ns]	25	25
ϵ_n (x,y)	[μm]	2.5	2.5
σ_z (rms)	[cm]	7.55	9.0
$\mathrm{IP}_{1,5}$ β^*	[cm]	55	20
Betatron Tunes	-	64.31, 59.32	62.31, 60.32
X-Angle: $2\phi_c$	[μrad]	300	590
Piwinski Angle	$\frac{\sigma_z}{\sigma^*}\phi_c$	0.65	3.14
RF Frequency	[MHz]	400.79	
Peak luminosity	[$10^{34}\mathrm{cm}^{-2}\mathrm{s}^{-1}$]	1.0	7.2

CRAB CAVITIES

Without crab crossing in the HL-LHC, the beams see each other at more than 128 locations excluding the collision points due to the fact that they share a common beam pipe in the four interaction regions. Separation between the counter rotating beams is accomplished by introducing a crossing angle at the interaction point (IP), which needs to increase with the inverse of the transverse beam size to maintain a constant normalized beam separation.

The non-zero crossing angle implies an inefficient overlap of the colliding bunches. The luminosity reduction compared to that of a zero crossing angle, assuming a Gaussian distribution, can be conveniently expressed by a reduction factor,

$$R_\Phi = \frac{1}{\sqrt{(1+\Phi^2)}} \tag{1}$$

where $\Phi = \sigma_z\phi/\sigma_x$ is the Piwinski angle, σ_z is the bunch length, σ_x is the beam size and ϕ is the half crossing angle at the IP. As shown in Table 2, a Piwinski angle as large as 3 results in a the peak luminosity loss of more than 70%.

Therefore, to fully exploit the available luminosity, a time-dependent transverse kick from an RF deflecting cavity applied. This action rotates the bunch in the $x-z$ (or $y-z$) plane about the barycentre of the bunch (see Fig. 2). The kick is transformed to a relative displacement of the head and the tail of the bunch at the IP after a phase advance of 90° to impose a head-on collision. The advantage of this technique is that the required beam separation to minimize parasitic collisions is still maintained without loss of luminosity. This effect can also be viewed as z-dependent dispersive orbit. The upstream RF deflector is used to reverse the kick to confine the bunch rotation to within the IR.

Figure 2: Schematic of the bunch crossings at the IP with and without crab cavities.

Since the crossing plane in the two high luminosity experiments is different, a local crab cavity system is a prerequisite. The required HL-LHC crossing angle together with the beam optics require the crab cavities to provide a total voltage of 12 – 13 MV per beam per side of each collision point at a frequency of 400.79 MHz. The present baseline for HL-LHC will use a two-cavity cryomodule as the basic unit on each side of the IP per beam. Each cryomodule will provide a total deflecting voltage of 6.8 MV (3.4 MV per cavity). The additional voltage required for the full compensation is kept optional with the infrastructure designed to accommodate

* Research supported by the HL-LHC project and the DOE, UK-STFC and KEK

Content from this work may be used under the terms of the CC BY 3.0 licence (© 2017). Any distribution of this work must maintain attribution to the author(s), title of the work, publisher, and DOI.

ISBN: 978-3-95450-191-5 doi:10.18429/JACoW-SRF2017-THXA04

Content from this work may be used under the terms of the CC BY 3.0 licence (© 2017). Any distribution of this work must maintain attribution to the author(s), title of the work, publisher, and DOI.

FABRICATION, TREATMENT AND TEST OF LARGE GRAIN CAVITIES*

Jiankui Hao, Shengwen Quan, Lin Lin, Feng Zhu, Fang Wang,
Liwen Feng, Huamu Xie, Kexin Liu, Jiaer Chen
Institute of Heavy Ion Physics & State Key Laboratory of Nuclear
Physics and Technology, Peking University, Beijing 100871, China

Abstract

Development of SRF technology has been included in the project of Soft X-ray FEL (SXFEL) for a hard X-ray FEL plan in China which would be operated in CW mode. Six 9-cell TESLA type cavities as well as several single-cell cavities made of Ningxia large grain niobium material have been fabricated by Peking University for achieving high gradient and high intrinsic quality factor Q_0. The measurements of gradient and Q_0 have been carried out with a new vertical test system at PKU. The process of fabrication, surface treatment and test results of these large grain cavities are presented in this paper.

INTRODUCTION

Researches on large grain superconducting cavities have been carried out for more than ten years. It is reported that the average intrinsic quality factor Q_0 of large grain niobium cavities at 2 K is higher than standard fine grain Nb cavities [1-3]. SRF technology has been developed at Peking University (PKU) since 1990's. Researches on large grain cavities were started from 2005. A series of large grain cavities were fabricated and tested, including single cell, 2-cell, 3.5-cell cavities. The gradient of a single cell and a 2-cell cavity made of large grain niobium was larger than 40 MV/m and the quality factor was higher than 1×10^{10} [4-5]. A 3.5-cell large grain cavity was fabricated for DC-SRF photoinjector and the gradient of the cavity reached 23.5 MV/m, Q_0 value is higher than 1.2×10^{10} in vertical test at Jlab [6]. 5 years ago, we fabricated four 9-cell TESLA type cavities, among which two large grain cavities PKU2 and PKU4 showed good performances. The maximum gradient of PKU2 reached 22.4 MV/m and Q_0 was about 2×10^{10} at the highest gradient at 2 K [7]. The E_{acc} of PKU4 was 32.6 MV/m and Q_0 was above 1.0×10^{10}, which fulfilled the requirement for ILC both in gradient and intrinsic quality factor [8]. PKU2 and PKU4 were installed in the 2×9-cell cryomodule and operated for electron beam loading experiments successfully.

In recent years, development of SRF technology has been included in the project of Soft X-ray FEL (SXFEL), which is the pre-research for a hard X-ray FEL plan in China which would be operated in CW mode. The purpose is to develop SRF technology and test the production capability of multi-cell superconducting cavities. Due to the advantage in Q_0, large grain cavities were chosen as the candidate for cavity production. Six 9-cell TESLA type large grain cavities were fabricated, treated and tested by Peking University. The results are presented in this paper.

*Work supported by National Key Programme for S&T Research and Development (Grant NO.:2016YFA0400400) and National Natural Science Foundation of China (Grant No. 11575012).

FABRICATION AND TREATMENT OF LARGE GRAIN CAVITIES

The fabrication and part of treatment of large grain cavities are finished at Ningxia Orient Superconductor Technology Co., Ltd. (OSTEC). OSTEC was founded jointly by Ningxia Orient Tantalum Industry Co. Ltd (OTIC) and Peking University in 2011, in order to promote the SRF technology and meet the increasing demand for superconducting cavities in China and around the world. Field flatness tuning, final treatment and vertical test are carried at Peking University.

Fabrication

Six large grain 9-cell cavities were fabricated with deep drawing, precise machining and vacuum electron beam welding in early 2017, see Fig. 1. The large grain niobium sheets with RRR > 250 was produced by OTIC. Investigation shows the phonon peak of OTIC large grain niobium can be recovered by heat treatment at a temperature of more than 800°C [9]. The length and frequency of the 6 cavities are given in Table 1. The length of NXPKU3 is shorter than the standard length because of technical reason.

Figure 1: Large grain 9-cell TESLA cavities.

Treatments

After fabrication and RF measurement, a series of treatments were applied to the cavities, including standard BCP, pure water rinsing, HPR and high temperature annealing, etc. A total of 210 μm of inner surface was removed by BCP for each cavity to remove the impurities during the fabrication. High pure water rinsing and HPR were used after BCP to remove the remaining acid. After BCP, the cavities were annealed in a high temperature furnace for fabrication stress releasing and hydrogen

ISBN: 978-3-95450-191-5 doi:10.18429/JACoW-SRF2017-THXA06

ADVANCED OST SYSTEM FOR THE SECOND-SOUND TEST OF FULLY DRESSED CAVITIES

Y. Tamashevich[1], Helmholtz-Zentrum Berlin for Materials and Energy (HZB), Berlin, Germany
[1]also at University of Hamburg/DESY, Hamburg, Germany

Abstract

Cavities which exhibit a low field quench are normally discarded from usage in accelerator projects. However, they can be repaired if the exact location of the quench is known. Optical inspection alone cannot reliably locate the source of a quench. Methods that directly measure the quench, such as thermometry or second sound detection, could so far only be performed at undressed cavities. A new, specially designed, second-sound system for the first time allows the localization of the quench in multicell cavities equipped with a helium vessel. It can be easily installed in the helium pipe of the cavity. Information on the quench location can be acquired during a standard rf test. A new algorithm localizes the quench based on the real path of the second-sound wave around the cavity surface, rather than using simple triangulation. The implemented pathfinding method leads to a high precision and high accuracy of the quench location. This was verified by testing standard dressed 9-cell XFEL cavities. The system can be easily applied to other cavity shapes and sizes.

DETECTORS

In the setup second sound oscillations are detected by oscillating superliquid transducers (OST) [1, 2]. Within the OST the electrical capacity changes due to oscillation of the ratio of the fractions of helium phases.

While the OST is biased, its capacitance changes leads to voltage changes on the measuring resistors. The voltage oscillations on this resistor can be easily measured after the amplification.

Single OST

Positioning OSTs around the cavity leads to the highest resolution and lowest uncertainties of the measurement results.

OSTs of the original [2] design with a porous membrane (see Fig. 1) are often suitable for second sound tests of naked cavities. While providing a high signal level, the relatively large area of the membrane doesn't allow positioning the OST in small volumes such as a helium tank or a helium nozzle pipe. At the same time reducing of the OST dimensions reduces the signal and requires a higher gain of the amplifier.

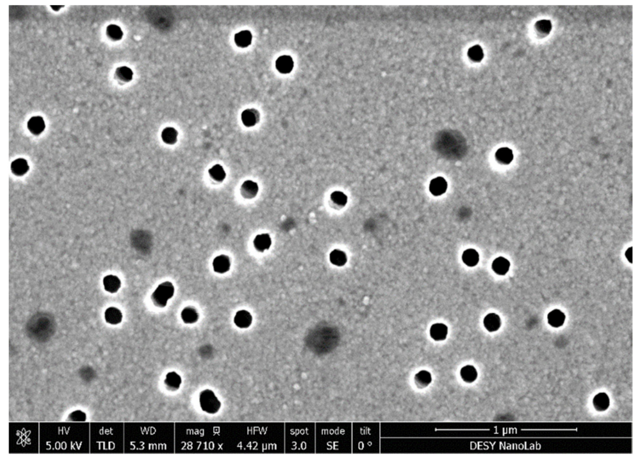

Figure 1: SEM image of the OST membrane [3].

A single OST with outer diameter of only 9 mm was developed to counter these challenges. It has an SMC connector significantly smaller than previously used SMA connector. The optional outer thread allows easy and rigid installation of such a sensor similar to a usual screw. Such sensors are used for example for horizontal test of bERLinPro booster cavities. As these cavities will be tested in HoBiCat only once, there is no need for a special holder which can provide repeated use. Therefore, four of such OSTs were installed on a plastic 3D printed holder (see Fig. 2) and positioned in a helium pipe (see Fig. 3). The holder provides precise and stable positioning of the OSTs which is important to exactly locate the quench. OSTs are connected by coaxial cables via vacuum feedthrough located on a helium pipe.

Figure 2: Four OSTs are assembled on a single plastic holder.

Content from this work may be used under the terms of the CC BY 3.0 licence (© 2017). Any distribution of this work must maintain attribution to the author(s), title of the work, publisher, and DOI.

ISBN: 978-3-95450-191-5 doi:10.18429/JACoW-SRF2017-THXA08

REVIEW OF HEAT TREATMENTS FOR LOW BETA CAVITIES: WHAT'S SO DIFFERENT FROM ELLIPTICAL CAVITIES

D. Longuevergne, IPNO, Orsay, France

Abstract

Heat treatments done for low beta (low frequency) cavities are usually, due to the lack of feedback, inspired from elliptical (high frequency) cavity results.

Is that still relevant now that experimental data are available thanks to the florishing business of low beta structures (Spiral2, ESS, FRIB, C-ADS, MYRRHA, PROJECTX, ...).

These two families are moreover not usually operating in the same resistance regime (BCS and residual).

The paper will review procedures applied and results obtained on different type of cavities (Quarter-Wave resonator, Half-Wave resonator and Spoke) and different temperature treatments (low temperature baking, hydrogen degassing, nitrogen doping, ...) and compare these to elliptical cavities.

INTRODUCTION

Heat treatments and specifically hydrogen degassing have been applied to L-band elliptical cavities to avoid severe irreversible degradations (see Figures 1 and 2) of the quality factor due to the precipitation of hydrogen (called Q-disease or 100K effect). This treatment typically done at 800°C during 3h under vacuum was compulsory to achieve performance requirements in terms of power dissipations ($Q_0 > 1E10$) at accelerating gradients targeted by superconducting linac projects ($E_{acc} > 20$ MV/m).

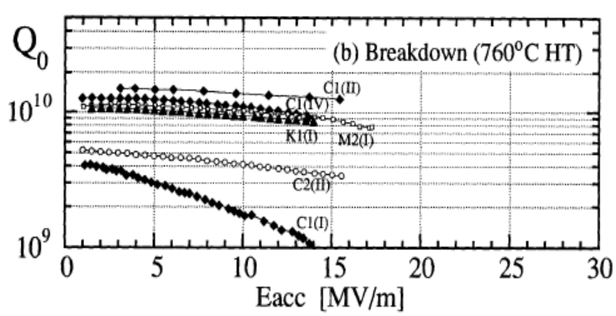

Figure 1: Study of the effect of heat treatments done on elliptical cavities at KEK in 1993. Curve C1(I) and Curve C1(II) represent respectively the quality factor at 2K versus accelerating gradient of a non-degassed and 760°C degassed cavity (figure extracted from [1]).

The heat treatment is followed by an Electro-Polishing (EP) or Buffered Chemical Polishing (BCP) of few tens of microns to remove the surface polluted by the residual gas re-absorbed by bulk Niobium at the end of the process. Indeed, at these temperatures, the oxide barrier is dissolved allowing any pollution to diffuse into the bulk.

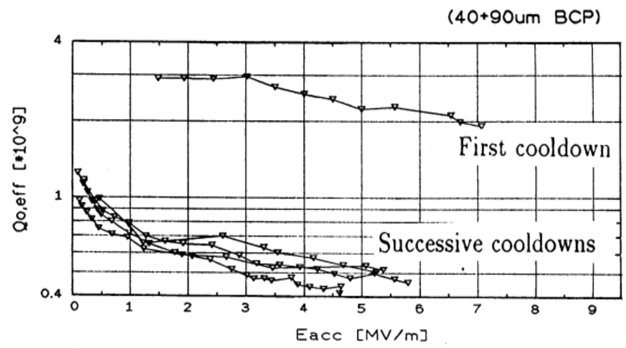

Figure 2: Irreversible degradation caused by hydrogen precipitation of an elliptical cavity after successive cooldown (figure extracted from [2])

Once this treatment optimized and part of the standard preparation of cavities, performances were then limited by what has been called the High Field Q-slope (HFQS). This very abrupt Q_0 degradation has been investigated for long. Even though the origin of this phenomenon is not totally understood, a cure has been reported by B. Visentin in 1998 [3]. Baking a cavity at 170°C during 70h would not only mitigate the HFQS but also decrease the BCS resistance as visible on Figure 3. Optimization of the baking treatment made it converge at 120°C during 48h.

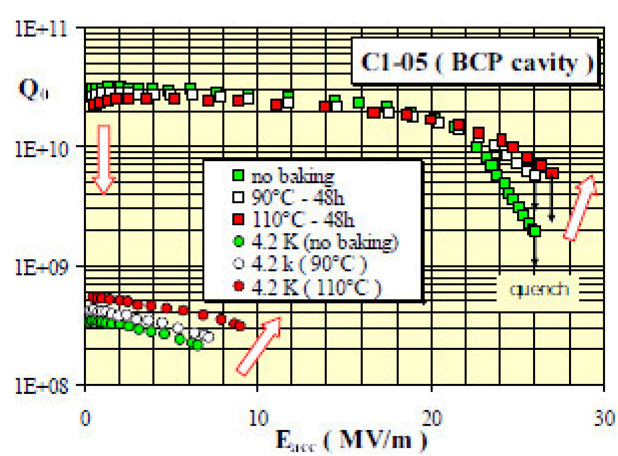

Figure 3: Improvement of the BCS resistance with a 110°C baking during 48h. A Q_0 improvement at 4.2K is the sign of reduction of BCS resistance. A Q_0 degradation at 2K is sign of residual resistance increase (figure extracted from [4]).

Content from this work may be used under the terms of the CC BY 3.0 licence (© 2017). Any distribution of this work must maintain attribution to the author(s), title of the work, publisher, and DOI.

ISBN: 978-3-95450-191-5 doi:10.18429/JACoW-SRF2017-THYA01

PERFORMANCE TESTING OF FRIB EARLY SERIES CRYOMODULES*

J.T. Popielarski†, C. Compton, A. Ganshyn, W. Hartung, D. Luo, S.J. Miller, D.G. Morris, P.N. Ostroumov, L. Popielarski, K. Saito, S. Shanab, S. Stark, T. Xu, S. Zhao, Z. Zheng
Facility for Rare Isotope Beams, Michigan State University, East Lansing, MI, USA

Abstract

Construction of a new accelerator for nuclear physics research, the Facility for Rare Isotope Beams (FRIB), is underway at Michigan State University (MSU). The FRIB linac will use superconducting resonators operating at a temperature of 2 K to accelerate ions to 200 MeV per nucleon. The linac requires 104 quarter wave resonators (80.5 MHz, β = 0.041 and 0.085) and 220 half wave resonators (322 MHz, β = 0.29 and 0.53), all made from sheet Nb. Production resonators are being fabricated by cavity vendors; the resonators are etched, rinsed, and tested in MSU's certification test facility. Cavity certification testing is done before the installation of the high-power input coupler and tuner. After certification and cryomodule assembly, the resonators are tested in the cryomodule before installation into the FRIB tunnel. The cryomodule test goals are to verify integrated operation of the resonators, RF couplers, tuners, RF controls, and superconducting solenoids. To date, 12 out of 46 cryomodules have been completed, and 9 have been certified. Cavity and cryomodule certification test results are presented in this paper.

FRIB CAVITIES

The FRIB linac will use 2 types of quarter wave resonators (QWRs), and 2 types of half wave resonators (HWRs). Drawings of the production cavities are shown in Figure 1; design parameters are given in Table 1. Prior to cavity production, all cavity designs were validated with pre-production cavities. The goal for Dewar certification testing of production cavities is to reach an accelerating gradient (E_a) 20% higher than the cryomodule performance goal, with the same intrinsic quality factor (Q_0).

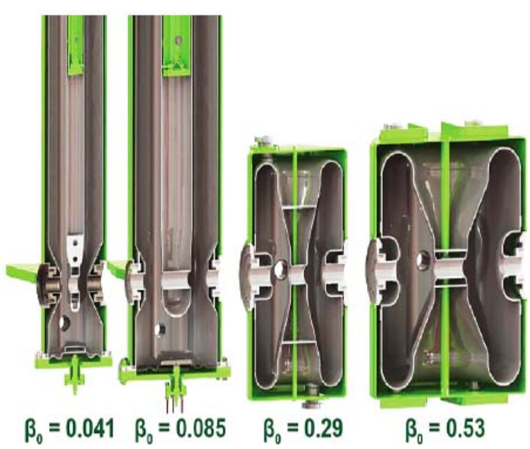

Figure 1: Isometric sectional views of FRIB production cavities.

*Work supported by the U.S. Department of Energy Office of Science under Cooperative Agreement DE-SC0000661
†popielar@frib.msu.edu

Table 1: FRIB Production Cavity Parameters

Cavity Type	QWR	QWR	HWR	HWR
β_0	0.041	0.085	0.29	0.53
f (MHz)	80.5	80.5	322	322
Accelerating voltage (MV)	0.81	1.78	2.09	3.70
E_a (MV/m)	5.1	5.6	7.7	7.4
Peak E field E_p (MV/m)	30.8	33.4	33.3	26.5
Peak B field B_p (mT)	54.6	68.9	59.6	63.2
Q_0 (VTA)	1.4E9	2.0E9	6.7E9	9.2E9
# of cavities/cryomodule	4	8	6	8
Total Dynamic load to cryoplant (2 K)	7.3	34.8	22.8	65.2
Control bandwith (Hz)	40	40	52	30
Maximum RF power (kW)	0.7	2.5	2.8	5.0
# of cavities needed	12	92	72	148
# of cavities certified	16	69	68	17
# of cryomodules needed	3	11	12	18
# of cryomodules certified	3	5	0	1

CAVITY PRODUCTION AND TESTING

As of July 2017, 240 cavities have been received out of 324 cavities needed for the FRIB linac; 208 cavities have been certified for installation in cryomodules. The remaining cavities will be received by the middle of 2018. Approximately 10% of the cavities were returned to the vendor before Dewar testing due to issues identified during acceptance checking (welds, dimensions, threads, etc.). More detailed cavity production information can be found in a separate paper [1].

After acceptance, production cavities are cleaned, etched (buffered chemical polishing, BCP), hydrogen degassed, and high-pressure water rinsed at MSU [1]. These steps are carried out in the FRIB SRF High Bay [2].

All cavities undergo a Dewar certification test before they are installed in a cryomodule. Up to 5 cavities can be Dewar tested per week. Less than 20% of the cavities require rework after the first Dewar test. Certified cavities are installed into cryomodules at MSU [3].

Dewar Test Procedures and Certification Requirements

Resonators are delivered with their helium jacket. The Dewar test is done in such a way as to approximate the cryomodule environment, with liquid helium in the jacket and the Dewar under vacuum (in contrast to the more customary Dewar dunk test of an unjacketed cavity). As seen in Figure 2, we use an insert with a helium reservoir, which provides a larger volume of helium for pumping to 2 K. The insert is prepared and installed into the Dewar the evening before the test begins. After the morning cooldown, testing is done at 4.3 K, along with thorough conditioning of multipacting barriers. Typically the 4.3 K testing

Content from this work may be used under the terms of the CC BY 3.0 licence (© 2017). Any distribution of this work must maintain attribution to the author(s), title of the work, publisher, and DOI.

ISBN: 978-3-95450-191-5 doi:10.18429/JACoW-SRF2017-THYA02

Content from this work may be used under the terms of the CC BY 3.0 licence (© 2017). Any distribution of this work must maintain attribution to the author(s), title of the work, publisher, and DOI.

ACHIEVEMENT OF STABLE PULSED OPERATION AT 36 MV/m IN STF-2 CRYOMODULE AT KEK

Y. Yamamoto†, T. Dohmae, M. Egi, K. Hara, T. Honma, E. Kako, Y. Kojima, T. Konomi, T. Kubo, T. Matsumoto, T. Miura, H. Nakai, K. Nakanishi, G. Park, T. Saeki, H. Shimizu, T. Shishido, T. Takenaka, K. Umemori
High Energy Accelerator Research Organization, Tsukuba, Japan

Abstract

In the Superconducting RF Test Facility (STF) in KEK, the cool-down test for the STF-2 cryomdoules with twelve cavities has been done three times since 2014. In 2016, the third cool-down test was successfully done including the capture cryomodule with two cavities, used for Quantum Beam Project in 2012. In this paper, the result of the third cool-down test is presented in detail.

INTRODUCTION

The STF-2 cryomodules are the one and half size cryomodule, defined "Type B" in Technical Design Report (TDR) for International Linear Collider (ILC) [1], with twelve 9-cell STF-type cavities, called CM1 and CM2a, respectively. In the center of CM1, there are one superconducting quadrupole magnet developed by the collaboration between KEK and FNAL [2], and one beam position monitor developed in Accelerator Test Facility (ATF) [3].

The table 1 shows the brief history of STF-2 project. The fabrication of cavities and power couplers started from 2010. In the period of 2013-2014, the cavity string assembly and the cryomodule assembly were done, the STF-2 cryomodules were successfully installed into the STF tunnel, and the investigation for the high pressure gas regulation was done by the local government. In 2014, the first cool-down test was done for the low power measurement by network analyser, the drive test for the slide-jack tuner, and the piezo tuner test by the induced voltage of 500 V [4]. In 2015, the second cool-down test was done for the performance check in the single cavity operation using the 5 MW klystron and the single waveguide system [5, 6]. Eight of twelve cavities in the STF-2 cryomodules achieved above 31.5 MV/m as the ILC specification.

After the second cool-down test, the RF system was drastically changed, that is, the change from 5 MW klystron to 10 MW (multi-beam) klystron including the modulator, and the single waveguide system for the single cavity to multi-waveguide system for eight cavities as shown in Figure 1. And, the LLRF control system was also changed.

The third cool-down test in late 2016 was done with the capture cryomodule. At this time, fourteen 9-cell cavities were cooled down in 2K. The main purpose in the third cool-down test was to do the vector-sum operation with eight cavities, including the feedforward system, at the average accelerating gradient of 31.5 MV/m. The others are the measurement for Lorentz Force Detuning (LFD), the heat load measurement, and the Low Level RF (LLRF) study [7], and so on.

† yasuchika.yamamoto@kek.jp

Table 1: History of the STF-2 Project

Date	Content
2011~2013	V.T. for 12 cavities / RF conditioning for 12 couplers
Jul/2013~Apr/2014	Cavity string assembly
Oct/2013~Jun/2014	Cryomodule assembly
Jul/2014	Certification for high pressure gas regulation
Oct/2014~Dec/2014	1st cool-down test
Apr/2015~Jul/2015	5 MW klystron prepared
Oct/2015~Dec/2015	2nd cool-down test
Jan/2016~Jul/2016	10 MW klystron prepared
Sep/2016~Nov/2016	3rd cool-down test

CAVITY PERFORMANCE AND RADIATION LEVEL

After the cool-down, the achievable accelerating gradient for each cavity was checked again including the radiation level. Regardless of the comparable radiation level as the 2nd cool-down test, almost all cavities had the performance degradation again. Moreover, two cavities in the capture cryomodule also had the degradation, although the beamline has been kept under vacuum since 2013. The left figure in Fig. 2 shows the summary of the achievable accelerating gradient for every cavity in the capture and STF-2 cryomodules. CAV#5, #6, #7, and #9 in the STF-2 cryomodules were not tested in the 3rd cool-down test. The right figure in Fig. 2 shows the correlation plot of achievable accelerating gradient for ten cavities measured in the previous and present cool-down tests. It is clear that almost every cavity had degradation again in the 3rd cool-down test. The causes for the "more" degraded cavities are the followings:

- Change of RF system from single to multi cavity
- Not-optimized forward power to power couplers
- Earthquake

The change of RF system means that klystron, modulator, waveguide, circulator, and LLRF changed from the single cavity to multi cavity operation. Generally, there is the systematic error between the different RF systems. The change of RF system in the 3rd cool-down test may generate the change of the cavity performance.

As for the second item, during the vector-sum operation, it is necessary to keep the optimum forward power to each power coupler; however, actually, too-much forward

ISBN: 978-3-95450-191-5 doi:10.18429/JACoW-SRF2017-THYA05

DEVELOPMENTS AND PROGRESS WITH ESS ELLIPTICAL CRYOMODULES AT CEA-SACLAY AND IPN-ORSAY

F. Peauger†, C. Arcambal, F. Ardellier, S. Berry, P. Bosland, A. Bouygues, E. Cenni, JP. Charrier, G. Devanz, F. Eozénou, A. Gaget, D. Gevaert, A. Gomes, T. Hamelin, X. Hanus, P. Hardy, V. Hennion, T. Joannem, C. Marchand, O. Piquet, J.P. Poupeau, B. Renard, P. Sahuquet, T. Trublet, Irfu, CEA, Université Paris-Saclay, F-91191 Gif-sur-Yvette, France
G. Olivier, IPN Orsay, France
C. Darve, ESS, Lund, Sweden

Abstract

CEA Saclay in collaboration with IPN Orsay is in charge of the ESS elliptical cavities cryomodule design, prototyping and series production. Two cryomodule prototypes are being developed and will be tested at CEA Saclay before starting the series production. The main cryomodule design features are first reminded. We present the cavities and couplers test results and the achieved assembly sequences of the first medium beta cavities cryomodule demonstrator M-ECCTD. The progress on the preparation of the CEA cryomodule test station is given. The procurement status and development plan of the second high beta demonstrator H-ECCTD are also reported. Finally we give the components procurement progress and the assembly strategy of the 30 series cryomodules to be integrated at CEA before delivery to ESS at Lund.

INTRODUCTION

The European Spallation Source ESS is under construction in Lund, Sweden [1]. It is composed of a 62.5 mA - 2 GeV proton LINAC operating in long pulsed mode 2.86 ms – 14 Hz. The high energy section consists in 352 MHz spoke and 704 MHz elliptical superconducting cavities working at 2 K [2]. The elliptical section is made of 36 medium beta (β=0.67) 6-cell cavities which accelerate the beam from 200 MeV to 570 MeV and 84 high beta (β=0.86) 5-cell cavities up to the final energy. The elliptical cavities are grouped four by four in a 6.6 meter long cryomodule which has a common design for medium beta and high beta cavities. A total of 30 elliptical cryomodules will be integrated in the next 3 years with a delivery rate of one cryomodule per month.

An international collaboration has been established to develop and construct the 30 elliptical cryomodules. CEA Saclay and IPN Orsay collaborate to design, build and test a first Medium beta Elliptical Cavities Cryomodule Demonstrator (M-ECCTD). A second demonstrator with high beta cavities (H-ECCTD) is being developed by CEA before starting the series cryomodule activities. The 36 β=0.67 cavities will be delivered by INFN LASA (Italy) and the 84 β=0.86 cavities by STFC (UK). CEA will provide all the other components, including the power couplers and their RF processing. All cryomodules assembled in CEA Saclay will be shipped to Lund. The qualification tests at high power will be performed in the ESS test stand before the integration in the tunnel.

This paper describes the developments and progress done at CEA Saclay and IPN Orsay. The prototyping phase will be detailed as well as the preparation for the series. This work has also been reported recently in [3].

CRYOMODULE DESCRIPTION

The design of the ESS elliptical cryomodule is shown in Figure 1. It hosts four high gradient cavities specified at Eacc = 16.7 MV/m (β=0.67) and 19.9 MV/m (β=0.86). Each cavity is equipped with a single window high power coupler able to transmit 1.1 MW peak power, a 600 kHz range 1 Hz resolution cold tuning system equipped with two piezo-actuators for fast tuning, and a 2 mm thick magnetic shield made of Cryophy material.

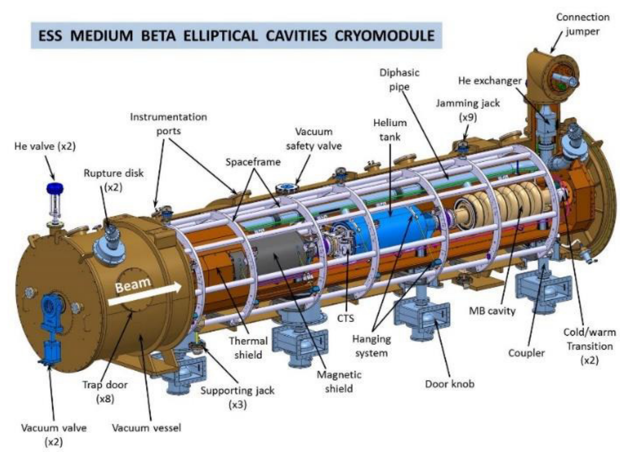

Figure 1: Elliptical cryomodule 3D view equipped with medium beta cavities.

The mechanical design of the cryomodule is based on the SNS cryomodule principle [4] where a rigid structure named spaceframe holds the four cavities and a 2 mm thick aluminium thermal shield. The spaceframe allows easy access to the cavity string and permits intermediate steps of mechanical alignment before integration inside the vacuum vessel. The segmented approach has been adopted so that independent cryomodule cool down, warm-up and replacement can be performed. Thus each cryomodule is linked to an individual valve box by a jumper connexion which provides the 4.5 K – 3 bars liquid helium (LHe) supply and return for the cavities and couplers cooling, as well as the 40 K – 19.5 bara helium cooling circuit of the thermal shield. The 2 K superfluid helium is produced inside the cryomodule by a Joule-Thomson valve. The cryomodule

Content from this work may be used under the terms of the CC BY 3.0 licence (© 2017). Any distribution of this work must maintain attribution to the author(s), title of the work, publisher, and DOI.

ISBN: 978-3-95450-191-5 doi:10.18429/JACoW-SRF2017-THYA06

LONG-TERM OPERATION EXPERIENCE WITH BEAMS IN COMPACT ERL CRYOMODULES

K. Umemori#, M. Egi, K. Enami, T. Furuya, Y. Honda, E. Kako, T. Konomi, H. Sakai, KEK, Ibaraki, Japan
M. Sawamura, QST, Ibraki, Japan, T. Okada, SOKENDAI, Japan

Abstract

Compact ERL (cERL) was constructed at KEK as a prototype for 3 GeV ERL light source. It consists of two types of SRF cavities. Three injector 2-cell SRF cavities and two main linac 9-cell SRF cavities. The beam operation started at 2013 with a few hundred nA. Beam current increased step by step and currently reached to 1mA (CW). Energy recovery has successfully achieved. Performance of the SRF cavities through long term beam operation has been investigated. cERL has suffered from heavy field emissions in operation. Field emissions of the main linac cavity started just after module assembly work, and during beam operation, performances of both the main linac and the injector SRF cavities sometimes degraded. One reason of degradation was discharges occurred at beamline components due to charge-up of electrons. Pulse aging technique helped to recover SRF performances. With the beam induced HOMs, the beam position and the beam timing studies were started. In this presentation, details of SRF beam operation, degradation, applied recovery methods are described.

INTRODUCTION

Now a day many SRF based accelerators are operated, constructed and designed [1-3]. Stable beam operation is essential for these facilities, however, sometimes degradations occur for SRF cryomodules [4]. Recovery method from degradation is also important [5,6].

Operation of cERL started at 2013. We had four years operation experiences since then. Beam current is updated to 1 mA (CW). Change of cavity performance during beam operation is summarized below.

COMPACT ERL

Compact ERL

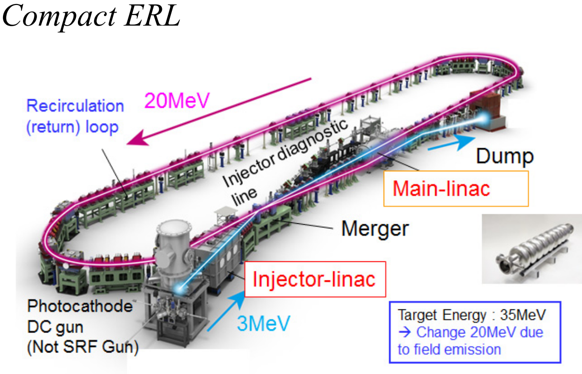

Figure 1: Schematic view of cERL.

Table 1: Design Parameter of the cERL

Nominal beam energy	35 MeV → 20 MeV
Nominal injection energy	5 MeV → 2.9 MeV
Beam current	10 mA (initial goal)
	100 mA (final goal)
Normalized emittance	0.1 – 1 mm-mrad
Bunch length	1-3 ps (usual)
(bunch compressed)	100 fs (short bunch)

Figure 1 shows schematic view of cERL [7,8] and Table 1 shows design parameters. High charge and low emittance electron beam from 500 kV DC photocathode gun come to the injector cavities and accelerated to 3 ~ 5 MeV. Beam pass through merger section accelerated to 20 MeV at the main linac cavity and then after circulation it is decelerated and dumped. Because of severe field emission occurred at the main linac cavities, beam energy is limited to 20 MeV.

Injector Cryomodule

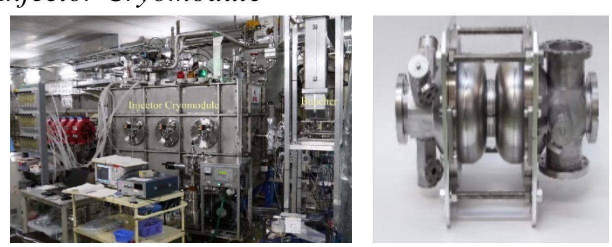

Figure 2: (left) Injector cryomodule and (right) injector 2-cell SRF cavity.

Left and right of Figure 2 shows the injector cryomodule [9] and the 2-cell SRF cavities [10]. Two input coupler ports and five HOM couplers are mounted on one cavity.

Main Linac Cryomodule

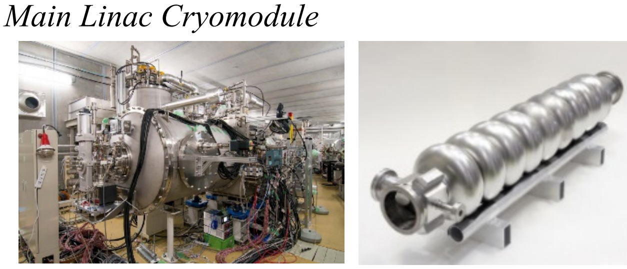

Figure 3: (left) Main linac cryomodule and (right) main linac 9-cell SRF cavity.

Left and right of Figure 3 shows the main linac cryomodule [11] and the 9-cell SRF cavities [12]. In order to achieve strong HOM damping for high-current ERL, iris diameter is increased to 80 mm. Epeak/Eacc becomes high and to be 3.0.

kensei.umemori@kek.jp

Content from this work may be used under the terms of the CC BY 3.0 licence (© 2017). Any distribution of this work must maintain attribution to the author(s), title of the work, publisher, and DOI.

ISBN: 978-3-95450-191-5 doi:10.18429/JACoW-SRF2017-THPB002

ROLE OF NITROGEN ON HYDRIDE NUCLEATION IN PURE NIOBIUM BY FIRST PRINCIPLES CALCULATIONS

P. Garg, S. Balachandran, I. Adlakha, P. J. Lee, T. R. Bieler, and K. N. Solanki

Abstract

It is well known that the formation and growth of niobium hydride degrades the superconducting radio frequency (SRF) properties of niobium cavities and the treatments that reduce hydrogen concentration improve the cavity quality factor. Recently it has also been shown that the addition of nitrogen through doping or infusion improves the quality factor of SRF niobium. Thus, in this work, the role of nitrogen solute addition in niobium on hydride precipitation is probed through first-principles calculations. In the presence of nitrogen the energetic preference for hydrogen to occupy interstitial sites in the vicinity is reduced. Furthermore, both interstitial octahedral and tetrahedral sites become equally favorable for hydrogen to occupy due to the presence of nitrogen. To examine the role of nitrogen on the nucleation of hydrides, we utilized valence charge transfer and density of states calculations. These quantum insights reveal a strong tendency for nitrogen to accumulate charge, thereby decreasing the bond strength of neighboring niobium and hydrogen atoms. These atomic scale results explain the lesser tendency of surface hydride formation in SRF niobium cavities in the presence of nitrogen and are applicable to dilute Nb-H solid solutions.

INTRODUCTION

Niobium is the primary material for manufacturing superconducting radio-frequency (SRF) cavities for many modern high-performance particle accelerators like the International Linear Collider [1, 2]. The selection of superconductors for SRF applications is based on the operating temperatures (1.8 K–4.2 K) required to minimize the surface resistance and provide and sustain high electromagnetic fields in order to accelerate the charged particles inside the cavities. Niobium has the highest critical temperature (T_c) of all the pure elements (9.25 K) as well as having high critical magnetic fields and high malleability as it can be formed into complex shapes; thus, it is well suited to make SRF cavities [2]. However, niobium can readily absorb hydrogen which may occupy interstitial sites, segregate at defects or precipitate into hydride phases, depending on the hydrogen concentration and temperature, which can significantly degrade the desired properties for SRF applications [3, 4]. The performance of SRF cavities is measured in terms of the quality factor $Q_0 = G/R_s$ where the geometric factor G depends on the cavity geometry and R_s is the average surface resistance of the inner cavity wall, as a function of the accelerating gradient field (E_{acc}) [5]. Typically, niobium cavities have a Q_0 value in the range of $10^{10} - 10^{11}$ but the absorbed hydrogen contaminates niobium and severely decreases the cavity Q_0 thereby making these SRF cavities useless [6, 7]. The formation of ordered hydride phases leads to hydrogen embrittlement and also affects the critical temperature of niobium properties since the hydride phases are not superconducting above 1-2 K [8, 9]. Therefore, improvement in the quality factor and acceleration gradients of SRF cavities is critical in the development of current and future accelerators.

Many experimental methods like X-ray, neutron and electron diffraction, differential thermal analysis (DTA), resistivity, optical microscopy, and transmission (TEM) and scanning (SEM) electron microscopyhave been used to study the niobium hydrogen system for different hydrogen concentrations [7, 10–12]. Barkov *et al.* [7, 10] observed hydride precipitates of different sizes in niobium samples using laser and optical microscopy. The shape of hydride precipitates was found to be dependent on the crystallographic orientation of each grain with the presence of small hydride precipitates near the grain boundaries [7]. The diffraction patterns obtained from temperature dependent nano-area electron diffraction and scanning electron nano-area diffraction techniques further showed that Nb_4H_3 and NbH, were respectively oriented along [110] direction of Nb at cryogenic temperatures [11]. To lower surface resistance, Grassellino *et al.* [13] reported a surface treatment technique involving nitrogen doping to improve the quality factor of SRF niobium cavities. Significantly higher Q_0 values were measured for the cavity surfaces treated in nitrogen atmosphere as compared to the Q_0 values for surfaces treated with standard methods, but the underlying mechanisms are unclear [5,13–15].Quantitative evaluation of hydrogen in SRF cavities is difficult and in situ observations have not been possible[7, 10, 12]. The first-principles calculations showed that hydrogen absorption occurs readily into niobium [2]. Hydrogen atoms occupy interstitial tetrahedral sites, expand the crystal lattice by displacing niobium atoms from their lattice sites and create lattice distortions which decrease the structural stability of niobium [3, 16]. Furthermore, first-principles calculations also show that oxygen acts as a trapping site for hydrogen by suppressing hydrogen-hydrogen interactions and inhibiting hydride formation in niobium [17, 18]. A similar inhibiting effect is expected from nitrogen doping but the understanding is limited since such calculations have not been performed yet.

In the current work, we examine the effect of nitrogen doping on the precipitation of hydride phases in niobium through first-principles calculations. Specifically, we start by calculating the interactions between hydrogen and the niobium lattice to understand the properties of hydride phases which precipitate in niobium during service conditions. Next, we investigate the effect of nitrogen on hydrogen absorption in the niobium matrix. We find that

Content from this work may be used under the terms of the CC BY 3.0 licence (© 2017). Any distribution of this work must maintain attribution to the author(s), title of the work, publisher, and DOI.

ISBN: 978-3-95450-191-5 doi:10.18429/JACoW-SRF2017-THPB003

AN INNOVATIVE DESIGN OF A FLEXIBLE TEMPERATURE-MAPPING SYSTEM*

M. Ge†, F. Furuta, P. Pamel, M. Liepe,
CLASSE, Cornell University, Ithaca, New York, 14853, USA

Abstract

A temperature-mapping (T-Map) system is an essential tool for fundamental SRF research as it provides spatial information of RF power dissipation and so allows localizing hot-spots on a cavity surface at cryogenic temperatures. However, the temperature sensors are mounted on rigid boards in most current systems, so each can only work for one specific cavity size and shape. In this paper, we proposed a flexible design, which allows this temperature mapping system to work for different cavity shapes.

INTRODUCTION

Superconducting radio-frequency (SRF) cavities are a key component of a state-of-the-art accelerator, because their ultra-low surface loss can dramatically reduce operating costs compared to normal-conducting cavities. The quality factor of a SRF cavity, defined by the cavity angular frequency (ω) multiply the stored energy (U) divided by the power dissipated on surface (P_c) (see Eq. 1), measures the efficiency of a cavity, i.e. higher Q_0 represents lower power loss on surfaces at a certain stored energy level.

$$Q_0 = \frac{\omega U}{P_c}. \tag{1}$$

The P_c can be written as an integral of the local surface resistance multiplied by the square of the magnetic field, integrated over the entire cavity surface,

$$P_c = \frac{1}{2}\int_A R_s(\vec{x})\,|H(\vec{x})|^2 da. \tag{2}$$

Eq. 2 manifests that a weighted summation of the local surface resistances determines the power loss of a cavity. A temperature-mapping (T-Map) system, which consists of a thermometer array positioned precisely on an exterior cavity wall, is capable of detecting small temperature increases on the surfaces. Therefore, it is an essential tool for SRF research, e.g. for studying localized hot-spots of an SRF cavity as well as studying quench mechanisms, etc.

Cornell University is one of the early developers of T-Map systems, has used a single-cell T-Map system since the 1980s [1, 2], and has constructed a multi-cell T-Map system [3, 4]. Today many SRF labs are equipped or plan to build a sophisticated T-Map system. Most existing T-Map systems, however, mount the temperature-sensors on rigid T-Map boards, which can only fit for one specific cavity size and shape. But the SRF cavity family has a quite large frequency range for different accelerator applications, e.g. the Cornell B-cell's frequency for the CESR is 500MHz [5], while the FLASH 3rd harmonic cavity [6] operates at a frequency of 3.9 GHz. Even at the same frequency, e.g. 1.3GHz, cavities have different shapes e.g. ILC-shape [7], Cornell ERL-shape [8], and re-entrant shape [9], etc.

In this paper, we proposed a flexible design based on the current Cornell T-Map systems, which allows it to work for different cavity sizes and shapes.

REVIEW OF THE CORNELL T-MAP SYSTEM

Before discussing the design of the flexible T-Map, we will review the Cornell T-Map systems.

T-Map Sensor and Board

The Cornell T-Map systems adopt Allen–Bradley carbon resistors (56 or 100 Ω, 1/8 W). The carbon resistor is embedded in G10 housing, which is 1 cm long by 0.4 cm wide; see Fig. 1. The leads of each resistor are connected to a Manganin wire. A clear phenolic varnish is painted on the resistor side and a spring loaded pogo stick is installed on the back side of the G10 housing hold in place by Stycast 2850 epoxy. The spring presses the sensor against cavity wall and APIEZON type N grease or Dow Corning vacuum grease is applied between the varnished side of the sensors and the cavity outside surface prior to T-Map installation. The grease fills the small gaps between the flat sensor and the curved cavity wall and so prevents superfluid helium from cooling the sensors and thereby improves thermal contact. With the grease, the thermal efficiency of the sensor is 25%-30% [2].

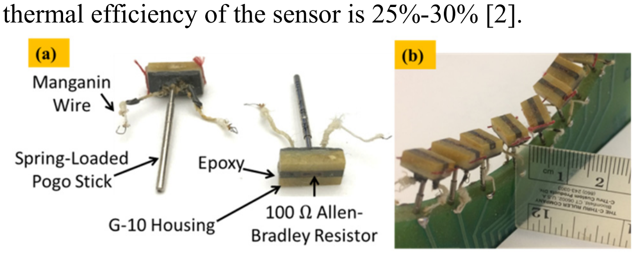

Figure 1: (a) Schematic of a carbon resistor based sensor; (b) Photograph of T-Map sensors with a ruler for size reference.

The T-Map board of the Cornell system is made of G10 material as well. There are two kinds of T-Map board in the Cornell systems: 3-cell boards and single-cell boards, as are shown in Fig. 2. The wires connecting the sensors and the blue connector are printed on the G10 board. The curvature of the board accommodates 1.3 GHz ILC-shape cavities and Cornell ERL-shape cavities, but not a re-entrant shape.

* The work is supported by NSF Award PHY-1416318
† mg574@cornell.edu

Content from this work may be used under the terms of the CC BY 3.0 licence (© 2017). Any distribution of this work must maintain attribution to the author(s), title of the work, publisher, and DOI.

ISBN: 978-3-95450-191-5 doi:10.18429/JACoW-SRF2017-THPB004

Content from this work may be used under the terms of the CC BY 3.0 licence (© 2017). Any distribution of this work must maintain attribution to the author(s), title of the work, publisher, and DOI.

IMPACT OF DURATION OF LOW TEMPERATURE DOPING ON SUPERCONDUCTING CAVITY PERFORMANCE *

P. N. Koufalis†, F. Furuta, J. J. Kaufman, M. Liepe, Cornell University, Ithaca, NY, USA

Abstract

Low temperature treatments of superconducting cavities in a low pressure atmosphere of nitrogen have been shown to introduce a 'Q-rise' up to moderate surface fields and an overall increase in quality factor, Q_0. We present preliminary results of a systematic study of the effect of doping time on superconducting cavity performance. We show that the introduction of impurities to the RF penetration layer can improve cavity performance and investigate the relationship between electron mean free path and the temperature-dependent component of the surface resistance.

INTRODUCTION

Low temperature treatments of niobium in a low pressure atmosphere of nitrogen introduces interstitial impurities in the RF penetration layer resulting in an increase in the density of scattering sites and, therefore, in a reduction of the electron mean free path, ℓ [1]. This leads to the ubiquitous 'Q-rise' – an increase in cavity quality factor Q_0 with increasing accelerating gradient, $E_{\rm acc}$, up to moderate fields – and overall higher Q_0 values with respect to 'clean' niobium cavities. Varying the doping time and temperature during the low temperature treatment leads to different impurity concentrations in the RF penetration layer ($\sim 2\lambda_L$) and, thus, results in a different ℓ, allowing one to control the strength of the 'Q-rise' of the cavity [1].

We heat treated two 1.3 GHz TESLA-shaped [2] cavities with different doping durations and vertically RF tested them to obtain measurements of Q_0 as a function of $E_{\rm acc}$ at various T, surface resistance, R_S, vs. T at low fields ($\sim$4.5 MV/m), and resonance frequency, f_0, vs. T near T_c. We then used these RF measurements to compare cavity performance and extract relevant material properties such as residual resistance, R_0, the energy gap, $\Delta(0)/k_B T_c$, and the mean free path, ℓ. Additionally, we investigated the field dependence of R_0 and the temperature-dependent component of the surface resistance, $R_{\rm BCS}$.

SURFACE TREATMENTS

Two 1.3 GHz TESLA-shaped niobium cavities were treated in a low temperature, low pressure atmosphere of continuously flowing nitrogen with different vacuum annealing times. One was a single-cell cavity, C4(P2), and the other a 9-cell cavity, MHI-02. A 'clean' single-cell niobium cavity, C1(P1), was prepared and tested to provide a baseline for cavity performance. Finally, a single-cell cavity, C4(P1), received a high-temperature nitrogen-doping (i.e.

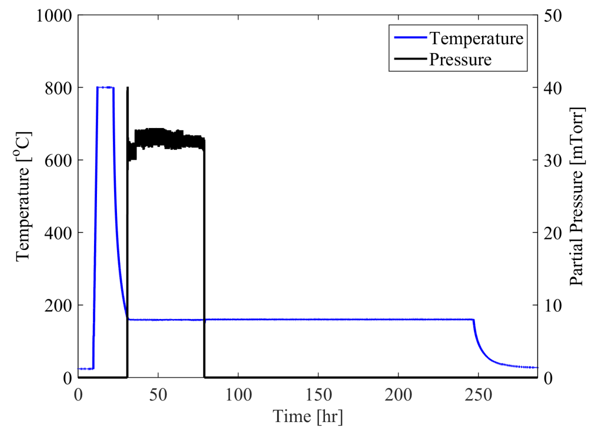

Figure 1: Temperature and nitrogen partial pressure profile for the heat treatment of cavity C4(P2).

800 °C) to compare the low temperature and high temperature treatments. The details of the cavity surface treatments are outlined in Table 1 and the bake profile for C4(P2) is shown in Fig. 1.

The nitrogen atmosphere used during the doping step of C4(P2) and MHI-02 was continuously flowing as to constantly replenish trace impurities in the gas. The nitrogen used had 5 ppm O_2, 3 ppm H_2O, and 1 ppm of CO and CO_2. The heat treatments were completed sequentially in the order: de-gas, dope, and anneal. The cavities were not removed from the furnace in between each step.

Prior to heat treatment each cavity received a vertical electro-polish (EP) to remove inclusions, defects, and surface roughness and an ultra-sonic methanol rinse. Prior to assembly the cavities were cleaned with de-ionized water on a high pressure rinsing system to ensure a clean surface for RF testing. Cavity C4(P1) received a 24 μm vertical EP post-heat treatment to remove the lossy nitride layer that forms on the surface during the doping procedure [3,4].

RF PERFORMANCE

The low temperature doped cavities C4(P2) and MHI-02 both displayed the Q-rise and higher overall Q_0 values that is typical of high-temperature nitrogen-doped cavities [3,4]. In particular, the performance of C4(P2) was remarkably similar to that of C4(P1) reaching a maximum Q_0 of 3.6×10^{10} at $E_{\rm acc}$ = 16 MV/m – a factor of 1.6 increase over the Q_0 of the baseline cavity, C1(P1), at this field. The maximum field, $E_{\rm max}$ = 25 MV/m, reached by C4(P2) was limited by quench. Cavity MHI-02 reached a maximum Q_0 of 2.9×10^{10} at 14.6 MV/m and quenched at 23 MV/m. The

* Work supported by NSF Award PHYS-1416318.
† pnk9@cornell.edu

ISBN: 978-3-95450-191-5 doi:10.18429/JACoW-SRF2017-THPB005

DESIGN UPDATES ON CAVITY TO MEASURE SUPPRESSION OF MICROWAVE SURFACE RESISTANCE BY DC MAGNETIC FIELDS *

J. T. Maniscalco†, M. Liepe, and R. Porter
CLASSE, Cornell University, Ithaca, NY, 14853, USA

Abstract

Our research has shown good agreement between experimental measurements of the anti-Q-slope in niobium SRF cavities and predictions from a recent theoretical model of the suppression of the microwave surface resistance with applied RF field. To confirm that this mechanism is indeed what causes the anti-Q-slope in impurity-doped niobium, it will be necessary to measure the theory's prediction that the same effect may be achieved by applying a constant (i.e. DC) magnetic field parallel to the RF surface. This will also allow for systematic studies of the proposed fundamental effect of the anti-Q-slope and of the behavior of the anti-Q-slope for many surface preparations and alternative materials, since it provides a cleaner measurement by eliminating the counteracting quasiparticle overheating and the complexifying oscillation of the screening currents. In this report we give an update on work at Cornell to design and build a coaxial cavity to measure this effect.

MOTIVATION

The "anti-Q-slope" is a perplexing phenomenon, exhibited by certain impurity-doped niobium cavities, in which the microwave surface resistance decreases as the strength of the field in the cavity increases [1–3]. Soon after the discovery of this effect, theoretical work proposed a mechanism for this decrease in resistance: high magnetic fields establish Meissner-state screening currents on the superconducting surface, which modify the electron density of states in such a way that the surface resistance decreases [4]. However, as the RF field dissipates energy into the electrons in the surface, inefficiencies in the transfer of thermal energy out to the refrigeration system lead to an increasing electron temperature; this counterbalances the decrease in surface resistance due to the strong temperature-dependence of BCS theory [5, 6], and the magnitude of the anti-Q-slope can be tuned by the magnitude of the energy transfer inefficiency. Recent work from Cornell showed that the magnitude of this inefficiency depends linearly on the electron mean free path, the principal measure of doping strength for impurity-doped SRF cavities [7].

In order to confirm that this mechanism indeed is the source of the anti-Q-slope, it is necessary to measure another of the theory's predictions, namely that externally-applied constant (DC) magnetic fields parallel to the superconducting surface will also reduce the surface resistance. In this

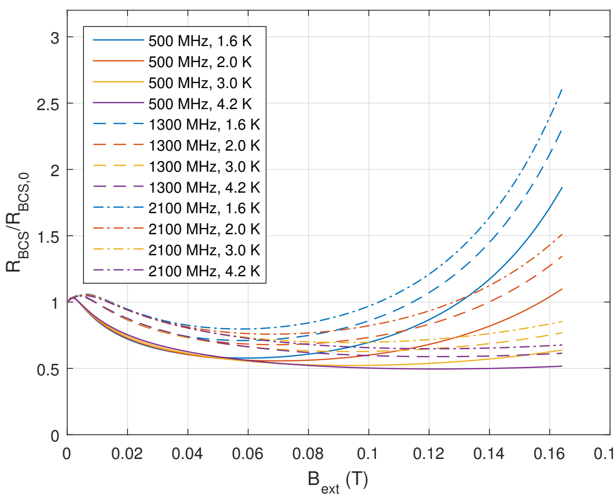

Figure 1: Theoretical predictions of the surface resistance (normalized to the zero-field value) for typical doped niobium parameters $\Delta/k_B T_c = 1.875$ and $\ell = 39$ nm.

variation of the effect, the strong external DC field excites screening currents just as the RF field did in the above case. An experiment measuring this effect by measuring quality factor Q_0 with a low-power RF field (relative to the external DC field) would benefit from two simplifications compared with the original case: first, the weak RF field means that the oscillations in electron density with the RF field would not be significant in comparison to the changes due to the DC field; second, the weak RF field would dissipate only a small amount of power, leading to insignificant electron overheating. Because of these simplifications, in a sense such an experiment would be a "purer" investigation of the theory than experiments of the strong-RF case.

Figure 1 shows theoretical predictions of the surface resistance as a function of DC field strength for several configurations of frequency and temperature. For magnetic fields up to ~ 50 mT, the greatest variation in the predictions of relative change in resistance depends on the RF frequency; for higher fields, on the other hand, the greatest variation in prediction comes from the dependence on temperature. To adequately investigate the theory experimentally, it will be necessary to probe both the frequency and temperature dependence of the effect.

The perfect diamagnetism of superconductors means that traditional cavities can not be used for such an experiment: superconducting cylinders are extremely efficient at shielding externally-applied magnetic fields [8]. As such, it is necessary to design a new cavity to perform these investiga-

* This work was supported in part by the U.S. National Science Foundation under Award No. PHY-1549132, the Center for Bright Beams, and under NSF Award No. PHY-1416318.
† jtm288@cornell.edu

Content from this work may be used under the terms of the CC BY 3.0 licence (© 2017). Any distribution of this work must maintain attribution to the author(s), title of the work, publisher, and DOI.

ISBN: 978-3-95450-191-5 doi:10.18429/JACoW-SRF2017-THPB007

NITROGEN INFUSION R&D ON SINGLE CELL CAVITIES AT DESY

M. Wenskat*, A. Prudnikava[1], D. Reschke, J. Schaffran
DESY, Hamburg, Germany
[1]Universität Hamburg, Hamburg, Germany

Abstract

A first series of single cell cavities underwent the "Nitrogen Infusion" treatment at DESY. Samples, which were in the furnace together with the cavities, underwent a series of SEM/EDX measurements and showed some unexpected structures. In parallel, the cavity performance deteriorated after the treatment. The furnace pressure and temperature and the residual gases during the treatment were analyzed to find the possible cause for the deterioration and next steps to prevent this deterioration in following treatments are discussed.

INTRODUCTION

Future upgrades of the European X-ray Free Electron Laser (XFEL) to operate in continuous wave (cw) mode at moderate to high gradients demand a high quality factor Q_0 at those gradients. A recently discovered treatment, the so called 'Nitrogen Infusion', seems to allow for such a behavior [1, 2], which could also lead to a cost reduction of a possible International Linear Collider.

FURNACE

The furnace in use has a volume of 7m^3 of which an effective volume of $1800 \times 625 \times 660\text{mm}^3$ has a homogenous temperature during baking, and was produced by the company Ipsen™. The maximum achievable, stable temperature is $T_{max} = 1100^o$C and the furnace has a temperature stability of ±2°C. The door of the furnace is double sealed by EPDM O-rings with vacuum in between. Other accessories like pumps, gauges etc. are sealed by standard EPDM seals. The pre-pumps are a rotary vane pumps and a roots pump. The main pumps are two turbo molecular pumps (TMP) by Varian™ with a pumping speed of 6000 l/s each. The installation of a single cell with niobium caps and two niobium samples on an aluminum-oxide ceramic in the furnace can be seen in Fig 1.

CAVITIES

Several single cell cavities are prepared for this R&D, and up till now, three of them have been baked. The first cavity which underwent the infusion treatment, 1DE18, underwent a minor HF treatment, prior to the baking, after a small fraction of the inner surface of one beam pipe was oxidized after the long term storage. All three cavities were tested last in 2006/2007 and have been stored since in double sealed clean room bags and with plastic caps. For the baking, all cavities were equipped with niobium caps, which underwent an etching and bake out before assembly onto a cavity. Table 1 shows a summary of the relevant cavity history details for each single cell. The nitrogen pressure was three order of magnitudes lower than the recipe for 1DE18 during the 120°C. The problem was the location of a gauge, used to steer and control the mass flow, which was placed directly at the inlet and the high throughput of the turbo molecular pumps. This caused a pressure gradient across the furnace

* marc.wenskat@desy.de

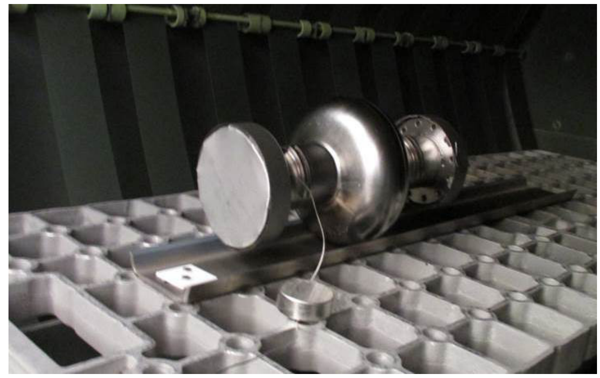

Figure 1: 1DE18 installed in furnace. Two samples are placed in front on a ceramic and the temperature sensor is attached to the cavity.

Table 1: Cavity History and RF Results

	1DE18	1DE17	1DE16
Material	Ningxia fine grain	Ningxia fine grain	Plansee fine grain
RRR	300	300	300
Final Chemistry	100 µm EP	82 µm BCP	100 µm EP
RF Test 1 @ 2K			
$E_{acc,max}[\frac{MV}{m}]$	37.7 - BD	31.2 - BD	32.2 - BD
$Q_0(4\,\text{MV/m})[\times 10^{10}]$	2.8	2.5	2.7
Baking Parameters			
p @ $800^o C$ [mbar]	2×10^{-5}	1.5×10^{-5}	1.3×10^{-6}
$p_{N=28}$ @ 800^oC [mbar]	2.2×10^{-7}	1.6×10^{-7}	2×10^{-8}
P_{N_2} @ 120°C [mbar]	7×10^{-5}	w/o	w/o
RF Test 2 @ 2K			
$E_{acc,max}[\frac{MV}{m}]$	20.2 no FE	19.5 no FE	-
$Q_0(4\,\text{MV/m})[\times 10^{10}]$	0.5	1.2	-

Content from this work may be used under the terms of the CC BY 3.0 licence (© 2017). Any distribution of this work must maintain attribution to the author(s), title of the work, publisher, and DOI.

ISBN: 978-3-95450-191-5 doi:10.18429/JACoW-SRF2017-THPB017

Content from this work may be used under the terms of the CC BY 3.0 licence (© 2017). Any distribution of this work must maintain attribution to the author(s), title of the work, publisher, and DOI.

INVESTIGATION OF TRAPPED MAGNETIC FLUX IN SUPERCONDUCTING NIOBIUM SAMPLES WITH NEUTRON RADIOGRAPHY

Oliver Kugeler*, Marc Krzyzagorski, Julia Köszegi, Ralf Ziesche, Luisa Riik, Tobias Junginger, Jens Knobloch, Wolfgang Treimer
Helmholtz Zentrum Berlin, Albert-Einstein-Straße 15, 12489 Berlin, Germany

Abstract

The dynamics of flux expulsion in Nb samples during superconducting transition has been investigated with neutron radiography. Aiming at a reduction of the trapped flux with respect to obtaining a small residual resistance it was attempted to influence the expulsion by applying external AC magnetic fields. The results of these experiments are presented.

INTRODUCTION

Trapped magnetic flux is a major contribution to the residual resistance of superconducting cavities. Minimizing the trapped flux can significantly reduce operation costs of superconducting CW accelerators. In order to gain a better understanding of the mechanisms, various techniques have been employed to measure it: Field probes like fluxgates [1] or AMR sensors [2] can only indirectly measure the trapped flux, by deducing it from the change in ambient field due to incomplete Meissner transition, taking into consideration the demagnetization behavior of the involved sample [3] or cavity [4]. Magneto-optic methods can visualize trapped flux on a surface at good resolution better than 10 µm [5–7]. We present a complimentary method, polarized neutron radiography [8–10], which measures the field directly and provides spatially resolved in-depth information from the entire volume of the investigated sample. We apply this method to the specific questions of SRF applications. The following issues were addressed with radiographies:

- Influence of cool-down speed on the amount of trapped flux
- Influence of applied field on trapped flux
- Influence of an AC external magnetic field on the flux trapping behaviour

EXPERIMENTAL

The presented neutron radiographies were recorded with PONTO II, an instrument of the University of Applied Sciences (Beuth Hochschule für Technik) Berlin that is operated at the BER II research reactor at HZB. PONTO II uses cold, spin-polarized neutrons at adjustable wavelengths of 2.9 Å $\leq \lambda \leq$ 4.5 Å. A photograph of the PONTO II experiment is shown in Figure 1.

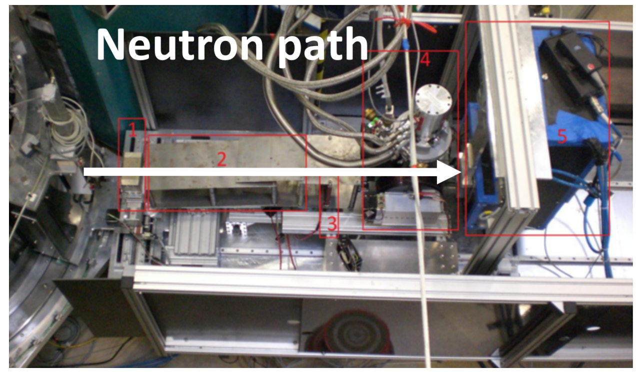

Figure 1: Photograph of the PONTO II set up from top: (1) polarizer, (2) guiding field, (3) spin flipper, (4) sample in cryostat and Helmholtz coils, and (5) neutron detector.

As illustrated in Figure 2, these neutrons are sent through a sample in a closed cycle cryostat that can be cooled down to T = 4.0 K. While there is negligible scattering of neutrons in the setup, their spin interacts only with the ambient magnetic field along the neutron path from the polarizing element, through the sample, up to the analysing element and the detector. A flat field offset measurement with sample in non-superconducting state allows for removing the effects of the inhomogeneous beam, attenuation of sample, sample-holder and temperature shielding and background field. After exposure to the field, neutrons are detected in an up to 40 mm x 40 mm field of view at a spatial resolution of 120 µm. The phase of the precession due to the amount of magnetic field can be detected by a second polarizer in front of the detector in multiples of 2π.

The samples were cut from a large grain ingot of high purity RRR300 Niobium provided by Heraeus. The obtained cylindrical discs were 5 mm in radius and 5 mm in height. They received a chemical polish at DESY in a beaker. The amount of removed material by the flash (1:1:2) BCP was not monitored. Samples were mounted into an aluminum sample holder with Titanium spring-loaded bolts. The holder is shown in the right part of Figure 3. The holder was installed in the cryostat and conduction cooled via a cold trap. A Helmholtz coil around the cryostat allowed to apply a homogeneous magnetic field during phase transition, see left part of Figure 3. The field cooling was always performed by starting from a stabilized temperature above T = 15 K above Tc = 9.2 K, then applying a certain cooling rate that could be

* oliver.kugeler@helmholtz-berlin.de

ISBN: 978-3-95450-191-5 doi:10.18429/JACoW-SRF2017-THPB018
Content from this work may be used under the terms of the CC BY 3.0 licence (© 2017). Any distribution of this work must maintain attribution to the author(s), title of the work, publisher, and DOI.

TOWARDS THE PERFECT MEISSNER STATE: A MAGNETO-OPTICAL STUDY ON COMPETING PINNING CENTERS IN NIOBIUM

J. Köszegi†, O. Kugeler, D. Abou-Ras, J. Knobloch, Helmholtz-Zentrum Berlin, Germany
R. Schäfer, IWF Dresden, Germany

Abstract

Over the past years trapped magnetic flux has emerged as a main limiting factor of high quality factors in SRF cavities. Several studies investigated how the ambient magnetic field can be minimized or how the flux expulsion during the phase transition can be improved. We now present a study that targets the pinning centers which allow for the flux to remain inside the superconductor in the first place. Using magneto-optical imaging we were able to not only measure the amount of trapped flux but in addition we managed to image its distribution with a resolution in the order of 10μm and correlate it with electron backscatter diffraction maps. As a result we found that the grain boundaries did not play a major role as pinning centers nor did the crystal orientation influence the amount of trapped flux significantly. However, niobium hydrides which formed during the cooldown to cryogenic temperatures were found to enhance trapping.

INTRODUCTION

SRF cavities are operated in the Meissner state of the superconducting (sc) material. In theory, all magnetic flux should be expelled during the phase transition into this state. However, pinning centers inside the material hinder the vortices from leaving. They get trapped and dissipate power once exposed to the RF field [1].

Therefore, the only pathway towards high quality factor SRF cavities leads through the elimination of all vortices inside the sc material. Since a cavity cannot be shielded completely from any magnetic field, e.g. because of thermocurrents [2-4], its expulsion during the sc phase transition must be maximized.

Recent studies investigated the influence of cooldown conditions on the efficiency of flux expulsion. The impact of the cooling rate and of the temperature gradient over the material during phase transition was studied [2, 5, 6]. In addition, a strong correlation was found for efficient expulsion and the grain size of the analyzed niobium [5, 7]. The study in Reference 7 investigated the change in the overall amount of trapped flux depending on the treatment history, especially high temperature heat treatment. It was found that a high average grain size was correlated with maximized flux expulsion. The results suggested that grain boundaries acted as the main pinning centers in niobium. The conclusion is reasonable since grain boundaries are known to act as pinning [8]. Following this argument, a higher average grain size would lead to fewer grain boundaries per area unit and hence to reduced pinning. However, there was no *direct* evidence that the grain boundaries are the main pinning centers. The high temperature heat treatment influences not only the morphology but also several other material properties which might impact flux trapping.

In this work, we report on a study using magneto-optical (MO) imaging adding further information. The detailed study can be found in Reference [9]. The investigation targets the distribution of trapped magnetic flux in niobium after it transitioned into the sc state with an applied magnetic field. This specific application of MO imaging is comparatively new. Previously, the method was largely applied to image flux penetration close to the critical field which occurs at several 10 mT [10, 11]. We now explore the field regime below 10 mT and focus on the trapped flux after field cooling.

Using MO imaging different pinning centers in the niobium used for SRF cavities are directly imaged and compared with one another. Furthermore, it is compared how the distribution of trapped flux changes before and after the heat treatment. The obtained information can be used to systematically reduce the flux trapping in the future.

METHOD

MO Imaging Setup

MO imaging commonly utilizes the Kerr and Faraday effects [12], which occur in materials with magnetic circular birefringence and dichroism. Niobium exhibits neither of the two effects hence an indicator material has to be used in order to image the trapped magnetic flux. The indicator is placed on top of the sample as shown in Figure 1.

Polarized light is used to image the magnetic stray field originating from the sample as it extends into the indicator material. It passes the indicator twice due to the mirror layer and the polarization is changed by the Faraday effect. The MO indicator features a ferrite garnet film with in-plane magnetic anisotropy as a detection layer. As a result, the imaged magnetic field is the projection onto the sensitive axis of the garnet. Furthermore, the black and white contrast in the final image does not correspond to zero and maximum field but to the two possible orientations of the indicator as is also indicated in Figure 1. The MO images presented here were acquired in a setup at IFW Dresden, Germany [13]. An in-plane indicator was used with magnifications of 2.5 and 20. Therefore, the resolution can be estimated to be approximately 10 μm.

† julia.koeszegi@helmholtz-berlin.de

ISBN: 978-3-95450-191-5 doi:10.18429/JACoW-SRF2017-THPB019

SIMULATION OF THE THERMOELECTRICALLY GENERATED MAGNETIC FIELD IN A SC NINE-CELL CAVITY

J. Köszegi†, O. Kugeler, J. Knobloch, Helmholtz-Zentrum Berlin, Germany

Abstract

Several studies [1-3] showed that thermocurrents generate a magnetic field in a horizontal cavity test assembly or cryomodule, which may get trapped during the superconducting phase transition. The trapped flux causes additional dissipation during operation and can therefore significantly degrade the cavity's quality factor. We simulated the distribution of the generated magnetic field for an asymmetric temperature distribution and compared the results to experimental findings. Furthermore, the impact of a growing superconducting area on the magnetic field distribution was investigated. The simulations complement the experimental studies because direct measurements are only feasible with a limited number of magnetic field probes and hence restricted to selected locations and orientations. The simulations allow to analyze the local data in the context of the whole system.

NUMERICAL SIMULATIONS

Setup

Figure 1 shows the model of a TESLA-style cavity which was used to simulate the magnetic field in the system. It includes the niobium cavity, the liquid helium vessel (titanium) and the magnetic shield. Several components of the setup were excluded (e.g. tuner, coupler) because they increased complexity as well as computation time without influencing the thermocurrent.

The bellow between cavity and tank was also omitted. However, its small wall thickness caused its DC resistance to be in the same order of magnitude as the helium tank itself. Hence, it had to be accounted to obtain a realistic thermocurrent value [4]. Thus, a thin ring was added to the vessel head. By use of this ring, the overall resistance of the system was tuned to simulate the experimental data from a vertical test which was presented in Reference [5]. The temperature dependent material properties needed for the calculations (heat capacity, thermal conductivity, electrical conductivity and thermopower) were taken from References [6-8].

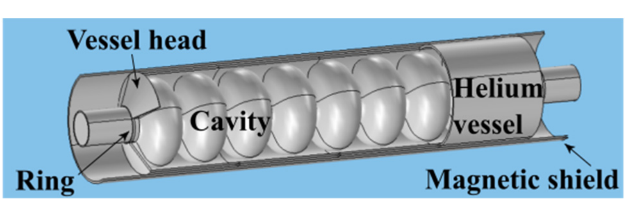

Figure 1: Model of cavity, magnetic shield and tank with ring for adjustment of electrical resistance.

† julia.koeszegi@helmholtz-berlin.de

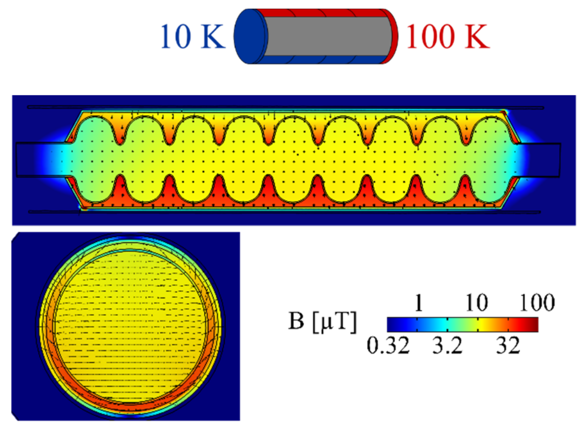

Figure 2: Magnetic field inside cavity and tank in a logarithmic scale for asymmetric temperature boundaries (displayed on top). The black arrows indicate the magnetic field vectors that point into and out of the paper plane in the middle figure and from left to right in the bottom figure.

Steady State Boundary Conditions

The thermocurrent in the cavity-tank-system is driven by large temperature differences which occur during the cool down procedure. In the cool down scheme commonly used in horizontal operation, the liquid helium is filled via a filling line at the bottom left of the tank.

Based on the experimental conditions, two temperature gradients were implemented in the simulations: first a gradient from left to right driving the thermocurrent. Second, a gradient from bottom to top which must be included because it breaks the symmetry of the current distribution. Without the second gradient, no magnetic field would be present at the RF surface inside the cavity [2, 3].

Results

Figure 2 shows the magnetic field obtained for asymmetric temperature distribution over the whole length of the cavity. The vessel heads were set to 10 K and 100 K for the first gradient and, in addition, the bottom quarter of the helium tank was set to 10 K and the top quarter to 100K for the second gradient as is depicted in the uppermost image.

The resulting distribution is in general comparable to simulations presented previously [2, 3]. In addition, we found that the magnetic field inside the cavity is more homogeneous due to the magnetic shield which is placed closely around the helium vessel.

Furthermore, the field inside the cavity is oriented orthogonally to the bottom to top gradient. Since the vessel

Content from this work may be used under the terms of the CC BY 3.0 licence (© 2017). Any distribution of this work must maintain attribution to the author(s), title of the work, publisher, and DOI.

ISBN: 978-3-95450-191-5 doi:10.18429/JACoW-SRF2017-THPB021

TRIAL OF NITROGEN INFUSION AND NITROGEN DOPING BY USING J-PARC FURNACE

T. Konomi†, T. Dohmae, Y. Hori, E. Kako, T. Kubo, G. T. Park
H. Sakai, K. Umemori, KEK, Tsukuba, Japan
J. Kamiya, K. Takeishi, JAEA/J-PARC, Tokai-mura, Japan
T. Nagata, ULVAC, Inc., Sammu, Japan

Abstract

KEK has been carrying out SRF cavity developments toward higher Q-values and higher accelerating gradients. In the past nitrogen-doping was tested using the KEK furnaces, but it did not succeed. This time nitrogen infusion and nitrogen doping are tested using the J-PARC's furnace, which has an oil-free pumping system and is mainly pumped by a 10000 L/s cryopump and three 3000 L/s turbo pumps. Nitrogen pressure is controlled by a variable leak valve and an additional turbo pump. To avoid performance degradation during heat treatment, flanges of cavities are covered by Nb caps and foils. Nitrogen infusion at 120 degrees was applied to a single cell cavity and cavity performance was measured by vertical tests after HPR and assembly. Nitrogen doping at 800 degrees is also applied to another single cell cavity. After applying EP and HPR, vertical tests were carried out. Nb samples were also installed into the furnace during heat treatment. Surfaces are analysed by SIMS and XPS. In this presentation, we report procedure of nitrogen infusion and doping, vertical test results and results of surface analysis.

INTRODUCTION

Nitrogen treatment of superconducting niobium cavity is getting a lot of attention as a new technology to improve the performance limit of ILC basic recipe. KEK is also researching to apply this technology to accelerators such as ILC and ERL. KEK measured the nitrogen doped cavity treated in KEK small and large furnace [1, 2]. KEK small furnace is used for mulch purpose such as niobium cavity annealing, brazing and so on. The pumping system is consists of a diffusion pump with liquid nitrogen trap, a mechanical booster pump and a roots pump (Osaka Vacuum, Ltd. RD600 500 m^3/h) (Fig. 1(a)). KEK large furnace is used only for superconducting cavity treatment. The pumping system is consists of a diffusion pump (ULVAC Inc. PFL-22 10000 L/sec), a mechanical booster pump (ULVAC Inc. PMB024CM 33300 L/min) and a rotary pump (ULVAC Inc. PKS-070 7000 L/min) (Fig. 1 (b)). Q values and accelerating gradient were lower than ILC recipe. The cause was considered to be oil contamination from the pumps. J-PARC furnace was selected because it consists of oil free pumps and good ultimate vacuum pressure. It is used for degassing of stainless chambers using for J-PRAC accelerators. The pumping system consists of three turbo pumps (SIMADZU Corp. TMP 3202M 300L/sec), three scroll pumps (ANEST IWATA Corp. ISP500 500 L/min) and one cryopump (CANON ANELVA Corp. CAP220 10000L/sec) (Fig. 1(c)).

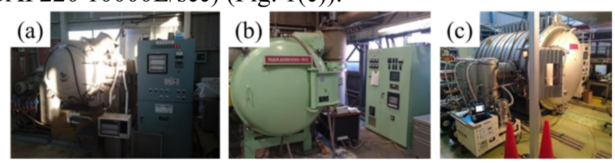

Figure 1: KEK furnaces (a) KEK small furnace. (b) KEK large furnace. (c) J-PRAC furnace.

DETAILS OF J-PARC FUANCE

Nitrogen gas line was added to J-PARC furnace. Figure 2 shows the main pumping systems and the nitrogen line. During the nitrogen introduction, the turbo pumps were stopped and gate valve of the cryopump was closed. There are no gate valves at head of turbo pumps. Purity of the nitrogen source is more than 99.99995 vol%. Nitrogen line was connected with ICF flanges and baked at around 120 ºC. The introduced gas was pumped by the portable pump unit which is consisted with turbo pump and scroll pump. Pressure is controlled by controllable variable leak valve.

Cavity was high pressure rinsed and double packed at class 1000 clean room before heat treatment. The pack was opened just before installing the J-PARC furnace. Figure 3 shows the cavity and samples installed in the furnace. Inner surface of the cavity was covered with niobium cap and foil. These careful treatments shut out the particles and contamination. The cavity was mounted on the Inconel stage and supported by niobium V block plate. Temperature is controlled far from the cavity. Thermoelectric coupler monitor was inserted between Inconel stage and V block. Various size niobium samples are heat treated with niobium cavity at same time. Niobium samples are shaved out from fine grain niobium plate. Samples are also covered with niobium.

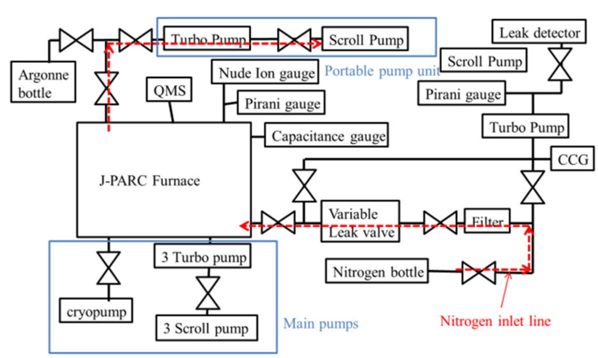

Figure 2: Diagram of J-PARC furnace.

† konomi@post.kek.jp

Content from this work may be used under the terms of the CC BY 3.0 licence (© 2017). Any distribution of this work must maintain attribution to the author(s), title of the work, publisher, and DOI.

ISBN: 978-3-95450-191-5 doi:10.18429/JACoW-SRF2017-THPB024

INVESTIGATION ON DEPTH PROFILING OF NIOBIUM SURFACE COMPOSITION AND WORK FUNCTION OF SRF CAVITIES*

A.D. Wu†, Q.W. Chu, F. Pan, H. Guo, L.Yang, L. Chen, Y.M. Li, S.H. Zhang, Y. He, H.W. Zhao
Institute of Modern Physics, CAS, Lanzhou, China

Abstract

The niobium samples were prepared by different surface treatments that commonly applied for the superconducting RF cavities preparation, as the following of electrochemical polishing, the buffered chemical polishing and high temperature annealing. In order to understand the property of niobium surface, especially the relationship between the composition and the work function value, the X-ray and ultraviolet photoelectron spectra depth profiling has been studied. The intensity photoelectrons signals of O1s, C1s and the Nb3d were identified for composition of the niobium oxide and the hydrocarbon contamination. And the work function of sample surface was measured via the means of the ultraviolet photoelectron spectra band width. To make a depth profiling, the sputtering of Argon ions was used to remove surface material gradually under by control the sputtering times. The results shown that the value of work function strongly depends on the chemical composition.

INTRODUCTION

The electrons load effects, such as the multipacting (MP) in the low field gradient and field emission occurred at the higher gradient, have adverse impact for superconducting RF operating to higher gradient and reliability. During the SRF cavities design and preparation, the multipacting effect can be eliminated by optimizing geometry of the inner conducting wall.

The field electrons emission is the tunneling effect that the electrons are pulled out from the inside material to the outside vacuum. The emission density is under control of the electric field enhancement factor on the surface and the work function of conducting wall material. The surface treatments, such as the chemical polish and high pressure rinsing by the DI water, are developed a lot to reduce the surface enhancement factor successfully. In the resent years, plasma in-situ cleaning for the elliptical cavities revealed that the field emission effect can be relieved, as the results of the surface composition modified and the work function improvement [1-2].

The changing of carbon contamination and the niobium oxides on the outmost surface as the main issues of cavities treatment, such as chemical polish, the high temperature annealing and the low temperature baking, have been studied under the in situ condition experiment for niobium samples from literatures [3-5]. Meanwhile, the cavities surface is hardly keeping a similar state with sample in situ condition during the surface preparation. To understanding the real station of SRF cavities, the niobium samples were prepared following the sequence of the cavity treatment, and the depth profiling was studied.

* Work supported by National Natural Science Foundation of China (91426303, 11505255)
† Email address: antonwoo@impcas.ac.cn

SAMPLE PREPARING

Square shapes, 10mm *10mm width, 3mm thick high with purity niobium (RRR>250) were cut from the niobium sheet used to fabricate the SRF cavities. To remove the surface damage layer and the metal impurities from the wire cutting progress, the buffered chemical polish (BCP) was used in the first step. The BCP solution was 1:1:2 volume mixture of HNO_3(69%), HF(40%) and H_3PO_4(80%), and keep the temperature under 20 0C during the reaction. 150 um thickness was removed, the surface roughness value monitored by the peak-to-valley (PV) and the arithmetic average (Ra) was 4.0um and 0.7um.

To increase the roughness to better, the electrochemical polish (EP) was used after the BCP treatment. The EP solution was 1:9 volume of HF(40%) and H_2SO_4(98%), the current density was about 35mA/cm2. The Figure 1 shows that Ra roughness can reduce to constant value about 100nm above 150um thickness removed. Finally, the samples polished to Rz of 0.6um and Ra of 100nm.

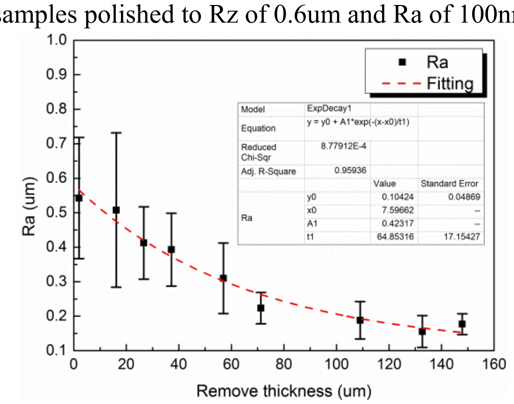

Figure 1: The arithmetic average roughness independence with the surface thickness remove by the EP treatment, the electric parameters set at 10V and 35mA/cm2.

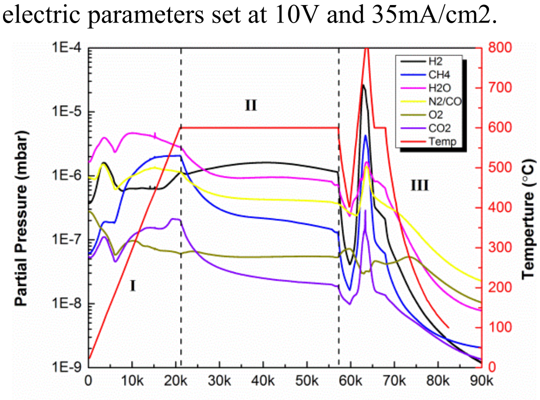

Figure 2: Temperature and partial data during the annealing treatment.

Content from this work may be used under the terms of the CC BY 3.0 licence (© 2017). Any distribution of this work must maintain attribution to the author(s), title of the work, publisher, and DOI.

ISBN: 978-3-95450-191-5 doi:10.18429/JACoW-SRF2017-THPB025

A CRYSTAL PLASTICITY STUDY ON INFLUENCE OF DISLOCATION MEAN FREE PATH ON STAGE II HARDENING IN Nb SINGLE CRYSTALS

T. Maiti, A. Chakraborty, P. Eisenlohr, D. Kang, and T.R. Bieler
Chemical Engineering and Materials Science
Michigan State University, East Lansing, MI 48824, USA

Abstract

Constitutive models based on thermally-activated stress-assisted dislocation kinetics have been successful in predicting deformation behavior of crystalline materials, particularly in face-centered cubic (fcc) metals. In body-centered cubic (bcc) metals, success has been more or less limited, owing to the ill-defined nature of slip planes and non-planar spreading of $1/2\langle 1\,1\,1\rangle$ screw dislocation cores. As a direct consequence of this, bcc metals show a strong dependence of flow stress on temperature and strain rate, and violation of Schmid law. We present high-resolution full-field crystal plasticity simulations of single crystal Niobium under tensile loading with an emphasis on multi-stage hardening, orientation dependence, and non-Schmid behavior. A dislocation density-based constitutive model with storage and recovery rates derived from Discrete Dislocation Dynamics is used to model strain hardening in stage II. The influence of dislocation mean free path and initial dislocation content on stage II hardening is simulated and compared with in-situ tensile experiments.

INTRODUCTION

When processing pure niobium into superconducting radio-frequency (SRF) cavities, the inherent deformation anisotropy of the individual grains leads to variability in the final cavity properties [1]. Deformation paths involving surface working, such as spinning, introduce gradients of deformation from the surface inward, with a higher density of defects near the surface. To gain precise control of a forming process, it is essential to understand the mesoscopic deformation behavior in terms of stresses necessary to activate dislocation slip on various slip systems and the work hardening behavior resulting from dislocation interactions. Identification of these criteria is important for predicting how crystal orientations and flow stresses will evolve in more complex forming operations.

Single crystal tensile deformation along four exemplary crystallographic directions illustrated in Fig. 1 exhibits a large variability in strain hardening. Capturing such multi-stage hardening with existing phenomenological constitutive descriptions, such as proposed by [2, 3], has seen limited success. In the present work, a constitutive model with dislocation storage and recovery rates based on Discrete Dislocation Dynamics is used to model strain hardening in stage II. Adjustable parameters in this model are identified based on an inverse strategy that uses a Nelder–Mead simplex approach to minimize the deviation between measured and simulated uniaxial single crystal tension experiments.

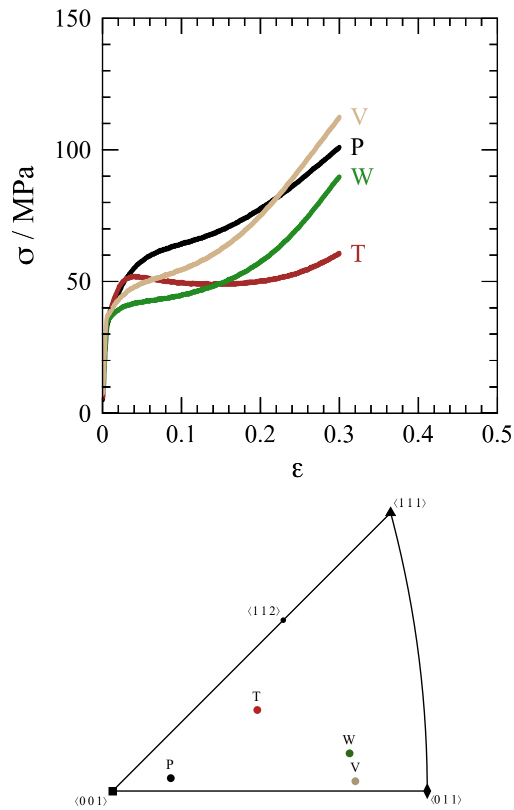

Figure 1: Strong orientation dependence of single crystal strain hardening in Nb ($\dot{\epsilon} \approx 10^{-3}\,\mathrm{s}^{-1}$ at room temperature) [4].

METHODS

Continuum Mechanics

A finite strain framework is adopted in which the total deformation gradient $\mathbf{F} = \mathbf{F}_\mathrm{e}\mathbf{F}_\mathrm{p}$ at each material point is multiplicatively decomposed into elastic $\mathbf{F}_\mathrm{e}$ and plastic $\mathbf{F}_\mathrm{p}$ components, thus introducing an intermediate (or 'lattice') configuration. The second Piola–Kirchhoff stress $\mathbf{S} = \mathbb{C} : \left(\mathbf{F}_\mathrm{e}{}^\mathrm{T}\mathbf{F}_\mathrm{e}\right)/2 = f\left(\dot{\mathbf{F}}, \boldsymbol{\eta}\right)$ reflects the elastic lattice distortion ($\mathbb{C}$ being the fourth-order elastic stiffness tensor) and drives the plastic velocity gradient $\mathbf{L}_\mathrm{p}(\mathbf{S}, \boldsymbol{\eta}) = \dot{\mathbf{F}}_\mathrm{p}\,\mathbf{F}_\mathrm{p}{}^{-1}$ as well as the evolution of internal state variables $\boldsymbol{\eta}$ (see [5] for details).

Content from this work may be used under the terms of the CC BY 3.0 licence (© 2017). Any distribution of this work must maintain attribution to the author(s), title of the work, publisher, and DOI.

ISBN: 978-3-95450-191-5 doi:10.18429/JACoW-SRF2017-THPB026

INVESTIGATION OF THE EFFECT OF STRATEGICALLY SELECTED GRAIN BOUNDARIES ON SUPERCONDUCTING PROPERTIES OF SRF CAVITY NIOBIUM*

M. Wang, T.R. Bieler, Michigan State University, East Lansing, MI 48824, USA
C.C. Compton, Facility for Rare Isotope Beams, East Lansing, MI 48824, USA
S. Balachandran, S. Chetri, A. A. Polyanskii, P. J. Lee, Applied Superconductivity Center, National High Magnetic Field Laboratory, Tallahassee, FL 32310, USA

Abstract

High purity Nb is commonly used for fabricating SRF cavities due to its high critical temperature and good formability. However, microstructural defects such as dislocations and grain boundaries in niobium can serve as favorable sites for pinning centers of magnetic flux that can degrade SRF cavity performance. In this study, six bi-crystal niobium samples extracted from strategically selected grain boundaries from two niobium disks were investigated for the effect of grain misorientation on magnetic flux behavior. Laue X-ray and EBSD-OIM crystallographic analysis were used to characterize grain orientations and orientation gradients. Cryogenic Magneto-Optical Imaging (MOI) was used to directly observe magnetic flux penetration at about 5-8 K. Flux penetration was observed along one of the grain boundaries, as well as along a low angle boundary that was not detected prior to MOI imaging. Hydride scars on the sample surface after MOI were examined using Atomic Force Microscopy (AFM) analysis. The relationships between dislocation content, cryo-cooling, flux penetration, and grain boundaries are examined.

INTRODUCTION

Superconducting radio-frequency (SRF) cavities, which have been used for charged particle accelerators for decades, are usually made from high purity niobium because of its highest critical temperature and magnetic field of elemental superconductors, as well as its good formability, reliable chemical stability, and sufficient availability on the market [1].

Achieving a high accelerating field and quality factor has always been the major motivations for the research and development of niobium cavities. Over the past decades, the theoretical limit of accelerating field for niobium has been achieved at about 42MV/m [2-4], however the high performance of SRF cavities cannot always be consistently reproduced due to the variability of the material.

Microstructural defects such as grain boundaries and dislocations, which are introduced during the fabrication and processing of niobium cavities, are capable of trapping magnetic flux, which would result in the loss of superconductivity in local regions and cause perturbation to the superconducting current in niobium [5-9]. Grain boundaries play a critical role in defining niobium cavity performance, since they are both a source and a sink for microstructural defects. During recrystallization, grain boundaries sweep across the grain and eliminate dislocations in their way, and hydrogen atoms and vacancies tend to be stored in grain boundaries, favoring precipitation of hydrides. Although magnetic flux trapped by grain boundaries and dislocations in niobium cavities is widely acknowledged as a common reason for RF losses, the mechanism is still not clear.

To pursue reproducible cavity performance, it is necessary to comprehensively understand the mechanism of flux trapping by grain boundaries of different types. This paper focuses on grain boundaries that were strategically chosen such that specific slip system, at different angles with respect to the grain boundaries, will be activated when tensile strain is imposed that favors shear along the boundary. Two bi-crystal samples were extracted with favored slip systems parallel to the grain boundaries, while four other samples have slip systems perpendicular to the grain boundaries. The purpose is to introduce dislocations under various orientations of grain boundaries of different types. Cryogenic Magneto-Optical Imaging (MOI) was used to directly observe magnetic flux behavior and the orientation gradient, and low angle grain boundary were characterized using Electron Backscattered Diffraction (EBSD) and Orientation Imaging Microscopy (OIM) crystallographic analysis. Only two undeformed samples will be described in this paper, which provides the basis for comparison that will be reported in future work.

MATERIALS AND SAMPLE EXTRACTION

Large Grain Niobium Disks

A niobium disk, with a thickness of 2.8 mm and a diameter of 270 mm, was sliced from a high purity large grain niobium ingot. It consists of several large grains with visible grain boundaries (Fig. 1a), which enables bi-crystal sample design along different boundaries. Prior tensile sample characterization is found in ref. [2].

Laue X-ray Diffraction and Grain Orientations

To obtain information of crystal orientations of those numbered grains in the niobium disk, Laue X-ray diffraction patterns of these grains were collected, which were then indexed using the OrientExpress software to

* Research supported by DOE/OHEP contracts DE-SC0009962, DE-SC0009960, NSF-DMR-1157490, and the State of Florida.

Content from this work may be used under the terms of the CC BY 3.0 licence (© 2017). Any distribution of this work must maintain attribution to the author(s), title of the work, publisher, and DOI.

ISBN: 978-3-95450-191-5 doi:10.18429/JACoW-SRF2017-THPB027

CHARACTERIZATION OF MICROSTRUCTURAL DEFECTS IN SRF CAVITY NIOBIUM USING ELECTRON CHANNELING CONTRAST IMAGING

M. Wang, D. Kang, T.R. Bieler, Michigan State University, East Lansing, MI 48824, USA
C. Compton, Facility for Rare Isotope Beams, East Lansing, MI 48824, USA

Abstract

Although the quality factor of niobium cavities has improved, performance variability arises from microstructural defects such as dislocations and grain boundaries that can trap magnetic flux, block heat transfer, and perturb superconducting currents. Microstructural defect evolution is compared in four samples extracted from a 2.8 mm thick large-grain niobium slice, with tensile axes chosen to generate desired dislocation structures during deformation. The four samples are 1) as-extracted, 2) extracted and annealed, 3) extracted and then deformed to 40% strain, and 4) extracted, annealed at 800 ℃ 2 hours, and deformed to 40% strain. Electron channeling contrast imaging (ECCI) was performed on all samples to characterize initial dislocation density, dislocation structure evolution due to annealing and deformation, and related to the mechanical behavior observed in stress-strain curves. Fundamental understanding of dislocation evolution in niobium is necessary to develop computational models to simulate cavity forming.

INTRODUCTION

High purity niobium has been used for the fabrication of superconducting radio frequency (SRF) cavities for decades due to its high critical temperature and good formability [1]. Investigations were carried out to optimize the performance of particle accelerators in different ways, to achieve high accelerating gradient and quality factors. Although great progress has been made to improve the accelerating gradient to a value close to the theoretical limit of niobium, cavity properties still suffer from variability that could be introduced anywhere along the materials processing fabrication path, including ingot remelt, rolling, deep drawing, and electron-beam welding (EBW) [1, 2]. These processing procedures involve plastic deformation that generates microstructural defects such as geometrically necessary dislocations and grain boundaries, which could lead to magnetic flux pinning and residual resistance [2-7].

An anomalous decrease of quality factor with increasing field, also known as Q drop, has been correlated with localized heating during the operation of cavities. The temperature map of the cavity shows hot spots in the high magnetic field regions of the cavity surface, which could be caused by the wiggling of magnetic flux trapped by dislocations and grain boundaries [5]. Low temperature baking eliminates the high field Q drop and reduces surface resistance [8].

Nevertheless, the relationship between microstructural defects and magnetic field behavior is not very clear, so it is necessary to investigate the dislocation structure evolution in niobium during deformation to understand conditions that may cause flux pinning by dislocations. Once understood, this will guide new processing methods to obtain an optimized microstructure for cavity niobium.

In recent years, large grain or single crystal cavities, which are less expensive and have fewer grain boundaries, have become a new alterative to the traditional fine grain cavities [9, 10]. Studies of slip systems during the deformation of single-crystal niobium have been presented at SRF 2013 and SRF 2015, which shows stress-strain behavior depends strongly on the initial grain orientations and changes resulting from annealing, as well as changes resulting from operation of preferred slip systems during tensile deformation [11, 12]. Better understanding of relationships between crystal orientation, slip systems, and stress-strain behavior are needed for modeling of deep drawing and computational simulation of cavity fabrication that can predict the microstructure and performance of cavities [11, 13].

Direct observation of dislocations in single crystal tensile samples from a previous study was done to build on previous work [11, 12], to enable identification of dislocation character (screw-mixed-edge) and the activity of slip systems underlying the highly orientation dependent stress-strain behavior of single-crystal niobium. This paper focuses on direct observation of dislocation evolution using electron channeling contrast imaging (ECCI), which is a convenient way to observe microstructural defects such as dislocations, stacking faults, nanotwins, and elastic strain fields in bulk materials [14] without destruction of the sample. Details about ECCI can be found in [14-16].

SAMPLE PREPARATION

Four single-crystal niobium samples with the same orientation were extracted from one large grain, and then different processing operations were applied. Sample 1 was as-extracted, Sample 2 extracted and annealed, Sample 3 extracted and deformed to 40% strain, and Sample 4 extracted, annealed at 800℃ for 2 hours, and then deformed to 40% strain. Details of the sample history is found in [11, 12], where crystal rotations indicated predominant slip on {110} planes in the annealed condition, but preferential activity of slip on {112} planes with increasing dislocation density [12].

The samples were then electro-polished in an electrolyte of 90vol% Sulfuric Acid and 10vol%

† Email: wangmi22@msu.edu

Content from this work may be used under the terms of the CC BY 3.0 licence (© 2017). Any distribution of this work must maintain attribution to the author(s), title of the work, publisher, and DOI.

ISBN: 978-3-95450-191-5 doi:10.18429/JACoW-SRF2017-THPB028

FLUX PINNING STUDY OF OTIC NIOBIUM MATERIAL*

Shu Chen, Jiankui Hao#, Shengwen Quan, Lin Lin, Kexin Liu
State Key Laboratory of Nuclear Physics and Technology & Institute of Heavy Ion Physics, Peking University, Beijing 100871, China

Abstract

The performance of superconducting cavities is influenced by the trapped flux during the cooling down through critical temperature, especially for nitrogen doped cavities which are more sensitive to flux trapping. We have investigated the flux trapping of OTIC niobium samples with different grain size. Samples were prepared and heat treated at 800 °C and 900 °C, followed with different surface removal by BCP. A series of measurements, including MPMS, TOF-SIMS, were carried out on the niobium samples. The results and analysis will be presented.

INTRODUCTION

Intrinsic quality factor Q_0 is one of the most important parameters of superconducting cavities. High quality factor can reduce the cryogenic load of superconducting cavity and reduce the considerable costs for the cryogenics. In 2012, FNAL colleagues discovered very high Q values on single cell cavities treated with nitrogen in high temperature furnace, which is called N-doping recipe [1] and discovered that "light doping" improves quench field while maintaining the benefit of high Q. Cornell colleagues found that "heavy doping", which needs longer nitrogen atmosphere and more EP removal, is effective to improve the performance of superconducting cavities. In 2014-2015, N-doping recipe was adopted as the baseline cavity surface processing protocol for LCLS-II [2].

It was reported that some superconducting cavities treated with 800 °C nitrogen doping recipe did not meet the spec of LCLS-II(2.7×10^{10} in 5mG field) [3]. To solve this problem, 900°C modified recipe was tried on material. Some material (ASTM<7.0) changed better, and met the high quality factor requirement. But some material (ASTM>7.0) did not change as much. After treated at 950°C and 970 °C, the material eventually can be used [3]. The difference in performance with different materials is caused by trapping magnetic flux. Flux expulsion behavior of cavities seems to be a great deal in different materials, even in batches from a single vendor. To investigate the problem, flux pinning study on OTIC niobium samples of different grain size and other vendor's niobium samples were carried out at Peking University.

Q_0 degradation by trapped flux can be considered as a three-step process [5]: 1.the cavity is cooled in external environment magnetic field B_{ext}. 2.some of the B_{ext} is trapped in cavity surface, called B_{trap}. 3.the B_{trap} introduces the residual resistance R_{res}, and increases the surface resistance R_s. So the quality factor of cavity is reduced. We focus on the second step, how much B_{ext} is trapped in the material. Some researches [3, 4] show that different niobium material has different flux expulsion behavior, and the flux expulsion behavior changes a lot after different temperature heat treatment. B_{trap} is the key factor to superconducting cavities whether N-doping works or not. We used the MPMS (Magnetic Property Measurement System) to measure the flux trapping in different samples, which can be helpful to understand the variability between the different materials and different treatments.

*Work supported by National Key Programme for S&T Research and Development (Grant No. 2016YFA0400400) and National Natural Science Foundation of China (Grant No. 11575012)
#E-mail: jkhao@pku.edu.cn

PREPARATION AND TREATMENTS OF NIOBIUM SAMPLES

Preparation of Different Kind of Niobium Samples

Two fine grain niobium strips from different vendors were used for the investigation. One niobium strip has grain size ASTM 4.5-5.0 and hardness HV49.8. Another niobium strip has the same grain size ASTM 4.5-5.0. And a large grain niobium strip was taken into account. All samples are listed in Table 1. Small samples were cut out from these niobium strips by wire electric discharge machining. Then they were etched by BCP (1:1:2) with the depth of about 250μm, to remove the mechanical damage layer. We use pure water to rinse the samples and clean the surface sufficiently in case of remaining acid from BCP process. After pure water (ρ>2MΩ-cm) rinsing, the samples were moved to clean room, rinsed by ultrapure water (ρ>18MΩ-cm) again, followed by drying and annealing at 800° C for 3 hours. The vacuum of the furnace is 10^{-4} Pa. The samples were put on niobium sheets that had been BCP treated to prevent pollution, see Figure 1. The whole heating process was divided into 7 stages as follow.

- The pressure in the furnace was pumped to 1.2×10^{-4}Pa
- Heating from room temperature to 500 °C in 30 minutes.
- Maintaining at 500 °C for 60 min
- Heating from 500 °C to 800°C in 30 minutes.
- Maintaining at 800 °C for 180 min
- Cooling down in vacuum.
- When temperature down to 60 °C, open the furnace.

The maintaining at 500 °C and 800 °C helps to degas the impurity in the niobium material. At the end, all samples were etched 40 μm by BCP and rinsed by ultrapure water. After all the above steps were accomplished, grain size of FG1 samples decrease to ASTM 3.5-4.5. And grain size of FG2 samples decrease to ASTM 3.0-3.5. By annealing at

Content from this work may be used under the terms of the CC BY 3.0 licence (© 2017). Any distribution of this work must maintain attribution to the author(s), title of the work, publisher, and DOI.

ISBN: 978-3-95450-191-5 doi:10.18429/JACoW-SRF2017-THPB029

Content from this work may be used under the terms of the CC BY 3.0 licence (© 2017). Any distribution of this work must maintain attribution to the author(s), title of the work, publisher, and DOI.

XPS STUDIES OF NITROGEN DOPING Nb SAMPLES BEFORE AND AFTER GCIB ETCHING*

Z. Q. Yang†, X. Y. Lu, W. W. Tan, D. Y. Yang, Y. J. Yang, J. F. Zhao
State Key Laboratory of Nuclear Physics and Technology, Peking University, Beijing, China

Abstract

The surface chemical composition of nitrogen doping Nb samples used for the fabrication of superconducting radio frequency (SRF) cavities, followed by the subsequent successive EP with different amounts of material removal, has been studied by XPS. The chemical composition of Nb, O, C and N was presented before and after Gas Cluster Ion Beams (GCIB) etching. No signals of bad superconducting nitrides NbN_x was found in any doped and un-doped samples before etching. However, in the depth range greater than 30nm, the content of N elements is below the XPS detection precision scope even in the samples directly after nitrogen doping treatment.

INTRODUCTION

Niobium used for cavity production undergoes several different treatments before it eventually becomes a superconducting radio frequency (SRF) cavity ready for test. The typical procedures not only includes rolling, deep drawing, electron beam welding and other mechanical treatments, but also includes chemical etching, high temperature degasing, high pressure rinsing, 120^{0}C baking and other post treatments. The subtle material details of the niobium surface largely influence the surface resistance of niobium below 2K. XPS analysis of the surface composition of niobium used for the fabrication of SRF cavity after procedures commonly employed in the preparation of SRF cavities have been reported [1-2]. Nitrogen doping is a new surface treatment discovered by A. Grassellino [3], which can systematically improve the quality factor of SRF niobium cavities up to a factor of about 3 compared to the standard surface treatment procedures. Presently, nitrogen doping treatment is being transferred from the prototyping and R&D stage to the production stage [4]. Fundamental understanding of the nitrogen doping mechanism is being carried out extensively, but yet remains unclear. The SRF cavity directly after nitrogen doping treatment showed quality factor in the range of 10^7 at 2K. That is far below the routinely achieved Q values of cavities with the standard surface treatment procedures at this frequency and temperature. This has always been thought to be caused by the formation of unwanted poorly superconducting nitrides [3]. Thus the aim of the present study is to investigate the elemental compositions and chemical structures of the niobium samples with different treatments. The X-ray Photoelectron Spectroscopy is suitable to provide this information. For this reason XPS studies of nitrogen doping samples before and after gas cluster ion beam (GCIB) etching has been carried out, with particular attention to the elemental compositions and chemical structures of nitrogen both on the surface and in the penetration depth range.

EXPERIMENTAL

To avoid heat generation, instead of wire electro-discharge machining (EDM), the niobium samples were manually processed. The niobium strips were polished smoothly on 180-grit sandpaper, 300-grit sandpaper and 1200-grit sandpaper. The samples' treatments were attempted to replicate that of the cavities. So the niobium strips were etched by EP ($HF:H_2SO_4$=1:9), with the material removal of about 150μm, to remove the mechanical damage layers and surface contaminations introduced during handling or exposing to the air.

Nitrogen Doping Treatment

The nitrogen doping treatments and 800^{0}C heat treatments of the niobium samples used for the magnetic measurements can be seen in [5].

XPS Measurements Before Etching

The elemental compositions and chemical structures of the niobium samples was analysed by using a Thermo Scientific ESCALab250Xi Multifunctional Photoelectron Spectrometer. Photoelectrons are excited by using a monochromatized source that produces Al Kα (hν=1486.6eV) radiation and the power is about 200W. The surface area of analysis of the sample is about 500μm×500μm. A base pressure of about 3×10^{-10}mbar is obtained in the analysis chamber. Both doped and un-doped samples from two groups were chosen for the XPS experiments. That is ND-1st-0μm, ND-2nd-0μm, ND-2nd-1μm, ND-2nd-7μm, ND-2nd-13μm, ND-2nd-21μm, HT-2nd-0μm 、 HT-2nd-20μm and noNDnoHT. The labels begin with ND, followed by a serial number and ended by a exact number means a doped sample from group 1 or group 2 with a certain amount of EP removal.

A lower resolution survey over the wide energy window with the bin size of 1 eV is used to get information about elements presentation the sample. High resolution scans around peaks corresponding to the elements of interest are then performed with the bin size of 0.05 eV to obtain the fine structure of the peaks, which contain the information about the chemical environment.

XPS Measurements After Etching

To obtain the elemental compositions and chemical structures in the penetration depth, XPS studies were

* Supported by Major Research Plan of National Natural Science Foundation of China (91426303) and National Major Scientific Instrument and Equipment Development projects (2011YQ130018).
† email address: ziqinyang@pku.edu.cn

ISBN: 978-3-95450-191-5 doi:10.18429/JACoW-SRF2017-THPB030

DIRECT OBSERVATION OF HYDRIDES FORMATION OF NITROGEN DOPING Nb SAMPLES*

Z. Q. Yang, X. Y. Lu, W. W. Tan, D. Y. Yang, Y. J. Yang, J. F. Zhao
State Key Laboratory of Nuclear Physics and Technology, Peking University, Beijing, China

Abstract

Direct observation of hydrides precipitates formation on both nitrogen doped and un-doped Nb samples at 80K has been carried out using Scanning Electron Microscope (SEM) with Cold Stand. We have found that, under our experimental conditions, when the subsequent EP removal is less than 7μm, the amounts of hydrides formed on the surface of doped samples can be effectively reduced. When the subsequent material removal is larger than 9μm, the amounts of precipitated hydrides increased with the EP removal. When the EP removal is 7-9μm, the amounts of hydrides can still be effectively reduced. Also, more hydrides were precipitated on the surface of un-doped samples. The amounts of hydrides of doped samples may be reduced to varying degrees with different amounts of material removal.

INTRODUCTION

The niobium hydrides are normal conducting at the typical cavity operating temperature of about 2K. Both previous and present studies have shown that the amounts of lossy non-superconducting niobium hydrides precipitated on the inner surface of the superconducting radio frequency (SRF) cavity have a significant influence on the Q value of the cavity. So hydride is an important source of residual resistance in the SRF niobium cavity. Therefore, special attention is needed to be paid to the changes of the precipitate of niobium hydrides on the surface of niobium samples before and after nitrogen doping treatment.

Nb-H systems have been widely studied in the 1970s for hydrogen storage as niobium figures among metals able to accept and restitute a large volume of hydrogen even at room temperature [1-3]. A complete equilibrium phase diagram is presented in Fig. 1. At room temperature, H atoms randomly distributed over tetrahedral sites in the crystal lattice. This is the α phase. The solubility limit of this phase extends up to 4 atomic percent of hydrogen at room temperature, which corresponds to more than 4×10^3 wt ppm of H concentration. So niobium hydrides do not form on the surface of RRR~300 high purity niobium, of which the H concentration is less than 2 wt ppm. As the temperature is lowered, the hydrogen concentration needed to form the hydride phases decreases. At 100K, solubility limit of the ε phase hydride is dramatically reduced to about 5 wt ppm. A well-known phenomenon about H in metals is its tendency to interact with crystal defects like impurity atoms, grain boundaries, and dislocations due to elastic stresses applied to the lattice. H keeps concentrated near the defect and can even reach niobium hydride precipitation limit, resulting in the formation of different stoichiometric hydrides. The diffusion rate of hydrogen between 150 K and 60 K remains quite significant, so that hydrogen can move to accumulate to critical concentrations at nucleation sites. When the temperature is reduced to below 60 K, the diffusion of hydrogen was slowed down so that hydrogen can no longer accumulate to the hydride centers.

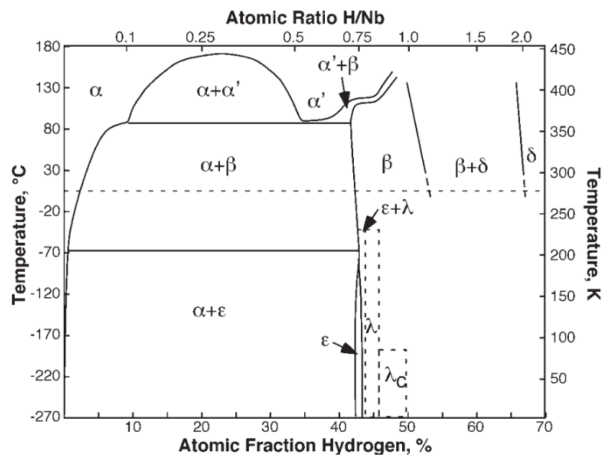

Figure 1: Phase diagram of Nb-H system [3].

To observe the hydrides precipitates formation on the surface of niobium, the niobium sample should be kept in a low temperature environment between 150 K and 60 K. Two methods have been used to the observation of niobium hydrides precipitation. One is the scanning transmission electron microscopy (STEM) [4]. Combined with the electron energy loss spectroscopy (EELS), the atomic scale structure information of niobium hydride can be observed. The other is the cryogenic laser scanning confocal microscopy (CLSCM) with a lateral resolution of the order of 1 μm in a temperature range 5-300 K [5]. The effect of different post treatments on the formation of hydrides on niobium surface at low temperature can be observed on the micron scale. Taking into account our experimental conditions and experimental requirements, the observation of hydrides precipitates formation on both nitrogen doped and un-doped Nb samples was carried out by using the scanning electron microscope (SEM) with a cold stand at 80K.

EXPERIMENTAL PROCEDURES

Sample Preparation

The sample preparation, nitrogen doping treatment and 800^0C heat treatment of the niobium samples can be seen in [6].

* Supported by Major Research Plan of National Natural Science Foundation of China (91426303) and National Major Scientific Instrument and Equipment Development projects (2011YQ130018).
† email address: ziqinyang@pku.edu.cn

Content from this work may be used under the terms of the CC BY 3.0 licence (© 2017). Any distribution of this work must maintain attribution to the author(s), title of the work, publisher, and DOI.

ISBN: 978-3-95450-191-5 doi:10.18429/JACoW-SRF2017-THPB031

MAGNETIC PROPERTIES OF NITROGEN DOPING NIOBIUM SAMPLES*

Z. Q. Yang, X. Y. Lu#, W. W. Tan, D. Y. Yang, Y. J. Yang, J. F. Zhao
State Key Laboratory of Nuclear Physics and Technology, Peking University, Beijing, China

Abstract

Nitrogen doping study on Niobium samples used for the fabrication of superconducting radio frequency (SRF) cavities was carried out. The samples' surface treatments were attempted to replicate that of the cavities, which included heavy electropolishing (EP), nitrogen doping and the subsequent successive EP with different amounts of material removal. The magnetization curves of both doped and un-doped samples have been measured, from which the lower critical field H_{ffp} (First Flux Penetration, ffp) and upper critical field H_{c2} was extracted. The thermodynamic critical field H_c, superheating field H_{sh} and superconducting parameters of samples with different treatments was calculated from the determined reversible magnetization curves. H_{sh} of doped samples is obviously smaller than that of un-doped samples, which may be a possible reason for the reduction of achievable accelerating gradient in SRF niobium cavities after nitrogen doping treatments.

INTRODUCTION

Fundamental understanding of the nitrogen doping mechanism is being carried out extensively [1-5], but yet remains unclear. Two years after the discovery of nitrogen doping phenomenon, A. Romanenko [6] discovered that fast cooling down through T_c in both single cell and 9-cell nitrogen doping cavities helps to much more efficient flux expulsion and results in lower residual resistance. While this effect is not so obvious for un-doped cavities, especially for the cavities with standard preparation which consists of EP 120μm, 800^0C heat treatment for 3 hours, EP 20μm and 120^0C baking for 24-48 hours. A. Gurevich and G. Ciovati [7] studied the impact of vortex on the residual resistance of SRF niobium cavities. They predicted that the residual resistance has a high sensitivity to trapped flux. Dan Gonnella [8] studied the sensitivity of surface resistance to trapped magnetic flux on both doped and un-doped cavities. Dan Gonnella's experiments showed that nitrogen doping cavities have higher sensitivity of residual resistance to trapped flux. Vertical tests also showed that the sensitivity decreases with the EP removal and will be reduced gradually to the level of un-doped cavities after a certain amount of material removal, which is determined by the specific nitrogen doping condition.

For the nitrogen doping cavities, vertical tests [9-10] showed that the residual resistance has minimum value when the EP removal reaches an optimized value, where also corresponds to the largest quality factor. When the EP removal is smaller or larger than the optimized value, the residual resistance becomes greater. So the variation of residual resistance with EP removal after nitrogen doping treatments is also an important aspect of the physical mechanism of nitrogen doping phenomenon. Limited to our experimental conditions, we tried to study the impact of nitrogen doping treatments on the residual resistance through experiments on Nb samples to seek the physical explanation of it.

As mentioned above, the diffused N may have an impact on the material's flux pinning behaviour and thereby affects the cavities' residual resistance. So it is necessary to study the magnetic properties of Nb samples before and after nitrogen doping treatment. Both doped and un-doped samples were electropolished with different amounts of material removal. Magnetic measurements on Nb samples were carried out with a SQUID magnetometer (Quantum Design MPMS-XL-7).

EXPERIMENTAL PROCEDURE

To avoid heat generation, instead of wire electro-discharge machining (EDM), the niobium samples were manually processed. The niobium strips were polished smoothly on 180-grit sandpaper, 300-grit sandpaper and 1200-grit sandpaper. The samples' treatments were attempted to replicate that of the cavities. So the niobium strips were etched by EP ($HF:H_2SO_4$=1:9), with the material removal of about 150μm, to remove the mechanical damage layers and surface contaminations introduced during handling or exposing to the air.

Nitrogen Doping Treatment

The nitrogen doping treatments and 800^0C heat treatments of the niobium samples used for the magnetic measurements can be seen in [11].

Magnetization Measurement

The magnetization was measured by using a commercial SQUID magnetometer (Quantum Design MPMS-XL-7) at Peking University. The weight of experimental samples lies between 80-260mg. For the considerations of measurement range, the DC module was used with the measurement accuracy of 1×10^{-8} emu. Mounted in a sample holder, the sample was transported to the sample space together with a rigid sample rod during which the sample was cooled from room temperature at zero field (ZFC). The sample's motion length is 4cm. The magnetic field is homogeneous to 0.05% for this regime. The measuring range of DC applied field H_a lies between zero

* Work supported by Major Research Plan of National Natural Science Foundation of China (91426303) and National Major Scientific Instrument and Equipment Development projects (2011YQ130018).
† Email address: xylu@pku.edu.cn

Content from this work may be used under the terms of the CC BY 3.0 licence (© 2017). Any distribution of this work must maintain attribution to the author(s), title of the work, publisher, and DOI.

ISBN: 978-3-95450-191-5 doi:10.18429/JACoW-SRF2017-THPB034

Content from this work may be used under the terms of the CC BY 3.0 licence (© 2017). Any distribution of this work must maintain attribution to the author(s), title of the work, publisher, and DOI.

DEVELOPMENT OF HIGH PURITY NIOBIUM COMPONENTS AND CAVITIES FOR SRF ACCELERATOR

T. Nagata#, H. Masui, S. Shinozawa, H. Murakami, ULVAC Inc., Chiba, Japan
H. Inoue, E. Kako, M. Yamanaka, KEK, Ibaraki, Japan

Abstract

Comprehensive cavity fabrication process from Nb ingot was investigated. In order to purify ingots, 600 kW electron beam melting furnace was introduced in ULVAC. It makes possible the stable quality of Nb sheets and tubes. In evaluation of chemical components and residual resistivity ratio (RRR) of our materials, all the value satisfies the ASTM Type 5 (superconducting grade) specification. We performed the trial manufacturing of welding-type and seamless-type cavities were made of our high purity Nb ingots (RRR > 300). Accelerating gradient over 40 MV/m at 2K was obtained both cavities. Trial manufacturing for 3-cell seamless-type cavity as scale up study was also performed. We succeed in hydro-forming from seamless tube to 3-cell cavity shape.

INTRODUCTION

Nb materials used as SRF cavity must be highly pure because they are used in the superconducting state that is sensitive to impurities. The upper limit on the amount of impurities are specified in the ASTM standards as the high purity superconducting grade (ASTM Type 5) [1]. Nb is rather expensive among pure metals and there are still some challenges with technologies for mass-producing cavities at present, so technologies for manufacturing cavities at low cost with high productivity are strongly demanded.

We have taken a two-pronged approach to developing SRF cavities in order to solve the problems mentioned above.

The first is to establish a technology for refining high purity Nb ingots. The goal is to discover a technology for supplying Nb materials that provide the required purity and acceleration performance at the lowest price possible. A 600 kW electron beam melting furnace with high vacuum system has been introduced in the factory of ULVAC Tohoku, Inc. to develop methods for manufacturing such Nb ingots.

The second part of our approach is a manufacturing technique called the seamless method. In this method, Nb seamless tubes that are produced by an ULVAC original technology are directly formed into cavities. The aim is to establish a method to manufacture SRF cavities at a lower cost than those manufactured by the welding method that is mainly used at present. Some research has suggested that the seamless method in which no welding is required for the main bodies of accelerator cavities has cost advantages [2, 3]. We believe manufacturing costs need to be closely re-examined throughout all the actual processes from purifying raw materials to fabricating cavities, as we have been doing.

tomohiro_nagata@ulvac.com

MANUFACTURING HIGH PURITY NIOBIUM INGOTS

In order to manufacture high purity Nb ingots by electron beam purification, it is best to purify them at high power under high vacuum to effectively remove impurities, especially gases and high melting-point metals. ULVAC designed a 600 kW electron beam melting furnace with high vacuum system for manufacturing high purity Nb ingot. Figure 1 shows the appearance of the electron beam melting furnace.

In the International Linear Collider (ILC) project, the RRR required for Nb materials is more than 250 as specifications. Currently, high purity ingots that satisfy such a value can be produced using this melting furnace. Table 1 shows the chemical analysis results of an ingot with the RRR of 330 as a typical example of high purity. This shows that the ingot is high purity superconducting grade (ASTM Type 5).

Figure 1: 600 kW electron beam melting furnace [4].

Table 1: Impurity Element Analysis of Nb Ingot.

(ppm)

	H	O	N	C	Zr	Fe
ASTM Type5	5	40	30	30	100	50
ULVAC	1	<10	<10	10	<10	<10
	Si	W	Ni	Ti	Al	Ta
ASTM Type5	50	70	30	50	50	1000
ULVAC	<10	10	<10	<5	<10	140

PROTOTYPING SEAMLESS CAVITIES

Single-cell

In order to reduce the cost of manufacturing cavities, we have been working to use seamless tubes to cavity

ISBN: 978-3-95450-191-5 doi:10.18429/JACoW-SRF2017-THPB035

HIGH POWER TESTING OF THE FIRST ESS SPOKE CAVITY PACKAGE

H. Li, M. Jobs, R. Santiago Kern, A. K. Bhattacharyya, L. Hermansson, R. Ruber,
FREIA Lab, Uppsala University, Sweden,

Abstract

The first double spoke cavity for the ESS project was tested with high power in the HNOSS cryostat at the FREIA Laboratory. This cavity is designed for 325.21MHz, pulsed mode with 14 Hz repetition rate, up to a peak power of 360 kW. The qualification of the cavity package in a horizontal test, involving a superconducting spoke cavity, a fundamental power coupler (FPC), LLRF system and RF station, represents an important verification before the module assembly. This paper presents the test configuration, RF conditioning history and first high power performance of this cavity.

INTRODUCTION

The superconducting spoke section of the ESS linac accelerates the beam from the normal conducting section to the first family of elliptical superconducting cavities [1]. This spoke section includes a single family of β=0.5 bulk niobium double spoke cavities operating at a temperature of 2 K and at a frequency of 352.21 MHz. A total of 26 spoke cavities are designed at IPN Orsay and will be grouped by 2 in 13 cryomodules [2].

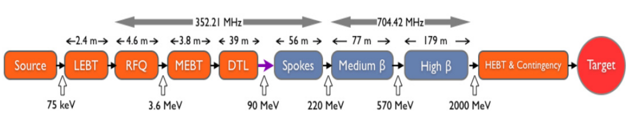

Figure 1: The layout of ESS accelerator.

Figure 1 shows the layout of ESS accelerator and the nominal operation parameters of spoke section are shown in table 1.

Table 1: Main Parameters of Spoke Cavities

Parameter	ESS Spoke cavity
Frequency [MHz]	352.21
Temperature [K]	2
Pulse duty factor [%]	4
Repetition rate [Hz]	14
Nominal gradient [MV/m]	9
Optimal Beta	0.5

A double spoke cavity (Romea) has been fabricated and selected for the horizontal test. It completed its vertical test at IPN Orsay with an excellent performance of maximum Eacc of 15 MV/m @ Q_0= 4×10^9, showing a successful cavity design and processing [3]. Equipped with the fundamental power coupler (FPC) and cold tuning system (CTS), this cavity package was shipped to FREIA and installed in the HNOSS cryostat. In this test, Romea has no magnetic shield and relies on the HNOSS magnetic shield which is located at room temperature in the vacuum vessel. The object of this test thus becomes the validation of the complete chain of high power RF amplifier, high power RF distribution, FPC, spoke cavity package and LLRF system. All these infrastructures provide a mechanical environment similar to its operation in the linac.

RF CONDITIONING

The warm and first cold coupler conditioning were done by using IPN Orsay's system followed by the new FREIA conditioning system to verify its performance. All coupler conditioning used a traditional signal generator driven loop. The warm RF processing before cooldown took about 40 hours, lots of outgassing occurred through the forward power region of 40-70kW at short pulses. At the first phase, the coupler conditioning finished when a forward power of 120 kW was reached with 2.86 ms pulse duration. The FREIA conditioning system was then tested with ESS cavity package to verify the logic and related hardware.

Compared to the FPC conditioning, the cavity RF conditioning is done by a self-excited loop (SEL). Since the tuner feedback controller is still under development, SEL naturally becomes a substitute for following the cavity resonant frequency without feedback. In order to produce pulses in the SEL, a RF switch controlled by a programmable trigger signal is introduced.

Cavity conditioning has been implemented in two phases. The first phase introduces a frequency modulation around the resonant frequency at a very low power level in order to sweep the field distribution forth and back along the coupler walls in a controlled manner. The subsequent phase is also completed with the SEL but by only ramping up the RF power with a fixed pulse length of 2.86 ms, with a procedure described in [4]. After about 30 hours of conditioning, the cavity package reached and was stably kept at 9 MV/m peak accelerating gradient.

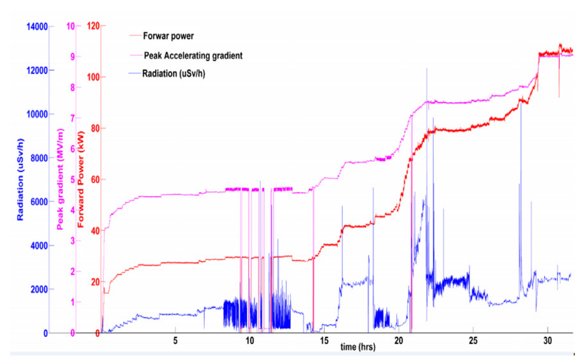

Figure 2: Cavity RF Conditioning history at FREIA.

Content from this work may be used under the terms of the CC BY 3.0 licence (© 2017). Any distribution of this work must maintain attribution to the author(s), title of the work, publisher, and DOI.

ISBN: 978-3-95450-191-5 doi:10.18429/JACoW-SRF2017-THPB036

FUNDAMENTAL SIMS ANALYSES FOR NITROGEN-ENRICHED NIOBIUM

J. Tuggle[1], U. Pudasaini[2], A.D. Palczewski[3], C.E. Reece[3], F.A. Stevie[4], M.J. Kelley[1,2,3,†]
[1]Virginia Polytechnic Institute and State University, Blacksburg, VA, USA
[2]The College of William and Mary, Williamsburg, VA, USA
[3]Thomas Jefferson National Accelerator Facility, Newport News, VA, USA
[4]Analytical Instrumentation Facility, North Carolina State University, Raleigh, NC, USA

Abstract

In order to fully understand nitrogen addition techniques it is vital to have a full understanding of the material, including the content, location, and speciation of nitrogen contained in the treated Nb. In this work Secondary Ion Mass Spectrometry (SIMS) is used to elucidate content and location. Dynamic SIMS nitrogen analysis is reported, for the first time, for "as-received" cavity grade niobium from three separate suppliers. In addition, a number of method and instrumental issues are discussed including depth resolution, detection limit, and quantification.

INTRODUCTION

SIMS obtains information by directing a beam of primary ions onto the surface of interest and measuring the mass distribution and intensity of the ejected (secondary) ions [1]. Of all analytical techniques including various types of SIMS (TOF, NanoSIMS, etc.) dynamic SIMS instruments, such as the CAMECA IMS-7f, have the lowest detection limits, making dynamic SIMS the instrument of choice when concerned for trace element quantification.

SIMS analysis requires proper sample preparation and method development in order to correctly quantify results. When conducting SIMS experiments, matrix effects, differential sputtering, surface topography, acceptable backgrounds, and other complications all must be considered. For a brief discussion of SIMS issues and the development of a method for the analysis of N in Nb please see Ref. [2]. For a more in depth discussion of SIMS method development in general please see Ref. [1].

EXPERIMENTAL

Sample Preparation

Unless otherwise noted all samples are 3 mm thick cavity grade niobium, cut to 10 x 10 mm coupons with "NanoPolished" surfaces. Normal BCP surface finishes have been found to be insufficiently smooth and produce poor depth resolution due to surface topography [2]. Standards used for quantification were prepared by ion implantation with ^{14}N to a dose of $1X10^{15}$ atoms/cm^2 at 160 keV and ^{16}O to a dose of $2x10^{15}$ atoms/cm^2 at 180 keV.

SIMS Instrumentation

SIMS analyses were collected on a CAMECA IMS-7fGEO magnetic sector instrument. A Cs^+ primary ion beam was used and rastered over an area of 150 x 150 µm with a 63µm diameter analysis area. An impact energy of 15 kV (10kV source/-5kV sample) was used with a current of 100nA. Negative secondary ions of $^{93}Nb^{14}N^-$ were detected, while $^{93}Nb^-$ was used as a reference signal. Data were collected, in at least two locations, on each sample to verify repeatability. Figure 1 shows a schematic of the Cameca 7f instrument.

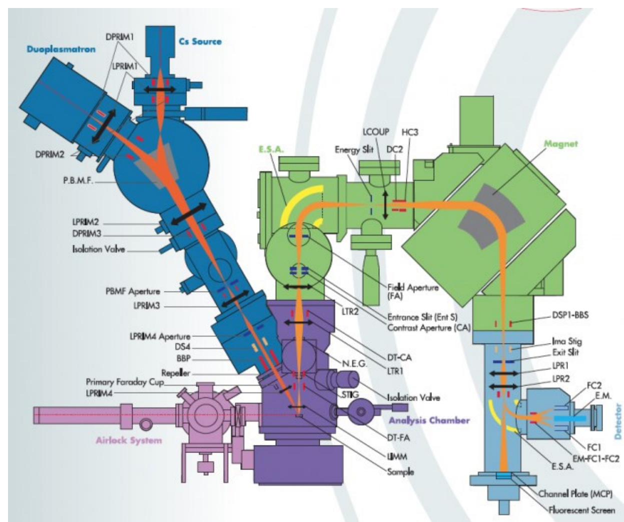

Figure 1: Schematic of Cameca IMS-7fGEO [3].

Quantification

The most common method for quantifying SIMS depth profiles is by utilizing ion implant standards. The ion of interest can by placed in the matrix of interest at a known dose by the ion implanter. Quantification is achieved by depth profiling the implant standard and using this data to calculate a relative sensitivity factor (RSF). The RSF can then be used to quantify the species of interest in depth profiles of the sample material. All concentrations were reported in atomic ppm and denoted by ppm(a). Ion implants are also useful to determine the detection limit of the method/instrument.

Detection Limit

Analysis of elements at low concentration, requires insuring the detection limit of the method and instrumentation is acceptable; i.e., lower than the subject species concentration. This is especially true when analyzing atmospherics such as nitrogen and oxygen, which are ever present in some amount. It can be difficult to know whether a baseline value for a sample is due to the species of interest

† mkelley@jlab.org

Content from this work may be used under the terms of the CC BY 3.0 licence (© 2017). Any distribution of this work must maintain attribution to the author(s), title of the work, publisher, and DOI.

ISBN: 978-3-95450-191-5 doi:10.18429/JACoW-SRF2017-THPB037

CAVITY FUNDAMENTAL MODE AND BEAM INTERACTION IN CEPC MAIN RING

D. J. Gong, J. Gao, J. Y. Zhai, D. Wang
Key Laboratory of Particle Acceleration Physics and Technology, Institute of High Energy Physics, CAS, Beijing 100049, China

Abstract

In this paper the preliminary study is undertaken for cavity fundamental mode and beam interaction of CEPC main ring. The baseline of CEPC main ring is DR scheme, the alternative is APDR scheme. Beam loading effects and the corresponding longitudinal beam dynamics of both CEPC DR and APDR are elaborated in this article. The phase shift and voltage decrease are calculated by the analytic formula and the program. Furthermore, the longitudinal coupled-bunch instability is also studied. At last, the RF parameters are calculated for CEPC 100km APDR, in order to match the machine parameters and relieve the beam loading effects.

INTRODUCTION

Circular Electron-Positron Collider (CEPC) is a 100km ring, an electron-positron collider serving as a Higgs factory in phase-I. It can be upgraded to a super proton-proton collider (SPPC) in phase-II [1]. The designed beam energy for CEPC is 120 GeV for Higgs study, 80 GeV for W and 45.5GeV for Z.

A Preliminary Conceptual Design Report (Pre-CDR) was published in March, 2015. In Pre-CDR, CEPC is a single ring machine with 50 equally spaced bunches [2]. The pretzel orbit was designed for *e+e-* beams, which is difficult to control and the luminosity of Z can't reach the target. To solve the problem, a partial double ring scheme (PDR) was raised [3]. The crab-waist scheme is used in two IPs, the luminosity is increased and the beam power is reduced [4].

The advanced partial double ring scheme (APDR) was put forward as an alternative plan last year. It's a main ring structure improved from PDR, which can save the cost but gives a challenge for the SRF system. Because of large gaps, the beam loading problem is serious in CEPC main ring, especially for Z pole. Afterwards, the 100km full partial double ring scheme (DR) becomes the baseline of CEPC main ring.

The SRF system is one of the most important system in CEPC. The beam loading effects due to RF-beam interaction is also the critical problem in CEPC SRF system. There are two particular beam loading effects presenting in large high-current storage rings: First, the phase shift between bunches due to gaps in the bunch train. Second, the longitudinal coupled bunch instability (CBI) due to the detuned fundamental RF resonance [5].

At last, we try to adjust the APDR machine parameters to both reach the luminosity target and control the beam loading effects within the limit. The phase shift and voltage decrease of the bunches in APDR and DR are calculated with K. Bane's formula and P. B. Wilson's formula [6,7]. The result is also checked with the program.

The analysis of longitudinal coupled bunch instability is also involved in this paper.

CEPC DR RF PARAMETERS

The analysis results of this paper are based on the CEPC DR RF parameter [8] in Table 1.

Table 1: CEPC DR RF Parameters

Parameter	Unit	Higgs	Z
Beam Energy	GeV	120	45.5
Circumference	km	100	100
SR loss/ turn	GeV	1.67	0.034
Beam current	mA	16.9	10.5
SR power/beam	MW	32	16
Bunch number		412	21300
Bunch length	mm	2.9	4.0
Bunch charge	nC	15.5	7.3
RF frequency	MHz	650	650
RF voltage	GeV	2.1	0.14
Cell number/ cavity		2	2
R/Q per cavity	Ohm	213	213
Harmonic number (10^5)		2.167	2.167
Cavity number/ beam		336	48
Synchrotron phase	deg	37.3	75.9
Input power/ cavity	kW	190	335
Loaded Q (10^5)		9.6	1.2
Optimal detuning	kHz	0.3	10.9
Cavity bandwidth	kHz	0.7	5.5
Momentum compaction (10^{-5})		1.14	4.49
Synchrotron tune	υ_s	0.065	0.068
Luminosity ($10^{34}cm^{-2}s^{-1}$)	L_0	2.96	2.01

Content from this work may be used under the terms of the CC BY 3.0 licence (© 2017). Any distribution of this work must maintain attribution to the author(s), title of the work, publisher, and DOI.

ISBN: 978-3-95450-191-5 doi:10.18429/JACoW-SRF2017-THPB038

LOCAL MAGNETOMETER: FIRST CRITICAL FIELD MEASUREMENT OF MULTILAYER SUPERCONDUCTORS

M. Aburas, C.Z. Antoine, A. Four
Irfu, CEA, Université Paris-Saclay, F-91191 Gif-sur-Yvette, France

Abstract

S-I-S (Superconductor-Insulator-Superconductor) nanometric superconducting multilayers have been proposed by Gurevich [1] to increase the maximum accelerating field of Nb RF cavities. This enhancement of Hc_1 may be done by coating Nb with thin layers of thickness less than the penetration depth ($d \leq \lambda$). Therefore, it is necessary to find a particular tool, which allows us measuring Hc_1 directly. In fact, DC magnetometers (e.g. SQUID magnetometers) are largely used for magnetic measurements but these last are strongly influenced by orientation, edge and shape effects, especially in the case of superconductor thin films. For that reason, we developed at Saclay a specific local magnetic measurement of first critical field Hc_1.

INTRODUCTION

The first critical field Hc_1 is one of the key physical parameters characterizing a superconducting material. This parameter is usually measured by conventional magnetometers (SQUID). For thin superconducting films, these measurements are strongly influenced by orientation, edge and shape effects. These devices give ambiguous results for very thin samples because of demagnetization effects (field on the back and sides, alignment issues (Fig. 1a). Samples exhibit a strong transverse moment, due to misalignment, which is sufficient to let vortices entered the material.

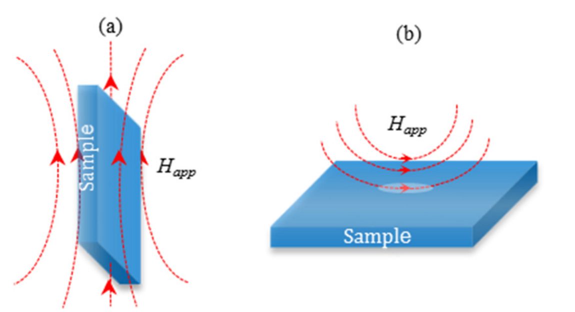

Figure 1: a) SQUID magnetometer principle. b) Local magnetometer principle.

Therefore, the development of a local magnetometer is necessary to measure directly the first critical field Hc_1 on superconductor sample without edge nor demagnetization effect.

When the coil is much smaller than the sample, the magnetic field decreases quickly away from the coil and the sample can be considered as an infinite plane for the field lines, with no edge and demagnetizing effect (Fig. 1b).

In this experimental set-up, the field configuration is similar to cavities, i.e. parallel to the surface and only on one side. In this paper, we will describe the evolution of the design of a local magnetometer specifically dedicated to measure thin films and multilayer samples, which is being developed at Saclay.

METHODOLOGY

The principle of our local magnetometer is based on the third-harmonic voltage method purposed by Claassen [2], it is non-destructive and contactless, but more importantly, without demagnetization effects The method of third harmonic analysis is currently used to study vortex behavior in superconducting (SC) samples (H_{irr} and/or J_C). Lamura showed in 2009 that it also can be used to measure Hc_1 [3].

By monitoring the intensity and/or the phase of the third harmonic signal (i. e. the higher harmonic) one can detect accurately the transition to the mixed state in a configuration that is close to the cavity operation conditions. In this configuration, if the samples were devoid of defects, we could in principle access to the superheating field. In the following we nevertheless will refer to it as Hc_1 as a precaution, meaning the transition of the composite sample to the mixed state.

The coil provides excitation as well as detection. It produces an AC magnetic field at the surface of the sample. As long as the sample keeps in the Meissner state, the sample acts as a perfect magnetic mirror: when the sample is in the Meissner state, the sample generates a magnetic moment opposed to the vertical component of H_{app} and the resulting induction is equals to twice the horizontal component of H_{app} : $2\mu_0\, H_{app}{}^{hor}$. The current (and voltage) in the coil keeps linear and shows the same sinusoidal curve as the reference signal at frequency ω. (Fig. 2).

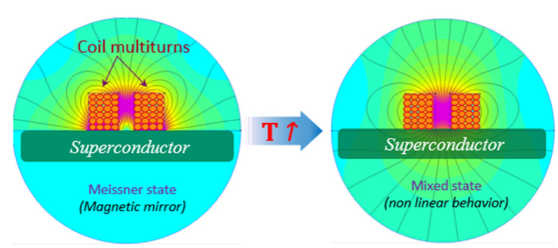

Figure 2: Repartition of the field lines in the Meissner state and in the mixed state.

Once vortices start to enter the sample (upon rising temperature or rising the current in the coil), they are pinned by defects, and the electrons from the coil experience a dragging force that gives rise to nonlinearity in the current/voltage inside the coil. In addition to the reference frequency ω, one start to observe higher odd harmonics. By monitoring the 3rd harmonic (most intense harmonic) one is able to determine the temperature of vortices penetration for a given field. The experiment is repeated for various

Content from this work may be used under the terms of the CC BY 3.0 licence (© 2017). Any distribution of this work must maintain attribution to the author(s), title of the work, publisher, and DOI.

ISBN: 978-3-95450-191-5 doi:10.18429/JACoW-SRF2017-THPB040

SRF THEORY DEVELOPMENTS FROM THE CENTER FOR BRIGHT BEAMS*

D. B. Liarte†, T. Arias, D. L. Hall, M. Liepe, J. P. Sethna, N. Sitaraman
Cornell University, Ithaca, NY, United States of America
A. Pack, M. K. Transtrum
Brigham Young University, Provo, UT, USA

Abstract

We present theoretical studies of SRF materials from the Center for Bright Beams. First, we discuss the effects of disorder, inhomogeneities, and materials anisotropy on the maximum parallel surface field that a superconductor can sustain in an SRF cavity, using linear stability in conjunction with Ginzburg-Landau and Eilenberger theory. We connect our disorder mediated vortex nucleation model to current experimental developments of Nb_3Sn and other cavity materials. Second, we use time-dependent Ginzburg-Landau simulations to explore the role of inhomogeneities in nucleating vortices, and discuss the effects of trapped magnetic flux on the residual resistance of weakly- pinned Nb_3Sn cavities. Third, we present first-principles density-functional theory (DFT) calculations to uncover and characterize the key fundamental materials processes underlying the growth of Nb_3Sn. Our calculations give us key information about how, where, and when the observed tin-depleted regions form. Based on this we plan to develop new coating protocols to mitigate the formation of tin depleted regions.

INTRODUCTION

The fundamental limit to the accelerating E-field in an SRF cavity is the ability of the superconductor to resist penetration of the associated magnetic field H (or equivalently B). SRF cavities are routinely run at peak magnetic fields above the maximum field H_{c1} sustainable in equilibrium; there is a metastable regime at higher fields due to an energy barrier at the surface [1]. $H_{\rm sh}$ marks the stability threshold of the Meissner state. In Fig. 1 we show results from linear stability analysis [2], valid near T_c, for $H_{\rm sh}$ as a function of the Ginzburg-Landau parameter κ, the ratio λ/ξ of the London penetration depth λ to the coherence length ξ. Niobium has $\kappa \approx 1.5$, most of the promising new materials have large κ. At lower temperatures, one must move to more sophisticated Eliashberg theories [3], for which $H_{\rm sh}$ is known analytically for large κ; numerical studies at lower κ are in progress [4]. Broadly speaking, the results so far for isotropic materials appear similar to those of Ginzburg-Landau.

This manuscript will briefly summarize theoretical work on $H_{\rm sh}$ (the threshold of vortex penetration and hence the quench field). First, we discuss the effect of materials anisotropy on $H_{\rm sh}$ [5]. Second, we discuss theoretical estimates of the effect of disorder [6], and preliminary unpublished simulations of the effects of surface roughness and materials inhomogeneity. Third, we discuss key practical implications of theoretically calculated point defect energies, interactions, relaxation times, and mobilities in the promising new cavity material Nb_3Sn. Finally, some magnetic flux is trapped in cavities during the cooldown phase, and the response of these flux lines to the oscillating external fields appears to be the dominant source of dissipation in modern cavities. We model potentially important effects of multiple weak-pinning centers on this dissipation due to trapped flux.

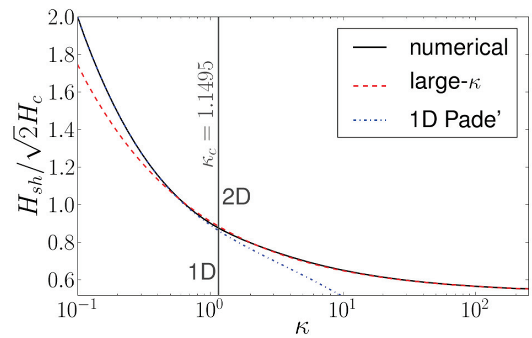

Figure 1: From Ref. [2], showing a numerical estimate of $H_{\rm sh}$ in Ginzburg-Landau theory over many orders of magnitude of κ (black solid line), along with a large-κ expansion (red dashed line), and a Padé approximation for small κ (blue dotted-dashed line).

THE EFFECT OF MATERIALS ANISOTROPY ON THE MAXIMUM FIELD

Some of the promising new materials are layered, with strongly anisotropic superconducting properties (MgB_2 and the pnictides, for example, but not Nb_3Sn or NbN). Figure 2 illustrates an anisotropic vortex (magnetized region blue, vortex core red) penetrating into the surface of a superconductor (grey). The anisotropy here is characteristic of MgB_2 at low temperatures, except that the vortex core is expanded by a factor of 30 to make it visible.

Near T_c, we find in Ref. [5] that a simple coordinate change and rescaling maps the anisotropic system onto the isotropic case (Fig. 1) above, as studied in Ref. [2]). We find, near T_c where Ginzburg-Landau theory is valid, that $H_{\rm sh}$ is nearly isotropic for large κ materials (Fig. 3. At lower temperatures, different heuristic estimates of the effects of anisotropy on $H_{\rm sh}$ yield conflicting results. Further work at lower temperatures could provide valuable insight into the

* This work was supported by the US National Science Foundation under Award OIA-1549132, the Center for Bright Beams.
† dl778@cornell.edu

Content from this work may be used under the terms of the CC BY 3.0 licence (© 2017). Any distribution of this work must maintain attribution to the author(s), title of the work, publisher, and DOI.

ISBN: 978-3-95450-191-5 doi:10.18429/JACoW-SRF2017-THPB041

Content from this work may be used under the terms of the CC BY 3.0 licence (© 2017). Any distribution of this work must maintain attribution to the author(s), title of the work, publisher, and DOI.

CAVITY QUENCH STUDIES IN Nb_3Sn USING TEMPERATURE MAPPING AND SURFACE ANALYSIS OF CAVITY CUT-OUTS*

D.L. Hall†, M. Liepe, R.D. Porter, P. Cueva, D.B. Liarte, D.A. Muller, J.P. Sethna
Cornell Laboratory for Accelerator-Based Sciences and Education (CLASSE),
Ithaca, NY 14853, USA

Abstract

Previous experimental studies on single-cell Nb_3Sn cavities have shown that the cause of quench is isolated to a localised defect on the cavity surface. Here, cavity temperature mapping has been used to investigate cavity quench behaviour in an Nb_3Sn cavity by measuring the temperature at the quench location as the RF field approaches the quench field. The heating profile observed at the quench location prior to quench appears to suggest quantised vortex entry at a defect. To investigate further, the quench region has been removed from the cavity and analysed using SEM methods. These results are compared to theoretical models describing two vortex entry defect candidates: regions of thin-layer tin-depleted Nb_3Sn on the cavity surface that lower the flux entry field, and grain boundaries acting as Josephson junctions with a lower critical current than the surrounding material. A theoretical model of layer growth developed using density functional theory is used to discuss alterations to the coating process that could mitigate the formation of such defects.

INTRODUCTION

Single-cell 1.3 GHz ILC-style niobium cavities coated with Nb_3Sn have outperformed the efficiency of their niobium equivalents while operating at 4.2 K and 16 MV/m [1–3]. However, all Nb_3Sn cavities coated at Cornell are limited to quench fields between 14 and 18 MV/m. Pulsed testing [4] has demonstrated that higher fields can be achieved, but fall still short of the theoretical maximum field that Nb_3Sn could achieve given its superheating field of approximately 400 mT.

To better understand this limitation in quench field, temperature mapping studies were performed on a single-cell 1.3 GHz Nb_3Sn cavity to observe the behaviour of the cavity near the quench field. Following data taking, the cavity was cut to remove the origin the quench region, as well as representative samples from other regions of the cavity.

EXPERIMENTAL METHOD

The temperature mapping system in use at Cornell University is an array of cryogenic temperature sensors that are mounted onto a single-cell 1.3 GHz cavity, as seen in Fig. 1. Composed of 646 sensors, each one a 100 Ω (at room temperature) carbon resistor, the array is mounted on 38 boards equipped with 17 sensors each that surround the cavity. Through the use of set screws, the resistors are pressed against the cavity surface, with good thermal contact being ensured through the application of thermal paste to each sensor head. Each sensor is capable of a resolution of 1 mK or less at a bath temperature of 2.0 K.

The temperature map can be operated in one of three modes. In the most basic mode, the cavity is kept at a constant RF power while the voltage across each sensor (equivalent to its temperature via a known calibration) is measured. Such a measurement takes approximately 15 minutes per acquisition. In the second mode, the cavity is allowed to quench multiple times while the system scans board-per-board, searching for sudden spikes in temperature associated with a cavity quench. In this mode, the resolution of the system is sorely impacted, but due to the large temperature spikes associated with a quench, this is not a problem for the purposes of the measurement. This particular mode results in a *quench map*, indicating the location(s) of the cavity quench.

A third mode was designed specifically for this experiment, dubbed *single-scan* mode, in which a single sensor is scanned at high speed – 20 kHz – while maintaining the high resolution of the temperature mapping basic mode. The sacrifice to be made is that only a single sensor can be operational at any one time. However, for the purposes of monitoring a specific location, such as the region known to be the centre of the cavity quench, this mode is ideal.

For this study of the quench dynamics, one of the best-performing Cornell Nb_3Sn cavities was chosen: a single-

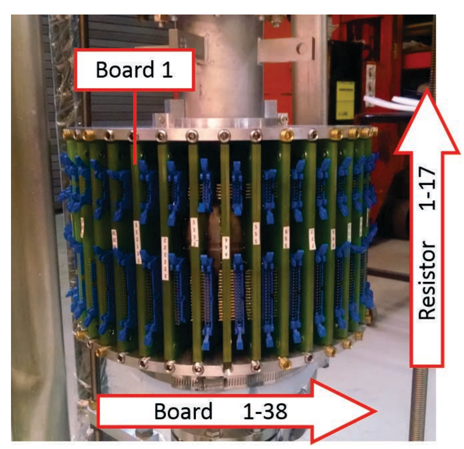

Figure 1: The single-cell temperature mapping system in use at Cornell University, mounted onto a 1.3 GHz single-cell ILC-style cavity coated with Nb_3Sn. The cables connecting the boards to the data acquisition system have been removed for better visibility.

* This work was primarily supported by U.S. DOE award DE-SC0008431.
† dlh269@cornell.edu

ISBN: 978-3-95450-191-5 doi:10.18429/JACoW-SRF2017-THPB042

Content from this work may be used under the terms of the CC BY 3.0 licence (© 2017). Any distribution of this work must maintain attribution to the author(s), title of the work, publisher, and DOI.

FIELD-DEPENDENCE OF THE SENSITIVITY TO TRAPPED FLUX IN Nb_3Sn*

D.L. Hall†, M.Liepe, R.D. Porter, D.B. Liarte, J.P. Sethna
Cornell Laboratory for Accelerator-Based Sciences and Education (CLASSE),
Ithaca, NY 14853, USA

Abstract

The amount of residual resistance gained per unit of trapped flux – referred to as the trapped flux sensitivity – in Nb_3Sn cavities has been found to be a function of the amplitude of the RF field. This behaviour is consistent with a scenario in which the trapped vortex dynamics are described by collective weak pinning. A model has been developed to describe this, and results in the observed linear dependence of trapped flux sensitivity with RF field. The model is used to discuss cavity preparation methods that might suppress this dependence, which would reduce the trapped flux requirements necessary to operate an Nb_3Sn cavity at simultaneous high quality factors and accelerating gradients.

INTRODUCTION

Niobium cavities coated with a layer of Nb_3Sn are a promising high-efficiency alternative to more conventional niobium for SRF applications [1–5]. In particular, the lower BCS resistance of Nb_3Sn allows operation of 1.3 GHz cavities at a bath temperature of 4.2 K, permitting the use of cryo-coolers or liquid helium without active pumping. To allow this to happen, however, the other components of the surface resistance, vis-à-vis residual resistance, must be minimised.

The greatest contributor to the surface resistance from source other than BCS are contributions from trapped magnetic flux. The losses from trapped flux are linearly proportional to the amount of flux trapped, and are quantified by the sensitivity to trapped flux, in nΩ of residual gained per mG of flux trapped. Results given here show that the sensitivity to trapped flux in Nb_3Sn films on niobium possess a noticeable dependence on the applied RF field, in a similar fashion seen to niobium films sputtered onto copper [6]. In this paper we demonstrate that this behaviour is consistent with a weak collective flux pinning scenario, in which a loss term from the presence of many weak pinning sites is introduced into the flux vortex equations of motion.

EXPERIMENTAL METHOD

An ILC-style single-cell 1.3 GHz cavity, niobium coated with Nb_3Sn, was utilised for this experiment. The cavity was tested in a vertical cryostat, using an experimental arrangement described by the diagram in Fig. 1. A Helmholtz coiled mounted over the cavity allowed the application of a near-constant magnetic field along the beam axis of the cavity, while a heater located at the base of the cryostat allowed the application of a thermal gradient across the cavity during the cool-down through T_c. The latter is necessary for the generation of thermoelectric currents from the metal bilayer interface of Nb/Nb_3Sn, which will result in the generation of a thermally-induced magnetic field. This measurement was used to demonstrate that the application of a thermal gradient during cool-down is equivalent to the application of an external magnetic field.

RESULTS

The equivalence of a thermal gradient to an externally applied magnetic field during cool-down is demonstrated in Fig. 2. In both cases, a linear increase in the ΔT across the cavity (measured in K/m) or an equivalent increase in the external magnetic field results in an increases in the residual resistance. This linear dependence allows us to quote an equivalence factor between the two sources for this cavity, which was found to be (6.2 ± 0.3) mG/(K/m).

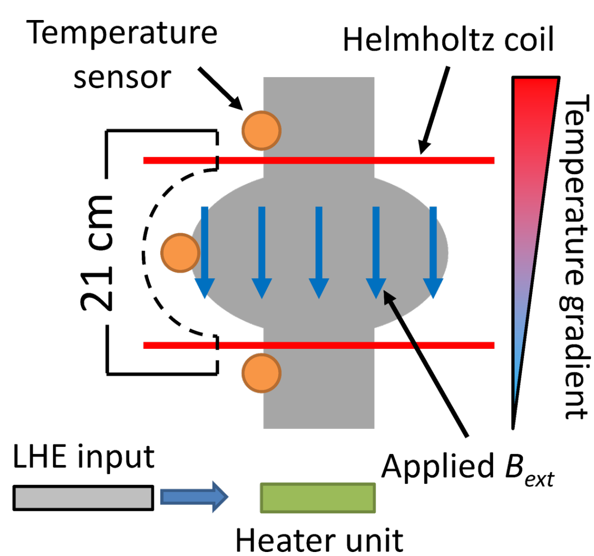

Figure 1: Diagram illustrating the experimental setup of the single-cell cavity. Liquid helium is introduced in a control fashion at the base of the cryostat, which, in the absence of power from the heater unit, allows cooling in an almost-uniform gradient. The Helmholtz coil allows the application of an external magnetic field, whilst the use of the heater develops a temperature gradient across the cavity, measured by the Cernox sensors mounted on the equator and irises.

* This work was primarily supported by U.S. DOE award DE-SC0008431. This work was supported in part by the U.S. National Science Foundation under Award PHY-1549132, the Center for Bright Beams.
† dlh269@cornell.edu

ISBN: 978-3-95450-191-5 doi:10.18429/JACoW-SRF2017-THPB043

EFFECTS OF CHEMICAL TREATMENTS ON THE SURFACE ROUGHESS AND SURFACE MAGNETIC FIELD EHANCEMENT OF NIOBIUM-3 TIN FILMS FOR SUPERCONDUCTING RADIO-FREQUENCY CAVITIES*

R. Porter†, F. Furuta, D. L. Hall, M. Liepe, and J. T. Maniscalco
Cornell Laboratory for Accelerator-Based Sciences and Education (CLASSE), Ithaca, NY, USA

Abstract

Current niobium-3 tin (Nb_3Sn) films produced via vapor diffusion have rougher surfaces than typical electropolished niobium surfaces causing significantly enhancement of the surface magnetic fields. Reducing surface roughness of Nb_3Sn surfaces may be necessary to achieve higher gradient accelerator cavities with high Q. Previous work at Cornell has shown the impact of several chemical treatments on the surface roughness of Nb_3Sn films; however, it had not been evaluated how the changes in surface roughness impact the surface magnetic field enhancement. In this paper we present simulations of the surface field enhancement of oxipolished Nb_3Sn, which was shown to be effective at reducing the surface roughness of Nb_3Sn. The surface magnetic field enhancement data is compared to those of unetched Nb_3Sn to find that the surface magnetic field enhancement (and surface roughness) has been roughly halved.

INTRODUCTION

Current niobium-3 tin coated niobium produced at Cornell University using tin vapor diffusion [1–5] has a significantly rougher surface than conventional electropolished niobium (see Fig. 1) [6, 7]. Previous work has shown that this roughness can significantly enhance the surface magnetic field (1% of the surface has magnetic fields enhanced by at least 45%), possibly lowering the maximum achievable quench field or causing other deleterious effects [6]. This is further supported by high-pulsed power klystron testing done near T_c (see Fig. 2) that suggests the maximal achievable quench field of Nb_3Sn (extrapolated to 0 K) would be 230 mT [8]. This is much less than theoretical predictions of 400 mT [9]. However, if 1% of the cavity becoming normal conducting was sufficient to cause quench then the data suggests a maximal quench field (extrapolated to 0 K) of 330 mT, much closer to the theoretical superheating field.

Work is being done to find chemical treatments that can reduce the surface roughness and destroy possible surface defects without destroying the thin (2 – 3 µm) Nb_3Sn surface layer [7, 10]. Recent results have found standard electropolishing and buffered chemical polish (1:1:2) to be ineffective for reducing the roughness of Nb_3Sn, but that oxipolishing

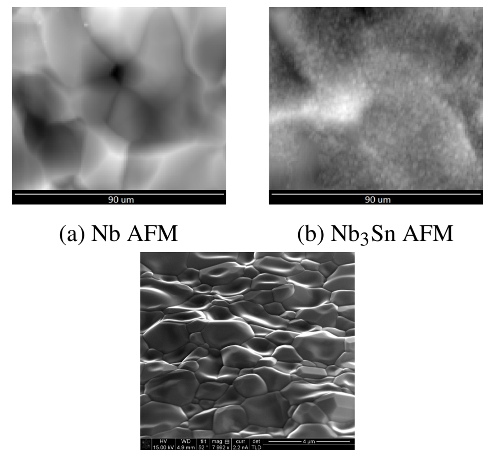

(a) Nb AFM (b) Nb_3Sn AFM

(c) Nb_3Sn SEM image.

Figure 1: Surface images of Nb and Nb_3Sn. Notice that the grain sizes of Nb_3Sn are on the order of microns, much smaller than Nb.

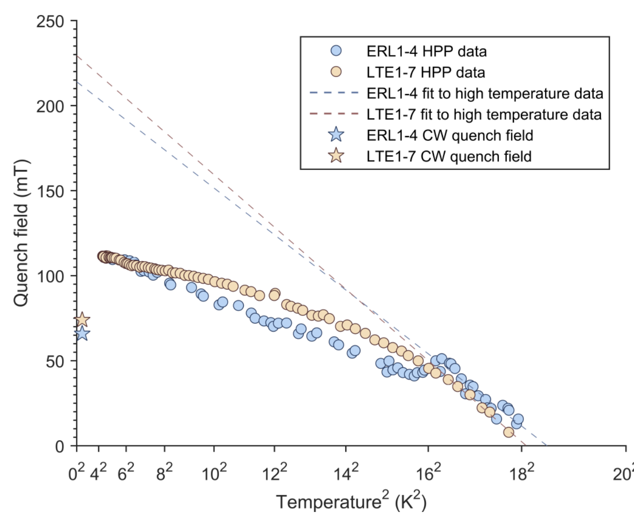

Figure 2: Plot of quench field (calculated from internal energy) versus T^2 from klystron high pulsed power measurements of Cornell Nb_3Sn cavities [8]

can half the surface roughness while etching away less than 1 µm (see Fig. 3) [7], with further reduction likely with additional polishing; however, it is has not been evaluated how this surface roughness reduction impacts the surface magnetic field enhancement. This paper uses surface height maps from Atomic Force Microscopy (AFM) to calculate

* This work was supported by the U.S. National Science Foundation under Award PHY-1549132, the Center for Bright Beams. This work was supported in part by U.S. DOE award DE-SC0008431. This work made use of the Cornell Center for Materials Research Shared Facilities which are supported through the NSF MRSEC program (DMR-1120296)
† rdp98@cornell.edu

Content from this work may be used under the terms of the CC BY 3.0 licence (© 2017). Any distribution of this work must maintain attribution to the author(s), title of the work, publisher, and DOI.

ISBN: 978-3-95450-191-5 doi:10.18429/JACoW-SRF2017-THPB044

UPDATE ON SAMPLE HOST CAVITY DESIGN WORK FOR MEASURING FLUX ENTRY AND QUENCH FIELD*

R. Porter† , M. Liepe, J. T. Maniscalco, and R. Strauss
Cornell Laboratory for Accelerator-Based Sciences and Education (CLASSE), Ithaca, NY, USA

Abstract

Current state-of-the-art Niobium superconducting radio-frequency (SRF) accelerator cavities have reached surface magnetic field close to the theoretical maximum set by the superheating field. Further increasing accelerating gradients will require new superconducting materials for accelerator cavities that are capable of supporting higher surface magnetic fields. This necessitates measuring the quench fields of new materials in high power RF fields. Previous work at Cornell University has used electromagnetic simulations to optimize the shape of a dipole mode sample host cavity such that the surface magnetic fields on the sample are high compared to the energy inside the cavity and the surface magnetic field on the rest of the cavity. In this paper we present an update of the design that includes how to mount samples in the cavity and the addition of a low field chamber.

INTRODUCTION

State-of-the-art niobium SRF cavities have reached surface magnetic fields close to the superheating field, the theoretical maximum [1, 2]. Further increasing accelerating gradients will require superconducting materials with superheating/quench fields that are greater than niobium's. This necessitates identifying materials with high superheating fields and processes for creating these materials that attain high quench fields. This can be measured using single cell cavity tests [3], but for some materials it might not yet be possible to create the complex cavity geometry, and creating full cavities is both time consuming and expensive.

This paper presents preliminary designs of a sample host cavity for measuring quench fields of material samples. We want this cavity to be capable of achieving peak magnetic fields on the sample that are greater than the superheating field of niobium, and capable of making measurements at a temperature greater than the critical temperature of niobium, ideally reaching T_c of whatever the sample material is so that the quench field can be explored near T_c.

DESIGN

The cavity consists of an upper and lower chamber, with the upper chamber being the resonant cavity (see Fig. 1). The upper chamber is based on a geometry created by Yi Xie at Cornell University [4]. The cavity geometry had been previously optimized to maximize the peak surface magnetic field in the center of the plate, achieving $48.9\,\mathrm{mT}/\sqrt{\mathrm{J}}$. The geometry was modified to change the frequency to 1.3 GHz so that we can use it with our high pulsed-power klystron.

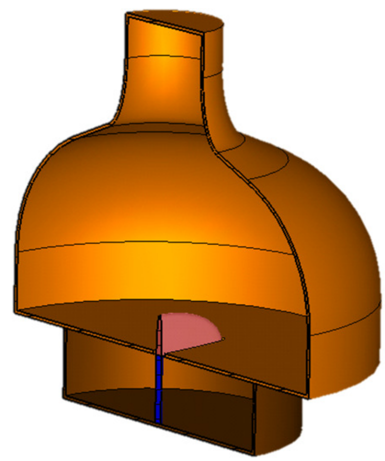

(a) Cross section of whole cavity. Note upper and lower chambers

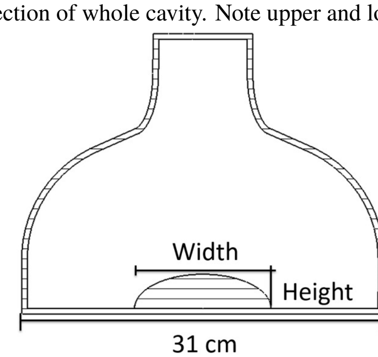

(b) x-z plane cross section of upper chamber.

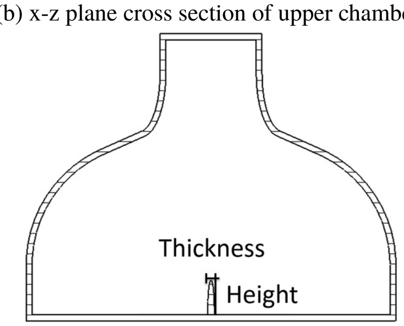

(c) y-z plane cross section of upper chamber.

Figure 1: Sample host cavity design.

To further increase the peak surface magnetic fields on the sample, the sample has been designed as an elliptical bump. This shape enhances the surface magnetic fields on the tip of the sample [5, 6]. Previous work [7] showed how the peak surface magnetic fields depends on the bump dimensions (see Fig. 4 and that peak fields of $400\,\mathrm{mT}/\sqrt{\mathrm{J}}$ or higher is possible.

---

* This work was supported by the U.S. National Science Foundation under Award PHY-1549132, the Center for Bright Beams

† rdp98@cornell.edu

Content from this work may be used under the terms of the CC BY 3.0 licence (© 2017). Any distribution of this work must maintain attribution to the author(s), title of the work, publisher, and DOI.

ISBN: 978-3-95450-191-5 doi:10.18429/JACoW-SRF2017-THPB048

DOUBLE CATHODE CONFIGURATION FOR THE Nb COATING OF HIE-ISOLDE CAVITIES*

A. Awais†[1], A.J.G. Lunt, A. Sublet, G. Rosaz, M. Taborelli, CERN, Geneva, Switzerland
[1]also at NCP, Islamabad, Pakistan

Abstract

The Quarter Wave Resonator (QWR) cavities for HIE-ISOLDE project at CERN have entered their ending phase of production. Some R&D is still required to improve the uniformity of the Nb layer thickness on the cavity surface. In order to improve this behaviour one approach which has been proposed is to replace the single cathode with a double cathode and test the suitability of different deposition techniques. With this change it is possible to control the plasma and power distribution separately for the inner and outer part of cavity and thereby potentially improve film uniformity throughout the cavity and coating duration. In this study a comparison between the deposition rates obtained using a single cathode and a double cathode using Direct Current (DC)-bias diode sputtering, DC-magnetron sputtering (DCMS) and Pulsed DC-magnetron sputtering (PDCMS) is presented. The morphology of the thin film samples were compared using Focused Ion Beam (FIB) cross section milling and Scanning Electron Microscopy (SEM) analysis.

INTRODUCTION

The technology of Nb sputtering on copper cavities was developed in early 1980's at CERN [1]. This technology was selected for QWR cavities for HIE-ISOLDE project in 2007 [2] while the work for establishing the setup and method for the series production was started in 2008 [3]. After passing this R&D stage, the first cryomodule cavities were produced between 2013 and 2014 [4]. With the completion of the fourth cryomodule [5] the project has reached its final stage, in which five spare cavities are being produced. Despite reaching its final production stage, R&D on QWR coatings continues in parallel, as advances in RF performance are still possible.

Coating layer thickness uniformity remains one of the aspects which requires further improvement. For example, current baseline cavities are known to show discrepancies between the inner and outer conductor thickness profiles [6]. Typically the minimum thickness required for a coating is defined by the penetration depth of the RF field (~ 40 nm) and must be thick enough to minimize losses with respect to material quality (dense layer, defect and contaminant free) and substrate influence. In practice we target to a thickness of tens of penetration depths with an additional safety margin resulting to a minimum 1 µm film. The maximum thickness is primarily limited by the residual stress induced in the film [7] and the associated adhesion issues between the film and the copper surface. It mostly depends on the coating method and surface preparation and can be validated by high pressure rinsing test up to 100 bars.

In order to achieve the desired cavity performances for the HIE-ISOLDE project [8] with the current baseline process we have to tune the outer conductor minimum thickness by increasing the overall coating time and consequently increasing the inner conductor thickness (up to 4 times larger [6]) and potentially the amount of impurities in the film.

To facilitate improved control of the coating process, and thereby ensure a more optimal coating thickness and deposition time, a new double cathode system has been designed. The increased flexibility of this two component system facilitates independent optimization of the inner and outer conductors coating rates and helps in reducing the amount of impurities.

In this paper the double cathode design will be introduced and comparisons will be drawn between the deposition rates obtained with double cathode and those obtained using conventional single cathode with different coating techniques. For each technique, the film morphology at different locations within the cavity will also be presented and discussed, along with the limitations of DC-magnetron sputtering technique for this geometry.

EXPERIMENTAL SETUP

Double Cathode Scheme

In this scheme two cathodes are used instead of a single one as used in production baseline process. Fig. 1 shows the comparison of the single and double cathode schemes.

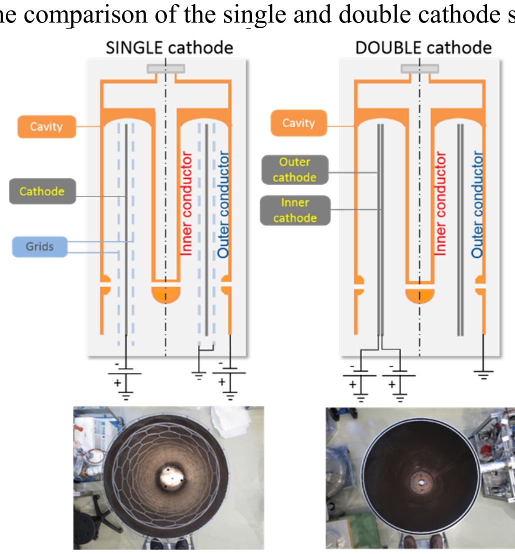

Figure 1: (a) single cathode scheme for DC-bias diode baseline, (b) double cathode scheme.

* Work supported by HIE-SIOLDE project at CERN
† ali.awais@cern.ch

Content from this work may be used under the terms of the CC BY 3.0 licence (© 2017). Any distribution of this work must maintain attribution to the author(s), title of the work, publisher, and DOI.

ISBN: 978-3-95450-191-5 doi:10.18429/JACoW-SRF2017-THPB052

ERROR ANALYSIS OF SURFACE RESISTANCE FITS TO EXPERIMENTAL DATA

S. Keckert*, O. Kugeler, J. Knobloch, Helmholtz-Zentrum Berlin, Berlin, Germany

Abstract

Superconducting material properties such as energy gap, mean free path or residual resistance are commonly extracted by fitting experimental surface resistance data. Depending on the measurement setup, both, temperature range and the number of points are limited. In order to obtain significant results, systematic as well as statistical uncertainties have to be taken into account. In this contribution different classes of errors and their impact on systematic and statistical deviations of the fitted parameters are discussed. In particular, past measurements by various groups have yielded contradictory conclusions that, we believe, result from the use of insufficient data in the necessary temperature range. Furthermore, this study is applied to the boundary conditions of the Quadrupole Resonator and its measurement accuracy.

INTRODUCTION

The RF surface resistance of a superconductor is an important contribution to the performance (quality) of an SRF cavity. A better understanding requires the knowledge of superconducting parameters such as energy gap and penetration depth. In order to access (superconducting) material properties from surface resistance data, measurements vs. temperature are compared to BCS theory. The methods available are typically as follows:

1. Approximation of the BCS surface resistance in the limit of low temperatures ($T < T_c/2$) and for frequencies $f \ll 2\Delta/h$.

$$R_s(T) = \frac{af^2}{T}\exp\left(-b\frac{T_c}{T}\right) + R_{\text{res}} \tag{1}$$

   with $a \propto \sigma\lambda^3\Delta$ taking into account several properties such as penetration depth or mean free path [1]. The exponential slope b can also be written as $b = \frac{\Delta}{kT_c}$.

2. Numerical simulation of the BCS surface resistance using SRIMP [2].

In both cases an temperature-independent residual resistance R_{res} is not intrinsic part of the model but has to be added to consider additional contributions to the surface resistance such as losses due to trapped magnetic flux. This work concentrates on the method of fitting using an exponential function as shown in Eq. (1).

Temperature Range and Experimental Data Sets

In a typical cavity test the cavity is cooled directly by a liquid helium bath. In horizontal tests this is provided by the helium tank welded to the cavity or – case of vertical testing – by means of a bath cryostat. In order to handle the RF heating of the inner side of the cavity wall while testing at relevant levels of accelerating field (several MV/m), this generally has to happen with superfluid helium at temperatures below 2.1 K. At frequencies of about 500 MHz measurements up to 4.2 K are possible. The minimum temperature is given by the cryoplant which is typically 1.5 K.

In contrast to this, measurements of the RF surface resistance of superconducting samples can be done using a Quadrupole Resonator (QPR) [3]. In that case the temperature limits look different: The minimum temperature again is given by the minimum helium bath temperature plus an offset given by the RF heating of the sample and the heat conductivity of the sample holder. At similar field levels as with cavity tests and for 'good' residual resistance below about 10 nΩ this is in the range of 1.8 – 2.0 K. Due to the calorimetric measurement principle of the QPR, the maximum accessible temperature is not limited by the helium bath. Here the limited validity of the exponential function in Eq. (1) has to be considered, which is also for Nb_3Sn the maximum temperature.

Both measurement methods have in common that the number of data points in the accessible temperature range is practically limited by the available time. In the following the number of data points is a matter of optimization in order to obtain sufficient accuracy with reasonable experimental effort.

We will show that fits limited to temperatures below 2.1 K show a significant error on the energy gap parameter b and an unacceptable high error on the parameter a.

Method

Discussing the significance of results, two different sources of errors are to be taken into account: Systematic errors and statistical uncertainties containing random error. While the actual determination of systematic errors can be very difficult, the impact on the final results can be calculated analytically. For statistical uncertainties this is different. Since the quantities of interest are extracted by fitting experimental data with the model shown above (see Eq. (1)), statistical uncertainties of the obtained values cannot be calculated by using classical propagation of uncertainties. In the following this will be done by numerical simulation of randomly distributed errors.

SYSTEMATIC ERRORS

Systematic errors are caused by the experimental setup and will in general depend on very experiment-specific parameters. With the QPR the surface resistance is measured using a calorimetric RF-DC compensation technique [3].

* sebastian.keckert@helmholtz-berlin.de

Content from this work may be used under the terms of the CC BY 3.0 licence (© 2017). Any distribution of this work must maintain attribution to the author(s), title of the work, publisher, and DOI.

ISBN: 978-3-95450-191-5 doi:10.18429/JACoW-SRF2017-THPB053

SURFACE RESISTANCE CHARACTERIZATION OF Nb_3Sn USING THE HZB QUADRUPOLE RESONATOR

S. Keckert*, O. Kugeler, J. Knobloch, Helmholtz-Zentrum Berlin, Berlin, Germany
D. L. Hall, M. Liepe, Cornell University, Ithaca, USA

Abstract

Nb_3Sn is a very promising candidate material for future SRF cavities. With a critical temperature more than twice as the one of bulk niobium, higher operational temperatures with still lower surface resistance are theoretically possible. The RF properties of a sample prepared by Cornell University were characterized using the HZB Quadrupole Resonator. In comparison to a coated cavity this device enables SRF measurements over an extended parameter space (frequency, temperature and RF field) and easy access to physical quantities such as critical field and penetration depth. In this contribution we present surface resistance and RF critical field measurements.

INTRODUCTION

Nb_3Sn is one of the most promising alternative materials to niobium for applications in SRF cavities. With its high critical temperature of about 18.5 K and superheating critical field $B_{sh} \approx 400$ mT [1], Nb_3Sn provides potential major improvements for both applications currently being investigated in the SRF community, high gradient accelerators as well as high-Q cavities with significantly reduced operating costs. Recent results with cavities have demonstrated R_s values of about 27 nΩ at 4.2 K far beyond the fundamental limit of niobium [2].

Sample Preparation

The sample characterized in this work was prepared at Cornell University using the coating procedure commonly applied to single cell cavities [2, 3]. As substrate a RRR 300 fine grain bulk niobium QPR sample was used. Prior to coating the substrate was characterized at HZB showing very good residual resistance of about 4 nΩ and high RF critical field $B_{c,RF} = 220$ mT [4].

For coating the substrate is placed into a UHV furnace with a $SnCl_2$ tin source inside. The process starts with heating up to 500 °C where tin evaporates from the source and forms nucleation sites on the niobium substrate. The actual coating consisting of diffusion of tin into niobium along with alloying to Nb_3Sn happens at a substrate temperature of 1100 °C with the source heated even further to 1200 °C. After 3 hours of coating the source heater is switched off while the sample is kept at high temperature for approximately 6.5 hours in order to allow for further annealing and grain growth.

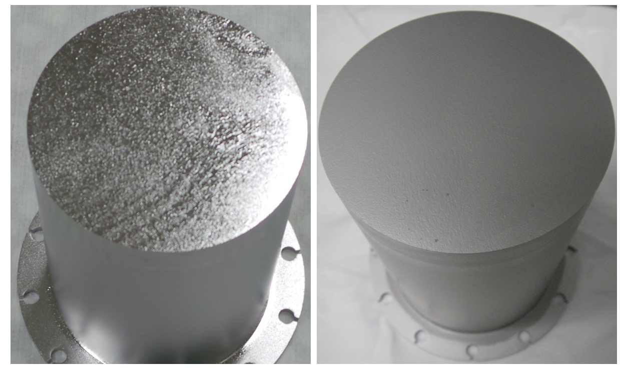

Figure 1: QPR sample before (left) and after (right) coating with Nb_3Sn.

EXPERIMENTAL SETUP: THE QUADRUPOLE RESONATOR

At HZB a Quadrupole Resonator (QPR) is available which enables SRF characterization of planar samples in a wide parameter space of temperature, RF field strength and frequency [5–7]. Up to now the sample had to be brazed into a stainless steel flange prior to mounting into the resonator. This joint limited the maximum temperature available for sample treatments to few hundred °C. Alternatively, brazing or an electron-beam weld had to be made after sample treatment which itself could affect relevant material properties. In order to allow for high temperature treatments of the sample – such as coating with Nb_3Sn – a modified sample chamber was developed [4]. In addition to available treatments this design makes samples exchangeable between the two existing QPRs at CERN and HZB. The main part as depicted in Fig. 1 is mounted into a double-sided CF100 flange using an indium wire gasket. This assembly is then inserted into the resonator (Fig. 2). As before, the planar surface on

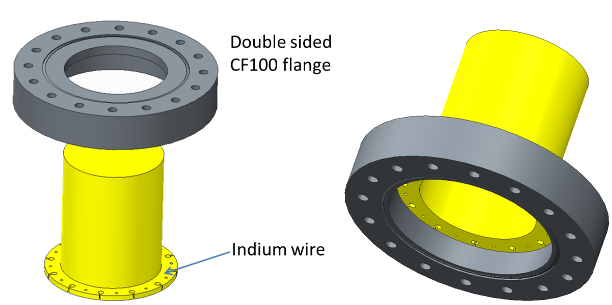

Figure 2: CAD sketch of the newly developed QPR sample chamber. Exploded view (left) and assembly ready for mounting into the QPR (right).

* sebastian.keckert@helmholtz-berlin.de

Content from this work may be used under the terms of the CC BY 3.0 licence (© 2017). Any distribution of this work must maintain attribution to the author(s), title of the work, publisher, and DOI.

ISBN: 978-3-95450-191-5 doi:10.18429/JACoW-SRF2017-THPB054

CALCULATING THE FIELD DEPENDENT SURFACE RESISTANCE FROM QUALITY FACTOR DATA

R. Kleindienst, S. Keckert, J. Knobloch, O. Kugeler, HZB, Berlin, Germany

Abstract

The quality factor of an RF cavity and the surface resistance are typically related with a constant geometry factor. The implicit assumption made is that the surface resistance is field independent, which is however not observed experimentally in superconducting cavities. The approximation error due to this assumption becomes larger the less homogeneous the magnetic field distribution along the cavity walls is. In this paper we calculate the surface resistance error for different cavity types. Correction factors as well as a numerical method to correct for this error are presented.

INTRODUCTION

The quality factor Q_0 of an RF cavity relates the stored energy U with the energy dissipated per RF cycle. It is calculated by:

$$Q_0 = \frac{\omega U}{P_{\mathrm{Dis}}} = \frac{\omega \int_{\mathrm{V}} |B|^2 \,\mathrm{d}v}{\mu_0 \int_{\mathrm{S}} R_{\mathrm{S}} \cdot |B|^2 \,\mathrm{d}s} \approx \frac{G}{R_{\mathrm{S}}} \qquad (1)$$

where P_{Dis} is the dissipated power and R_{S} is the surface resistance. In the last term, the geometry factor G is introduced which directly links the quality factor with the surface resistance. This factor is independent of the material and of the size of the cavity and is calculated with:

$$G = \frac{\omega \int_V |B|^2 \cdot \mathrm{d}v}{\mu_0 \int_{\mathrm{S}} |B|^2 \cdot \mathrm{d}s} \qquad (2)$$

Calculating the surface resistance from a quality factor measurement using $R_{\mathrm{S}}^{\mathrm{meas}} = G/Q_0$ will return a mean surface resistance which is only identical to the local material surface resistance $R_{\mathrm{S}}(B)$ if it is field independent or if the field distribution on the cavity surface is uniform. The less homogenous the surface magnetic field is distributed, the larger the approximation error becomes.

The effect of this is shown in Figures 1 and 2. In these plots, the hypothetically measured surface resistance $R_{\mathrm{S}}^{\mathrm{meas}}$ is shown for various different cavity types:

- Two elliptical cavities, a stadard TESLA geometry and low-loss ERL cavity
- An idealized half-wave resonator (HWR), modelled as a coaxial transmission line shorted at both ends [1].
- Two cavities used for sample testing - a TE_{011} host cavity [2, 3] and a Quadrupole Resonator (QPR) [4, 5]

In Figure 1, the assumed 'true' surface resistance is monotonically increasing and has a quadratic and an exponential component. In Figure 1, a linear term with a negative sign is added, giving a shape similiar to those produced with N-doped cavities [6]. As expected, the ERL cavity which has the most homogeneous field distribution produces the smallest error. The cavities in our study with a very inhomogenous surface magnetic field, the HWR and the QPR, have errors as large as 30% at high fields. For the N-doped case one also observes that the surface resistance minium gets shifted significantly.

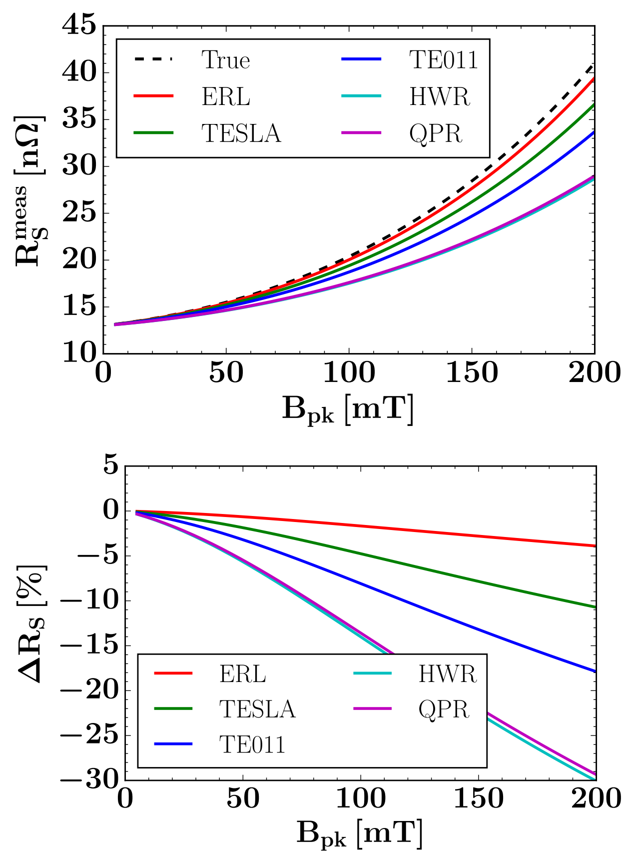

Figure 1: Hypothetical measurement of the same material with different cavities. Shown in the dotted black line is the assumed surface resistance which has a quadratic and an exponential contribution. For cavities types with very inhomogenous surface magnetic fields, the error when calculating the surface resistance as $R_{\mathrm{S}}^{\mathrm{meas}} = G/Q_0$ can be as large as 30%.

For calculating these results, Equation (1) was used together with an explicit calculation of P_{Dis}. For the eliptical cavities which have cylindrical symmetry one can use the wall profile $r(z)$ and the surface field $B(z)$ to reduce the calculation to a line integral:

Content from this work may be used under the terms of the CC BY 3.0 licence (© 2017). Any distribution of this work must maintain attribution to the author(s), title of the work, publisher, and DOI.

ISBN: 978-3-95450-191-5 doi:10.18429/JACoW-SRF2017-THPB055

PLASMA-ENHANCED ALD SYSTEM FOR SRF CAVITY

S. Kato† and H. Hayano
High Energy Accelerator Research Organization (KEK), Tsukuba, Japan

Abstract

A remote PEALD (Plasma-enhanced Atomic Layer Deposition) system which would offer a high conformality and a low deposition temperature has been being developed in KEK to aim deposition of multilayer systems like a NbN/Al_2O_3 multilayer on an SRF cavity. The deposition equipment was designed to carry out ALD not only on planar silicon wafer substrates in a reaction chamber but also on inner surface of a 1.3GHz single cell cavity just by replacement of reaction chamber with the cavity. An RF plasma exciter was utilized for an ALD reactant gas in order to reduce ALD temperature. Prepared precursors were tris [ethylmethylamido][tert-butylimido] niobium (TBTEMN) and trimethylaluminium (TMA) with reactants of ammonia, hydrogen and water for NbN and Al_2O_3 deposition. Surface analyses confirmed preliminary results of NbN_x ALD with homogeneous and smooth film growth and a GPC (growth per cycle) of around 0.1 nm. However noticeable concentration of oxygen and carbon found in the film requires further improvements of the ALD system and the operation conditions.

INTRODUCTION

To enhance a breakdown magnetic field in a superconducting radio frequency (SRF) cavity, a nano-scaled multilayer system of combination of high Hc superconducting material and insulator was proposed [1-3]. A remote PE-ALD (Plasma-enhanced Atomic Layer Deposition) system [4] was developed in order to deposit multilayers on planar substrates or on an inner surface of a SRF cavity with a high conformality, a low deposition temperature and a low density of contaminants [5]. Recently PE-ALD for NbN formation was also tried with a commercially available equipment from Oxford Instruments [6, 7]. A type of remote plasma would bring a better conformality in comparison with a type of non remote plasma even for a large coating area with a longitudinal configuration like a 1.3GHz 9-cell SRF cavity. In this study, we present our remote PE-ALD system design and results of our first deposition of NbN_x on samples which were analyzed with a scanning electron microscope (SEM), energy dispersive x-ray spectroscopy (EDX) and x-ray photoelectron spectroscopy (XPS) with sputter-etching.

EXPERIMENT

Our in-house made ALD system consists of a reaction chamber, a remote plasma exciter, a precursor supply system, vacuum pumps, a quartz crystal microbalance (QCM) as a film growth rate meter, a detoxifying system and a control sequencer shown in Fig. 1 [4]. The substrate holder can be heated up to 600 ℃ and the almost whole system can be baked out up to 200 ℃. An RF frequency of 13.56MHz was used for the inductively coupled plasma exciter of a reactant gas. The whole equipment is in a draft booth for operation safety. Though the reaction chamber accepts only coupon samples including a silicon wafer substrate up to 2", the ALD system allows to easily replace the reaction chamber with a single cell niobium cavity when ALD conditions are well found.

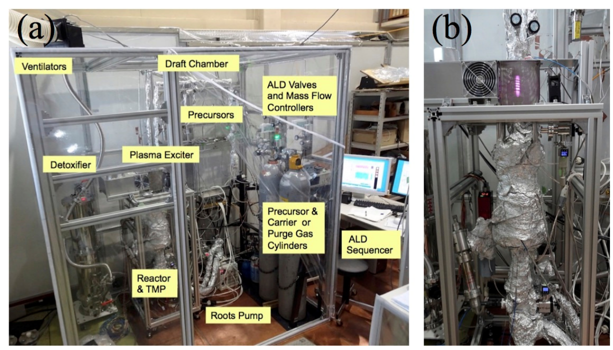

Figure 1: (a) ALD System for SRF Cavity in KEK (b) zoomed-in 13.56MHz plasma exciter and reaction chamber.

The precursors for this study are tris [ethylmethylamido][tert-butylimido] niobium (TBTEMN) with ammonia or hydrogen gas as the reactants.

Typical ALD conditions are the following:

* Precursor: TBTEMN
* Reactant: NH_3 (6 SCCM) + Ar (1 SCCM)
* RF Power: 50 W / 1 min / cycle
* Cycle: ~4 min
* Substrate temperature: 150 ºC

Deposited films on silicon substrates were analysed with SEM-EDX and XPS with sputter-etching capability to know film morphology and its atomic compositions.

RESULTS AND DISCUSSION

SEM images of a 200 cycle film and a 300 cycle film on silicon substrates are shown in Fig. 2 (a) and (b), respectively. Thickness of each film was measured to be around 20 and 35 nm with SEM observation. This results in a GPC (growth per cycle) of around 0.1 nm. It was found that the ALD films were quite homogeneous and the surfaces were smooth. To check conformity of our ALD, surfaces of a couple of silicon substrates were set in the reactor with different angles. The all samples showed a similar deposition thickness.

† Email address: shigeki.kato@kek.jp

Content from this work may be used under the terms of the CC BY 3.0 licence (© 2017). Any distribution of this work must maintain attribution to the author(s), title of the work, publisher, and DOI.

ISBN: 978-3-95450-191-5 doi:10.18429/JACoW-SRF2017-THPB057

INVESTIGATION OF NUCLEATION STAGE IN DIFFUSION COATING OF Nb_3Sn ON Nb*

F. Pan, T. Tan, A.D. Wu, L. Yang, L. Cheng, Y.M. Li, S.H. Zhang and Y. He
IMP, CAS, Lanzhou 730000, China
P. Zhu and F. Huang, Ningbo Institute of Industrial Technologies, CAS, Ningbo, China
J. Shi, Lanzhou University, Lanzhou, China

Abstract

Nb_3Sn has the potential to improve properties of SRF cavities, such as the gradients and the working temperatures. Institute of Modern Physics has launched its Nb_3Sn thin film coated SRF cavity project in 2016. Samples have been successfully coated to study the process of tin vapor diffusion. The main part of the deposition system is a tube furnace, which working temperature can reach 1100℃. Basic material characterization of the Sn-Nb film will be presented in this work.

INTRODUCTION

Niobium is the most widely used material for the present SRF accelerators. While the niobium cavities are approaching the material limit. The next superconducting for SRF cavities should have a higher T_c (the critical temperature) and H_{sh} (the superheating field) for higher working temperature and quality factor. The T_c and H_{sh} of Nb_3Sn are nearly twice that of niobium [1]. So Nb_3Sn has the potential to improve properties of SRF cavities, such as the gradients and the working temperatures.

The Nb_3Sn for SRF applications has a long history. Siemens AG and University of Wuppertal started to developed a diffusion coating recipe to get Nb3Sn cavities in 1970's. They successfully fabricated Nb3Sn cavities with tin vapor diffusion technology. Their susceptibility to ambient magnetic flux has resulted in a $Q_0 \approx 10^{10}$ at 5 MV/m at 4.2 K, but then suffered a precipitous drop [1]. The possible reason is an implicit property of Nb_3Sn. However, all studies of Nb_3Sn cavities fell off by the end of 1990`s until Cornell stated Nb_3Sn programs in 1990's. Now, Nb3Sn programs are now on going at Cornell and Jefferson.

Institute of Modern Physics has launched its Nb_3Sn thin film coated SRF cavity project with Sn vapor diffusion technique in 2016. The coating consists for the process of tin vapor diffusion we used is based on that in Cornell shown in Fig. 1:

I. A degas stage lasting hours
II. Nucleation
III. Ramp-up
IV. Coating
V. Annealing

*Work supported by the Key Research Program of Frontier Sciences, CAS, Grant NO. QYZDY-SSW-JSC019 and the National Natural Science Foundation of China (91426303).

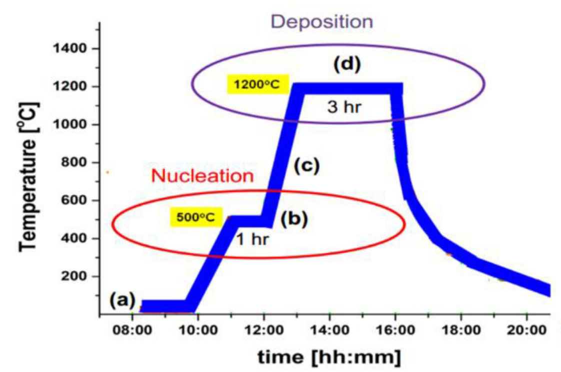

Figure 1: Heating profile used for sample coating. The nucleation step followed by deposition [2].

When researchers at Siemens AG (1970`s) began their Nb_3Sn programs, they found niobium spots not covered with Nb_3Sn film. While the coating process used tin halides or pre-anodized, the problem disappeared. They finally found tin halide (high vapor pressure) initiates Nb-Sn nucleation early by more availability of tin [3]. My study focuses on the parameters of the nucleation step.

THE EXPERIMENTAL

Experimental Set-up

For better monitoring the temperature and vacuum, a tube furnace system was used to perform experiments to imitate the nucleation step. The details of the experimental set-up are shown in the Fig. 2.

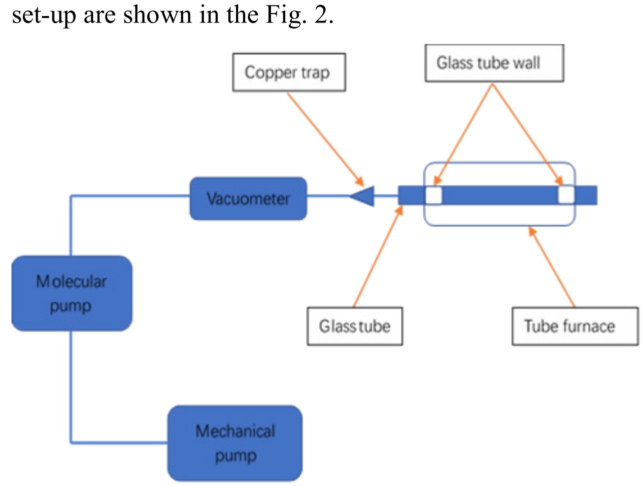

Figure 2: The coating system for samples.

A vacuum port is connected on the quartz glass tube. The system vacuum can reach 1×10^-4 Pa, and the working

Content from this work may be used under the terms of the CC BY 3.0 licence (© 2017). Any distribution of this work must maintain attribution to the author(s), title of the work, publisher, and DOI.

ISBN: 978-3-95450-191-5 doi:10.18429/JACoW-SRF2017-THPB058

R&D OF THIN FILM COATING ON SUPERCONDUCTORS

Y. Iwashita, R. Katayama, H. Tongu , ICR, Kyoto University, Uji, Kyoto, Japan
H. Hayano, T. Kubo, T. Saeki, KEK, Ibaraki, Japan
M. Hino KURRI, Kyoto University, Osaka, Japan
H. Oikawa, Utsunomiya University, Tochigi, Japan

Abstract

A measurement system for superconducting thin film coating is constructed, in order to investigate performances of superconducting thin film coatings. It is based on the third order harmonic measurement, which measure the nonlinear behaviour of an inductance of a coil put on a superconducting film around the critical magnetic field B_{c1}. Samples are cooled down through a copper plate tab whose bottom end is immersed in liquid Helium. The tab is fixed under a sample stage and the temperature of the stage is controlled by a heater on the stage. The temperature is monitored by Cernox sensors. We could obtain a preliminary results using the system

INTRODUCTION

Multilayer thin film coating of superconducting materials is a promising technology to enhance performance of superconducting cavities. Until recently, principal parameters to achieve the sufficient performance had not been known, such as the thickness of each layer. We proposed a method to deduce a set of the parameters to exhibit a good performance [1,2] (see Figure 1). In order to verify the scheme, we prepared the third order harmonic measurement system at Kyoto University[3].

MEASUREMENT METHOD

In order to evaluate the performance of the thin film coated material, we selected the third order harmonic detection method [4,5,6]. Figure 2 shows the schematic diagram of the prepared system, where the FPGA controls the generation of a sinusoidal wave and the amplified current excites the coil to generate the AC magnetic field. The FPGA is controlled by a PC through USB. The magnetic field is applied to superconducting samples and the excitation current and the self-induced voltage of the coil are monitored. The third harmonic component is measured through a high pass filter (HPF) cutting the fundamental frequency component. Figure 3 shows the measurement system for the third order harmonic component. When the applied magnetic field is less than B_{c1} of the superconducting film material, the Meissner effect completely repels the magnetic flux and the magnetic field flux does not penetrate the superconducting films (see Fig. 4). The self-induced voltage of the coil is proportional to the time derivative of the coil current as long as the Meissner effect is maintained. This linear behavior is

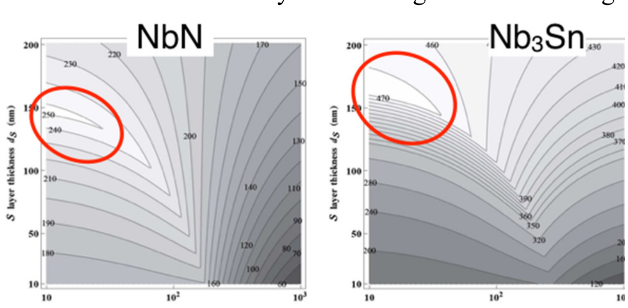

Figure 1: Parameters for enhancing a gradient limit by the multilayer thin film coating on superconducting bulk surface. A thin S layer pushes up B_v, but it cannot protect the bulk SC from an applied field if d_S << London depth. Not only B_v, but also the shielded magnetic field on the bulk SC must be considered simultaneously.

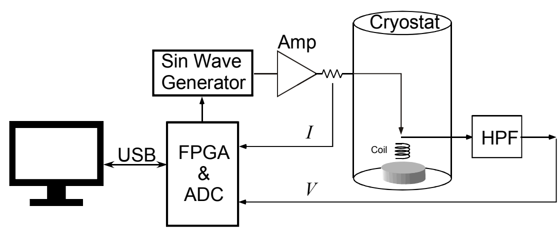

Figure 2: Block diagram of the measurement system of the third order harmonic component.

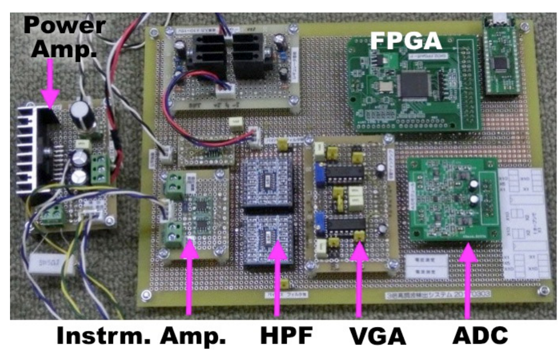

Figure 3: Circuits of the measurement system for the third order harmonic component.

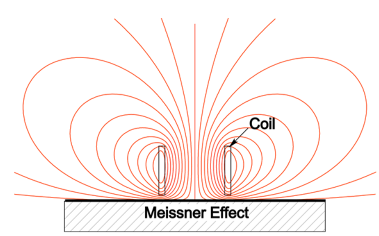

Figure 4: Meissner effect completely repels the magnetic flux from the superconductor film and the magnetic stored energy around the coil is reduced compared with the coil without the film.

Content from this work may be used under the terms of the CC BY 3.0 licence (© 2017). Any distribution of this work must maintain attribution to the author(s), title of the work, publisher, and DOI.

ISBN: 978-3-95450-191-5 doi:10.18429/JACoW-SRF2017-THPB059

SIMULATION AND MEASUREMENTS OF CRAB CAVITY HOMS AND HOM COUPLERS FOR HL-LHC*

J. A. Mitchell[†1, 2], R. Apsimon[2], G. Burt[2], T. Jones[2], N. Shipman[1, 2]
Lancaster University, Lancaster, UK
I. Ben-Zvi, S.Verdú-Andrés, B. Xiao, BNL, Upton, NY 11973, USA
R. Calaga, A. Castilla, A. Macpherson, A. Zwozniak, CERN, Geneva, Switzerland
T. Powers, H. Wang, JLab, Newport News, VA 23606, USA
[1]also at CERN, Geneva, Switzerland
[2]also at the Cockcroft Institute, Daresbury, UK

Abstract

Two Superconducting Radio-Frequency (SRF) crab cavities are foreseen for the High Luminosity LHC (HL-LHC) upgrade. Preliminary beam tests of the Double Quarter Wave (DQW) crab cavity will take place in the Super Proton Synchrotron (SPS) in 2018. For damping of the cavity's Higher Order Modes (HOMs) the DQW has three identical on-cell, superconducting HOM couplers. The couplers are actively cooled by liquid heluim. In this paper, electromagnetic simulations of the HOMs and HOM couplers are presented. A novel approach to pre-installation spectral analysis of the HOM couplers is then presented, detailing both simulated and measured data. Measurements of the cavity HOMs at warm and in Vertical Test Facilities (VTFs) at both JLAB and CERN are detailed, comparing the measured characteristics of each mode to that of the simulated data-sets. Finally, the measured cavity data is compared with the test box measurements to see by what extent any reduction in damping can be predicted.

INTRODUCTION

To damp the HOMs in the DQW crab cavity, the transmission response of the three identical HOM couplers was deigned to provide high transmission at the frequencies of high impedance modes, whilst rejecting the fundamental mode at ~ 400 MHz. The high transmission peaks are notated as the 'filter interaction regions' and the rejection of the fundamental mode is achieved with a band-stop response at this frequency.

with a band-stop response centred around this frequency. The HOM coupler designed for the SPS DQW crab cavity [1] is shown in Fig. 1 and it's S_{21} response is plotted in Fig. 2.

HOM COUPLER TEST BOXES

Complex HOM coupler geometries could result in a deviation from RF performance criteria due to inaccuracies in machining processes. From this, a motivation for test-stands capable of accurately defining the coupler's spectral response produced two 'test-boxes' [2]. The manufactured test-boxes can be seen in Fig. 3.

* This work is supported by the HL-LHC project, Lancaster University and the Cockcroft core grant.
† j.a.mitchell@lancaster.ac.uk

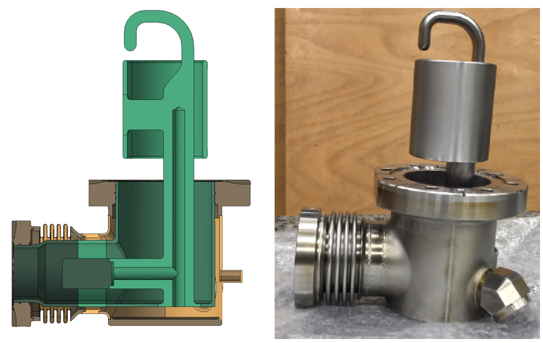

Figure 1: CAD model (left) and photograph (right) of the HOM coupler for the SPS DQW crab cavity.

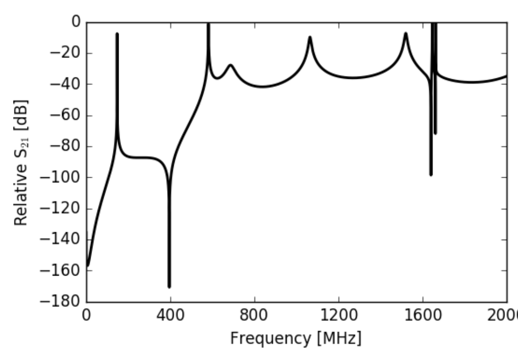

Figure 2: Transmission characteristics for the SPS HOM coupler. Relative amplitude is used as a waveguide port is located on open vacuum.

Although the test boxes were designed to give an accurate representation of the coupler's spectral response, minor differences between the test-box and coupler response were still present. This difference was optimised to best represent

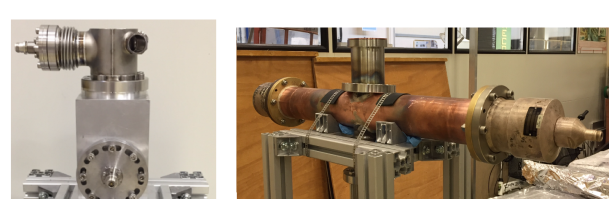

Figure 3: Test box designs for the DQW crab cavity HOM couplers. The designs are denoted the L-bend transmission (left) and coaxial chamber (right) test-boxes.

Content from this work may be used under the terms of the CC BY 3.0 licence (© 2017). Any distribution of this work must maintain attribution to the author(s), title of the work, publisher, and DOI.

ISBN: 978-3-95450-191-5 doi:10.18429/JACoW-SRF2017-THPB061

Content from this work may be used under the terms of the CC BY 3.0 licence (© 2017). Any distribution of this work must maintain attribution to the author(s), title of the work, publisher, and DOI.

EFFECT OF DISLOCATIONS ON THE THERMAL CONDUCTIVITY OF SUPERCONDUCTING Nb

Peng Xu, Neil T. Wright, Mechanical Engineering
Thomas R. Bieler, Chemical Engineering and Materials Science
Michigan State University, East Lansing, MI, 48823, USA

Abstract

The thermal conductivity of Niobium (Nb) often experiences a local maximum (a phonon peak) at a temperature between 1.8 and 3 K. While the magnitude of the phonon peak has been shown to be related to the dislocation density and may be influenced by manufacturing processes, little has been discussed as to the temperature at which the peak occurs. In examining these phenomena, it has been determined that more explicit accounting of phonon–dislocation scattering in a popular model better represents the thermal conductivity at temperatures colder than 3 K. Scaled sensitivity coefficients show this term to have similar influence as the phonon-electron and phonon-boundary scattering terms. Results using the enhanced model also show an apparent threshold of dislocation density ($N_d < 10^{12}$ m^{-2}) below which there is little contribution to the thermal conductivity of Nb.

INTRODUCTION

Manufacturing superconducting radio frequency (SRF) cavities from large grain niobium (Nb) may reduce cost and improve the quality factor as compared with polycrystalline Nb [1]. Processing Nb to obtain the largest thermal conductivity possible is an important component of the improved performance. Even in the superconducting regime, small imperfections at the RF surface can cause local heating that leads to loss of performance. Large values of thermal conductivity can mitigate local temperature excursions and prevent cavity quench, thus improving cavity performance [2].

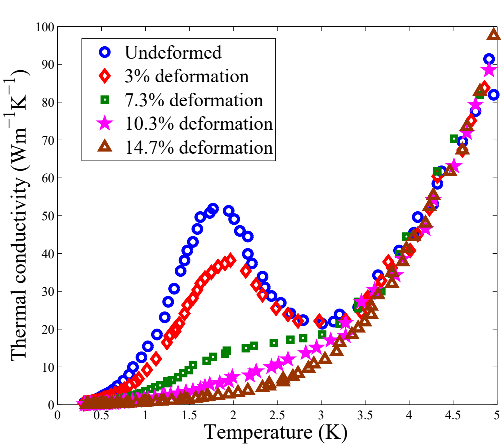

Figure 1: Thermal conductivity of sample K6 from Wasserbäch with different deformation, replotted from [3].

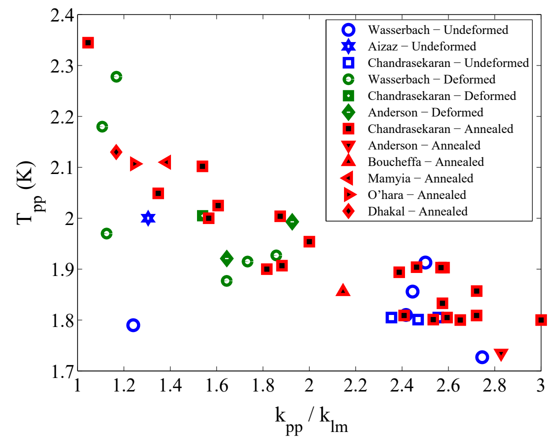

Figure 2: Measured phonon peak temperatures T_{pp} for undeformed, deformed and annealed specimens as a function of the ratio of the thermal conductivity at phonon peak k_{pp} to that at local minimum temperature k_{lm}.

Manufacturing SRF cavities from Nb sheets requires large deformations that increase dislocation density [4], which has been shown to reduce the thermal conductivity of superconducting large grain Nb [3, 5–9]. Wasserbäch measured the thermal conductivity of Nb after uniaxial straining of up to 22.2% [3]. An example of these data for a single specimen that has undergone increasing levels of deformation is replotted in Fig. 1, where the thermal conductivity k for temperatures colder than 3 K decreases with increasing deformation. Of particular note is the local maximum in k (*i.e.*, the phonon peak in conductivity k_{pp}) at approximately 2 K that diminishes with increasing deformation. Wasserbäch examined the effect of deformation on conduction [9] by using a relaxation time approximation [10, 11]. Phonon-electron scattering, which is a significant factor at the working temperatures of SRF cavities (about 2 K), was not included in the analysis. Chandrasekaran [8] measured the effect of deformation on k and quantified the role of subsequent heat treatment on the recovery of the local maximum phonon peak and the decrease in dislocation density. A phonon peak that has disappeared after deformation can be partially recovered with heat treatment of appropriate temperature and duration [12]. In the analysis of effect of deformation on conductivity, only k_{pp} was used to estimate the dislocation density. Koechlin and Bonin [13] used a simplified equation based on the Bardeen-Rickayzen-Tewordt (BRT) model [14] to fit the experimental data. This equation was reparameterized by Chandrasekaran [15] for analysis and

ISBN: 978-3-95450-191-5 doi:10.18429/JACoW-SRF2017-THPB066

INTRODUCING THE VERTICAL HIGH-TEMPERATURE UHV FURNACE OF THE S-DALINAC FOR FUTURE CAVITY MATERIAL STUDIES*

R. Grewe†, L. Alff, M. Arnold, J. Conrad, S. Flege, M. Major, N. Pietralla,
Technische Universität Darmstadt, Darmstadt, Germany
F. Hug, Johannes Gutenberg-Universität Mainz, Mainz, Germany

Abstract

Since 2005 the Institute for Nuclear Physics in Darmstadt operates a high temperature UHV furnace for temperatures of up to 1750°C. It has been used several times for hydrogen bake-out of the SRF cavities of the S-DALINAC with proven success. In 2013, studies at FNAL have shown that cavities treated with nitrogen reached an up to four times higher q-factor. The cavities are exposed to N_2 at 850°C at the end of the H_2 bake-out. A thin layer of normal conducting (nc) hexagonal niobium nitride (NbN) forms at the surface which is removed by electropolishing while the higher quality factors are attributed to the N_2 diffusion into the bulk Nb. At temperatures from 1300°C to 1700°C a thin layer of the superconducting (sc) cubic phase of NbN can be observed, e.g. δ-phase NbN, which has a higher critical field and higher critical temperature and thus is very intereresting for applications for SRF cavities. The UHV furnace has been prepared for future treatments of Nb samples and cavities in an N_2 atmosphere at high temperatures for research on cubic NbN. The material properties of the samples will be analyzed at the ATFT group at the Department for Materials Science of TU Darmstadt.

INTRODUCTION

Research on doping of niobium cavities with nitrogen at temperatures of 850°C results in an up to four times higher quality factor compared to untreated cavities [1]. At even higher temperatures in the range between 1300°C and 1700°C the δ-phase of NbN forms [2], as shown in the phase diagram in Fig. 1. The δ-phase is highly interesting for superconducting accelerator technology applications. Due to different nitrogen concentrations along the depth of the niobium, different phases of NbN form. In Fig. 2 the microstructure of NbN along the depth profile is shown.

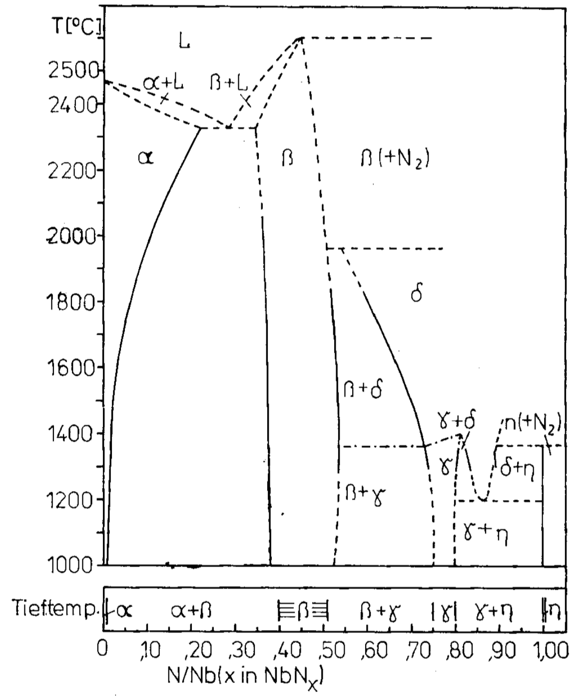

Figure 1: Phase diagram of NbN. The δ-phase of NbN forms at temperatures between 1300°C and 1700°C [3].

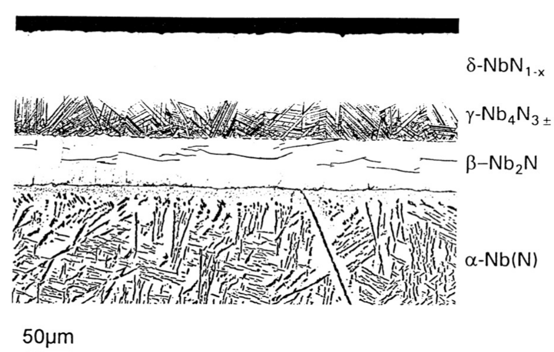

Figure 2: Cross section of the microstructure of NbN. The sc δ-phase forms at the highest nitrogen concentration at the top, followed by the nc β-phase and the sc α-phase at the bottom. During cooldown the δ-phase transforms into the sc γ-phase [4].

UHV-FURNACE

The UHV-furnace at the S-DALINAC [5] was built at the University of Wuppertal in 1983 [6] and moved to Technische Universität Darmstadt in 2002. It was designed to reach temperatures of up to 1800°C with vacuum pressures lower then 10^{-4} mbar. Since 2005 it has been used for hydrogen bakeout of several superconducting niobium cavities at 850°C with proven success [7]. Due to technical constraints at TU Darmstadt the temperature was limited to 850°C. Beginning in 2015 the furnace has been upgraded and recommissioned to operate at temperatures of up to 1800°C again [8]. The cross-section in Fig. 3 illustrates the main parts of the furnace [9]. The inner part of the UHV-furnace is a hot-pot made of niobium. The niobium samples

* Work supported by the Federal Ministry of Education and Research through grant No. 05H15RDRBA.
† rgrewe@ikp.tu-darmstadt.de

Content from this work may be used under the terms of the CC BY 3.0 licence (© 2017). Any distribution of this work must maintain attribution to the author(s), title of the work, publisher, and DOI.

ISBN: 978-3-95450-191-5 doi:10.18429/JACoW-SRF2017-THPB069

Content from this work may be used under the terms of the CC BY 3.0 licence (© 2017). Any distribution of this work must maintain attribution to the author(s), title of the work, publisher, and DOI.

SURFACE STUDIES OF Nb_3Sn COATED SAMPLES PREPARED UNDER DIFFERENT COATING CONDITIONS*

Uttar Pudasaini[1], G. Eremeev[2], Charles E. Reece[2], J. Tuggle[3], and M. J. Kelley[1,2,3]
[1]Applied Science Department, The College of William and Mary, Williamsburg, VA 23185, USA
[2]Thomas Jefferson National Accelerator Facility, Newport News, VA 23606, USA
[3]Virginia Polytechnic Institute and State University, Blacksburg, VA 24061, USA

Abstract

The promise of better performance and significant cost reduction make Nb_3Sn-coated Nb SRF cavities an attractive option when compared to traditional Nb SRF cavities. Historically, the vapor diffusion technique for coating Nb cavities with Nb_3Sn has proven to be the most successful, and is currently practiced in several research facilities with minor variations. Using modern characterization tools, we examined the Nb_3Sn coating prepared in different systems and/or under different conditions. Identically prepared high RRR (~ 300) Nb samples were coated using existing standard protocols at different coating facilities. The microstructure and composition of Nb_3Sn coatings were found to be similar when examined with scanning electron microscopy (SEM) and energy dispersive X-ray spectroscopy (EDS). Atomic force microscopy (AFM) was performed on each sample and the topographies of the samples were then compared in terms of power spectral densities (PSDs). Secondary ion mass spectrometry (SIMS) depth profiles revealed trace amounts of Ti in some of the samples.

INTRODUCTION

Presently, Nb_3Sn is the front running candidate for replacing Nb in SRF accelerator cavities and as such, it has become an active topic of research and development efforts [1-4]. The goal of these efforts is to more fully understand both the limitations of Nb_3Sn and methods by which to optimize its SRF cavity performance enhancing capabilities. Since the application of this material is limited to the form of a coating, SRF cavities should be prepared by depositing Nb_3Sn of 2-3 micron thickness inside of accelerating structures. The tin vapor diffusion technique has been the leading technique for fabricating Nb_3Sn-coated Nb cavities since the 1970's [5-7]. The typical coating procedure involves vaporizing both tin and tin chloride inside an ultra-high vacuum (UHV) furnace, where they interact with a Nb substrate to form the Nb_3Sn coating. The temperature profile inside the furnace often includes two plateaus. The first plateau at about 500 °C is known as the nucleation step, where tin chloride is evaporated and creates early tin deposition sites. During the second plateau at about 1200 °C, or the deposition step, tin is transported to the substrate where Nb_3Sn is subsequently formed. The exact mechanism for the Nb_3Sn formation is not well understood. The importance of understanding the effects of varying coating parameters (such as nucleation time and temperature, deposition time and temperature, and the amounts of tin and tin chloride vaporized) is paramount for controlling and optimizing the final coating structure. Several experiments were performed in order to investigate the effects of varying coating process parameters on the kinetics and growth of the Nb_3Sn coating. In this contribution, an analysis of coatings produced using a number of different coating process parameter combinations are reported.

*Partially authored by Jefferson Science Associates under contract no. DEAC0506OR23177. Work at College of William & Mary supported by Office of High Energy Physics under grant SC0014475. This material is based upon work supported by the U.S. Department of Energy, Office of Science, Office of Nuclear Physics.

VARIATION OF NUCLEATION PROFILE

The current Nb_3Sn coating protocol in practice at different research facilities includes a nucleation step at a low temperature plateau of 500 °C for 1 - 5 hours. The purpose of this step is to generate tin enriched Nb-Sn nucleation sites on the Nb substrate through evaporation and decomposition of tin chloride. Nucleation step was evolved to prevent non-uniform and incomplete layers of Nb_3Sn from early coating experiments [5]. Recent surface studies following nucleation steps with different process parameter combinations show that, in general, both a tin film and a distribution of tin particles cover the Nb substrate surface [8]. However, variation in duration and temperature of the nucleation step, as well as the amount of tin chloride utilized, produced differences in the surfaces. A systematic set of coating experiments was performed in order to determine the effect of varying nucleation parameters on the final Nb_3Sn coatings. In each case, the nucleation step was followed by a three-hour deposition step at 1200 °C with 1 g (~ 2 - 3 mg/cm^2) of tin and an equal amount of tin chloride. The chemical composition and microstructure of the final Nb_3Sn coatings were examined using SEM/EDS. Figure 1 shows that no significant differences in the final coatings were observed for three distinct nucleation temperature-duration profiles. This suggests that the properties of the final Nb_3Sn coating are instead dominated by the higher temperature, tin-rich deposition step.

A set of nanopolished Nb samples were pre-nucleated (300 - 500 °C for 1 to 5 hours) using typical amounts of tin and tin chloride. Subsequent to atmospheric exposure, the samples were subjected to the standard coating procedure. SEM/EDS examination showed that coatings do not depend significantly on pre-nucleation history. The chemical composition of the coating for each sample demonstrated usual ~24 atomic % of Sn. A comparison of

ISBN: 978-3-95450-191-5 doi:10.18429/JACoW-SRF2017-THPB070

Content from this work may be used under the terms of the CC BY 3.0 licence (© 2017). Any distribution of this work must maintain attribution to the author(s), title of the work, publisher, and DOI.

ELECTROCHEMICAL FINISHING TREATMENT OF Nb_3Sn DIFFUSION-COATED NIOBIUM*

Uttar Pudasaini[1], G. Eremeev[2], Charles E. Reece[2], H. Tian[2], and M. J. Kelley[1,2]
[1]Applied Science Department, The College of William and Mary, Williamsburg, VA 23185, USA
[2]Thomas Jefferson National Accelerator Facility, Newport News, VA 23606, USA

Abstract

Nb_3Sn cavities are now routinely prepared by depositing few micron thick Nb_3Sn coatings on Nb cavities using tin vapor diffusion process. For the case of niobium there is a significant improvement after electropolishing (EP), but electrochemical finishing treatment on Nb_3Sn coatings has not been studied. Controlled removal of the first few layers could lead to a smoother and cleaner surface that is conducive to better RF performance. Several samples, which were coated with Nb_3Sn by vapor diffusion process in a JLab sample chamber, were used to explore polishing parameters, such as I-V characteristics, removal rate, topography, etc. Preliminary results from the first runs are discussed here.

INTRODUCTION

After decades of R&D efforts, the performance of SRF cavities made from niobium is approaching the fundamental limits set by the material. Nb_3Sn is a promising superconducting material (Tc ~ 18K and H_{sh} ~ 410 mT) and has the potential to substitute niobium in SRF cavities for better performance and cost reduction [1]. It is a brittle material with thermal conductivity three orders of magnitude lower than niobium, which precludes its application as a bulk material to fabricate cavities. Nb_3Sn cavities are commonly fabricated by depositing a Nb_3Sn coating inside the Nb cavities using tin vapor diffusion technique [2-4]. Such cavities are able to achieve an accelerating gradient as high as 16 MV/m with quality factor 10^{10} at 4.2 K [4]. Degradation of RF performance beyond a certain gradient is not well understood yet. It is suspected that the roughness of an as-coated surface may play some role in such degradation. Note that Nb_3Sn develops a characteristic topography independent of substrate preparation method [5]. A typical example of such a surface is shown in Figure 1. It is thought that controlled removal of the top few layers of material could lead to better RF performance due to a smoother and cleaner surface. Material removal techniques commonly used for niobium pose several challenges for Nb_3Sn, primarily because the material available to process for the latter is only a few microns thick. Also, the response of an intermetallic compound may be dissimilar to that of a pure metal. Different material removal techniques applied for niobium were surveyed for Nb_3Sn [6-7]. It was found that buffered chemical polishing (BCP) is very reactive and etches the surface non-uniformly within only a few seconds. Oxypolishing and electrochemical treatments, however, did show some potential to apply to a Nb_3Sn-coated surface.

Since electropolishing significantly enhances cavity performance for the case of niobium, electrochemical treatment of Nb_3Sn was explored. In this contribution, preliminary results are presented from recent first experiments.

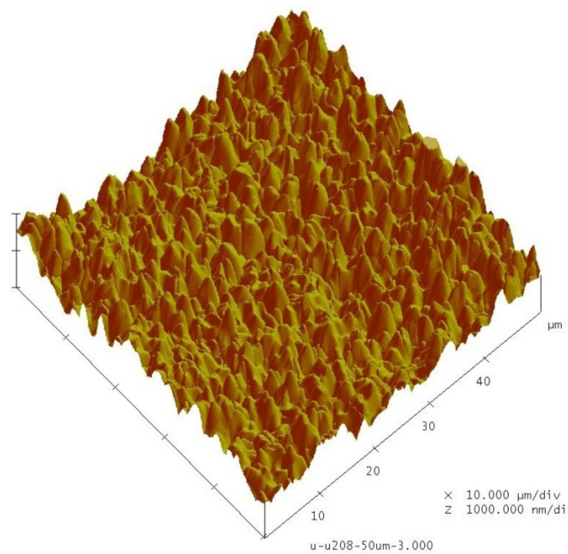

Figure 1: Typical topography of a Nb_3Sn coating on a niobium substrate.

EXPERIMENTAL

Nb_3Sn Sample Preparation

A standard set of 10 cm x 10 cm coupons and cylindrical samples with surface area 1.96 cm^2 were produced from high RRR sheet material of the type used for cavity fabrication. Each sample received ~100 microns BCP removal using a solution of 49% HF, 70% HNO_3 and 85% H_3PO_4 in the ratio of 1:1:1 by volume. These samples were then coated with the Nb_3Sn coating procedure at Jefferson Lab. A detailed description of the coating procedure is available in [5]. The temperature profile and amount of tin supplied was slightly changed to make the Nb_3Sn coating thicker. The temperature profile included a six-hour deposition step at 1200 ˚C instead of the usual three hours, and the initial amount of tin loading was increased from 3 mg/cm^2 to 4 mg/cm^2. A few nanopolished samples with the usual Nb_3Sn coating were also used in some experiments.

*Partially authored by Jefferson Science Associates under contract no. DEAC0506OR23177. Work at College of William & Mary supported by Office of High Energy Physics under grant SC0014475. This material is based upon work supported by the U.S. Department of Energy, Office of Science, Office of Nuclear Physics.

ISBN: 978-3-95450-191-5 doi:10.18429/JACoW-SRF2017-THPB075

Content from this work may be used under the terms of the CC BY 3.0 licence (© 2017). Any distribution of this work must maintain attribution to the author(s), title of the work, publisher, and DOI.

GaN-BASED PHOTOCATHODES FOR HIGH BRIGHTNESS ELECTRON BEAMS

M. Schumacher#, M. Vogel, X. Jiang, University of Siegen, Germany

Abtract

Prospective light sources require photocathodes with high quantum efficiency (QE), long lifetime and minimized thermal emittance. One promising candidate meeting the aforementioned specifications is gallium nitride (GaN). Due to its wide band gap ($E_g = 3{,}4$ eV), GaN can be excited by UV-light sources. Its thermal and chemical stability are added bonuses [1-3]. In the framework of the present activity, the synthesis of GaN films on copper, niobium, tantalum, molybdenum and silicon (Si) by means of RF magnetron sputtering is proposed. In this context, gallium (Ga), gallium arsenic (GaAs) and GaN are suitable source material candidates, which are sputtered in a Nitrogen (N) and Argon (Ar) plasma discharge. The conductivity as well as the band gap (E_g) of the corresponding films can be modified by dopants like magnesium (Mg) and indium (In), respectively [1, 3]. Standard materials science characterization techniques such as SEM, EDX, XRD or XPS are used to explore the growth mechanism of GaN alongside with a morphological and chemical examination. To assess and optimize the performance of the photocathode the abovementioned requirements are tested in an in-situ setup. Hence, the coating chamber is connected with a contamination chamber for the QE measurement to transfer the synthesized GaN films under UHV conditions. Following, a project outline, first experimental results of GaN films, synthesized based on a GaAs source sputtered in a pure N_2 plasma discharge are presented.

INTRODUCTION

Superconducting radiofrequency photoinjectors (SRF gun), which are for instance operated at Helmholtz-Zentrum Dresden-Rossendorf (HZDR) and Helmholtz-Zentrum Berlin (HZB), require photocathodes providing high brightness electron beams. In addition, a high current and operating in a continuous wave mode are required. Hence, photocathodes with high QE, long life time, minimized thermal emittance as well as reduced dark current are necessary. One promising candidate meeting the aforementioned specifications is GaN [1-3]. Due to its wide band gap ($E_g = 3{,}4$ eV), GaN can be excited by UV-light sources, which are used e.g. at HZDR.

The thermal and chemical stability of GaN are added bonuses. In the framework of the present activity, GaN films are synthesized and subsequently modified. As shown in the schematic band diagram in Figure 1, for undoped and non-modified GaN, there is a high potential barrier. Accordingly, the vacuum energy level (E_{vac}) is higher than the conduction band energy level (E_c) whereby excited electrons can not leave the surface of the film [2].

marc.schumacher@uni-siegen.de

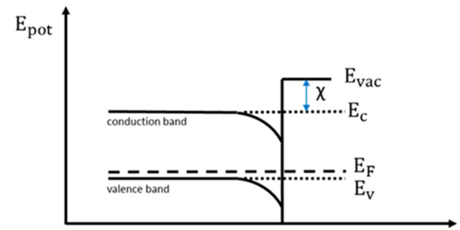

Figure 1: Schematic band diagram of non-modified GaN [2].

By p-type doping with Mg, the diffusion length of the excited electrons within the bulk material can be increased. Hence, generated holes are drifting to energetically favourable surface locations and the emerging electric field causes a bending of the band gap. However, after p-type doping, E_{vac} is still higher than the E_c. Hence, another preparation step is required.

To achieve a negative electron affinity (NEA), the film surface can be activated by a Cs deposition [1-3].

$$NEA = E_{vac} - E_c < 0 \tag{1}$$

Accordingly, electrons of the adsorpt Cs-atoms diffuse to unsaturated surface atoms, where an electric dipole occurs. The excited electrons can tunnel through a small potential barrier and leave the film surface (Figure 2) [1, 2].

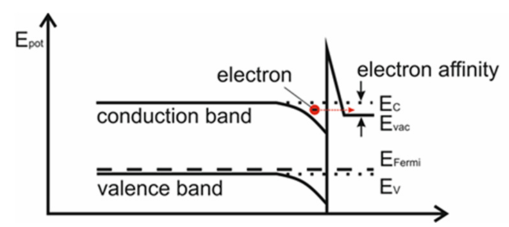

Figure 2: Schematic band diagram of GaN after Cesium deposition [1, 2].

After the preparation, the films will be characterized in situ, to correlate their QE with the preparation parameters. QE is defined as the ratio of incident photon to emitted electron, described by the photoelectric effect (Figure 3). For the emission of an electron, the GaN film is excited by a light source, where the energy of the absorbed photons needs to be higher than E_g.

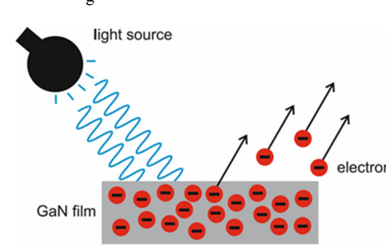

Figure 3: The main principle of the photoelectric effect.

ISBN: 978-3-95450-191-5 doi:10.18429/JACoW-SRF2017-THPB076

CARBON-BASED COATINGS FOR ELECTRON CLOUD MITIGATION IN SRF PHOTOCATHODES

M. Vogel†, C. Schlemper, X. Jiang, Institute of Materials Engineering, University Siegen, Siegen, Germany

Abstract

Multipacting is a common issue in the context of cathode units of superconducting radiofrequency photoinjectors (SRF-guns) utilized in linear accelerators under resonant conditions. During the past three years, we developed a coating along with a corresponding in-situ characterization process in order to realize SRF-gun surfaces featuring low secondary electron yield (SEY). Important aspects that have been accounted for are the homogeneity and adhesion of the coatings deposited on the cylindrical SRF-gun mantle. Furthermore, the correlation between SEY and crystallinity, morphology, and contamination was studied in detail. The SEY maximum can be tuned between 1.5 and less than 0.7 depending on the deposition conditions. In this work, we recap the results and present a general strategy for the effective mitigation of electron cloud multiplication.

INTRODUCTION

The unwanted resonant electron multiplication in high-frequency structures is called multipacting (MP). This phenomenon arises at the cathode module of superconducting photoinjectors for linear accelerators and prevent its operation [1]. Principally, there are four strategies for MP mitigation on a srf-gun:

1. DC-biasing of the coaxial cathode system [2],
2. structuring the cathode surface on a micrometer-scale [3],
3. geometrical optimization of the system [4],
4. coating the cathode by a low secondary electron emission yield material.

This work focusses on the fourth strategy of coating the srf-gun mantle with a low SEY carbon coating. Carbon has been shown to have a SEY below 1 [5, 6]. The latter is the requirement for effectively suppressing the electron multiplication. Compared to other methods, a coating system is cost effective, applicable to 3D structures and clean in terms of vacuum compatibility.

One of the main concerns in an accelerator is the pollution of the system by particles. A coating must provide a good adhesion to its substrate material in order to make sure that no delamination happens. An area-wide or even a partly delamination of the coating would be disastrous. Therefore, increasing the adhesion of the coating is one of the main topics of this research.

In this study, the prototype was based on the design of the FELBE srf-gun used at HZDR. This design uses two different metals, namely the cathode body and the cathode plug. The former is made of copper, the latter is made of molybdenum sitting on the very tip of the cathode body [7]. In conjunction with aforementioned adhesion requirements the two substrate materials Cu and Mo making things even more challenging. Both materials do not react chemically with carbon thus do not form any chemical bonds. Hence, the adhesion of carbon on both metals will be poor. Still, to go for a good adhesion a titanium interlayer was implemented. On the one hand, Ti easily forms metallic bonding with Cu and Mo. On the other hand, Ti chemically reacts with carbon forming chemical bonds (TiC). This increase the adhesion dramatically and makes the top coating somewhat independent from the actual substrate material. The following results are based on this interlayer concept.

In this contribution, we show the dependencies of deposition parameters on microstructure and the resulting SEY.

EXPERIMENTAL

Carbon coatings were prepared on coin-shaped Cu and Mo samples with a diameter of 25 mm and on cylindrical srf-gun dummy-samples having a diameter of 10 mm and length of 100 mm. The latter have been prepared to mimic the FELBE srf-gun at HZDR. To coat the mantle of the cylinder-shaped samples a new substrate holder was engineered. With this, it is possible to coat a fully assembled FELBE-style srf-gun homogenously (Fig. 1).

Figure 1: Coated srf-gun dummy sitting in its specially designed coating sample holder system.

Before deposition, samples have been cleaned in ethanol ultrasonically and rinsed in distilled water. Additionally, various surface pre-treatments like polishing, sandblasting, wet chemical etching and plasma etching have been investigated in order to get different roughness, a good cleanliness and contamination free substrate surface.

† email address: michael.vogel@uni-siegen.de

Content from this work may be used under the terms of the CC BY 3.0 licence (© 2017). Any distribution of this work must maintain attribution to the author(s), title of the work, publisher, and DOI.

ISBN: 978-3-95450-191-5 doi:10.18429/JACoW-SRF2017-THPB077

Content from this work may be used under the terms of the CC BY 3.0 licence (© 2017). Any distribution of this work must maintain attribution to the author(s), title of the work, publisher, and DOI.

DESIGN STUDY OF MUSHROOM SHAPED CAVITY FOR EVALUATION OF RF CRITICAL MAGNETIC FIELD OF THIN-FILM SUPERCONDUCTOR

H. Oikawa, Utsunomiya University, Utsunomiya, Tochigi 321-8585, Japan
T. Higashiguchi, Center for Optical Research and Education, Utsunomiya University, Utsunomiya, Tochigi 321-8585, Japan
H. Hayano, KEK, Tsukuba, Ibaraki 305-0801, Japan

Abstract

For future accelerator, superconducting RF cavity has high gradient of 45 MV/m or more is demanded. To obtain such a higher gradient, there has been proposed a method of increasing an RF critical magnetic field of the cavity inner surface by coating of multi-layer thin-film superconductor. Their thickness is close to the London penetration depth. By producing a multilayer film structure in cavity inner surface, it is believed to improve the RF critical magnetic field, and to connect directly to high gradient. To demonstrate a creation of a thin film on a surface of Nb samples, an RF cavity with a thin film coated Nb sample is needed to measure the RF critical field of the sample. To adapt it to the cavity, to cool to cryogenic temperature and to establish the sample to supply the RF power, it is necessary to design a cavity to produce a strong RF magnetic field parallel to the surface of the thin film sample. We designed a mushroom shaped cavity made of Nb and input coupler. Resonant frequency is 5.2 GHz by calculation. We calculated the resonant frequency and the field distribution, compared with the measured values for the model cavity.

MULTI-LAYER THIN-FILM SUPECONDUCTOR

A superconducting thin film for a high electric field of an accelerator cavity application was proposed by Gurevitch 2006 [1]. The study of multilayer thin-film superconductor is being on a way in many institutes [2]. In order to achieve high acceleration gradients for the superconducting cavity of the second stage ILC accelerator, we started the study to evaluate a critical magnetic field of superconducting thin-films such as Nb_3Sn and NbN and MgB_2 deposited on the Nb samples. We chose an atomic layer deposition (ALD) method of film formation, which has an advantage of uniform and nm controllability for thickness on a complex inner-surface structure of cavity. In order to develop application method of ALD on Nb surface, we need to measure lower critical field at a frequency of several kHz using a small coil, a superheating critical magnetic field of RF frequency using RF cavity respectively, as well as RRR for thin-film on a sample. There is theoretical study to evaluate a thickness of each layer for the best performance of multi-layer thin film superconductor. We have shown that there is an optimum thickness of formed thin layer to get maximum superheating critical magnetic field [3]. Those are the target structure in this study.

DESIGN AND MANUFACTURE OF THE ALUMINUM MUSHROOM-SHAPED CAVITY

Calculation of Electromagnetic Field in the Cavity

A mushroom-shaped cavity has a shape of half hemisphere with flat bottom plate. It has an advantage to make strong magnetic field closing well inside of the cavity and facing to the sample surface of the bottom plate, on the other hand, a magnetic field on the hemisphere surface can be reduced compare to the bottom surface.

The previously designed mushroom-shaped cavity has high field sensitivity with dimension change of protrusion inward. In addition, it has also high sensitivity to the axisymmetric disturbance of the electromagnetic field by the insertion of the antenna, and the internal electromagnetic field is easily disturbed by the antenna. Furthermore, the resonance frequency of the target mode was close to the resonance frequency of the adjacent modes, so the mode separation was not enough. Since it was found that mode separation tends to improve by increasing the order of the mode, we newly changed the resonance frequency from 3.9 GHz to 5.2 GHz of the next higher order. Furthermore, by adopting an antenna shape which does not disturb the axisymmetry, more stable electromagnetic field design can be performed.

Resonant frequency corresponds to a fourth-order harmonics of 1.3 GHz which is the resonant frequency of the superconducting accelerating cavity of ILC. The shape of the cavity was based on the mushroom-shaped cavity of the SLAC study [4]. The stored RF power is limited by thermal superconductivity destruction of Nb of the cavity. We have designed a cavity so that the magnetic field of the sample surface to the magnetic field of the inner hemisphere wall holds a value twice or more. The electric field in the cavity inner wall has been designed to have minimum, in order not to generate field emission. A cylinder shape port at the top of the mushroom-shaped cavity is a coupled RF amplifier to put RF power into the cavity. The port is also used for a vacuum pumping port installation. CST MW STUDIO was used to design the cavity. By starting from the shape of SLAC cavity, model dimensions were optimized to have 5.2 GHz with similar elec-

ISBN: 978-3-95450-191-5 doi:10.18429/JACoW-SRF2017-THPB078

FABRICATION OF LARGE-AREA MgB_2 FILMS ON COPPER SUBSTRATES*

Xin Guo, Zhimao Ni, Kexin Liu†, School of Physics and State Key Laboratory of Nuclear Physics and Technology, Peking University, Beijing, China
Can Yang, Qingrong Feng, School of Physics and State Key Laboratory for Artificial Microstructure and Mesoscopic Physics, Applied Superconductivity Research Center, Peking University, Beijing, China

Abstract

Magnesium diboride (MgB_2) is a promising candidate material for SRF cavities because of its higher transition temperature and critical field compared with niobium. To meet the demand of RF test devices, the fabrication of large-area MgB_2 films on metal substrates is needed. In this work, MgB_2 films with 50-mm diameter were fabricated on Cu substrates by using an improved HPCVD setup at Peking University. The transition temperatures of MgB_2 film on Cu substrate and with Mo buffer layer on Cu substrate are 36.2 K and 36.5 K, respectively. The fabrication processes, surface morphology, superconducting properties of these large-area MgB_2 films are presented.

INTRODUCTION

Bulk niobium superconducting radio frequency (SRF) cavities for particle accelerators have been in operation for more than 50 years, and the RF performance is approaching the theoretical limit. To further improve the RF performance, it is important to investigate alternative materials with higher superheating critical fields to satisfy the demands for higher accelerating gradients and lower operating cost. MgB_2 has shown potential as an alternative material for the application of SRF cavities [1, 2]. With a higher transition temperature (39 K), a larger energy gap, a higher critical field, it is expected to have a high quality factor (Q_0) and high accelerating gradient (E_{acc}) for MgB_2 coated cavities.

Considering mechanical and thermal stability of cavities, it is necessary to fabricate MgB_2 films on metal substrates. Characterization of the RF properties of these MgB_2 films is an important step to evaluate the feasibility of MgB_2 coated SRF cavity. Hence, large-area MgB_2 films are needed to meet the demand of RF test devices, in which the MgB_2 coating is a part of the test cavity. In our previous work, we reported the results of large-area MgB_2 films on niobium substrates. T_c values measured at different positions on the film range from 38.4 to 40.6 K, showing good uniformity. In RF tests, the film exhibits a low R_s of about 120 μΩ at 4 K and 11.4 GHz, close to that of bulk Nb [3].

Cu is an ideal thin film cavity body material because of its good thermal conductivity and machinability. However, the reaction between Cu and Mg make it challenging to fabricate MgB_2 film on Cu substrate. It has been reported previously that lower reaction temperature can help to fabricate MgB_2 thin films on Cu substrates [4-6]. Sputtering Mo on Cu substrate may further suppress the Mg-Cu reaction. In this work, we fabricated 50-mm diameter MgB_2 films on copper substrates using a modified hybrid physical-chemical vapor deposition (HPCVD) setup. The fabrication process, superconducting properties of the large-area MgB_2 films on Cu substrate as well as Cu substrate with Mo buffer layer are investigated.

* Work supported by National Natural Science Foundation of China (Grant No. 11575012) and National Key Programme for S&T Research and Development (Grant No. 2016YFA0400400).
† email address: kxliu@pku.edu.cn

LARGE-AREA MgB_2 FILMS ON COPPER SUBSTRATES

Film Preparation

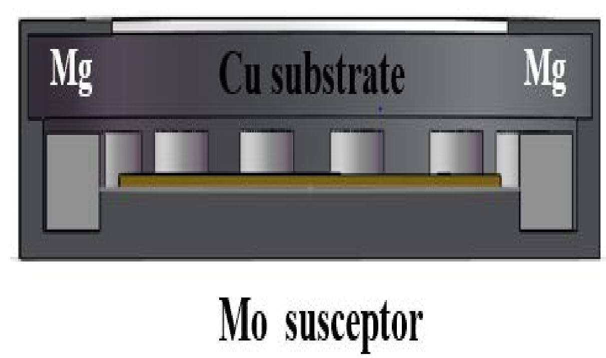

Figure 1: The profile of the improved susceptor for MgB_2 film fabrication on Cu substrate.

The modified HPCVD setup for 50-mm diameter MgB_2 films fabrication on Nb substrates has been described in detail in our previous work [3]. In particular, adding a wall about 9 mm in height surrounding the molybdenum susceptor to achieve uniform Mg vapor distribution over the substrate. To improve the quality of MgB_2 film on copper substrate, the reaction temperature is lower. Then the structure of the susceptor need to be modified further to help Mg vapour move towards the centre of the substrate. On the basis of the susceptor for deposition MgB_2 on niobium substrate, one more wall was added on the top of Mg ignots. Other changes, the height of Mg ignots and Cu substrate, contribute to forming a lower temperature at the centre of the substrate. These changes help Mg distribution on the top of the Cu substrate more uniform. The profile of the improved susceptor for MgB_2 film fabrication on Cu substrate is shown in Figure 1.

Content from this work may be used under the terms of the CC BY 3.0 licence (© 2017). Any distribution of this work must maintain attribution to the author(s), title of the work, publisher, and DOI.

18th International Conference on RF Superconductivity SRF2017, Lanzhou, China JACoW Publishing
ISBN: 978-3-95450-191-5 doi:10.18429/JACoW-SRF2017-THPB079

Content from this work may be used under the terms of the CC BY 3.0 licence (© 2017). Any distribution of this work must maintain attribution to the author(s), title of the work, publisher, and DOI.

SIMULATIONS OF RF FIELD-INDUCED THERMAL FEEDBACK IN NIOBIUM AND Nb_3Sn CAVITIES*

Jixun Ding†, Daniel Leslie Hall, Matthias Liepe
Cornell Laboratory for Accelerator-Based Sciences and Education (CLASSE),
Ithaca, NY 14853, USA

Abstract

Thermal feedback is a known limitation for SRF cavities made of low-purity niobium, as the increased losses at higher temperature described by BCS theory create a feedback mechanism that can eventually result in a runaway effect and associated cavity quench. In a similar manner, niobium cavities coated with Nb_3Sn may also be subject to increased losses from thermal feedback, as Nb_3Sn is possessed of a much lower thermal conductivity than niobium, although this effect will be mitigated by the thin film nature of the coating. In order to better understand the degree to which thermal feedback plays a role in the performance of Nb_3Sn cavities, it is necessary to understand how the various components of the problem play a role in the outcome. In this paper, we present the first results from simulations performed at Cornell University that model RF induced thermal feedback in both conventional niobium cavities and niobium cavities coated with a thin film of Nb_3Sn. The impacts of layer thickness, niobium substrate thermal conductivity, and trapped flux on the performance of the cavity are discussed.

INTRODUCTION

The effect of RF heating on niobium cavity performance has been studied via the thermal feedback model (TFBM) [1–5] . Heat produced by RF fields at cavity inner surfaces must be transported across a typically 3mm thick layer of niobium and a niobium-Helium interface into liquid Helium. Both niobium and the Nb-He interface have finite thermal conductance, so RF heat production increases the inner surface temperature of a cavity, which in turn increases BCS resistance and heat dissipation, creating a positive feedback loop. At low to moderate fields, the feedback effect is small enough that the temperature inside the cavity reaches a stationary state. The stationary inner surface temperature (and hence surface resistance) can be written as a function of accelerating field strength, which may contribute to the so called "mid-field Q-slope" [5, 6]. Under certain conditions, the feedback mechanism is strong enough that there exists a "thermal breakdown field" H_b, above which no stationary temperature can be sustained [1, 3]. This can manifest as "high field Q-drop" [3] followed by a cavity quench, and is considered the thermal stability limit of a SRF cavity. No work has yet been done to probe the thermal stability limit of niobium cavities coated with Nb_3Sn. To this end, thermal simulations were developed at Cornell University to extend the well established TFBM to apply to Nb_3Sn coated cavities.

* This work was primarily supported by U.S. DOE award DE-SC0008431. This work was supported in part by the U.S. National Science Foundation under Award PHY-1549132, the Center for Bright Beams.
† jd664@cornell.edu

SIMULATION METHOD

Bulk Niobium

Our niobium simulations build upon and improve existing HEAT simulations, previously also developed at Cornell [5,7]. We model the cavity wall locally as an infinite slab of niobium and define x as distance from cavity inner surface. The temperature profile in niobium induced by RF heating is shown schematically in Fig. 1. A temperature gradient forms in the cavity bulk, and a temperature jump forms at the Nb-He interface.

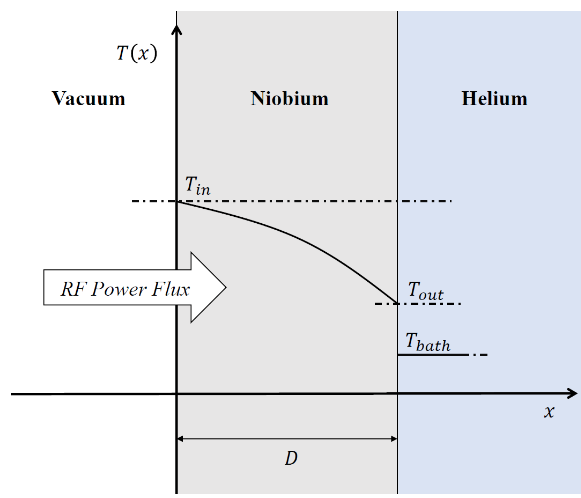

Figure 1: Sketch of steady state temperature profile in niobium.

Using Matlab's Partial Differential Equation Toolbox [8], we look for a stationary solution $T(x)$ of the one dimensional heat equation

$$\frac{d}{dx}\left(\kappa(T)\frac{dT}{dx}\right) = 0$$

with mixed boundary conditions

$$q = \kappa(T_{in})\frac{\partial T}{\partial x} \quad \text{at } x = 0 \qquad (1)$$

$$q = (T_{out} - T_{bath})H_k(T_{out}, T_{bath}) \quad \text{at } x = D \qquad (2)$$

In the above equations, Eq. 1 defines a Neumann boundary condition and Eq. 2 defines a Dirichlet boundary condition

ISBN: 978-3-95450-191-5 doi:10.18429/JACoW-SRF2017-THPB080

MEASUREMENTS OF FREQUENCY, TEMPERATURE, RF FIELD DEPENDENT SURFACE RESISTANCE USING SRF HALF WAVE CAVITY*

H. Park[1] †, S. U. De Silva, J. R. Delayen[1]
Old Dominion University, Norfolk, VA, USA
[1] also at Thomas Jefferson National Accelerator Facility, Newport News, VA, USA

Abstract
A theory of surface resistance of superconductor was rigorously formulated by Bardeen, Cooper, Schrieffer more than 50 years ago. Since then the accelerator community has been used the theory as a guideline to improve the surface resistance of the superconducting cavity. It has been observed that the surface resistance is dependent on frequency, temperature and rf field strength, and surface preparation. To verify these dependences, a well-controlled study is required. Although many different types of cavities have been tested, the typical superconducting cavities are built for specific frequencies of their application. They do not provide data other than at its own frequency. A superconducting half wave cavity [1] is a cavity that enables us to collect the surface resistance data across frequencies of interest for particle accelerators and evaluate preparation techniques. This paper will present the design of the half wave cavity, its electromagnetic mode characteristics and experimental results in order to better understand the contributions of the various physical processes to the surface resistance of superconductors.

INTRODUCTION

So far, the origin of residual resistance is believed to be a result of extrinsic mechanisms such as trapped vortices, metallic suboxide layers at the surface, non-superconducting precipitates (hydrides, etc) [2]. The full theory should include residual resistance. Extracting frequency, temperature, rf field dependence will provide significant insight to a better understanding.

Because of the statistical nature of multiple materials defect, technological contributions to surface resistance and the lack of reproducibility, it is difficult to extract accurate frequency dependence of the surface resistance when different cavities of different frequencies are tested. Coaxial half wave resonator provides the frequencies reasonably separated and the same location where the high surface magnetic field is distributed.

CAVITY DESIGN

For our research purpose a cavity should meet a certain requirements as listed below.

- Cavity should provide a wide range of frequency, preferably frequencies used in accelerators.
- Different modes should be widely separate so the measurement can be easily made.
- Cavity should be able to reach high rf surface field.
- Mechanically compatible with various cavity treatment.

We chose a half wave coaxial cavity. The TEM modes of this cavity can provide the frequencies of interest: 325, 650, 975, 1300 MHz. These TEM modes are sufficiently separated by other TM and TE modes by strategically dimensioning the cavity inner radius (20 mm) and outer diameter (101 mm). The rf properties of each mode are shown in Table 1. Surface field distribution of each mode is shown in Figure 1.

Table 1: RF Properties of Half Wave Coaxial Cavity

Mode	Frequency [MHz]	Geometric factor	R/Q [Ohm]
TEM1	325.4	59	124
TEM2	650.8	119	62
TEM3	976.1	179	41
TEM4	1301.3	239	31

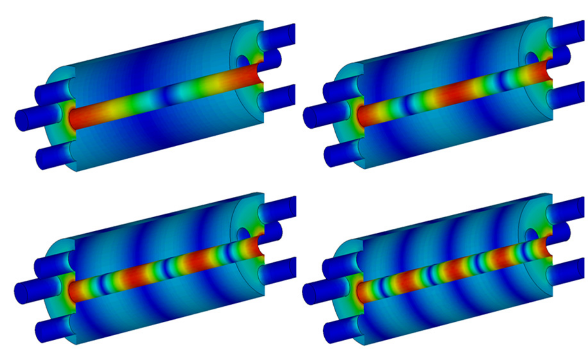

Figure 1: Surface magnetic field distribution from top left to right TEM1, TEM2, and from bottom left to right TEM3 and TEM4.

EXPERIMENTAL METHODS

As a baseline, we prepared the cavity using following typical cavity processing.

- Bulk BCP 150 μm removal.
- Heat treatment at 600 °C for 10 hours.
- Light BCP 10 μm removal.
- High pressure rinse.
- Evacuation and leak check.
- Bake at 120 °C for 24 hours.

*Work supported by NSF Award PHY-1416051
†hkpark@jlab.org

Content from this work may be used under the terms of the CC BY 3.0 licence (© 2017). Any distribution of this work must maintain attribution to the author(s), title of the work, publisher, and DOI.

ISBN: 978-3-95450-191-5 doi:10.18429/JACoW-SRF2017-FRXAA01

PRODUCTION STATUS OF SUPERCONDUCTING CRYOMODULES FOR THE FACILITY FOR RARE ISOTOPE BEAMS (FRIB) PROJECT*

C. Compton†, H. Ao, J. Asciutto, B. Bird, S. Drake, S. Enness, K. Curtain, W. Hartung, J. Holbert, S. Miller, J. Popielarski, L. Popielarski, M. Reaume, K. Saito, M. Shuptar, S. Stark, T. Stine, B. Tousignant, J. VanAken, E. Wellman, K. Witgen, T. Xu, W. Zheng
Facility for Rare Isotope Beams, Michigan State University, East Lansing, MI, 48824, U.S.A.

Abstract

The Facility for Rare Isotope Beams (FRIB) is an SRF accelerator project in full production at Michigan State University (MSU). With the civil construction nearly complete, the installation of accelerator equipment into the tunnel has taken center stage. A total of 46 superconducting cryomodules are needed for the FRIB linac to reach 200 MeV per nucleon. The linac consist of four cavity types (beta = 0.041, 0.085, 0.29, and 0.53) and 6 different cryomodule designs. Cryomodule assembly is done in 5 parallel bays, each one compatible with every cryomodule type. Completed cryomodules undergo full system testing in bunkers before being accepted and delivered to the tunnel. The current status of the cryomodule assembly effort will be presented, including lessons learned and overall experience to date.

INTRODUCTION

The Facility for Rare Isotope Beams (FRIB) at Michigan State University (MSU) is an approved project funded by a cooperative agreement between MSU and The US Department of Energy (DOE) for advancement in the study of rare isotopes. The driver linac for the FRIB project is a 200 MeV/u superconducting linac with final beam power reaching 400 kW [1].

The FRIB linac will require the fabrication of 46 cryomodules housing both superconducting cavities and superconducting solenoids. There are 4 main cryomodule types; utilizing 6 cryomodule designs. There are 4 accelerating cavity designs; beta=0.041 quarter-wave (80.5MHz), beta=0.085 quarter-wave (80.5 MHz), beta=0.29 half-wave (322MHz), and 0.53 half-wave (322MHz). There are also two matching cryomodule designs, one housing beta=0.085 cavities and one housing beta=0.53 cavities, which do not install solenoids. These FRIB all cryomodules are shown in Figure 1.

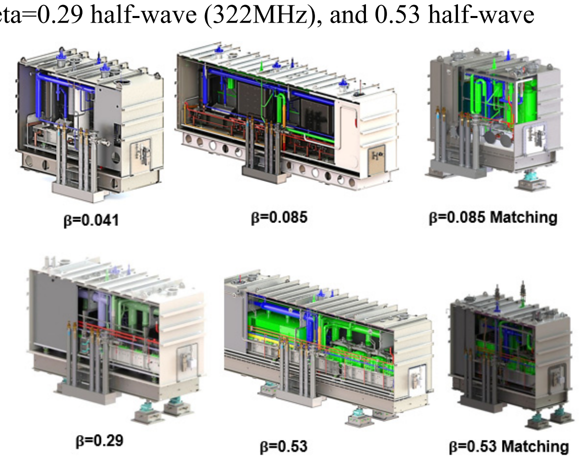

Figure 1: FRIB cryomodule designs.

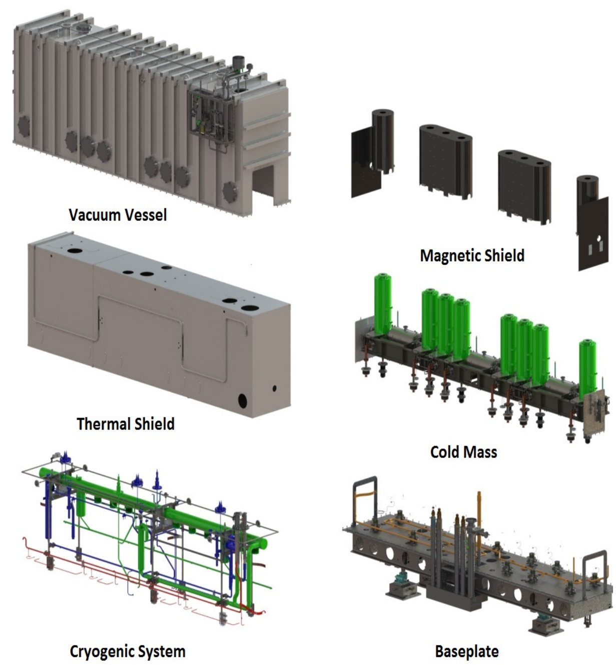

Figure 2: Bottom-up cryomodule design approach.

CRYOMODULE DESIGN AND CRYOMODULE ASSEMBLY

All cryomodule designs use the bottoms-up assembly concept [2]. The major cryomodule components are illustrated in Figure 2. The designs have two cooling lines: cavities at 2 K and solenoid package at 4.5 K. In this building approach, a coldmass which cavities dressed helium jacket and solenoid packages with helium jacket are mounted on multi alignment rails tightly connected into one, is put on a cryomodule base plate. The coldmass is thermally insulated using mounting posts constructed from a glass composite (G-10). G-10 supports of 4 to 6 pieces are used depending on the rail length. One is fixed and

* Work supported by *the U.S. Department of Energy Office of Science under Cooperative Agreement DE-SC0000661*
† compton@frib.mes.edu

Content from this work may be used under the terms of the CC BY 3.0 licence (© 2017). Any distribution of this work must maintain attribution to the author(s), title of the work, publisher, and DOI.

ISBN: 978-3-95450-191-5 doi:10.18429/JACoW-SRF2017-FRXAA02

HIGH-EFFICIENCY, HIGH-CURRENT OPTIMIZED MAIN-LINAC ERL CRYOMODULE*

F. Furuta, N. Banerjee, A. Bartnik, J. Dobbins, R. Eichhorn, M. Ge, G. Hoffstaetter, M. Liepe, P. Quigley, D. Sabol, J. Sears, E. Smith, V. Veshcherevich, CLASSE, Cornell University, USA

Abstract

The Main Linac Cryomodule (MLC) prototype is a key component of the Cornell-BNL ERL Test Accelerator (CBETA) project, which is a 4-turn FFAG ERL currently under construction at Cornell University. This novel cryomodule is the first SRF module ever to be fully optimized simultaneously for high efficient SRF cavity operation and for supporting very high CW beam currents. After a successful initial MLC testing, the MLC has now been moved into its final location for the CBETA ring. For a first beam test of the MLC and CBETA, the Cornell ERL high voltage DC gun and SRF injector cryomodule were connected to MLC via an entry beam line; a beam stop assembly was also installed at the exit line. In this paper, we summarize the performance of this novel ERL cryomodule including results of the first beam test and additional tests focused on RF field stability and cavity microphonics.

INTRODUCTION

The Cornell-BNL ERL Test Accelerator (CBETA) is a collaboration project between BNL and Cornell to investigate eRHIC's non-scaling Fixed Field Alternating Gradient (NS-FFAG) optics and its multi-turn Energy Recovery Linac (ERL) by building a 4-turn, one-cryomodule ERL at Cornell (Fig. 1) [1-3]. CBETA will be built in the L0E area of Wilson Lab at Cornell with many components that have been developed at Cornell under previous R&D programs for a hard x-ray ERL [4].

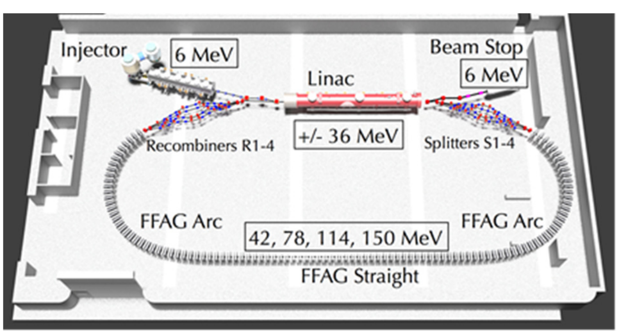

Figure 1: The layout of CBETA project at Cornell.

The main accelerator module, one of the key components for CBETA, will be the Cornell Main Linac Cryomodule (MLC) which will provide 36MeV beam energy gain per pass through the MLC. The MLC was built as a prototype for the Cornell hard x-ray ERL project and designed to operate in CW at 1.3GHz with 2ps bunch length, normalized emittance of 0.3mm-mrad, and 100mA average current in each of the accelerating and decelerating beams [5]. Some other key components, such as the Cornell high voltage DC-gun, Injector Cryomodule (ICM), and Beam stop, shown in Fig. 1, already exist at Cornell, have been commissioned, and are ready for CBETA. In this paper, we report on initial commissioning test results of the MLC, microphonics studies and its compensations, and initial beam acceleration test through the MLC.

MAIN LINAC CRYOMODULE PROTOTYPE

Figure 2 shows an image of the Main Linac Cryomodule prototype in its final location for the CBETA ring. The design of the MLC for the Cornell ERL had been completed in 2012 [4]. One of the unique design goals of the MLC is a combination of a high cavity quality factor Q_0, targeted 2×10^{10} at 16.2MV/m, 1.8K, and a high loaded-Q design of $\sim6\times10^7$, which is equivalent to a narrow half bandwidth of ~10Hz. In order to meet strict beam energy stability requirements, the required amplitude stability and phase stability are 1×10^{-4} in rms and 0.05° in rms, respectively. In addition, as a high current machine, the suppression of high order modes (HOMs) excited by the beam in the SRF cavities in the MLC is also essential.

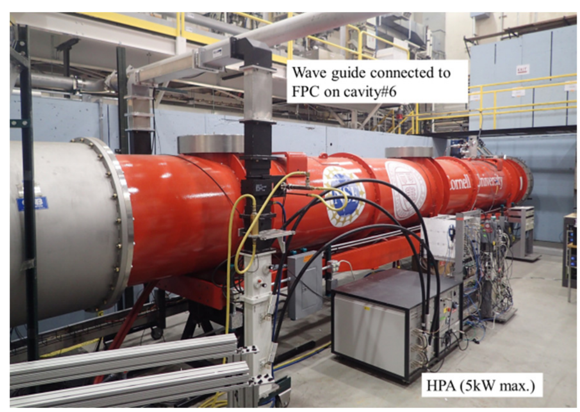

Figure 2: The MLC prototype in its final location.

A general description of the MLC is given in the following. The MLC is 9.8m long and houses six 1.3GHz 7-cell superconducting cavities. Three of them are stiffened cavities, and another three are un-stiffened. Individual HOM beamline absorbers are located between the cavities. Each cavity has a single 10kW coaxial RF input coupler, which transfers power from a solid-state RF power source to the cavity (the designed Q_{ext} of RF input coupler is 6.5×10^7). The fabrication and testing of MLC

* This work was performed with the support of NYSERDA (New York State Energy Research and Development Agency) and of the National Science Foundation (Award No. NSF-DMR 0807731).
#ff97@cornell.edu

Content from this work may be used under the terms of the CC BY 3.0 licence (© 2017). Any distribution of this work must maintain attribution to the author(s), title of the work, publisher, and DOI.

ISBN: 978-3-95450-191-5 doi:10.18429/JACoW-SRF2017-FRXBA01

LLRF COMMISSIONING AT THE EUROPEAN XFEL

M. Omet*, V. Ayvazyan, J. Branlard, L. Butkowski, M. Fenner, M. Grecki, M. Hierholzer, M. Hoffmann, M. Killenberg, D. Kuehn, F. Ludwig, U. Mavric, S. Pfeiffer, H. Pryschelski, K. Przygoda, R. Rybaniec, H. Schlarb, C. Schmidt, B. Szczepanski, H. Weddig, Deutsches Elektronen-Synchrotron, Hamburg, Germany
W. Cichalewski, D. Makowski, F. Makowski, A. Mielczarek
TUL-DMCS, Lodz, Poland
K. Czuba, B. Gasowski, S. Hanasz, P. Jatczak, D. Kolcz, T. Lesniak, D. Sikora
Warsaw University of Technology, Warsaw, Poland

Abstract

The European X–ray Free–Electron Laser (XFEL) at Deutsches Elektronen–Synchrotron (DESY), Hamburg, Germany is a user facility under commissioning, providing ultrashort X–ray flashes with a high brilliance. All LLRF stations of the injector, covering the normal conducting RF gun, A1 (8 1.3 GHz superconducting cavities (SCs)) and AH1 (8 3.9 GHz SCs), were successfully commissioned by the end of 2015. The injector was operated with beam transmission to the injector dump since then. After the conclusion of the construction work in the XFEL accelerator tunnel (XTL), the commissioning of 22 LLRF stations (A2 to A23) started with the beginning of 2017. At every station the LLRF system is organized in a master–slave configuration, controlling 32 1.3 GHz SCs. Stable operation with beam transport to the main dump (TLD) was achieved. The commissioning procedure applied, experience gained and performance reached are described.

INTRODUCTION

The Deutsches Elektronen–Synchrotron (DESY) in Hamburg is currently commissioning the European X–ray Free Electron Laser (E-XFEL) [1]. Once finished, up to 27000 coherent laser pulses per second with a duration of less than 100 fs and a wavelength down to 0.05 nm will be generated. For this, electrons have to be accelerated using a 2 km particle accelerator based on superconducting radio frequency technology. The maximum design energy is 17.5 GeV [1]. Precision regulation of the RF fields inside the accelerating cavities is essential to provide a highly reproducible and stable electron beam. The RF field regulation is done by measuring the stored electromagnetic field inside the cavities. This information is further processed by the feedback controller to modulate the driving RF source. The standard in which the low level radio frequency (LLRF) systems are realized is Micro Telecommunications Computing Architecture (MicroTCA.4) [2]. Figure 1 shows a schematic of European XFEL, focusing on the accelerator sections, cryostrings (CS) and RF stations. Every RF station has its own power source and LLRF system. In the case of the XTL, the LLRF systems have a master–slave configuration [3].

COMMISSIONING OF THE LLRF SYSTEM

The following commissioning denominates the procedure necessary to ready an RF station from a finished precommissioning for beam acceleration. For a detailed description of the installation and first commissioning see [4].
Due to the large number of RF stations to be commissioned, a commissioning team of 14 members of DESY personal was established. This team was supported by five guests from the SLAC National Accelerator Laboratory and one from the Helmholtz–Zentrum Dresden–Rossendorf (HZDR). The work was organized in two 8–hour shifts per day. It was planned to commission the RF stations SC–wise. The estimated required time was two weeks for L1 (one RF station), two weeks for L2

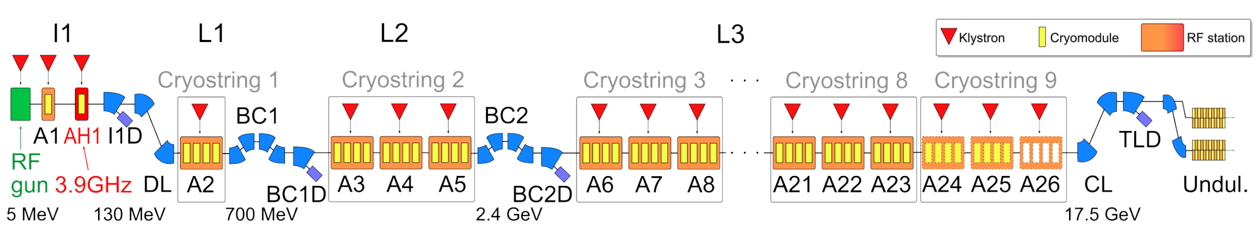

Figure 1: Layout of the European XFEL.

* mathieu.omet@desy.de

Content from this work may be used under the terms of the CC BY 3.0 licence (© 2017). Any distribution of this work must maintain attribution to the author(s), title of the work, publisher, and DOI.

ISBN: 978-3-95450-191-5 doi:10.18429/JACoW-SRF2017-FRXBA02

Content from this work may be used under the terms of the CC BY 3.0 licence (© 2017). Any distribution of this work must maintain attribution to the author(s), title of the work, publisher, and DOI.

HIGH PRECISION RF CONTROL FOR SRF CAVITIES IN LCLS-II

L. Doolittle*, K. Campbell, Q. Du, G. Huang, J. Jones,
C. Serrano, V. Vytla, LBNL, Berkeley, CA 94720, USA
S. Babel, A. Benwell, M. Boyes, G. Brown, D. Cha, G. Dalit, J. DeLong, J. Diaz-Cruz,
B. Hong, R. Kelly, A. McCollough, A. Ratti, C. Rivetta, SLAC, Menlo Park, CA 94720, USA
R. Bachimanchi, C. Hovater, D. Seidman, JLab, Newport News, VA 23606, USA
B. Chase, E. Cullerton, J. Einstein, D. Klepec, FNAL, Batavia, IL 60555, USA

ABSTRACT

The unique properties of SRF cavities enable a new generation of X-ray light sources in XFEL and LCLS-II. The LCLS-II design calls for 280 L-band cavities to be operated in CW mode with a Q_L of 4×10^7, using Single-Source Single-Cavity control. The target RF field stability is 0.01% and 0.01° for the band above 1 Hz. Hardware and software implementing a digital LLRF system has been constructed by a four-lab collaboration to minimize known contributors to cavity RF field fluctuation. Efforts include careful attachment to the phase reference line, and minimizing the effects of RF crosstalk by placing forward and reverse signals in chassis separate from the cavity measurement. A low-noise receiver/digitizer section will allow feedback to operate with high proportional gain without excessive noise being sent to the drive amplifier. Test results will show behavior on prototype cryomodules at FNAL and JLab, ahead of the 2018 final accelerator installation.

INTRODUCTION

LCLS-II is an X-ray Free Electron Laser (FEL) under construction at SLAC, driven by a superconducting RF Linac [1]. The electron beam quality will directly translate to the quality of the X-ray beams produced in undulators and used for scientific research in the end stations; hence strict requirements have been placed on the stability of the accelerating cavity fields. An initial stability goal of 0.01° in phase and 0.01% amplitude has been set for the main Linac, composed of 280 nine-cell 1300 MHz superconducting cavities [2].

Plans for the RF controls for the 1.3 GHz cavities have been described elsewhere [3] [4] [5] [6]. It is based on mainstream digital LLRF technology, and incorporates many ideas developed for LBNL's NGLS proposal [7]. The controls use a Single Source Single Cavity (SSSC) architecture, where each cavity has a dedicated amplifier. SSSC has enormous value for simplifying control of narrow-band SRF cavities, It is also a sensible choice for a CW machine, where Solid-State Amplifier technology has approximately matched Klystrons in price, and they are considered easier to operate and maintain.

The LLRF subsystem of LCLS-II is itself a four-laboratory collaboration: LBNL for architecture, FPGA hardware and RF DSP programming, and ADC/DAC hardware development; Fermilab for downconverters, upconverters and piezo drivers; JLab for interlocks, stepper controls, and power supplies; and SLAC for LO distribution, MO and PRL, global control system integration, commissioning, transition to operations, and project management.

* lrdoolittle@lbl.gov; This work supported under DOE Contract DE-AC02-76SF00515

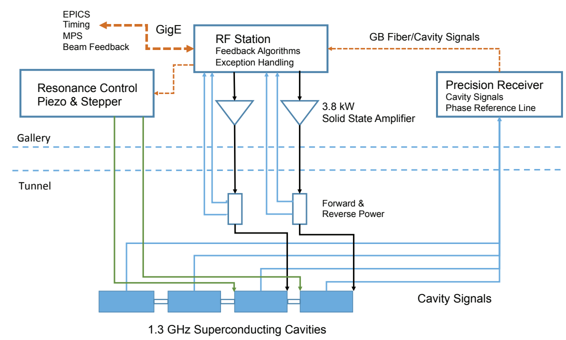

Figure 1: System hardware configuration supporting half of a cryomodule (one of two RF Station chassis shown).

SYSTEM DESIGN

Each rack (supporting four cavities) includes a separate Precision Receiver Chassis (PRC), linked only by optical fiber to two RF Control Chassis (RFS), as shown in figure 1. This density of rack equipment matches the civil layout of the accelerator, where one LLRF rack is cabled to one penetration to the tunnel. The physical separation between PRC and RFS maximizes isolation between the critical stabilized cavity signals and the wildly fluctuating forward and reverse monitoring channels. Preliminary measurements show that this separation has succeeded, in that the measured isolation is at least 125 dB.

The system bypasses some of the usual compromises in choosing an IF by means of an unusual split-LO design, where a low-frequency IF (20 MHz) is used for RF downconversion, and a higher-frequency IF (145 MHz) is used for RF upconversion.

The downconversion IF is 7/33 of the ADC clock rate, yielding near-IQ sampling [8]. The low downconversion IF is good for selecting low-$1/f$-noise amplifiers, and for reducing crosstalk. The 94.3 MHz ADC clock rate is high enough that the whole 9-cell TM_{010} passband (1274-1300 MHz) fits in the first Nyquist zone. The high upconversion IF allows commercial four-section tubular filters with 45 MHz bandwidth to remove the undesired sideband after mixing.